ISSN 2307-8960 (online)

World Journal of *Clinical Cases*

World J Clin Cases 2022 February 16; 10(5): 1457-1753

Published by Baishideng Publishing Group Inc

World Journal of Clinical Cases

Contents

Thrice Monthly Volume 10 Number 5 February 16, 2022

REVIEW

1457 Nonalcoholic fatty liver disease shows significant sex dimorphism

Chen XY, Wang C, Huang YZ, Zhang LL

MINIREVIEWS

1473 Management of procedural pain in the intensive care unit

Guo NN, Wang HL, Zhao MY, Li JG, Liu HT, Zhang TX, Zhang XY, Chu YJ, Yu KJ, Wang CS

ORIGINAL ARTICLE

Clinical and Translational Research

1485 Effect of prior malignancy on the prognosis of gastric cancer and somatic mutation

Yin X, He XK, Wu LY, Yan SX

Retrospective Cohort Study

1498 Elemene-containing hyperthermic intraperitoneal chemotherapy combined with chemotherapy for elderly patients with peritoneal metastatic advanced gastric cancer

Chen ZX, Li J, Liu WB, Zhang SR, Sun H

Retrospective Study

1508 Timing theory continuous nursing, resistance training: Rehabilitation and mental health of caregivers and stroke patients with traumatic fractures

Shen YL, Zhang ZQ, Zhu LJ, Liu JH

1517 Effect of precise nursing service mode on postoperative urinary incontinence prevention in patients with prostate disease

Zheng XC, Luo TT, Cao DD, Cai WZ

1527 Significance of serum glucagon-like peptide-1 and matrix Gla protein levels in patients with diabetes and osteoporosis

Xie FF, Zhang YF, Hu YF, Xie YY, Wang XY, Wang SZ, Xie BQ

1536 Castleman disease and TAFRO syndrome: To improve the diagnostic consciousness is the key

Zhou QY

Observational Study

1548 Correlation of myopia onset and progression with corneal biomechanical parameters in children

Lu LL, Hu XJ, Yang Y, Xu S, Yang SY, Zhang CY, Zhao QY

World Journal of Clinical Cases

Thrice Monthly Volume 10 Number 5 February 16, 2022

Contents

META-ANALYSIS

1557 Intensive *vs* non-intensive statin pretreatment before percutaneous coronary intervention in Chinese patients: A meta-analysis of randomized controlled trials

Yang X, Lan X, Zhang XL, Han ZL, Yan SM, Wang WX, Xu B, Ge WH

CASE REPORT

1572 Giant nodular fasciitis originating from the humeral periosteum: A case report

Yu SL, Sun PL, Li J, Jia M, Gao HW

1580 Tumor-related cytokine release syndrome in a treatment-naïve patient with lung adenocarcinoma: A case report

Deng PB, Jiang J, Hu CP, Cao LM, Li M

1586 Submucosal protuberance caused by a fish bone in the absence of preoperative positive signs: A case report

Du WW, Huang T, Yang GD, Zhang J, Chen J, Wang YB

1592 Misdiagnosis of unroofed coronary sinus syndrome as an ostium primum atrial septal defect by echocardiography: A case report

Chen JL, Yu CG, Wang DJ, Chen HB

1598 Uncommon complication of nasoenteral feeding tube: A case report

Jiang YP, Zhang S, Lin RH

1602 Treatment of extracranial internal carotid artery dissecting aneurysm with SUPERA stent implantation: Two case reports

Qiu MJ, Zhang BR, Song SJ

1609 Combination of atezolizumab and chidamide to maintain long-term remission in refractory metastatic extranodal natural killer/T-cell lymphoma: A case report

Wang J, Gao YS, Xu K, Li XD

1617 Hemangioma in the lower labial vestibule of an eleven-year-old girl: A case report

Aloyouny AY, Alfaifi AJ, Aladhyani SM, Alshalan AA, Alfayadh HM, Salem HM

1623 Primary orbital monophasic synovial sarcoma with calcification: A case report

Ren MY, Li J, Li RM, Wu YX, Han RJ, Zhang C

1630 Small-cell carcinoma of the prostate with negative CD56, NSE, Syn, and CgA indicators: A case report

Shi HJ, Fan ZN, Zhang JS, Xiong BB, Wang HF, Wang JS

1639 Disseminated peritoneal leiomyomatosis with malignant transformation involving right ureter: A case report

Wen CY, Lee HS, Lin JT, Yu CC

World Journal of Clinical Cases

Thrice Monthly Volume 10 Number 5 February 16, 2022

Contents

1645 Arthroscopic surgery for synovial chondroma of the subacromial bursa with non-traumatic shoulder subluxation complications: Two case reports

Tang XF, Qin YG, Shen XY, Chen B, Li YZ

1654 Wilkie's syndrome as a cause of anxiety-depressive disorder: A case report and review of literature

Apostu RC, Chira L, Colcear D, Lebovici A, Nagy G, Scurtu RR, Drasovean R

1667 Gastric schwannoma misdiagnosed as gastrointestinal stromal tumor by ultrasonography before surgery: A case report

Li QQ, Liu D

1675 Giant retroperitoneal lipoma presenting with abdominal distention: A case report and review of the literature

Chen ZY, Chen XL, Yu Q, Fan QB

1684 Pneumothorax during retroperitoneal laparoscopic partial nephrectomy in a lupus nephritis patient: A case report

Zhao Y, Xue XQ, Xia D, Xu WF, Liu GH, Xie Y, Ji ZG

1689 Bulbar conjunctival vascular lesion combined with spontaneous retrobulbar hematoma: A case report

Lei JY, Wang H

1697 Hepatitis B virus in cerebrospinal fluid of a patient with purulent bacterial meningitis detected by multiplex-PCR: A case report

Gao DQ, Hu YQ, Wang X, Zhang YZ

1702 Aseptic abscess in the abdominal wall accompanied by monoclonal gammopathy simulating the local recurrence of rectal cancer: A case report

Yu Y, Feng YD, Zhang C, Li R, Tian DA, Huang HJ

1709 Tacrolimus treatment for relapsing-remitting chronic inflammatory demyelinating polyradiculoneuropathy: Two case reports

Zhu WJ, Da YW, Chen H, Xu M, Lu Y, Di L, Duo JY

1716 Vedolizumab-associated diffuse interstitial lung disease in patients with ulcerative colitis: A case report

Zhang J, Liu MH, Gao X, Dong C, Li YX

1723 Unusual magnetic resonance imaging findings of brain and leptomeningeal metastasis in lung adenocarcinoma: A case report

Li N, Wang YJ, Zhu FM, Deng ST

1729 Diffuse invasive signet ring cell carcinoma in total colorectum caused by ulcerative colitis: A case report and review of literature

Zhang Z, Yu PF, Gu GL, Zhang YH, Wang YM, Dong ZW, Yang HR

1738 Neurothekeoma located in the hallux and axilla: Two case reports

Huang WY, Zhang YQ, Yang XH

1747 Subclavian artery stenting *via* bilateral radial artery access: Four case reports

Qiu T, Fu SQ, Deng XY, Chen M, Dai XY

Contents

Thrice Monthly Volume 10 Number 5 February 16, 2022

ABOUT COVER

Editorial Board Member of *World Journal of Clinical Cases*, Prashanth Panta, MDS, Reader (Associate Professor), Department of Oral Medicine and Radiology, Malla Reddy Institute of Dental Sciences, Suraram 500055, Telangana, India. maithreya.prashanth@gmail.com

AIMS AND SCOPE

The primary aim of *World Journal of Clinical Cases* (*WJCC*, *World J Clin Cases*) is to provide scholars and readers from various fields of clinical medicine with a platform to publish high-quality clinical research articles and communicate their research findings online.

WJCC mainly publishes articles reporting research results and findings obtained in the field of clinical medicine and covering a wide range of topics, including case control studies, retrospective cohort studies, retrospective studies, clinical trials studies, observational studies, prospective studies, randomized controlled trials, randomized clinical trials, systematic reviews, meta-analysis, and case reports.

INDEXING/ABSTRACTING

The *WJCC* is now indexed in Science Citation Index Expanded (also known as SciSearch®), Journal Citation Reports/Science Edition, Scopus, PubMed, and PubMed Central. The 2021 Edition of Journal Citation Reports® cites the 2020 impact factor (IF) for *WJCC* as 1.337; IF without journal self cites: 1.301; 5-year IF: 1.742; Journal Citation Indicator: 0.33; Ranking: 119 among 169 journals in medicine, general and internal; and Quartile category: Q3. The *WJCC*'s CiteScore for 2020 is 0.8 and Scopus CiteScore rank 2020: General Medicine is 493/793.

RESPONSIBLE EDITORS FOR THIS ISSUE

Production Editor: *Lin-YuTong Wang*; **Production Department Director:** *Xiang Li*; **Editorial Office Director:** *Jin-Lei Wang*.

NAME OF JOURNAL
World Journal of Clinical Cases

ISSN
ISSN 2307-8960 (online)

LAUNCH DATE
April 16, 2013

FREQUENCY
Thrice Monthly

PUBLICATION DATE
February 16, 2022

World Journal of Clinical Cases

Submit a Manuscript: https://www.f6publishing.com

World J Clin Cases 2022 February 16; 10(5): 1457-1472

DOI: 10.12998/wjcc.v10.i5.1457

ISSN 2307-8960 (online)

REVIEW

Nonalcoholic fatty liver disease shows significant sex dimorphism

Xing-Yu Chen, Cong Wang, Yi-Zhou Huang, Li-Li Zhang

ORCID number: Xing-Yu Chen 0000-0003-0244-3721; Cong Wang 0000-0002-1209-4978; Yi-Zhou Huang 0000-0002-7151-205X; Li-Li Zhang 0000-0001-9007-5281.

Author contributions: Chen XY was the main author of the review, and completed the collection and analysis of relevant literature and the writing of the first draft of the paper; Wang C and Huang YZ participated in the analysis and collation of literature materials; Zhang LL is the principal of the project, supervising the thesis writing; all authors have read and approve the final manuscript.

Conflict-of-interest statement: The authors declare no conflicts of interest associated with this article.

Country/Territory of origin: China

Specialty type: Gastroenterology and hepatology

Provenance and peer review: Invited article; Externally peer reviewed.

Peer-review model: Single blind

Peer-review report's scientific quality classification

Grade A (Excellent): 0
Grade B (Very good): B
Grade C (Good): C
Grade D (Fair): 0
Grade E (Poor): E

Xing-Yu Chen, Cong Wang, Yi-Zhou Huang, Li-Li Zhang, The Second Affiliated Hospital, Chongqing Medical University, Chongqing 404100, China

Corresponding author: Li-Li Zhang, MD, PhD, Associate Professor, Doctor, Postdoc, Research Fellow, The Second Affiliated Hospital, Chongqing Medical University, No. 74 Linjiang Road, Yuzhong District, Chongqing 404100, China. zhanglili.jl@foxmail.com

Abstract

Nonalcoholic fatty liver disease (NAFLD), which has been renamed metabolic dysfunction-associated fatty liver disease, is a growing global medical problem. The incidence of NAFLD and its associated end-stage liver disease is increasing each year, and many research advancements have been achieved to date. This review focuses on the current knowledge of the sex differences in NAFLD and does not elaborate on areas without differences. Studies have revealed significant sex differences in the prevalence, influencing factors, pathophysiology, complications and therapies of NAFLD. Men have a higher incidence than women. Compared with women, men exhibit increased visceral fat deposition, are more susceptible to leptin resistance, lack estrogen receptors, and tend to synthesize fatty acids into fat storage. Male patients will experience more severe hepatic fibrosis and a higher incidence of liver cancer. However, once NAFLD occurs, women show a faster progression of liver fibrosis, higher levels of liver cell damage and inflammation and are less likely to undergo liver transplantation than men. In general, men have more risk factors and more severe pathophysiological reactions than women, whereas the development of NAFLD is faster in women, and the treatments for women are more limited than those for men. Thus, whether sex differences should be considered in the individualized prevention and treatment of NAFLD in the future is worth considering.

Key Words: Nonalcoholic fatty liver disease; Metabolic dysfunction-associated fatty liver disease; Sex differences; Estrogen; Steatosis; Cirrhosis

Core Tip: Nonalcoholic fatty liver disease (NAFLD) is a sexual dimorphic disease, and its prevalence worldwide is increasing each year. However, our understanding of sex differences in NAFLD remains insufficient. The incidence in males is significantly higher than that in females, and studies have also revealed significant sex differences in

Received: October 5, 2021
Peer-review started: October 5, 2021
First decision: November 15, 2021
Revised: December 2, 2021
Accepted: December 31, 2021
Article in press: December 31, 2021
Published online: February 16, 2022

P-Reviewer: Machado M, Tarantino G, Ulasoglu C
S-Editor: Liu JH
L-Editor: A
P-Editor: Liu JH

influencing factors, pathophysiology, complications and therapies. This review summarizes the current research progress on sex differences in NAFLD and indicates that whether sex differences in NAFLD can be considered in future research, treatment and prevention is worth exploring.

Citation: Chen XY, Wang C, Huang YZ, Zhang LL. Nonalcoholic fatty liver disease shows significant sex dimorphism. *World J Clin Cases* 2022; 10(5): 1457-1472
URL: https://www.wjgnet.com/2307-8960/full/v10/i5/1457.htm
DOI: https://dx.doi.org/10.12998/wjcc.v10.i5.1457

INTRODUCTION

Nonalcoholic fatty liver disease (NAFLD), which has been renamed metabolic dysfunction-associated fatty liver disease, affects approximately a quarter of adults worldwide[1]. In the past, NAFLD was considered a Western disease, but with improvements in living standards, the prevalence of this disease in Asia is increasing each year, particularly in China[2], where the incidence has exceeded that in Europe and North America. NAFLD should be regarded as a global disease. Moreover, NAFLD, which manifests as nonalcoholic fatty liver or nonalcoholic steatohepatitis (NASH), is a growing worldwide cause of chronic liver disease, which may gradually lead to severe liver disease, such as liver cirrhosis, hepatocellular carcinoma, and even death. The increasing prevalence of this disease and the serious complications it may cause pose a substantial medical and economic burden to the whole world[3]. With the development of research on NAFLD, an increasing number of findings have revealed significant sex differences regarding this disease. This review focuses on the current knowledge of sex differences in NAFLD and does not elaborate on the areas without differences. The review mainly focuses on the following aspects: Epidemiology, influencing factors, pathophysiology, complications and treatments.

EPIDEMIOLOGY

The prevalence of NAFLD is increasing annually and has exceeded 25% of the global population. The increasing trend of NAFLD is closely related to the increasing standard of life and the increasing prevalence of obesity[4]. A large number of studies have proven that obesity is an important risk factor for hepatic steatosis and promotes the formation of NAFLD[5-7]. Considering the continuing increase in NAFLD, this disease will be the main cause of cirrhosis and hepatocellular carcinoma (HCC) and is the fastest growing cause of orthotopic liver transplantation[8].

Previous epidemiological studies revealed a significant sex difference in the incidence rate of NAFLD, which is strongly related to age. Overall, the prevalence of NAFLD in men is higher than that in women[7,9-11]. Interestingly, studies in pediatric populations have also found that the prevalence of NAFLD is higher in boys than in girls[12]. A study performed in Korea using data from 6648 subjects found that the prevalence of NAFLD in women increased with age, and the prevalence increased sharply with age among women older than 50 years, particularly after the perimenopausal period. However, the prevalence in men shows minimal differences according to age. The prevalence among men under 50 years of age is significantly higher than that among women (22.6% *vs* 6.8%), whereas the sex difference is not significant among participants over 50 years of age (23.6% *vs* 24.2%)[7]. Similar conclusions have been reached by studies conducted in Shanghai and Japan[10,11]. Compared with men and postmenopausal women, premenopausal women are at a significantly lower risk for NAFLD. Moreover, hormone replacement therapy can reduce the prevalence of NAFLD in postmenopausal women, which suggests that estrogen is protective against NAFLD[13]. Men are more susceptible to NAFLD at a younger age than women, which is a problem worthy of attention. Men are exposed to high metabolic risk for a longer period of time.

INFLUENCING FACTORS

Adipose distribution, adipocytokines and lipid metabolism

The main sex differences in adipose distribution are well recognized: Men store more adipose tissue in their intra-abdominal depots, whereas women tend to have enlarged peripheral adipose tissue, and these differences are associated with the deleterious metabolic consequences of men and the lower cardiometabolic risk of women[14]. Estrogen promotes and maintains typical female fat by reducing the lipolysis of subcutaneous fat without affecting visceral fat[15]. Peripheral adipocytes exhibit a lower lipolytic response[16]. Heine *et al*[17] found that estrogen regulates the amount of adipose tissue. The absence of estrogen receptor α (ERα) causes adipocyte hyperplasia and hypertrophy. Postmenopausal women exhibit increased central fat deposition[18]. For a given waist circumference or body mass index, women have higher levels of subcutaneous adipose tissue than men[19]. Sex also influences lipid storage within the liver and muscle. Fat can be stored in adipose tissue, liver and skeletal muscle as triglycerides (TGs). Excessive liver TG storage leads to NAFLD. Studies have found that men have higher levels of TGs stored in the liver than women, and women store more intramyocellular lipids than men, which explains the higher prevalence of NAFLD in men[20,21]. Skeletal muscle is one of the major organs responsible for peripheral glucose disposal, and a higher intramyocellular lipid content is associated with insulin resistance, which decreases the skeletal muscle glucose uptake[22]. However, the increased levels of intramyocellular lipids in women are not related to a higher risk of diabetes, which may be related to the mechanism through which lipids are stored and metabolized in muscles[20].

Adipose tissue releases a multitude of secretory products, which are collectively called adipocytokines. The related sex differences are mainly reflected by the levels of leptin, adiponectin and prohibitin. Leptin is a metabolic regulator that can reduce food intake and inhibit the synthesis of lipids, and its secretion is proportional to the fat mass. However, in some cases, hyperleptinemia can lead to insulin resistance and participates in hepatic steatosis. Studies have repeatedly shown that adiponectin enhances insulin sensitivity and increases lipolysis, which is inversely correlated with the fat mass[23-25]. Many studies have proven that the levels of leptin and adiponectin in males are lower than those in females[26,27]. The serum leptin levels in men and women with NAFLD are higher than those in individuals without NAFLD, whereas the opposite trend has been found for adiponectin. A previous study showed that the leptin level is correlated with the severity of steatosis in men and women, whereas the serum adiponectin level is inversely correlated with the severity of steatosis in men ($P < 0.01$) but not in women ($P = 0.4$)[26]. Prohibitin plays a sex-dimorphic role in adipose tissue functions[28]. Its overexpression induces the upregulation of mitochondrial organisms, which leads to obesity and impairments in glucose homeostasis and insulin sensitivity, but this issue is specific to males.

The retention of TGs within the liver is a prerequisite for the development of NAFLD. The synthesis of fatty acids (FAs) in the liver is an important determinant of the development of hepatic steatosis[29]. The oxidation of FAs removes TGs from the liver[30]. To some extent, the occurrence of NAFLD depends on the imbalance between liver FA synthesis and oxidation. Individuals with a similar age, BMI, and liver fat content were assessed using metabolic substrates labeled with stable isotope tracers, and the results revealed clear differences in hepatic FA partitioning. Specifically, females tended to favor oxidation pathways, and increased levels of ^{13}C in breath CO_2 and plasma 3-hydroxybutyrate are found in females, whereas males tend to favor synthetic pathways. In both men ($r_s = 0.75$, $P < 0.05$) and women ($r_s = 0.79$, $P < 0.01$), de novo lipogenesis (DNL) is positively correlated with the plasma very low-density lipoprotein (VLDL) cholesterol concentration[31]. As many studies have revealed, premenopausal women have better lipid profiles than men, as demonstrated by higher high-density lipoprotein cholesterol levels and lower low-density lipoprotein cholesterol, VLDL cholesterol and total plasma TG levels[32,33]. The disposal of FAs *via* the oxidation pathway may play an important role in preventing the accumulation of TG in the liver, which may partially explain the sex difference in the prevalence of NAFLD.

In addition, glucocorticoids exert certain effects on the human body during the process of lipid metabolism. Excessive glucocorticoids are related to the pathogenesis of NAFLD, which can cause the decomposition of adipose tissue, hyperlipidemia, visceral fat generation and insulin resistance[34]. One study found hepatic steatosis in 20% of patients with Cushing's syndrome[35]. It is important to note that gender differences remain during the process. Among mice administered high levels of cortisol, male mice exhibit more severe insulin resistance, and female mice show more

protective adaptations to adipose tissue, such as increased adiponectin levels[36].

Estrogen and hepatic ERα

Based on the abovementioned differences in prevalence between men and women and the findings that women of postmenopausal age are at increased risk of developing NAFLD, that hormone replacement therapy is protective against NAFLD after menopause[13], and that women are at increased risk of developing NAFLD after using an anti-estrogen drug or undergoing surgical ovariectomy[37,38], we can assume that the resistance to NAFLD in premenopausal women depends on estrogen. A large number of studies have shown that estrogen regulates almost all steps of lipid metabolism. Estrogen reduces the lipolysis of subcutaneous adipocytes by upregulating alpha2A-adrenergic receptors[15] and thereby reduce the delivery of FAs to the liver. Estrogen regulates liver lipid metabolism through ERα. Estrogen signaling reduces DNL to prevent hepatic steatosis. The lack of estrogen signaling will reduce the VLDL output, promote the accumulation of TGs in the liver, and lead to hepatic insulin resistance[39]. In female mammals, estrogen receptor is highly expressed in the liver, but this finding has rarely been observed in males. This receptor plays an important role in the regulation of the synthesis of receptors for cholesterol uptake, cholesterol transport proteins, and enzymes for lipoprotein remodeling[40]. A recent study found that hepatic ERα shows opposite lipid metabolism regulation in men and women that consume diets high in lipids: the male liver exceeds its compensatory capacity, and liver ERα promotes the accumulation of liver lipids by stimulating the input and synthesis of lipids. While the female liver can handle the excess lipids, and the ERα in the female liver is able to reduce lipid synthesis and absorption and promote FA oxidation[41]. In general, hepatic ERα plays an important role in the sex difference in NAFLD.

Androgen

Polycystic ovary syndrome (PCOS) is a female endocrine disease characterized by hyperandrogenemia. Many studies have documented a higher incidence of NAFLD in women with PCOS. However, only patients with PCOS and high androgen levels are associated with a higher risk of NAFLD[42]. It can be inferred that high androgen levels play an important role in this process. Biological studies have shown that androgen can induce cell cycle arrest and initiate hepatocyte apoptosis[43]. High androgen levels can promote inflammation by activating mononuclear cells[44]. Increased androgen levels increase the visceral fat mass by decreasing the activation of adenosine 5' and monophosphate-activated protein kinase and increasing the expression of lipogenic genes in visceral fat[45]. In men, however, decreased androgen levels are independently associated with NAFLD[46]. Low serum testosterone levels increase visceral fat accumulation and inflammation, and these effects lead to insulin resistance and hepatic steatosis[47-49]. Therefore, further studies may be needed to clarify the mechanism related to androgen and NAFLD.

Mitochondria and liver pyruvate kinase

Mitochondrial dysfunction contributes to the development of NAFLD, which predates insulin dysfunction and hepatic steatosis[50]. Exercise enhances mitochondrial function[51]. In general, females exhibited an improved mitochondrial quality than males. Men often need to exercise to maintain a stronger mitochondrial respiratory function, whereas women can maintain this function even without exercise[52]. A recent study reported a close relationship between liver pyruvate kinase (LPK) and NAFLD. As demonstrated by mouse experiments, LPK affects liver lipids, mitochondrial respiration, glucose metabolism and insulin sensitivity. LPK expression is increased in men under the influence of testosterone. LPK overexpression aggravates insulin resistance, increases the plasma cholesterol levels and exacerbates liver steatosis by changing liver mitochondrial respiration, whereas LPK silencing attenuates these effects. Studies have also found a positive correlation between hepatic LPK expression and the liver TG levels in males but not in females, which shows that LPK is only slightly involved in the development of steatosis in females. Researchers have performed liver biopsies in patients with NASH and observed a strong positive correlation between liver LPK expression and the NAFLD activity score in men but no correlation in women[53]. LPK overexpression exerts a male-specific effect on NAFLD.

Vitamin D deficiency

Vitamin D deficiency can increase hepatic fat accumulation and mildly reduce insulin sensitivity[54]. Studies have found that low serum levels of 25-hydroxyvitamin D are

associated with dyslipidemia and cardiovascular disease[55,56]. Vitamin D increases intestinal calcium absorption, and this finding is more obvious in males than in females[57]. Calcium supplements can improve blood lipids[58]. Estrogen can also affect calcium absorption[59]. A sex disparity has been found for the association of vitamin D deficiency with NAFLD. A cross-sectional study revealed that vitamin D deficiency is positively associated with NAFLD in men, whereas no significant interaction has been observed in women. Vitamin D deficiency is an independent risk factor for NAFLD in men and may be associated with testosterone levels[60]. Women may respond differently to vitamin D supplementation than men, and women show improvements in blood lipids in response to this supplementation[61].

Serum uric acid

Elevated serum uric acid (SUA) is a risk factor for NAFLD[62,63]. The mechanism may be related to the insulin resistance induced by high SUA levels[64]. According to basic studies, SUA can directly induce and regulate hepatic steatosis and stimulate hepatic fat accumulation[65-67]. Many population-based studies have revealed a sex difference in the association between SUA and NAFLD: The correlation between SUA and NAFLD is significantly higher in women than in men[68,69]. However, a study of patients with type 2 diabetes mellitus (T2DM) revealed that although SUA is associated with NAFLD, an increase in the SUA level is independently associated with a higher risk of NAFLD only in male patients[70]. Therefore, whether diabetes is one of the causes of the inconsistent results is worth further study.

Fructose and dietary intake, sleep quality and the gut microbiota

Regarding food choices, women tend to eat more fruits, vegetables and grains, whereas men tend to choose more meat products, eggs and certain types of poultry [71]. Studies have shown that women tend to eat better-quality diets. The negative correlation between diet quality and obesity is similar in both men and women[72]. However, the diet-induced increases in serum TGs are more significant in females[73]. With a high consumption of fructose, the role of fructose in inducing NAFLD has become increasingly important. Fructose can increase insulin resistance and induce an increase in plasma TGs. In a study of a high-fructose diet, female mice that were fed this diet for a long time showed extensive steatosis and ballooning, whereas males showed only a slight increase in hepatic steatosis[73]. These findings suggest that after the long-term consumption of high-fructose foods, women are more likely than men to develop NAFLD/NASH.

Poor sleep affects the production of hormones and increases the risk of metabolic syndrome. However, poor sleep quality can be more detrimental to women than men by increasing the risk of T2DM and cardiovascular disease, and this finding may be related to the higher testosterone levels in men and sex differences in peroxisome proliferator-activated receptor-α[74]. The sex differences in gut microbes may be influenced by age, race, and diet. Intestinal microbiota-dependent metabolites, such as short-chain fatty acids and trimethylamine *N*-oxide, are involved in the regulation of cholesterol metabolism and insulin sensitivity. Women are more vulnerable to adverse effects[75]. Bile acids are important signaling molecules that activate receptors such as farnesoid X receptor, and these receptors have been shown to promote hepatic steatosis[76]. Intestinal microorganisms can mediate the metabolism of bile acids. The gut microbiota differs according to sex, which leads to differences in the synthesis and metabolism of bile acids and other metabolites between males and females and thus affects the metabolism of liver fat[77].

PATHOPHYSIOLOGY

Hepatic fibrosis

NAFLD includes a spectrum of liver disorders consisting of nonalcoholic fatty liver and NASH, which range from simple hepatic steatosis to inflammation and fibrosis and even progress to cirrhosis. Hepatic stellate cells are one of the primary target cells of hepatic inflammatory stimulation and play a major role during liver repair reactions, including fibrosis[78]. In mice, estrogen inhibits the activation of stellate cells and suppresses the induction of hepatic fibrosis through estrogen receptors[79]. A cross-sectional study revealed that postmenopausal women and men are at a higher risk (60% to 70%) of developing severe fibrosis than premenopausal women. In postmenopausal women, estrogen replacement treatment appears to reduce the risk of advanced fibrosis[80]. A recent systematic review and meta-analysis of 62239

individuals also found that women have a lower risk of developing NAFLD than men pooled risk ratio (RR), 0.81; 95%CI, 0.68-0.97; I^2 = 97.5%]. However, after the development of NAFLD, women face a higher risk of developing advanced fibrosis than men (RR, 1.56; 95%CI, 1.36-1.80; I^2 = 0), and this finding is particularly obvious among individuals older than 50 years[81]. This finding suggests the protective effect of estrogen on hepatic fibrosis in patients with NASH, and the effect is more pronounced in patients with hepatitis C virus[82]. However, the severity of hepatocyte injury and inflammation in NAFLD shows the opposite trend. Premenopausal women exhibit increased levels of lobular inflammation, hepatocyte ballooning and Mallory-Denk bodies than men and postmenopausal women. Hormone replacement therapy is related to a risk of more severe hepatocyte inflammation in postmenopausal women [83]. This association may be related to an increase in the progesterone levels, but this hypothesis needs further study.

Branched-chain amino acids

Branched-chain amino acids (BCAAs) are amino acids with nonlinear aliphatic side chains and include the essential amino acids leucine, valine and isoleucine. High plasma BCAA levels may contribute to insulin resistance and increase the risks of metabolic syndrome and T2DM[84,85]. Intestinal microorganisms are also related to the synthesis of BCAAs[86]. The level of plasma BCAAs in patients with NAFLD is increased, and its changes show sex dimorphism. Studies have shown that the plasma BCAA concentration is positively correlated with the severity of NAFLD[87]. However, a recent study found that only the female BCAA concentration is positively associated with the level of steatosis and fibrosis in NAFLD, whereas no correlation has been detected in males, as demonstrated by a moderate negative correlation between the plasma valine level and lobular inflammation. Additionally, menopause alone has no significant effect on the plasma BCAA concentration in NAFLD[88]. The mechanism of BCAAs involved in NAFLD remains unclear. BACCs are associated with activation of the mammalian target of rapamycin pathway and liver injury in mice[89-91]. However, BCAA supplementing can reduce further liver injury in patients with liver cirrhosis[92].

Macrophages and inflammation

A large number of experimental and clinical studies have shown that macrophages play a critical role in the development and progression of NAFLD. Liver-resident macrophages, which are also known as Kupffer cells, are important participants in liver metabolism disorders and inflammation. These cells activate the inflammatory response, recruit monocytes into the liver, and then differentiate into proinflammatory macrophages to promote the development of NAFLD. Kupffer cells are closely associated with insulin resistance, FA accumulation, and inflammatory injury to promote the progression of fibrosis[93]. High fructose intake triggers the activation of Kupffer cells, which leads to an inflammatory response. As mentioned above, fructose plays an important role in inducing NAFLD. The main types of macrophages can be divided into proinflammatory and anti-inflammatory subgroups (M1 and M2), and both estrogen and androgen receptors can be found in murine macrophages and promote M2 phenotype differentiation[94]. The effect of sex on the differentiation of hepatic macrophages in patients with NAFLD has not been reported. However, accumulating evidence shows that testosterone reduces the secretion of proinflammatory cytokines by macrophages and exerts anti-inflammatory effects[95].

COMPLICATIONS

HCC

HCC is the fourth leading cause of cancer-related death worldwide, and its morbidity and mortality rates are both increasing[96,97]. With improvements in the prevention, diagnosis and treatment of viral hepatitis, the proportion of end-stage liver disease caused by NAFLD progression is increasing. NAFLD is the most common cause of chronic liver disease in the world. HCC is one of the major complications of NASH-associated cirrhosis[98]. NASH-related liver disease has become the leading indicator of liver transplantation (LT)[99]. The incidence of liver cancer in males is significantly higher than that in females. Premenopausal women are also at a lower risk of NAFLD than men. Some studies have found that estrogen may prevent the occurrence of liver cancer and can play a beneficial biological role once HCC develops[100]. Among patients with nonsurgical liver cancer and patients undergoing surgical resection, the

prognosis of women is better than that of men[101,102], but the benefits from LT in patients exhibit no significant gender differences[101]. Moreover, under the current organ allocation system, the proportion of women who receive a LT is lower than that of men. The explanations of this sex difference in LT may include size mismatch and lower creatinine levels in women, which leads to lower Model for End-Stage Liver Disease scores[103,104].

Cardiovascular disease

An increasing number of studies have shown that NAFLD can increase the incidence and prevalence of cardiovascular disease (CVD). In addition, the incidence of CVD presents a sex difference similar to that of NAFLD: Men younger than 50 years are at a higher risk of developing CVD than women, but the incidence of CVD in postmenopausal women is higher[105]. Women are also at a lower risk of death from CVD than men[106]. As mentioned above, women exhibit better blood lipid values than men, and men with NAFLD have worse TG and high-density lipoprotein levels than women[107]. In addition, the incidence of other cardiovascular risk factors in patients with NASH, such as hypertension, renal failure and smoking, is lower in women than in men. Women are more likely to develop obesity and diabetes. A retrospective observational cohort study of 41005 adult patients with NASH conducted by Gayatri Pemmasani found that males have a higher incidence of most CVDs, such as coronary artery disease, myocardial infarction, and heart failure, than females[108]. However, another previous study showed that women with NAFLD lose the protective effect that women have against cardiovascular disease[109]. These researchers found that women and men with NAFLD have a similar risk of CVD and that women with NAFLD develop CVD earlier than women without NAFLD. This finding may be due to the high metabolic burden of patients with NAFLD because these metabolites neutralize the protective effect of estrogen.

T2DM

NAFLD is associated with an increased risk of T2DM, is involved in the pathogenesis of T2DM and promotes insulin resistance. Obesity is a risk factor for NAFLD and T2DM. However, a recent study obtained a novel finding that NAFLD has a hazard ratio of 2.331 for the incidence of diabetes. Among lean patients with NAFLD, the effect appeared to be more pronounced in women, particularly postmenopausal women, than in men (5.53 *vs* 2.02)[110]. A study conducted in Japan also showed that the female sex is an independent risk factor for T2DM through the follow-up of patients diagnosed with NAFLD[111].

Others

A previous study showed that the serum insulin levels are directly correlated with a higher risk of colorectal adenomas (OR, 1.5; 95%CI, 1.1-2.0; $P = 0.005$) and hyperplastic polyps (OR, 1.3; 95%CI, 1.0-1.7; $P = 0.075$)[112]. Disorders of insulin and adipocytokine metabolism are now thought to influence the development of colon tumors[113]. Patients with NAFLD always show fat metabolism disorders, insulin resistance, and high insulin levels. A large number of studies have shown that NAFLD is a risk factor for adenomatous polyps and hyperplastic polyps[114,115]. However, the correlation exhibits significant sex differences: NAFLD is associated with an increased risk of colorectal adenomatous and hyperplastic polyps in men (OR = 1.53, 95%CI: 1.18-2.00, $P < 0.05$; OR = 1.42, 95%CI: 1.04-1.95, $P < 0.05$) but is not a significant risk factor in women (OR = 0.44, 95%CI: 0.18-1.04, $P > 0.05$; OR = 1.18, 95%CI: 0.50-2.78, $P > 0.05$) [115]. The promoting mechanism of NAFLD on colorectal adenoma and hyperplastic polyps is unclear, but some researches believe that this mechanism may be related to the metabolic disorder of adipocytes and the effect of inflammatory cytokines[113]; thus hypothesis needs further exploration.

Abdominal obesity and insulin resistance are risk factors for erosive esophagitis (EO). Metabolic syndrome (MS) and NAFLD are significantly associated with EO. A previous study revealed significant sex differences in the effects of NAFLD and MS on EO: MS (OR 1.26; 95%CI 1.09 to 1.45) shows a greater detrimental effect on EO in males, NAFLD (OR 1.93; 95%CI 1.43 to 2.59) is significantly associated with EO in females, and the relationship between NAFLD and EO is stronger in premenopausal females than in postmenopausal females (51.1% *vs* 48.9%)[116]. In addition, MS is independently associated with EO through increased serum cytokines. Men exhibit increased visceral obesity deposition than women, and visceral obesity increases the esophageal reflux by increasing the serum cytokine levels[117]. The sex difference between NAFLD and EO may be related to estrogen, which reduces oxidative stress

and serum cytokines. Hence, the decrease in estrogen levels found in female patients with NAFLD leads to a decrease in the protective effect on EO.

THERAPY

Very low-carbohydrate ketogenic diets

Obesity is a risk factor for NAFLD. Very low-carbohydrate ketogenic diets (VLCKDs) constitute a new treatment for obesity that functions by reducing the caloric intake and promoting the transformation of energy metabolism from carbohydrates to TGs to reduce weight. Previous studies have suggested that VLCKDs are associated with inducing the activity of lysosomal acid lipase and improving hepatic steatosis, which can benefit patients with NAFLD[118]. Studies have shown that men benefit more from this therapy than women, particularly premenopausal women[119]. This finding may be related to the fact that men have more visceral adipose tissue and exhibit a higher basal energy expenditure.

Inhibition of protein tyrosine phosphatase 1B

Protein tyrosine phosphatase 1B (PTP1B) is an enzyme with multiple functions that can inhibit leptin and insulin signal transduction, which results in abnormal glucose tolerance and hepatic steatosis. PTP1B inhibition may be a potential weight loss therapy that increases energy consumption, weight loss and insulin sensitivity[120]. A study of the role of proopiomelanocortin neuronal-specific PTP1B deficiency in metabolic regulation after consumption of a high-fat diet found that male but not female mice fed this diet exhibit significantly reduced liver lipid accumulation than control mice[121]. This result may indicate that PTP1B is a potential target in the treatment of NAFLD in men.

Others

At present, the treatment of NAFLD remains focused on prevention, as reflected by the control of risk factors, such as weight loss, reduced fat and fructose intake, increased exercise, and vitamin D supplementation. Men lose weight mainly by reducing their visceral adipose tissue and exhibit better histological improvement than women[122,123]. Women are more affected by dietary factors than men. Reducing lipid and fructose intake is more beneficial for female patients. Physical activities are beneficial to the prevention of NAFLD, and exercise can reduce liver enzymes in postmenopausal women[124]. Vitamin D deficiency is an independent risk factor for NAFLD in men, and men should be screened early and administered timely supplementation. Therefore, the optimal prevention of NAFLD may differ by sex, but no consensus has been reached, and further exploration is still needed.

CONCLUSION

As mentioned above, NAFLD exhibits significant sex dimorphism in many aspects, particularly in influencing factors, pathophysiology (Figure 1) and intrahepatic and extrahepatic damage (Figure 2). In general, the higher incidence among males than females is related to adipose distribution, adipose metabolism, differences in estrogen and its receptors, liver metabolism and other factors. The protective effects of estrogen reduce the degree of liver fibrosis in women. Robust evidence shows that NAFLD is closely associated with liver cancer, cardiovascular disease, T2DM and other diseases, and men with NAFLD are at a higher risk of experiencing these complications than women. However, once NAFLD occurs, the inflammation and disease progression is markedly worse among female than male patients, and the treatments for females are more limited than those for men. Although we found a large number of sex differences in NAFLD, the relevant principles are unclear, and further research is needed. Whether sex differences should be considered in future research and whether they can be applied to clinical personalized treatment and prevention are still worth exploring.

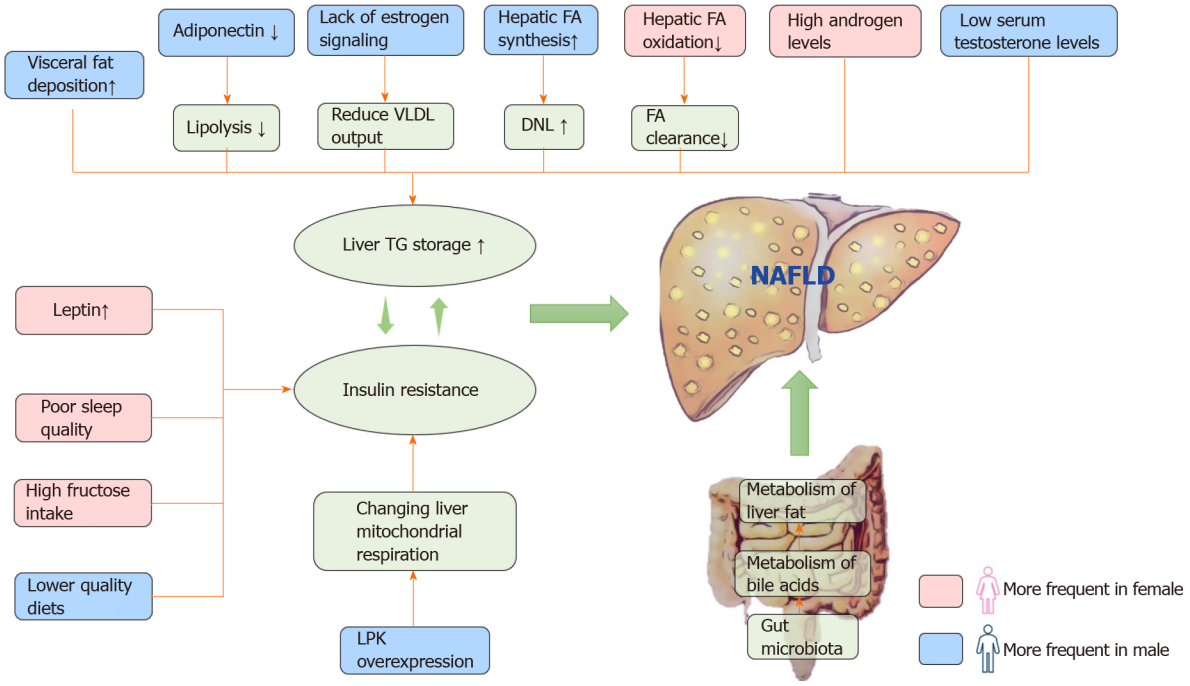

Figure 1 Overview of sex differences in etiology and pathogenesis of nonalcoholic fatty liver disease. Men store more visceral adipose tissue than women. Adipokines mediate fat metabolism, and adiponectin can increase lipolysis; however, excessive leptin can lead to insulin resistance and steatosis. The estrogen receptor plays an important role in the regulation of fat metabolism. Increased androgen levels in women and low testosterone in men are prone to visceral fat accumulation. In the process of fatty acid metabolism, men tend to synthesize, and women tend to oxidize. We found that the overexpression of liver pyruvate kinase can lead to changes in liver mitochondrial function, which leads to the deformation of liver fat. The difference in intestinal microflora between men and women also plays a role in the sex difference in nonalcoholic fatty liver disease (NAFLD). In addition, sleep quality, high sugar intake and diet quality can also affect the formation of NAFLD. VLDL: Very low-density lipoprotein; DNL: De novo lipogenesis; TG: Triglyceride; LPK: Liver pyruvate kinase; FA: Fatty acid; NAFLD: Nonalcoholic fatty liver disease.

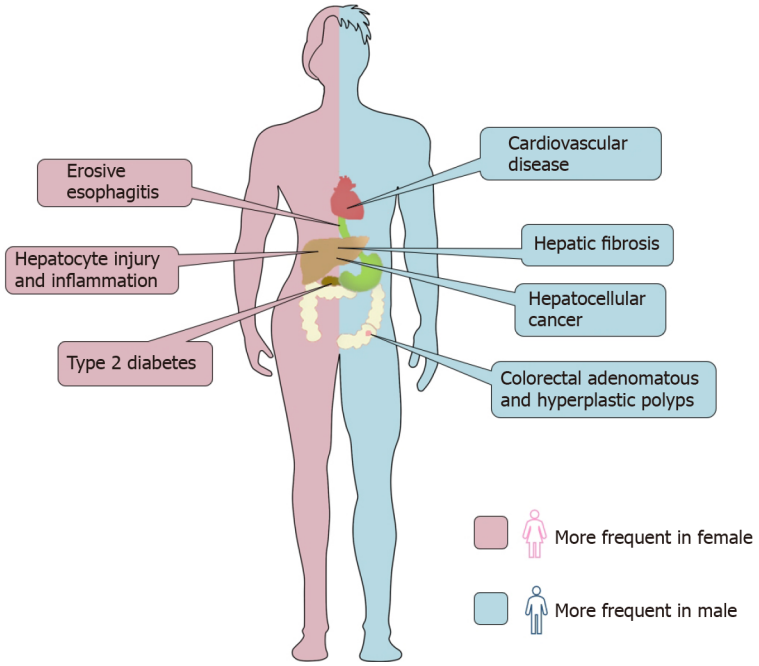

Figure 2 Sex differences in intrahepatic and extrahepatic outcomes in nonalcoholic fatty liver disease. As a metabolic disorder, nonalcoholic fatty liver disease (NAFLD) is related not only to liver injury but also to a variety of extrahepatic diseases. The picture summarizes the differences between men and women in this respect. Without the protection of estrogen, men have more serious liver fibrosis than women and are more likely to develop liver cancer. The incidence of cardiovascular events and colorectal adenoma in men with NAFLD is higher than that in women. However, female patients have more severe hepatocyte injury and inflammation than male patients and have a higher risk of erosive esophagitis and type 2 diabetes.

REFERENCES

1 **Eslam M**, Sanyal AJ, George J; International Consensus Panel. MAFLD: A Consensus-Driven Proposed Nomenclature for Metabolic Associated Fatty Liver Disease. *Gastroenterology* 2020; **158**: 1999-2014.e1 [PMID: 32044314 DOI: 10.1053/j.gastro.2019.11.312]

2 **Zhou F**, Zhou J, Wang W, Zhang XJ, Ji YX, Zhang P, She ZG, Zhu L, Cai J, Li H. Unexpected Rapid Increase in the Burden of NAFLD in China From 2008 to 2018: A Systematic Review and Meta-Analysis. *Hepatology* 2019; **70**: 1119-1133 [PMID: 31070259 DOI: 10.1002/hep.30702]

3 **Younossi Z**, Anstee QM, Marietti M, Hardy T, Henry L, Eslam M, George J, Bugianesi E. Global burden of NAFLD and NASH: trends, predictions, risk factors and prevention. *Nat Rev Gastroenterol Hepatol* 2018; **15**: 11-20 [PMID: 28930295 DOI: 10.1038/nrgastro.2017.109]

4 **Finucane MM**, Stevens GA, Cowan MJ, Danaei G, Lin JK, Paciorek CJ, Singh GM, Gutierrez HR, Lu Y, Bahalim AN, Farzadfar F, Riley LM, Ezzati M; Global Burden of Metabolic Risk Factors of Chronic Diseases Collaborating Group (Body Mass Index). National, regional, and global trends in body-mass index since 1980: systematic analysis of health examination surveys and epidemiological studies with 960 country-years and 9·1 million participants. *Lancet* 2011; **377**: 557-567 [PMID: 21295846 DOI: 10.1016/S0140-6736(10)62037-5]

5 **Festi D**, Colecchia A, Sacco T, Bondi M, Roda E, Marchesini G. Hepatic steatosis in obese patients: clinical aspects and prognostic significance. *Obes Rev* 2004; **5**: 27-42 [PMID: 14969505 DOI: 10.1111/j.1467-789x.2004.00126.x]

6 **Morita S**, Neto Dde S, Morita FH, Morita NK, Lobo SM. Prevalence of Non-alcoholic Fatty Liver Disease and Steatohepatitis Risk Factors in Patients Undergoing Bariatric Surgery. *Obes Surg* 2015; **25**: 2335-2343 [PMID: 25920616 DOI: 10.1007/s11695-015-1696-5]

7 **Park SH**, Jeon WK, Kim SH, Kim HJ, Park DI, Cho YK, Sung IK, Sohn CI, Keum DK, Kim BI. Prevalence and risk factors of non-alcoholic fatty liver disease among Korean adults. *J Gastroenterol Hepatol* 2006; **21**: 138-143 [PMID: 16706825 DOI: 10.1111/j.1440-1746.2005.04086.x]

8 **Shingina A**, DeWitt PE, Dodge JL, Biggins SW, Gralla J, Sprague D, Bambha K. Future Trends in Demand for Liver Transplant: Birth Cohort Effects Among Patients With NASH and HCC. *Transplantation* 2019; **103**: 140-148 [PMID: 30451739 DOI: 10.1097/TP.0000000000002497]

9 **Eguchi Y**, Hyogo H, Ono M, Mizuta T, Ono N, Fujimoto K, Chayama K, Saibara T; JSG-NAFLD. Prevalence and associated metabolic factors of nonalcoholic fatty liver disease in the general population from 2009 to 2010 in Japan: a multicenter large retrospective study. *J Gastroenterol* 2012; **47**: 586-595 [PMID: 22328022 DOI: 10.1007/s00535-012-0533-z]

10 **Fang JG**, Zhu J, Li XJ, Li R, Dai F, Song XM, Chen L, Li F, Chen SY. [Epidemiological survey of prevalence of fatty liver and its risk factors in a general adult population of Shanghai]. *Zhonghua Gan Zang Bing Za Zhi* 2005; **13**: 83-88 [PMID: 15727689]

11 **Hamaguchi M**, Kojima T, Ohbora A, Takeda N, Fukui M, Kato T. Aging is a risk factor of nonalcoholic fatty liver disease in premenopausal women. *World J Gastroenterol* 2012; **18**: 237-243 [PMID: 22294826 DOI: 10.3748/wjg.v18.i3.237]

12 **Anderson EL**, Howe LD, Jones HE, Higgins JP, Lawlor DA, Fraser A. The Prevalence of Non-Alcoholic Fatty Liver Disease in Children and Adolescents: A Systematic Review and Meta-Analysis. *PLoS One* 2015; **10**: e0140908 [PMID: 26512983 DOI: 10.1371/journal.pone.0140908]

13 **McKenzie J**, Fisher BM, Jaap AJ, Stanley A, Paterson K, Sattar N. Effects of HRT on liver enzyme levels in women with type 2 diabetes: a randomized placebo-controlled trial. *Clin Endocrinol (Oxf)* 2006; **65**: 40-44 [PMID: 16817817 DOI: 10.1111/j.1365-2265.2006.02543.x]

14 **Karastergiou K**, Smith SR, Greenberg AS, Fried SK. Sex differences in human adipose tissues - the biology of pear shape. *Biol Sex Differ* 2012; **3**: 13 [PMID: 22651247 DOI: 10.1186/2042-6410-3-13]

15 **Pedersen SB**, Kristensen K, Hermann PA, Katzenellenbogen JA, Richelsen B. Estrogen controls lipolysis by up-regulating alpha2A-adrenergic receptors directly in human adipose tissue through the estrogen receptor alpha. Implications for the female fat distribution. *J Clin Endocrinol Metab* 2004; **89**: 1869-1878 [PMID: 15070958 DOI: 10.1210/jc.2003-031327]

16 **Leibel RL**, Edens NK, Fried SK. Physiologic basis for the control of body fat distribution in humans. *Annu Rev Nutr* 1989; **9**: 417-443 [PMID: 2669880 DOI: 10.1146/annurev.nu.09.070189.002221]

17 **Heine PA**, Taylor JA, Iwamoto GA, Lubahn DB, Cooke PS. Increased adipose tissue in male and female estrogen receptor-alpha knockout mice. *Proc Natl Acad Sci U S A* 2000; **97**: 12729-12734 [PMID: 11070086 DOI: 10.1073/pnas.97.23.12729]

18 **Ambikairajah A**, Walsh E, Tabatabaei-Jafari H, Cherbuin N. Fat mass changes during menopause: a metaanalysis. *Am J Obstet Gynecol* 2019; **221**: 393-409.e50 [PMID: 31034807 DOI: 10.1016/j.ajog.2019.04.023]

19 **Camhi SM**, Bray GA, Bouchard C, Greenway FL, Johnson WD, Newton RL, Ravussin E, Ryan DH, Smith SR, Katzmarzyk PT. The relationship of waist circumference and BMI to visceral, subcutaneous, and total body fat: sex and race differences. *Obesity (Silver Spring)* 2011; **19**: 402-408 [PMID: 20948514 DOI: 10.1038/oby.2010.248]

20 **Beaudry KM**, Devries MC. Sex-based differences in hepatic and skeletal muscle triglyceride storage and metabolism [1]. *Appl Physiol Nutr Metab* 2019; **44**: 805-813 [PMID: 30702924 DOI: 10.1139/apnm-2018-0635]

21 **Høeg L**, Roepstorff C, Thiele M, Richter EA, Wojtaszewski JF, Kiens B. Higher intramuscular

triacylglycerol in women does not impair insulin sensitivity and proximal insulin signaling. *J Appl Physiol (1985)* 2009; **107**: 824-831 [PMID: 19574502 DOI: 10.1152/japplphysiol.91382.2008]

22 **van Loon LJ**. Use of intramuscular triacylglycerol as a substrate source during exercise in humans. *J Appl Physiol (1985)* 2004; **97**: 1170-1187 [PMID: 15358749 DOI: 10.1152/japplphysiol.00368.2004]

23 **Kim JY**, van de Wall E, Laplante M, Azzara A, Trujillo ME, Hofmann SM, Schraw T, Durand JL, Li H, Li G, Jelicks LA, Mehler MF, Hui DY, Deshaies Y, Shulman GI, Schwartz GJ, Scherer PE. Obesity-associated improvements in metabolic profile through expansion of adipose tissue. *J Clin Invest* 2007; **117**: 2621-2637 [PMID: 17717599 DOI: 10.1172/jci31021]

24 **Berg AH**, Combs TP, Du X, Brownlee M, Scherer PE. The adipocyte-secreted protein Acrp30 enhances hepatic insulin action. *Nat Med* 2001; **7**: 947-953 [PMID: 11479628 DOI: 10.1038/90992]

25 **Yamauchi T**, Kamon J, Minokoshi Y, Ito Y, Waki H, Uchida S, Yamashita S, Noda M, Kita S, Ueki K, Eto K, Akanuma Y, Froguel P, Foufelle F, Ferre P, Carling D, Kimura S, Nagai R, Kahn BB, Kadowaki T. Adiponectin stimulates glucose utilization and fatty-acid oxidation by activating AMP-activated protein kinase. *Nat Med* 2002; **8**: 1288-1295 [PMID: 12368907 DOI: 10.1038/nm788]

26 **Ayonrinde OT**, Olynyk JK, Beilin LJ, Mori TA, Pennell CE, de Klerk N, Oddy WH, Shipman P, Adams LA. Gender-specific differences in adipose distribution and adipocytokines influence adolescent nonalcoholic fatty liver disease. *Hepatology* 2011; **53**: 800-809 [PMID: 21374659 DOI: 10.1002/hep.24097]

27 **Valencak TG**, Osterrieder A, Schulz TJ. Sex matters: The effects of biological sex on adipose tissue biology and energy metabolism. *Redox Biol* 2017; **12**: 806-813 [PMID: 28441629 DOI: 10.1016/j.redox.2017.04.012]

28 **Ande SR**, Nguyen KH, Padilla-Meier GP, Wahida W, Nyomba BL, Mishra S. Prohibitin overexpression in adipocytes induces mitochondrial biogenesis, leads to obesity development, and affects glucose homeostasis in a sex-specific manner. *Diabetes* 2014; **63**: 3734-3741 [PMID: 24947361 DOI: 10.2337/db13-1807]

29 **Lambert JE**, Ramos-Roman MA, Browning JD, Parks EJ. Increased de novo lipogenesis is a distinct characteristic of individuals with nonalcoholic fatty liver disease. *Gastroenterology* 2014; **146**: 726-735 [PMID: 24316260 DOI: 10.1053/j.gastro.2013.11.049]

30 **Hodson L**, Frayn KN. Hepatic fatty acid partitioning. *Curr Opin Lipidol* 2011; **22**: 216-224 [PMID: 21494141 DOI: 10.1097/MOL.0b013e3283462e16]

31 **Pramfalk C**, Pavlides M, Banerjee R, McNeil CA, Neubauer S, Karpe F, Hodson L. Sex-Specific Differences in Hepatic Fat Oxidation and Synthesis May Explain the Higher Propensity for NAFLD in Men. *J Clin Endocrinol Metab* 2015; **100**: 4425-4433 [PMID: 26414963 DOI: 10.1210/jc.2015-2649]

32 **Magkos F**, Mittendorfer B. Gender differences in lipid metabolism and the effect of obesity. *Obstet Gynecol Clin North Am* 2009; **36**: 245-265, vii [PMID: 19501312 DOI: 10.1016/j.ogc.2009.03.001]

33 **Johnson JL**, Slentz CA, Duscha BD, Samsa GP, McCartney JS, Houmard JA, Kraus WE. Gender and racial differences in lipoprotein subclass distributions: the STRRIDE study. *Atherosclerosis* 2004; **176**: 371-377 [PMID: 15380461 DOI: 10.1016/j.atherosclerosis.2004.05.018]

34 **Papanastasiou L**, Fountoulakis S, Vatalas IA. Adrenal disorders and non-alcoholic fatty liver disease. *Minerva Endocrinol* 2017; **42**: 151-163 [PMID: 27973460 DOI: 10.23736/S0391-1977.16.02583-9]

35 **Rockall AG**, Sohaib SA, Evans D, Kaltsas G, Isidori AM, Monson JP, Besser GM, Grossman AB, Reznek RH. Hepatic steatosis in Cushing's syndrome: a radiological assessment using computed tomography. *Eur J Endocrinol* 2003; **149**: 543-548 [PMID: 14640995 DOI: 10.1530/eje.0.1490543]

36 **Kaikaew K**, Steenbergen J, van Dijk TH, Grefhorst A, Visser JA. Sex Difference in Corticosterone-Induced Insulin Resistance in Mice. *Endocrinology* 2019; **160**: 2367-2387 [PMID: 31265057 DOI: 10.1210/en.2019-00194]

37 **Nishino M**, Hayakawa K, Nakamura Y, Morimoto T, Mukaihara S. Effects of tamoxifen on hepatic fat content and the development of hepatic steatosis in patients with breast cancer: high frequency of involvement and rapid reversal after completion of tamoxifen therapy. *AJR Am J Roentgenol* 2003; **180**: 129-134 [PMID: 12490491 DOI: 10.2214/ajr.180.1.1800129]

38 **Matsuo K**, Gualtieri MR, Cahoon SS, Jung CE, Paulson RJ, Shoupe D, Muderspach LI, Wakatsuki A, Wright JD, Roman LD. Surgical menopause and increased risk of nonalcoholic fatty liver disease in endometrial cancer. *Menopause* 2016; **23**: 189-196 [PMID: 26173075 DOI: 10.1097/GME.0000000000000500]

39 **Palmisano BT**, Zhu L, Stafford JM. Role of Estrogens in the Regulation of Liver Lipid Metabolism. *Adv Exp Med Biol* 2017; **1043**: 227-256 [PMID: 29224098 DOI: 10.1007/978-3-319-70178-3_12]

40 **Della Torre S**, Mitro N, Fontana R, Gomaraschi M, Favari E, Recordati C, Lolli F, Quagliarini F, Meda C, Ohlsson C, Crestani M, Uhlenhaut NH, Calabresi L, Maggi A. An Essential Role for Liver ERα in Coupling Hepatic Metabolism to the Reproductive Cycle. *Cell Rep* 2016; **15**: 360-371 [PMID: 27050513 DOI: 10.1016/j.celrep.2016.03.019]

41 **Meda C**, Barone M, Mitro N, Lolli F, Pedretti S, Caruso D, Maggi A, Della Torre S. Hepatic ERα accounts for sex differences in the ability to cope with an excess of dietary lipids. *Mol Metab* 2020; **32**: 97-108 [PMID: 32029233 DOI: 10.1016/j.molmet.2019.12.009]

42 **Ramezani-Binabaj M**, Motalebi M, Karimi-Sari H, Rezaee-Zavareh MS, Alavian SM. Are women with polycystic ovarian syndrome at a high risk of non-alcoholic Fatty liver disease; a meta-analysis. *Hepat Mon* 2014; **14**: e23235 [PMID: 25598791 DOI: 10.5812/hepatmon.23235]

43 **Dai R**, Yan D, Li J, Chen S, Liu Y, Chen R, Duan C, Wei M, Li H, He T. Activation of PKR/eIF2α signaling cascade is associated with dihydrotestosterone-induced cell cycle arrest and apoptosis in human liver cells. *J Cell Biochem* 2012; **113**: 1800-1808 [PMID: 22228470 DOI: 10.1002/jcb.24051]

44 **González F**, Nair KS, Daniels JK, Basal E, Schimke JM. Hyperandrogenism sensitizes mononuclear cells to promote glucose-induced inflammation in lean reproductive-age women. *Am J Physiol Endocrinol Metab* 2012; **302**: E297-E306 [PMID: 22045316 DOI: 10.1152/ajpendo.00416.2011]

45 **McInnes KJ**, Corbould A, Simpson ER, Jones ME. Regulation of adenosine 5',monophosphate-activated protein kinase and lipogenesis by androgens contributes to visceral obesity in an estrogen-deficient state. *Endocrinology* 2006; **147**: 5907-5913 [PMID: 16990341 DOI: 10.1210/en.2006-0879]

46 **Kim S**, Kwon H, Park JH, Cho B, Kim D, Oh SW, Lee CM, Choi HC. A low level of serum total testosterone is independently associated with nonalcoholic fatty liver disease. *BMC Gastroenterol* 2012; **12**: 69 [PMID: 22691278 DOI: 10.1186/1471-230X-12-69]

47 **Tsai EC**, Boyko EJ, Leonetti DL, Fujimoto WY. Low serum testosterone level as a predictor of increased visceral fat in Japanese-American men. *Int J Obes Relat Metab Disord* 2000; **24**: 485-491 [PMID: 10805506 DOI: 10.1038/sj.ijo.0801183]

48 **Tarantino G**, Savastano S, Colao A. Hepatic steatosis, low-grade chronic inflammation and hormone/growth factor/adipokine imbalance. *World J Gastroenterol* 2010; **16**: 4773-4783 [PMID: 20939105 DOI: 10.3748/wjg.v16.i38.4773]

49 **Tsai EC**, Matsumoto AM, Fujimoto WY, Boyko EJ. Association of bioavailable, free, and total testosterone with insulin resistance: influence of sex hormone-binding globulin and body fat. *Diabetes Care* 2004; **27**: 861-868 [PMID: 15047639 DOI: 10.2337/diacare.27.4.861]

50 **Rector RS**, Thyfault JP, Uptergrove GM, Morris EM, Naples SP, Borengasser SJ, Mikus CR, Laye MJ, Laughlin MH, Booth FW, Ibdah JA. Mitochondrial dysfunction precedes insulin resistance and hepatic steatosis and contributes to the natural history of non-alcoholic fatty liver disease in an obese rodent model. *J Hepatol* 2010; **52**: 727-736 [PMID: 20347174 DOI: 10.1016/j.jhep.2009.11.030]

51 **Fletcher JA**, Meers GM, Linden MA, Kearney ML, Morris EM, Thyfault JP, Rector RS. Impact of various exercise modalities on hepatic mitochondrial function. *Med Sci Sports Exerc* 2014; **46**: 1089-1097 [PMID: 24263979 DOI: 10.1249/MSS.0000000000000223]

52 **Bellissimo CA**, Perry CGR. Sex differences in the regulation of hepatic mitochondrial turnover following physical activity: do males need more quality control than females? *J Physiol* 2018; **596**: 6125-6126 [PMID: 30284737 DOI: 10.1113/JP276896]

53 **Chella Krishnan K**, Floyd RR, Sabir S, Jayasekera DW, Leon-Mimila PV, Jones AE, Cortez AA, Shravah V, Péterfy M, Stiles L, Canizales-Quinteros S, Divakaruni AS, Huertas-Vazquez A, Lusis AJ. Liver Pyruvate Kinase Promotes NAFLD/NASH in Both Mice and Humans in a Sex-Specific Manner. *Cell Mol Gastroenterol Hepatol* 2021; **11**: 389-406 [PMID: 32942044 DOI: 10.1016/j.jcmgh.2020.09.004]

54 **Giblin RJ**, Bennett EJ, Zosky GR, Dwyer RM. The Impact of Sex and 25(OH)D Deficiency on Metabolic Function in Mice. *Nutrients* 2017; **9** [PMID: 28880231 DOI: 10.3390/nu9090985]

55 **Dobnig H**, Pilz S, Scharnagl H, Renner W, Seelhorst U, Wellnitz B, Kinkeldei J, Boehm BO, Weihrauch G, Maerz W. Independent association of low serum 25-hydroxyvitamin d and 1,25-dihydroxyvitamin d levels with all-cause and cardiovascular mortality. *Arch Intern Med* 2008; **168**: 1340-1349 [PMID: 18574092 DOI: 10.1001/archinte.168.12.1340]

56 **Karhapää P**, Pihlajamäki J, Pörsti I, Kastarinen M, Mustonen J, Niemelä O, Kuusisto J. Diverse associations of 25-hydroxyvitamin D and 1,25-dihydroxy-vitamin D with dyslipidaemias. *J Intern Med* 2010; **268**: 604-610 [PMID: 20831628 DOI: 10.1111/j.1365-2796.2010.02279.x]

57 **Uhland-Smith A**, DeLuca HF. 1,25-dihydroxycholecalciferol analogs cannot replace vitamin D in normocalcemic male rats. *J Nutr* 1993; **123**: 1777-1785 [PMID: 8229291 DOI: 10.1093/jn/123.11.1777]

58 **Major GC**, Alarie F, Doré J, Phouttama S, Tremblay A. Supplementation with calcium + vitamin D enhances the beneficial effect of weight loss on plasma lipid and lipoprotein concentrations. *Am J Clin Nutr* 2007; **85**: 54-59 [PMID: 17209177 DOI: 10.1093/ajcn/85.1.54]

59 **Dong XL**, Zhang Y, Wong MS. Estrogen deficiency-induced Ca balance impairment is associated with decrease in expression of epithelial Ca transport proteins in aged female rats. *Life Sci* 2014; **96**: 26-32 [PMID: 24378673 DOI: 10.1016/j.lfs.2013.12.025]

60 **Park D**, Kwon H, Oh SW, Joh HK, Hwang SS, Park JH, Yun JM, Lee H, Chung GE, Ze S, Bae Y, Lee A. Is Vitamin D an Independent Risk Factor of Nonalcoholic Fatty Liver Disease? *J Korean Med Sci* 2017; **32**: 95-101 [PMID: 27914137 DOI: 10.3346/jkms.2017.32.1.95]

61 **Sharifi N**, Amani R, Hajiani E, Cheraghian B. Women may respond different from men to vitamin D supplementation regarding cardiometabolic biomarkers. *Exp Biol Med (Maywood)* 2016; **241**: 830-838 [PMID: 26811103 DOI: 10.1177/1535370216629009]

62 **Xu C**, Yu C, Xu L, Miao M, Li Y. High serum uric acid increases the risk for nonalcoholic Fatty liver disease: a prospective observational study. *PLoS One* 2010; **5**: e11578 [PMID: 20644649 DOI: 10.1371/journal.pone.0011578]

63 **Shih MH**, Lazo M, Liu SH, Bonekamp S, Hernaez R, Clark JM. Association between serum uric acid and nonalcoholic fatty liver disease in the US population. *J Formos Med Assoc* 2015; **114**: 314-320 [PMID: 25839764 DOI: 10.1016/j.jfma.2012.11.014]

64 **Zhu Y**, Hu Y, Huang T, Zhang Y, Li Z, Luo C, Luo Y, Yuan H, Hisatome I, Yamamoto T, Cheng J.

High uric acid directly inhibits insulin signalling and induces insulin resistance. *Biochem Biophys Res Commun* 2014; **447**: 707-714 [PMID: 24769205 DOI: 10.1016/j.bbrc.2014.04.080]

65 **Lanaspa MA**, Sanchez-Lozada LG, Choi YJ, Cicerchi C, Kanbay M, Roncal-Jimenez CA, Ishimoto T, Li N, Marek G, Duranay M, Schreiner G, Rodriguez-Iturbe B, Nakagawa T, Kang DH, Sautin YY, Johnson RJ. Uric acid induces hepatic steatosis by generation of mitochondrial oxidative stress: potential role in fructose-dependent and -independent fatty liver. *J Biol Chem* 2012; **287**: 40732-40744 [PMID: 23035112 DOI: 10.1074/jbc.M112.399899]

66 **Wan X**, Xu C, Lin Y, Lu C, Li D, Sang J, He H, Liu X, Li Y, Yu C. Uric acid regulates hepatic steatosis and insulin resistance through the NLRP3 inflammasome-dependent mechanism. *J Hepatol* 2016; **64**: 925-932 [PMID: 26639394 DOI: 10.1016/j.jhep.2015.11.022]

67 **Choi YJ**, Shin HS, Choi HS, Park JW, Jo I, Oh ES, Lee KY, Lee BH, Johnson RJ, Kang DH. Uric acid induces fat accumulation *via* generation of endoplasmic reticulum stress and SREBP-1c activation in hepatocytes. *Lab Invest* 2014; **94**: 1114-1125 [PMID: 25111690 DOI: 10.1038/labinvest.2014.98]

68 **Wu SJ**, Zhu GQ, Ye BZ, Kong FQ, Zheng ZX, Zou H, Shi KQ, Lin L, Braddock M, Huang WJ, Chen YP, Zheng MH. Association between sex-specific serum uric acid and non-alcoholic fatty liver disease in Chinese adults: a large population-based study. *Medicine (Baltimore)* 2015; **94**: e802 [PMID: 25929934 DOI: 10.1097/MD.0000000000000802]

69 **Hwang IC**, Suh SY, Suh AR, Ahn HY. The relationship between normal serum uric acid and nonalcoholic fatty liver disease. *J Korean Med Sci* 2011; **26**: 386-391 [PMID: 21394307 DOI: 10.3346/jkms.2011.26.3.386]

70 **Fan N**, Zhang L, Xia Z, Peng L, Wang Y, Peng Y. Sex-Specific Association between Serum Uric Acid and Nonalcoholic Fatty Liver Disease in Type 2 Diabetic Patients. *J Diabetes Res* 2016; **2016**: 3805372 [PMID: 27382573 DOI: 10.1155/2016/3805372]

71 **Shiferaw B**, Verrill L, Booth H, Zansky SM, Norton DM, Crim S, Henao OL. Sex-based differences in food consumption: Foodborne Diseases Active Surveillance Network (FoodNet) Population Survey, 2006-2007. *Clin Infect Dis* 2012; **54** Suppl 5: S453-S457 [PMID: 22572669 DOI: 10.1093/cid/cis247]

72 **Maskarinec G**, Namatame LA, Kang M, Buchthal SD, Ernst T, Monroe KR, Shepherd JA, Wilkens LR, Boushey CJ, Marchand LL, Lim U. Differences in the association of diet quality with body fat distribution between men and women. *Eur J Clin Nutr* 2020; **74**: 1434-1441 [PMID: 31980746 DOI: 10.1038/s41430-020-0563-1]

73 **Hyer MM**, Dyer SK, Kloster A, Adrees A, Taetzsch T, Feaster J, Valdez G, Neigh GN. Sex modifies the consequences of extended fructose consumption on liver health, motor function, and physiological damage in rats. *Am J Physiol Regul Integr Comp Physiol* 2019; **317**: R903-R911 [PMID: 31553663 DOI: 10.1152/ajpregu.00046.2019]

74 **Suarez EC**. Self-reported symptoms of sleep disturbance and inflammation, coagulation, insulin resistance and psychosocial distress: evidence for gender disparity. *Brain Behav Immun* 2008; **22**: 960-968 [PMID: 18328671 DOI: 10.1016/j.bbi.2008.01.011]

75 **Razavi AC**, Potts KS, Kelly TN, Bazzano LA. Sex, gut microbiome, and cardiovascular disease risk. *Biol Sex Differ* 2019; **10**: 29 [PMID: 31182162 DOI: 10.1186/s13293-019-0240-z]

76 **Jiang C**, Xie C, Li F, Zhang L, Nichols RG, Krausz KW, Cai J, Qi Y, Fang ZZ, Takahashi S, Tanaka N, Desai D, Amin SG, Albert I, Patterson AD, Gonzalez FJ. Intestinal farnesoid X receptor signaling promotes nonalcoholic fatty liver disease. *J Clin Invest* 2015; **125**: 386-402 [PMID: 25500885 DOI: 10.1172/JCI76738]

77 **Xie G**, Wang X, Zhao A, Yan J, Chen W, Jiang R, Ji J, Huang F, Zhang Y, Lei S, Ge K, Zheng X, Rajani C, Alegado RA, Liu J, Liu P, Nicholson J, Jia W. Sex-dependent effects on gut microbiota regulate hepatic carcinogenic outcomes. *Sci Rep* 2017; **7**: 45232 [PMID: 28345673 DOI: 10.1038/srep45232]

78 **Kobold D**, Grundmann A, Piscaglia F, Eisenbach C, Neubauer K, Steffgen J, Ramadori G, Knittel T. Expression of reelin in hepatic stellate cells and during hepatic tissue repair: a novel marker for the differentiation of HSC from other liver myofibroblasts. *J Hepatol* 2002; **36**: 607-613 [PMID: 11983443 DOI: 10.1016/s0168-8278(02)00050-8]

79 **Zhang B**, Zhang CG, Ji LH, Zhao G, Wu ZY. Estrogen receptor β selective agonist ameliorates liver cirrhosis in rats by inhibiting the activation and proliferation of hepatic stellate cells. *J Gastroenterol Hepatol* 2018; **33**: 747-755 [PMID: 28884481 DOI: 10.1111/jgh.13976]

80 **Yang JD**, Abdelmalek MF, Pang H, Guy CD, Smith AD, Diehl AM, Suzuki A. Gender and menopause impact severity of fibrosis among patients with nonalcoholic steatohepatitis. *Hepatology* 2014; **59**: 1406-1414 [PMID: 24123276 DOI: 10.1002/hep.26761]

81 **Balakrishnan M**, Patel P, Dunn-Valadez S, Dao C, Khan V, Ali H, El-Serag L, Hernaez R, Sisson A, Thrift AP, Liu Y, El-Serag HB, Kanwal F. Women Have a Lower Risk of Nonalcoholic Fatty Liver Disease but a Higher Risk of Progression vs Men: A Systematic Review and Meta-analysis. *Clin Gastroenterol Hepatol* 2021; **19**: 61-71.e15 [PMID: 32360810 DOI: 10.1016/j.cgh.2020.04.067]

82 **Codes L**, Asselah T, Cazals-Hatem D, Tubach F, Vidaud D, Paraná R, Bedossa P, Valla D, Marcellin P. Liver fibrosis in women with chronic hepatitis C: evidence for the negative role of the menopause and steatosis and the potential benefit of hormone replacement therapy. *Gut* 2007; **56**: 390-395 [PMID: 17005762 DOI: 10.1136/gut.2006.101931]

83 **Yang JD**, Abdelmalek MF, Guy CD, Gill RM, Lavine JE, Yates K, Klair J, Terrault NA, Clark JM,

Unalp-Arida A, Diehl AM, Suzuki A; Nonalcoholic Steatohepatitis Clinical Research Network. Patient Sex, Reproductive Status, and Synthetic Hormone Use Associate With Histologic Severity of Nonalcoholic Steatohepatitis. *Clin Gastroenterol Hepatol* 2017; **15**: 127-131.e2 [PMID: 27523635 DOI: 10.1016/j.cgh.2016.07.034]

84 **Wang TJ**, Larson MG, Vasan RS, Cheng S, Rhee EP, McCabe E, Lewis GD, Fox CS, Jacques PF, Fernandez C, O'Donnell CJ, Carr SA, Mootha VK, Florez JC, Souza A, Melander O, Clish CB, Gerszten RE. Metabolite profiles and the risk of developing diabetes. *Nat Med* 2011; **17**: 448-453 [PMID: 21423183 DOI: 10.1038/nm.2307]

85 **Bloomgarden Z**. Diabetes and branched-chain amino acids: What is the link? *J Diabetes* 2018; **10**: 350-352 [PMID: 29369529 DOI: 10.1111/1753-0407.12645]

86 **Pedersen HK**, Gudmundsdottir V, Nielsen HB, Hyotylainen T, Nielsen T, Jensen BA, Forslund K, Hildebrand F, Prifti E, Falony G, Le Chatelier E, Levenez F, Doré J, Mattila I, Plichta DR, Pöhö P, Hellgren LI, Arumugam M, Sunagawa S, Vieira-Silva S, Jørgensen T, Holm JB, Trošt K; MetaHIT Consortium, Kristiansen K, Brix S, Raes J, Wang J, Hansen T, Bork P, Brunak S, Oresic M, Ehrlich SD, Pedersen O. Human gut microbes impact host serum metabolome and insulin sensitivity. *Nature* 2016; **535**: 376-381 [PMID: 27409811 DOI: 10.1038/nature18646]

87 **Lake AD**, Novak P, Shipkova P, Aranibar N, Robertson DG, Reily MD, Lehman-McKeeman LD, Vaillancourt RR, Cherrington NJ. Branched chain amino acid metabolism profiles in progressive human nonalcoholic fatty liver disease. *Amino Acids* 2015; **47**: 603-615 [PMID: 25534430 DOI: 10.1007/s00726-014-1894-9]

88 **Grzych G**, Vonghia L, Bout MA, Weyler J, Verrijken A, Dirinck E, Chevalier Curt MJ, Van Gaal L, Paumelle R, Francque S, Tailleux A, Haas JT, Staels B. Plasma BCAA Changes in Patients With NAFLD Are Sex Dependent. *J Clin Endocrinol Metab* 2020; **105** [PMID: 32271385 DOI: 10.1210/clinem/dgaa175]

89 **Krebs M**, Brunmair B, Brehm A, Artwohl M, Szendroedi J, Nowotny P, Roth E, Fürnsinn C, Promintzer M, Anderwald C, Bischof M, Roden M. The Mammalian target of rapamycin pathway regulates nutrient-sensitive glucose uptake in man. *Diabetes* 2007; **56**: 1600-1607 [PMID: 17329620 DOI: 10.2337/db06-1016]

90 **Um SH**, D'Alessio D, Thomas G. Nutrient overload, insulin resistance, and ribosomal protein S6 kinase 1, S6K1. *Cell Metab* 2006; **3**: 393-402 [PMID: 16753575 DOI: 10.1016/j.cmet.2006.05.003]

91 **Zhang F**, Zhao S, Yan W, Xia Y, Chen X, Wang W, Zhang J, Gao C, Peng C, Yan F, Zhao H, Lian K, Lee Y, Zhang L, Lau WB, Ma X, Tao L. Branched Chain Amino Acids Cause Liver Injury in Obese/Diabetic Mice by Promoting Adipocyte Lipolysis and Inhibiting Hepatic Autophagy. *EBioMedicine* 2016; **13**: 157-167 [PMID: 27843095 DOI: 10.1016/j.ebiom.2016.10.013]

92 **Yoshiji H**, Nagoshi S, Akahane T, Asaoka Y, Ueno Y, Ogawa K, Kawaguchi T, Kurosaki M, Sakaida I, Shimizu M, Taniai M, Terai S, Nishikawa H, Hiasa Y, Hidaka H, Miwa H, Chayama K, Enomoto N, Shimosegawa T, Takehara T, Koike K. Evidence-based clinical practice guidelines for Liver Cirrhosis 2020. *J Gastroenterol* 2021; **56**: 593-619 [PMID: 34231046 DOI: 10.1007/s00535-021-01788-x]

93 **Kazankov K**, Jørgensen SMD, Thomsen KL, Møller HJ, Vilstrup H, George J, Schuppan D, Grønbæk H. The role of macrophages in nonalcoholic fatty liver disease and nonalcoholic steatohepatitis. *Nat Rev Gastroenterol Hepatol* 2019; **16**: 145-159 [PMID: 30482910 DOI: 10.1038/s41575-018-0082-x]

94 **Becerra-Díaz M**, Strickland AB, Keselman A, Heller NM. Androgen and Androgen Receptor as Enhancers of M2 Macrophage Polarization in Allergic Lung Inflammation. *J Immunol* 2018; **201**: 2923-2933 [PMID: 30305328 DOI: 10.4049/jimmunol.1800352]

95 **Corcoran MP**, Meydani M, Lichtenstein AH, Schaefer EJ, Dillard A, Lamon-Fava S. Sex hormone modulation of proinflammatory cytokine and C-reactive protein expression in macrophages from older men and postmenopausal women. *J Endocrinol* 2010; **206**: 217-224 [PMID: 20484148 DOI: 10.1677/JOE-10-0057]

96 **Bray F**, Ferlay J, Soerjomataram I, Siegel RL, Torre LA, Jemal A. Global cancer statistics 2018: GLOBOCAN estimates of incidence and mortality worldwide for 36 cancers in 185 countries. *CA Cancer J Clin* 2018; **68**: 394-424 [PMID: 30207593 DOI: 10.3322/caac.21492]

97 **Ryerson AB**, Eheman CR, Altekruse SF, Ward JW, Jemal A, Sherman RL, Henley SJ, Holtzman D, Lake A, Noone AM, Anderson RN, Ma J, Ly KN, Cronin KA, Penberthy L, Kohler BA. Annual Report to the Nation on the Status of Cancer, 1975-2012, featuring the increasing incidence of liver cancer. *Cancer* 2016; **122**: 1312-1337 [PMID: 26959385 DOI: 10.1002/cncr.29936]

98 **Khan FZ**, Perumpail RB, Wong RJ, Ahmed A. Advances in hepatocellular carcinoma: Nonalcoholic steatohepatitis-related hepatocellular carcinoma. *World J Hepatol* 2015; **7**: 2155-2161 [PMID: 26328027 DOI: 10.4254/wjh.v7.i18.2155]

99 **Noureddin M**, Vipani A, Bresee C, Todo T, Kim IK, Alkhouri N, Setiawan VW, Tran T, Ayoub WS, Lu SC, Klein AS, Sundaram V, Nissen NN. NASH Leading Cause of Liver Transplant in Women: Updated Analysis of Indications For Liver Transplant and Ethnic and Gender Variances. *Am J Gastroenterol* 2018; **113**: 1649-1659 [PMID: 29880964 DOI: 10.1038/s41395-018-0088-6]

100 **Yang W**, Lu Y, Xu Y, Xu L, Zheng W, Wu Y, Li L, Shen P. Estrogen represses hepatocellular carcinoma (HCC) growth *via* inhibiting alternative activation of tumor-associated macrophages (TAMs). *J Biol Chem* 2012; **287**: 40140-40149 [PMID: 22908233 DOI: 10.1074/jbc.M112.348763]

101 **Yang D**, Hanna DL, Usher J, LoCoco J, Chaudhari P, Lenz HJ, Setiawan VW, El-Khoueiry A. Impact of sex on the survival of patients with hepatocellular carcinoma: a Surveillance,

Epidemiology, and End Results analysis. *Cancer* 2014; **120**: 3707-3716 [PMID: 25081299 DOI: 10.1002/cncr.28912]

102 **Wang R**, Liu Y, Sun H, Wang T, Li C, Fan J, Wang Z. Estradiol is significantly associated with prognosis in non-surgical liver cancer patients: from bench to bedside. *Aging (Albany NY)* 2021; **13**: 3483-3500 [PMID: 33428602 DOI: 10.18632/aging.202280]

103 **Mindikoglu AL**, Regev A, Seliger SL, Magder LS. Gender disparity in liver transplant waiting-list mortality: the importance of kidney function. *Liver Transpl* 2010; **16**: 1147-1157 [PMID: 20879013 DOI: 10.1002/lt.22121]

104 **Mindikoglu AL**, Emre SH, Magder LS. Impact of estimated liver volume and liver weight on gender disparity in liver transplantation. *Liver Transpl* 2013; **19**: 89-95 [PMID: 23008117 DOI: 10.1002/lt.23553]

105 **Wells GL**. Cardiovascular Risk Factors: Does Sex Matter? *Curr Vasc Pharmacol* 2016; **14**: 452-457 [PMID: 27456107 DOI: 10.2174/1570161114666160722113116]

106 **Kim C**, Cushman M, Khodneva Y, Lisabeth LD, Judd S, Kleindorfer DO, Howard VJ, Safford MM. Risk of Incident Coronary Heart Disease Events in Men Compared to Women by Menopause Type and Race. *J Am Heart Assoc* 2015; **4** [PMID: 26133958 DOI: 10.1161/jaha.115.001881]

107 **Du T**, Sun X, Yuan G, Zhou X, Lu H, Lin X, Yu X. Sex differences in the impact of nonalcoholic fatty liver disease on cardiovascular risk factors. *Nutr Metab Cardiovasc Dis* 2017; **27**: 63-69 [PMID: 27956025 DOI: 10.1016/j.numecd.2016.10.004]

108 **Pemmasani G**, Yandrapalli S, Aronow W. Sex differences in cardiovascular diseases and associated risk factors in non-alcoholic steatohepatitis. *Am J Cardiovasc Dis* 2020; **10**: 362-366 [PMID: 33224584]

109 **Allen AM**, Therneau TM, Mara KC, Larson JJ, Watt KD, Hayes SN, Kamath PS. Women With Nonalcoholic Fatty Liver Disease Lose Protection Against Cardiovascular Disease: A Longitudinal Cohort Study. *Am J Gastroenterol* 2019; **114**: 1764-1771 [PMID: 31577570 DOI: 10.14309/ajg.0000000000000401]

110 **Wei L**, Cheng X, Luo Y, Yang R, Lei Z, Jiang H, Chen L. Lean non-alcoholic fatty liver disease and risk of incident diabetes in a euglycaemic population undergoing health check-ups: A cohort study. *Diabetes Metab* 2021; **47**: 101200 [PMID: 33075504 DOI: 10.1016/j.diabet.2020.08.008]

111 **Akuta N**, Kawamura Y, Arase Y, Saitoh S, Fujiyama S, Sezaki H, Hosaka T, Kobayashi M, Suzuki Y, Suzuki F, Ikeda K, Kumada H. Hepatocellular carcinoma is the most common liver-related complication in patients with histopathologically-confirmed NAFLD in Japan. *BMC Gastroenterol* 2018; **18**: 165 [PMID: 30400829 DOI: 10.1186/s12876-018-0900-1]

112 **Yoshida I**, Suzuki A, Vallée M, Matano Y, Masunaga T, Zenda T, Shinozaki K, Okada T. Serum insulin levels and the prevalence of adenomatous and hyperplastic polyps in the proximal colon. *Clin Gastroenterol Hepatol* 2006; **4**: 1225-1231 [PMID: 16979948 DOI: 10.1016/j.cgh.2006.07.002]

113 **Saxena A**, Chumanevich A, Fletcher E, Larsen B, Lattwein K, Kaur K, Fayad R. Adiponectin deficiency: role in chronic inflammation induced colon cancer. *Biochim Biophys Acta* 2012; **1822**: 527-536 [PMID: 22198319 DOI: 10.1016/j.bbadis.2011.12.006]

114 **Hwang ST**, Cho YK, Park JH, Kim HJ, Park DI, Sohn CI, Jeon WK, Kim BI, Won KH, Jin W. Relationship of non-alcoholic fatty liver disease to colorectal adenomatous polyps. *J Gastroenterol Hepatol* 2010; **25**: 562-567 [PMID: 20074156 DOI: 10.1111/j.1440-1746.2009.06117.x]

115 **Chen QF**, Zhou XD, Sun YJ, Fang DH, Zhao Q, Huang JH, Jin Y, Wu JS. Sex-influenced association of non-alcoholic fatty liver disease with colorectal adenomatous and hyperplastic polyps. *World J Gastroenterol* 2017; **23**: 5206-5215 [PMID: 28811715 DOI: 10.3748/wjg.v23.i28.5206]

116 **Hung WC**, Wu JS, Sun ZJ, Lu FH, Yang YC, Chang CJ. Gender differences in the association of non-alcoholic fatty liver disease and metabolic syndrome with erosive oesophagitis: a cross-sectional study in a Taiwanese population. *BMJ Open* 2016; **6**: e013106 [PMID: 27852719 DOI: 10.1136/bmjopen-2016-013106]

117 **Chung SJ**, Kim D, Park MJ, Kim YS, Kim JS, Jung HC, Song IS. Metabolic syndrome and visceral obesity as risk factors for reflux oesophagitis: a cross-sectional case-control study of 7078 Koreans undergoing health check-ups. *Gut* 2008; **57**: 1360-1365 [PMID: 18441006 DOI: 10.1136/gut.2007.147090]

118 **Ministrini S**, Calzini L, Nulli Migliola E, Ricci MA, Roscini AR, Siepi D, Tozzi G, Daviddi G, Martorelli EE, Paganelli MT, Lupattelli G. Lysosomal Acid Lipase as a Molecular Target of the Very Low Carbohydrate Ketogenic Diet in Morbidly Obese Patients: The Potential Effects on Liver Steatosis and Cardiovascular Risk Factors. *J Clin Med* 2019; **8** [PMID: 31067824 DOI: 10.3390/jcm8050621]

119 **D'Abbondanza M**, Ministrini S, Pucci G, Nulli Migliola E, Martorelli EE, Gandolfo V, Siepi D, Lupattelli G, Vaudo G. Very Low-Carbohydrate Ketogenic Diet for the Treatment of Severe Obesity and Associated Non-Alcoholic Fatty Liver Disease: The Role of Sex Differences. *Nutrients* 2020; **12** [PMID: 32916989 DOI: 10.3390/nu12092748]

120 **Klaman LD**, Boss O, Peroni OD, Kim JK, Martino JL, Zabolotny JM, Moghal N, Lubkin M, Kim YB, Sharpe AH, Stricker-Krongrad A, Shulman GI, Neel BG, Kahn BB. Increased energy expenditure, decreased adiposity, and tissue-specific insulin sensitivity in protein-tyrosine phosphatase 1B-deficient mice. *Mol Cell Biol* 2000; **20**: 5479-5489 [PMID: 10891488 DOI: 10.1128/mcb.20.15.5479-5489.2000]

121 **Aberdein N**, Dambrino RJ, do Carmo JM, Wang Z, Mitchell LE, Drummond HA, Hall JE. Role of PTP1B in POMC neurons during chronic high-fat diet: sex differences in regulation of liver lipids

and glucose tolerance. *Am J Physiol Regul Integr Comp Physiol* 2018; **314**: R478-R488 [PMID: 29351427 DOI: 10.1152/ajpregu.00287.2017]

122 **Doucet E**, St-Pierre S, Alméras N, Imbeault P, Mauriège P, Pascot A, Després JP, Tremblay A. Reduction of visceral adipose tissue during weight loss. *Eur J Clin Nutr* 2002; **56**: 297-304 [PMID: 11965505 DOI: 10.1038/sj.ejcn.1601334]

123 **Vilar-Gomez E**, Martinez-Perez Y, Calzadilla-Bertot L, Torres-Gonzalez A, Gra-Oramas B, Gonzalez-Fabian L, Friedman SL, Diago M, Romero-Gomez M. Weight Loss Through Lifestyle Modification Significantly Reduces Features of Nonalcoholic Steatohepatitis. *Gastroenterology* 2015; **149**: 367-78.e5; quiz e14 [PMID: 25865049 DOI: 10.1053/j.gastro.2015.04.005]

124 **Barsalani R**, Riesco E, Lavoie JM, Dionne IJ. Effect of exercise training and isoflavones on hepatic steatosis in overweight postmenopausal women. *Climacteric* 2013; **16**: 88-95 [PMID: 22530610 DOI: 10.3109/13697137.2012.662251]

World Journal of Clinical Cases

Submit a Manuscript: https://www.f6publishing.com

World J Clin Cases 2022 February 16; 10(5): 1473-1484

DOI: 10.12998/wjcc.v10.i5.1473

ISSN 2307-8960 (online)

MINIREVIEWS

Management of procedural pain in the intensive care unit

Na-Na Guo, Hong-Liang Wang, Ming-Yan Zhao, Jian-Guo Li, Hai-Tao Liu, Ting-Xin Zhang, Xin-Yu Zhang, Yi-Jun Chu, Kai-Jiang Yu, Chang-Song Wang

ORCID number: Na-Na Guo 0000-0001-6652-4964; Hong-Liang Wang 0000-0002-1407-0072; Ming-Yan Zhao 0000-0003-4287-8586; Jian-Guo Li 0000-0001-5569-9603; Hai-Tao Liu 0000-0002-3052-8709; Ting-Xin Zhang 0000-0001-7265-5370; Xin-Yu Zhang 0000-0002-1622-1620; Yi-Jun Chu 0000-0003-1436-7121; Kai-Jiang Yu 0000-0001-8456-9664; Chang-Song Wang 0000-0002-0079-5259.

Author contributions: Wang CS and Yu KJ provided design and guidance; Guo NN, Zhang TX, Zhang XY and Chu YJ consulted the literature and completed the writing; Wang HL, Zhao MY, Li JG and Liu HT assisted in the literature review; all authors read and approved the final manuscript.

Conflict-of-interest statement: Authors declare no conflict of interests for this article.

Country/Territory of origin: China

Specialty type: Medicine, research and experimental

Provenance and peer review: Invited article; Externally peer reviewed.

Peer-review model: Single blind

Peer-review report's scientific quality classification

Grade A (Excellent): 0
Grade B (Very good): B
Grade C (Good): 0

Na-Na Guo, Hai-Tao Liu, Xin-Yu Zhang, Yi-Jun Chu, Chang-Song Wang, Department of Critical Care Medicine, Harbin Medical University Cancer Hospital, Harbin 150081, Heilongjiang Province, China

Hong-Liang Wang, Department of Critical Care Medicine, The Second Affiliated Hospital of Harbin Medical University, Harbin 150081, Heilongjiang Province, China

Ming-Yan Zhao, Kai-Jiang Yu, Department of Critical Care Medicine, The First Affiliated Hospital of Harbin Medical University, Harbin 150081, Heilongjiang Province, China

Jian-Guo Li, Department of Intensive Care Unit, Zhongnan Hospital of Wuhan University, Wuhan 430000, Hubei Province, China

Ting-Xin Zhang, Department of Orthopedics, The Second Affiliated Hospital of Harbin Medical University, Harbin 150081, Heilongjiang Province, China

Corresponding author: Chang-Song Wang, PhD, Professor, Department of Critical Care Medicine, Harbin Medical University Cancer Hospital, No. 150 Haping Road, Nangang District, Harbin 150081, Heilongjiang Province, China. changsongwangicu@163.com

Abstract

Pain is a common experience for inpatients, and intensive care unit (ICU) patients undergo more pain than other departmental patients, with an incidence of 50% at rest and up to 80% during common care procedures. At present, the management of persistent pain in ICU patients has attracted considerable attention, and there are many related clinical studies and guidelines. However, the management of transient pain caused by certain ICU procedures has not received sufficient attention. We reviewed the different management strategies for procedural pain in the ICU and reached a conclusion. Pain management is a process of continuous quality improvement that requires multidisciplinary team cooperation, pain-related training of all relevant personnel, effective relief of all kinds of pain, and improvement of patients' quality of life. In clinical work, which involves complex and diverse patients, we should pay attention to the following points for procedural pain: (1) Consider not only the patient's persistent pain but also his or her procedural pain; (2) Conduct multimodal pain management; (3) Provide combined sedation on the basis of pain management; and (4) Perform individualized pain management. Until now, the pain management of procedural pain in the ICU has not attracted extensive attention. Therefore, we expect additional studies to solve the existing problems of procedural pain management in the ICU.

Grade D (Fair): 0
Grade E (Poor): 0

Received: February 3, 2021
Peer-review started: February 3, 2021
First decision: July 16, 2021
Revised: July 22, 2021
Accepted: January 19, 2022
Article in press: January 19, 2022
Published online: February 16, 2022

P-Reviewer: Ewers A
S-Editor: Gao CC
L-Editor: A
P-Editor: Gao CC

Key Words: Procedural pain; Persistent pain; Transient pain; Pain management; Topical anesthesia; Intensive care unit

Core Tip: In clinical work, which involves complex and diverse patients, we should pay attention to the following points for procedural pain: (1) Consider not only the patient's persistent pain but also his or her procedural pain; (2) Conduct multimodal pain management; (3) Provide combined sedation on the basis of pain management; and (4) Perform individualized pain management.

Citation: Guo NN, Wang HL, Zhao MY, Li JG, Liu HT, Zhang TX, Zhang XY, Chu YJ, Yu KJ, Wang CS. Management of procedural pain in the intensive care unit. *World J Clin Cases* 2022; 10(5): 1473-1484
URL: https://www.wjgnet.com/2307-8960/full/v10/i5/1473.htm
DOI: https://dx.doi.org/10.12998/wjcc.v10.i5.1473

INTRODUCTION

Pain is a common experience for inpatients, and intensive care unit (ICU) patients undergo more pain than other departmental patients, with an incidence of 50% at rest and up to 80% during common care procedures[1]. The inducing factors of pain in the ICU include primary disease, various monitoring devices, treatment, long-term bed rest, and environmental and psychological factors[2]. In terms of its duration, pain in the ICU is divided into persistent pain (with inducing factors including mechanical ventilation, surgical incision, *etc.*) and transient pain (with inducing factors including arteriovenous puncture, abdominocentesis, *etc.*). At present, the management of persistent pain in ICU patients has attracted considerable attention, and there are many related clinical studies[3-5] and guidelines[6,7]. However, the management of transient pain caused by certain ICU procedures has not received sufficient attention. In 2018, although the PADIS guidelines[7] and "The Guidelines for the Management of Pain, Agitation in Adult Patients in the Intensive Care Unit"[2] refer to the prevalence of pain in ICU patients and recommend pain management and sedation to reduce patient discomfort, there are no specific recommendations for managing pain caused by procedures performed in the ICU. Therefore, the purpose of this article is to review the different management strategies for procedural pain in the ICU.

CLASSIFICATION OF PROCEDURAL PAIN IN THE ICU

Due to the severity and complexity of diseases in the ICU, various procedures are performed for monitoring, treatment, nursing care and other reasons. According to the procedural purposes, we defined the source of procedural pain into the following four categories: (1) Establishment of vascular access; (2) Noninvasive catheterization of a natural lumen; (3) Percutaneous catheterization and extubation of a natural lumen; and (4) Other procedures (Table 1). Although the above classifications are distinguished for operational purposes, the causes of each type of procedural pain have similar physiological anatomical foundations.

MANAGEMENT OF DIFFERENT CATEGORIES OF PROCEDURAL PAIN

In the past decade, the prevention and treatment concepts of pain, anxiety, and delirium have been updated: treatment based on pain management is emphasized, focusing on early intervention and paying more attention to patient-centered humanistic care while minimizing the side effects of analgesic and sedative drugs[6,8,9]. "The Guidelines for the Management of Pain, Agitation in Adult Patients in the Intensive Care Unit" recommend the preadministration of analgesics or nonpharmaco-

Table 1 Classification of procedural pain in the intensive care unit

Category	Specific operation					
Establishment of vascular access	Arterial puncture and catheterization	Peripherally inserted central catheters	Central venous catheter	Extracorporeal membrane oxygenation	Continuous renal replacement therapy *etc.*	
Natural cavity noninvasive catheterization	Endotracheal intubation	Bronchofiberscopy	Nasogastric tube intubation	Nasal jejunal intubation	Urethral catheterization *etc.*	
Natural cavity percutaneous catheterization and extubation	Pericardiocentesis	Thoracentesis	Thoracic closed drainage	Tracheotomy	Abdominocentesis	Extraction of chest tube *etc.*
Others	Turn *etc.*					

logical interventions to relieve pain before procedures that may cause pain[2].

The generation of pain involves both physiological and psychological factors. At present, clinical pain management includes pharmacological and nonpharmacological treatments. These drugs include opioid analgesics, nonopioid analgesics, nonsteroidal anti-inflammatory drugs (NSAIDs), and local anesthetics. Nonpharmacological pain management, including hypnosis and distraction by virtual reality, has been used as an adjunct for procedural pain management in ICUs. To date, there is not enough evidence to support the value of nonpharmacological pain management in ICUs[10]. Therefore, this review mainly compares the existing pain management approaches from the perspective of drug analgesia according to the different types of procedural pain mentioned above.

MANAGEMENT OF PAIN CAUSED BY THE ESTABLISHMENT OF VASCULAR ACCESS

Establishing vascular access is an essential operation in the ICU (Figure 1). For example, arterial puncture and catheterization can enable blood gas analysis and continuous arterial pressure monitoring, and central venous catheters (CVCs) and peripherally inserted central catheters (PICCs) can facilitate central venous pressure monitoring and the rapid administration of liquid and vasoactive drugs. Extracorporeal membrane oxygenation (ECMO) and continuous renal replacement therapy (CRRT) are important organ support methods in the ICU. Both procedures require deep venous catheterization to establish extracorporeal circulation. Improving the patient's oxygenation and excreting metabolic waste from the blood saves valuable time.

At present, pain caused by arterial puncture and catheterization, deep venous catheterization, and PICCs in the ICU is usually managed by local infiltration anesthesia. However, local infiltration anesthesia has the following limitations: (1) Local infiltration anesthesia itself can cause pain; (2) The effect of partial local infiltration anesthesia is not perfect; (3) After local infiltration, superficial arteriovenous structures may be difficult to identify, increasing the difficulty of puncture; and (4) Improper operation of local infiltration anesthesia may cause local anesthetic poisoning. Therefore, some clinical studies have attempted to apply more pain management methods to alleviate the pain caused by the establishment of vascular access.

Pain management during arterial puncture and catheterization and PICCs

There are few studies on arterial puncture and catheterization or on PICCs with general anesthesia as pain management methods. Zeng *et al*[11] found that a subanesthetic dose of ketamine (0.5 mg/kg) combined with midazolam (0.05 mg/kg) for arterial puncture has good analgesic and sedative effects, and most patients can awaken within 5 min to 8 min. When adopting this method, local infiltration anesthesia is not needed, and swelling of the puncture site during local anesthesia is avoided, which is beneficial to improving the success rate of puncture. This method has little effect on the patient's breathing and circulation, but for individuals who are elderly and infirm, it is still necessary to pay attention to transient respiratory depression. Because of the side effects of ketamine on pulmonary arterial pressure and intracranial pressure, patients with pulmonary hypertension or intracranial

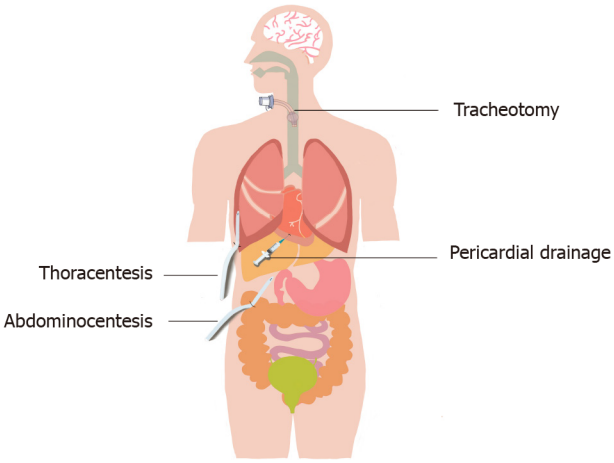

Figure 1 Establishment of vascular access.

hypertension should be treated with caution[11].

Most studies on the management of pain caused by arterial puncture and catheterization and PICCs focus on topical anesthesia. A review published in 2006 suggested that the use of lidocaine topical anesthesia before arterial puncture can significantly reduce pain and does not affect the success rate of puncture[12]. In 2012, a randomized double-blind trial examined topical anesthesia induced *via* a lidocaine/tetracaine patch in arterial puncture and showed that both the lidocaine/tetracaine patch and a subcutaneous injection of lidocaine effectively relieved pain during arterial puncture; however, the subcutaneous injection of lidocaine caused discomfort during the injection. In contrast, the lidocaine/tetracaine patch should be placed for 20 min before the operation, and the analgesic effect is better if given enough time[13]. A study published in 2016 compared the analgesic effects of vapocoolant sprays (ethyl chloride and alkane mixtures) with lidocaine local anesthesia during radial artery cannulation. The results showed that vapocoolant sprays can replace local anesthesia with lidocaine to relieve pain and discomfort caused by arterial catheterization[14]. A trial conducted in 2001 evaluated the effectiveness of two types of local anesthesia (buffered lidocaine and EMLA cream, which is a eutectic mixture of 2.5% lidocaine, 2.5% prilocaine, an emulsifier, and a thickener) compared to no anesthesia. The results showed that buffered lidocaine was superior to EMLA cream or no anesthesia in reducing PICC-related pain[15].

Topical anesthesia with different types or formulations of local anesthetics has been used to relieve pain caused by arterial puncture and catheterization and by PICCs in an increasing number of studies. Although topical anesthesia does not cause stabbing pain or local anesthetic poisoning, its anesthetic effect needs to be confirmed by more clinical studies.

Pain management of central venous catheterization

A 2014 study by Samantaray and Rao[16] evaluated the efficacy of fentanyl combined with local infiltration anesthesia with lidocaine for CVCs. The results showed that fentanyl is effective in relieving pain and can be safely used in conscious patients. The same team compared the effects of dexmedetomidine, fentanyl, and placebo during CVC placement in a trial conducted in 2016. The study concluded that both dexmedetomidine and fentanyl achieved good analgesia. Dexmedetomidine is superior to fentanyl and placebo in providing comfort to patients but is associated with excessive sedation and cardiovascular adverse events[17]. The latest study conducted in 2019 compared the target-controlled infusion of remifentanil plus local lidocaine infiltration and placebo plus local lidocaine infiltration in conscious patients. Remifentanil is effective in reducing the pain associated with local lidocaine infiltration during CVC placement[18].

The pain management of CVC placement is mostly focused on the intravenous administration of opioid analgesics (remifentanil, fentanyl) combined with lidocaine local infiltration, which can achieve a good analgesic effect while keeping patients awake. Although general anesthesia is more comfortable than local anesthesia, respiratory and circulatory inhibition by general anesthesia cannot be ignored.

Pain management of ECMO

The essence of ECMO is an improved artificial heart-lung machine that can be used for both extracorporeal respiratory support and cardiac support. There is currently no independent study on pain management during the establishment of extracorporeal circulation for ECMO. However, some studies have focused on pain management after extracorporeal circulation establishment.

Two recent case studies and one review suggest that ketamine infusion can be used as an analgesic for ECMO patients, reducing sedatives and opioid doses without changing the Richmond Agitation and Sedation Scale (RASS) score[19-21]. Based on the above findings, ketamine combined with local lidocaine infiltration may be an option for analgesia in ECMO patients during the establishment of extracorporeal circulation.

Pain management for CRRT

There is no independent study on the pain management of extracorporeal circulation establishment before CRRT. Mostly, these cases involve renal insufficiency in patients with CRRT. The choice of pain management should avoid nephrotoxic drugs such as tramadol and NSAIDs and may be patterned after pain management for CVC. The management of pain caused by establishing different types of vascular access is shown in Table 2.

In addition to the management of procedural pain caused by the establishment of vascular access, we should also pay attention to improving the success rate of vascular access and avoiding repeated procedures that cause patients more pain. A large number of studies have confirmed that ultrasound guidance in arterial puncture, PICCs and CVCs can not only improve the success rate of puncture but also reduce the incidence of adverse events and improve the satisfaction and comfort of patients[22, 23]. Moreover, bedside ultrasound can also identify malpositioning of the CVC and pneumothorax faster than an X-ray examination[24,25].

MANAGEMENT OF PAIN CAUSED BY NONINVASIVE CATHETERIZATION THROUGH A NATURAL CAVITY

Natural cavities are channels that connect the inside and outside of the human body, and they are sensitive and highly reactive. When a fiberoptic bronchoscope, stomach tube or urinary catheter enters a natural cavity, the device stimulates the mucous membrane, causing discomfort or even pain (Figure 2). Therefore, proper pain management combined with sedation can not only relieve the patient's discomfort and pain but also improve the success rate of intubation and avoid additional pain caused by repeated operations.

Pain management for bronchofiberscopy

A 2013 study found that remifentanil target-controlled infusion analgesia was reliable in ICU patients who required bronchoscopy with spontaneous breathing[26].

Kundra *et al*[27] evaluated the efficacy of upper airway anesthesia produced by nebulized lidocaine against a combined regional block (CRB) for awake fiberoptic nasotracheal intubation. The results showed that both nebulization and CRB produced satisfactory anesthesia of the upper airway, but CRB provided better patient comfort and hemodynamic stability[27]. A randomized controlled study was performed to compare two methods of airway anesthesia, namely, ultrasonic nebulization of a local anesthetic and the performance of airway blocks. The results showed that upper airway blocks provided better quality anesthesia than lidocaine nebulization[28].

The above studies indicate that the analgesic effect of topical anesthesia combined with a nerve block is superior, but it may be difficult for some clinicians to achieve. On the basis of adequate topical anesthesia, combining intravenous analgesic sedative drugs may have a better effect, but this option needs to be confirmed by clinical research.

Pain management of nasogastric tube intubation

Nasal tube intubation is a common operation in the ICU but a painful process for patients[29]. Pain management for nasal tube intubation mainly involves topical anesthesia.

Table 2 The management of pain caused by establishing different vascular access

Operational type	Ref.	Drugs	Advantages	Disadvantages
Arterial puncture and catheterization	Zeng *et al*[11], 2007	Subanesthetic dose of ketamine (0.5 mg/kg) combined with midazolam (0.05 mg/kg)	The effect of pain management is 100%, with less side effect on breathing and circulation	Older and infirm should pay attention to transient respiratory depression
	Rüsch *et al*[14], 2017	Vapocoolant sprays	Can replace lidocaine to relieve discomfort caused by arterial catheterization	Not mentioned
	Ruetzler *et al* [13], 2012	Lidocaine/tetracaine patch	Effectively relieve pain	Need enough time before operation
PICC	Fry and Aholt [15], 2001	Buffered lidocaine	Effectively relieve pain	With short-term stability
CVC	Vardon Bounes *et al*[18], 2019	Remifentanil combined with lidocaine	Effectively relieve pain and has a short half-life	Extended operating time
	Samantaray *et al*[17], 2016	Fentanyl	Effectively relieve pain, less adverse respiratory and cardiovascular events	It is not as good as dexmedetomidine in providing comfort to patients
	Samantaray and Rao[16], 2014	Fentanyl	Effectively relieve pain	Respiratory depression may occur
ECMO	Maybauer *et al* [21], 2019	Ketamine	Provides relatively stable hemodynamic stability while maintaining airway reflex	There may be dose-related hallucinations, paralysis, tearing, tachycardia, and possibly increased intracranial pressure, and coronary ischemia
	Floroff *et al* [20], 2016	Ketamine	Less respiratory depression, better pain control, boosting, and increased cardiac output	There may be dose-related hallucinations, sputum, hooliganism
	Tellor *et al*[19], 2015	Ketamine	Can reduce the amount of opioids used in surgical patients	The safety and efficacy of patients requiring ECMO therapy have not been determined

PICC: Peripherally inserted central catheter; CVC: Central venous catheter; ECMO: Extracorporeal membrane oxygenation.

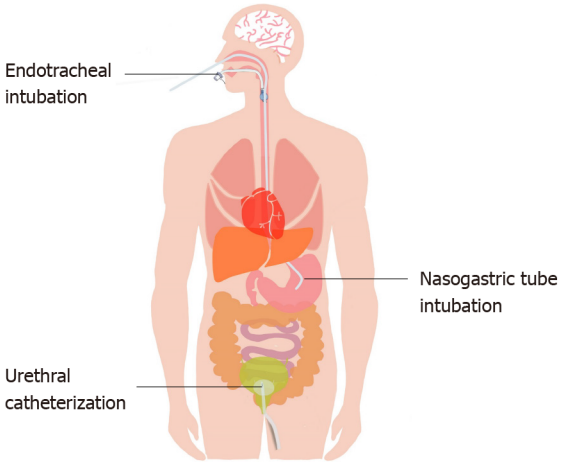

Figure 2 Noninvasive catheterization through a natural cavity.

A randomized controlled trial by Singer and Konia[30] showed that using topical lidocaine and phenylephrine for the nose and tetracaine with benzocaine spray for the throat prior to nasogastric (NG) intubation resulted in significantly less pain and discomfort than using a nasal surgical lubricant alone. Widespread use of topical anesthetics and vasoconstrictors prior to NG intubation is recommended[30]. Studies by Wolfe *et al*[31] have shown that atomized nasopharyngeal and oropharyngeal 4% lidocaine results in clinically and statistically significant reductions in pain during NG tube (NGT) placement. Ducharme and Matheson[32] compared atomized lidocaine, atomized cocaine, and lidocaine gel and found that 2% lidocaine gel appeared to

provide the best option for a topical anesthetic during NGT insertion. A randomized controlled trial by Cullen *et al*[33] showed that nebulized lidocaine decreases the discomfort of NGT insertion and should be considered before passing an NGT.

Both nebulized and topical local anesthetics (lidocaine, tetracaine, cocaine) can alleviate the pain of NG intubation. The combined application of both nebulized and topical local anesthetics may be a better option during NG intubation.

There is little research on analgesia after nasal jejunal intubation. In fact, management for nasal jejunal intubation may be patterned after pain management for NG tube intubation.

Pain management of urethral catheterization

A randomized controlled trial in 2004 determined whether pretreatment of the urethra with topical lidocaine reduces the pain associated with urethral catheterization. The results showed that using a topical lidocaine gel can reduce the pain associated with male urethral catheterization in comparison with topical lubricants only[34]. Another randomized controlled trial in 2007 compared the effects of a lidocaine gel and a water-based lubricating gel for female urethral catheterization. The results showed that compared with the water-based lubricating gel, the lidocaine gel substantially reduced the procedural pain caused by female urethral catheterization[35].

All of the above studies have shown that topical anesthesia with a lidocaine gel can effectively reduce the pain experienced during urethral catheterization. The management of pain caused by natural cavity noninvasive catheterization is shown in Table 3.

MANAGEMENT OF PAIN CAUSED BY NATURAL CAVITY PERCUTANEOUS CATHETERIZATION AND EXTUBATION

Natural cavity percutaneous catheterization is common in the ICU (Figure 3). Tracheotomy can quickly establish a respiratory passage and save patients' lives; thoracentesis, thoracic closed drainage, pericardial drainage, and abdominocentesis can drain effusions or gas to relieve symptoms and to diagnose and treat diseases. Since these operations require puncture through the skin and muscle layers, pain management is necessary.

Pain management of tracheotomy

Mechanical ventilation is an important means of respiratory support for critically ill patients. The clinical application guidelines for mechanical ventilation clearly suggest that patients who cannot have their artificial airways removed in the short term should be selected for replacement with tracheotomy as soon as possible[36]. A 2010 study showed that compared with tracheal intubation, tracheotomy may increase survival rates in mechanical ventilation patients. However, during tracheotomy, some patients are conscious and experience a certain fear of the procedure. Therefore, appropriate preoperative pain management and sedation are inevitable[37].

A 2011 trial compared local anesthesia (2% lidocaine tracheal mucosal-surface anesthesia and local-infiltration anesthesia) and monitored anesthesia (midazolam, propofol and fentanyl given intravenously after surface and local anesthesia) during tracheotomy. Monitored anesthesia gave patients a higher level of comfort, no memory of the tracheotomy and more stable hemodynamics[38]. A recent study evaluated the pain management and side effects of remifentanil in percutaneous dilatational tracheostomy. The results showed that based on propofol general anesthesia, combined treatment with remifentanil and lidocaine for local anesthesia can result in a shorter recovery time and more tolerable pain after recovery[39].

Tracheotomy pain management has mostly focused on intravenous analgesia (fentanyl, remifentanil), sedative drugs (propofol, midazolam) and combination treatment with local infiltration anesthesia (lidocaine), which can provide good pain management and sedative effects. According to the patient's circulatory state and the original pain management sedation plan, the pain management sedation combination and the local infiltration anesthesia method can be selected.

Pain management for the extraction of a chest tube

A 2004 study compared morphine and ketorolac in cardiac surgery patients undergoing chest tube removal. The findings confirmed that if used correctly, either an opioid (morphine) or an NSAID (ketorolac) can substantially reduce pain during chest

Table 3 The management of pain caused by the natural cavity noninvasive catheterization

Operational type	Ref.	Drugs	Advantages	Disadvantages
Fiberbronchoscopy	Chalumeau-Lemoine *et al*[26], 2013	Remifentanil	Shorten the operational time, reduce discomfort, and have better antitussive effect	May cause respiratory arrest
	Gupta *et al*[28], 2014	2% lignocaine and viscous lignocaine gargles	Effectively relieve pain and provide comfort	Not mentioned
	Kundra *et al*[27], 2000	Translaryngeal block, bilateral superior laryngeal nerve block and three 4% lignocaine-soaked cotton swabs in the nose (CRB group)	Provided better patient comfort and haemodynamic stability	Not mentioned
Nasogastric tube intubation	Cullen *et al*[33], 2004	Nebulized lidocaine	Can significantly alleviate pain	Can cause complications such as nosebleeds
	Ducharme and Matheson[32], 2003	2% lidocaine gel	Effectively alleviate pain and is easy to use	Not mentioned
	Wolfe *et al*[31], 2000	4% Nebulized lidocaine	Significantly alleviate pain	Not mentioned
	Singer and Konia [30], 1999	Lidocaine, tetracaine	Alleviate pain	Adverse events such as vomiting and nosebleeds
Urethral catheterization	Chung *et al*[35], 2007	Lidocaine gel	Alleviate pain	Not mentioned
	Siderias *et al*[34], 2004	Lidocaine gel	Alleviate pain	Not mentioned

CRB: Combined regional block.

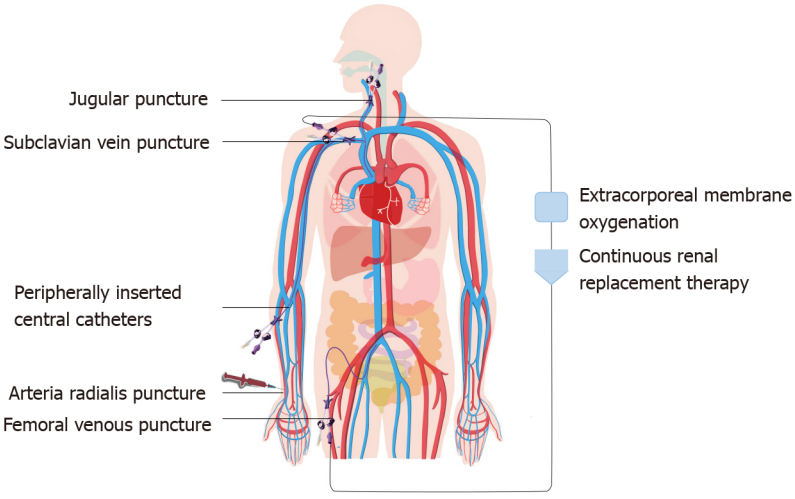

Figure 3 Natural cavity percutaneous catheterization and extubation.

tube removal without causing adverse sedative effects[40]. However, a review published in 2005 suggested that morphine alone does not provide satisfactory pain management for chest tube removal pain. NSAIDs, local anesthetics and inhalation agents may play a role in providing more effective analgesia[41].

A prospective, randomized, double-blind, placebo-controlled study conducted in 2005 evaluated the efficacy of topical valdecoxib as an analgesic during chest tube removal in postcardiac surgical patients. The results showed that compared with liquid paraffin, valdecoxib is a safe and effective topical analgesic[42].

In addition, three studies compared whether the preuse of ice packs can alleviate the pain of chest tube removal. Integration of the three studies in a meta-analysis showed that the preuse of ice packs can alleviate the pain of patients with chest tubes. The pain score was reduced after removal of the chest tube, SMD=0.30, [95% confidence interval (CI): 0.01-0.59, P = 0.04, I^2 = 0%][43-45].

There are many pain management methods, such as intravenous opioid analgesics, NSAIDs and cold compresses, for the extraction of chest tubes. There are few studies on local infiltration anesthesia, but it may be a better pain management method for the extraction of chest tubes because local infiltration anesthesia not only reduces pain during extubation but also reduces pain after extubation. The effect of local infiltration anesthesia in the extraction of chest tubes needs to be confirmed by clinical studies.

There are few pain management studies on thoracentesis and abdominocentesis. The traditional pain management method is local lidocaine infiltration anesthesia, which can provide effective analgesic effects. However, short-term pain management and sedation combined with local infiltration anesthesia may be a better choice, and we expect more clinical studies to confirm this option. The management of pain caused by natural cavity percutaneous catheterization and extubation is shown in Table 4.

MANAGEMENT OF PAIN CAUSED BY OTHER PROCEDURES

Some nursing care in the ICU can also cause discomfort to the patient, and appropriate pain management can reduce the incidence of pain and adverse events.

Pain management of turning

Turning is part of routine nursing care that is beneficial to sputum discharge and can even prevent hemorrhoids. However, due to the patient's own disease and the presence of various tubes, the patient may suffer from pulling and friction pain during turning. Even if the movement is slow and gentle, it will cause discomfort and pain to the patient.

In a randomized controlled trial conducted by Robleda *et al*[46], patients who underwent mechanical ventilation in the ICU were randomized to a fentanyl group (39 patients) and a placebo group (36 patients). Fentanyl or placebo was administered before turning. The incidence of pain in the fentanyl group was lower than that in the control group, and the incidence of adverse events was not statistically significant in the fentanyl group[46].

A prospective intervention study by de Jong *et al*[47] found that planned analgesia treatment (analgesic drugs combined with music) before turning can reduce the incidence of severe pain from 16% to 6% (odds ratio = 0.33, 95%CI: 0.11-0.98, $P = 0.04$) and the incidence of serious adverse events from 37% to 17%.

At present, no more attention is being paid to pain management during patient turning. Because the pain caused by turning is mostly systemic, general anesthesia may be a good choice. Remifentanil can be chosen because it has a quick effect and a short half-life; moreover, its analgesic effect and side effects are dose-dependent, so it is suitable for turning. The management of pain caused by other procedures is shown in Table 5.

Since some ICU patients are already in a state of analgesia and sedation during the above operations, the combination of local anesthesia (surface anesthesia or local infiltration anesthesia) on the basis of deepening their analgesia and sedation may be a more effective pain management method for procedural pain. However, for patients who are not under analgesic sedation, the pain management methods mentioned above can be referred to.

Critical care medicine aims to provide the most comprehensive and effective life support for patients with multiple organ dysfunction and severe nonterminal diseases to save their lives, improve their prognosis to the greatest extent and increase their quality of life. Contemporary medicine focuses on human care. Pain management in the ICU can eliminate or alleviate pain and discomfort, reduce adverse stimuli and excessive sympathetic nervous system excitement, facilitate and improve sleep, induce procedural amnesia, reduce memory in the ICU, alleviate or reduce anxiety, incite or even paralyze, prevent unconscious movements, reduce the metabolic rate and decrease oxygen consumption to ensure organ metabolism.

CONCLUSION

Pain management is a process of continuous quality improvement that requires multidisciplinary team cooperation, pain-related training of all relevant personnel, effective relief of all kinds of pain, and improvement of patients' quality of life. In clinical work, which involves complex and diverse patients, we should pay attention

Table 4 The management of pain caused by the natural cavity percutaneous catheterization and extubation

Operational type	Ref.	Drugs/physical method	Advantages	Disadvantages
Tracheotomy	Chang[39], 2017	Remifentanil and lidocaine combined with propofol	Can result in a shorter recovery time and more pain tolerable after recovery	Inhibition of heart and breathing
	Dong *et al*[38], 2011	Monitored anesthesia care	Give patients a higher level of comfort, no memory for tracheotomy and the hemodynamics is more stable	Intravenous administration to patients with difficulty in ventilation or intubation should be cautious
Extraction of chest tube	Puntillo and Ley[40], 2004	Morphine and ketorolac	Alleviate pain	Morphine may cause sedation
	Singh and Gopinath[42], 2005	Valdecoxib	Can alleviate pain safely and effectively	Can't completely alleviate pain
	Gorji *et al*[43], 2014	Ice packs	Effectively alleviate pain	Not mentioned

Table 5 The management of pain caused by other operations

Operational type	Ref.	Drugs/physical method	Advantages	Disadvantages
Turn	Robleda *et al* [46], 2016	Fentanyl	Effectively alleviate pain	Non-tracheal intubation patients use caution and may cause respiratory depression or apnea
	de Jong *et al*[47], 2013	Analgesic drug combined music	Effectively alleviate pain	The feasibility and impact of large-scale routine implementation has not been evaluated

to the following points for procedural pain: (1) Consider not only the patient's persistent pain but also his or her procedural pain; (2) Conduct multimodal pain management; (3) Provide combined sedation on the basis of pain management; and (4) Perform individualized pain management. Until now, the pain management of procedural pain in the ICU has not attracted extensive attention. There are few studies and there is no clear standard for the application of drugs; thus, there is no adequate guidance for clinicians to use exact treatment methods to reduce patients' pain and improve their prognosis. Moreover, for some special procedures, such as ECMO and CRRT, we should provide individualized pain management based on pharmacokinetics and pharmacodynamics. Therefore, we expect additional studies to solve the existing problems of procedural pain management in the ICU.

REFERENCES

1 **Skrobik Y**, Chanques G. The pain, agitation, and delirium practice guidelines for adult critically ill patients: a post-publication perspective. *Ann Intensive Care* 2013; **3**: 9 [PMID: 23547921 DOI: 10.1186/2110-5820-3-9]

2 **Chinese Medical Association Critical Care Medicine Branch**. The Guidelines for the Management of Pain, Agitation in Adult Patients in the Intensive Care Unit. *Zhonghua Zhongzheng Yixue Dianzi Zazhi* 2018; **4**: 90-113 [DOI: 10.3877/cma.j.issn.2096-1537.2018.02.002]

3 **Garber PM**, Droege CA, Carter KE, Harger NJ, Mueller EW. Continuous Infusion Ketamine for Adjunctive Analgosedation in Mechanically Ventilated, Critically Ill Patients. *Pharmacotherapy* 2019; **39**: 288-296 [PMID: 30746728 DOI: 10.1002/phar.2223]

4 **Zhu Y**, Wang Y, Du B, Xi X. Could remifentanil reduce duration of mechanical ventilation in comparison with other opioids for mechanically ventilated patients? *Crit Care* 2017; **21**: 206 [PMID: 28774327 DOI: 10.1186/s13054-017-1789-8]

5 **Zhao H**, Yang S, Wang H, Zhang H, An Y. Non-opioid analgesics as adjuvants to opioid for pain management in adult patients in the ICU: A systematic review and meta-analysis. *J Crit Care* 2019; **54**: 136-144 [PMID: 31446231 DOI: 10.1016/j.jcrc.2019.08.022]

6 **Barr J**, Fraser GL, Puntillo K, Ely EW, Gélinas C, Dasta JF, Davidson JE, Devlin JW, Kress JP, Joffe AM, Coursin DB, Herr DL, Tung A, Robinson BR, Fontaine DK, Ramsay MA, Riker RR, Sessler CN, Pun B, Skrobik Y, Jaeschke R; American College of Critical Care Medicine. Clinical practice guidelines for the management of pain, agitation, and delirium in adult patients in the intensive care unit. *Crit Care Med* 2013; **41**: 263-306 [PMID: 23269131 DOI: 10.1097/CCM.0b013e3182783b72]

7 **Devlin JW**, Skrobik Y, Gélinas C, Needham DM, Slooter AJC, Pandharipande PP, Watson PL,

Weinhouse GL, Nunnally ME, Rochwerg B, Balas MC, van den Boogaard M, Bosma KJ, Brummel NE, Chanques G, Denehy L, Drouot X, Fraser GL, Harris JE, Joffe AM, Kho ME, Kress JP, Lanphere JA, McKinley S, Neufeld KJ, Pisani MA, Payen JF, Pun BT, Puntillo KA, Riker RR, Robinson BRH, Shehabi Y, Szumita PM, Winkelman C, Centofanti JE, Price C, Nikayin S, Misak CJ, Flood PD, Kiedrowski K, Alhazzani W. Clinical Practice Guidelines for the Prevention and Management of Pain, Agitation/Sedation, Delirium, Immobility, and Sleep Disruption in Adult Patients in the ICU. *Crit Care Med* 2018; **46**: e825-e873 [PMID: 30113379 DOI: 10.1097/CCM.0000000000003299]

8 **Balas M**, Buckingham R, Braley T, Saldi S, Vasilevskis EE. Extending the ABCDE bundle to the post-intensive care unit setting. *J Gerontol Nurs* 2013; **39**: 39-51 [PMID: 23758115 DOI: 10.3928/00989134-20130530-06]

9 **Vincent JL**, Shehabi Y, Walsh TS, Pandharipande PP, Ball JA, Spronk P, Longrois D, Strøm T, Conti G, Funk GC, Badenes R, Mantz J, Spies C, Takala J. Comfort and patient-centred care without excessive sedation: the eCASH concept. *Intensive Care Med* 2016; **42**: 962-971 [PMID: 27075762 DOI: 10.1007/s00134-016-4297-4]

10 **He ZH**, Yang CL. Pain assessment and treatment progress in critically ill patients in ICU. *Jiangxi Yixue Zazhi* 2011; **46**: 290-293

11 **Zeng J**, Wu JL, Ma L. Application of subanesthetic dose of ketamine combined with midazolam during arterial puncture. *Guangxi Yixue Zazhi* 2007; **29**: 1001-1002

12 **Hudson TL**, Dukes SF, Reilly K. Use of local anesthesia for arterial punctures. *Am J Crit Care* 2006; **15**: 595-599 [PMID: 17053266]

13 **Ruetzler K**, Sima B, Mayer L, Golescu A, Dunkler D, Jaeger W, Hoeferl M, You J, Sessler DI, Grubhofer G, Hutschala D. Lidocaine/tetracaine patch (Rapydan) for topical anaesthesia before arterial access: a double-blind, randomized trial. *Br J Anaesth* 2012; **109**: 790-796 [PMID: 22831890 DOI: 10.1093/bja/aes254]

14 **Rüsch D**, Koch T, Seel F, Eberhart L. Vapocoolant Spray Versus Lidocaine Infiltration for Radial Artery Cannulation: A Prospective, Randomized, Controlled Clinical Trial. *J Cardiothorac Vasc Anesth* 2017; **31**: 77-83 [PMID: 27590462 DOI: 10.1053/j.jvca.2016.06.008]

15 **Fry C**, Aholt D. Local anesthesia prior to the insertion of peripherally inserted central catheters. *J Infus Nurs* 2001; **24**: 404-408 [PMID: 11758266 DOI: 10.1097/00129804-200111000-00009]

16 **Samantaray A**, Rao MH. Effects of fentanyl on procedural pain and discomfort associated with central venous catheter insertion: A prospective, randomized, double-blind, placebo controlled trial. *Indian J Crit Care Med* 2014; **18**: 421-426 [PMID: 25097353 DOI: 10.4103/0972-5229.136069]

17 **Samantaray A**, Hanumantha Rao M, Sahu CR. Additional Analgesia for Central Venous Catheter Insertion: A Placebo Controlled Randomized Trial of Dexmedetomidine and Fentanyl. *Crit Care Res Pract* 2016; **2016**: 9062658 [PMID: 27200187 DOI: 10.1155/2016/9062658]

18 **Vardon Bounes F**, Pichon X, Ducos G, Ruiz J, Samier C, Silva S, Sommet A, Fourcade O, Conil JM, Minville V. Remifentanil for Procedural Sedation and Analgesia in Central Venous Catheter Insertion: A Randomized, Controlled Trial. *Clin J Pain* 2019; **35**: 691-695 [PMID: 31094935 DOI: 10.1097/AJP.0000000000000725]

19 **Tellor B**, Shin N, Graetz TJ, Avidan MS. Ketamine infusion for patients receiving extracorporeal membrane oxygenation support: a case series. *F1000Res* 2015; **4**: 16 [PMID: 26309726 DOI: 10.12688/f1000research.6006.1]

20 **Floroff CK**, Hassig TB, Cochran JB, Mazur JE. High-Dose Sedation and Analgesia During Extracorporeal Membrane Oxygenation: A Focus on the Adjunctive Use of Ketamine. *J Pain Palliat Care Pharmacother* 2016; **30**: 36-40 [PMID: 26865321 DOI: 10.3109/15360288.2015.1101637]

21 **Maybauer MO**, Koerner MM, Maybauer DM. Perspectives on adjunctive use of ketamine for analgosedation during extracorporeal membrane oxygenation. *Expert Opin Drug Metab Toxicol* 2019; **15**: 349-351 [PMID: 30913933 DOI: 10.1080/17425255.2019.1593963]

22 **Wang Q**, Wang N, Sun Y. Clinical effect of peripherally inserted central catheters based on modified seldinger technique under guidance of vascular ultrasound. *Pak J Med Sci* 2016; **32**: 1179-1183 [PMID: 27882017 DOI: 10.12669/pjms.325.10384]

23 **Kim YO**, Chung CR, Gil E, Park CM, Suh GY, Ryu JA. Safety and feasibility of ultrasound-guided placement of peripherally inserted central catheter performed by neurointensivist in neurosurgery intensive care unit. *PLoS One* 2019; **14**: e0217641 [PMID: 31150465 DOI: 10.1371/journal.pone.0217641]

24 **Bou Chebl R**, Kiblawi S, El Khuri C, El Hajj N, Bachir R, Aoun R, Abou Dagher G. Use of Contrast-Enhanced Ultrasound for Confirmation of Central Venous Catheter Placement: Systematic Review and Meta-analysis. *J Ultrasound Med* 2017; **36**: 2503-2510 [PMID: 28660688 DOI: 10.1002/jum.14296]

25 **Ablordeppey EA**, Drewry AM, Beyer AB, Theodoro DL, Fowler SA, Fuller BM, Carpenter CR. Diagnostic Accuracy of Central Venous Catheter Confirmation by Bedside Ultrasound Versus Chest Radiography in Critically Ill Patients: A Systematic Review and Meta-Analysis. *Crit Care Med* 2017; **45**: 715-724 [PMID: 27922877 DOI: 10.1097/CCM.0000000000002188]

26 **Chalumeau-Lemoine L**, Stoclin A, Billard V, Laplanche A, Raynard B, Blot F. Flexible fiberoptic bronchoscopy and remifentanil target-controlled infusion in ICU: a preliminary study. *Intensive Care Med* 2013; **39**: 53-58 [PMID: 23052952 DOI: 10.1007/s00134-012-2697-7]

27 **Kundra P**, Kutralam S, Ravishankar M. Local anaesthesia for awake fibreoptic nasotracheal intubation. *Acta Anaesthesiol Scand* 2000; **44**: 511-516 [PMID: 10786733 DOI: 10.1034/j.1399-6576.2000.00503.x]

28 **Gupta B**, Kohli S, Farooque K, Jalwal G, Gupta D, Sinha S, Chandralekha. Topical airway anesthesia for awake fiberoptic intubation: Comparison between airway nerve blocks and nebulized lignocaine by ultrasonic nebulizer. *Saudi J Anaesth* 2014; **8**: S15-S19 [PMID: 25538514 DOI: 10.4103/1658-354X.144056]

29 **Singer AJ**, Richman PB, Kowalska A, Thode HC Jr. Comparison of patient and practitioner assessments of pain from commonly performed emergency department procedures. *Ann Emerg Med* 1999; **33**: 652-658 [PMID: 10339680]

30 **Singer AJ**, Konia N. Comparison of topical anesthetics and vasoconstrictors *vs* lubricants prior to nasogastric intubation: a randomized, controlled trial. *Acad Emerg Med* 1999; **6**: 184-190 [PMID: 10192668 DOI: 10.1111/j.1553-2712.1999.tb00153.x]

31 **Wolfe TR**, Fosnocht DE, Linscott MS. Atomized lidocaine as topical anesthesia for nasogastric tube placement: A randomized, double-blind, placebo-controlled trial. *Ann Emerg Med* 2000; **35**: 421-425 [PMID: 10783403]

32 **Ducharme J**, Matheson K. What is the best topical anesthetic for nasogastric insertion? *J Emerg Nurs* 2003; **29**: 427-430 [PMID: 14583715 DOI: 10.1016/s0099-1767(03)00295-2]

33 **Cullen L**, Taylor D, Taylor S, Chu K. Nebulized lidocaine decreases the discomfort of nasogastric tube insertion: a randomized, double-blind trial. *Ann Emerg Med* 2004; **44**: 131-137 [PMID: 15278085 DOI: 10.1016/j.annemergmed.2004.03.033]

34 **Siderias J**, Gaudio F, Singer AJ. Comparison of topical anesthetics and lubricants prior to urethral catheterization in males: a randomized controlled trial. *Acad Emerg Med* 2004; **11**: 703-706 [PMID: 15175214]

35 **Chung C**, Chu M, Paoloni R, O'Brien MJ, Demel T. Comparison of lignocaine and water-based lubricating gels for female urethral catheterization: a randomized controlled trial. *Emerg Med Australas* 2007; **19**: 315-319 [PMID: 17655633 DOI: 10.1111/j.1742-6723.2007.00961.x]

36 **Chinese Medical Association Critical Care Medicine Branch**. Clinical Application Guidelines for Mechanical Ventilation (2006). *Zhongguo Jijiu Yixue* 2007; **19**

37 **Wu YK**, Tsai YH, Lan CC, Huang CY, Lee CH, Kao KC, Fu JY. Prolonged mechanical ventilation in a respiratory-care setting: a comparison of outcome between tracheostomized and translaryngeal intubated patients. *Crit Care* 2010; **14**: R26 [PMID: 20193057 DOI: 10.1186/cc8890]

38 **Dong YC**, Su RX, Wu WM, Li G. Clinical application of monitoring anesthesia management in percutaneous dilatation tracheotomy. *Huaxi Kouqiang Yixue Zazhi* 2011; **29**: 626-628 [DOI: 10.3969/j.issn.1000-1182.2011.06.016]

39 **Chang SY**. Analgesic study of remifentanil in short operation of ICU. M.D. Thesis, Zhengzhou University. 2017. Available from: https://t.cnki.net/kcms/detail?v=i8RQNj_vMVRYPe5jP8kzRPhbPTZW21wxREglgzGTPk_VKNcaBqGeQX-0c1pzIg3u87glUmwYzKtHLLjT2PCoEPL5Xc0eIfu0Wpz4xUcUULjDUYxJQkwpG1m4EBAVuvYF&uniplatform=NZKPT

40 **Puntillo K**, Ley SJ. Appropriately timed analgesics control pain due to chest tube removal. *Am J Crit Care* 2004; **13**: 292-301; discussion 302; quiz 303 [PMID: 15293581]

41 **Bruce EA**, Howard RF, Franck LS. Chest drain removal pain and its management: a literature review. *J Clin Nurs* 2006; **15**: 145-154 [PMID: 16422731 DOI: 10.1111/j.1365-2702.2006.01273.x]

42 **Singh M**, Gopinath R. Topical analgesia for chest tube removal in cardiac patients. *J Cardiothorac Vasc Anesth* 2005; **19**: 719-722 [PMID: 16326294 DOI: 10.1053/j.jvca.2005.07.024]

43 **Gorji HM**, Nesami BM, Ayyasi M, Ghafari R, Yazdani J. Comparison of Ice Packs Application and Relaxation Therapy in Pain Reduction during Chest Tube Removal Following Cardiac Surgery. *N Am J Med Sci* 2014; **6**: 19-24 [PMID: 24678472 DOI: 10.4103/1947-2714.125857]

44 **Sauls J**. The use of ice for pain associated with chest tube removal. *Pain Manag Nurs* 2002; **3**: 44-52 [PMID: 12050835 DOI: 10.1053/jpmn.2002.123017]

45 **Demir Y**, Khorshid L. The effect of cold application in combination with standard analgesic administration on pain and anxiety during chest tube removal: a single-blinded, randomized, double-controlled study. *Pain Manag Nurs* 2010; **11**: 186-196 [PMID: 20728068 DOI: 10.1016/j.pmn.2009.09.002]

46 **Robleda G**, Roche-Campo F, Sendra MÀ, Navarro M, Castillo A, Rodríguez-Arias A, Juanes-Borrego E, Gich I, Urrutia G, Nicolás-Arfelis JM, Puntillo K, Mancebo J, Baños JE. Fentanyl as pre-emptive treatment of pain associated with turning mechanically ventilated patients: a randomized controlled feasibility study. *Intensive Care Med* 2016; **42**: 183-191 [PMID: 26556618 DOI: 10.1007/s00134-015-4112-7]

47 **de Jong A**, Molinari N, de Lattre S, Gniadek C, Carr J, Conseil M, Susbielles MP, Jung B, Jaber S, Chanques G. Decreasing severe pain and serious adverse events while moving intensive care unit patients: a prospective interventional study (the NURSE-DO project). *Crit Care* 2013; **17**: R74 [PMID: 23597243 DOI: 10.1186/cc12683]

World Journal of Clinical Cases

Submit a Manuscript: https://www.f6publishing.com

World J Clin Cases 2022 February 16; 10(5): 1485-1497

DOI: 10.12998/wjcc.v10.i5.1485

ISSN 2307-8960 (online)

ORIGINAL ARTICLE

Clinical and Translational Research

Effect of prior malignancy on the prognosis of gastric cancer and somatic mutation

Xin Yin, Xing-Kang He, Ling-Yun Wu, Sen-Xiang Yan

ORCID number: Xin Yin 0000-0002-4177-3048; Xing-Kang He 0000-0002-1586-2266; Ling-Yun Wu 0000-0001-7753-6143; Sen-Xiang Yan 0000-0001-6902-0892.

Author contributions: Yin X, Yan SX, and He XK conceived and designed the study, conducted data extraction statistical analyses, interpreted the study results, and wrote the first draft of the manuscript; Wu LY extracted and analyzed the data, and interpreted the study results; All authors edited and critically revised the final version of the manuscript.

Institutional review board statement: The data that support the findings of this study are publicly available. The current study does not require approval from an ethics committee.

Conflict-of-interest statement: The authors declare that they have no competing interests.

Data sharing statement: The data that support the findings of this study are publicly available.

Country/Territory of origin: China

Specialty type: Medicine, research and experimental

Provenance and peer review:

Xin Yin, Ling-Yun Wu, Sen-Xiang Yan, Department of Radiation Oncology, The First Affiliated Hospital, College of Medicine, Zhejiang University, Hangzhou 310000, Zhejiang Province, China

Xing-Kang He, Department of Gastroenterology, Sir Run Run Shaw Hospital, Hangzhou 310000, Zhejiang Province, China

Corresponding author: Sen-Xiang Yan, MD, Chief Doctor, Department of Radiation Oncology, the First Affiliated Hospital, College of Medicine, Zhejiang University, the First Affiliated Hospital, College of Medicine, Zhejiang University, 79 Qingchun Road, Hangzhou, Zhejiang 310003, PR China, Hangzhou 310000, Zhejiang Province, China. yansenxiang@zju.edu.cn

Abstract

BACKGROUND

Cancer survivors have a higher risk of developing secondary cancer, with previous studies showing heterogeneous effects of prior cancer on cancer survivors.

AIM

To describe the features and clinical significance of a prior malignancy in patients with gastric cancer (GC).

METHODS

We identified eligible patients from the Surveillance, Epidemiology, and End Results (SEER) database, and compared the clinical features of GC patients with/without prior cancer. Kaplan-Meier curves and Cox analyses were used to assess the prognostic impact of prior cancer on overall survival (OS) and cancer-specific survival (CSS) outcomes. We also validated our results in The Cancer Genome Atlas (TCGA) cohort and compared mutation patterns.

RESULTS

In the SEER dataset, of the 35492 patients newly diagnosed with GC between 2004 and 2011, 4,001 (11.3%) had at least one prior cancer, including 576 (1.62%) patients with multiple cancers. Patients with a prior cancer history tended to be elderly, with a more localized stage and less positive lymph nodes. The prostate (32%) was the most common initial cancer site. The median interval from initial cancer diagnosis to secondary GC was 68 mo. By using multivariable Cox analyses, we found that a prior cancer history was not significantly associated with OS (hazard ratio [HR]: 1.01, 95% confidence interval [CI]: 0.97–1.05).

Unsolicited article; Externally peer reviewed.

Peer-review model: Single blind

Peer-review report's scientific quality classification
Grade A (Excellent): 0
Grade B (Very good): B
Grade C (Good): 0
Grade D (Fair): 0
Grade E (Poor): 0

Received: July 10, 2021
Peer-review started: July 10, 2021
First decision: November 8, 2021
Revised: November 8, 2021
Accepted: January 6, 2022
Article in press: January 6, 2022
Published online: February 16, 2022

P-Reviewer: Kotelevets SM
S-Editor: Wang LL
L-Editor: Filipodia
P-Editor: Wang LL

However, a prior cancer history was significantly associated with better GC-specific survival (HR: 0.82, 95% CI: 0.78–0.85). In TCGA cohort, no significant difference in OS was observed for GC patients with or without prior cancer. Also, no significant differences in somatic mutations were observed between groups.

CONCLUSION
The prognosis of GC patients with previous diagnosis of cancer was not inferior to that of primary GC patients.

Key Words: Gastric cancer; Secondary cancer; Survivorship; Prognosis; Lymph nodes

Core Tip: We identified eligible cases during 2004-2011 from the Surveillance, Epidemiology, and End Results database and compared the clinical features of gastric cancer (GC) patients with/without prior cancer. We found that patients with a history of prior cancer tended to be elderly, with a more localized stage and less positive lymph nodes. The prognosis of GC patients with diagnosis of prior cancer was not inferior to primary GC.

Citation: Yin X, He XK, Wu LY, Yan SX. Effect of prior malignancy on the prognosis of gastric cancer and somatic mutation. *World J Clin Cases* 2022; 10(5): 1485-1497
URL: https://www.wjgnet.com/2307-8960/full/v10/i5/1485.htm
DOI: https://dx.doi.org/10.12998/wjcc.v10.i5.1485

INTRODUCTION

With the successful eradication of *Helicobacter pylori* and healthier lifestyles, gastric cancer (GC) incidence and mortality have steadily declined in the United States[1,2]. In recent decades, thanks to active cancer screening and effective therapies, many cancer survivors now enjoy relatively longer lives. Although risk factors for primary GC incidence and prognosis are well documented[2,3], little is known about secondary GC occurrence in cancer survivors.

With the increasing aging populations, it is anticipated that the prevalence of secondary cancer in cancer survivors will increase[4]. A recent study revealed that approximately 17.8% of elderly (≥ 65 years) and 7.3% of young adults (< 65 years) with newly diagnosed GC have a prior cancer history[5].

Due to inadequate selection criteria, patients with prior cancers are routinely excluded from oncology clinical trials[5,6]; thus, a substantial number of patients may have lost access to cutting-edge therapies and care. The impact of prior cancer on a current malignancy is often inconsistent and varies by cancer type (*e.g.*, pancreatic, prostate, esophageal, Non-Hodgkin's lymphoma, gastrointestinal, and lung cancers)[7-16]. To the best of our knowledge, there is a dearth of data on the characteristics and survival outcomes of GC patients with prior cancer. Similarly, there is a lack of real-world evidence to address these issues.

In this study, we characterized GC patients with a prior cancer history and estimated survival outcomes from real-world data. Understanding the prognostic impact of prior cancer on GC patients may have significant implications for improved therapeutic strategies and surveillance.

MATERIALS AND METHODS

Data sources and populations

We identified eligible patients with newly diagnosed and histopathologically proven GC between 2004 and 2011 in 18 Surveillance, Epidemiology, and End Results (SEER) registries (https://seer.cancer.gov/), which covered approximately 30% of the United States population[17]. We included patients aged ≥ 18 with active follow-up to the end of 2014. Tumor 83 site codes (C16.0, C16.1, C16.2, C16.3, C16.4, C16.5, C16.6, C16.8, and

C16.9) were used for GC identification according to the International Classification of Diseases for Oncology 3rd edition. A sequence number was used to identify the number of multiple primaries. A sequence number = 0 indicated that an individual had only one primary cancer, and a larger number indicated more than one primary cancer. To reduce the possibility of misclassifying synchronous metastases, a latency period of at least 6 mo was required from initial prior cancer diagnosis to secondary GC. For initial prior cancer, we excluded cases termed as GC. We categorized prior malignancies of interest including prostate, gastrointestinal, hematologic, breast, genitourinary, and lung cancers.

The following information was collected from the SEER database: age, sex, race, marital status, tumor sites for the prior malignancy and GC, lymph nodes examined, positive lymph nodes, SEER stage, GC grade, and current and prior cancer therapies. To validate the impact of prior cancer on GC patient survival, we used The Cancer Genome Atlas (TCGA) database as an external validation source. Primary gastric adenocarcinoma in TCGA with or without prior malignancy was included. Clinicopathological and genomic data were also queried in TCGA database.

Statistical analyses

Baseline characteristics from GC patients with or without prior cancer were summarized and investigated using the χ^2 test. For patients with prior cancer, site distribution, stages, and main therapies were classified. To investigate the impact of a prior cancer, we calculated overall GC survival and cancer-specific 3-year survival rates with and without prior cancer, stratified by age. Kaplan-Meier curves were constructed for patients with and without prior cancer, and survival differences were examined using the log-rank test. Furthermore, to validate our results, we adopted a multivariate Cox proportional hazards model to estimate hazard ratios (HRs). Using the maftools package in R, the frequency and visualization of gene mutations in TCGA was performed. Differentially expressed genes (DEGs) in TCGA samples, with and without prior malignancy, were analyzed using the Limma package. DEGs were considered genes where fold change > 2 and $^aP < 0.05$. All P values were two-sided and statistical significance was accepted at $P < 0.05$. All statistical analyses were performed using STATA version 13.0 (StataCorp, College Station, TX, United States) and R software version 3.40 (www.r-project.org).

RESULTS

Demographic and clinicopathological characteristics

In the SEER dataset, from 2004 to 2011, 35492 patients were identified with newly diagnosed GC, of which, 4,001 (11.27%) had one or more prior malignancy, including 576 (1.62%) patients with multiple malignancies. Baseline patient demographic and clinicopathological characteristics are described in Table 1. When compared with patients with primary GC only, those with a history of prior cancer were more likely to be elderly, male, white, and married. The proportion of cancers arising at cardia and fundus sites, with negative lymph nodes, at a localized stage, and with well/moderate differentiation, were higher in patients with prior cancer. In terms of GC therapeutic options, no significant differences were observed in the percentage of surgeries. In patients without prior cancer, radiotherapy and chemotherapy were more common. From TCGA dataset, 13 patients had one or more prior malignancy and 376 patients had no prior malignancy.

Regarding initial cancer sites, the prostate (32%) was the most common site, followed by gastrointestinal tract (17%), genitourinary (15%), breast (14%), others (10%), hematological system (7%), and the lung (5%) (Figure 1A). Unsurprisingly, the majority of prior cancers were either at localized (37%) or localized/regional stages (28%), with only 5% at distant stages (Figure 1B). Regarding therapeutic options for initial cancers, surgery was the most common modality, with most cases receiving multiple therapies (Figure 1C). The median time of initial malignancy to the time of subsequent GC diagnosis varied across initial cancer sites (from 50-78 mo, average = 68 mo; Supplementary Table 1). For breast and genitourinary cancer survivors, this interval exceeded 68 mo, whereas it was only 50 mo for lung cancer survivors.

Effects of prior cancer on GC patient survival in the SEER dataset

Among the primary GC patients in the SEER dataset, 25,592 (81%) died and 22,223 (87%) GC-related deaths were recorded during follow-up. In GC patients with prior cancer, 3407 (85.28%) died, including 544 initial cancer-related deaths and 2,353 GC-

Table 1 Baseline characteristics of patients diagnosed with gastric cancer (*n* = 35, 492) by prior cancer status

Characteristics	No previous cancer, *n* = 31491 (88.73%)		With prior cancer, *n* = 4001 (11.27%)		*P* value
Age (yr)					< 0.001
< 65	13160	(41.79%)	714	(17.85%)	
≥ 65	18331	(58.21%)	3287	(82.15%)	
Sex					< 0.001
Male	19479	(61.86%)	2777	(69.41%)	
Female	12012	(38.14%)	1224	(30.59%)	
Race					< 0.001
White	22087	(70.14%)	2926	(73.13%)	
Black	4090	(12.99%)	555	(13.87%)	
AI/AN	285	(0.91%)	16	(0.4%)	
AP	4898	(15.55%)	504	(12.6%)	
Unknown	131	(0.42%)	0	(0%)	
Marital status					< 0.001
Married	17571	(55.80%)	2366	(59.14%)	
Unmarried	12473	(39.61%)	1416	(35.39%)	
Unknown	1447	(4.59%)	219	(5.47%)	
Site					
Cardia and Fundus	10537	(33.46%)	1486	(37.14%)	
Body of stomach	6340	(20.13%)	844	(21.09%)	
Antrum and Pylorus	7370	(23.40%)	862	(21.54%)	
Stomach, NOS	7244	(23.00%)	809	(20.22%)	
Lymph nodes examined					< 0.001
No examined	16884	(53.62%)	2287	(57.16%)	
1-15	7020	(22.29%)	909	(22.72%)	
≥ 16	6338	(20.13%)	686	(17.15%)	
Unknown	1249	(3.97%)	119	(2.97%)	
Positive lymph nodes					< 0.001
0	4914	(36.79%)	693	(43.45%)	
1-2	2599	(19.46%)	327	(20.50%)	
3-6	2399	(17.96%)	276	(17.30%)	
7-15	2355	(17.63%)	207	(12.98%)	
≥ 16	1066	(7.98%)	89	(5.58%)	
Unknown	25	(0.19%)	3	(0.19%)	
SEER stage					< 0.001
Localized	7209	(22.89%)	1190	(29.74%)	
Regional	8978	(28.51%)	1051	(26.27%)	
Distant	12615	(40.06%)	1242	(31.04%)	
Unstaged	2689	(8.54%)	518	(12.95%)	
Grade					< 0.001
G1	1087	(3.45%)	181	(4.52%)	
G2	7012	(22.27%)	1027	(25.67%)	

G3	18112	(57.51%)	2108	(52.69%)	
G4	567	(1.80%)	68	(1.70%)	
Unknown	4713	(14.97%)	617	(15.42%)	
Surgery					0.088
No	16692	(53.01%)	2194	(54.84%)	
Yes	14630	(46.46%)	1785	(44.61%)	
Unknown	169	(0.54%)	22	(0.55%)	
Radiation					< 0.001
None	23413	(74.35 %)	3098	(77.43%)	
Radiation	7789	(24.73%)	866	(21.64%)	
Unknown	289	(0.92%)	37	(0.92%)	
Chemotherapy					< 0.001
No/Known	17189	(54.58%)	2569	(64.21%)	
Chemotherapy	14302	(45.42%)	1432	(35.79%)	

AI/AN: American Indian/Alaska Native; AP: Asian or Pacific Islander; G1: Well-differentiated; G2: Moderately differentiated; G3: Poorly differentiated; G4: Undifferentiated.

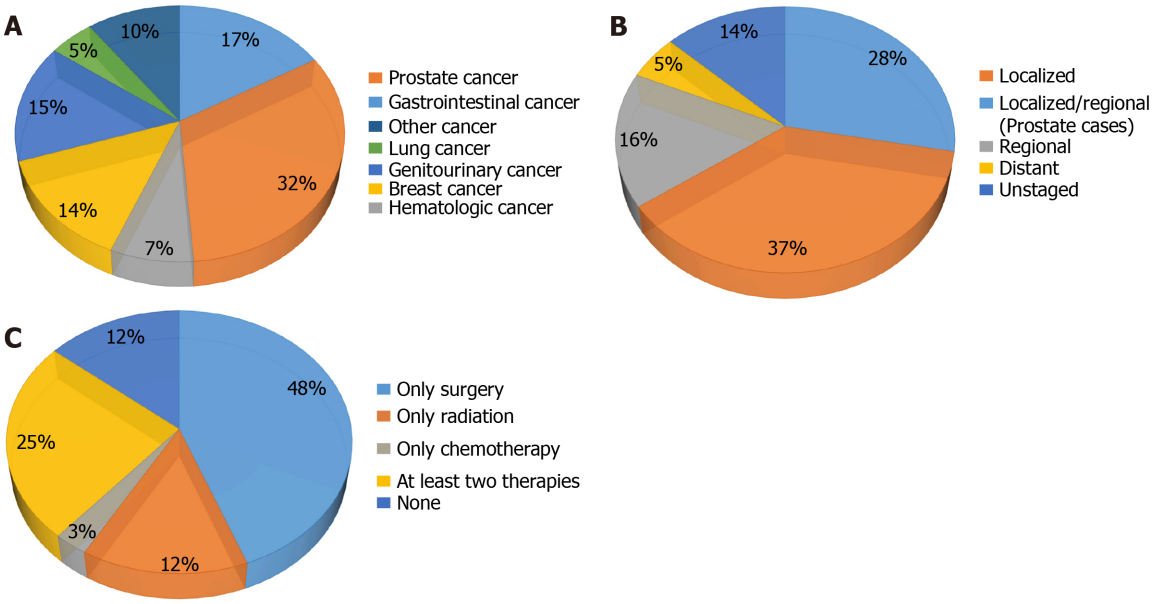

Figure 1 Distribution of initial site (A), stage (B) and therapeutic options (C) of prior cancers in gastric cancer patients with a history of cancer.

related deaths (Supplementary Table 2). The all-cause and GC-specific 3-year survival rates of primary GC patients were 26.42% (95% confidence interval [CI]: 25.90%–26.94%) and 30.91% (95%CI: 30.34%–31.47%), respectively, while for patients with a history of prior cancer, theses rates were 25.20% (95%CI: 23.80%–26.63%) and 38.03 (95%CI: 36.27%–39.79%), respectively (Table 2, Supplementary Table 3). Thus, it appeared that patients with prior cancer had a higher GC-related survival rate. Considering age may have had a role, we calculated the survival rates stratified by age. In either young or elderly patients, a higher GC-specific survival rate was observed in those with prior cancer. In terms of different initial cancer sites, lung cancer survivors had lower all-cause and cancer-specific survival (CSS) rates than those with other initial cancer sites. From Kaplan-Meier curves, patients with prior cancer had a significantly worse overall-survival (OS) and better GC-specific survival rate (log-rank tests both $P < 0.05$) (Figure 2). We also constructed multivariable Cox regression models to confirm the effects of prior cancer on survival outcomes. A

Table 2 Overall 3-year survival rate of gastric patients stratified by age

Prior initial cancer site	All-cause survival (95%CI)		
	Overall	Age < 65 yr (%)	Age ≥ 65 yr (%)
No prior cancer	26.42 (25.90, 26.94)	28.95 (28.14, 29.77)	24.49 (23.82, 25.16)
With prior cancer	25.20 (23.80, 26.63)	30.12 (26.68, 33.62)	24.08 (22.55, 25.65)
Prostate	24.79 (21.39, 28.32)	23.33 (16.23, 31.21)	25.16 (21.35, 29.14)
Gastrointestinal	26.47 (23.96, 29.04)	31.13 (22.60, 40.03)	26.00 (23.38, 28.68)
Hematologic	28.06 (22.75, 33.58)	42.17 (31.11, 52.80)	22.16 (16.49, 28.38)
Breast	26.80 (22.96, 30.78)	33.27 (25.47, 41.25)	24.36 (20.04, 28.92)
Genitourinary	23.64 (20.14, 27.30)	34.29 (25.39, 43.35)	21.06 (17.36, 25.02)
Lung	19.32 (13.87, 25.45)	12.50 (3.95, 26.23)	20.83 (14.64, 27.79)
Other	22.90 (18.79, 27.26)	24.61 (16.44, 33.66)	22.33 (17.66, 27.35)

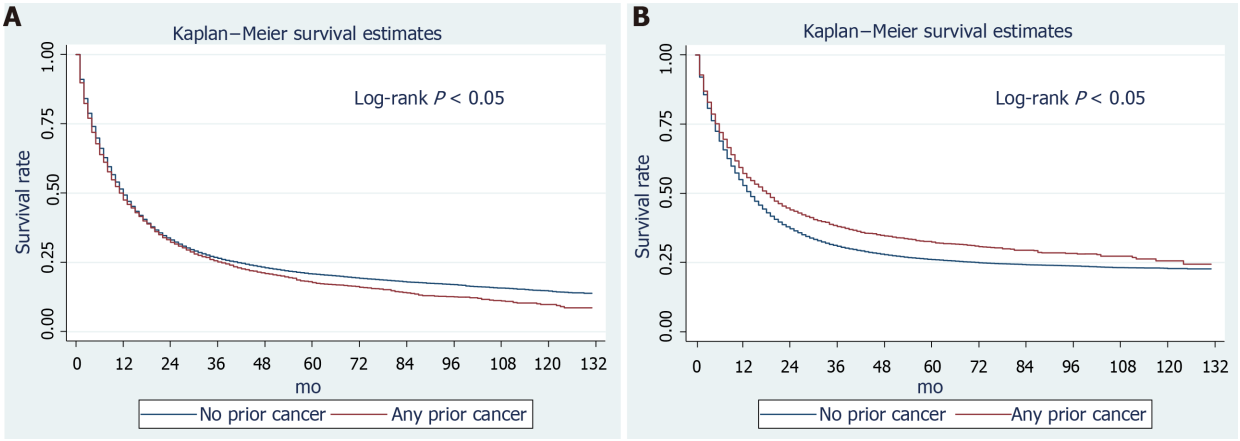

Figure 2 Kaplan–Meier survival curves of gastric cancer patients with and without a history of prior cancer. A: All-cause survival; B: Gastric cancer-specific cancer survival.

history of previous malignancies was not independently associated with all-cause death (HR: 1.01, 95%CI: 0.97–1.05, P = 0.644) after adjusting for other variables (Table 3). By contrast, it was significantly associated with a superior GC-specific survival (HR: 0.82, 95%CI: 0.78–0.85, P < 0.001). When stratified by initial cancer site, a history of other malignancies was related to worse OS, with prior breast cancer associated with superior OS (Supplementary Table 4). For CSS, a history of prostate, gastrointestinal, hematological, breast, and lung cancers was associated with a better prognosis (Supplementary Table 4). To validate our results, we performed subgroup analyses stratified by age, tumor size, and stage. In both < 65 and ≥ 65 age groups, a prior cancer history was unrelated to OS and was associated with superior CSS (Table 4). For different GC stages, prior cancer had an inconsistent impact on OS (Table 4) and significantly increased the overall mortality risk of localized stage GC (HR = 1.10), whereas, it reduced the mortality risk of distant-stage GC (HR = 0.92). (Table 4) Consistently, prior cancer was an independent factor for GC-specific survival, regardless of stage (Table 4). The timing of prior cancer was unrelated to GC OS. However, the timing of a prior cancer was associated with a better GC-specific survival rate.

Effects of prior cancer on GC patient survival in TCGA

We observed that 329 patients (329/376, 87.5%) without prior cancer had molecular alterations; the top mutated genes were titin (TTN), tumor protein 53 (TP53), mucin 16 (MUC16), AT-rich interactive domain-containing protein 1A, and lipoprotein receptor-related protein 1B (LRP1B) (Figure 3A). Ten patients (10/13, 76.92%) with prior cancer had molecular alterations; the top mutation genes were MUC16, TP53, TTN, contactin associated protein 2, and LRP1B (Figure 3B). We observed no significant differences in

Table 3 Multivariable Cox regression analysis of survival in patients with gastric cancer[1]

Characteristics	All-cause adjusted HR	*P* value	Cancer-specific adjusted HR	*P* value
Age (yr; *vs* < 65)				
≥ 65	1.32 (1.28, 1.35)	< 0.001	1.25 (1.22, 1.29)	< 0.001
Sex (*vs* male)				
Female	0.93 (0.91, 0.96)	< 0.001	0.95 (0.92, 0.98)	< 0.001
Race (*vs* white)				
Black	1.09 (1.05, 1.13)	< 0.001	1.07 (1.03, 1.12)	< 0.001
AI/AN	1.14 (1.01, 1.29)	0.033	1.16 (1.02, 1.32)	0.023
AP	0.79 (0.76, 0.82)	< 0.001	0.79 (0.76, 0.82)	< 0.001
Marital status (*vs* married)				
Unmarried	1.14 (1.12, 1.17)	< 0.001	1.11 (1.08, 1.14)	< 0.001
Gastric cancer site (*vs* cardia and fundus)				
Body of stomach	0.96 (0.92, 0.99)	0.013	0.93 (0.90, 0.97)	< 0.001
Antrum and Pylorus	0.99 (0.96, 1.03)	0.727	0.97 (0.93, 1.01)	0.114
Lymph nodes examined (*vs* no examined)				
1-15	0.73 (0.69, 0.77)	< 0.001	0.72 (0.68, 0.77)	< 0.001
≥ 16	0.65 (0.61, 0.68)	< 0.001	0.66 (0.62, 0.71)	< 0.001
Prior history of cancer (*vs* none)				
Yes	1.01 (0.97, 1.05)	0.644	0.82 (0.78, 0.85)	< 0.001
SEER stage (*vs* localized)				
Regional	2.34 (2.26, 2.44)	< 0.001	2.83 (2.70, 2.96)	< 0.001
Distant	3.43 (3.31, 3.57)	< 0.001	4.35 (4.16, 4.54)	< 0.001
Grade (*vs* G1)				
G2	1.19 (1.10, 1.28)	< 0.001	1.27 (1.16, 1.38)	< 0.001
G3	1.56 (1.45, 1.67)	< 0.001	1.75 (1.61, 1.91)	< 0.001
G4	1.60 (1.43, 1.79)	< 0.001	1.85 (1.63, 2.09)	< 0.001
Surgery (*vs* none)				
Yes	0.45 (0.43, 0.48)	< 0.001	0.44 (0.42, 0.47)	< 0.001
Radiation (*vs* none)				
Radiation	0.92 (0.89, 0.95)	0.007	0.92 (0.89, 0.96)	< 0.001
Chemotherapy (*vs* none)				
Chemotherapy	0.52 (0.51, 0.54)	< 0.001	0.53 (0.51, 0.55)	< 0.001

[1]Adjusted for age, race, sex, marital status, grade, stage, size, radiation, surgery, chemotherapy. AI/AN: American Indian/Alaska Native; AP: Asian or Pacific Islander; CI: Confidence interval; G1: Well-differentiated; G2: Moderately differentiated; G3: Poorly differentiated; G4: Undifferentiated; HR: Hazard ratio.

somatic mutations between GC patients with or without prior cancer (Figure 3C). Distinct to the SEER dataset, TCGA appeared to show a survival benefit toward patients with prior cancer. Due to insufficient sample numbers, we observed no significant OS between GC patients with or without prior cancer (Figure 3D). Also, we identified 42 DEGs between cancer groups, with 15 upregulated and 27 downregulated genes identified in the prior cancer group. Additionally, we constructed a volcano map (Figure 3E) to show the distribution of these 42 DEGs.

Table 4 Multivariable Cox regression analysis of survival in gastric cancer patients stratified by age, stage, and timing of prior cancer (prior cancer *vs* < none)

Characteristics	All-cause survival (CI)	*P* value	Gastric cancer-specific survival (CI)	*P* value
Age (yr)				
< 65	1.08 (1.00, 1.18)	0.064	0.77 (0.69, 0.85)	< *0.001*
≥ 65	1.00 (0.96, 1.04)	0.843	0.83 (0.79, 0.87)	< *0.001*
Stage				
Localized	1.10 (1.02, 1.19)	0.012	0.82 (0.74, 0.91)	< *0.001*
Regional	0.99 (0.92, 1.06)	0.777	0.84 (0.78, 0.92)	< *0.001*
Distant	0.92 (0.87, 0.98)	0.014	0.79 (0.73, 0.85)	< *0.001*
Timing of prior cancer				
< 5	1.03 (0.98, 1.09)	0.275	0.77 (0.72, 0.82)	< *0.001*
5-10	0.98 (0.92, 1.04)	0.525	0.84 (0.78, 0.90)	< *0.001*
≥ 10	1.01 (0.94, 1.08)	0.811	0.88 (0.81, 0.95)	*0.001*

Adjusted for age, race, sex, marital status, grade, stage, size, radiation, surgery, chemotherapy. AHR: Adjusted hazard ratio; CI: Confidence interval.

DISCUSSION

Cancer survivors are at higher risk of developing secondary malignancies[18,19]. With increasing numbers of cancer survivors having complicated dual or even multiple malignancies, the prognostic impact of previous cancer on cancer survival remains controversial. A pan-cancer study investigated the distinct effects of prior cancer across 20 cancer types[20]. For colorectal, sarcoma, melanoma, breast, cervical, endometrial, prostate, urothelial, orbital, and thyroid cancers, a prior cancer history contributed to a poor OS, while nasopharynx, gastrointestinal tract, lung, ovary, and brain cancer patients, with prior cancer, had a similar OS to patients without prior cancer[20]. In our population-based study, more than 10% of patients with newly diagnosed GC had a prior cancer history, similar to that reported by Murphy *et al*[5]. Newly diagnosed GC patients with prior cancer were older, suggesting that age is an independent risk factor for secondary malignancies[21]. The proportion of localized stages and negative lymph nodes were higher in patients with a prior cancer history, suggesting that cancer survivors may receive more active surveillance and that their cancer may be incidentally diagnosed at earlier stages[22,23]. Unsurprisingly, prostate cancer was the most common prior tumor type, suggesting an indolent clinical course. Similar results were identified for lung cancer patients[24]. The interval between initial malignancy and GC suggested the GC risk increased after five years of prior cancer diagnoses.

In oncology clinical trials, a substantial proportion of cancer survivors are excluded due to stringent eligibility criteria, and the assumption that these patients have inferior survival[6,24-27]. A previous study reported that the heterogeneous impact of a prior cancer history should be reconsidered according to the specific cancer type[20]. Thus, it is inappropriate to assume a prior cancer is a risk factor for mortality in a newly diagnosed cancer. In our study, using the SEER database, GC patients with a prior cancer history had similar 3-year survival rates compared to those without a prior cancer history. Despite a survival benefit trend, these data were not significant for patients with prior cancer.

A similar result was identified and validated in TCGA cohort, and suggested that a prior cancer history did not adversely affect the overall prognosis in GC patients. Regarding CSS, patients with prior cancer had superior GC-specific survival after particular variables were adjusted. It is unclear why a prior cancer history could improve GC-specific survival. Cancer survivors may undergo active cancer surveillance, thereby having an early cancer stage and improved survival, which may cause length bias and lead-time bias[28-30]. As gene mutations underlie most cancers, we hypothesized that patients with prior cancers harbored more molecular mutations, however, no significant mutation counts were associated with prior cancer status in the TCGA cohort.

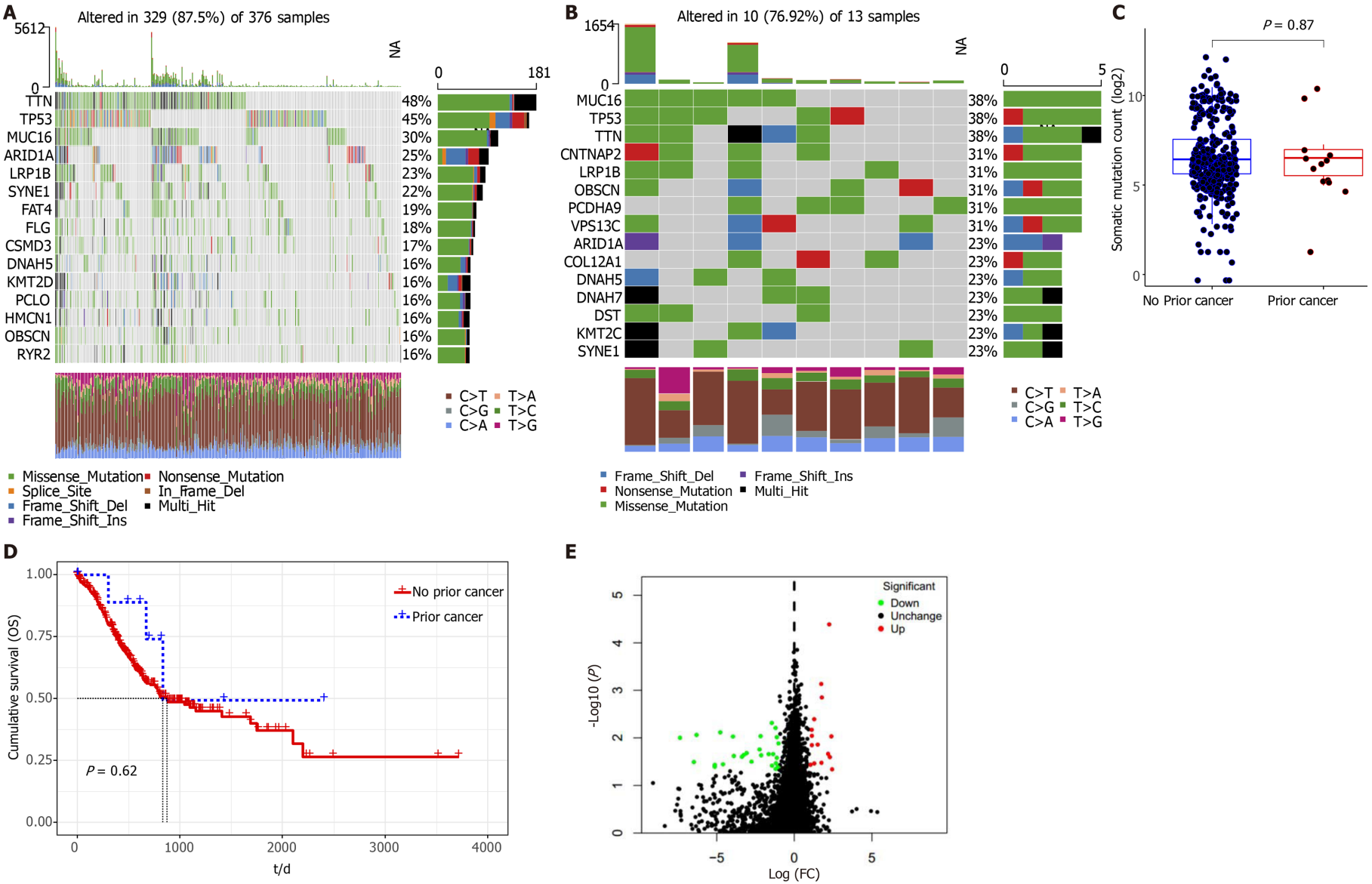

Figure 3 Effect of prior cancer on the survival of patients with gastric cancer in The Cancer Genome Atlas. A: Oncoplot of the top frequently mutated genes in patients without prior cancer; B: Oncoplot of the top frequently mutated

genes in patients without prior cancer patients with prior cancer; C: Distribution of somatic mutation counts between patients with and without prior cancer; D: Kaplan–Meier survival curves of overall survival in patients with and without prior cancer; E: Volcano plot of differentially expressed genes between patients with and without prior cancer.

In our study, we could not avoid bias as the percentage of early stage GC was more frequent in patients with prior cancer. However, we did not believe this bias was responsible for GC-specific survival advantages because a prior cancer was also associated with better GC-specific survival in the localized stages (HR = 0.82, 95%CI: 0.74–0.91). We speculated that higher competing mortality risks (either due to prior cancer or other factors) in patients with prior cancer may have accounted for GC-specific survival benefits[31]. Further studies are required to address these observations.

In subgroup analyses, age did not affect the impact of a prior cancer diagnosis. A prior cancer had no significant influence on OS, but improved CSS in GC patients. We also noted that the prognostic impact of a prior cancer was independent of the time of previous cancer diagnosis, suggesting that GC patients with a prior cancer diagnosis could be considered for trial enrollment regardless of the time.

We observed that the impact of a prior cancer history on survival was varied across different cancer types. In 2009, Pulte *et al*[10] reported that non-Hodgkin's lymphoma patients with prior malignancies had worse prognoses than those without prior cancer. Youn *et al*[32] subsequently showed a reduced survival time for Hodgkin's lymphoma survivors with secondary gastrointestinal cancer. In contrast, opposite trends were identified in other studies: Smyth *et al*[11] showed that gastrointestinal cancer patients with/without prior cancer had comparable OS and gastrointestinal cancer-specific survival times. Also, in early or advanced lung cancer stages, no differences in OS were noted between patients with and without prior cancer[24,33]. Pruitt *et al*[24] demonstrated improved lung CSS outcomes in patients with prior cancer. For stage IV esophageal cancer, a prior malignancy had no impact on OS[9]. A recent study explored the prognostic effect landscape across 20 prior cancer types[20]. However, this study primarily focused on pan-cancer and did not characterize specific clinical features and the specific impact of GC with a prior cancer history. Thus, our study filled this knowledge gap.

Our study had several limitations. The SEER database did not provide detailed chemotherapy and radiation information, and the efficacy and tolerability of prior therapies were unclear. Other covariates, such as *Helicobacter pylori* infection status, genetic information, and comorbidities were unavailable. Also, we could not completely exclude the possibility of GC metastatic misclassifications from earlier tumors. Finally, our findings were based on the SEER database and TCGA cohorts, thereby limiting overall generalizability to other populations. Further studies or independent cohorts are required to validate our findings and conclusions.

CONCLUSION

In the SEER database, 11.3% of newly diagnosed GC patients had a prior cancer history, with GC occurring within 6 years after prior cancer diagnosis. GC patients with a prior cancer history had a non-inferior OS, and the CSS was slightly improved. We suggest that in future clinical trials, broader inclusion criteria for GC patients with previous cancer should be considered in order to obtain the best inclusion rate and generalizable results.

ARTICLE HIGHLIGHTS

Research background

Cancer survivors had a higher risk of developing secondary cancer, and previous studies have indicated the heterogeneous effects of prior cancer on cancer survivors.

Research motivation

To evaluate prior malignancy on patients with gastric cancer (GC).

Research objectives

To describe the features and clinical significance of a prior malignancy on patients with GC.

Research methods

We identified eligible cases from the Surveillance, Epidemiology, and End Results (SEER) database and compared clinical features of GC patients with/without prior cancer. We adopted Kaplan-Meier curves and Cox analyses to assess the prognostic impact of a prior cancer on the overall survival (OS) and GC-specific survival outcomes. We also validated these results in The Cancer Genome Atlas (TCGA) cohort and compared mutation patterns.

Research results

In the SEER dataset, 35,492 patients newly diagnosed with GC during 2004-2011, 4,001 (11.3%) cases had at least one prior cancer, including 576 (1.62%) cases with multiple prior cancers. Patients with a history of prior cancer tended to be elderly, with a more localized stage and less positive lymph nodes. Prostate (32%) was the most common initial cancer site. The median interval from the initial diagnosis of malignancy to secondary gastric cancer was 68 mo. A history of prior cancer was not significantly associated with overall (hazard ratio:1.01, 95% confidence interval: 0.97-1.05) survival in multivariable Cox analyses.

Research conclusions

The prognosis for GC patients with a diagnosis of prior cancer was not inferior to primary GC patients.

Research perspectives

The prognosis for GC patients with a diagnosis of prior cancer was not inferior to primary GC patients. Our results suggest that a wide range of conclusions should be considered in the clinical trials of GC patients with a previous cancer to obtain the best inclusion rate and generalizable results.

REFERENCES

1 Jim MA, Pinheiro PS, Carreira H, Espey DK, Wiggins CL, Weir HK. Stomach cancer survival in the United States by race and stage (2001-2009): Findings from the CONCORD-2 study. *Cancer* 2017; 123 Suppl 24: 4994-5013 [PMID: 29205310 DOI: 10.1002/cncr.30881]

2 Karimi P, Islami F, Anandasabapathy S, Freedman ND, Kamangar F. Gastric cancer: descriptive epidemiology, risk factors, screening, and prevention. *Cancer Epidemiol Biomarkers Prev* 2014; 23: 700-713 [PMID: 24618998 DOI: 10.1158/1055-9965.EPI-13-1057]

3 Sitarz R, Skierucha M, Mielko J, Offerhaus GJA, Maciejewski R, Polkowski WP. Gastric cancer: epidemiology, prevention, classification, and treatment. *Cancer Manag Res* 2018; 10: 239-248 [PMID: 29445300 DOI: 10.2147/CMAR.S149619]

4 Morrell S, Young J, Roder D. The burden of cancer on primary and secondary health care services before and after cancer diagnosis in New South Wales, Australia. *BMC Health Serv Res* 2019; 19: 431 [PMID: 31248405 DOI: 10.1186/s12913-019-4280-1]

5 Murphy CC, Gerber DE, Pruitt SL. Prevalence of Prior Cancer Among Persons Newly Diagnosed With Cancer: An Initial Report From the Surveillance, Epidemiology, and End Results Program. *JAMA Oncol* 2018; 4: 832-836 [PMID: 29167866 DOI: 10.1001/jamaoncol.2017.3605]

6 Kim ES, Bernstein D, Hilsenbeck SG, Chung CH, Dicker AP, Ersek JL, Stein S, Khuri FR, Burgess E, Hunt K, Ivy P, Bruinooge SS, Meropol N, Schilsky RL. Modernizing Eligibility Criteria for Molecularly Driven Trials. *J Clin Oncol* 2015; 33: 2815-2820 [PMID: 26195710 DOI: 10.1200/JCO.2015.62.1854]

7 He X, Li Y, Su T, Lai S, Wu W, Chen L, Si J, Sun L. The impact of a history of cancer on pancreatic ductal adenocarcinoma survival. *United European Gastroenterol J* 2018; 6: 888-894 [PMID: 30023066 DOI: 10.1177/2050640618765505]

8 Abhyankar N, Hoskins KF, Abern MR, Calip GS. Descriptive characteristics of prostate cancer in patients with a history of primary male breast cancer - a SEER analysis. *BMC Cancer* 2017; 17: 659 [PMID: 28946846 DOI: 10.1186/s12885-017-3640-7]

9 Saad AM, Al-Husseini MJ, Elgebaly A, Aboshady OA, Salahia S, Abdel-Rahman O. Impact of prior malignancy on outcomes of stage IV esophageal carcinoma: SEER based study. *Expert Rev Gastroenterol Hepatol* 2018; 12: 417-423 [PMID: 29316808 DOI: 10.1080/17474124.2018.1426458]

10 Pulte D, Gondos A, Brenner H. Long-term survival of patients diagnosed with non-Hodgkin lymphoma after a previous malignancy. *Leuk Lymphoma* 2009; 50: 179-186 [PMID: 19197735 DOI: 10.1080/10428190802645061]

11 Smyth EC, Tarazona N, Peckitt C, Armstrong E, Mansukhani S, Cunningham D, Chau I. Exclusion of Gastrointestinal Cancer Patients With Prior Cancer From Clinical Trials: Is This Justified? *Clin Colorectal Cancer* 2016; 15: e53-e59 [PMID: 26747392 DOI: 10.1016/j.clcc.2015.11.003]

12 Dinh KT, Mahal BA, Ziehr DR, Muralidhar V, Chen YW, Viswanathan VB, Nezolosky MD, Beard CJ, Choueiri TK, Martin NE, Orio PF, Sweeney CJ, Trinh QD, Nguyen PL. Risk of prostate cancer mortality in men with a history of prior cancer. *BJU Int* 2016; 117: E20-E28 [PMID: 25845283 DOI: 10.1111/bju.13144]

13 Pandurengan RK, Dumont AG, Araujo DM, Ludwig JA, Ravi V, Patel S, Garber J, Benjamin RS, Strom SS, Trent JC. Survival of patients with multiple primary malignancies: a study of 783 patients with gastrointestinal stromal tumor. *Ann Oncol* 2010; 21: 2107-2111 [PMID: 20348145 DOI: 10.1093/annonc/mdq078]

14 Hattori A, Suzuki K, Aokage K, Mimae T, Nagai K, Tsuboi M, Okada M. Prognosis of lung cancer patients with a past history of colorectal cancer. *Jpn J Clin Oncol* 2014; 44: 1088-1095 [PMID: 25156681 DOI: 10.1093/jjco/hyu122]

15 Liu J, Zhou H, Zhang Y, Fang W, Yang Y, Hong S, Chen G, Zhao S, Chen X, Zhang Z, Xian W, Shen J, Huang Y, Zhao H, Zhang L. Impact of prior cancer history on the overall survival of younger patients with lung cancer. *ESMO Open* 2020; 5 [PMID: 32054633 DOI: 10.1136/esmoopen-2019-000608]

16 He C, Zhang Y, Cai Z, Lin X. Effect of prior cancer on survival outcomes for patients with pancreatic adenocarcinoma: a propensity score analysis. *BMC Cancer* 2019; 19: 509 [PMID: 31142278 DOI: 10.1186/s12885-019-5744-8]

17 Surveillance E, and End Results (SEER) Program (www.seer.cancer.gov). SEER*Stat Database: Incidence-SEER 18 Regs excluding AK Research Data, Nov 2016 Sub (2000-2014) - Linked To County Attributes - Total U.S., 1969-2015 Counties, National Cancer Institute, DCCPS, Surveillance Research Program, 2018

18 Donin N, Filson C, Drakaki A, Tan HJ, Castillo A, Kwan L, Litwin M, Chamie K. Risk of second primary malignancies among cancer survivors in the United States, 1992 through 2008. *Cancer* 2016; 122: 3075-3086 [PMID: 27377470 DOI: 10.1002/cncr.30164]

19 Hayat MJ, Howlader N, Reichman ME, Edwards BK. Cancer statistics, trends, and multiple primary cancer analyses from the Surveillance, Epidemiology, and End Results (SEER) Program. *Oncologist* 2007; 12: 20-37 [PMID: 17227898 DOI: 10.1634/theoncologist.12-1-20]

20 Zhou H, Huang Y, Qiu Z, Zhao H, Fang W, Yang Y, Zhao Y, Hou X, Ma Y, Hong S, Zhou T, Zhang Y, Zhang L. Impact of prior cancer history on the overall survival of patients newly diagnosed with cancer: A pan-cancer analysis of the SEER database. *Int J Cancer* 2018; 143: 1569-1577 [PMID: 29667174 DOI: 10.1002/ijc.31543]

21 Rowland JH, Bellizzi KM. Cancer survivorship issues: life after treatment and implications for an aging population. *J Clin Oncol* 2014; 32: 2662-2668 [PMID: 25071099 DOI: 10.1200/JCO.2014.55.8361]

22 Corkum M, Hayden JA, Kephart G, Urquhart R, Schlievert C, Porter G. Screening for new primary cancers in cancer survivors compared to non-cancer controls: a systematic review and meta-analysis. *J Cancer Surviv* 2013; 7: 455-463 [PMID: 23645522 DOI: 10.1007/s11764-013-0278-6]

23 Miller KD, Nogueira L, Mariotto AB, Rowland JH, Yabroff KR, Alfano CM, Jemal A, Kramer JL, Siegel RL. Cancer treatment and survivorship statistics, 2019. *CA Cancer J Clin* 2019; 69: 363-385 [PMID: 31184787 DOI: 10.3322/caac.21565]

24 Pruitt SL, Laccetti AL, Xuan L, Halm EA, Gerber DE. Revisiting a longstanding clinical trial exclusion criterion: impact of prior cancer in early-stage lung cancer. *Br J Cancer* 2017; 116: 717-725 [PMID: 28196065 DOI: 10.1038/bjc.2017.27]

25 Jin S, Pazdur R, Sridhara R. Re-Evaluating Eligibility Criteria for Oncology Clinical Trials: Analysis of Investigational New Drug Applications in 2015. *J Clin Oncol* 2017; 35: 3745-3752 [PMID: 28968168 DOI: 10.1200/JCO.2017.73.4186]

26 Gerber DE, Laccetti AL, Xuan L, Halm EA, Pruitt SL. Impact of prior cancer on eligibility for lung cancer clinical trials. *J Natl Cancer Inst* 2014; 106 [PMID: 25253615 DOI: 10.1093/jnci/dju302]

27 Sorbye H, Pfeiffer P, Cavalli-Björkman N, Qvortrup C, Holsen MH, Wentzel-Larsen T, Glimelius B. Clinical trial enrollment, patient characteristics, and survival differences in prospectively registered metastatic colorectal cancer patients. *Cancer* 2009; 115: 4679-4687 [PMID: 19562777 DOI: 10.1002/cncr.24527]

28 Duffy SW, Nagtegaal ID, Wallis M, Cafferty FH, Houssami N, Warwick J, Allgood PC, Kearins O, Tappenden N, O'Sullivan E, Lawrence G. Correcting for lead time and length bias in estimating the effect of screen detection on cancer survival. *Am J Epidemiol* 2008; 168: 98-104 [PMID: 18504245 DOI: 10.1093/aje/kwn120]

29 Sankila R, Hakulinen T. Survival of patients with colorectal carcinoma: effect of prior breast cancer. *J Natl Cancer Inst* 1998; 90: 63-65 [PMID: 9428785 DOI: 10.1093/jnci/90.1.63]

30 Shen M, Boffetta P, Olsen JH, Andersen A, Hemminki K, Pukkala E, Tracey E, Brewster DH, McBride ML, Pompe-Kirn V, Kliewer EV, Tonita JM, Chia KS, Martos C, Jonasson JG, Colin D, Scé lo G, Brennan P. A pooled analysis of second primary pancreatic cancer. *Am J Epidemiol* 2006; 163: 502-511 [PMID: 16421239 DOI: 10.1093/aje/kwj073]

31 Al-Husseini MJ, Saad AM, Mohamed HH, Alkhayat MA, Sonbol MB, Abdel-Rahman O. Impact of prior malignancies on outcome of colorectal cancer; revisiting clinical trial eligibility criteria. *BMC Cancer* 2019; 19: 863 [PMID: 31470823 DOI: 10.1186/s12885-019-6074-6]

32 Youn P, Li H, Milano MT, Stovall M, Constine LS, Travis LB. Long-term survival among Hodgkin's lymphoma patients with gastrointestinal cancer: a population-based study. *Ann Oncol* 2013; 24: 202-208 [PMID: 22855552 DOI: 10.1093/annonc/mds218]

33 Laccetti AL, Pruitt SL, Xuan L, Halm EA, Gerber DE. Effect of prior cancer on outcomes in advanced lung cancer: implications for clinical trial eligibility and accrual. *J Natl Cancer Inst* 2015; 107 [PMID: 25667420 DOI: 10.1093/jnci/djv002]

World Journal of Clinical Cases

Submit a Manuscript: https://www.f6publishing.com

World J Clin Cases 2022 February 16; 10(5): 1498-1507

DOI: 10.12998/wjcc.v10.i5.1498

ISSN 2307-8960 (online)

ORIGINAL ARTICLE

Retrospective Cohort Study

Elemene-containing hyperthermic intraperitoneal chemotherapy combined with chemotherapy for elderly patients with peritoneal metastatic advanced gastric cancer

Zhi-Xiong Chen, Jin Li, Wen-Bin Liu, Shou-Ru Zhang, Hao Sun

ORCID number: Zhi-Xiong Chen 0000-0002-7942-5903; Jin Li 0000-0001-8943-1197; Wen-Bin Liu 0000-0002-7944-918X; Shou-Ru Zhang 0000-0001-8106-0037; Hao Sun 0000-0003-2805-6826.

Author contributions: Sun H and Chen ZX concepted and designed; Chen ZX and Li J; Chen ZX, Liu WB, and Zhang SR analysed the data and interpretation; all authors wrote the manuscript and approval of the final manuscript.

Institutional review board statement: All procedures performed in studies that involved human participants were in accordance with the ethical standards of the institutional and/or national research committee, and the 1964 Helsinki declaration and its later amendments or comparable ethical standards. The present study was approved by the Ethics Committee of CUCH.

Informed consent statement: All study participants or their legal guardian provided informed written consent about personal and medical data collection prior to study enrolment.

Conflict-of-interest statement: The

Zhi-Xiong Chen, Hao Sun, Department of Gastrointestinal Cancer Center, Chongqing University Cancer Hospital, Chongqing 400030, China

Jin Li, Department of Ultrasound, The Fifth People's Hospital of Chongqing, Chongqing 400062, China

Wen-Bin Liu, Department of Hepatobiliary and Pancreatic Oncology, Chongqing University Cancer Hospital, Chongqing 400030, China

Shou-Ru Zhang, Department of Teaching and Research Section, Chongqing University Cancer Hospital, Chongqing 400030, China

Corresponding author: Hao Sun, MM, Department of Gastrointestinal Cancer Center, Chongqing University Cancer Hospital, No. 181 Hanyu Road, Sha pingba District, Chongqing 400030, China. sunhao68@sina.com

Abstract

BACKGROUND

Almost all elderly patients with peritoneal metastatic gastric cancer (PGC) are unlikely to tolerate cytoreductive surgery combined with hyperthermic intraperitoneal chemotherapy (HIPEC) and adjuvant chemotherapy. However, determining how to optimize the treatment strategy for such patients has always been a clinical problem. Both HIPEC and palliative adjuvant chemotherapy can benefit patients with PGC. Therefore, optimizing HIPEC and chemotherapy regimens has potential clinical value in reducing side effects, and improving treatment tolerance and clinical effectiveness.

AIM

To explore the effect of HIPEC containing elemene, which is an anti-cancer component extracted in traditional Chinese herbal medicine, combined with reduced capecitabine and oxaliplatin (CapeOx) chemotherapy regimens, in elderly patients with PGC.

METHODS

In the present study, 39 of 52 elderly PGC patients were included and assigned to different HIPEC treatment groups [lobaplatin group (group L) and mixed group

authors declare that they have no conflict of interest.

Data sharing statement: The datasets generated and analyzed in the present study are available from the corresponding author on reasonable request.

STROBE statement: The authors have read the STROBE Statement-checklist of items, and the manuscript was prepared and revised according to the STROBE Statement-checklist of items.

Country/Territory of origin: China

Specialty type: Gastroenterology and hepatology

Provenance and peer review: Unsolicited article; Externally peer reviewed.

Peer-review model: Single blind

Peer-review report's scientific quality classification
Grade A (Excellent): 0
Grade B (Very good): B
Grade C (Good): 0
Grade D (Fair): D
Grade E (Poor): 0

Received: September 18, 2021
Peer-review started: September 18, 2021
First decision: October 27, 2021
Revised: November 19, 2021
Accepted: January 11, 2022
Article in press: January 11, 2022
Published online: February 16, 2022

P-Reviewer: Kawabata H,

(group M)] for analysis. Lobaplatin was used for all three HIPECs in group L. In group M, lobaplatin was used in the middle of the three HIPECs, and elemene was used for the first and third HIPEC. After HIPEC, patients received CapeOx chemotherapy. The incidence of complications (abdominal infection, lung infection, and urinary tract infection), myelosuppression, immune function (CD4/CD8 ratio), average length of hospital stay, and prognosis were compared between these two groups.

RESULTS
There was no significant difference in the incidence of complications between the two groups during hospitalization ($P > 0.05$). Compared to patients in group M, patients in group L exhibited severe myelosuppression ($P = 0.027$) and increased length of hospital stay ($P = 0.045$). However, no overall survival benefit was observed in group M. Furthermore, the immune function of patients in group M was less affected ($P < 0.001$), when compared to that of patients in group L. The multivariate analysis suggested that the cycles of chemotherapy after perfusion significantly affected the prognosis of patients in both groups.

CONCLUSION
Compared to the lobaplatin-based HIPEC regimen, the administration of elemene reduced the myelosuppression incidence in elderly PGC patients. The present study sheds light on the implementation of this therapeutic strategy for this set of patients.

Key Words: Gastric cancer; Hyperthermic intraperitoneal chemotherapy; Peritoneal metastasis; Oxaliplatin; Capecitabine

Core Tip: Elderly patients with advanced gastric cancer (GC) cannot tolerate high-intensity treatment. In addition, intraperitoneal hyperthermic perfusion chemotherapy (HIPEC) and capecitabine and oxaliplatin (CapeOx) regimens have limited therapeutic effects on advanced GC. On the other hand, the extracted Chinese herbal medicine, elemene, has anti-cancer effects and negligible side effects. In the present study, the use of elemene-containing HIPEC combined with a CapeOx chemotherapy regimen was proven to be more tolerant for elderly patients with peritoneal metastatic gastric cancer, making this a clinical choice for such patients.

Citation: Chen ZX, Li J, Liu WB, Zhang SR, Sun H. Elemene-containing hyperthermic intraperitoneal chemotherapy combined with chemotherapy for elderly patients with peritoneal metastatic advanced gastric cancer. *World J Clin Cases* 2022; 10(5): 1498-1507
URL: https://www.wjgnet.com/2307-8960/full/v10/i5/1498.htm
DOI: https://dx.doi.org/10.12998/wjcc.v10.i5.1498

INTRODUCTION

In 2020, it was reported that there were approximately 1089103 new gastric cancer (GC) cases and 789793 gastric cancer-related deaths worldwide[1]. The lack of typical clinical symptoms at the early stage has made GC one of the malignancies with the highest incidence in the gastroenterological tract in China. Furthermore, a recent study demonstrated that more than half of patients were diagnosed at the advanced stage [2]. In addition, nearly 20%-30% of diagnosed GC patients were found to develop peritoneal metastasis[3]. Despite the advances achieved by treatment approaches, the median survival time still ranges within 3-4 mo[3,4]. Cytoreductive surgery (CRS) with hyperthermic intraperitoneal chemotherapy (HIPEC) has been shown to be an effective therapeutic strategy for prolonging survival in a variety of peritoneal malignancies[5-7]. Most recent evidence has shown that CRS-HIPEC can improve the prognosis of GC patients with peritoneal metastasis[8-10]. However, it has been reported that elderly patients have an increased risk for postoperative morbidity[11].

Mohamed SY
S-Editor: Ma YJ
L-Editor: A
P-Editor: Ma YJ

Therefore, this group of patients may not be able to tolerate regular CRS-HIPEC. Thus, developing an effective therapeutic strategy for elderly GC patients with peritoneal metastasis is urgently important.

An increasing body of evidence has revealed that HIPEC combined with systemic chemotherapy using capecitabine and oxaliplatin (CapeOx) can significantly improve the outcome of GC patients with peritoneal metastasis[12,13]. It is noteworthy that CapeOx has been accepted as a regimen with acceptable toxicity for metastatic or advanced GC[14,15]. Furthermore, it has been reported that elderly patients with advanced GC can tolerate and benefit from CapeOx treatment, even at lower doses [16]. However, the use of HIPEC combined with systemic chemotherapy for elderly patients with advanced GC has not been described to date. Furthermore, a recommended treatment paradigm to achieve optimum therapeutic effects and minimum side-effects for patients with advanced GC has not been established.

Accumulating evidence has revealed that β-elemene, an active ingredient in the ginger family of Chinese herbal medicine Wenyujin, has anti-cancer activity. Importantly, it has been shown that β-elemene can increase the susceptibility of multidrug-resistant cancer cells and exhibit synergistic anti-cancer effects[17] with neglectable side effects. Furthermore, it has been reported that elemene can be utilized to treat a variety of cancers, including lung cancer[18], liver cancer[19], brain cancer [20], breast cancer[21], and GC[22,23]. Moreover, elemene has been shown to increase the susceptibility of cancer cells to chemotherapy and radiotherapy[17,24]. In addition, it has fewer side effects, and can inhibit M2 macrophage-mediated immunosuppressive effects[24]. Its extremely high penetrating potential[23] also enables elemene to penetrate the blood-brain barrier and prolong the survival of patients with glioma [25]. The therapeutic efficacy of elemene for malignant pleural and ascites has been well-documented[26-28]. Therefore, it was speculated that the β-elemene-containing HIPEC paradigm might be a promising therapeutic strategy for elderly patients with advanced GC. In line with this, the present study evaluated the efficacy and safety of the elemene-supplemented HIPEC combined with CapeOx regimen in elderly GC patients with peritoneal metastasis.

MATERIALS AND METHODS

Study design and patients

A single-center research was conducted for patients recruited at the Gastrointestinal Cancer Center of Chongqing University Cancer Hospital (CUCH) between July 2016 and April 2020. All patients (n = 52) who participated in the present study provided a signed informed consent. The inclusion criteria were, as follows: (1) Age ≥ 65 years old; (2) Diagnosed with advanced GC and peritoneal metastasis; (3) Eastern Cooperative Oncology group (ECOG) score ≤ 2; (4) No severe organ or metabolic dysfunction; (5) No hypertension; (6) Mentally capable to adapt to intervention; and (7) > 3 mo of expected survival time. Finally, 39 patients who met the inclusion criteria were analyzed for the present study (Figure 1), and none of these cases were HER2-positive.

Groupings: A total of 52 recruited elderly peritoneal metastatic gastric cancer (PGC) patients were randomly assigned to two groups: lobaplatin group (group L), in which lobaplatin was used during HIPEC; mixed group (group M), in which both elemene and lobaplatin were used during HIPEC.

Treatment information

Before HIPEC, patients underwent preventive fasting, gastric intubation, intravenous fluid replacement, nebulization, and sputum suction. Then, patients received laparoscopic puncture and catheterization, and no postoperative ICU admission was needed. Three cycles of HIPEC were performed for each patient. The first cycle was administered upon completion of the catheterization, and while the patient was still under anesthesia. The remaining cycles were performed when the patient was transferred to the ward (within 36, 72, or 120 h after surgery). In general, the HIPEC system (BR-TRG-I, BRM, Guangzhou, China) was perfused with 3000 mL of 0.9% sodium chloride, and pre-heated for 15 minutes until the ambiance temperature reached 43 °C. Then, the chemotherapy agents were delivered into the system in different groups. In particular, for patients in group L, lobaplatin [State Drug Administration (SDA) approval number: H20050308, 50 mg/m^2] supplemented in 250 mL of 5% glucose was added into the system for all three HIPEC cycles. For patients in group M, elemene (SDA approval number: H20110114, 0.6 g) supplemented in 250 mL of 5%

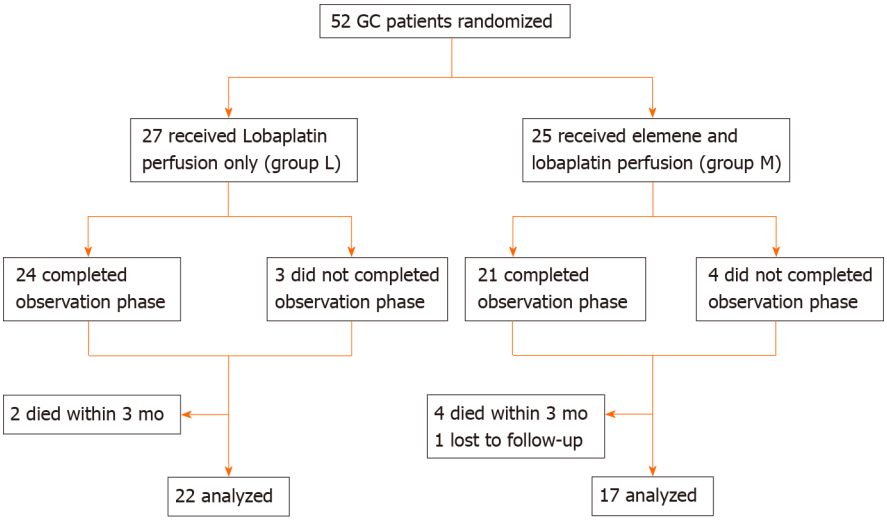

Figure 1 Overall study design flowchart.

glucose was administered at the first and third HIPEC cycles. For the second HIPEC cycle, these patients were administered with the same HIPEC chemotherapy reagent as that administered for patients in group L. The perfusion machine was operated according to manufacturer's instructions. The perfusion time ranged within 30-90 min, based on the tolerance of each recipient (patients who failed to achieve a perfusion speed higher than 350 mL/min were excluded from the present study). Morphine and tramadol were used to relieve the pain before and after the perfusion. Oxygen was given to patients during the perfusion. In group M, 1.5 g of lidocaine was administered into the HIPEC system at five minutes before the administration of elemene to reduce peritoneal irritation. After the HIPEC treatment, case-specific supportive care was provided based on the complications (analgesia, acid suppression, antiemetic, maintenance of electrolyte balance, albumin infusion, and blood transfusion; subcutaneous injection of granulocyte stimulating factor, thrombopoietin [300 μg, once], and/or interleukin-11 (IL-11; 3 mg, per day, 5-7 d, according to the manual; Qilu Pharmaceutical Co., Ltd.); partial parenteral nutrition support therapy). Within two weeks after discharge, these patients received CapeOx chemotherapy (60% or 80%, or the standard CapeOx dose). The dose was gradually reduced to 60% from 80% for some patients. Each cycle was repeated every 21 d.

Data collection

The vital signs of each patient were collected during hospitalization, and these patients were followed up monthly. The average follow-up time for the entire cohort was 9.04 mo (range: 3.0-17.9 mo), and the follow-up of all patients recruited for the present study was concluded in April 2020. After perfusion, the abdominal drainage was sent to the laboratory for bacterial test. In addition, during the CapeOx chemotherapy, the results for the routine blood test, liver and kidney function evaluation, immune function analysis (CD4/CD8 ratio), and serum markers for gastric cancer (CEA, CA-125 and CA-199; any serum marker level that increases to two or becomes more than two times of the normal threshold was defined as high; otherwise, the level was defined as normal) were recorded for each patient.

Statistical analysis

The data were analyzed using the SPSS software package (version 22.0). The measurement data were presented as mean ± SD, categorical variables were analyzed by Chi-square test or Fisher's exact test, and ordinal data were analyzed by nonparametric Mann-Whitney *U*-test. Furthermore, the survival differences were analyzed using the Kaplan-Meier survival curve and Log-rank test. In addition, univariate analysis and Cox multivariate risk ratio regression analysis were performed to identify the potential factors related to the prognosis. A P value of < 0.05 in the two-sided test was considered statistically significant.

RESULTS

Patients' clinical data

A total of 39 GC patients were analyzed (Figure 1). The clinical characteristics of these patients are summarized in Table 1. There were 22 GC patients in group L (n = 22, 69.9 ± 3.6 years old), and 17 GC patients in group M (n = 17, 68.6 ± 3.0 years old). There were no significant differences between the two groups, in terms of gender, ECOG score, age, tumor site composition ratio, tumor size, and occurrence of complications during the first hospitalization (except for myelosuppression). However, patients in group L developed severe myelosuppression during the first hospitalization, when compared to patients in group M (P = 0.027). In addition, the average length of hospital stay was 18.7 d for patients in group L. This was a slightly longer than that for patients in group M, which was merely 16.1 d (P = 0.045).

Follow-up results

The average follow-up duration for all patients was 9.04 ± 4.30 mo (3.00-17.90 mo). The follow-up duration was 9.60 ± 4.20 mo (3.40-17.90 mo) for patients in group L, and 8.30 ± 4.40 mo (3.00-16.10 mo) for patients in group M. There was no significant difference in follow-up duration between these two groups (9.60 ± 4.20 mo (3.40-17.90 mo) *vs* 8.30 ± 4.40 mo (3.00-16.10 mo), P = 0.292). Three patients were lost to follow-up during the follow-up period, and 33 patients became deceased, while three patients survived at the end of the follow-up period. There were no significant differences in survival performance, in terms of HIPEC regimen (P = 0.29, Figure 1). Furthermore, both groups' median overall survival (OS) was 9.90 mo (95%CI: 5.30-13.50). The median survival was 10.80 mo (95%CI: 8.50-13.10) and 9.40 mo (95%CI: 5.30-13.50) for patients in groups L and M, respectively.

Prognostic factors

In order to identify the potential prognostic factors, independent variables, including gender, age, treatment regimen, serum tumor marker levels, immune function (CD4/CD8 ratio), myelosuppression status, cycles of chemotherapy (CapeOx chemotherapy) after HIPEC, peritoneal cancer index (PCI), and observation/presence of malignant ascites during catheterization, were analyzed using univariate analysis, followed by multivariate analysis. The results revealed that high-level serum tumor markers, low CD4/CD8 ratio (< 1), fewer cycles of chemotherapy (reduced CapeOx regimen) after HIPEC (< 6 times), high PCI (not < 20), and the appearance of ascites during laparoscopic catheter placement indicates poor prognosis (Table 2).

DISCUSSION

Compared to the OS of simple systemic palliative chemotherapy, the present study revealed that the elemene-containing HIPEC combined with CapeOx regimen can extend the OS (the median OS was approximately 9.40 mo) of elderly PGC patients, which is consistent with the report of Blum Murphy *et al*[29] (the OS was approximately 12 mo). It is noteworthy that clinical studies have revealed that multiple chemotherapy regimens, including fluorouracil plus leucovorin, oxaliplatin (FLOT4), and docetaxel and docetaxel, cisplatin, and 5-fluorouracil (DCF), are poorly tolerated by elderly patients[30,31]. The present study provides the possibility that the tolerance of these regimens by elderly PGC patients could be potentially elevated. However, further investigations are needed to determine whether implementing elemene to lobaplatin-based HIPEC can improve the chemotherapy efficacy of FLOT4 or DCF to be as potent as that of CapeOx. The present finding revealed that the implementation of the lobaplatin-based HIPEC combined with CapeOx regimen resulted in a high occurrence of myelosuppression in elderly GC patients (27.3%). Although the addition of elemene in the lobaplatin-based HIPEC combined with CapeOx regimen did not improve the OS of these patients, when compared to that in group L (Figure 2), this significantly reduced the incidence of myelosuppression in the recipients (P = 0.027). It is noteworthy that elderly patients with advanced cancer, such as GC, often undergo myelosuppression after receiving high-intensity chemotherapies, including lobaplatin-based regimens[32]. Notably, such complications would lead to treatment delay, and some can be life-threatening[33]. Although the OS of patients was not directly influenced, this complication increased the cost of treatment and length of hospital stay of these patients. In addition, the subgroup analysis revealed that the cycles of CapeOx treatment after HIPEC, PCI, and the CD4/CD8 ratio are prognostic factors in

Table 1 Clinical characteristics of patients with gastric cancer

Clinical parameters	Group L	Group M	*P* value
Gender			0.531
Male	14	9	
Female	8	8	
Age group (yr)			0.748
65-69	11	10	
70-75	11	7	
ECOG score			0.561
0	14	8	
1	5	5	
2	3	4	
Tumor location			0.667
Proximal	2	3	
Middle	4	2	
Distal	16	12	
Tumor stage			0.192
cT3	12	5	
cT4a	9	9	
cT4b	1	3	
PCI scores			0.508
< 20	15	9	
≥ 20	7	8	
Abdominal infection (cases)	2	0	0.495
pulmonary infection (cases)	1	1	1.000
Urinary tract infection (cases)	0	1	0.436
Myelosuppression system (grade 3/4, cases)	6	0	0.027
Blood transfusion therapy (cases)	4	0	0.118
Average length of stay (d)	18.7	16.1	0.045

PCI: Peritoneal cancer index; ECOG: Eastern Cooperative Oncology group.

elderly patients. The finding that a low CD4/CD8 ratio indicates poor prognosis is in line with the findings reported by previous studies, suggesting that GC patients with impaired immune function have a poor prognosis[34,35].

The present study has the following limitations. First, the sample size was small, and a control group that only used elemene HIPEC was not added. Hence, a larger cohort is needed in future studies. Second, it has been reported that reduced CapeOx doses can affect the clinical outcomes of elderly patients with advanced GC[16]. In the present study, the reduced dose of CapeOx was utilized during the treatment for part of the patients, and this may have led to biased results. Third, further exploration is needed to determine whether patients can benefit from the intravenous administration of elemene combined with CapeOx after HIPEC. Lastly, a control group for systemic chemotherapy should also be considered. Finally, it has been reported that NCT03333967[36], TAGS[37] and EPOC1201[38] can improve the prognosis of patients with advanced GC. Therefore, in future studies, it should be determined whether elemene-containing HIPEC can improve the therapeutic effects of these drugs.

Table 2 Univariate and multivariate analysis of prognostic factors of gastric cancer patients

Clinical parameters	Univariate analysis		Multivariate analysis	
	HR (95%CI)	*P* value	HR (95%CI)	*P* value
Gender (male *vs* female)	0.858 (0.424-1.734)	0.670		
Age (< 70 *vs* ≥ 70)	1.139 (0.564-2.301)	0.717		
Group (L *vs* M)	1.467 (0.714-3.016)	0.297		
T stage (T3 *vs*T4 or above)	2.403 (1.118-5.163)	0.025	1.457 (0.554-3.832)	0.445
Tumor marker (normal *vs* high)	1.009 (0.473-2.153)	0.981		
CD4/CD8 (< 1 *vs* ≥ 1)	2.505 (1.147-5.467)	0.021	2.051 (0.8534.933)	0.109
Myelosuppression (1/2 *vs* 3/4)	3.570 (1.291-9.874)	0.014	3.220 (0.985-10.530)	0.053
Times of chemotherapy after HIPEC (< 6 *vs* ≥ 6)	0.143 (0.060-0.343)	0.000	0.210 (0.070-0.634)	0.006
PCI (< 20 *vs* ≥ 20)	2.444 (1.105-5.404)	0.027	1.247 (0.417-3.725)	0.693
Ascites (exist[1] *vs* none)	4.106 (1.746-9.658)	0.001	3.084 (0.948-10.027)	0.061

[1]Discernible malignant ascites in surgery.

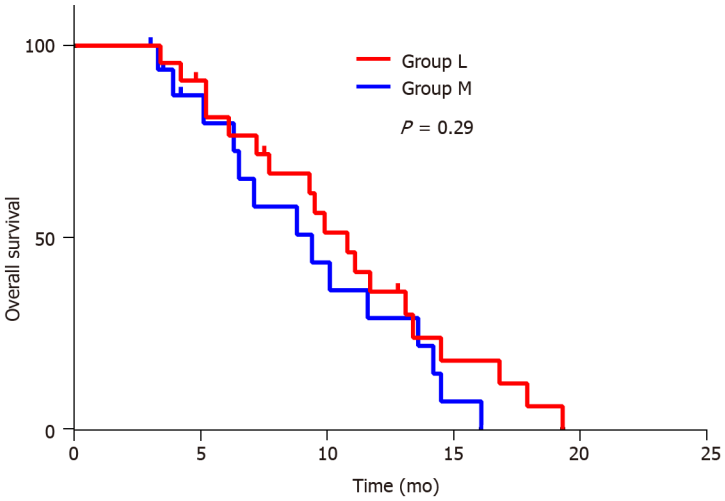

Figure 2 Survival curves for gastric cancer patients, according to the treatment regimen (*P* = 0.29).

CONCLUSION

The elemene-containing HIPEC combined with CapeOX regimen has fewer side effects, and is safe for elderly PGC patients. However, further exploration is needed to determine how to further optimize the dose and combine this with other chemotherapy regimens.

ARTICLE HIGHLIGHTS

Research background

Elderly patients with peritoneal metastatic gastric cancer (PGC) have poor tolerance to intensive treatment, such as cytoreductive surgery plus hyperthermic perfusion chemotherapy (HIPEC). To date, no guidelines or consensus has standardized the HIPEC composition. However, elemene, a Chinese herbal extract with anti-cancer activity and low toxicity, turns out to be a promising ingredient for HIPEC.

Research motivation

The study aims to determine whether implementing elemene in lobaplatin-based

HIPEC benefits elderly PGC patients during chemotherapy.

Research objectives

The study aims to explore the clinical effectiveness and potential side effects of elemene-containing lobaplatin-based HIPEC in elderly PGC patients.

Research methods

The included patients were assigned into two groups: patients who received elemene-containing lobaplatin-based HIPEC plus oxaliplatin and capecitabine (CapeOx) treatment (group M) and patients who received elemene-free lobaplatin-based HIPEC plus CapeOx treatment (group L). The incidence of complications such as myelosuppression, immune function (CD4/CD8 ratio), average length of hospital stay, and prognosis were compared between these two groups.

Research results

There was no significant difference in the incidence of complications and overall survival between the two groups during hospitalization. In addition, supplementing elemene in HIPEC lessened the myelosuppression (P = 0.027) and shortened the length of hospital stay (P = 0.045) of elderly PGC patients.

Research conclusions

The administration of elemene led to the amelioration of myelosuppression in elderly PGC patients.

Research perspectives

The present study sheds light on the implemention of an elemene-containing HIPEC therapeutic strategy for elderly patients with PGC.

REFERENCES

1 **Sung H**, Ferlay J, Siegel RL, Laversanne M, Soerjomataram I, Jemal A, Bray F. Global Cancer Statistics 2020: GLOBOCAN Estimates of Incidence and Mortality Worldwide for 36 Cancers in 185 Countries. *CA Cancer J Clin* 2021; **71**: 209-249 [PMID: 33538338 DOI: 10.3322/caac.21660]

2 **Nguyen HV**, Nguyen HV, Nguyen LT, Pham NQ, Nguyen HX, Nguyen VT. A Case of Advanced Gastric Cancer with Folfiri as a Preoperative Chemotherapy. *Case Rep Oncol Med* 2019; **2019**: 1352173 [PMID: 31871804 DOI: 10.1155/2019/1352173]

3 **Thomassen I**, van Gestel YR, van Ramshorst B, Luyer MD, Bosscha K, Nienhuijs SW, Lemmens VE, de Hingh IH. Peritoneal carcinomatosis of gastric origin: a population-based study on incidence, survival and risk factors. *Int J Cancer* 2014; **134**: 622-628 [PMID: 23832847 DOI: 10.1002/ijc.28373]

4 **Sarela AI**, Miner TJ, Karpeh MS, Coit DG, Jaques DP, Brennan MF. Clinical outcomes with laparoscopic stage M1, unresected gastric adenocarcinoma. *Ann Surg* 2006; **243**: 189-195 [PMID: 16432351 DOI: 10.1097/01.sla.0000197382.43208.a5]

5 **Yan TD**, Deraco M, Baratti D, Kusamura S, Elias D, Glehen O, Gilly FN, Levine EA, Shen P, Mohamed F, Moran BJ, Morris DL, Chua TC, Piso P, Sugarbaker PH. Cytoreductive surgery and hyperthermic intraperitoneal chemotherapy for malignant peritoneal mesothelioma: multi-institutional experience. *J Clin Oncol* 2009; **27**: 6237-6242 [PMID: 19917862 DOI: 10.1200/JCO.2009.23.9640]

6 **Chua TC**, Moran BJ, Sugarbaker PH, Levine EA, Glehen O, Gilly FN, Baratti D, Deraco M, Elias D, Sardi A, Liauw W, Yan TD, Barrios P, Gómez Portilla A, de Hingh IH, Ceelen WP, Pelz JO, Piso P, González-Moreno S, Van Der Speeten K, Morris DL. Early- and long-term outcome data of patients with pseudomyxoma peritonei from appendiceal origin treated by a strategy of cytoreductive surgery and hyperthermic intraperitoneal chemotherapy. *J Clin Oncol* 2012; **30**: 2449-2456 [PMID: 22614976 DOI: 10.1200/JCO.2011.39.7166]

7 **Goéré D**, Malka D, Tzanis D, Gava V, Boige V, Eveno C, Maggiori L, Dumont F, Ducreux M, Elias D. Is there a possibility of a cure in patients with colorectal peritoneal carcinomatosis amenable to complete cytoreductive surgery and intraperitoneal chemotherapy? *Ann Surg* 2013; **257**: 1065-1071 [PMID: 23299520 DOI: 10.1097/SLA.0b013e31827e9289]

8 **Bonnot PE**, Piessen G, Kepenekian V, Decullier E, Pocard M, Meunier B, Bereder JM, Abboud K, Marchal F, Quenet F, Goere D, Msika S, Arvieux C, Pirro N, Wernert R, Rat P, Gagnière J, Lefevre JH, Courvoisier T, Kianmanesh R, Vaudoyer D, Rivoire M, Meeus P, Passot G, Glehen O; FREGAT and BIG-RENAPE Networks. Cytoreductive Surgery With or Without Hyperthermic Intraperitoneal Chemotherapy for Gastric Cancer With Peritoneal Metastases (CYTO-CHIP study): A Propensity Score Analysis. *J Clin Oncol* 2019; **37**: 2028-2040 [PMID: 31084544 DOI: 10.1200/JCO.18.01688]

9 **Ellison LM**, Man Y, Stojadinovic A, Xin H, Avital I. Cytoreductive surgery and hyperthermic intraperitoneal chemotherapy in treatment of gastric cancer with peritoneal carcinomatosis. *Chin J*

Cancer Res 2017; **29**: 86-92 [PMID: 28373757 DOI: 10.21147/j.issn.1000-9604.2017.01.10]
10 **Chia CS**, Seshadri RA, Kepenekian V, Vaudoyer D, Passot G, Glehen O. Survival outcomes after cytoreductive surgery and hyperthermic intraperitoneal chemotherapy for peritoneal carcinomatosis from gastric cancer: a systematic review. *Pleura Peritoneum* 2016; **1**: 67-77 [PMID: 30911610 DOI: 10.1515/pp-2016-0010]
11 **Votanopoulos KI**, Shen P, Stewart JH, Levine EA; Wake Forest HIPEC Group. Outcomes of Cytoreductive Surgery (CRS) with Hyperthermic Intraperitoneal Chemotherapy (HIPEC) in Patients Older than 70 Years; Survival Benefit at Considerable Morbidity and Mortality: A Reply. *Ann Surg Oncol* 2017; **24**: 602 [PMID: 29134373 DOI: 10.1245/s10434-017-6220-9]
12 **Yu P**, Ye Z, Dai G, Zhang Y, Huang L, Du Y, Cheng X. Neoadjuvant systemic and hyperthermic intraperitoneal chemotherapy combined with cytoreductive surgery for gastric cancer patients with limited peritoneal metastasis: a prospective cohort study. *BMC Cancer* 2020; **20**: 1108 [PMID: 33198674 DOI: 10.1186/s12885-020-07601-x]
13 **Bittoni A**, Faloppi L, Giampieri R, Cascinu S. Selecting the best treatment for an individual patient. *Recent Results Cancer Res* 2012; **196**: 307-318 [PMID: 23129382 DOI: 10.1007/978-3-642-31629-6_20]
14 **Xie BW**, Zang L, Ma JJ, Sun J, Yang X, Wang ML, Lu AG, Hu WG, Zheng MH. [Safety and effectiveness of oxaliplatin combined with capecitabine or oxaliplatin combined with S-1 neoadjuvant chemotherapy in the treatment of advanced gastric cancer]. *Zhonghua Wei Chang Wai Ke Za Zhi* 2021; **24**: 138-144 [PMID: 33508919 DOI: 10.3760/cma.j.cn.441530-20200721-00433]
15 **Satake H**, Yasui H, Kotake T, Okita Y, Hatachi Y, Kotaka M, Kato T, Tsuji A. First-line chemotherapy with capecitabine/oxaliplatin for advanced gastric cancer: A phase I study. *Mol Clin Oncol* 2017; **7**: 347-350 [PMID: 28894576 DOI: 10.3892/mco.2017.1335]
16 **Hwang IG**, Ji JH, Kang JH, Lee HR, Lee HY, Chi KC, Park SW, Lee SJ, Kim ST, Lee J, Park SH, Park JO, Park YS, Lim HY, Kang WK. A multi-center, open-label, randomized phase III trial of first-line chemotherapy with capecitabine monotherapy *vs* capecitabine plus oxaliplatin in elderly patients with advanced gastric cancer. *J Geriatr Oncol* 2017; **8**: 170-175 [PMID: 28119041 DOI: 10.1016/j.jgo.2017.01.002]
17 **Jiang Z**, Jacob JA, Loganathachetti DS, Nainangu P, Chen B. β-Elemene: Mechanistic Studies on Cancer Cell Interaction and Its Chemosensitization Effect. *Front Pharmacol* 2017; **8**: 105 [PMID: 28337141 DOI: 10.3389/fphar.2017.00105]
18 **Zhou K**, Wang L, Cheng R, Liu X, Mao S, Yan Y. Elemene Increases Autophagic Apoptosis and Drug Sensitivity in Human Cisplatin (DDP)-Resistant Lung Cancer Cell Line SPC-A-1/DDP By Inducing Beclin-1 Expression. *Oncol Res* 2017 [PMID: 28550680 DOI: 10.3727/096504017X14954936991990]
19 **Mao Y**, Zhang J, Hou L, Cui X. The effect of beta-elemene on alpha-tubulin polymerization in human hepatoma HepG2 cells. *Chin J Cancer Res* 2013; **25**: 770-776 [PMID: 24385707 DOI: 10.3978/j.issn.1000-9604.2013.12.12]
20 **Zhu T**, Li X, Luo L, Wang X, Li Z, Xie P, Gao X, Song Z, Su J, Liang G. Reversion of malignant phenotypes of human glioblastoma cells by β-elemene through β-catenin-mediated regulation of stemness-, differentiation- and epithelial-to-mesenchymal transition-related molecules. *J Transl Med* 2015; **13**: 356 [PMID: 26563263 DOI: 10.1186/s12967-015-0727-2]
21 **Zhang J**, Zhang Hd, Chen L, Sun DW, Mao Cf, Chen W, Wu JZ, Zhong SL, Zhao JH, Tang JH. β-elemene reverses chemoresistance of breast cancer *via* regulating MDR-related microRNA expression. *Cell Physiol Biochem* 2014; **34**: 2027-2037 [PMID: 25562151 DOI: 10.1159/000366398]
22 **Zhai B**, Zeng Y, Zeng Z, Zhang N, Li C, You Y, Wang S, Chen X, Sui X, Xie T. Drug delivery systems for elemene, its main active ingredient β-elemene, and its derivatives in cancer therapy. *Int J Nanomedicine* 2018; **13**: 6279-6296 [PMID: 30349250 DOI: 10.2147/IJN.S174527]
23 **Zhang Y**, Mu XD, Li EZ, Luo Y, Song N, Qu XJ, Hu XJ, Liu YP. The role of E3 ubiquitin ligase Cbl proteins in β-elemene reversing multi-drug resistance of human gastric adenocarcinoma cells. *Int J Mol Sci* 2013; **14**: 10075-10089 [PMID: 23665906 DOI: 10.3390/ijms140510075]
24 **Yu X**, Xu M, Li N, Li Z, Li H, Shao S, Zou K, Zou L. β-elemene inhibits tumor-promoting effect of M2 macrophages in lung cancer. *Biochem Biophys Res Commun* 2017; **490**: 514-520 [PMID: 28624450 DOI: 10.1016/j.bbrc.2017.06.071]
25 **Ma C**, Zhou W, Yan Z, Qu M, Bu X. β-Elemene treatment of glioblastoma: a single-center retrospective study. *Onco Targets Ther* 2016; **9**: 7521-7526 [PMID: 28003765 DOI: 10.2147/OTT.S120854]
26 **Wang QT**, Zhang ZL, Xiong H, Zhou DS, Li J, Liang J, Wang YF. Evaluation of the efficacy and safety of elemene in treating malignant pleural effusion caused by tumors: A PRISMA guided meta-analysis. *Medicine (Baltimore)* 2018; **97**: e12542 [PMID: 30383624 DOI: 10.1097/MD.0000000000012542]
27 **Wang X**, Wang H, Li L. A meta-analysis of elemene *vs* DDP intrapleural injection in the treatment of malignant pleural effusion caused by lung cancer. *J Cancer Res Ther* 2016; **12**: C244-C247 [PMID: 28230027 DOI: 10.4103/0973-1482.200748]
28 **Jiang ZY**, Qin SK, Yin XJ, Chen YL, Zhu L. Synergistic effects of Endostar combined with β-elemene on malignant ascites in a mouse model. *Exp Ther Med* 2012; **4**: 277-284 [PMID: 23139716 DOI: 10.3892/etm.2012.583]
29 **Blum Murphy M**, Ikoma N, Wang X, Estrella J, Roy-Chowdhuri S, Das P, Minsky BD, Song S, Mansfield P, Ajani J, Badgwell B. Phase I Trial of Hyperthermic Intraperitoneal Chemoperfusion

(HIPEC) with Cisplatin, Mitomycin, and Paclitaxel in Patients with Gastric Adenocarcinoma and Associated Carcinomatosis or Positive Cytology. *Ann Surg Oncol* 2020; **27**: 2806-2811 [PMID: 31974712 DOI: 10.1245/s10434-020-08226-x]

30 **Al-Batran SE**, Homann N, Pauligk C, Goetze TO, Meiler J, Kasper S, Kopp HG, Mayer F, Haag GM, Luley K, Lindig U, Schmiegel W, Pohl M, Stoehlmacher J, Folprecht G, Probst S, Prasnikar N, Fischbach W, Mahlberg R, Trojan J, Koenigsmann M, Martens UM, Thuss-Patience P, Egger M, Block A, Heinemann V, Illerhaus G, Moehler M, Schenk M, Kullmann F, Behringer DM, Heike M, Pink D, Teschendorf C, Löhr C, Bernhard H, Schuch G, Rethwisch V, von Weikersthal LF, Hartmann JT, Kneba M, Daum S, Schulmann K, Weniger J, Belle S, Gaiser T, Oduncu FS, Güntner M, Hozaeel W, Reichart A, Jäger E, Kraus T, Mönig S, Bechstein WO, Schuler M, Schmalenberg H, Hofheinz RD; FLOT4-AIO Investigators. Perioperative chemotherapy with fluorouracil plus leucovorin, oxaliplatin, and docetaxel *vs* fluorouracil or capecitabine plus cisplatin and epirubicin for locally advanced, resectable gastric or gastro-oesophageal junction adenocarcinoma (FLOT4): a randomised, phase 2/3 trial. *Lancet* 2019; **393**: 1948-1957 [PMID: 30982686 DOI: 10.1016/S0140-6736(18)32557-1]

31 **Wagner AD**, Syn NL, Moehler M, Grothe W, Yong WP, Tai BC, Ho J, Unverzagt S. Chemotherapy for advanced gastric cancer. *Cochrane Database Syst Rev* 2017; **8**: CD004064 [PMID: 28850174 DOI: 10.1002/14651858.CD004064.pub4]

32 **Wang Z**, Xu L, Wang H, Li Z, Lu L, Li X, Zhang Q. Lobaplatin-based regimens outperform cisplatin for metastatic breast cancer after anthracyclines and taxanes treatment. *Saudi J Biol Sci* 2018; **25**: 909-916 [PMID: 30108440 DOI: 10.1016/j.sjbs.2018.01.011]

33 **Pan L**, Zhang T, Cao H, Sun H, Liu G. Ginsenoside Rg3 for Chemotherapy-Induced Myelosuppression: A Meta-Analysis and Systematic Review. *Front Pharmacol* 2020; **11**: 649 [PMID: 32477128 DOI: 10.3389/fphar.2020.00649]

34 **Yuan XL**, Chen L, Li MX, Dong P, Xue J, Wang J, Zhang TT, Wang XA, Zhang FM, Ge HL, Shen LS, Xu D. Elevated expression of Foxp3 in tumor-infiltrating Treg cells suppresses T-cell proliferation and contributes to gastric cancer progression in a COX-2-dependent manner. *Clin Immunol* 2010; **134**: 277-288 [PMID: 19900843 DOI: 10.1016/j.clim.2009.10.005]

35 **Li F**, Sun Y, Huang J, Xu W, Liu J, Yuan Z. CD4/CD8 + T cells, DC subsets, Foxp3, and IDO expression are predictive indictors of gastric cancer prognosis. *Cancer Med* 2019; **8**: 7330-7344 [PMID: 31631566 DOI: 10.1002/cam4.2596]

36 **Du Y**, Cao Q, Jiang C, Liang H, Ning Z, Ji C, Wang J, Zhou C, Jiang Z, Yu C, Li L, Zhao Y, Xu Y, Xu T, Hu W, Wang D, Cheng H, Wang G, Zhou J, Wang S, Zhang Y, Hu Z, Li X, Lu D, Zhang J, Xie H, Sun G. Effectiveness and safety of low-dose apatinib in advanced gastric cancer: A real-world study. *Cancer Med* 2020; **9**: 5008-5014 [PMID: 32441892 DOI: 10.1002/cam4.3105]

37 **Shitara K**, Doi T, Dvorkin M, Mansoor W, Arkenau HT, Prokharau A, Alsina M, Ghidini M, Faustino C, Gorbunova V, Zhavrid E, Nishikawa K, Hosokawa A, Yalçın Ş, Fujitani K, Beretta GD, Cutsem EV, Winkler RE, Makris L, Ilson DH, Tabernero J. Trifluridine/tipiracil *vs* placebo in patients with heavily pretreated metastatic gastric cancer (TAGS): a randomised, double-blind, placebo-controlled, phase 3 trial. *Lancet Oncol* 2018; **19**: 1437-1448 [PMID: 30355453 DOI: 10.1016/S1470-2045(18)30739-3]

38 **Bando H**, Doi T, Muro K, Yasui H, Nishina T, Yamaguchi K, Takahashi S, Nomura S, Kuno H, Shitara K, Sato A, Ohtsu A. A multicenter phase II study of TAS-102 monotherapy in patients with pre-treated advanced gastric cancer (EPOC1201). *Eur J Cancer* 2016; **62**: 46-53 [PMID: 27208903 DOI: 10.1016/j.ejca.2016.04.009]

World Journal of Clinical Cases

Submit a Manuscript: https://www.f6publishing.com

World J Clin Cases 2022 February 16; 10(5): 1508-1516

DOI: 10.12998/wjcc.v10.i5.1508

ISSN 2307-8960 (online)

ORIGINAL ARTICLE

Retrospective Study

Timing theory continuous nursing, resistance training: Rehabilitation and mental health of caregivers and stroke patients with traumatic fractures

Ya-Li Shen, Zong-Qun Zhang, Li-Juan Zhu, Jing-Hua Liu

ORCID number: Ya-Li Shen 0000-0002-3673-7157; Zong-Qun Zhang 0000-0002-6687-0688; Li-Juan Zhu 0000-0003-3093-5264; Jing-Hua Liu 0000-0002-6040-5291.

Author contributions: Shen YL and Zhang ZQ design the experiment; Zhu LJ drafted the work, Liu JH and Shen YL collected the data; Zhang ZQ and Zhu LJ analyzed and interpreted data, Liu JH and Shen YL wrote and revised the manuscript.

Institutional review board statement: This study was Approved by the Ethics Committee of Chengde Central Hospital.

Informed consent statement: Patients were not required to give informed consent to the study because the analysis used anonymous clinical data that were obtained after each patient agreed to treatment by written consent.

Conflict-of-interest statement: The authors declared that there is no conflict of interest between them.

Data sharing statement: No additional data are available.

Country/Territory of origin: China

Ya-Li Shen, Li-Juan Zhu, Department of Orthopedics, Chengde Central Hospital, Chengde 067000, Hebei Province, China

Zong-Qun Zhang, Department of Neurology, Chengde Central Hospital, Chengde 067000, Hebei Province, China

Jing-Hua Liu, Department of Nursing, Chengde Central Hospital, Chengde 067000, Hebei Province, China

Corresponding author: Jing-Hua Liu, MD, Nurse, Department of Nursing, Chengde Central Hospital, No. 11 Guangren Street, Shuangqiao District, Chengde 067000, Hebei Province, China. 5446468liu@163.com

Abstract

BACKGROUND

Stroke is the leading cause of adult lifelong disability worldwide. A stroke is an acute cerebrovascular disease with a variety of causes and corresponding clinical symptoms. Around 75% of surviving stroke patients experience impaired nerve function, and some suffer from traumatic fractures, which can lead to special care needs.

AIM

To determine the effect of timing theory continuous care, with resistance training, on the rehabilitation and mental health of caregivers and stroke patients with traumatic fractures.

METHODS

Between January 2017 to March 2021, we selected 100 hospital admissions with post-stroke hemiplegia complicated with a traumatic fracture. Two participant groups were created: (1) Control group: given resistance training; and (2) Observation group: given timing theory continuous care combined with resistance training. The degree of satisfaction and differences in bone and phosphorus metabolism indexes between the two groups were compared. The self-perceived burden scale (SPBS) and caregiver burden questionnaire were used to evaluate the psychological health of patients and caregivers. The Harris hip function score, ability of daily living (ADL) scale, and global quality of life

Specialty type: Nursing

Provenance and peer review: Unsolicited article; Externally peer reviewed.

Peer-review model: Single blind

Peer-review report's scientific quality classification

Grade A (Excellent): 0
Grade B (Very good): B, B
Grade C (Good): 0
Grade D (Fair): 0
Grade E (Poor): 0

Received: November 14, 2021
Peer-review started: November 14, 2021
First decision: December 9, 2021
Revised: December 19, 2021
Accepted: January 8, 2022
Article in press: January 8, 2022
Published online: February 16, 2022

P-Reviewer: Aferu T, Regasa T
S-Editor: Wang JL
L-Editor: A
P-Editor: Wang JL

questionnaire (GQOL-74) were used to evaluate hip function, ability of daily living, and quality of life.

RESULTS

Data were collected prior to and after intervention. Alkaline phosphatase (ALP), osteocalcin, and vitamin D3 in the observation group and control group increased after intervention ($P < 0.05$), and carboxy-terminal peptide of type I collagen β Special sequence (β-CTX) decreased ($P < 0.05$). ALP and osteocalcin in the observation group were higher than in the control group ($P < 0.05$). There was no significant difference in β-CTX and vitamin D3 between the two groups ($P > 0.05$). The SPBS score of the observation group was lower and the ADL score was higher than the control group. The burden score was lower and the Harris hip function and GQOL-74 scores were higher than that of the control group ($P < 0.05$). The observation group's satisfaction rating was 94.00%, which was higher than the rating from the control group ($P < 0.05$).

CONCLUSION

Timing theory continuous nursing with resistance training can reduce hip dysfunction in stroke patients with a traumatic fracture and enhance quality of life and mental health of patients and caregivers.

Key Words: Timing theory continuous nursing; Resistance training; Stroke; Traumatic fracture; Mental health

Core Tip: Through a retrospective study of patients with hemiplegia and traumatic fractures after stroke, we proved that the timing theory and continuous nursing combined with resistance training can reduce hip dysfunction in patients with traumatic fractures after stroke, and improve the quality of life of patients and nursing staff.

Citation: Shen YL, Zhang ZQ, Zhu LJ, Liu JH. Timing theory continuous nursing, resistance training: Rehabilitation and mental health of caregivers and stroke patients with traumatic fractures. *World J Clin Cases* 2022; 10(5): 1508-1516
URL: https://www.wjgnet.com/2307-8960/full/v10/i5/1508.htm
DOI: https://dx.doi.org/10.12998/wjcc.v10.i5.1508

INTRODUCTION

Patients with stroke that is complicated by a traumatic fracture after surgery often experience a partial or total loss of self-care ability, causing them to require assistance in their daily life and activities[1,2]. Currently, China's medical resources tend to be insufficient and unevenly available, and there is a lack of health human resources. Therefore, caregivers undertake a large part of patients' daily care[3-6]. Caring for patients who have experience both stroke and fracture require more difficult care. Patients often have limb dysfunction, and severe osteonecrosis can occur. Therefore, effective rehabilitation care can significantly improve the patient's prognosis. This study showed that caregivers are under considerable pressure, which is related in part to the health status of the patient. Adverse emotions, such as depression, seriously affect the recovery of patients, and the existence and influence of the burden of care is long-lasting[7]. However, there are very few reports about the continuation of nursing care in stroke patients with fractures.

This study analyzed the effect of timing theory continuous nursing combined with resistance training on the rehabilitation of stroke patients with traumatic fractures and the mental health of caregivers. The purpose is to provide guidance and a basis for clinical practice.

MATERIALS AND METHODS

Participant inclusion and exclusion criteria

Inclusion criteria: (1) Stroke was diagnosed by CT or MRI and stroke had not occurred previously; (2) ≥ 40 years old and ≤ 75 years old; (3) Disease duration was ≥ 6 mo; (4) Diagnosed with hemiplegia and muscle strength < grade 4; (5) Diagnosed with a femoral neck fracture who had undergone hip arthroplasty; and (6) Complete clinical data.

Exclusion criteria: (1) Cognitive dysfunction and comprehension disorder; (2) Complications with brainstem and cerebellar infarction; (3) Long-term use of hormones and other drugs that can affect calcium and phosphorus metabolism; (4) Malignant tumor; (5) Liver and kidney dysfunction; and (6) Illiteracy.

Baseline data

A total of 100 patients with post-stroke hemiplegia combined with trauma fractures that had been admitted to our hospital from January 2017 to March 2021 were divided into two groups according to the intervention plan. The comparison of general data between the two groups was not statistically significant ($P > 0.05$) (Table 1).

Method

The control group completed resistance training, and patients were guided on active ankle flexion training. Ankle flexion actions were performed with patients' maximum strength, and nursing staff held the lower third of their calf with the left hand to enable patients to perform the resistance training in the opposite direction with equal strength. In active ankle dorsiflexion exercises, patients performed active ankle dorsiflexion with their maximum strength, and nursing staff crossed their hands and placed them on the dorsum of patients' feet. The training was conducted with equal strength in the opposite direction. Each training session lasted for 5 s, 300 times each day, and patients were divided into 5 groups to gradually complete the exercise.

For the observation group, timing theory continuous care combined with resistance training was conducted and divided into 5 stages, which were determined based on literature reviews and expert consultation. The intervention content at each stage was based on the specific needs of the caregivers, and targeted intervention was implemented. A health education manual for patient caregivers was formulated according to the results of qualitative studies, from admission to 3 mo after discharge. Each manual included basic information about the disease, treatment methods, rehabilitation exercise guidance, daily nursing, discharge procedures, and post-operative complications and prevention. An intervention group was established to jointly control data collection, implementation of health education, follow-up after discharge, and the construction of a public platform. Duties were divided between team members depending on their personal expertise. They regularly shared reviewed articles and videos related to rehabilitation training, answered patients' questions, and encouraged the exchange of experiences among patients to form a mutual assistance team. Patients regularly attended group face-to-face lectures. Concurrently, those in the intervention group were asked to conduct three 30-minute lectures. Hand-in-hand demonstrations were performed. The resistance training method was the same as in the control group.

Standard for evaluation

The self-perceived burden scale (SPBS)[8] and caregiver burden questionnaire[9] were used to evaluate the mental health of the patients and caregivers, respectively. The Harris hip function score[10] (HHS), ability of daily living (ADL) scale, and comprehensive quality of life questionnaire (GQOL-74)[11] were used to evaluate the patients' hip function, ability of daily living and quality of life.

Detection method

Fasting venous blood (3 mL) was drawn and centrifugated at 2000 r/min for 30 min. The concentrations of ALP, osteocalcin, vitamin D3 and β-CTX were determined by Enzyme-linked immunosorbent assay using the Hitachi 7600i automatic biochemical analyzer provided by Nanjing Jianchi Biological Products Co. Ltd.

Statistical analysis

SPSS19.0 was used for data analysis and measurement data was expressed as mean ± SD, a *t*-test was applied for comparison, and an χ^2 test was used for comparison of

Table 1 Comparison of two groups of general data, *n* (%)

General information	Control group (*n* = 50)	Observation group (*n* = 50)
Gender		
Male	29 (58.00)	27 (54.00)
Female	21 (42.00)	23 (46.00)
Age (yr)	62.32 ± 8.92	61.69 ± 9.22
Course of stroke (yr)	2.12 ± 0.56	2.09 ± 0.54
Body mass index (kg/m^2)	22.85 ± 3.23	22.80 ± 3.37
Stroke type		
Cerebral infarction	32 (64.00)	28 (56.00)
Cerebral hemorrhage	18 (36.00)	22 (44.00)
Education		
Primary plus junior	9 (18.00)	10 (20.00)
Technical secondary school, high school and College	23 (46.00)	19 (38.00)
Bachelor degree or above	18 (36.00)	21 (42.00)
Caregiver patient relationship		
Children	17 (34.00)	15 (30.00)
Spouse	24 (48.00)	24 (48.00)
Other	9 (18.00)	11 (22.00)

enumeration data. $P < 0.05$ was statistically significant.

RESULTS

The comparison of bone phosphorus metabolism indexes between the two groups

Before the intervention, there was no statistically significant difference in the bone phosphorus metabolism indexes between the two groups ($P > 0.05$). After intervention, ALP, osteocalcin, and vitamin D3 increased in both the observation group and control group ($P < 0.05$), and carboxy-terminal peptide of type I collagen β Special sequence (β-CTX) decreased ($P < 0.05$) in both groups. ALP and osteocalcin in the observation group were higher than they were in the control group ($P < 0.05$) and there was no significant difference in β-CTX and vitamin D3 between the observation and control group ($P > 0.05$). Before intervention, there was no statistically significant difference in the SPBS scores between groups ($P > 0.05$). After intervention, the SPBS scores of patients in both groups decreased ($P < 0.05$), but they were lower for patients in the observation group than for those in the control group ($P < 0.05$). Before intervention, there was no statistically significant difference in ADL scores between groups ($P > 0.05$). After intervention, ADL scores of both groups increased ($P < 0.05$), and the ADL scores of the observation group were higher than those of the control group ($P < 0.05$) (Table 2).

Comparison of burden scores of caregivers between the two groups

Before intervention, there was no statistically significant difference between the two groups regarding the burden scores of caregivers ($P > 0.05$). After intervention, time-dependent, development-constrained, physiological, social, and emotional load and total score in the observation and control group decreased ($P < 0.05$) and the burden scores of caregivers in the observation group were lower than the control group ($P < 0.05$) (Table 3).

Comparison of HHS between the two groups

Before intervention, there was no statistically significant difference in the HHS ($P > 0.05$) between the two groups. After intervention, pain, function, gait, walking aid, walking distance, deformity, range of joint motion, and the total HHS between the two

Table 2 Comparison of bone phosphorus metabolism, self-perceived burden scale, ability of daily living in two groups (mean ± SD)

Group		Control group (*n* = 50)	Observation group (*n* = 50)
ALP (IU/L)	Before intervention	82.36 ± 12.05	83.01 ± 10.15
	After intervention	95.25 ± 13.65[a]	101.14 ± 14.58[a,c]
β-CTX (ng/mL)	Before intervention	182.02 ± 23.36	179.85 ± 25.11
	After intervention	164.02 ± 15.34[a]	159.03 ± 12.74[a]
Osteocalcin (μg/L)	Before intervention	9.56 ± 1.21	9.53 ± 1.26
	After intervention	12.36 ± 1.52[a]	13.02 ± 1.61[a,c]
Vitamin D3 (ng/L)	Before intervention	9.66 ± 2.85	9.71 ± 2.91
	After intervention	13.65 ± 3.12[a]	14.02 ± 3.05[a]
SPBS score	Before intervention	35.23 ± 4.56	34.95 ± 5.02
	After intervention	28.65 ± 3.36[a]	22.01 ± 3.77[a,c]
ADL score	Before intervention	31.25 ± 3.69	30.98 ± 4.05
	After intervention	65.74 ± 5.69[a]	79.14 ± 6.33[a,c]

[a]$P < 0.05$ *vs* pre-intervention.
[c]$P < 0.05$ *vs* the control group.
ALP: Alkaline phosphatase; β-CTX: carboxy-terminal peptide of type I collagen β Special sequence; SPBS: self-perceived burden scale; ADL: Ability of daily living.

Table 3 Comparison of burden scores of caregivers between the two groups (mean ± SD, min)

Parameter	Control group (*n* = 50)		Observation group (*n* = 50)	
	Before intervention	After intervention	Before intervention	After intervention
Time dependent load	16.23 ± 3.24	10.23 ± 2.12[a]	16.09 ± 3.36	7.82 ± 1.92[a,c]
Development-constrained load	14.25 ± 2.96	7.56 ± 2.01[a]	14.06 ± 3.11	5.23 ± 1.49[a,c]
Physiological load	10.26 ± 2.13	5.87 ± 1.41[a]	10.21 ± 2.06	3.96 ± 0.95[a,c]
Social load	6.21 ± 1.25	2.58 ± 0.45[a]	6.09 ± 1.33	1.51 ± 0.38[a,c]
Emotional load	4.02 ± 1.02	1.85 ± 0.23[a]	3.97 ± 0.91	1.02 ± 0.18[a,c]
Total score	50.56 ± 5.36	28.63 ± 4.02[a]	51.04 ± 4.98	19.85 ± 3.47[a,c]

[a]$P < 0.05$ *vs* pre-intervention.
[c]$P < 0.05$ *vs* the control group.

groups increased ($P < 0.05$) and were higher in the observation than in the control group ($P < 0.05$) as illustrated in Table 4.

Comparison of GQOL-74 scores between the two groups

Before intervention, there was no statistically significant difference in GQOL-74 scores between the two groups ($P > 0.05$). After intervention, GQOL-74 scores for physical and mental health, material life, and social function in the two groups increased ($P < 0.05$), and the GQOL-74 score in the observation group was higher than the control group ($P < 0.05$) (Table 5).

Comparison of satisfaction between the two groups

In the observation group, there were 30 very satisfied cases and 17 basically satisfied cases; the overall satisfaction rating was 94.00%, which was higher than the control group. The difference was statistically significant ($P < 0.05$) (Table 6).

Table 4 Comparison of Harris hip function scores between the two groups (mean ± SD, min)

Parameter	Control group (*n* = 50)		Observation group (*n* = 50)	
	Before intervention	After intervention	Before intervention	After intervention
Pain degree	8.56 ± 1.65	35.69 ± 4.12[a]	8.70 ± 1.71	40.52 ± 4.56[a,c]
Daily activity function	2.96 ± 0.52	10.12 ± 2.02[a]	3.05 ± 0.45	11.89 ± 2.14[a,c]
Gait	1.85 ± 0.63	7.12 ± 1.63[a]	1.87 ± 0.59	9.36 ± 1.45[a,c]
Walking aid	1.63 ± 0.36	5.24 ± 0.96[a]	1.68 ± 0.30	7.11 ± 1.41[a,c]
Walking distance	1.98 ± 0.37	6.36 ± 1.32[a]	1.95 ± 0.31	8.05 ± 1.17[a,c]
Deformity	2.03 ± 0.41	3.12 ± 0.29[a]	2.06 ± 0.35	3.56 ± 0.31[a,c]
Joint range of motion	1.98 ± 0.29	3.22 ± 0.37[a]	2.03 ± 0.26	3.69 ± 0.41[a,c]
Total score	20.36 ± 2.12	70.52 ± 6.02[a]	20.13 ± 2.23	83.12 ± 7.02[a,c]

[a]$P < 0.05$ *vs* pre-intervention.
[c]$P < 0.05$ *vs* the control group.

Table 5 Comparison of global quality of life questionnaire scores between the two groups (mean ± SD, min)

Group		Control group (*n* = 50)	Observation group (*n* = 50)
Physical health	Before intervention	51.02 ± 9.63	50.29 ± 10.13
	After intervention	75.69 ± 11.05[a]	82.34 ± 10.53[a,c]
Mental health	Before intervention	68.36 ± 10.26	66.95 ± 12.97
	After intervention	81.36 ± 8.66[a]	87.96 ± 9.43[a,c]
Material life	Before intervention	61.62 ± 8.63	62.05 ± 9.34
	After intervention	66.36 ± 7.44[a]	73.05 ± 8.05[a,c]
Social function	Before intervention	59.02 ± 7.14	58.36 ± 7.74
	After intervention	67.36 ± 5.98[a]	75.45 ± 8.06[a,c]

[a]$P < 0.05$ *vs* pre-intervention.
[c]$P < 0.05$ *vs* the control group.

Table 6 Comparison of satisfaction between the two groups, *n* (%)

Group	Number of cases	Very satisfied	Basically satisfied	Dissatisfied	Satisfaction
Control group	50	21 (42.00)	18 (36.00)	11 (22.00)	39 (78.00)
Observation group	50	30 (60.00)	17 (34.00)	3 (6.00)	47 (94.00)[a]

[a]$P < 0.05$ *vs* the control group.

DISCUSSION

Timing theory advocates that during hospitalization, nurses provide appropriate interventions for caregivers by identifying the stage of the patient and strengthening the caregivers' performance through repeated guidance. The goal is to improve caregivers' ability to provide care, the quality of care, and the effectiveness of patients' rehabilitation[9]. A continuous nursing care plan, guided by post-discharge timing theory, can reduce the pressure on caregivers' through the application of a variety of intervention tools and measures, ensuring the effectiveness of post-discharge patient rehabilitation[12]. The continuous nursing model based on timing theory and combined with resistance training was used for patients with stroke that had been complicated with a traumatic fracture and incorporated both patients and caregivers.

Caregivers have multidimensional needs during the nursing period, and the primary needs changed over time depending on the patient's stage of disability. Therefore, to better meet the needs of caregivers, nursing staff should be cognizant of the characteristics of caregivers' needs when formulating health education content and nursing intervention measures to achieve comprehensive and multi-dimensional support. Staff should also be aware of changes in caregivers' needs so they can provide timely and corresponding needs support. After discharge, through regular telephone follow-up, WeChat groups, and public account information pushes, caregivers and patients can continue to acquire health knowledge. This can assist the caregivers in regularly evaluating the patient's disease status and adjusting their individualized care plan accordingly. This can help them to effectively manage a variety of problems in the process of rehabilitation and can encourage multi-directional and multi-channel access to health resources.

In this study, the SPBS and load scores of both patients and caregivers in the observation group was lower after intervention, suggesting that the use of timing theory continuous nursing, combined with resistance training, can reduce patients' sense of self-burden as well as caregivers' sense of load in patients with stroke combined with a traumatic fracture. Continuous nursing based on timing theory can effectively reduce the caregivers' psychological pressure and improve their caring ability[13-17]. Caregivers can share their caring experiences and emotional communication, thereby effectively relieving the psychological pressure. The study also found that the ADL score of the observation group after intervention was higher than that of the control group, and the Harris hip function score of the observation group after intervention was higher than that of the control group. By improving the hip joint function score, the quality of daily life is improved.

According to the study, after intervention, ALP, osteocalcin, and ADL scores in the observation group were higher than those in the control group, suggesting that timing theory continuous nursing, combined with resistance training, can be conducive to bone phosphorus metabolism recovery and improvement. Both ALP and osteocalcin are important indicators in the process of bone metabolism, so active rehabilitation care is of great significance for regulating human bone metabolism. The quality of daily life in patients with stroke combined with a traumatic fracture. The GQOL-74 and HHS in the observation group, after intervention, were higher than those in the control group, indicating that the application of this model can enable patients and caregivers to adapt to the new role of caring more quickly for patients and rearranging their work and life. Over time, the caregivers can slowly accept the reality of the disease, adapt to the reality of caregiving, and accumulate further care experience, while the patients' own functional defects and their self-care ability can gradually improve[18].

Timing theory has been applied in a variety of disease groups abroad, but it is rarely applied in stroke patients with a traumatic fracture in China[19,20]. In this study, the specific needs of patients at different stages and the timing to meet these needs were analyzed. An investigation was conducted according to patients' needs. Based on this, intervention measures conforming to the characteristics of caregivers' needs were formulated and implemented, and positive intervention effects were achieved. However, there was a short follow-up time in this study, so the long-term effects cannot be identified. The sample size and sampling range were small. Future studies should increase the sample size and conduct longer continuous intervention studies to understand their long-term effects.

CONCLUSION

In conclusion, timing theory continuous nursing combined with resistance training can reduce the hip function of stroke patients with a traumatic fracture, improve their ability of daily life and quality of life, and promote the mental health of both patients and their caregivers.

ARTICLE HIGHLIGHTS

Research background

Stroke is the main cause of lifelong disability in adults worldwide. It refers to acute cerebrovascular diseases with multiple etiologies and corresponding clinical

symptoms. Approximately 75% of surviving stroke patients have neurological impairment. Because of this, some patients are prone to traumatic fractures and require special care.

Research motivation

Provide new methods and ideas for the nursing of patients with traumatic fracture and stroke.

Research objectives

The authors aimed to determine the effect of timing theory continuous care, with resistance training, on rehabilitation and mental health of caregivers and stroke patients with traumatic fractures.

Research methods

We conducted a study on 100 patients with traumatic fractures who came to our hospital from January 2017 to March 2021 due to post-stroke hemiplegia.

Research results

After the intervention, compared with before the intervention, the observation group and the control group increased alkaline phosphatase (ALP), osteocalcin, and vitamin D3, and type I collagen β-carboxy terminal peptide (β-CTX) decreased. ALP and osteocalcin in the observation group were higher than those in the control group. There was no statistically significant difference between the two groups of β-CTX and vitamin D3. The SPBS score of the observation group was lower than that of the control group, and the ability of daily living score of the observation group was higher than that of the control group. The burden score was lower than that of the control group, Harris hip joint function and global quality of life questionnaire scores were higher than that of the control group, and the satisfaction degree was higher than that of the control group.

Research conclusions

Timing theory continuous nursing with resistance training can reduce hip dysfunction of stroke patients with a traumatic fracture and enhance quality of life and mental health of patients and caregivers.

Research perspectives

In the subsequent treatment, it can improve the ability of daily living and quality of life of patients with traumatic fracture of stroke, and promote the mental health of patients and their caregivers.

REFERENCES

1 **Cao Y**, DiPiro N, Krause JS. Association of Secondary Health Conditions With Future Chronic Health Conditions Among Persons With Traumatic Spinal Cord Injury. *Top Spinal Cord Inj Rehabil* 2020; **26**: 283-289 [PMID: 33536734 DOI: 10.46292/sci20-00020]

2 **Hoffman H**, Bunch KM, Protas M, Chin LS. Risk Factors and Outcomes Associated with Blunt Cerebrovascular Injury in Patients with Mild or Moderate Traumatic Brain Injury. *Ann Vasc Surg* 2021; **71**: 157-166 [PMID: 32768544 DOI: 10.1016/j.avsg.2020.07.031]

3 **Macovei L**, Magopet R, Tanasa A, Raileanu C, Prisacariu C, Presura MR, Balasanian MO. Coronary artery bypass graft surgery versus percutaneous coronary intervention in unprotected left main coronary artery disease: A systematic review. *Rev Cardiovasc Med* 2020; **21**: 65-73 [PMID: 32259905 DOI: 10.31083/j.rcm.2020.01.590]

4 **Paterno R**, Folweiler KA, Cohen AS. Pathophysiology and Treatment of Memory Dysfunction After Traumatic Brain Injury. *Curr Neurol Neurosci Rep* 2017; **17**: 52 [PMID: 28500417 DOI: 10.1007/s11910-017-0762-x]

5 **Bishop NA**, Lu T, Yankner BA. Neural mechanisms of ageing and cognitive decline. *Nature* 2010; **464**: 529-535 [PMID: 20336135 DOI: 10.1038/nature08983]

6 **Braun T**, Marks D. Comment on: "Evaluating the effectiveness of aquatic therapy on mobility, balance, and level of functional independence in stroke rehabilitation: a systematic review and meta-analysis". *Clin Rehabil* 2020; **34**: 845-847 [PMID: 32380862 DOI: 10.1177/0269215520919057]

7 **Khodadadi M**, Shayanfar H, Maghooli K, Hooshang Mazinan A. Fuzzy cognitive map based approach for determining the risk of ischemic stroke. *IET Syst Biol* 2019; **13**: 297-304 [PMID: 31778126 DOI: 10.1049/iet-syb.2018.5128]

8 **McFarlane TD**, Love J, Hanley S, Dixon BE, Hammond FM. Increased Risk of Stroke Among

Young Adults With Serious Traumatic Brain Injury. *J Head Trauma Rehabil* 2020; **35**: E310-E319 [PMID: 31834059 DOI: 10.1097/HTR.0000000000000539]

9 **Davies L**, Delcourt C. Current approach to acute stroke management. *Intern Med J* 2021; **51**: 481-487 [PMID: 33890368 DOI: 10.1111/imj.15273]

10 **Giubertoni A**, Boggio E, Ubertini E, Zanaboni J, Calcaterra E, Degiovanni A, Bellacosa I, Marino PN; from the Novara Atrial Fibrillation (NAIF) Study Group. Atrial conduit function quantitation precardioversion predicts early arrhythmia recurrence in persistent atrial fibrillation patients. *J Cardiovasc Med (Hagerstown)* 2019; **20**: 169-179 [PMID: 30829875 DOI: 10.2459/JCM.0000000000000756]

11 **Vieira CS**, de Nadai MN, de Melo Pereira do Carmo LS, Braga GC, Infante BF, Stifani BM, Ferriani RA, Quintana SM. Timing of postpartum etonogestrel-releasing implant insertion and bleeding patterns, weight change, 12-month continuation and satisfaction rates: a randomized controlled trial. *Contraception* 2019; **100**: 258-263 [PMID: 31145885 DOI: 10.1016/j.contraception.2019.05.007]

12 **Lee CK**, Gong J. Fokker-Planck equation with arbitrary dc and ac fields: continued fraction method. *Phys Rev E Stat Nonlin Soft Matter Phys* 2011; **84**: 011104 [PMID: 21867110 DOI: 10.1103/PhysRevE.84.011104]

13 **Wang XQ**, Bo QY, Liu Y, Geng R, Zhang B, Wang JY. [Study on the relationship between occupational stress and metabolic syndrome in operating room nursing staff of a third-class A hospital]. *Zhonghua Lao Dong Wei Sheng Zhi Ye Bing Za Zhi* 2020; **38**: 839-842 [PMID: 33287478 DOI: 10.3760/cma.j.cn121094-20191015-00496]

14 **Wollesen B**, Hagemann D, Pabst K, Schlüter R, Bischoff LL, Otto AK, Hold C, Fenger A. Identifying Individual Stressors in Geriatric Nursing Staff-A Cross-Sectional Study. *Int J Environ Res Public Health* 2019; **16** [PMID: 31557867 DOI: 10.3390/ijerph16193587]

15 **Conradie M**, Erwee D, Serfontein I, Visser M, Calitz FJ, Joubert G. A profile of perceived stress factors among nursing staff working with intellectually disabled in-patients at the Free State Psychiatric Complex, South Africa. *Curationis* 2017; **40**: e1-e8 [PMID: 28397510 DOI: 10.4102/curationis.v40i1.1578]

16 **Tran DT**, Johnson M, Fernandez R, Jones S. A shared care model vs. a patient allocation model of nursing care delivery: comparing nursing staff satisfaction and stress outcomes. *Int J Nurs Pract* 2010; **16**: 148-158 [PMID: 20487060 DOI: 10.1111/j.1440-172X.2010.01823.x]

17 **Glozier N**, Hough C, Henderson M, Holland-Elliott K. Attitudes of nursing staff towards co-workers returning from psychiatric and physical illnesses. *Int J Soc Psychiatry* 2006; **52**: 525-534 [PMID: 17294598 DOI: 10.1177/0020764006066843]

18 **Salášek M**, Šlechtová J, Pavelk T. [Heparin-Induced Thrombocytopenia after Total Knee Replacement]. *Acta Chir Orthop Traumatol Cech* 2020; **87**: 129-133 [PMID: 32396515]

19 **Sonaglioni A**, Lonati C, Lombardo M, Rigamonti E, Binda G, Vincenti A, Nicolosi GL, Bianchi S, Harari S, Anzà C. Incremental prognostic value of global left atrial peak strain in women with new-onset gestational hypertension. *J Hypertens* 2019; **37**: 1668-1675 [PMID: 30950977 DOI: 10.1097/HJH.0000000000002086]

20 **Nazzari H**, Chue CD, Toma M. Mechanical circulatory support in the heart failure population. *Curr Opin Cardiol* 2019; **34**: 194-201 [PMID: 30633077 DOI: 10.1097/HCO.0000000000000600]

World Journal of Clinical Cases

Submit a Manuscript: https://www.f6publishing.com

World J Clin Cases 2022 February 16; 10(5): 1517-1526

DOI: 10.12998/wjcc.v10.i5.1517

ISSN 2307-8960 (online)

ORIGINAL ARTICLE

Retrospective Study

Effect of precise nursing service mode on postoperative urinary incontinence prevention in patients with prostate disease

Xi-Chun Zheng, Ting-Ting Luo, Dan-Dan Cao, Wen-Zhi Cai

ORCID number: Xi-Chun Zheng 0000-0003-2044-0364; Ting-Ting Luo 0000-0003-4735-1767; Dan-Dan Cao 0000-0003-3773-2339; Wen-Zhi Cai 0000-0002-2354-5199.

Author contributions: Zheng XC and Cai WZ designed this retrospective study, Zheng XC and Luo TT wrote this paper; Zheng XC, Luo TT, Cao DD and Cai WZ were responsible for sorting the data.

Institutional review board statement: This study was reviewed and approved by the Ethics Committee Shenzhen Hospital of Southern Medical University (Approval No. NYSZYYEC20210005).

Conflict-of-interest statement: Nothing to disclose.

Data sharing statement: No additional data are available.

Supported by Nursing Scientific Research Project Fund of Nursing Society of Guangdong Province, No. gdhlxueh2019zx218; Shenzhen Bao'an District Science and Technology Plan, No. 20200515053525001.

Country/Territory of origin: China

Specialty type: Urology and

Xi-Chun Zheng, Ting-Ting Luo, Dan-Dan Cao, Department of Urology, Shenzhen Hospital of Southern Medical University, Shenzhen 518000, Guangdong Province, China

Wen-Zhi Cai, Nursing Department, Southern Medical University, Shenzhen 518000, Guangdong Province, China

Corresponding author: Wen-Zhi Cai, PhD, Chief Nurse, Nursing Department, Southern Medical University, No. 1333 Xinhu Road, Bao'an District, Shenzhen 518000, Guangdong Province, China. caiwzh@smu.edu.cn

Abstract

BACKGROUND

Patients with benign prostatic disease often experience detrusor morphological changes and dysfunction. In severe cases, it leads to bladder detrusor dysfunction, resulting in dysuria, frequent urination, urgent urination, incomplete urination, and other symptoms including renal function injury. An operation to restore normal urination function and to control postoperative complications, as far as possible, is the most common method for benign prostatic disease.

AIM

To observe the effect of precise nursing service mode on postoperative urinary incontinence prevention in patients with prostate disease.

METHODS

In total, 130 patients diagnosed with benign prostatic disease, from January 2018 to June 2021, in our hospital, were selected and divided into observation and control groups according to their treatment options. Sixty-five cases in the control group were given routine nursing mode intervention and 65 cases in the observation group received precise nursing service mode intervention. The intervention with the observation group included psychological counseling about negative emotions, pelvic floor exercises, and post-hospital discharge care. The complications of the two groups were counted, and the general postoperative conditions of the two groups were recorded. The urinary flow dynamics indexes of the two groups were detected, and differences in clinical international prostate system score (IPSS) and urinary incontinence quality of life questionnaire (I-QOL) scores were evaluated.

RESULTS

Nephrology

Provenance and peer review: Unsolicited article; Externally peer reviewed.

Peer-review model: Single blind

Peer-review report's scientific quality classification

Grade A (Excellent): 0
Grade B (Very good): B
Grade C (Good): C
Grade D (Fair): 0
Grade E (Poor): 0

Received: November 14, 2021
Peer-review started: November 14, 2021
First decision: December 9, 2021
Revised: December 26, 2021
Accepted: January 8, 2022
Article in press: January 8, 2022
Published online: February 16, 2022

P-Reviewer: Agarwal N, Lecouvet FE
S-Editor: Wang JL
L-Editor: A
P-Editor: Wang JL

Postoperative exhaust time (18.65 ± 3.23 h and 24.63 ± 4.51 h), the time of indwelling catheter (4.85 ± 1.08 d and 5.63 ± 1.24 d), and hospitalization time (8.78 ± 2.03 d and 10.23 ± 2.28 d) in the observation group were lower than in the control group. The difference was statistically significant ($P < 0.05$). After the operation, the maximum urinary flow rate (Qmax) increased ($P < 0.05$), the residual urine volume (RUV) decreased ($P < 0.05$), and the maximum closed urethral pressure (MUCP) was not statistically significant ($P > 0.05$) compared to pre-operation. The Qmax of the observation group was higher than that of the control group, while the RUV was lower than that of the control group. There was no significant difference in MUCP between the observation and control groups ($P > 0.05$). The I-QOL score of the two groups improved ($P < 0.05$), and the IPSS decreased ($P < 0.05$). After the operation, the I-QOL score of the observation group was higher than that of the control group, and the IPSS was lower than that of the control group ($P < 0.05$). There were no significant differences in the incidence of urethral injury (1.54% and 3.08%), bladder spasm (0.00% and 1.54%), and secondary bleeding (1.54% and 4.62) between the observation and control groups ($P > 0.05$).

CONCLUSION

The precise nursing service mode can reduce the incidence of postoperative urinary incontinence in patients with prostate disease, thus improving postoperative urodynamics and rehabilitation, and quality of life.

Key Words: Precise nursing service mode; Prostate disease; Urinary incontinence; Urodynamics; Life quality

Core Tip: The precise nursing service mode can reduce the incidence of postoperative urinary incontinence in patients with prostate disease, thus improving postoperative urodynamics and rehabilitation, as well as patients' quality of life.

Citation: Zheng XC, Luo TT, Cao DD, Cai WZ. Effect of precise nursing service mode on postoperative urinary incontinence prevention in patients with prostate disease. *World J Clin Cases* 2022; 10(5): 1517-1526
URL: https://www.wjgnet.com/2307-8960/full/v10/i5/1517.htm
DOI: https://dx.doi.org/10.12998/wjcc.v10.i5.1517

INTRODUCTION

Urinary incontinence is one of the most common postoperative complications in patients with benign prostate disease who fail to respond to conservative treatment. Urinary incontinence can not only cause local skin eczema, erosion, incontinence dermatitis, and other complications but also exert psychological pressure on patients, seriously affecting their physical and mental health after surgery[1,2]. Previous studies have found that postoperative local edema, a long catheter indwelling time, hyperplastic gland compression, hemostatic balloon placement, and psychological factors were related to urinary incontinence. The postoperative nursing quality has greatly influenced the care for urinary incontinence; however, routine nursing mode focuses on basic nursing. Therefore, targeted interventions for urinary incontinence are often inadequate[3].

Precise nursing service mode is a novel nursing mode, providing care based on patients' needs rather than care being imposed on them by the nursing staff. Hence, this intervention administers the right care to the right patient at the right time. Comprehensive precision nursing intervention helps to improve patients' cognition, compliance, and satisfaction while reducing complications. It has been applied in many areas such as in intensive care units, surgery, orthopedics, gynecology, and pediatrics, and has achieved beneficial results[4,5]. Neurogenic bladder, caused by dysuria, has no completely effective treatment in China or abroad. Urinary

incontinence can be alleviated by using a bladder therapy instrument after the prostate operation. Our study aimed to observe the effect of precise nursing service mode on the prevention of postoperative urinary incontinence in patients with prostate disease.

MATERIALS AND METHODS

Case data

A total of 130 patients, on average (62.89 ± 11.71) years old, diagnosed with benign prostatic disease from January 2018 to June 2021, in our hospital, were selected and divided into observation and control groups according to their treatment options. Sixty-five cases in the control group were given routine nursing mode intervention, and 65 cases in the observation group received precise nursing service mode intervention. There was no statistical significance of the baseline data between the two groups ($P > 0.05$). Written informed consent was given by patients in this study.

Selection of cases

Inclusion criteria: (1) Preoperative biopsy was performed on patients with prostate specific antigen < 4 ng/mL, which met the criteria of benign prostatic hyperplasia in The Guidelines for Diagnosis and Treatment of Diseases of Urology in China. Cystoscopy, urodynamic examination, and digital rectal examinations were performed to confirm the diagnosis; (2) Patients were ≥ 50 years old, ≤ 85 years old; (3) Electro prostatectomy was performed after invalid conservative observation and drug treatment; (4) Neurogenic bladder was excluded; (5) Patients had no history of lower urinary tract trauma; and (6) They understood the purpose and methods of this study, voluntarily participated in it, and signed the informed consent.

Exclusion criteria: (1) Obstruction of urination due to urinary calculi, urethral stricture, and other reasons; (2) skin disease or severe skin damage in the perineal region; (3) psychological urinary incontinence or previous urethral trauma; (4) mental abnormalities; and (5) serious heart, liver, kidney, and other organ diseases.

Methods

The control was given routine nursing mode intervention, including vital signs' monitoring, proper catheter fixation and unobstructed, continuous bladder irrigation, dietary guidance, psychological counseling, prevention of falls and pressure sores, and analgesic drugs as directed by doctors.

The observation group was given precise nursing service mode intervention. Moreover, psychological intervention occurred first to understand the factors causing patients' negative emotions, to correct patients' wrong ideas through health education, to ensure patients realize the impact of negative emotions on postoperative urinary incontinence, and to help patients establish recovery confidence.

Stepped pelvic floor functional exercise was adopted, and patients were guided to engage in pelvic floor muscle rehabilitation training three days before the operation. Training method: the nursing staff wore disposable gloves; inserted the right index finger into the patient's anus after smearing paraffin oil and asked the patient to relax the abdominal and thigh muscles, contract the anus and urethra, relax for 5–10 s after holding for more than 3 s, and gradually extended the contraction time for 5–10 s, depending on the feeling of tightness of the anus by the pressure on the fingers. The training time was 20 min/*t*, 3 times/d. The training was suspended from the day of the operation to 2d after the operation, and the tube training was started on the third day after operation. The duration and intensity of the exercise was gradually increased.

Patients were guided to conduct bladder function training. When the urinary catheter was just removed, the nurse responsible told the patients to urinate again immediately after urination, to avoid holding urine, to urinate regularly within a short time, and then gradually extend the interval. Once urination had occurred, they did not urinate again immediately, but maintained a relaxed and pleasant mood to relax the bladder and inhibit urination.

Intermittent micturition training was conducted to stop or slow down the speed of urinary flow during micturition. Attention was paid to contract the pelvic floor muscles to prevent urine outflow before urinary incontinence caused by coughing, laughing and other actions. For patients with urinary incontinence, clothes were changed in time and perineum area cleaned, to prevent urine odor and skin irritation.

The patient was guided to use the Lihe household low-frequency electronic pulse bladder instrument correctly after discharge from the hospital. Precision nursing permeates all stages of preoperative nursing, postoperative nursing, and continuous nursing to establish an out of hospital follow-up platform for specific diseases and to build a patient discharge system on effective supervision and communication.

Observation indexes and test method

The postoperative exhaust time, time of indwelling catheter, hospitalization time, urethral orifice injury, bladder spasm, secondary hemorrhage, and urinary incontinence were recorded.

Clinical international prostate system score (IPSS) and urinary incontinence quality of life questionnaire (I-QOL) scores were used to evaluate the symptoms and life quality[6,7]. There are 7 IPSSs, and the individual score is 0–5. The lower the score, the lighter the symptoms. There are 22 questions in the I-QOL score, with a total score of 0–100. The higher the score, the better the quality of life.

Statistical analysis

SPSS 19.0 was used for data analysis; measurement data were expressed by mean ± SD; *t*-test was used for comparative application; enumeration data were expressed by the number of cases (percentage); χ^2 test was used for comparative application. The inspection level was 0.05.

RESULTS

The comparison of baseline data between the two groups

There were no significant differences in age, course of the disease, IPSS, prostate volume, rectal digital examination, and basic diseases between the two groups ($P > 0.05$), as indicated in Table 1.

The comparison of postoperative outcomes between the two groups

Postoperative exhaust time, time of indwelling catheter, and hospitalization time for the observation group were lower than for the control group. The difference was significant ($P < 0.05$) (Table 2).

Comparisons of urinary flow mechanics index, IPSS, and I-QOL scores of the two groups

The urinary flow mechanics index before the operation was consistent ($P > 0.05$), After the operation, the maximum urinary flow rate (Qmax) increased ($P < 0.05$), the residual urine volume (RUV) decreased ($P < 0.05$), and the maximum closed urethral pressure (MUCP) was not statistically significant ($P > 0.05$) compared with during pre-operation. The Qmax of the observation group was higher than that of the control group, while the RUV was lower than that of the control group. There were no significant differences in MUCP between the observation and control groups ($P > 0.05$). Preoperative IPSS and I-QOL scores were similar ($P > 0.05$). After the operation, the I-QOL score of the two groups improved ($P < 0.05$), and the IPSS decreased ($P < 0.05$). The I-QOL score of the observation group was higher than that of the control group, and the IPSS was lower than that of the control group ($P < 0.05$), as demonstrated in Table 3.

Comparison of complications between two groups

There were no significant differences in urethral orifice injury, bladder spasm, and secondary bleeding between the two groups ($P > 0.05$) (Table 4).

Comparison of urinary incontinence between the two groups

In the observation group, there were 14 cases of temporary urinary incontinence on the day the catheter was introduced; the incidence rate was 21.54%; mainly mild. Among the 14 cases of urinary incontinence in the observation group, 9 cases returned to normal within 1 wk, and 5 cases returned to normal within 1 to 4 wk. In the control group, 25 cases of temporary urinary incontinence occurred on the same day; the incidence rate was 38.46%; mainly moderate. Among the 25 cases of urinary incontinence in the control group, 13 cases returned to normal within 1 wk, and 8 cases returned to normal within 1 to 4 wk. The incidence of urinary incontinence in the observation group was lower than that in the control group, and there was no

Table 1 Comparison of baseline data between the two groups, *n* (%)

Parameters	Control group (*n* = 65)	Observation group (*n* = 65)	χ^2/t	*P* value
Age (yr)	63.12 ± 12.05	62.85 ± 11.54	0.130	0.896
Course of disease (yr)	12.24 ± 3.02	12.31 ± 2.84	0.136	0.892
IPSS score	30.56 ± 4.63	31.02 ± 4.81	0.555	0.580
Prostate volume (mL)	45.96 ± 7.86	46.21 ± 7.37	0.187	0.852
Rectal digital examination				
II degree	36 (55.38)	41 (63.08)	0.796	0.372
III degree	29 (44.62)	24 (36.92)		
Basic diseases				
Bladder stones	24 (36.92)	19 (29.23)	0.869	0.351
Hypertension	36 (55.38)	39 (60.00)	0.284	0.594
Diabetes	18 (27.69)	20 (30.77)	0.149	0.700
Coronary heart disease	27 (41.54)	22 (33.85)	0.819	0.366
Chronic obstructive pulmonary disease	25 (38.46)	23 (35.38)	0.132	0.716

IPSS: International prostate system score.

Table 2 Comparison of postoperative outcomes between the two groups (mean ± SD)

Group	Number of cases	Postoperative exhaust time (h)	Time of indwelling catheter (d)	Hospitalization time (d)
Control group	65	24.63 ± 4.51	5.63 ± 1.24	10.23 ± 2.28
Observation Group	65	18.65 ± 3.23	4.85 ± 1.08	8.78 ± 2.03
t		8.691	3.824	3.829
P value		0.000	0.000	0.000

significant difference in the duration of urinary incontinence between the observation and control groups ($P > 0.05$) as indicated in Table 5.

DISCUSSION

Postoperative urinary incontinence is the common complication affecting the quality of life, with a harmful influence on patients' bodies and minds[8,9]. The main treatment for postoperative urinary incontinence is prevention, and nursing intervention plays a vital role in this process[10]. The Lihe household low-frequency electronic pulse bladder instrument provides a type of intervention. It is a non-invasive, painless physical therapeutic apparatus, multidimensional bladder stimulus with a low frequency, which can help patients to improve the bladder smooth muscle, pelvic floor muscles, and urethral sphincter function, to solve the increased residual urine, urinary retention, and urination dysfunction. The instrument can be used in professional medical institutions and at home.

In the postoperative care of patients with prostate disease, it is necessary to consider patients as the center and to implement the targeted nursing plan based on fully evaluating the patient's condition, which is the essence of the precision nursing model [11]. Since its advent, the precise nursing service mode has played a key role in various clinical fields. The precision nursing emergency management system in emergency rescue, and found that it could improve the emergency response rate and overall standards of nursing staff and ensure the safety of patients' lives[12,13]. Moreover, Spiers *et al*[14] applied the improved scheme based on precision nursing to the care of patients with the replantation of an amputated finger, and found that it could effectively reduce the risks of complications such as vascular crisis, postoperative infection, constipation, and could help relieve the pain.

Table 3 Comparison of urinary flow mechanics index, international prostate system score and incontinence quality of life questionnaire score in the two groups (mean ± SD)

Group		Control group (*n* = 65)	Observation group (*n* = 65)	*t*	*P* value
MUCP (cmH2O)	Preoperative	24.12 ± 4.33	24.05 ± 4.56	0.09	0.929
	Postoperative	25.69 ± 4.13	25.47 ± 4.32	0.297	0.767
RUV (mL)	Preoperative	74.21 ± 15.66	73.25 ± 16.74	0.338	0.736
	Postoperative	16.23 ± 3.21[a]	13.14 ± 2.57[a]	6.058	0
Qmax (mL/s)	Preoperative	4.26 ± 1.23	4.31 ± 1.27	0.228	0.82
	Postoperative	11.45 ± 2.03[a]	13.65 ± 2.41[a]	5.629	0
IPSS score	Preoperative	30.56 ± 4.63	31.02 ± 4.81	0.555	0.58
	Postoperative	8.96 ± 1.56[a]	5.74 ± 1.04[a]	13.846	0
I-QOL score	Preoperative	40.43 ± 4.52	40.68 ± 5.06	0.297	0.767
	Postoperative	48.74 ± 3.62[a]	51.14 ± 3.05[a]	4.088	0

[a]*P* < 0.05 *vs* the pre-operation of this group.

MUCP: Maximum closed urethral pressure; RUV: Residual urine volume; Qmax: Maximum urinary flow rate; IPSS: International prostate system score; I-QOL: Incontinence quality of life questionnaire score.

Table 4 Comparison of complications between two groups, *n* (%)

Group	Number of cases	Urethral orifice injury	Bladder spasm	Secondary bleeding
Control group	65	2 (3.08)	1 (1.54)	3 (4.62)
Observation group	65	1 (1.54)	0 (0.00)	1 (1.54)
χ^2		0.341	1.008	1.032
P value		0.559	0.315	0.310

Table 5 Comparison of urinary incontinence between two groups, *n* (%)

Group	Number of cases	Urinary incontinence				Duration of urinary incontinence		
		Mild	Moderate	Severe	Total	< 1 wk	1 wk-4 wk	> 4 wk
Control group	65	10 (40.00)	11 (44.00)	4 (16.00)	25 (38.46)	13 (52.00)	8 (32.00)	4 (16.00)
Observation group	65	7 (50.00)	5 (35.71)	2 (14.29)	14 (21.54)	9 (64.29)	5 (35.71)	0 (0.00)
χ^2					4.322	2.517		
P value					0.035	0.284		

In our study, precise nursing service mode was applied to prevent postoperative urinary incontinence in patients with prostate disease, and it was found to shorten postoperative exhaust time, the time of indwelling catheter and hospitalization time, and the incidence of urinary incontinence. However, there were no significant differences in urethral orifice injury, bladder spasm, and secondary bleeding between the two groups. This is because the psychological intervention was given first under the precision nursing service mode, which could have helped patients to reduce psychological pressure and to reduce the adverse psychological effects on urinary incontinence.

Before and after the operation, patients were guided to implement intervention measures such as pelvic floor muscle rehabilitation training to improve the strength of pelvic floor muscle groups and to reduce urinary incontinence caused by pelvic floor muscle relaxation. They were guided to increase urinary continence with intermittent training. Furthermore, patients were educated on how to use Lihe household low-frequency electronic pulse bladder instrument correctly after discharge. This was to help them improve urinary continence ability, to promote local blood circulation,

accelerate the damage of nerve repair which can help patients recover automatic micturition function as soon as possible, and accelerate the removal of catheters. The removal of the urethra is more conducive to the early cessation of the patient's rehabilitation, which can promote the faster recovery of intestinal function[15].

The urinary flow mechanics index is important to evaluate the effects of the operation and assess patients' urination function. In patients with prostate disease, the abnormality of the urinary flow mechanics index is related to not only the prostate disease but also the surgical trauma[16,17]. In our study, the urination function was evaluated through Qmax, RUV, and MUCP testing in the two groups. IPSSs were used to evaluate the prostate symptoms, and I-QOL scores were used to evaluate the quality of life. We found that the precision nursing service model could improve postoperative urinary flow mechanics, promote rehabilitation, and improve the quality of life of patients. This is because this nursing model can guide patients to avoid the occurrence of urinary incontinence Furthermore, it provides timely treatment after the occurrence of urinary incontinence, thus relieving the pain of patients and allowing their quality of life to improve[18]. The early removal of the catheter can not only reduce the triggering factors of urinary incontinence but also help patients to implement urination training and improve the urinary flow mechanics index. Operation on the prostate may affect the sexual function of patients, which is related to the damage of the penile anatomy, penile blood vessels, and the erectile nerve[19,20].

Nursing care for patients with prostate disease who have undergone surgery has a direct and important impact on patients' rehabilitation. However, existing conventional nursing interventions fail to achieve satisfactory results and have no significant effect on the prevention of patient complications. Precision nursing through psychological intervention, stepped pelvic floor exercises, and home training after discharge facilitates recovery and yields satisfactory results. Compared with conventional care, precision care encompasses all stages of preoperative, postoperative, and continuous care. Moreover, it is effective in preventing urinary incontinence. However, the findings are limited by the study sample because only patients who underwent prostatectomy for the treatment of benign prostatic hyperplasia were included. Patients with urinary dysfunction caused by urinary calculi, urethral stricture, and other reasons; skin diseases or severe skin damage in the perineum; psychological urinary incontinence; a previous history of urethral trauma; mental disorders; severe heart, liver, kidney, and other organic diseases were excluded. However, such patients are not uncommon in clinical settings, so future studies should explore targeted and precise care for such patients.

CONCLUSION

The precise nursing service mode can reduce the incidence of postoperative urinary incontinence in patients with prostate disease; thus, it improves postoperative urodynamics and rehabilitation, and the patients' quality of life.

ARTICLE HIGHLIGHTS

Research background

An operation to restore normal urination function and to control postoperative complications, as far as possible, is the most common method for benign prostatic disease. The postoperative nursing quality has greatly influenced the care for urinary incontinence.

Research motivation

In order to find a reasonable nursing way to improve postoperative urinary incontinence of patients with prostate disease.

Research objectives

This study aimed to observe the effect of precise nursing service mode on postoperative urinary incontinence prevention in patients with prostate disease.

Research methods

A total of 130 patients diagnosed with benign prostatic disease were selected and divided into observation and control groups according to their treatment options. The control was given routine nursing mode intervention; The observation group was given precise nursing service mode intervention. The postoperative exhaust time, time of indwelling catheter, hospitalization time, urethral orifice injury, bladder spasm, secondary hemorrhage, and urinary incontinence were recorded. Clinical international prostate system score (IPSS) and urinary incontinence quality of life questionnaire (I-QOL) scores were used to evaluate the symptoms and life quality.

Research results

Postoperative exhaust time, time of indwelling catheter and hospitalization time in the observation group were lower than in the control group. After the operation, the maximum urinary flow rate increased, the residual urine volume decreased, and the maximum closed urethral pressure was not statistically significant compared with during pre-operation; After the operation, the I-QOL score of the two groups improved, and the IPSS decreased. The I-QOL score of the observation group was higher than that of the control group, and the IPSS was lower than that of the control group. The incidence of urinary incontinence in the observation group was lower than that in the control group, and there was no statistical significance in the duration of urinary incontinence between the observation group and the control group.

Research conclusions

The precise nursing service mode can reduce the incidence of postoperative urinary incontinence in patients with prostate disease; thus, it improves postoperative urodynamics and rehabilitation, and the patients' quality of life.

Research perspectives

Next, we want to explore the improvement effect of precision nursing service mode on the prognosis of patients undergoing surgery for other urinary diseases

REFERENCES

1 **Valdivieso R**, Hueber PA, Meskawi M, Belleville E, Ajib K, Bruyere F, Te AE, Chughtai B, Elterman D, Misrai V, Zorn KC. Multicentre international experience of 532-nm laser photoselective vaporization with GreenLight XPS in men with very large prostates. *BJU Int* 2018; **122**: 873-878 [PMID: 29570929 DOI: 10.1111/bju.14208]

2 **Irwin GM**. Urinary Incontinence. *Prim Care* 2019; **46**: 233-242 [PMID: 31030824 DOI: 10.1016/j.pop.2019.02.004]

3 **Ghiasi B**, Sarokhani D, Najafi F, Motedayen M, Dehkordi AH. The Relationship Between Prostate Cancer and Metformin Consumption: A Systematic Review and Meta-analysis Study. *Curr Pharm Des* 2019; **25**: 1021-1029 [PMID: 30767734 DOI: 10.2174/1381612825666190215123759]

4 **Reed PG**. Explanatory Power and Nursing Theory. *Nurs Sci Q* 2020; **33**: 229-233 [PMID: 32605488 DOI: 10.1177/0894318420920584]

5 **Lee MJ**, Park DA, Lee SH. Utility after robot-assisted radical prostatectomy compared to conventional approaches for localized prostate cancer [socioeconomic perspective study]. *Prostate Cancer Prostatic Dis* 2019; **22**: 461-466 [PMID: 30679761 DOI: 10.1038/s41391-018-0119-9]

6 **Global Burden of Disease Cancer Collaboration**, Fitzmaurice C, Abate D, Abbasi N, Abbastabar H, Abd-Allah F, Abdel-Rahman O, Abdelalim A, Abdoli A, Abdollahpour I, Abdulle ASM, Abebe ND, Abraha HN, Abu-Raddad LJ, Abualhasan A, Adedeji IA, Advani SM, Afarideh M, Afshari M, Aghaali M, Agius D, Agrawal S, Ahmadi A, Ahmadian E, Ahmadpour E, Ahmed MB, Akbari ME, Akinyemiju T, Al-Aly Z, AlAbdulKader AM, Alahdab F, Alam T, Alamene GM, Alemnew BTT, Alene KA, Alinia C, Alipour V, Aljunid SM, Bakeshei FA, Almadi MAH, Almasi-Hashiani A, Alsharif U, Alsowaidi S, Alvis-Guzman N, Amini E, Amini S, Amoako YA, Anbari Z, Anber NH, Andrei CL, Anjomshoa M, Ansari F, Ansariadi A, Appiah SCY, Arab-Zozani M, Arabloo J, Arefi Z, Aremu O, Areri HA, Artaman A, Asayesh H, Asfaw ET, Ashagre AF, Assadi R, Ataeinia B, Atalay HT, Ataro Z, Atique S, Ausloos M, Avila-Burgos L, Avokpaho EFGA, Awasthi A, Awoke N, Ayala Quintanilla BP, Ayanore MA, Ayele HT, Babaee E, Bacha U, Badawi A, Bagherzadeh M, Bagli E, Balakrishnan S, Balouchi A, Bärnighausen TW, Battista RJ, Behzadifar M, Bekele BB, Belay YB, Belayneh YM, Berfield KKS, Berhane A, Bernabe E, Beuran M, Bhakta N, Bhattacharyya K, Biadgo B, Bijani A, Bin Sayeed MS, Birungi C, Bisignano C, Bitew H, Bjørge T, Bleyer A, Bogale KA, Bojia HA, Borzì AM, Bosetti C, Bou-Orm IR, Brenner H, Brewer JD, Briko AN, Briko NI, Bustamante-Teixeira MT, Butt ZA, Carreras G, Carrero JJ, Carvalho F, Castro C, Castro F, Catalá-López F, Cerin E, Chaiah Y, Chanie WF, Chattu VK, Chaturvedi P, Chauhan NS, Chehrazi M, Chiang PP, Chichiabellu TY, Chido-Amajuoyi OG, Chimed-Ochir O, Choi JJ, Christopher DJ, Chu

DT, Constantin MM, Costa VM, Crocetti E, Crowe CS, Curado MP, Dahlawi SMA, Damiani G, Darwish AH, Daryani A, das Neves J, Demeke FM, Demis AB, Demissie BW, Demoz GT, Denova-Gutiérrez E, Derakhshani A, Deribe KS, Desai R, Desalegn BB, Desta M, Dey S, Dharmaratne SD, Dhimal M, Diaz D, Dinberu MTT, Djalalinia S, Doku DT, Drake TM, Dubey M, Dubljanin E, Duken EE, Ebrahimi H, Effiong A, Eftekhari A, El Sayed I, Zaki MES, El-Jaafary SI, El-Khatib Z, Elemineh DA, Elkout H, Ellenbogen RG, Elsharkawy A, Emamian MH, Endalew DA, Endries AY, Eshrati B, Fadhil I, Fallah Omrani V, Faramarzi M, Farhangi MA, Farioli A, Farzadfar F, Fentahun N, Fernandes E, Feyissa GT, Filip I, Fischer F, Fisher JL, Force LM, Foroutan M, Freitas M, Fukumoto T, Futran ND, Gallus S, Gankpe FG, Gayesa RT, Gebrehiwot TT, Gebremeskel GG, Gedefaw GA, Gelaw BK, Geta B, Getachew S, Gezae KE, Ghafourifard M, Ghajar A, Ghashghaee A, Gholamian A, Gill PS, Ginindza TTG, Girmay A, Gizaw M, Gomez RS, Gopalani SV, Gorini G, Goulart BNG, Grada A, Ribeiro Guerra M, Guimaraes ALS, Gupta PC, Gupta R, Hadkhale K, Haj-Mirzaian A, Hamadeh RR, Hamidi S, Hanfore LK, Haro JM, Hasankhani M, Hasanzadeh A, Hassen HY, Hay RJ, Hay SI, Henok A, Henry NJ, Herteliu C, Hidru HD, Hoang CL, Hole MK, Hoogar P, Horita N, Hosgood HD, Hosseini M, Hosseinzadeh M, Hostiuc M, Hostiuc S, Househ M, Hussen MM, Ileanu B, Ilic MD, Innos K, Irvani SSN, Iseh KR, Islam SMS, Islami F, Jafari Balalami N, Jafarinia M, Jahangiry L, Jahani MA, Jahanmehr N, Jakovljevic M, James SL, Javanbakht M, Jayaraman S, Jee SH, Jenabi E, Jha RP, Jonas JB, Jonnagaddala J, Joo T, Jungari SB, Jürisson M, Kabir A, Kamangar F, Karch A, Karimi N, Karimian A, Kasaeian A, Kasahun GG, Kassa B, Kassa TD, Kassaw MW, Kaul A, Keiyoro PN, Kelbore AG, Kerbo AA, Khader YS, Khalilarjmandi M, Khan EA, Khan G, Khang YH, Khatab K, Khater A, Khayamzadeh M, Khazaee-Pool M, Khazaei S, Khoja AT, Khosravi MH, Khubchandani J, Kianipour N, Kim D, Kim YJ, Kisa A, Kisa S, Kissimova-Skarbek K, Komaki H, Koyanagi A, Krohn KJ, Bicer BK, Kugbey N, Kumar V, Kuupiel D, La Vecchia C, Lad DP, Lake EA, Lakew AM, Lal DK, Lami FH, Lan Q, Lasrado S, Lauriola P, Lazarus JV, Leigh J, Leshargie CT, Liao Y, Limenih MA, Listl S, Lopez AD, Lopukhov PD, Lunevicius R, Madadin M, Magdeldin S, El Razek HMA, Majeed A, Maleki A, Malekzadeh R, Manafi A, Manafi N, Manamo WA, Mansourian M, Mansournia MA, Mantovani LG, Maroufizadeh S, Martini SMS, Mashamba-Thompson TP, Massenburg BB, Maswabi MT, Mathur MR, McAlinden C, McKee M, Meheretu HAA, Mehrotra R, Mehta V, Meier T, Melaku YA, Meles GG, Meles HG, Melese A, Melku M, Memiah PTN, Mendoza W, Menezes RG, Merat S, Meretoja TJ, Mestrovic T, Miazgowski B, Miazgowski T, Mihretie KMM, Miller TR, Mills EJ, Mir SM, Mirzaei H, Mirzaei HR, Mishra R, Moazen B, Mohammad DK, Mohammad KA, Mohammad Y, Darwesh AM, Mohammadbeigi A, Mohammadi H, Mohammadi M, Mohammadian M, Mohammadian-Hafshejani A, Mohammadoo-Khorasani M, Mohammadpourhodki R, Mohammed AS, Mohammed JA, Mohammed S, Mohebi F, Mokdad AH, Monasta L, Moodley Y, Moosazadeh M, Moossavi M, Moradi G, Moradi-Joo M, Moradi-Lakeh M, Moradpour F, Morawska L, Morgado-da-Costa J, Morisaki N, Morrison SD, Mosapour A, Mousavi SM, Muche AA, Muhammed OSS, Musa J, Nabhan AF, Naderi M, Nagarajan AJ, Nagel G, Nahvijou A, Naik G, Najafi F, Naldi L, Nam HS, Nasiri N, Nazari J, Negoi I, Neupane S, Newcomb PA, Nggada HA, Ngunjiri JW, Nguyen CT, Nikniaz L, Ningrum DNA, Nirayo YL, Nixon MR, Nnaji CA, Nojomi M, Nosratnejad S, Shiadeh MN, Obsa MS, Ofori-Asenso R, Ogbo FA, Oh IH, Olagunju AT, Olagunju TO, Oluwasanu MM, Omonisi AE, Onwujekwe OE, Oommen AM, Oren E, Ortega-Altamirano DDV, Ota E, Otstavnov SS, Owolabi MO, P A M, Padubidri JR, Pakhale S, Pakpour AH, Pana A, Park EK, Parsian H, Pashaei T, Patel S, Patil ST, Pennini A, Pereira DM, Piccinelli C, Pillay JD, Pirestani M, Pishgar F, Postma MJ, Pourjafar H, Pourmalek F, Pourshams A, Prakash S, Prasad N, Qorbani M, Rabiee M, Rabiee N, Radfar A, Rafiei A, Rahim F, Rahimi M, Rahman MA, Rajati F, Rana SM, Raoofi S, Rath GK, Rawaf DL, Rawaf S, Reiner RC, Renzaho AMN, Rezaei N, Rezapour A, Ribeiro AI, Ribeiro D, Ronfani L, Roro EM, Roshandel G, Rostami A, Saad RS, Sabbagh P, Sabour S, Saddik B, Safiri S, Sahebkar A, Salahshoor MR, Salehi F, Salem H, Salem MR, Salimzadeh H, Salomon JA, Samy AM, Sanabria J, Santric Milicevic MM, Sartorius B, Sarveazad A, Sathian B, Satpathy M, Savic M, Sawhney M, Sayyah M, Schneider IJC, Schöttker B, Sekerija M, Sepanlou SG, Sepehrimanesh M, Seyedmousavi S, Shaahmadi F, Shabaninejad H, Shahbaz M, Shaikh MA, Shamshirian A, Shamsizadeh M, Sharafi H, Sharafi Z, Sharif M, Sharifi A, Sharifi H, Sharma R, Sheikh A, Shirkoohi R, Shukla SR, Si S, Siabani S, Silva DAS, Silveira DGA, Singh A, Singh JA, Sisay S, Sitas F, Sobngwi E, Soofi M, Soriano JB, Stathopoulou V, Sufiyan MB, Tabarés-Seisdedos R, Tabuchi T, Takahashi K, Tamtaji OR, Tarawneh MR, Tassew SG, Taymoori P, Tehrani-Banihashemi A, Temsah MH, Temsah O, Tesfay BE, Tesfay FH, Teshale MY, Tessema GA, Thapa S, Tlaye KG, Topor-Madry R, Tovani-Palone MR, Traini E, Tran BX, Tran KB, Tsadik AG, Ullah I, Uthman OA, Vacante M, Vaezi M, Varona Pérez P, Veisani Y, Vidale S, Violante FS, Vlassov V, Vollset SE, Vos T, Vosoughi K, Vu GT, Vujcic IS, Wabinga H, Wachamo TM, Wagnew FS, Waheed Y, Weldegebreal F, Weldesamuel GT, Wijeratne T, Wondafrash DZ, Wonde TE, Wondmieneh AB, Workie HM, Yadav R, Yadegar A, Yadollahpour A, Yaseri M, Yazdi-Feyzabadi V, Yeshaneh A, Yimam MA, Yimer EM, Yisma E, Yonemoto N, Younis MZ, Yousefi B, Yousefifard M, Yu C, Zabeh E, Zadnik V, Moghadam TZ, Zaidi Z, Zamani M, Zandian H, Zangeneh A, Zaki L, Zendehdel K, Zenebe ZM, Zewale TA, Ziapour A, Zodpey S, Murray CJL. Global, Regional, and National Cancer Incidence, Mortality, Years of Life Lost, Years Lived With Disability, and Disability-Adjusted Life-Years for 29 Cancer Groups, 1990 to 2017: A Systematic Analysis for the Global Burden of Disease Study. *JAMA Oncol* 2019; **5**: 1749-1768 [PMID: 31560378 DOI: 10.1001/jamaoncol.2019.2996]

7 **Jeihooni AK**, Kashfi SM, Hatami M, Avand A, Bazrafshan MR. The Effect of Educational Program

Based on PRECEDE Model in Promoting Prostate Cancer Screening in a Sample of Iranian Men. *J Cancer Educ* 2019; **34**: 161-172 [PMID: 28913671 DOI: 10.1007/s13187-017-1282-8]

8 **Averbeck MA**, Marcelissen T, Anding R, Rahnama'i MS, Sahai A, Tubaro A. How can we prevent postprostatectomy urinary incontinence by patient selection, and by preoperative, peroperative, and postoperative measures? *Neurourol Urodyn* 2019; **38** Suppl 5: S119-S126 [PMID: 31821626 DOI: 10.1002/nau.23972]

9 **Lv Z**, Jiang H, Hu X, Yang C, Chand H, Tang C, Li Y. Efficacy and safety of periprostatic nerve block combined with perineal subcutaneous anaesthesia and intrarectal lidocaine gel in transrectal ultrasound guided transperineal prostate biopsy: A Prospective Randomised Controlled Trial. *Prostate Cancer Prostatic Dis* 2020; **23**: 74-80 [PMID: 31160805 DOI: 10.1038/s41391-019-0155-0]

10 **Ding S**, Gu Z, Yan R, Tang Y, Miao P. A novel mode of DNA assembly at electrode and its application to protein quantification. *Anal Chim Acta* 2018; **1029**: 24-29 [PMID: 29907286 DOI: 10.1016/j.aca.2018.04.073]

11 **Pan LH**, Lin MH, Pang ST, Wang J, Shih WM. Improvement of Urinary Incontinence, Life Impact, and Depression and Anxiety With Modified Pelvic Floor Muscle Training After Radical Prostatectomy. *Am J Mens Health* 2019; **13**: 1557988319851618 [PMID: 31092098 DOI: 10.1177/1557988319851618]

12 **Dorsey SG**, Pickler RH. Precision Science in Nursing Research. *Nurs Res* 2019; **68**: 85 [PMID: 30829923 DOI: 10.1097/NNR.0000000000000333]

13 **Lemoine C**. Precision medicine for nurses: 101. *Semin Oncol Nurs* 2014; **30**: 84-99 [PMID: 24794082 DOI: 10.1016/j.soncn.2014.03.002]

14 **Spiers E**. Managing vascular compromise of hand and digit replantation following traumatic amputation. *Br J Nurs* 2018; **27**: S50-S56 [PMID: 30418845 DOI: 10.12968/bjon.2018.27.Sup20.S50]

15 **Ercan M**, Alp HH, Kocaturk H, Bakan N, Gul M. Oxidative stress before and after surgery in benign prostatic hyperplasia patients. *Andrologia* 2019; **51**: e13326 [PMID: 31158928 DOI: 10.1111/and.13326]

16 **Privitera S**, Russo GI, La Vignera S, Condorelli RA, Calogero AE, Cantiello F, Damiano R, Favilla V, Cimino S, Morgia G. Benign prostatic hyperplasia and intraprostatic inflammation are associated with liver inflammation: it's time for prevention. *Andrology* 2018; **6**: 737-741 [PMID: 29858538 DOI: 10.1111/andr.12505]

17 **van Mastrigt R**, Boevé ER, Groen J, de Zeeuw S. Urinary Bladder Contractility Revisited. Correlation of Noninvasively and Invasively Measured Contractility Parameters in Patients Eligible for Transurethral Resection of the Prostate. *Urology* 2015; **86**: 128-132 [PMID: 26142597 DOI: 10.1016/j.urology.2015.03.031]

18 **Bardsley A**. An overview of urinary incontinence. *Br J Nurs* 2016; **25**: S14-S21 [PMID: 27734727 DOI: 10.12968/bjon.2016.25.18.S14]

19 **Strope SA**. Evidence-based guidelines in lower urinary tract symptoms secondary to benign prostatic hyperplasia and variation in care. *Curr Opin Urol* 2018; **28**: 262-266 [PMID: 29601306 DOI: 10.1097/MOU.0000000000000504]

20 **Piechota H**. [Prevention of Catheter-Associated Urinary Tract Infections]. *Aktuelle Urol* 2016; **47**: 220-228 [PMID: 27271450 DOI: 10.1055/s-0042-101845]

World Journal of Clinical Cases

Submit a Manuscript: https://www.f6publishing.com

World J Clin Cases 2022 February 16; 10(5): 1527-1535

DOI: 10.12998/wjcc.v10.i5.1527

ISSN 2307-8960 (online)

ORIGINAL ARTICLE

Retrospective Study

Significance of serum glucagon-like peptide-1 and matrix Gla protein levels in patients with diabetes and osteoporosis

Fei-Fei Xie, Yu-Fang Zhang, Yan-Fang Hu, Yun-Yun Xie, Xiao-Ying Wang, Shu-Zhen Wang, Bao-Qiang Xie

ORCID number: Fei-Fei Xie 0000-0002-9837-3045; Yu-Fang Zhang 0000-0002-6711-8834; Yan-Fang Hu 0000-0002-0980-7666; Yun-Yun Xie 0000-0003-2662-747X; Xiao-Ying Wang 0000-0001-7575-6046; Shu-Zhen Wang 0000-0002-8491-0022; Bao-Qiang Xie 0000-0002-7724-3380.

Author contributions: Xie FF and Zhang YF designed the experiment; Hu YF drafted the work; Xie YY, Wang XY, and Wang SZ collected the data; Xie BQ and Xie FF analyzed and interpreted the data; and Zhang YF, Hu YF, and Xie YY wrote the article.

Institutional review board statement: This study was approved by the Medical Ethics Committee of Guangdong Provincial People's Hospital Ganzhou Hospital.

Informed consent statement: Patients were not required to give informed consent to the study because the analysis used anonymous clinical data that were obtained after each patient agreed to treatment by written consent.

Conflict-of-interest statement: No conflict of interest.

Data sharing statement: No additional data are available.

Fei-Fei Xie, Yu-Fang Zhang, Yan-Fang Hu, Yun-Yun Xie, Xiao-Ying Wang, Shu-Zhen Wang, Bao-Qiang Xie, Department of Endocrinology, Guangdong Provincial People's Hospital Ganzhou Hospital (Ganzhou Municipal Hospital), Ganzhou 341000, Jiangxi Province, China

Corresponding author: Bao-Qiang Xie, BM BCh, Chief Doctor, Department of Endocrinology, Guangdong Provincial People's Hospital Ganzhou Hospital (Ganzhou Municipal Hospital), No. 49 Dagong Road, Zhanggong District, Ganzhou 341000, Jiangxi Province, China. xiebaoqiang1629@163.com

Abstract

BACKGROUND

Osteoporosis is a systemic bone disease characterized by decreased bone mass, impaired bone mass, and reduced bone strength that leads to increased bone fragility and fracture. Type 2 diabetes mellitus (T2DM) complicated with osteoporosis is a common systemic metabolic bone disease, and reduced bone mass and bone strength are considered the main clinical features; however, the pathogenesis of this disease has not been fully clarified. Its occurrence is considered related to sex, age, and genetic factors. There are many risk factors for diabetes complicated with osteoporosis. Therefore, exploring these risk factors will help prevent it.

AIM

To investigate the relationships among serum glucagon-like peptide-1 (GLP-1) levels, matrix Gla protein (MGP) levels, and diabetes with osteoporosis.

METHODS

Sixty patients with T2DM complicated with osteoporosis confirmed by the endocrinology department of our hospital were selected as the case group. Sixty T2DM patients with bone loss were selected as the control group. Sixty healthy participants were selected as the healthy group. The general data, bone mineral density index, and bone metabolic markers of the three groups were compared. The relationships among GLP-1 levels, MGP levels, and the bone mineral density index of the case group were analyzed using linear correlation analysis and a logistic regression model.

RESULTS

Differences in sex, smoking, and drinking among the case group, control group, and healthy group were not statistically significant ($P > 0.05$). The mean age of the

Supported by Jiangxi Provincial Health and Family Planning Commission "Science and Technology Plan".

Country/Territory of origin: China

Specialty type: Endocrinology and Metabolism

Provenance and peer review: Unsolicited article; Externally peer reviewed.

Peer-review model: Single blind

Peer-review report's scientific quality classification
Grade A (Excellent): 0
Grade B (Very good): B, B
Grade C (Good): 0
Grade D (Fair): 0
Grade E (Poor): 0

Received: November 14, 2021
Peer-review started: November 14, 2021
First decision: December 9, 2021
Revised: December 27, 2021
Accepted: January 11, 2022
Article in press: January 11, 2022
Published online: February 16, 2022

P-Reviewer: Botta A, Ward LM
S-Editor: Wang JL
L-Editor: A
P-Editor: Wang JL

case group was older than those of the control and healthy groups ($P < 0.05$). The body mass index, fasting plasma glucose level, HbA1c level, hypertension rate, and coronary heart disease rate of the case and control groups were higher than those of the healthy group ($P < 0.05$). The serum GLP-1 and MGP levels of the case group were lower than those of the control and healthy groups; these differences were statistically significant ($P < 0.05$). The serum GLP-1 and MGP levels of the control group were lower than those of the healthy group; these differences were statistically significant ($P < 0.05$). The serum GLP-1 and MGP levels of the case group were significantly positively correlated with the bone mineral density values of the hip and lumbar spine ($P < 0.05$). The results of the logistic regression model showed that age and duration of diabetes were independent risk factors for osteoporosis in diabetic patients ($P < 0.05$) and that increased GLP-1 and MGP values were protective factors against osteoporosis in diabetic patients ($P < 0.05$).

CONCLUSION
Serum GLP-1 and MGP levels of diabetic patients with osteoporosis were significantly decreased and positively correlated with bone mineral density and were independent risk factors for osteoporosis in diabetic patients.

Key Words: Glucagon-like peptide-1; Matrix Gla protein; Diabetes mellitus; Osteoporosis; Bone mineral density; Systemic bone disease

Core Tip: Serum glucagon-like peptide-1 (GLP-1) and matrix Gla protein (MGP)levels were significantly positively correlated with bone mineral density values of the hip joint and lumbar vertebrae. They were significantly negatively correlated with type 1 procollagen amino-terminal propeptide, osteocalcin, and special sequence of carboxy-terminal peptide β of type 1 collagen. Older age and duration of diabetes were independent risk factors for osteoporosis for diabetic patients. Increased GLP-1 and MGP levels were protective factors against osteoporosis for diabetic patients. GLP-1 and MGP levels should be used as auxiliary evaluation indexes to evaluate the risk of osteoporosis for patients with diabetes to enable early detection of and intervention for diabetes with osteoporosis and improve its prognosis.

Citation: Xie FF, Zhang YF, Hu YF, Xie YY, Wang XY, Wang SZ, Xie BQ. Significance of serum glucagon-like peptide-1 and matrix Gla protein levels in patients with diabetes and osteoporosis. *World J Clin Cases* 2022; 10(5): 1527-1535
URL: https://www.wjgnet.com/2307-8960/full/v10/i5/1527.htm
DOI: https://dx.doi.org/10.12998/wjcc.v10.i5.1527

INTRODUCTION

Type 2 diabetes mellitus (T2DM) is a systemic metabolic disorder that can cause metabolic abnormalities of sugar, lipids, and proteins. It can also cause an imbalance of water and electrolytes and abnormal metabolism of bone minerals, resulting in massive losses of calcium, magnesium, phosphorus, and other trace elements, resulting in osteopenia. Additionally, the relative lack of insulin leads to decreased bone matrix synthesis, thereby causing decreased bone mineral density. Therefore, patients with T2DM are more likely to have osteoporosis[1]. When fracture healing occurs slowly in patients with T2DM, they are prone to infectious complications that have adverse effects on their physical and mental health. Therefore, early detection of and interventions for osteoporosis are particularly essential for patients with T2DM[2].

Glucagon-like peptide-1 (GLP-1) is an endocrine hormone that can stimulate insulin secretion in a glucose-dependent manner and protect islet β cells through various mechanisms. It has been widely used for the diagnosis and treatment of T2DM. Recent studies have suggested that GLP-1 can inhibit bone resorption by promoting the secretion of calcitonin[3]. Matrix Gla protein (MGP) is a circulating protein related to vitamin K that can inhibit calcium and phosphorus deposition and play a role in the

regulation of bone metabolism[4]. However, there are few studies of its effect on diabetic patients. This study explored the relationships among serum GLP-1 Levels, MGP levels, and diabetes with osteoporosis.

MATERIALS AND METHODS

Data

Sixty patients with T2DM complicated with osteoporosis diagnosed by the staff of the endocrinology department of our hospital from April 2019 to January 2020 were selected as the case group. Sixty patients with T2DM complicated with osteopenia were selected as the control group. Sixty healthy participants were selected as the healthy group. The flow chart of the selection of the three groups of study participants is presented in Figure 1. Inclusion criteria were as follows: T2DM diagnosed according to the criteria of the Guidelines for the Prevention and Treatment of Type 2 Diabetes in China (2017 edition)[5]; age 52 to 81 years; and bone mass reduction indicated by a bone mineral density T value of 1 to -2.5 (the diagnostic criteria for osteoporosis were a bone mineral density T value < -2.5 and/or one or more fractures)[6]. The healthy group included volunteers who underwent a physical examination. Exclusion criteria were as follows: complicated infectious diseases; thyroid disease; long-term use of hormone drugs; malignant tumors and tuberculosis; and use of drugs related to bone metabolism within 6 mo.

Patients and their families were advised about this study before its implementation and signed informed consent forms. This study was performed after approval was obtained from the medical ethics committee of our hospital. The baseline data of the participants in the three groups are shown in Table 1. The case group and control group had good equilibrium and comparability.

Serum GLP-1 and MGP testing methods

Venous blood samples (2 mL) were extracted from all participants during the morning after fasting for more than 8 h; they were kept at room temperature for 2 h after centrifugation. Serum was obtained after centrifugation at 3000 rpm for 10 min, and GLP-1 and MGP were detected using an enzyme-linked immunoassay. Serum samples were encapsulated, sealed, combined, incubated with the primary antibody, washed, incubated with the secondary antibody, washed, colored, and analyzed. The optical density was read using a 450-nm wavelength and substituted into the standard curve to calculate the concentration (the kit was from Wuhan Youersheng Technology Co., Ltd., Wuhan, China; the test instrument was the Elx88 automatic enzyme label instrument from Bertin Corporation, Rockville, MD, USA).

Measurement of bone density and bone metabolic marker levels

The bone mineral density values of the lumbar spine (L1-L4) and hip joint and levels of serum bone alkaline phosphatase (BALP), type 1 procollagen amino-terminal propeptide (P1NP), osteocalcin (BGP), and special sequence of carboxy-terminal peptide β of type 1 collagen (β-CTX) of the three groups were measured.

Venous blood samples (5 mL) were extracted from all participants during the morning after fasting for more than 8 h; they were kept at room temperature for 2 h after centrifugation. After centrifugation at 3000 rpm for 10 min, the serum was obtained. BALP, P1NP, BGP, and β-CTX were detected using electrochemiluminescence (the kit was from Beijing Boorsen Biological Co., Ltd., Beijing, China; the detection instrument was the Unicel DxI800 automatic chemiluminescence immunoassay analyzer from Beckman-Coulter, Brea, CA, USA).

All participants underwent testing to determine the bone mineral density values of the lumbar spine (L1-L4) and hip joint. Low-energy and high-energy photon peaks were obtained using an X-ray tube ball, and the data were transferred to the computer for processing and converted to bone mineral density values (DiscoveryA dual-energy X-ray bone mineral density instrument; GE, Madison, WI, USA).

Statistical analysis

Data processing software SPSS (v21.0; IBM, Cary, NC, USA) was used. The measurement indexes, including body mass index (BMI), fasting plasma glucose (FPG) level, and HbA1c level, during this study were tested using the normal distribution test, and the results were in line with the approximate normal distribution or normal distribution represented by mean ± SD. The *t*-test or single-factor analysis was used for

Table 1 Single factor analysis of general data of the three groups of study participants, *n* (%)

Factors	Case group (*n* = 60)	Control group (*n* = 60)	Healthy group (*n* = 60)	$F/\chi^2/t$	*P* value
Age (yr)	66.78 ± 5.85	61.83 ± 5.36	61.92 ± 5.48	15.563	0.000
Course of disease (yr)	12.99 ± 4.01	8.98 ± 3.83	-	5.601	0.000
BMI (kg/m^2)	24.52 ± 2.32	24.73 ± 2.49	23.68 ± 2.05	3.510	0.032
FPG (mmol/L)	8.50 ± 1.50	8.27 ± 1.24	5.77 ± 0.61	99.314	0.000
HbA1c (%)	9.18 ± 1.12	8.76 ± 1.26	5.89 ± 0.70	184.683	0.000
Sex				5.896	0.052
Male	15 (25.00)	25 (41.67)	27 (45.00)		
Female	45 (75.00)	35 (58.33)	33 (55.00)		
Smoking				2.553	0.279
Yes	9 (15.00)	16 (26.67)	14 (23.33)		
No	51 (85.00)	44 (73.33)	46 (76.67)		
Drinking				2.182	0.336
Yes	7 (11.67)	11 (18.33)	13 (21.67)		
No	53 (88.33)	49 (81.67)	47 (78.33)		
Hypertension				23.054	0.000
Yes	15 (25.00)	20 (33.33)	0 (0.00)		
No	45 (75.00)	40 (66.67)	60 (100.00)		
Coronary heart disease				9.449	0.009
Yes	5 (8.33)	9 (15.00)	0 (0.00)		
No	55 (91.67)	51 (85.00)	60 (100.00)		

BMI: body mass index; FPG: Fasting plasma glucose.

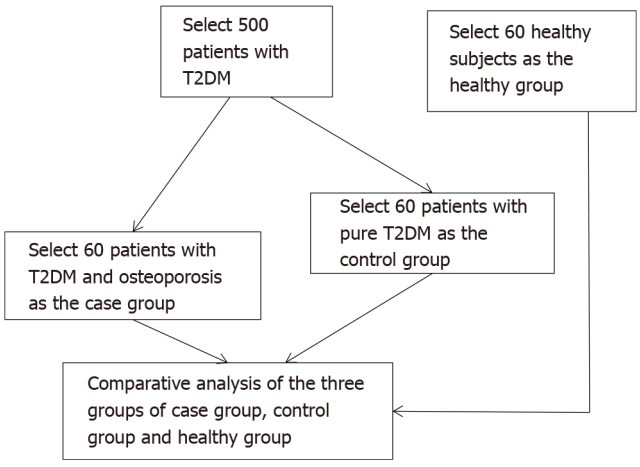

Figure 1 Flow chart of the selection of the three groups of study participants. T2DM: Type 2 diabetes mellitus.

comparisons between groups, and the least significant difference *t*-test was used for comparisons at any time point. The enumeration data were analyzed and compared using the χ^2 test. The Pearson linear correlation method was used for correlation analyses and the logistic regression model was used for multivariate analyses (α = 0.05).

RESULTS

Single-factor analysis of general data of the three groups

Differences in sex, smoking, and drinking among the case group, control group, and healthy group were not statistically significant ($P > 0.05$). The mean age of the case group was higher than those of the control and healthy groups ($P < 0.05$). The BMI, FPG level, HbA1c level, hypertension rate, and coronary heart disease rate of the case and control groups were higher than those of the healthy group ($P < 0.05$) (Table 1).

Comparison of serum GLP-1 and MG levels among the three groups

The serum GLP-1 and MGP levels of the case group were lower than those of the control and healthy groups; these differences were statistically significant ($P < 0.05$). The serum GLP-1 and MGP levels of the control group were lower than those of the healthy group; these differences were statistically significant ($P < 0.05$) (Table 2).

Comparison of bone mineral density and bone metabolic markers among the three groups

The bone mineral density values of the lumbar vertebrae (L1-L4) and hip joint of the case group were lower than those of the control and healthy groups; these differences were statistically significant ($P < 0.05$). The bone mineral density values of the lumbar vertebrae (L1-L4) and hip joint of the control group were lower than those of the healthy group; these differences were statistically significant ($P < 0.05$). The serum P1NP, BGP, and β-CTX levels of the case group were higher than those of the control and healthy group; these differences were statistically significant ($P < 0.05$). The serum P1NP, BGP, and β-CTX levels of the control group were higher than those of the healthy group; these differences were statistically significant ($P < 0.05$) (Table 3).

Correlations of serum GLP-1 and MGP levels with bone mineral density of the case group

The serum GLP-1 and MGP levels of the case group were significantly positively correlated with the bone mineral density values of the hip joint and lumbar vertebrae ($P < 0.05$) (Table 4).

Correlations of serum GLP-1 and MGP levels with bone metabolic markers of the case group

The serum GLP-1 and MGP levels of the case group were significantly negatively correlated with the serum P1NP, BGP, and β-CTX levels ($P < 0.05$) (Table 5).

Multivariate analysis

The logistic regression model was established with osteoporosis as the dependent variable and BMI, FPG level, HbA1c level, hypertension, coronary heart disease, GLP-1 Level, MGP level, P1NP level, BGP level, and β-CTX level as the independent variables. The results showed that older age and duration of diabetes were independent risk factors for osteoporosis in diabetic patients ($P < 0.05$) and that increased GLP-1 and MGP levels were protective factors against osteoporosis in diabetic patients ($P < 0.05$) (Table 6).

DISCUSSION

T2DM is characterized by reduced insulin secretion or decreased insulin sensitivity resulting in elevated blood glucose levels; it is often accompanied by metabolic disorders involving fat, protein, water, and electrolytes[7]. An epidemiological survey found that the worldwide incidence of T2DM exceeded 6.87%. Furthermore, diabetic complications result from disease progression and can cause disability or death[8]. The bone metabolism of patients with osteoporosis is abnormal, and their bone loss is aggravated, thus leading to decreased bone strength and increasing their risk of fractures. If patients with T2DM develop osteoporosis, then their risk of disability is increased, thereby adversely affecting their prognosis[9].

During this study, the lumbar vertebrae (L1-L4) and hip bone mineral density values were grouped and compared with the general data. Patients with T2DM complicated with osteoporosis were older than patients with T2DM complicated with decreased bone mass and healthy participants. The BMI, FPG level, HbA1c level,

Table 2 Comparison of serum glucagon-like peptide-1 and matrix Gla protein levels in the three groups of study participants (mean ± SD)

Group	*n*	GLP-1 (pmol/L)	MGP (nmol/L)
Case group	60	9.19 ± 1.10	7.88 ± 0.92
Control group	60	13.88 ± 1.65	9.77 ± 1.52
Healthy group	60	17.07 ± 2.48	10.79 ± 1.63
F		280.527	67.487
P value		0.000	0.000

GLP-1: Glucagon-like peptide-1; MGP: Matrix Gla protein.

Table 3 Comparison of bone density and bone metabolic marker levels of the three groups of study participants (mean ± SD)

Group	*n*	Lumbar spine (g/m²)	Hip joint (g/m²)	BALP (μg/mL)	P1NP (ng/mL)	BGP (μgmL)	β-CTX (ng/mL)
Case group	60	0.69 ± 0.08	0.66 ± 0.09	4.08 ± 1.20	49.16 ± 4.08	15.92 ± 4.08	0.49 ± 0.08
Control group	60	0.95 ± 0.14	0.83 ± 0.10	4.03 ± 0.84	44.41 ± 2.75	14.40 ± 2.75	0.44 ± 0.08
Healthy group	60	1.08 ± 0.16	0.99 ± 0.14	4.07 ± 0.82	31.59 ± 2.38	12.14 ± 2.38	0.41 ± 0.10
F		142.637	130.422	0.036	122.211	21.822	14.496
P value		0.000	0.000	0.965	0.000	0.000	0.000

BALP: Bone alkaline phosphatase; P1NP: Type 1 procollagen amino-terminal propeptide; BGP: Osteocalcin; β-CTX: Special sequence of carboxy-terminal peptide β of type 1 collagen.

Table 4 Correlation analysis results

Index	Relativity	Lumbar spine (g/m²)	Hip joint (g/m²)
GLP-1 (pmol/L)	*r*	0.707	0.691
	P value	0.000	0.000
MGP (nmol/L)	*r*	0.571	0.546
	P value	0.000	0.000

GLP-1: Glucagon-like peptide-1; MGP: Matrix Gla protein.

Table 5 Correlation between serum glucagon-like peptide-1, matrix Gla protein levels, and bone metabolism marker levels

Index	Relativity	BALP (μg/mL)	P1NP (ng/mL)	BGP (μgmL)	β-CTX (ng/mL)
GLP-1 (pmol/L)	*r*	0.192	-0.401	-0.386	-0.377
	P value	0.163	0.000	0.003	0.005
MGP (nmol/L)	*r*	0.155	-0.421	-0.419	-0.351
	P value	0.227	0.000	0.000	0.010

GLP-1: Glucagon-like peptide-1; MGP: Matrix Gla protein; BALP: Bone alkaline phosphatase; P1NP: Type 1 procollagen amino-terminal propeptide; BGP: Osteocalcin; β-CTX: Special sequence of carboxy-terminal peptide β of type 1 collagen.

hypertension rate, and coronary heart disease rate of diabetic patients were higher than those of healthy participants, suggesting that elderly patients with T2DM are more likely to have osteoporosis. Diabetes patients have a higher risk of obesity, hypertension, coronary heart disease, and other complications. P1NP is a peptide secreted by osteoblasts that can sensitively reflect the synthesis rate of type 1 collagen.

Table 6 Factor analysis of the logistic regression model

Index		SE	Walds	*P* value	OR	95%CI	
Age	0.551	0.225	5.997	0.007	1.735	1.116	2.697
Course of disease	0.494	0.240	4.237	0.048	1.639	1.024	2.623
BMI	0.381	0.211	3.261	0.094	1.464	0.968	2.213
FPG	0.307	0.184	2.784	0.116	1.359	0.948	1.950
HbA1c	0.502	0.316	2.524	0.131	1.652	0.889	3.069
Hypertension	0.484	0.408	1.407	0.248	1.623	0.729	3.610
Coronary heart disease	0.490	0.411	1.421	0.241	1.632	0.729	3.653
GLP-1	-0.616	0.277	4.945	0.039	0.540	0.314	0.930
MGP	-0.573	0.254	5.089	0.037	0.564	0.343	0.928
β-CTX	0.184	0.152	1.465	0.237	1.202	0.892	1.619
BALP	0.207	0.182	1.294	0.301	1.230	0.861	1.757
BGP	0.118	0.104	1.287	0.316	1.125	0.918	1.380

BMI: body mass index; FPG: Fasting plasma glucose; GLP-1: Glucagon-like peptide-1; MGP: Matrix Gla protein; BALP: Bone alkaline phosphatase; P1NP: Type 1 procollagen amino-terminal propeptide; BGP: Osteocalcin; β-CTX: Special sequence of carboxy-terminal peptide β of type 1 collagen.

BGP is a non-collagen acidic glycoprotein synthesized by osteoblasts and chondrocytes. P1NP and BGP are bone formation markers recommended by the International Osteoporosis Foundation[10]. BALP can directly reflect the osteoblast activity, which is the best indicator of human bone mineralization disorders[11]. β-CTX is an index of bone absorption and collagen degradation during bone remodeling[12]. During this study, the serum P1NP, BGP, BALP, and β-CTX levels of the three groups were compared. These levels were higher in patients with T2DM complicated with osteoporosis than in those of patients with T2DM complicated with decreased bone mass and healthy participants. The serum P1NP, BGP, and β-CTX levels of patients with T2DM complicated with bone loss were higher than those of healthy participants, suggesting that diabetic patients with osteoporosis have more severe bone metabolism disorders related to their lack of insulin, increased thyroid hormone secretion, insufficient collagen synthesis, and decreased osteoblast function. The abnormal bone metabolism in diabetic patients is one of the important mechanisms underlying their osteoporosis.

GLP-1 is a hormone secreted by ileal endocrine cells that can protect islet β cells, stimulate insulin secretion, and inhibit glucagon secretion to reduce blood glucose levels. GLP-1 exhibits low expression in patients with T2DM because of the impaired incretin effect[13-15]. GLP-1 receptor agonists promote the secretion of GLP-1 by binding to the receptor, thereby producing a hypoglycemic effect[16]. MGP is a strong inhibitor of calcium and phosphorus deposition that can bind to bone morphogenetic protein-2 to inhibit its biological activity and affect the transformation of mesenchymal cells into chondrocytes or osteoid cells[17-20]. In this study, serum GLP-1 and MGP levels were compared among the three groups. It was found that serum GLP-1 and MGP levels of patients with T2DM complicated with osteoporosis were lower than those of patients with T2DM complicated with bone loss and healthy participants. Furthermore, serum GLP-1 and MG levels of patients with T2DM and bone loss were lower than those of healthy participants, suggesting that decreased serum GLP-1 and MGP levels may be related to osteoporosis in patients with T2DM. GLP-1 can regulate bone metabolism by regulating calcium balance and affecting the proliferation and apoptosis of osteoclasts and osteoblasts. The decrease in serum GLP-1 Levels can lead to abnormal bone metabolism and osteoporosis. MGP is an inhibitor of vascular and cartilage calcification. MGP deficiency can trigger the differentiation of chondrocytes and cartilage formation in the middle layer of blood vessels and affect bone formation.

Furthermore, the correlation analysis results indicated that serum GLP-1 and MGP levels were significantly positively correlated with the bone mineral density values of the hip joint and lumbar vertebrae. The serum GLP-1 and MGP levels were significantly negatively correlated with the serum P1NP, BGP, and β-CTX levels. The results of the logistic regression model indicated that older age and duration of

diabetes were independent risk factors for osteoporosis in diabetic patients and that increased GLP-1 and MGP levels were protective factors against osteoporosis in diabetic patients. Future clinical studies should involve osteoporosis screening for elderly patients with long durations of diabetes, and the serum GLP-1 and MGP levels should be used as auxiliary evaluation indexes to evaluate the risk of osteoporosis in patients with T2DM to allow early detection of and intervention for diabetes with osteoporosis and improve the prognosis.

CONCLUSION

In summary, serum GLP-1 and MGP levels of diabetic patients with osteoporosis were markedly decreased and significantly positively correlated with bone mineral density. Furthermore, they were independent risk factors for osteoporosis in patients with diabetes.

ARTICLE HIGHLIGHTS

Research background

Osteoporosis is a systemic bone disease characterized by decreased bone mass, damaged bone mass, and decreased bone strength, leading to increased bone fragility and fractures. Type 2 diabetes (T2DM) complicated by osteoporosis is a common systemic metabolic bone disease. The reduction of bone mass and bone strength is considered to be the main clinical feature; its occurrence is considered to be related to gender, age and genetic factors.

Research motivation

Explore the risk factors of T2DM complicated with osteoporosis, and provide reasonable guidance for preventing this problem.

Research objectives

This study aimed to investigate the relationships among serum glucagon-like peptide-1 (GLP-1) levels, matrix Gla protein (MGP) levels, and diabetes with osteoporosis.

Research methods

Sixty T2DM patients with osteoporosis were selected as the case group, and 60 T2DM patients with bone loss were selected as the control group. Sixty healthy subjects were selected as the healthy group for the study.

Research results

Serum GLP-1 and MGP levels in diabetic osteoporosis patients are independent risk factors for osteoporosis in diabetic patients.

Research conclusions

Serum GLP-1 and MGP levels of diabetic patients with osteoporosis were significantly decreased and positively correlated with bone mineral density and were independent risk factors for osteoporosis in diabetic patients.

Research perspectives

Provide for the prevention of osteoporosis in diabetic patients.

REFERENCES

1 **Elena C**, Chiara M, Angelica B, Chiara MA, Laura N, Chiara C, Claudio C, Antonella F, Nicola G. Hyperglycemia and Diabetes Induced by Glucocorticoids in Nondiabetic and Diabetic Patients: Revision of Literature and Personal Considerations. *Curr Pharm Biotechnol* 2018; **19**: 1210-1220 [PMID: 30605054 DOI: 10.2174/1389201020666190102145305]

2 **Cortet B**, Lucas S, Legroux-Gerot I, Penel G, Chauveau C, Paccou J. Bone disorders associated with diabetes mellitus and its treatments. *Joint Bone Spine* 2019; **86**: 315-320 [PMID: 30098423 DOI: 10.1016/j.jbspin.2018.08.002]

3 **Bird GH**, Fu A, Escudero S, Godes M, Opoku-Nsiah K, Wales TE, Cameron MD, Engen JR, Danial

NN, Walensky LD. Hydrocarbon-Stitched Peptide Agonists of Glucagon-Like Peptide-1 Receptor. *ACS Chem Biol* 2020; **15**: 1340-1348 [PMID: 32348108 DOI: 10.1021/acschembio.0c00308]

4 **Sasaki M**, Hasegawa T, Yamada T, Hongo H, de Freitas PH, Suzuki R, Yamamoto T, Tabata C, Toyosawa S, Oda K, Li M, Inoue N, Amizuka N. Altered distribution of bone matrix proteins and defective bone mineralization in klotho-deficient mice. *Bone* 2013; **57**: 206-219 [PMID: 23954506 DOI: 10.1016/j.bone.2013.08.008]

5 **Cui JY**, Zhou RR, Han S, Wang TS, Wang LQ, Xie XH. Statin therapy on glycemic control in type 2 diabetic patients: A network meta-analysis. *J Clin Pharm Ther* 2018; **43**: 556-570 [PMID: 29733433 DOI: 10.1111/jcpt.12690]

6 **US Preventive Services Task Force**, Curry SJ, Krist AH, Owens DK, Barry MJ, Caughey AB, Davidson KW, Doubeni CA, Epling JW Jr, Kemper AR, Kubik M, Landefeld CS, Mangione CM, Phipps MG, Pignone M, Silverstein M, Simon MA, Tseng CW, Wong JB. Screening for Osteoporosis to Prevent Fractures: US Preventive Services Task Force Recommendation Statement. *JAMA* 2018; **319**: 2521-2531 [PMID: 29946735 DOI: 10.1001/jama.2018.7498]

7 **Gortázar AR**, Ardura JA. Osteocytes and Diabetes: Altered Function of Diabetic Osteocytes. *Curr Osteoporos Rep* 2020; **18**: 796-802 [PMID: 33184775 DOI: 10.1007/s11914-020-00641-z]

8 **Pothof AB**, O'Donnell TFX, Swerdlow NJ, Liang P, Li C, Varkevisser RRB, de Borst GJ, Schermerhorn ML. Risk of insulin-dependent diabetes mellitus in patients undergoing carotid endarterectomy. *J Vasc Surg* 2019; **69**: 814-823 [PMID: 30714571 DOI: 10.1016/j.jvs.2018.05.250]

9 **Minami M**, Ikoma K, Horii M, Sukenari T, Onishi O, Fujiwara H, Ogi H, Itoh K, Kubo T. Usefulness of Sweep Imaging With Fourier Transform for Evaluation of Cortical Bone in Diabetic Rats. *J Magn Reson Imaging* 2018; **48**: 389-397 [PMID: 29360263 DOI: 10.1002/jmri.25955]

10 **Hansen S**, Shanbhogue VV, Jørgensen NR, Beck-Nielsen SS. Elevated Bone Remodeling Markers of CTX and P1NP in Addition to Sclerostin in Patients with X-linked Hypophosphatemia: A Cross-Sectional Controlled Study. *Calcif Tissue Int* 2019; **104**: 591-598 [PMID: 30710161 DOI: 10.1007/s00223-019-00526-z]

11 **Maly IP**, Eppler E, Müller-Gerbl M. High metabolic activity of tissue-nonspecific alkaline phosphatase not only in young but also in adult bone as demonstrated using a new histochemical detection protocol. *Gen Comp Endocrinol* 2018; **258**: 109-118 [PMID: 28502741 DOI: 10.1016/j.ygcen.2017.05.008]

12 **Vallet S**, Hoyle NR, Kyle RA, Podar K, Pecherstorfer M. A role for bone turnover markers β-CrossLaps (CTX) and amino-terminal propeptide of type I collagen (PINP) as potential indicators for disease progression from MGUS to multiple myeloma. *Leuk Lymphoma* 2018; **59**: 2431-2438 [PMID: 29345175 DOI: 10.1080/10428194.2017.1421757]

13 **Singh P**, Taufeeq M, Pesavento TE, Washburn K, Walsh D, Meng S. Comparison of the glucagon-like-peptide-1 receptor agonists dulaglutide and liraglutide for the management of diabetes in solid organ transplant: A retrospective study. *Diabetes Obes Metab* 2020; **22**: 879-884 [PMID: 31943645 DOI: 10.1111/dom.13964]

14 **Frías JP**. Tirzepatide: a glucose-dependent insulinotropic polypeptide (GIP) and glucagon-like peptide-1 (GLP-1) dual agonist in development for the treatment of type 2 diabetes. *Expert Rev Endocrinol Metab* 2020; **15**: 379-394 [PMID: 33030356 DOI: 10.1080/17446651.2020.1830759]

15 **Andrikou E**, Tsioufis C, Andrikou I, Leontsinis I, Tousoulis D, Papanas N. GLP-1 receptor agonists and cardiovascular outcome trials: An update. *Hellenic J Cardiol* 2019; **60**: 347-351 [PMID: 30528435 DOI: 10.1016/j.hjc.2018.11.008]

16 **Granhall C**, Donsmark M, Blicher TM, Golor G, Søndergaard FL, Thomsen M, Bækdal TA. Safety and Pharmacokinetics of Single and Multiple Ascending Doses of the Novel Oral Human GLP-1 Analogue, Oral Semaglutide, in Healthy Subjects and Subjects with Type 2 Diabetes. *Clin Pharmacokinet* 2019; **58**: 781-791 [PMID: 30565096 DOI: 10.1007/s40262-018-0728-4]

17 **Mhalhal TR**, Washington MC, Newman KD, Heath JC, Sayegh AI. Combined gastrin releasing peptide-29 and glucagon like peptide-1 reduce body weight more than each individual peptide in diet-induced obese male rats. *Neuropeptides* 2018; **67**: 71-78 [PMID: 29180139 DOI: 10.1016/j.npep.2017.11.009]

18 **Buyukterzi Z**, Can U, Alpaydin S, Guzelant A, Karaarslan S, Mustu M, Kocyigit D, Gurses KM. Enhanced serum levels of matrix Gla protein and bone morphogenetic protein in acute coronary syndrome patients. *J Clin Lab Anal* 2018; **32** [PMID: 28605143 DOI: 10.1002/jcla.22278]

19 **Zhang Y**, Cai S, Tseng SCG, Zhu YT. Isolation and Expansion of Multipotent Progenitors from Human Trabecular Meshwork. *Sci Rep* 2018; **8**: 2814 [PMID: 29434243 DOI: 10.1038/s41598-018-21098-2]

20 **Kühnisch J**, Seto J, Lange C, Stumpp S, Kobus K, Grohmann J, Elefteriou F, Fratzl P, Mundlos S, Kolanczyk M. Neurofibromin inactivation impairs osteocyte development in Nf1Prx1 and Nf1Col1 mouse models. *Bone* 2014; **66**: 155-162 [PMID: 24947449 DOI: 10.1016/j.bone.2014.06.012]

World Journal of Clinical Cases

Submit a Manuscript: https://www.f6publishing.com

World J Clin Cases 2022 February 16; 10(5): 1536-1547

DOI: 10.12998/wjcc.v10.i5.1536

ISSN 2307-8960 (online)

ORIGINAL ARTICLE

Retrospective Study

Castleman disease and TAFRO syndrome: To improve the diagnostic consciousness is the key

Qian-Yun Zhou

ORCID number: Qian-Yun Zhou 0000-0003-0157-7752.

Author contributions: Zhou QY designed the research, collected and analyzed data, and wrote the paper.

Institutional review board statement: This study was approved by the Ethics Committee of Peking University Shougang Hospital (approval number: IRBK-2021-010-01).

Informed consent statement: Written informed consent was waived by the Ethics Committee of Peking University Shougang Hospital for retrospective nature of the study.

Conflict-of-interest statement: We have no financial relationships to disclose.

Data sharing statement: The datasets used and/or analyzed during the current study are available from the corresponding author on reasonable request.

Supported by the Key Medical Projects of Technical College Development of Shijingshan District.

Country/Territory of origin: China

Qian-Yun Zhou, Department of Critical Care Medicine, Peking University Shougang Hospital, Beijing 100144, China

Corresponding author: Qian-Yun Zhou, MD, Doctor, Department of Critical Care Medicine, Peking University Shougang Hospital, No. 9 Jinyuan Zhuang Road, Shijingshan District, Beijing 100144, China. 13521349450@163.com

Abstract

BACKGROUND

Castleman disease (CD) and TAFRO syndrome are very rare in clinical practice. Most clinicians, especially non-hematological clinicians, do not know enough about the two diseases, so it often leads to misdiagnosis or missed diagnosis.

AIM

To explore the clinical features and diagnosis of CD and TAFRO syndrome.

METHODS

We retrospectively collected the clinical and laboratory data of 39 patients who were diagnosed with CD from a single medical center.

RESULTS

Clinical classification identified 18 patients (46.15%) with unicentric Castleman disease (UCD) and 21 patients (53.85%) with multicentric Castleman disease (MCD), the latter is further divided into 13 patients (33.33%) with idiopathic multicentric Castleman disease-not otherwise specified (iMCD-NOS) and 8 patients (20.51%) with TAFRO syndrome. UCD and iMCD are significantly different in clinical manifestations, treatment, and prognosis. However, a few patients with MCD were diagnosed as UCD in their early stage. There was a correlation between two of Thrombocytopenia, anasarca and elevated creatinine, which were important components of TAFRO syndrome. In UCD group, the pathologies of lymph modes were mostly hyaline vascular type (13/18, 72.22%), however plasma cell type or mixed type could also appear. In iMCD-NOS group and TAFRO syndrome group, the pathologies of lymph mode shown polarity of plasma cell type and hyaline vascular type respectively. Compared with patients with TAFRO syndrome, patients with iMCD-NOS were diagnosed more difficultly.

CONCLUSION

Specialty type: Emergency medicine

Provenance and peer review: Unsolicited article; Externally peer reviewed

Peer-review model: Single blind

Peer-review report's scientific quality classification

Grade A (Excellent): A
Grade B (Very good): B
Grade C (Good): 0
Grade D (Fair): 0
Grade E (Poor): 0

Received: August 23, 2021
Peer-review started: August 23, 2021
First decision: October 16, 2021
Revised: October 29, 2021
Accepted: January 5, 2022
Article in press: January 5, 2022
Published online: February 16, 2022

P-Reviewer: Corte-Real A, Srivastava D
S-Editor: Zhang H
L-Editor: A
P-Editor: Zhang H

The clinical and pathological types of CD are not completely separate, there is an intermediate situation or mixed characteristics between two ends of clinical and pathological types. The clinical manifestations of patients with CD are determined by their pathological type. TAFRO syndrome is a special subtype of iMCD with unique clinical manifestations.

Key Words: Castleman disease; Diagnosis; Lymph node biopsy; TAFRO syndrome

Core Tip: This study is a real-world study. Through a retrospective analysis of the diagnosis and treatment process of 39 patients with Castleman disease (CD), we conclude that the clinical classification and pathological classification of CD are not completely independent, and there is an intermediate state or transition state between the two extreme manifestations. TAFRO syndrome is still classified as a special subtype of idiopathic multicentric Castleman disease (iMCD). TAFRO syndrome is easier to identify than iMCD-not otherwise specified because of its unique pathological and clinical features.

Citation: Zhou QY. Castleman disease and TAFRO syndrome: To improve the diagnostic consciousness is the key. *World J Clin Cases* 2022; 10(5): 1536-1547
URL: https://www.wjgnet.com/2307-8960/full/v10/i5/1536.htm
DOI: https://dx.doi.org/10.12998/wjcc.v10.i5.1536

INTRODUCTION

Emergency medicine is a symptomatic discipline. The diagnosis and differential diagnosis of diseases need the combination of general thinking and specialized knowledge, while lymph node enlargement is an area often involved in the differential diagnosis of diseases. A disease in this field has gained increasing attention of doctors in recent years, namely, Castleman disease (CD). CD is reactive lymphadenopathy with unknown causes. It was first officially reported by Professor Castleman in 1954. The reported lesion was a tumor-like mass confined to the mediastinum. Histology shown obvious hyperplasia of lymphoid follicles and capillaries[1]. In 1969, Flendrig *et al*[2] proposed another morphological subtype of CD characterized by plasma cell proliferation and often accompanied by systemic symptoms. With the deepening of clinical and pathological research, CD was clinically divided into unicentric CD (UCD) and multicentric CD (MCD)[3,4]; Pathologically, it was divided into hyaline vascular type, plasma cell type, and mixed type. UCD generally involves only a single lymph node region, and the pathological type is mostly hyaline vascular type, mainly relying on surgical treatment. MCD mostly involves multiple lymph node regions. The pathological type is mostly plasma cell type, accompanied by systemic symptoms. Drugs are the main treatment.

From 2004 to 2005, Kojima *et al*[5,6] reported many cases of cryptogenic MCD and pointed out that unlike Western researchers who reported that MCD was mostly human herpesvirus (HHV)-8 positive, Japanese MCD was mostly HHV-8 negative, that is, idiopathic multicentric Castleman disease (iMCD). In 2008, Kojima *et al*[7] classified 28 patients with iMCD into idiopathic plasmacytic lymphadenopathy (IPL) and non-IPL according to their pathological characteristics and summarized their clinical characteristics. In 2010, Takai *et al*[8] first named TAFRO syndrome: T (thrombocytopenia), A (anasarca), F (fever), R (reticulin fibrosis), and O (organomegaly). In 2012, the Fukushima and Nagoya conferences in Japan clearly defined TAFRO syndrome as a systemic inflammatory disease accompanied by a series of clinical symptoms such as thrombocytopenia, systemic edema, myelofibrosis, renal dysfunction, and organ enlargement[9]. Studies have found that the non-IPL MCD reported by Carbone *et al*[10] is highly similar to TAFRO syndrome in clinical features, therefore, TAFRO syndrome is also called Caslteman–Kojima disease. In 2016, Iwaki *et al*[11] divided iMCD into TAFRO syndrome and unspecified iMCD (idiopathic multicentric Castleman disease-not otherwise specified, iMCD-NOS).

TAFRO syndrome was first proposed by Japanese scholars, and subsequent reports and studies were mainly came from Japan[12]. At present, the most authoritative diagnostic criteria for TAFRO syndrome were put forward by Iwaki *et al*[11] and Masaki *et al*[13] respectively in 2016, and Masaki *et al*[14] updated the diagnostic criteria in 2019.

The research on iMCD and TAFRO syndrome is still in the clinical exploration stage, and its etiology and pathogenesis are unclear. TAFRO syndrome or MCD is rare clinically, patients often seek medical treatment with systemic symptoms, and non-hematological doctors often do not know enough about this disease. Hence, it is easy to cause misdiagnosis or missed diagnosis. In 2020, we reported two consecutive cases who were diagnosed with TAFRO syndrome according to their findings of lymph node and renal biopsy[15]. To further understand the clinical features of various types of CD and the internal relationship between TAFRO syndrome and iMCD, we collected CD cases diagnosed and treated in Peking University People's Hospital in the last 5 years and etrospectively analyzed their clinical data.

MATERIALS AND METHODS

Ethics

This study was approved by the Ethics Committee of Peking University Shougang Hospital (approval number: IRBK-2021-010-01). Written informed consent was waived by the Ethics Committee of Peking University Shougang Hospital for retrospective nature of the study.

Criteria

The selection of CD cases mainly depended on the pathological diagnosis. Patients with single or multiple lymph node enlargement in a single region were classified as UCD, and patients with lymph node enlargement in two or more regions were classified as MCD.

The diagnosis criteria of TAFRO syndrome adopted the updated Masaki standard in 2019[14] which were shown in Table 1.

Patients

Using "Castleman disease" or "TAFRO syndrome" as the key words, with either of them included in discharge diagnosis,we searched in the inpatient medical record system from January 2015 to October 2019. 48 cases were eligibable. The exclusion criteria were as follows: (1) no lymph node biopsy results, and CD was a clinically suspected diagnosis; (2) CD was a previous diagnosis, not the cause of this admission; (3) other definite diagnosis were present, such as POEMS syndrome (P, polyneuropathy; O, organomegaly; E, endocrinopathy; M, monoclonal; S, skin changes), lymphoma, systemic lupus erythematosus (SLE), *etc.*; (4) authoritative pathological institutions denied the diagnosis of CD; and (5) age < 18 years. A total of nine cases (including one case of POEMS syndrome, one case of lymphoma, two cases of SLE, one case of Sjogren's syndrome, one case with a past history of CD, one case without lymph node biopsy, and two cases with uncertain clinical diagnosis). Finally, 39 cases were enrolled.

Statistical analysis

SPSS 23.0 was used for statistical analysis. Counting data were expressed as a constituent ratio or percentage, and measurement data were expressed as mean ± SD (normal-distribution data) or median and quartile (non-normal-distribution data). The difference analysis was performed using t test (normal-distribution measurement data), nonparametric test (non-normal-distribution measurement data), and Fisher accurate test (sample size less than 40, counting data or classified variables). $P < 0.05$ indicated that the difference was statistically significant.

RESULTS

See Table 2. The enrolled patients were all Chinese, mainly distributed in North China. Both HHV-8 and human immunodeficiency virus (HIV) were negative. The rage of age was from 21 years to 80 years. The average age of the three groups was not statistically significantly different. But the minimum and maximum age were distributed in

Table 1 Diagnostic criteria for TAFRO syndrome proposed by Masaki *et al* (updated in 2019)

Diagnostic criteria for TAFRO syndrome
Primary criteria
Edema: Including pleural and abdominal effusion and systemic edema
Thrombocytopenia: Platelet count ≤ 10^5/uL before myelosuppression
Systemic inflammation: Fever of unknown origin, body temperature exceeding 37.5°C, and/or serum CRP ≥ 2 mg/dL
Secondary criteria
Pathological manifestations of CD-like lymph nodes
Bone marrow reticular fibrosis and/or increased bone marrow megakaryocyte count
Mild organ enlargement: Including liver, spleen, and lymph node enlargement
Progressive renal dysfunction
TAFRO syndrome can be diagnosed after meeting at least two of all three main criteria and four secondary criteria, and excluding malignant tumor, autoimmune disease, infection, POEMS syndrome, liver cirrhosis, TTP/HUS, *etc.*

CRP: C-reactive protein; CD: Castleman disease; TTP: Thrombotic thrombocytopenic purpura; HUS: Hemolytic uremic syndrome.

the iMCD-NOS group, including the only child patient (< 18 years old) enrolled in this study. The ratio of male and female in three grops was similar. Urban patients were dominant in the UCD group, while rural patients were dominant in the TAFRO syndrome group. A statistically significant difference was found between the two groups.

UCD

Most patients with UCD were diagnosed by chance or by physical examination (10/18, 55.56%), followed by symptoms caused by enlarged lymph node compression, including irritating dry cough (3/18, 16.67%), local pain (2/18, 11.11%), obstructive jaundice (1/18, 5.56%), and chest tightness (1/18, 5.56%). The distribution of enlarged lymph nodes is shown in Figure 1. Only a few patients also had a fever (2/18, 11.11%).

The patients with intraperitoneal lymphadenopathy would be at risk to have more complicated conditions than those with lymphadenopathy in other areas. 5 of 18 cases had complications, which were pancreatic cancer, paraneoplastic pemphigus and bronchiolitis obliterans, acute myeloid leukemia-M_2, thyroid cancer, and bronchiolitis obliterans respectively. The locations of lymphadenopathy in the first 3 patients with complications were retroperitoneal and/or intraperitoneal.

Because C-creative protein, direct antiglobulin test, interleukin (IL)-6, and vascular endothelial growth factor (VEGF) were not tested in most cases, we hadn't made statistical analysis for these indicators. All 18 patients underwent a lymph node biopsy. Most of them were hyaline vascular type (13/18, 72.22%), and a few were plasma cell type/mixed type (5/18, 27.78%). Compared with patients with hyaline vascular type, patients with plasma cell type/mixed-type UCD were more prone to have laboratory abnormalities and complications, as shown in Figure 2.

iMCD

Most patients with iMCD (18/21, 85.71%) had a fever, and fever was the first symptom in 15 patients (71.43%). Skin complications (10/39, 25.64%) were recorded in the course of 9 cases diagnosed with iMCD, including red papules (7/21, 33.33%) which were often treated as an allergy, mouth ulcer or skin blisters at hand which were diagnosed with paraneoplastic pemphigus (2/21, 4.76%). Kidney involvement was common, and most patients showed positive urine protein and/or occult blood (14/21, 66.67%), among which three cases had massive proteinuria (urine protein level more than 2 g in 24 h). The creatinine levels increased in 9 cases, of which two patients were treated with renal replacement therapy and the other seven patients had an slight and transient elevation of creatinine level.

TAFRO syndrome

By analyzing the clinical manifestations of patients with iMCD, we found that the triad of thrombocytopenia, anasarca (polyserositis and edema) and renal insufficiency, which were exactly the core components of TAFRO syndrome, often occurred at the

Table 2 Basic clinical data of 39 patients with Castleman disease (*n* = 39)

	UCD (*n* = 18)	iMCD-NOS (*n* = 13)	TAFRO (*n* = 8)	*P* value
Age (yr)	41.17 ± 18.23	47.23 ± 22.09	40.50 ± 9.04	0.530
Male/female	10/8	7/6	4/4	1.000
Rural/urban	5/13[a]	6/7	6/2[a]	0.085
Time of diagnosis (median, months)	NA	12	1	0.000
Systemic manifestations				
Fever	2	10	8	
Splenomegaly	0	5	3	
Edema/polyserous cavity effusion	0	0	8	
Bronchiolitis obliterans	2	0	0	
Rash	0	5	3	
Paraneoplastic pemphigus	1	1	0	
Abnormal renal function	0	1	7	
Laboratory examination				
White blood cell[1]				
Decreased	0	2	0	
Raise	1	4	3	
Hemoglobin[1]				0.000
Decrease (*n*)	2			
Average (g/L)	132.00 ± 19.985	99.31 ± 27.41	79.57 ± 21.08	
Platelet[1]				
Decreased	0	3	8t	
Raise	2	6	0	
CRP (mg/L)	NA	91.09 ± 59.14	141.55 ± 64.31	0.000
Albumin (g/L)[1]	39.61 ± 5.52	31.65 ± 7.39	22.79 ± 9.26	0.000
Direct anti-human ball test was positive (*n*, %)	NA	9/13	6/6	
IL-6 (median, pg/mL) (*n*)	NA	47.35 (8)	12.65 (8)	0.040
VGEF (median, pg/mL) (*n*)	NA	NA	> 800 (5)	
Ferritin > five times normal value	NA	4/13	1/8	
Elevated LDH	0	2	2	
Elevated ALP	1/18	3/13	6/8	
ANA positive (titer > 1:40)	2/18	8/13	2/8	
Elevated polyclonal immunoglobulin	0	9/13	1/8	
Hemophilia syndrome	0	0	1/8	
Pathological type				
Hyaline vascular type	13	0	5/8	
Plasma cell type	3	4	0	
Mixed type	2	9	2/8	
No evidence of lymph node biopsy	0	0	1/8	
Treatment				
Biopsy only, treatment unknown	0	5	0	

Symptomatic treatment only	0	0	1
Simple surgical resection	18	0	0
Glucocorticoid alone	0	2	3
Hormones combined with chemotherapy[2]	0	5[1]	2
Hormone combined with rituximab	0	0	1
Hormone combined with tozumab	0	1	1
Prognosis			
Loss of contact	0	3	0
Improved	16	6	7
Relapse	0	0	1
Solid cancer occurred during the follow-up	2[b]	1[c]	0
Transformation into lymphoma	0	1[d]	0
Death	0	2	0

[a]A statistically significant difference between the two groups.
[b]Two cases with pancreatic head cancer and thyroid.
[c]One case with pancreatic cancer.
[d]One case with non-Hodgkin lymphoma.
[1]Normal reference value: white blood cell count 3.5–9.5 × 10^9/L; hemoglobin 130–175 g/L (male), 115–150 g/L (female); platelet count 125–350 × 10^9/L; 40–55 g/L albumin.
[2]Chemotherapy regimens included CP (cyclophosphamide + prednisone), COP (cyclophosphamide + ciac/vincristine + prednisone), and CHOP (cyclophosphamide + doxorubicin + vincristine + prednisone).
iMCD-NOS: Idiopathic multicentric Castleman disease-not otherwise specified; UCD: Unicentric Castleman disease; ALP: Alkaline phosphatase; ANA: Antinuclear antibody; CRP: C-reactive protein; IL-6: Interleukin 6; LDH: Lactate dehydrogenase; VGEF: Vascular endothelial growth factor.

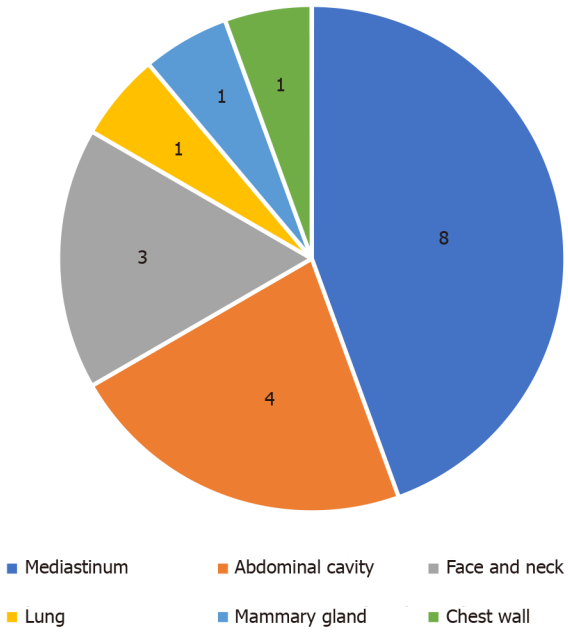

Figure 1 Distribution of enlarged lymph nodes in patients unicentric Castleman disease (*n* = 18).

same time or in succession in the same patient. The correlations between two variables of the triad were verified by Fisher's exact probability method ($P < 0.05$). 8 patients finally met the diagnostic criteria of TAFRO syndrome proposed by Masaki *et al*.

The clinical data and the diagnosis process of patients with TAFRO syndrome or iMCD-NOS were compared (Table 1 and Figures 3-5): (1) IL-6 and VEGF levels: Patients in iMCD-NOS group were more likely to show higher levels of IL-6 in blood than those with TAFRO syndrome because of the higher average rank of serum IL-6 Levels in iMCD-NOS group ($P < 0.05$).Because blood VEGF level was not a routine test

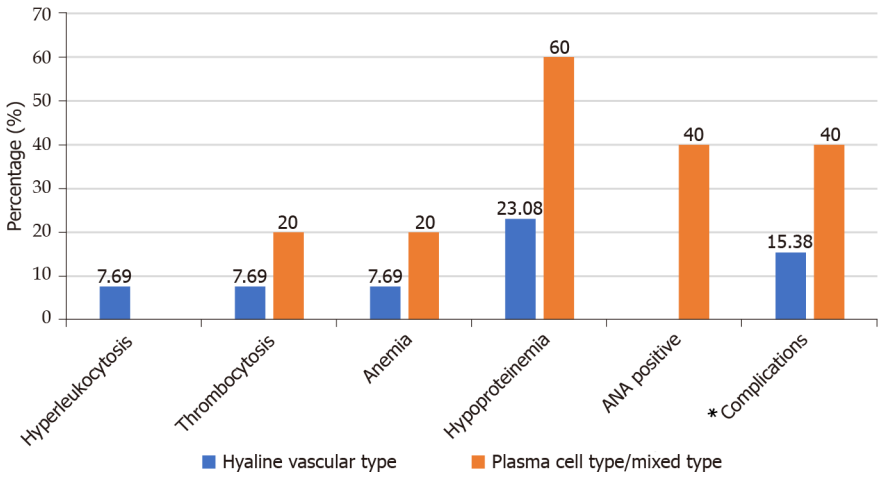

Figure 2 Relationship between unicentric Castleman disease clinical manifestations and pathological classification (*n* = 18). *Complications include paraneoplastic pemphigus, malignant tumor, bronchiolitis obliterans, *etc.*

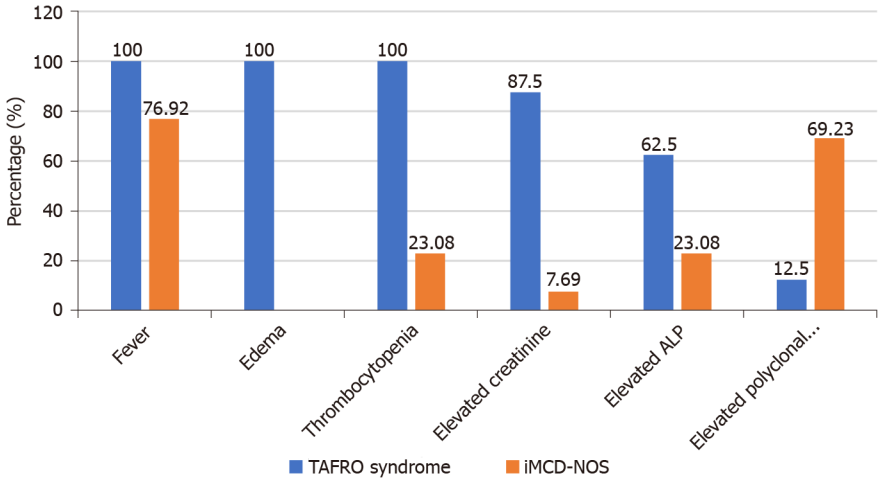

Figure 3 Comparison of clinical manifestations between TAFRO syndrome (*n* = 8) and idiopathic multicentric Castleman disease-not otherwise specified (*n* = 13).

in our hospital, so the records of serum VEGF levels only could be found in five patients diagnosed with TAFRO syndrome, all of the five patients showed significantly elevated serum VEGF levels (four cases > 800 pg/mL, one case 231.47 pg/mL); (2) Diagnosis process: The median time interval from onset to diagnosis in iMCD-NOS group was significantly prolonged than that in TAFRO syndrome group. In TAFRO syndrome group, except for one patient who rejected the suggestion of lymph node biopsy and renal biopsy at 1 mo after the onset of his symptoms; the other seven patients were all diagnosed within 1 to 1.5 mo after the onset of their symptoms. Among patients with iMCD-NOS, the median interval from the onset of their symptoms to the diagnosis of CD was 12 mo with the minimum and maxmum being 1 mo and 4 years respectively. The average time of lymph node biopsies and pathological consultations of iMCD-NOS group (1.69 and 2.38, respectively) were more than those of TAFRO syndrome group (1 and 1.375, respectively) ($P < 0.05$), and the poor consistencies of consultations were more likely happened in iMCD-NOS group (Figure 5).

Renal biopsies were performed in three patients who were diagnosed with TAFRO syndrome. Those findings of biopsies of lymph nodes and renal were thrombotic microangiopathy (TMA) and hyalin vascular type, TMA and absence, and membrano proliferative glomerulonephritis and mixed type, respectively.

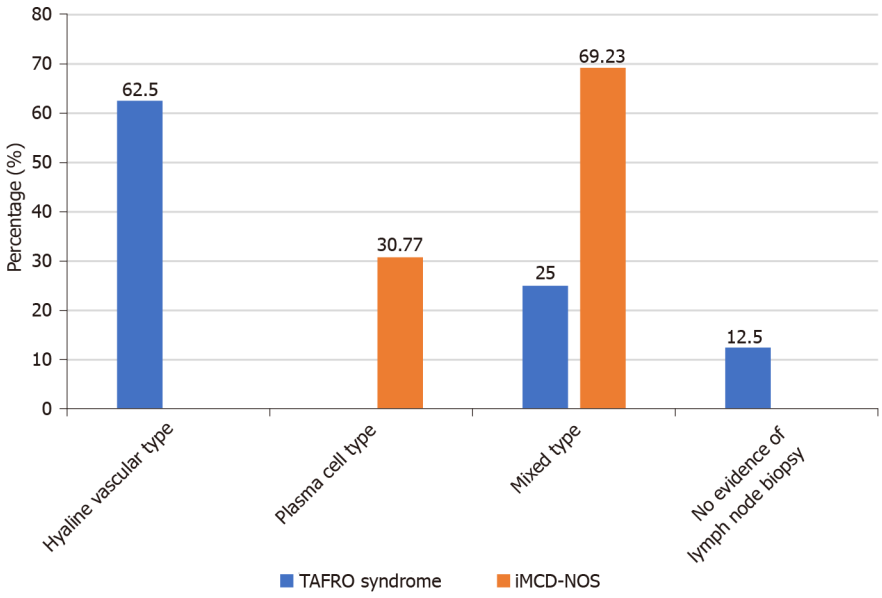

Figure 4 Comparison of pathological classification of TAFRO syndrome (*n* = 8) and idiopathic multicentric Castleman disease-not otherwise specified (*n* = 13).

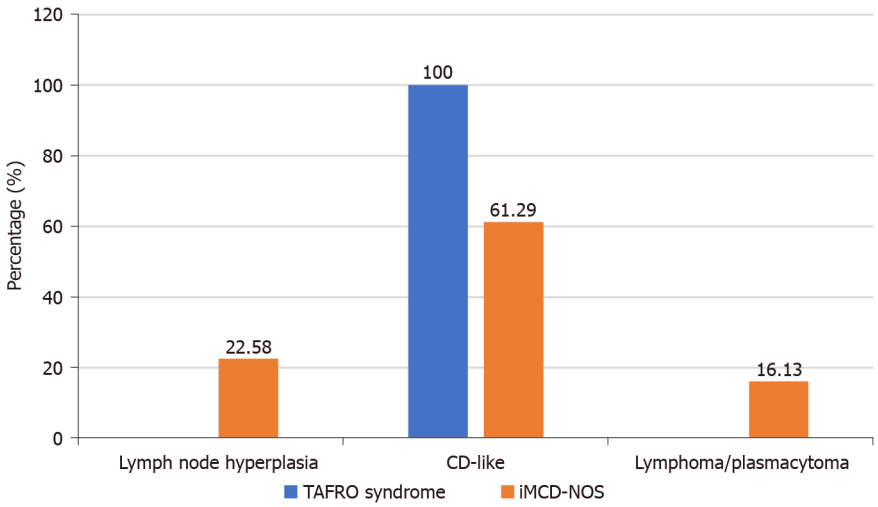

Figure 5 Comparison of distribution of lymph node pathological results in patients with idiopathic multicentric Castleman disease.

DISCUSSION

The study of CD has gone through the following stages: naming of CD for the first time[1]-the discovery of plasma cell type[2]–the discovery of MCD[3]–recognition of HIV as one of the causes of MCD[16,17]–proposal of the concept of iMCD[18]–proposal of the concept of TAFRO syndrome[8]. Although more than 60 years have passed since CD was proposed, the understanding of CD is still in the exploratory stage. What is the nature of CD? What are the internal relations and differences between different clinical and pathological types of CD? Can UCD tranform into MCD? TAFRO syndrome is a special subtype of iMCD? Or is it just a new special group whose clinical manifestations overlap with iMCD and are different from iMCD? The aforementioned problems are the focus of discussion in our study.

UCD and MCD are significantly different in clinical manifestations, treatment, and prognosis. However, these two clinical types are not completely independent: (1) There is an intermediate situation existing between single lymph node enlargement and multicentric lymph node enlargement, that is, multiple lymph node enlargement in a single region. At present, the latter is still classified as UCD, but what we need to think about is whether this single-region multiple lymph node enlargement is an intermediate or transitional state between single lymph node enlargement and

multicenter lymph node enlargement. Oksenhendler *et al*[19] compared 38 cases of UCD with single lymph node enlargement and 19 cases of UCD with multiple lymph node enlargement in a single center. The results showed that five cases with fever and two cases with death all distributed in the latter; (2) UCD may be the early stage of MCD: Two patients diagnosed with MCD were enrolled in our study that were diagnosed with UCD and underwent surgical resection in their past history. Therefore, for patients diagnosed with UCD, the scan of systemic lymph nodes and the careful following-up should be necessary to rule out MCD; (3) Some clinical manifestations of UCD and iMCD overlap, such as PNP and ANA positive, which also suggests that UCD and iMCD are not completely independent[20].

The pathological types of CD, namely hyalin vascular type and plasma cell type, are not completely independent too. Typical hyalin vascular type and plasma cell type are two extremes of a pathological spectrum consistent with a CD, which are characterized by hyalinization of small blood vessels and interfollicular plasmacytosis respectively. However many patients may show mixed characteristics, that is mixed type. Patients with hyaline vascular type usually could have a definite diagnosis according to its specific morphology. Nevertheless, plasma cell type is not a specific morphological feature of CD. Many diseases, such as autoimmune diseases (SLE and IgG4-related diseases), POEMS syndrome, plasma cell tumor, and non-Hodgkin lymphoma, all can show pathological features similar with plasma cell type of CD. Therefore, the diagnosis of CD of plasma cell type must require the combination of clinical and pathology[21,22]. Our study also showed that the patients with iMCD-NOS usually lacked specific clinical manifestations, and their lymph node pathology often needed to be differentiated from reactive lymph node hyperplasia and plasmacytoma /Lymphoma, which led to a significantly longer time interval from onset to diagnosis and a less consistency of diagnosis from different institution than those with TAFRO syndrome.

TAFRO syndrome was first proposed as a special subtype of iMCD[8]. The patients with TAFRO syndrome usually showed a group of similar clinical features which included thrombocytopenia, renal dysfunction, systemic edema and polyserous cavity effusion. Compared with those with iMCD-NOS, they were more likely to have a more acute course of disease, a worse general condition at the time of onset, smaller lymph nodes, not-elevated blood immunoglobulin levels, lower IL-6 levels in the serum, and higher levels of VEGF in the serum[11]. The lymph node pathology of patients with TAFRO syndrome reported in the literature was usually hyaline vascular type or mixed type, while the pathology of patients with iMCD-NOS was usually plasma cell type[13,23]. At present, the most authoritative diagnostic criteria for TAFRO syndrome are the Iwaki's criteria and the Masaki's criteria. These two diagnostic criteria have divergence on whether the pathological feature of lymph node in conformity with CD being necessary of diagnosis. Iwaki *et al*[11] advocated that TAFRO syndrome should be classified as a special subtype of iMCD, and pathological compliance with CD should be a necessary part of diagnosis of TAFRO syndrome. In Iwaki's criteria, the pathological features of lymph node of patients with TAFRO syndrome were defined as atrophy of the germinal center with enlargement of endothelial cell nucleus, proliferation of interfollicular endothelial vein, and rare mature plasma cells. Masaki *et al*[13,14] believed that the clinical manifestations of patients with TAFRO syndrome were quite different from those with iMCD, so they advocated that TAFRO syndrome might be a special group that overlapped with iMCD but was different from iMCD. In Masaki's criteria, pathological feature of lymph node was only regarded as one of the four secondary criteria rather than an essential part of diagnosis. Their explanation was that biopsy of lymph node might be unachievable for some patients due to anasarca, bleeding tendency or the smallness of the target lymph node, however early diagnosis and appropriate treatment without delay would be essential for favorable outcomes. We don't think the two diagnostic criteria are in conflict in essence. The pathological features of patients with TAFRO syndrome reported by Masaki *et al*[13] were consistent with those reported by Iwaki *et al*[11]. Masaki *et al*[13] reported that the pathological classifications of most patients with TAFRO syndrome were mixed type, and a few were hyaline vascular type. Our study also confirmed that the special clinical manifestations of patients with TAFRO syndrome were determined by their pathological features. In our study, we screened patients whose clinical characteristics were in conformity with the definition of TAFRO syndrome (thrombocytopenia, multiple serosal effusion/edema, and renal insufficiency). The results showed that the pathological types of lymph nodes of 7 patients with TAFRO syndrome whose pathology of lymph nodes were achievable were as hyaline vascular type (5/8, 62.5%) and mixed type (2/8, 25%).

Except the role of pathological features, there are two other differences between Iwaki's criteria and Masaki's criteria which are gamma globulinemia and renal insufficiency. The level of gamma globulin in the serum being not-elevated was regarded as one major category in Iwaki's criteria but was not mentioned in Masaki's criteria. On the contrary, progressive renal insufficiency was regarded as one minor category in Masaki's criteria as with pathological features but while was not mentioned in Iwaki's criteria. We advocate that whether patients be diagnosed with TAFRO syndrome should be based on the combination of clinical manifestations and pathological features of patients, and the focus should be on the nature of the syndrome rather than be confined to a specific diagnosis item. In the series of TAFRO syndrome cases of our study, one patient was diagnosed according to his massive proteinuria and TMA feature of renal biopsy although biopsy of lymph node was absent. Another patient was diagnosed according to his typical clinical manifestations (thrombocytopenia, renal dysfunction, anasarca and polyserous cavity effusion) and pathological feature of lymph node being hyaline vascular type although the polyclonal gamma globulin level was slightly elevated.

The present study has several obvious limitations. First, it was a retrospective study and some laboratory data were not available. Second, A bias is inevitable because the CD patient population come from a single medical centre and the sample size is small. Despite these limitations, this study provides a useful panoramic view of CD and attempt to probe into the internal relationship between various types of CD.

CONCLUSION

In conclusion, the etiology and pathogenesis of both CD and TAFRO syndrome remain unclear. Further clinical and pathophysiological evidence are necessary for understanding this new entity. At the same time, clinicians, especially non-hematology specialists, should pay more attention to this entity and improve the awareness of diagnosis.

ARTICLE HIGHLIGHTS

Research background

Castleman disease (CD) and TAFRO syndrome are very rare in clinical practice. Most clinicians, especially non-hematological clinicians, do not know enough about the two diseases, so it often leads to misdiagnosis or missed diagnosis.

Research motivation

What is the nature of CD? What are the internal relations and differences between different clinical and pathological types of CD? Can unicentric Castleman disease (UCD) transform into multicentric Castleman disease (MCD)? TAFRO syndrome is a special subtype of idiopathic MCD (iMCD)? Or is it just a new special group whose clinical manifestations overlap with iMCD and are different from iMCD? The aforementioned problems are the research motivation of our study.

Research objectives

This study aimed to explore the clinical features and diagnosis of CD and TAFRO syndrome.

Research methods

We retrospectively collected the clinical and laboratory data of 39 patients who were diagnosed with CD from a single medical center.

Research results

UCD and iMCD are significantly different in clinical manifestations, treatment, and prognosis. However, a few patients with MCD were diagnosed as UCD in their early stage. There was a correlation between two of Thrombocytopenia, anasarca and elevated creatinine, which were important components of TAFRO syndrome. In UCD group, the pathologies of lymph modes were mostly hyaline vascular type (13/18, 72.22%), however plasma cell type or mixed type could also appear. In iMCD-NOS group and TAFRO syndrome group, the pathologies of lymph mode shown polarity of

plasma cell type and hyaline vascular type respectively. Compared with patients with TAFRO syndrome, patients with iMCD-NOS were diagnosed more difficultly.

Research conclusions

The clinical and pathological types of CD are not completely separate, there is an intermediate situation or mixed characteristics between two ends of clinical and pathological types. The clinical manifestations of patients with CD are determined by their pathological type. TAFRO syndrome is a special subtype of iMCD with unique clinical manifestations.

Research perspectives

In the future, further research should be carried out on the pathological manifestations of lymph nodes and kidneys in patients with CD and TAFRO syndrome.

REFERENCES

1 **Castleman B**, Iverson L, Menendez VP. Localized mediastinal lymphnode hyperplasia resembling thymoma. *Cancer* 1956; **9**: 822-830 [PMID: 13356266 DOI: 10.1002/1097-0142(195607/08)9:4<822::aid-cncr2820090430>3.0.co;2-4]

2 **Flendrig J**, Schillings P. Benign giant lymphoma: the clinical signs and symptoms and the morphological aspectsy. *Folia Med Neerl* 1969; **12**: 119-120

3 **Frizzera G**, Banks PM, Massarelli G, Rosai J. A systemic lymphoproliferative disorder with morphologic features of Castleman's disease. Pathological findings in 15 patients. *Am J Surg Pathol* 1983; **7**: 211-231 [PMID: 6837832 DOI: 10.1097/00000478-198304000-00001]

4 **Weisenburger DD**, Nathwani BN, Winberg CD, Rappaport H. Multicentric angiofollicular lymph node hyperplasia: a clinicopathologic study of 16 cases. *Hum Pathol* 1985; **16**: 162-172 [PMID: 2579015 DOI: 10.1016/s0046-8177(85)80065-4]

5 **Kojima M**, Nakamura S, Shimizu K, Itoh H, Yamane Y, Murayama K, Tanaka H, Sugihara S, Shimano S, Sakata N, Masawa N. Clinical implication of idiopathic plasmacytic lymphadenopathy with polyclonal hypergammaglobulinemia: a report of 16 cases. *Int J Surg Pathol* 2004; **12**: 25-30 [PMID: 14765269 DOI: 10.1177/106689690401200104]

6 **Kojima M**, Nakamura S, Nishikawa M, Itoh H, Miyawaki S, Masawa N. Idiopathic multicentric Castleman's disease. A clinicopathologic and immunohistochemical study of five cases. *Pathol Res Pract* 2005; **201**: 325-332 [PMID: 15991840 DOI: 10.1016/j.prp.2005.01.006]

7 **Kojima M**, Nakamura N, Tsukamoto N, Otuski Y, Shimizu K, Itoh H, Kobayashi S, Kobayashi H, Murase T, Masawa N, Kashimura M, Nakamura S. Clinical implications of idiopathic multicentric castleman disease among Japanese: a report of 28 cases. *Int J Surg Pathol* 2008; **16**: 391-398 [PMID: 18499694 DOI: 10.1177/1066896908315812]

8 **Takai K**, Nikkuni K, Shibuya H, Hashidate H. [Thrombocytopenia with mild bone marrow fibrosis accompanied by fever, pleural effusion, ascites and hepatosplenomegaly]. *Rinsho Ketsueki* 2010; **51**: 320-325 [PMID: 20534952]

9 **Kawabata H**, Takai K, Kojima M, Nakamura N, Aoki S, Nakamura S, Kinoshita T, Masaki Y. Castleman-Kojima disease (TAFRO syndrome) : a novel systemic inflammatory disease characterized by a constellation of symptoms, namely, thrombocytopenia, ascites (anasarca), microcytic anemia, myelofibrosis, renal dysfunction, and organomegaly : a status report and summary of Fukushima (6 June, 2012) and Nagoya meetings (22 September, 2012). *J Clin Exp Hematop* 2013; **53**: 57-61 [PMID: 23801135 DOI: 10.3960/jslrt.53.57]

10 **Carbone A**, Pantanowitz L. TAFRO syndrome: An atypical variant of KSHV-negative multicentric Castleman disease. *Am J Hematol* 2016; **91**: 171-172 [PMID: 26663467 DOI: 10.1002/ajh.24274]

11 **Iwaki N**, Fajgenbaum DC, Nabel CS, Gion Y, Kondo E, Kawano M, Masunari T, Yoshida I, Moro H, Nikkuni K, Takai K, Matsue K, Kurosawa M, Hagihara M, Saito A, Okamoto M, Yokota K, Hiraiwa S, Nakamura N, Nakao S, Yoshino T, Sato Y. Clinicopathologic analysis of TAFRO syndrome demonstrates a distinct subtype of HHV-8-negative multicentric Castleman disease. *Am J Hematol* 2016; **91**: 220-226 [PMID: 26805758 DOI: 10.1002/ajh.24242]

12 **Coutier F**, Meaux Ruault N, Crepin T, Bouiller K, Gil H, Humbert S, Bedgedjian I, Magy-Bertrand N. A comparison of TAFRO syndrome between Japanese and non-Japanese cases: a case report and literature review. *Ann Hematol* 2018; **97**: 401-407 [PMID: 28956126 DOI: 10.1007/s00277-017-3138-z]

13 **Masaki Y**, Kawabata H, Takai K, Kojima M, Tsukamoto N, Ishigaki Y, Kurose N, Ide M, Murakami J, Nara K, Yamamoto H, Ozawa Y, Takahashi H, Miura K, Miyauchi T, Yoshida S, Momoi A, Awano N, Ikushima S, Ohta Y, Furuta N, Fujimoto S, Kawanami H, Sakai T, Kawanami T, Fujita Y, Fukushima T, Nakamura S, Kinoshita T, Aoki S. Proposed diagnostic criteria, disease severity classification and treatment strategy for TAFRO syndrome, 2015 version. *Int J Hematol* 2016; **103**: 686-692 [PMID: 27084250 DOI: 10.1007/s12185-016-1979-1]

14 **Masaki Y**, Kawabata H, Takai K, Tsukamoto N, Fujimoto S, Ishigaki Y, Kurose N, Miura K, Nakamura S, Aoki S; Japanese TAFRO Syndrome Research Team. 2019 Updated diagnostic criteria

and disease severity classification for TAFRO syndrome. *Int J Hematol* 2020; **111**: 155-158 [PMID: 31782045 DOI: 10.1007/s12185-019-02780-1]

15 **Zhou Q**, Zhang Y, Zhou G, Zhu J. Kidney biopsy findings in two patients with TAFRO syndrome: case presentations and review of the literature. *BMC Nephrol* 2020; **21**: 499 [PMID: 33225930 DOI: 10.1186/s12882-020-02119-7]

16 **Lowenthal DA**, Filippa DA, Richardson ME, Bertoni M, Straus DJ. Generalized lymphadenopathy with morphologic features of Castleman's disease in an HIV-positive man. *Cancer* 1987; **60**: 2454-2458 [PMID: 3478119 DOI: 10.1002/1097-0142(19871115)60:10<2454::aid-cncr2820601018>3.0.co;2-i]

17 **Oksenhendler E**, Duarte M, Soulier J, Cacoub P, Welker Y, Cadranel J, Cazals-Hatem D, Autran B, Clauvel JP, Raphael M. Multicentric Castleman's disease in HIV infection: a clinical and pathological study of 20 patients. *AIDS* 1996; **10**: 61-67 [PMID: 8924253]

18 **Fajgenbaum DC**, van Rhee F, Nabel CS. HHV-8-negative, idiopathic multicentric Castleman disease: novel insights into biology, pathogenesis, and therapy. *Blood* 2014; **123**: 2924-2933 [PMID: 24622327 DOI: 10.1182/blood-2013-12-545087]

19 **Oksenhendler E**, Boutboul D, Fajgenbaum D, Mirouse A, Fieschi C, Malphettes M, Vercellino L, Meignin V, Gérard L, Galicier L. The full spectrum of Castleman disease: 273 patients studied over 20 years. *Br J Haematol* 2018; **180**: 206-216 [PMID: 29143319 DOI: 10.1111/bjh.15019]

20 **Jia N**, Ping L, Rengui W, Liangchun W, Wanzhong Z. Clinicopathological Observation of Castleman's Disease. *Zhonghua Bing Li Xue Za Zhi* 2003; **32**: 521-524

21 **Yong L**, Guozhang C. Suggestions on Diagnostic Criteria of Castleman's Disease. *Zhonghua Bing Li Xue Za Zhi* 2013; **42**: 644-647 [DOI: 10.3760/cma.j.issn.0529-5807.2013.09.020]

22 **Frizzera G**. Atypical lymphoproliferative disorders. In: Knowles D. Neoplastic Hematopathology. 2 nd ed. Baltimore, MD: Lippincott William & Wilkins, 2000: 569-622

23 **Srkalovic G**, Marijanovic I, Srkalovic MB, Fajgenbaum DC. TAFRO syndrome: New subtype of idiopathic multicentric Castleman disease. *Bosn J Basic Med Sci* 2017; **17**: 81-84 [PMID: 28135567 DOI: 10.17305/bjbms.2017.1930]

World Journal of Clinical Cases

Submit a Manuscript: https://www.f6publishing.com

World J Clin Cases 2022 February 16; 10(5): 1548-1556

DOI: 10.12998/wjcc.v10.i5.1548

ISSN 2307-8960 (online)

ORIGINAL ARTICLE

Observational Study

Correlation of myopia onset and progression with corneal biomechanical parameters in children

Li-Li Lu, Xiao-Juan Hu, Yan Yang, Shen Xu, Shi-Yong Yang, Cui-Yu Zhang, Qing-Ya Zhao

ORCID number: Li-Li Lu 0000-0003-2713-1150; Xiao-Juan Hu 0000-0003-0562-8908; Yan Yang 0000-0002-4313-8275; Shen Xu 0000-0002-4650-6125; Shi-Yong Yang 0000-0001-5687-2818; Cui-Yu Zhang 0000-0001-5278-5629; Qing-Ya Zhao 0000-0003-0743-9430.

Author contributions: Lu LL contributed to study conception, design, and writing of the article; Hu XJ, Yang Y contributed to collection of clinical data; Xu S, Yang SY contributed to data acquisition, data analysis, and interpretation; Zhang CY, Zhao QY contributed to editing, reviewing, and final approval of the article.

Institutional review board statement: This study was approved by the Cangzhou Aier Eye Hospital Ethics Committee.

Informed consent statement: All study participants, or their legal guardian, provided informed written consent prior to study enrollment.

Conflict-of-interest statement: The authors declare that there is no conflict of interest to disclose.

Data sharing statement: No additional data are available.

STROBE statement: The authors

Li-Li Lu, Xiao-Juan Hu, Yan Yang, Shen Xu, Shi-Yong Yang, Cui-Yu Zhang, Qing-Ya Zhao, Department of Ophthalmology, Cangzhou Aier Eye Hospital, Cangzhou 061000, Hebei Province, China

Corresponding author: Li-Li Lu, MBChB, Attending Doctor, Department of Ophthalmology, Cangzhou Aier Eye Hospital, No. 35 Huanghe West Road, Yongan South Avenue, Yunhe District, Cangzhou 061000, Hebei Province, China. lili5lu@163.com

Abstract

BACKGROUND

Recent epidemiological studies have shown that general eye measurement parameters and corneal biomechanical properties can predict the speed of myopic progression in children.

AIM

To investigate the correlation between the onset and progression of myopia and corneal biomechanical parameters in children.

METHODS

The study included 102 cases in the emmetropia group, 207 cases in the myopic group, and 109 cases in the hyperopic group. The correlation between the change in corneal biomechanical indexes and the change in general ocular measurement parameters was analyzed. A one-way ANOVA test compared general ocular measurement and corneal biomechanical parameters. Pearson's correlation coefficient was analyzed to correlate corneal biomechanical and general ocular measurement parameters.

RESULTS

The general ophthalmometric parameters: Spherical equivalent (SE), intraocular pressure (IOP), and axial length (AL), differed significantly among subjects in myopia, emmetropia, and hyperopic groups. Children's SE positively correlated with corneal biomechanical parameters: Second velocity of applanation (A2V), peak distance (PD), and deformation amplitude (DA) ($P < 0.05$), and second applanation length (A2L) ($P < 0.05$). But it was negatively correlated with PD, DA and integral radius (IR) ($P < 0.05$). Also, IOP was negatively correlated with A2L and IR ($P < 0.05$). AL positively correlated with A2V and negatively correlated with second applanation time (A2T), highest concavity, and PD. Central corneal thickness positively correlated with first applanation length, first applanation

have read the STROBE Statement-checklist of items, and the manuscript was prepared and revised according to the STROBE Statement-checklist of items.

Country/Territory of origin: China

Specialty type: Ophthalmology

Provenance and peer review: Unsolicited article; Externally peer reviewed.

Peer-review model: Single blind

Peer-review report's scientific quality classification

Grade A (Excellent): 0
Grade B (Very good): B
Grade C (Good): C
Grade D (Fair): 0
Grade E (Poor): 0

Received: October 15, 2021
Peer-review started: October 15, 2021
First decision: December 1, 2021
Revised: December 15, 2021
Accepted: December 31, 2021
Article in press: December 31, 2021
Published online: February 16, 2022

P-Reviewer: Baird PN, Lee CH
S-Editor: Wang JL
L-Editor: A
P-Editor: Wang JL

time, first applanation deformation amplitude, A2V, A2L, A2T, second applanation deformation amplitude, central curvature radius at highest concavity (HCR), PD, DA, IR, ambrosia relational thickness-horizontal, first applanation stiffness parameter, corvis biomechanical index, topographic and biomechanics index and the first velocity of applanation. The general ocular Km in children positively correlated with corneal biomechanical parameters DA and IR and negatively correlated with A2L, HCR, and PD. There was a positive correlation between the general ocular measurement parameters ΔSE and corneal biomechanical parameters ΔA2V and ΔA2L, and a negative correlation with ΔIR. The increase in general ocular measurement parameter ΔKm positively correlated with changes in corneal biomechanical parameters, ΔDA and ΔIR, and negatively correlated with ΔHCR and ΔPD.

CONCLUSION
Myopia development in children was associated with multiple corneal biomechanical parameters.

Key Words: Children; Myopia; Corneal biomechanical parameters; Correlation

Core Tip: A total of 207 elementary school students aged 9-11 years, 142 males and 65 females, who presented to our hospital from November 2019 to April 2020, were enrolled for myopia study. We found a correlation between myopia development and various corneal biomechanical parameters in children. These findings may allow clinicians to take preventive measures to minimize a further increase in axial length.

Citation: Lu LL, Hu XJ, Yang Y, Xu S, Yang SY, Zhang CY, Zhao QY. Correlation of myopia onset and progression with corneal biomechanical parameters in children. *World J Clin Cases* 2022; 10(5): 1548-1556
URL: https://www.wjgnet.com/2307-8960/full/v10/i5/1548.htm
DOI: https://dx.doi.org/10.12998/wjcc.v10.i5.1548

INTRODUCTION

Refractive error is one of the leading causes of visual impairment in Chinese school-age children and is associated with a significant decrease in self-perceived visual function[1]. Patients with myopia, especially those with high myopia, could be much more likely to have serious complications, such as retinal detachment and open-angle glaucoma, than normal patients. Their reduced visual acuity and impaired visual function greatly affect their work, study, and daily activities. The progression of myopia is closely related to an increased eye axis. One possible reason for the accelerated growth of the eye axis is the weakening of the structure or function of the corneoscleral[2-5]. Therefore, the development of myopia may be related to corneoscleral stiffness, and the mechanical properties of the biological tissue play an important role in the increase of the ocular axis. Reducing scleral matrix metalloproteinase activity, decreasing the loss of extracellular matrix, and enhancing scleral biomechanical strength may slow down myopia progression. Therefore, it is crucial to learn about the correlation among children's ocular parameters, including corneal biomechanical parameters, and their alterations in children's myopia development. This study aimed to investigate the correlation between the occurrence and progression of myopia and corneal biomechanical parameters in children.

MATERIALS AND METHODS

General information

The study included elementary school students aged 9–11 years who visited our

hospital from November 2019 to April 2020. Our hospital ethics committee approved the study, and all enrolled subjects provided informed consent. Inclusion criteria: (1) best-corrected vision acuity ≥ 0.5 (LogMAR); and (2) no history of wearing special glasses, such as keratoplasty lenses. Exclusion criteria: (1) other eye diseases, such as amblyopia, strabismus, cone cornea, and lid entropion; (2) history of previous ophthalmic surgery, such as retinal, congenital cataract, and ptosis surgery; and (3) systemic diseases affecting the eye, such as diabetes mellitus. We grouped the subjects according to their spherical equivalent lens degree: (1) myopic group: SE < -0.50 D; (2) emmetropia group: -0.50 D ≤ SE ≤ + 0.50 D; and (3) hyperopic group: SE > + 0.50 D. There were 207 cases in the myopic group, including 142 males and 65 females, with a mean age of 10.23 ± 0.58 years. There were 102 cases in the emmetropia group, including 61 males and 41 females, with a mean age of 10.04 ± 0.64 years. There were 109 cases in the hyperopia group, including 59 males and 50 females, with a mean age of 10.19 ± 0.84 years. We followed up on patients in the myopia group every 3 mo, recording the axial measurement, medical optometry, and corneal biomechanical parameters. After 1 year of follow-up, we compared changes in corneal biomechanical indexes and other clinical characteristics.

Methods

After enrollment, all subjects underwent routine ophthalmic examinations, including naked eye visual acuity, best-corrected visual acuity, anterior segment, fundus, medical optometry, and other ophthalmic examinations. Subjects' intraocular pressure (IOP), anterior chamber depth, corneal curvature, spherical equivalent (SE), flat-axis corneal curvature, and steep-axis corneal curvature were recorded. IOLMaster measured axial length (AL). Corvis ST measured corneal biomechanical parameters and biological parameters, including the first velocity of applanation (A1V), first applanation length (A1L), first applanation time (A1T), first applanation deformation amplitude (A1DA), the second velocity of applanation (A2V), second applanation length (A2L), second applanation time (A2T), second applanation deformation amplitude (A2DA), time from the start until the highest concavity (HCT), central curvature radius at highest concavity (HCR), peak distance (PD), deformation amplitude (DA), central corneal thickness (CCT), integrated radius (IR), ambrosia relational thickness-horizontal (ARTh), first applanation stiffness parameter (SP-A1), corvis biomechanical index (CBI), and topographic and biomechanics index (TBI).

Statistical analysis

The Kolmogorov–Smirnov test analyzed the distribution of variables. Normally, distributed data were expressed as the mean ± SD. The one-ANOVA test compared the three groups' general ocular measurement and corneal biomechanical parameters. Correlations between corneal biomechanical and general ocular measurement parameters were analyzed using a Pearson correlation coefficient. All statistical analyses were performed using the SPSS 23.0 software package and MedCalc 15.2.2 software. $P < 0.05$ was considered a statistically significant difference.

RESULTS

Comparison of general ocular measurement parameters among the three groups of subjects

There were statistically significant ($P < 0.05$) differences in the general ocular measurement parameters SE, IOP, and AL among subjects in three groups. However, there were no significant differences in the general ocular measurement parameters CCT and Km among subjects in three groups ($P > 0.05$), as shown in Table 1.

Comparison of corneal biomechanical parameters among the three groups of subjects

The corneal biomechanical parameters A1V, A1L, A1T, A1DA, A2V, A2DA, HCR, PD, IR, ARTh, SP-A1, CBI, and TBI were significantly different ($P < 0.05$) among subjects in three groups. However, the corneal biomechanical A2L, A2T, HCT, DA were not significantly different subjects in three groups ($P > 0.05$, Table 2).

Table 1 Comparison of general ocular measurement parameters among the three groups of subjects

	Number of cases	SE (D)	IOP (mmHg)	AL (mm)	CCT (μm)	Km
Myopia group	207	-2.543 ± 0.493	17.04 ± 2.88	25.61 ± 0.77	560.31 ± 36.13	43.15 ± 2.05
Emmetropia group	102	-0.104 ± 0.025	15.40 ± 2.09	23.35 ± 0.68	559.23 ± 38.43	43.05 ± 1.96
Hyperopia group	109	2.465 ± 1.025	15.32 ± 2.93	22.08 ± 0.79	561.92 ± 40.50	43.61 ± 2.34
F		2321	19.94	855.1	0.1364	2.279
P value		< 0.0001	< 0.0001	< 0.0001	0.8725	0.1036

SE: Spherical equivalent; IOP: Intraocular pressure; AL: Axial length; CCT: Central corneal thickness.

Correlation of general ocular measurement parameters with corneal biomechanical parameters in children

Children's general ocular measurement parameter SE positively correlated with corneal biomechanical parameters A2V and A2L while negatively correlated with PD, DA, and IR. In children, the general ocular measurement parameter IOP was positively correlated with corneal biomechanical parameters PD and DA and negatively correlated with A2L and IR. The general ocular measurement parameter AL positively correlated with corneal biomechanical parameter A2V and negatively correlated with A2T, HCT, and PD. The general ocular measurement parameter CCT in children was positively correlated with corneal biomechanical parameters A1L, A1T, A2V, A2L, A2T, A2DA, HCR, PD, DA, IR, ARTh, SP-A1, CBI, and TBI and negatively correlated with A1V. Children's general ocular measurement parameter Km positively correlated with corneal biomechanical parameters DA and IR but negatively correlated with A2L, HCR, and PD (all $P < 0.05$), as shown in Table 3.

The general ocular measurement parameters ΔIOP was positively correlated with the corneal biomechanical parameters ΔDA, ΔIR, and negatively with ΔA2L, and increased ΔAL was positively correlated with corneal biomechanical parameters ΔA2V and ΔPD.

Correlation between myopia development and corneal biomechanical parameters in children

There was a positive correlation between the increase in general ocular measurement ΔSE and the change in corneal biomechanical parameters ΔA2V and ΔA2L and a negative correlation with ΔIR. There was a positive correlation between ΔIOP and ΔDA and a negative correlation between ΔA2L and ΔIR. There was a positive correlation between the increase in the general ocular measurement parameter ΔAL and the change in the corneal biomechanical parameters ΔA2V and ΔPD in children. There was a positive correlation between the general ocular measurement parameter ΔCCT and the corneal biomechanical parameters ΔA1L, ΔA1T, ΔA2V, ΔA2L, ΔA2T, ΔA2DA, ΔHCR, ΔPD, ΔDA, ΔIR, ΔARTh, ΔSP-A1, ΔCBI, and ΔTBI and a negative correlation with ΔA1V. There was a positive correlation between the increase in general ocular measurement parameter ΔKm and the change in corneal biomechanical parameters ΔDA and ΔIR and a negative correlation with ΔHCR and ΔPD in children (all $P < 0.05$), as shown in Table 4.

The corneal biomechanical parameters A1V, A1L, A1T, A1DA, A2V, A2DA, HCR, PD, IR, ARTh, SP-A, CBI, and TBI were statistically different in the myopic, emmetropia, and hyperopic groups (all $P < 0.05$).

DISCUSSION

The prevalence of myopia is rather high worldwide, reaching 80% in some Asian populations[6]. Well-documented changes in myopia include prolonged AL, deeper anterior chamber and vitreous depth, thinner retina, higher incidence of retinal detachment, and reduced scleral thickness and elasticity[6]. This study measured general ocular and corneal biomechanical parameters in myopic, emmetropic, and hyperopic children. The analysis revealed statistically significant ($P < 0.05$) differences in general ocular measurement parameters SE, IOP, and AL among subjects in three groups. Corneal biomechanical parameters A1V, A1L, A1T, A1DA, A2V, A2DA, HCR,

Table 2 Comparison of corneal biomechanical parameters among the three groups of subjects

	Number of cases	A1V (ms^{-1})	A1L (mm)	A1T (ms)	A1DA (mm)	A2V (ms^{-1})	A2L (mm)	A2T (ms)	A2D (mm)	HCT (ms)	HCR (mm)	PD (mm)	DA (mm)	IR	ARTh	SP-A1	CBI	TBI
Myopia group	207	0.13 ± 0.02	1.85 ± 0.29	7.63 ± 0.29	0.12 ± 0.01	0.29 ± 0.06	1.73 ± 0.39	21.33 ± 0.93	0.37 ± 0.08	16.70 ± 0.79	7.59 ± 0.73	3.42 ± 0.88	0.98 ± 0.09	9.23 ± 1.93	472.03 ± 131.43	102.01 ± 18.43	0.53 ± 0.35	0.56 ± 0.25
Emmetropia group	102	0.15 ± 0.05	1.93 ± 0.33	7.41 ± 0.22	0.13 ± 0.01	0.30 ± 0.02	1.70 ± 0.55	21.57 ± 1.24	0.41 ± 0.09	16.73 ± 0.49	6.42 ± 0.89	3.77 ± 0.92	0.99 ± 0.09	9.05 ± 2.61	451.61 ± 111.43	107.32 ± 14.62	0.23 ± 0.14	0.33 ± 0.23
Hyperopia group	109	0.14 ± 0.03	1.77 ± 0.39	7.39 ± 0.29	0.13 ± 0.02	0.31 ± 0.05	1.63 ± 0.53	21.35 ± 1.29	0.47 ± 0.13	16.59 ± 0.66	6.69 ± 1.02	3.02 ± 0.61	0.99 ± 0.10	11.34 ± 1.34	256.45 ± 46.34	108.42 ± 14.45	0.02 ± 0.01	0.12 ± 0.07
F		13.57	6.258	36.89	29.34	5.780	1.610	1.706	37.52	1.267	78.85	21.67	0.6079	47.99	145.7	6.681	150.6	158.2
P value		< 0.0001	0.0021	< 0.0001	< 0.0001	0.0033	0.2011	0.1829	< 0.0001	0.2829	< 0.0001	< 0.0001	0.5450	< 0.0001	< 0.0001	0.0014	< 0.0001	< 0.0001

A1V: First velocity of applanation; A1L: First applanation length; A1T: First applanation time; A1DA: First applanation deformation amplitude; A2V: Second velocity of applanation; A2L: Second applanation length; A2T: Second applanation time; A2D: Second applanation deformation; HCT: Time from the start until the highest concavity; HCR: Central curvature radius at highest concavity; PD: Peak distance; DA: Deformation amplitude; IR: Integrated radius; ARTh: ambrosia relational thickness-horizontal; SP-A1: First applanation stiffness parameter; CBI: Corvis biomechanical index; TBI: Topographic and biomechanics index.

PD, IR, ARTh, SP-A1, CBI, and TBI were significantly different ($P < 0.05$) in three groups. Despite the limited tracking time and the number of participants compared to the large scale of clinic studies, our data were effectively valid because of highly professional supervision and appropriate statistics.

IOP is an important biometric parameter in myopic eyes. Previous studies have shown that thinner corneas may lead to underestimation errors in IOP measurements [7]. However, recent studies have found significantly higher mean IOP values in myopic children than in non-myopic children[8]. In this study, children's general eye measurement parameter IOP was positively correlated with corneal biomechanical parameters PD and DA and negatively correlated with A2L and IR. The change in ΔIOP was positively correlated with the corneal biomechanical parameter ΔDA and negatively correlated with ΔA2L and ΔIR (all $P < 0.05$). Glaucoma is a blinding eye disease and the major ocular disease causing vision loss and blindness worldwide that shows characteristic damage to the optic nerve and loss of visual function[9]. Primary open-angle glaucoma is the most common form of glaucoma globally, where the degree of visual field damage is already severe, and the damage to visual acuity and visual field is irreversible[10]. Elevated IOP is considered the most important risk factor for developing and progression of primary open-angle glaucoma[11]. Therefore, alterations in DA in myopia development in children can be used as potential markers for glaucoma development.

In the present study, the general ocular measurement parameter CCT in children positively correlated ($P < 0.05$) with the corneal biomechanical parameters A1L, A1T, A2V, A2L, A2T, A2DA, HCR, PD, DA, IR, ARTh, SP-A1, CBI, and TBI, while it was

Table 3 Correlation of corneal biomechanical parameters with general ocular measurement parameters

	SE (D)		IOP (mmHg)		AL (mm)		CCT (μm)		Km	
	ρ	*P* value	ρ	*P* value	ρ	*P* value	ρ	*P* value	ρ	*P* value
A1V	-0.042	0.3917	0.053	0.2797	-0.003	0.9512	-0.583	< 0.0001	0.103	0.0353
A1L	0.033	0.5010	-0.061	0.2133	-0.077	0.1160	0.483	< 0.0001	-0.089	0.692
A1T	0.024	0.6246	-0.091	0.0631	-0.082	0.0941	0.562	< 0.0001	0.008	0.8705
A1DA	0.038	0.4384	-0.073	0.1362	0.053	0.2797	0.358	0.2367	0.048	0.3276
A2V	0.235	< 0.0001	-0.114	0.0197	0.302	< 0.0001	0.542	< 0.0001	0.043	0.3805
A2L	0.124	0.0112	-0.139	0.0044	-0.094	0.0548	0.382	< 0.0001	-0.117	0.0167
A2T	0.093	0.0575	-0.088	0.0723	-0.110	0.0245	0.421	< 0.0001	0.021	0.6686
A2DA	0.041	0.4031	-0.038	0.4383	0.074	0.1309	0.345	< 0.0001	0.033	0.5010
HCT	0.004	0.9350	-0.008	0.8705	-0.109	0.0258	0.049	0.3176	0.063	0.1986
HCR	0.009	0.8705	-0.039	0.4265	-0.049	0.3176	0.482	< 0.0001	-0.285	< 0.0001
PD	-0.130	0.0078	0.117	0.0167	0.545	< 0.0001	0.381	< 0.0001	-0.394	< 0.0001
DA	-0.119	0.0149	0.193	0.0001	0.038	0.4384	0.295	< 0.0001	0.234	< 0.0001
IR	-0.204	< 0.0001	0.244	< 0.0001	0.025	0.6103	0.421	< 0.0001	0.283	< 0.0001
ARTh	0.062	0.2059	-0.072	0.1417	0.017	0.7289	0.274	< 0.0001	-0.085	0.0826
SP-A1	0.032	0.5141	-0.024	0.6246	-0.059	0.2287	0.362	< 0.0001	0.008	0.8705
CBI	0.039	0.4265	-0.019	0.6985	-0.06	0.2209	0.385	< 0.0001	0.087	0.0756
TBI	0.027	0.5820	-0.020	0.6835	-0.016	0.7443	0.0235	< 0.0001	0.064	0.1916

SE: Spherical equivalent; IOP: Intraocular pressure; AL: Axial length; CCT: Central corneal thickness; A1V: First velocity of applanation; A1L: First applanation length; A1T: First applanation time; A1DA: First applanation deformation amplitude; A2V: Second velocity of applanation; A2L: Second applanation length; A2T: Second applanation time; A2D: Second applanation deformation; HCT: Time from the start until the highest concavity; HCR: Central curvature radius at highest concavity; PD: Peak distance; DA: Deformation amplitude; IR: Integrated radius; ARTh: ambrosia relational thickness-horizontal; SP-A1: First applanation stiffness parameter; CBI: Corvis biomechanical index; TBI: Topographic and biomechanics index.

negatively correlated ($P < 0.05$) with A1V. The general ocular measurement parameter ΔCCT in children positively correlated with corneal biomechanical parameters ΔA1L, ΔA1T, ΔA2V, ΔA2L, ΔA2T, ΔA2DA, ΔHCR, ΔPD, ΔDA, ΔIR, ΔARTh, ΔSP-A1, ΔCBI, and ΔTBI ($P < 0.05$), while negatively correlated with ΔA1V ($P < 0.05$). Studies of CCT in children of different ages have shown that CCT increases with age so that the average CCT is thicker in older than in young children[12]. CCT and the change in CCT positively correlated with most corneal biomechanics except for A1V and ΔA1V, so these corneal biomechanical parameters may also increase with the child's age.

The refractive error results from a mismatch between various optical components of the eye, one of the most important parts of which is AL[13]. In the present study, there was a positive correlation between the general ocular measurement parameter AL and the corneal biomechanical parameter A2V ($P < 0.05$) and a negative correlation with A2T, HCT, and PD ($P < 0.05$) in children. There was a positive correlation between the increased general ocular measurement parameter ΔAL and the change in the corneal biomechanical parameter ΔA2V and ΔPD in children ($P < 0.05$). This usually corresponds to an AL ≥ 26 mm, which significantly increases the risk of serious complications later in life, including myopic macular degeneration, retinal detachment, and glaucoma[14,15]. The mean AL of the subjects in the myopic group included in this study was 25.61 ± 0.77 mm. Therefore, the corneal biomechanical parameters A2V, A2T, HCT, and PD may identify children at low risk. The application of corneal biomechanical parameters will allow clinicians to implement preventive measures to minimize the further increase in AL. These measures include pharmacological agents, such as atropine, and optical applications, such as multifocal contact lenses. There are still limitations in this study, including that this study is a prospective study and cannot determine the causal relationship between various variables. At the same time, this study only collected children from the same hospital, and the sample size is small. There may still be other influencing factors that have not

Table 4 Correlation between spherical equivalent, intraocular pressure, and axial length growth and the change in corneal biomechanical parameters in subjects in the myopic group

	ΔSE (D)		ΔIOP (mmHg)		ΔAL (mm)		CCT (μm)		Km	
	ρ	*P* value	ρ	*P* value	ρ	*P* value	ρ	*P* value	ρ	*P* value
ΔA1V	-0.0391	0.5758	0.0460	0.5107	-0.0032	0.9631	-0.5873	< 0.0001	0.1010	0.1478
ΔA1L	0.0370	0.5962	-0.0673	0.3350	-0.0818	0.2415	0.4236	< 0.0001	-0.0716	0.3053
ΔA1T	0.0257	0.7133	-0.0917	0.1889	-0.0909	0.1926	0.4629	< 0.0001	0.0080	0.9084
ΔA1DA	0.0344	0.6230	-0.0586	0.4013	0.0455	0.5147	0.3530	< 0.0001	0.0475	0.4966
ΔA2V	0.2027	0.0034	-0.1075	0.1232	0.3121	< 0.0001	0.5029	< 0.0001	0.0472	0.4994
ΔA2L	0.1397	0.0446	-0.1459	0.0360	-0.0971	0.1640	0.4505	< 0.0001	-0.0972	0.1637
ΔA2T	0.0772	0.2691	-0.0718	0.3042	-0.0897	0.1987	0.4920	< 0.0001	0.0244	0.7268
ΔA2DA	0.0462	0.5089	-0.0321	0.6459	0.0677	0.3327	0.3561	< 0.0001	0.0331	0.6357
ΔHCT	0.0035	0.9601	-0.0073	0.9171	-0.1120	0.1082	0.0465	0.5061	0.0717	0.3047
ΔHCR	0.0081	0.9073	-0.0323	0.6446	-0.0508	0.4669	0.5378	< 0.0001	-0.3190	< 0.0001
ΔPD	-0.1331	0.0559	0.1361	0.0505	0.4427	< 0.0001	0.3246	< 0.0001	-0.3320	< 0.0001
ΔDA	-0.1130	0.1049	0.1814	0.0089	0.0391	0.5763	0.2474	0.0003	0.2125	0.0021
ΔIR	-0.1841	0.0079	0.2674	0.0001	0.0228	0.7439	0.4886	< 0.0001	0.2615	0.0001
ΔARTh	0.0542	0.4378	-0.0671	0.3365	0.0164	0.8150	0.3274	< 0.0001	-0.0726	0.2983
ΔSP-A1	0.0372	0.5951	-0.0209	0.7655	-0.0623	0.3727	0.4282	< 0.0001	0.0074	0.9161
ΔCBI	0.0321	0.6461	-0.0160	0.8187	-0.0534	0.4450	0.3329	< 0.0001	0.1010	0.1474
ΔTBI	0.0234	0.7378	-0.0187	0.7888	-0.0143	0.8381	0.0247	0.7238	0.0589	0.3988

SE: Spherical equivalent; IOP: Intraocular pressure; AL: Axial length; CCT: Central corneal thickness; A1V: First velocity of applanation; A1L: First applanation length; A1T: First applanation time; A1DA: First applanation deformation amplitude; A2V: Second velocity of applanation; A2L: Second applanation length; A2T: Second applanation time; A2D: Second applanation deformation; HCT: Time from the start until the highest concavity; HCR: Central curvature radius at highest concavity; PD: Peak distance; DA: Deformation amplitude; IR: Integrated radius; ARTh: ambrosia relational thickness-horizontal; SP-A1: First applanation stiffness parameter; CBI: Corvis biomechanical index; TBI: Topographic and biomechanics index.

been found. The age range of children included in this study is not large enough. In addition, due to time constraints, the children were not followed up for a longer time.

CONCLUSION

Myopia development in children was associated with multiple corneal biomechanical parameters. These findings may help clinics take preventive measures to minimize the further increase in myopic children's axial length.

ARTICLE HIGHLIGHTS

Research background

Patients with myopia, especially those with high myopia, are much more likely to have serious complications such as retinal detachment and open-angle glaucoma than normal patients. High myopia may have a degenerative disorder, including cornea, sclera, choroid, optic disc, vitreous, macula, and peripheral retina.

Research motivation

The increasingly high incidents of myopia in children and the association with multiple corneal biomechanical parameters in local community and worldwide.

Research objectives
This study is to determine the change of corneal biomechanical parameters after onset and progression of myopia.

Research methods
A total of 207 myopic subjects were enrolled according to local clinic criteria and one-way ANOVA test was applied to determine whether there is statistical evidence between different general ocular measurement parameters.

Research results
There is a correlation between the development of myopia and various corneal biomechanical parameters in children.

Research conclusions
There are positive and negative correlations between myopia and general eye measurement parameters, corneal biomechanical parameters and other multiple parameters.

Research perspectives
Corneal ophthalmometric parameters and biomechanical properties including multiple baselines may be able to predict the development of myopia.

REFERENCES

1 **Grzybowski A**, Kanclerz P, Tsubota K, Lanca C, Saw SM. A review on the epidemiology of myopia in school children worldwide. *BMC Ophthalmol* 2020; **20**: 27 [PMID: 31937276 DOI: 10.1186/s12886-019-1220-0]

2 **Wang J**, Li Y, Musch DC, Wei N, Qi X, Ding G, Li X, Li J, Song L, Zhang Y, Ning Y, Zeng X, Hua N, Li S, Qian X. Progression of Myopia in School-Aged Children After COVID-19 Home Confinement. *JAMA Ophthalmol* 2021; **139**: 293-300 [PMID: 33443542 DOI: 10.1001/jamaophthalmol.2020.6239]

3 **Walline JJ**, Walker MK, Mutti DO, Jones-Jordan LA, Sinnott LT, Giannoni AG, Bickle KM, Schulle KL, Nixon A, Pierce GE, Berntsen DA; BLINK Study Group. Effect of High Add Power, Medium Add Power, or Single-Vision Contact Lenses on Myopia Progression in Children: The BLINK Randomized Clinical Trial. *JAMA* 2020; **324**: 571-580 [PMID: 32780139 DOI: 10.1001/jama.2020.10834]

4 **Yam JC**, Tang SM, Kam KW, Chen LJ, Yu M, Law AK, Yip BH, Wang YM, Cheung CYL, Ng DSC, Young AL, Tham CC, Pang CP. High prevalence of myopia in children and their parents in Hong Kong Chinese Population: the Hong Kong Children Eye Study. *Acta Ophthalmol* 2020 [PMID: 31981300 DOI: 10.1111/aos.14350]

5 **Liu XN**, Naduvilath TJ, Wang J, Xiong S, He X, Xu X, Sankaridurg PR. Sleeping late is a risk factor for myopia development amongst school-aged children in China. *Sci Rep* 2020; **10**: 17194 [PMID: 33057123 DOI: 10.1038/s41598-020-74348-7]

6 **McCullough S**, Adamson G, Breslin KMM, McClelland JF, Doyle L, Saunders KJ. Axial growth and refractive change in white European children and young adults: predictive factors for myopia. *Sci Rep* 2020; **10**: 15189 [PMID: 32938970 DOI: 10.1038/s41598-020-72240-y]

7 **Ku PW**, Steptoe A, Lai YJ, Hu HY, Chu D, Yen YF, Liao Y, Chen LJ. The Associations between Near Visual Activity and Incident Myopia in Children: A Nationwide 4-Year Follow-up Study. *Ophthalmology* 2019; **126**: 214-220 [PMID: 29934268 DOI: 10.1016/j.ophtha.2018.05.010]

8 **Modjtahedi BS**, Abbott RL, Fong DS, Lum F, Tan D; Task Force on Myopia. Reducing the Global Burden of Myopia by Delaying the Onset of Myopia and Reducing Myopic Progression in Children: The Academy's Task Force on Myopia. *Ophthalmology* 2021; **128**: 816-826 [PMID: 33388160 DOI: 10.1016/j.ophtha.2020.10.040]

9 **Bouhenni RA**, Ricker I, Hertle RW. Prevalence and Clinical Characteristics of Childhood Glaucoma at a Tertiary Care Children's Hospital. *J Glaucoma* 2019; **28**: 655-659 [PMID: 30950965 DOI: 10.1097/IJG.0000000000001259]

10 **Ji X**, Zhang Z, Shi J, He B. Clinical application of NGS-based SNP haplotyping for the preimplantation genetic diagnosis of primary open angle glaucoma. *Syst Biol Reprod Med* 2019; **65**: 258-263 [PMID: 30977407 DOI: 10.1080/19396368.2019.1590479]

11 **Gedde SJ**, Vinod K, Wright MM, Muir KW, Lind JT, Chen PP, Li T, Mansberger SL; American Academy of Ophthalmology Preferred Practice Pattern Glaucoma Panel. Primary Open-Angle Glaucoma Preferred Practice Pattern®. *Ophthalmology* 2021; **128**: P71-P150 [PMID: 34933745 DOI: 10.1016/j.ophtha.2020.10.022]

12 **Dong L**, Kang YK, Li Y, Wei WB, Jonas JB. Prevalence and Time Trends of Myopia in Children and Adolescents in China: A Systemic Review and Meta-Analysis. *Retina* 2020; **40**: 399-411 [PMID:

31259808 DOI: 10.1097/IAE.0000000000002590]
13 **Wei S**, Li SM, An W, Du J, Liang X, Sun Y, Zhang D, Tian J, Wang N. Safety and Efficacy of Low-Dose Atropine Eyedrops for the Treatment of Myopia Progression in Chinese Children: A Randomized Clinical Trial. *JAMA Ophthalmol* 2020; **138**: 1178-1184 [PMID: 33001210 DOI: 10.1001/jamaophthalmol.2020.3820]
14 **Rozema J**, Dankert S, Iribarren R, Lanca C, Saw SM. Axial Growth and Lens Power Loss at Myopia Onset in Singaporean Children. *Invest Ophthalmol Vis Sci* 2019; **60**: 3091-3099 [PMID: 31323091 DOI: 10.1167/iovs.18-26247]
15 **Tideman JWL**, Polling JR, Jaddoe VWV, Vingerling JR, Klaver CCW. Environmental Risk Factors Can Reduce Axial Length Elongation and Myopia Incidence in 6- to 9-Year-Old Children. *Ophthalmology* 2019; **126**: 127-136 [PMID: 30146089 DOI: 10.1016/j.ophtha.2018.06.029]

World Journal of Clinical Cases

Submit a Manuscript: https://www.f6publishing.com

World J Clin Cases 2022 February 16; 10(5): 1557-1571

DOI: 10.12998/wjcc.v10.i5.1557

ISSN 2307-8960 (online)

META-ANALYSIS

Intensive *vs* non-intensive statin pretreatment before percutaneous coronary intervention in Chinese patients: A meta-analysis of randomized controlled trials

Xian Yang, Xi Lan, Xin-Lin Zhang, Zhong-Lin Han, Si-Min Yan, Wen-Xiao Wang, Biao Xu, Wei-Hong Ge

ORCID number: Xian Yang 0000-0003-1477-5117; Xi Lan 0000-0002-1647-9840; Xin-Lin Zhang 0000-0001-9236-7632; Zhong-Lin Han 0000-0002-0982-7755; Si-Min Yan 0000-0002-5987-5333; Wen-Xiao Wang 0000-0003-1489-1994; Biao Xu 0000-0002-8743-1406; Wei-Hong Ge 0000-0002-6124-8742.

Author contributions: Ge WH and Xu B designed the research; Yang X, Lan X, Zhang XL and Yan SM collected the data; Lan X and Zhang XL analyzed the data; Yang X and Lan X supervised the research; Yang X, Lan X, Zhang XL, Han ZL and Wang WX wrote the paper.

Conflict-of-interest statement: The authors deny any conflict of interest.

PRISMA 2009 Checklist statement: The authors have read the PRISMA 2009 Checklist, and the manuscript was prepared and revised according to the PRISMA 2009 Checklist

Supported by the Scientific Research Project of Nanjing Clinical Medical Centre, No. 1 Ning Health Science Education [2020].

Country/Territory of origin: China

Xian Yang, Si-Min Yan, Wei-Hong Ge, Department of Pharmacy, Nanjing Drum Tower Hospital, The Affiliated Hospital of Nanjing University Medical School, Nanjing 210000, Jiangsu Province, China

Xian Yang, Si-Min Yan, Wei-Hong Ge, Department of Pharmacy, Nanjing Medical Center for Clinical Pharmacy, Nanjing 210000, Jiangsu Province, China

Xi Lan, Xin-Lin Zhang, Zhong-Lin Han, Biao Xu, Department of Cardiology, Nanjing Drum Tower Hospital, The Affiliated Hospital of Nanjing University Medical School, Nanjing 210000, Jiangsu Province, China

Wen-Xiao Wang, Department of Pharmacy, The Affiliated Hospital of Qingdao University, Qingdao 266000, Shandong Province, China

Corresponding author: Wei-Hong Ge, MS, Department of Pharmacy, Nanjing Drum Tower Hospital, The Affiliated Hospital of Nanjing University Medical School, No. 321 Zhongshan Road, Gulou District, Nanjing 210000, Jiangsu Province, China.
wh.ge.drumtower@outlook.com

Abstract

BACKGROUND

The results of intensive statin pretreatment before percutaneous coronary intervention (PCI) is inconsistent between Chinese and Western populations, and there are no corresponding meta-analyses involving hard clinical endpoints in the available published literature.

AIM

To evaluate the efficacy and safety of high-dose statin loading before PCI in Chinese patients through a meta-analysis.

METHODS

Relevant studies were identified by searching the electronic databases of PubMed, Embase and Cochrane's Library to December 2019. The outcomes included an assessment of major adverse cardiovascular event (MACE), non-fatal myocardial infarction (MI), cardiac death, target vessel revascularization (TVR), myalgia /myasthenia and abnormal alanine aminotransferase (ALT) in all enrolled patients. Random effect model and fixed effect model were applied to combine

Specialty type: Medicine, research and experimental

Provenance and peer review: Unsolicited article; Externally peer reviewed.

Peer-review model: Single blind

Peer-review report's scientific quality classification

Grade A (Excellent): 0
Grade B (Very good): 0
Grade C (Good): C, C
Grade D (Fair): 0
Grade E (Poor): 0

Received: August 12, 2021
Peer-review started: August 12, 2021
First decision: October 20, 2021
Revised: November 9, 2021
Accepted: December 31, 2021
Article in press: December 31, 2021
Published online: February 16, 2022

P-Reviewer: Lee PN
S-Editor: Wang LL
L-Editor: Filipodia
P-Editor: Wang LL

the data, which were further analyzed by χ^2 test and I^2 test. The main outcomes were then analyzed through the use of relative risks (RR) and its 95% confidence interval (95%CI).

RESULTS

Eleven studies involving 3123 individuals were included. Compared with patients receiving placebo or no statin treatment before surgery, intensive statin treatment was associated with a clear reduction of risk of MACE (RR = 0.44, 95%CI: 0.31-0.61, P < 0.00001). However, compared with the patients receiving moderate-intensity statin before surgery, no advantage to intensive statin treatment was seen (RR = 1.04, 95%CI: 0.82-1.31, P = 0.74). In addition, no significant difference was observed between intensive statin therapy and non-intensive statin therapy on the incidence of TVR (RR = 0.43, 95%CI: 0.18-1.02, P = 0.06) , myalgia /myasthenia (RR = 1.35, 95%CI: 0.30-5.95, P = 0.69) and abnormal alanine aminotransferase (RR = 1.47, 95%CI: 0.54-4.02, P = 0.45) except non-fatal MI (RR = 0.54, 95%CI: 0.33-0.88, P = 0.01).

CONCLUSION

Compared with placebo or no statin pretreatment, intensive statin before PCI displayed reduced incidence of MACE. However, there was no significant benefit between high and moderate-intensity statin. In addition, no significant difference was observed between intensive statin therapy and non-intensive statin therapy on the incidence of TVR, myalgia/myasthenia and abnormal alanine aminotransferase except non-fatal MI.

Key Words: Intensive; Non-intensive; Statin; Percutaneous coronary intervention; Chinese; Meta-analysis

Core Tip: As the cornerstone of primary and secondary prevention of arteriosclerotic cardiovascular disease, statins have been widely used in clinical practice. However, whether intensive statin therapy before percutaneous coronary intervention (PCI) could benefit the Chinese population remains debatable. A meta-analysis was performed to evaluate the efficacy and safety of the strategy. The results showed that compared with placebo or no statin pretreatment, Chinese patients receiving intensive statin therapy before PCI could further reduce the incidence of major adverse cardiovascular events. In addition, there was no significant benefit to using high-intensity and moderate-intensity statin therapy.

Citation: Yang X, Lan X, Zhang XL, Han ZL, Yan SM, Wang WX, Xu B, Ge WH. Intensive *vs* non-intensive statin pretreatment before percutaneous coronary intervention in Chinese patients: A meta-analysis of randomized controlled trials. *World J Clin Cases* 2022; 10(5): 1557-1571
URL: https://www.wjgnet.com/2307-8960/full/v10/i5/1557.htm
DOI: https://dx.doi.org/10.12998/wjcc.v10.i5.1557

INTRODUCTION

At present, the burden of cardiovascular and cerebrovascular disease is very heavy in China. There are about 290 million patients presenting with these conditions, including 11 million patients with coronary heart disease[1]. Despite the rapid development of percutaneous coronary intervention (PCI), which has increased from 500000 in 2014 to more than 915000 in 2018, and also surpassed the numbers of presenting cases in the United States[2], the overall mortality rate of coronary heart disease and acute myocardial infarction in China is still on the rise[1]. This suggests that there is room for optimizing perioperative therapy.

As the cornerstone of primary and secondary prevention of arteriosclerotic cardiovascular disease, statins have been widely used in clinical practice. In recent years, a number of studies in Europe and the United States suggested that intensive statin therapy before PCI could significantly reduce the level of postoperative myocardial damage markers and reduce the incidence of perioperative myocardial infarction and short-term cardiovascular events[3-5].

However, whether the strategy could benefit the Chinese population remains debatable. The ALPACS study, which included the Chinese population, suggested that patients did not benefit from intensive statin therapy as compared with a control population in major adverse cardiovascular events (MACE) (P = 0.80)[6]. The ISCAP study also found no difference in the incidence of MACE between treatment with high-intensity and moderate-intensity statins after 30 d and 6 mo of follow-up (P = 0.43 and P = 0.63, respectively)[7]. Considering the differences in lipid metabolism between Chinese and Western populations, it was unknown whether or not race influences the outcome of intensive statin treatment[8]. Thus, the lack of available meta-analyses of clinically defined hard endpoints has affected the general perioperative application of statins in China.

This current article intended to evaluate the efficacy and safety of intensive statin therapy as compared to non-intensive statin pretreatment before PCI in the Chinese population through a meta-analysis investigation.

MATERIALS AND METHODS

Search strategy

A comprehensive search of electronic databases including PubMed, EMBASE and the Cochrane Library was performed by two researchers. The search was limited from inception of the database collections up to December 2019 and of the English language. Search terms included "intensive," "intensity," "high," "load," "loading," "statin," "atorvastatin," "rosuvastatin," "percutaneous coronary intervention" and "PCI" and connected using the logical search modifiers "AND" or "OR" in standard Boolean search strategies. It is worth mentioning that in order to inadvertently avoid missing important literature, the retrieval type did not include some terms such as "China" or "Chinese." We checked the location of the research center and the specific inclusion criteria in the article to comprehensively determine that the patient was indeed Chinese. The references of the identified articles and relevant reviews were screened to include other potentially suitable trials.

Inclusion and exclusion criteria

Studies satisfying the following criteria were eligible: (1) Randomized controlled trials (RCTs); (2) The patient was Chinese; (3) The patient presented with an emergency or elective PCI; (4) Preoperative interventions for intensive and non-intensive statin therapy, which included moderate-intensity statin therapy, placebo and no statin pretreatment; (5) High-intensity statin therapy that referred to atorvastatin ≥ 40 mg/d or rosuvastatin ≥ 20 mg/d and moderate-intensity statin therapy that referred to atorvastatin < 40 mg/d or rosuvastatin < 20 mg/d or an equivalent dose of the statin; (6) Outcome indicators that included effectiveness and safety of the treatment. The former referred to MACE and the latter referred to myalgia/myasthenia and abnormal alanine aminotransferase (ALT) levels. MACE is defined as cardiac death, non-fatal myocardial infarction (MI) and target vessel revascularization (TVR). Abnormal ALT is defined as ALT levels that increased more than three-fold the upper limit of the normal reference range; (7) The follow-up lasted for 1-3 mo after PCI; and (8) The published literature language was English. Exclusion criteria included any of the following: chronic high-intensity statin therapy before PCI; abnormal liver enzymes [ALT or aspartate aminotransferase that exceeded 40 U/L]; blood creatinine levels > 2 mg/dL; or a history of muscle disease. The studies were reviewed by two independent investigators to determine whether they met the set inclusion criteria. In the case of any disagreement, this was resolved by consensus.

Data extraction

The baseline data involving study characteristics (*i.e.* first author, year of publication, sample size, intervention and follow-up time), patient characteristics (*i.e.* clinical presentation and statin medication history) and outcome indicators were extracted directly from the articles. Differences in assessments were resolved by discussion with a third investigator.

Quality assessment

The RCTs were evaluated according to the following methodological criteria as recommended by the Cochrane Collaboration: sequence generation, concealment of allocation, blinding, incomplete outcome data, selective outcome reporting and other sources of bias.

Statistical analysis

We used RevMan (Version 5.3; Cochrane Collaboration, Oxford, UK) and Stata software (version 12.0; Stata Corporation, College Station, TX, United States) for meta- and statistical analyses. Dichotomous data were presented as risk ratios (RR) with 95% confidence intervals (CI). The heterogeneity was evaluated using I^2 and a P value that was based on the χ^2 test. $I^2 \leq 50\%$ or $P \geq 0.1$ did not demonstrate significant heterogeneity, and a fixed-effects model was used. $I^2 > 50\%$ or $P < 0.1$ indicated significant heterogeneity, and thus a randomeffects model was applied. Potential publication bias was assessed with a funnel plot and Egger's regression asymmetry test. All P values were twosided, and the results were considered statistically significant at an alpha value of $P < 0.05$.

The statistical methods of this study were reviewed by Xue B, who is an assistant researcher from the department of Cardiology, Nanjing Drum Tower Hospital.

RESULTS

Study selection and quality assessment

As shown in Figure 1, 4020 potentially relevant articles were identified in the initial analysis. Among them, 3418 articles were identified after removal of duplicate studies. Only 27 articles were retained after screening the title and abstract. Of note, one study was excluded as there was zero occurrence of each of the six conditions considered in both treated and control[9]. Finally, 11 studies involving 3123 patients were included in the present metaanalysis[7,10-19]. Among them, 1524 patients belonged to the intensive statin treatment group, and 1599 patients belonged to the non-intensive statin treatment group. Furthermore, the non-intensive statin treatment group that received moderate-intensity statin therapy, the placebo group and the no statin pretreatment group, included 738, 244 and 617 patients, respectively. All patients were female in one study[17]. A meta-analyses was not performed for cardiac death because of an extremely low occurrence, only one case in all studies. The characteristics of the included studies are shown in Table 1. The baseline clinical, angiographic and procedural characteristics of the patients are listed in Table 2. Quality assessment results are described in Table 3.

Effectiveness analysis

There were seven studies that compared the effects of preoperative high-intensity statin therapy and placebo or no statin therapy on the incidence of MACE[10,11,13-15,17,19]. The results showed that the incidence of MACE (RR = 0.44, 95%CI: 0.31-0.61, $P < 0.00001$, Figure 2) between the two groups were statistically significant. In addition, there were two studies that compared the effects of preoperative high-intensity statin therapy and moderate-intensity statin therapy on the incidence of MACE[7,16]. The indicator was not statistically significant (RR = 1.04, 95%CI: 0.82-1.31, $P = 0.74$, Figure 3).

Due to the limitations of the included literature, it was difficult to perform meta-analysis between the high-intensity statin group with placebo or no statin group or moderate-dose statin group in non-fatal MI and TVR. Therefore, we compared intensive statin therapy and non-intensive statin therapy for these endpoints. The results showed that the incidence of TVR[7,12-14,16,17,19] (RR = 0.43, 95%CI: 0.18-1.02, $P = 0.06$, Figure 4) between the two groups were not statistically significant, whlie there was a significant difference in the incidence of non-fatal MI[7,10,11,13-15,17,19] (RR = 0.54, 95%CI: 0.33-0.88, $P = 0.01$ Figure 5).

Safety analysis

There were two studies that compared the effects of preoperative intensive statin therapy and non-intensive statin therapy on the incidence of myalgia/myasthenia[10,12] and abnormal ALT[10,18]. No significant difference was observed between the groups (RR = 1.35, 95%CI: 0.30-5.95, $P = 0.69$, Figure 6A; RR = 1.47, 95%CI: 0.54-4.02, $P = 0.45$, Figure 6B, respectively).

Table 1 Characteristics of the included studies

Ref.	Sample size (intensive/non-intensive statin)	Clinical presentation	Statin medication history	Primary/elective PCI	Statin regimen before PCI	Statin regimen after PCI	Follow-up (d)	Outcome indicators	
								Effectiveness	Safety
Liu *et al* [10], 2016	616 (307/309)	Stable angina, ACS	Statin-naïve or atorvastatin ≤ 20mg/d, or equivalent dose statin	Elective PCI	Atorvastatin 80 mg 12 h before PCI *vs* no statin pretreatment	40 mg/d *vs* 20 mg/d	30	MACE, non-fatal MI	Myalgia/myasthenia
	182 (93/89)	STEMI	Statin-naïve or atorvastatin ≤ 20mg/d, or equivalent dose statin	Primary PCI	Atorvastatin 80 mg just before primary PCI *vs* no statin pretreatment	40 mg/d *vs* 20 mg/d	90		ALT
Jiao *et al* [11], 2015	72 (33/39)	NSTE-ACS	Not mentioned	Elective PCI	Rosuvastatin 20 mg 12 h before PCI + 20 mg just before PCI *vs* no statin pretreatment	10 mg/d	30	MACE, cardiac death, non-fatal MI, TVR	
Jiao *et al* [12], 2015	126 (62/64)	NSTE-ACS	Not mentioned	Elective PCI	Rosuvastatin 20 mg 12 h before PCI + 20 mg just before PCI *vs* no statin pretreatment	10 mg/d	30		Myalgia/myasthenia
Zheng *et al*[7], 2015	1202 (573/629)	Stable angina, NSTE-ACS	Statin-naïve or atorvastatin ≤ 20mg/d or equivalent dose statin	Elective PCI	Atorvastatin 80 mg at night before PCI for 2 d *vs* atorvastatin ≤ 20 mg or equivalent dose statin at night before PCI	40 mg/d *vs* ≤ 20 mg/d or equivalent dose statin	30	MACE, cardiac death, non-fatal MI, TVR	
Xie *et al* [13], 2014	159 (79/80)	NSTE-ACS	Statin-naïve	Elective PCI	Rosuvastatin 20 mg 12 h before PCI + 20 mg 2 h before PCI ***vs*** no statin pretreatment	10 mg/d	30	MACE, cardiac death, non-fatal MI, TVR	
Luo *et al* [14], 2013	67 (31/36)	NSTE-ACS	Statin-naïve	Elective PCI	Rosuvastatin 20 mg 12 h before PCI + 20 mg 2 h before PCI ***vs*** no statin pretreatment	10 mg/d	30	MACE, cardiac death, non-fatal MI, TVR	
Wang *et al*[15], 2013	125 (62/63)	NSTE-ACS	Statin-naïve	Elective PCI	Rosuvastatin 20 mg 2-4 h before PCI *vs* placebo 2-4 h before PCI	10 mg/d	30	MACE, cardiac death, non-fatal MI, TVR	
Li *et al* [16], 2013	215 (106/109)	Stable angina	Regular statin for at least 3 mo	Elective PCI	Atorvastatin 80 mg 12 h before PCI ***vs*** 20 mg 12 h before PCI	20 mg/d	30	MACE, cardiac death, non-fatal MI, TVR	
Gao *et al* [17], 2012	117 (59/58)	NSTE-ACS	Statin-naïve	Elective PCI	Rosuvastatin 20 mg 12 h before PCI + 10 mg 2 h before PCI *vs* placebo 12 h before PCI + 2 h before PCI	10 mg/d	90	MACE, cardiac death, non-fatal MI, TVR	
Li *et al* [18], 2012	161 (78/83)	STEMI	Statin-naïve	Primary PCI	Atorvastatin 80 mg 1.5 h before PCI *vs* placebo 1.5 h before PCI	40 mg/d	30		ALT
Yu *et al* [19], 2011	81 (41/40)	NSTE-ACS	Statin-naïve	Elective PCI	Atorvastatin 80 mg 12 h before PCI + 40 mg 2 h before PCI *vs* placebo 12 h before PCI + 2 h before PCI	20 mg/d	30	MACE, cardiac death, non-fatal MI, TVR	

PCI: Percutaneous coronary intervention; MACE: Major adverse cardiac events; MI: Myocardial infarction; NSTE-ACS: Non-ST segment elevation acute coronary syndrome; STEMI: ST segment elevation myocardial infarction; TVR: Target vessel revascularization; ALT: Alanine aminotransferase; ACS: Acute coronary syndrome.

Publication bias

The plots were symmetrical on visual inspection, indicating a risk of publication bias (Figure 7). Egger's regression test also demonstrated risk of publication bias (P = 0.004; Figure 8). The small number of studies included in the overall population and subgroup might represent one of the key reasons for publication bias.

DISCUSSION

Some studies have completed investigations of intensive statin therapy before PCI. In 2013, the ALPACS study took the lead in exploring similar work in Asia[6]. This was a prospective, multicenter, randomized, open-label study involving 499 patients with Non-ST segment elevation acute coronary syndrome (26 clinical centers in China and South Korea). None of the enrolled patients had previously received statins. The intensive treatment group received additional atorvastatin loading doses of 80 mg at 12 h and 40 mg at 2 h pre-PCI. The conventional treatment group was only treated with atorvastatin at a dose of 40 mg/d after PCI. The results suggested that the intensive treatment group failed to significantly reduce the occurrence of MACE at 30 d after PCI as compared with the conventional treatment group (15.7% *vs* 14.7%; P = 0.80). The study also demonstrated that the Asian population could tolerate high-intensity atorvastatin during the perioperative period.

Unfortunately, the ALPACS were not included in this meta-analysis because of the mixed data from the Korean population. The ISCAP study that was subsequently published in 2015 was a large-scale, multicenter, randomized, prospective, open-label, blinded, parallel controlled clinical study with Chinese patients[7]. Follow-up results showed no significant differences in the incidence of MACE at 30 d when comparing the intensive statin treatment group and the conventional treatment group (19.4% *vs* 18.3%; P = 0.43). When followed up at 6 mo, there was still no difference between the groups (20.1% *vs* 18.3%; P = 0.63). In terms of safety, no significant differences were found in terms of liver enzymes, creatine kinase levels and other objective indicators.

In addition to multicenter clinical studies, many scholars have attempted to identify further answers with meta-analyses. In 2013, Guo[20] conducted a meta-analysis on the impact of sequential statin therapy on the prognosis of Chinese patients with PCI. Ten studies that included 1015 patients were investigated. The results from that published study suggested a significant reduction in the incidence of MACE within 6 mo. Since some patients in the experimental group only received intensive statin treatment after PCI, the subjects were not entirely consistent with the characteristics discussed in this paper. In 2017, a systematic review and meta-analysis involving 11

Table 2 Baseline clinical, angiographic and procedural characteristics in the overall population

Variable	High-intensity statin/population (%)	Moderate-intensity statin/population (%)	Placebo or no statin pretreatment/population (%)
Number of patients	1524/3123 (48.8)	738/3123 (23.6)	861/3123 (27.6)
Male	1052/1524 (69.0)	521/738 (70.6)	566/861 (65.7)
Hypertension	9441524 (61.9)	489/738 (66.3)	533/861 (61.9)
Diabetes mellitus	439/1429 (30.7)	232/758 (30.6)	246/778 31.6)
Dyslipidemia	193/751 (25.7)	147/649 (22.7)	75/201 (37.3)
Smokers	537/1524 (35.2)	279/758 (36.8)	280/881 (31.8)
Previous MI	88/610 (14.4)	0/20 (0)	84/632 (13.3)
Previous PCI	159/1183 (13.4)	51/629 (8.1)	103/612 (15.2)
Previous CABG	6/500 (1.2)	0/0 (0)	6/496 (1.2)
Stable angina	230/506 (45.5)	109/109 (100)	118/398 (29.6)
NSTE-ACS	518/767 (67.5)	0/0 (0)	539/778 (69.3)
STEMI	203/478 (42.5)	0/20 (0)	204/501 (40.7)
Single vessel	59/172 (34.3)	0/20 (0)	55/200 (27.5)
Double vessel	66/172 (38.4)	0/20 (0)	71/200 (35.5)
More than three and triple vessels	47/172 (27.3)	0/20 (0)	54/200 (27.0)
Target vessel LM	36/877 (4.1)	25/629 (4.0)	7/320 (2.2)
Target vessel LAD	622/1018 (61.1)	418/649 (64.4)	249/483 (51.6)
Target vessel LCX	328/1018 (32.2)	199/649 (30.7)	155/483 (32.1)
Target vessel RCA	346/1018 (34.0)	234/649 (36.1)	164/483 (34.0)
B2/C lesions	346/609 (56.8)	0/0 (0)	333/615 (54.1)
Multivessel lesions	33/78 (42.3)	0/0 (0)	39/83 (47.0)
Multivessel intervention	244/773 (31.6)	215/629 (34.2)	62/201 (30.8)
Aspirin	1375/1491 (92.2)	622/738 (84.3)	802/822 (97.6)
Clopidogrel/Ticlopidine	1300/1385 (93.9)	541/629 (86.0)	807/822 (98.2)
β-blockers	1104/1491 (74.0)	495/738 (67.1)	630/822 (76.6)
ACEI/ARB	1045/1491 (70.1)	404/738 (54.7)	667/822 (81.1)
Glycoprotein IIb/IIIa inhibitors	89/350 (25.4)	0/20 (0)	101/380 (29.7)
DES	822/851 (96.6)	701/738 (95.0)	176/179 (98.3)

MI: Myocardial infarction; PCI: Percutaneous coronary intervention; CABG: Coronary artery bypass grafting; NSTE-ACS: Non-ST segment elevation acute coronary syndrome; STEMI: ST segment elevation myocardial infarction; LM: Left main; LAD: Left anterior descending; LCX: Left circumflex; RCA: Right coronary artery; ACEI: Angiotensin-converting enzyme inhibitor; ARB: Angiotensin receptor blockers; DES: Drug-eluting stent.

RCTs with 802 patients was performed by Ye *et al*[21]. Compared with preoperative rosuvastatin 10 mg/d therapy, it was found that using a loading dose of 20 mg/d before PCI significantly reduced cardiac troponin T and high sensitivity C-reactive protein levels by 24 h and low-density lipoprotein cholesterol, total cholesterol and triglyceride levels by 30 d after PCI. However, the clinical indicators that were analyzed and evaluated in this article were surrogate indicators, which did not involve cardiovascular endpoint events nor did they examine the safety. In 2018, Cao *et al*[22] discussed the effectiveness of high-dose statin therapy before PCI in reducing cardiovascular events in Asian populations. The systematic review included 7 RCTs involving 1381 patients, all of whom were Chinese or Korean. The results indicated that the incidence of MACE and perioperative MI in the intensive statin group were significantly lower than those in the control group. This article did not discuss the benefits of treatment to the Chinese population through subgroup analysis.

Table 3 Assessment of randomized controlled trials

Ref.	Randomization sequence generation	Allocation concealment	Blinding of participants, personnel and outcome assessors	Incomplete outcome data	Selective reporting	Other sources of bias
Liu *et al* [10], 2016	Low risk	Low risk	High risk	Unclear risk	Unclear risk	Unclear risk
Jiao *et al* [11], 2015	Unclear risk	Unclear risk	Unclear risk	High risk	Unclear risk	Unclear risk
Jiao *et al* [12], 2015	Low risk	Low risk	Unclear risk	Unclear risk	Unclear risk	Unclear risk
Zheng *et al* [7], 2015	Unclear risk	Unclear risk	High risk	Low risk	Low risk	Unclear risk
Xie *et al* [13], 2014	Unclear risk	Unclear risk	Unclear risk	Unclear risk	Unclear risk	Unclear risk
Luo *et al* [14], 2013	Unclear risk	Unclear risk	Unclear risk	Unclear risk	Unclear risk	Unclear risk
Wang *et al* [15], 2013	Unclear risk	Unclear risk	Unclear risk	Unclear risk	Unclear risk	Unclear risk
Li *et al*[16], 2013	Low risk	Low risk	Low risk	Unclear risk	Unclear risk	Unclear risk
Gao *et al* [17], 2012	Unclear risk	Unclear risk	High risk	Unclear risk	Unclear risk	Unclear risk
Li *et al*[18], 2012	Unclear risk	Unclear risk	Low risk	Unclear risk	Unclear risk	Unclear risk
Yu *et al* [19], 2011	Unclear risk	Unclear risk	Unclear risk	High risk	Unclear risk	Unclear risk

Compared with the previously published meta-analysis, this article was improved in the following ways. First, four new studies published after 2014 were included in this paper[7,10-12]. The full paper included 11 RCTs with 3123 patients, which meant that the total number of studies and patients exceeded any previously published meta-analysis. Second, the population studied in this paper were all Chinese; thus, the interference of other Asian populations such as inclusion of the Korean population was removed. Third, new outcome indicators such as TVR were established to make the data more complete.

An important finding of this study is that the benefits of differential treatment were inconsistent. Compared with patients receiving placebo or no statin treatment before surgery, intensive statin treatment was associated with a clear reduction of risk of MACE. This conclusion was consistent with the results of previous studies involving Western populations. However, compared with the patients receiving moderate-intensity statin before surgery, no advantage to intensive statin treatment was seen, which suggested that both regimens promoted a consistent effect on short-term outcomes. In fact, there is a lack of data on the effect of high-intensity and moderate-intensity statins in Western populations.

Racial differences in the pharmacokinetics of statins have also been reported. With a single dose of 20 mg or 40 mg rosuvastatin, the area under the curve and peak blood concentration of Chinese patients were 1.79, 1.89, 2.31 and 2.36 times that of Caucasians, respectively[23,24]. Birmingham also found that relative to Caucasians the mean area under the curve was 86% higher for single oral doses of rosuvastatin 20 mg and 53% higher for atorvastatin 40 mg in Chinese subjects. In addition, the geometric mean maximum drug concentration was proportionally higher for each statin[25]. Differences in race sensitivity to statins might also be related to genetic factors. Common polymorphisms in genes encoding drug transporters such as *ABCB1*, *ABCG2* and *SLCO1B1* between Chinese and Caucasian populations might partially account for this phenomenon[26]. However, based on the results of this paper and those of prior studies, we did not find any racial differences in terms of the efficacy and safety of preoperative intensive statin therapy.

Another thing that introduces attention was that the data for the meta-analysis comparing high-intensity statins and moderate-intensity statins virtually all come from one study: ISCAP, which was the largest clinical study to date targeting Chinese

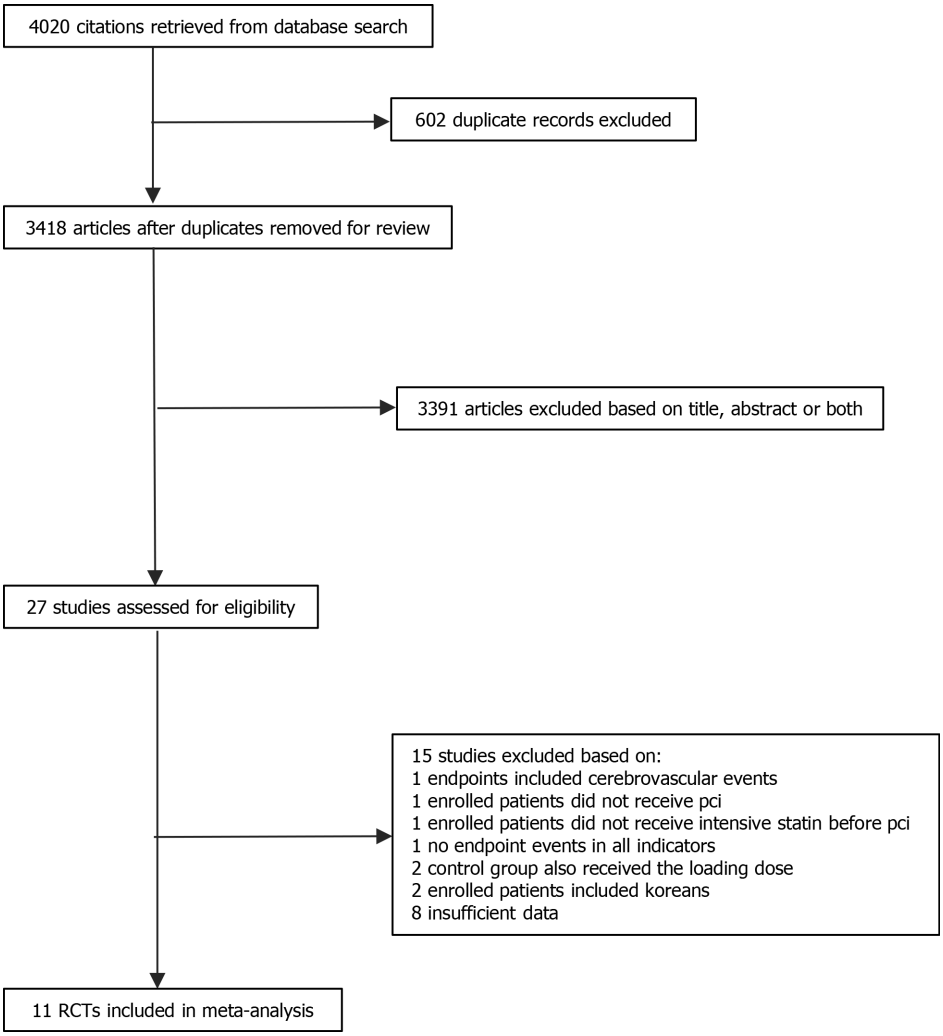

Figure 1 Flowchart of the literature search strategy for this metaanalysis. PCI: Percutaneous coronary intervention; RCT: Randomized controlled trial.

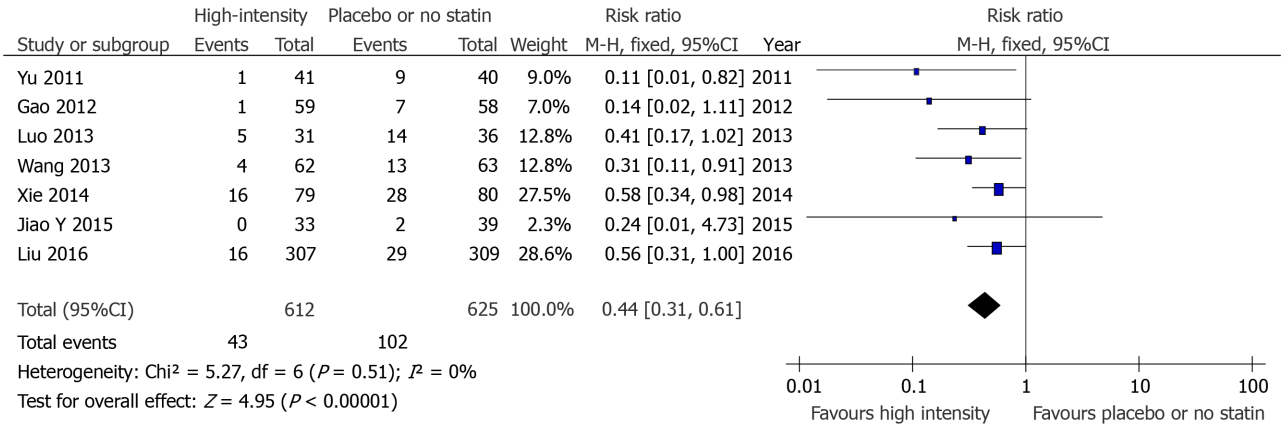

Figure 2 A forest plot of major adverse cardiovascular events with preoperative high-intensity and placebo or no statin therapy in acute coronary syndrome patients. M-H: Mantel-Haenszel method; CI: Confidence interval.

patients. Although negative results were obtained, we also noticed there might be some confounding factors that affected the final conclusions. First, about 60% of enrolled patients had previously taken low-intensity and even moderate-intensity statins, and only 40% were statin-naïve patients. It was unclear whether statin history could have dampened the benefits from the effects of intensive treatment in Chinese patients. Secondly, the timing of drug administration in ISCAP was performed at night before the operation, and it was not exactly fixed. Distinct from the aforementioned

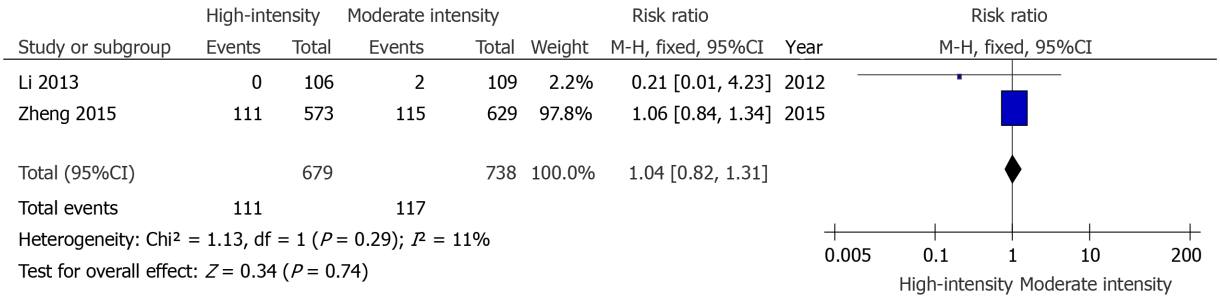

Figure 3 A forest plot of major adverse cardiovascular event with preoperative high-intensity and moderate-intensity statin therapy in acute coronary syndrome patients. M-H: Mantel-Haenszel method; CI: Confidence interval.

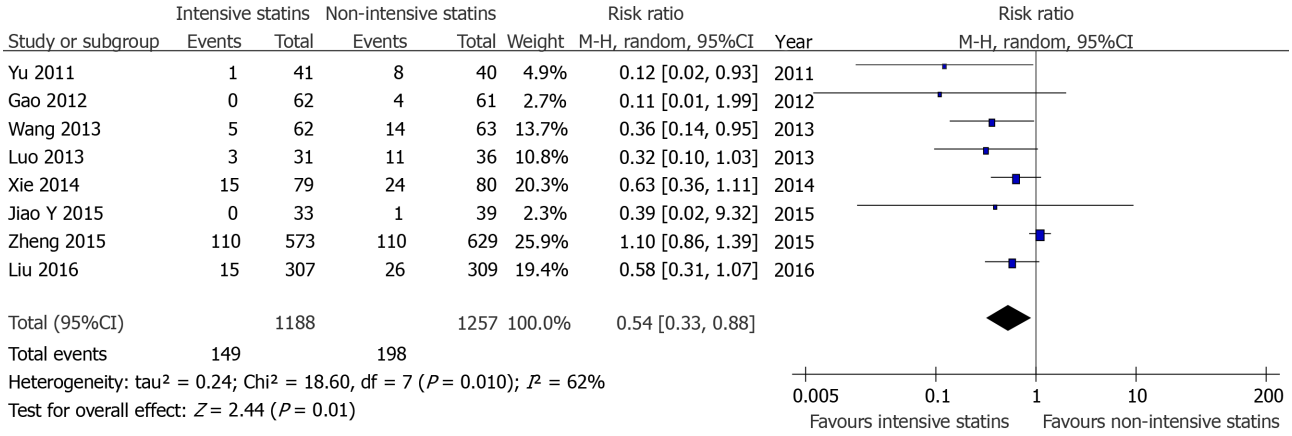

Figure 4 A forest plot of target vessel revascularization with preoperative intensive and non-intensive statins therapy in acute coronary syndrome patients. M-H: Mantel-Haenszel method; CI: Confidence interval.

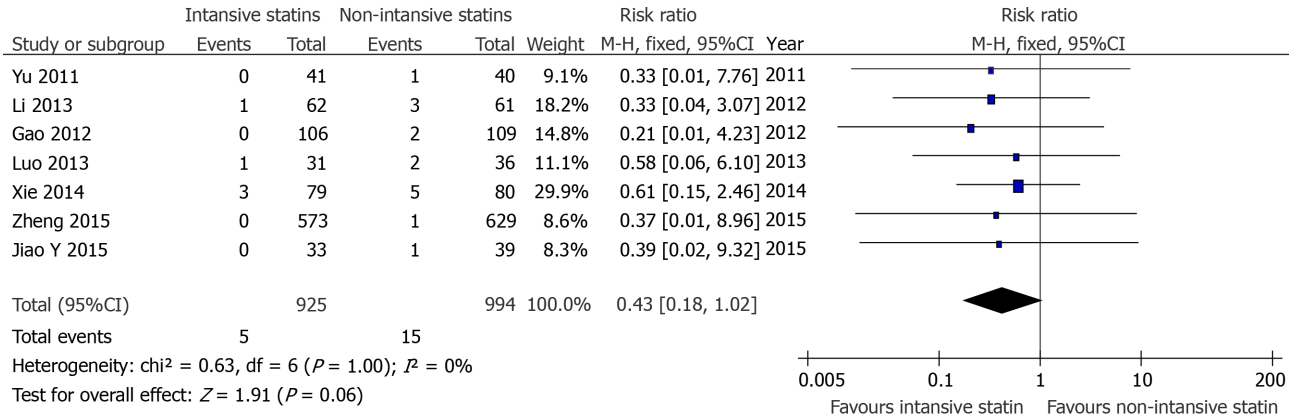

Figure 5 A forest plot of non-fatal myocardial infarction with preoperative intensive and non-intensive statin therapy in acute coronary syndrome patients. M-H: Mantel-Haenszel method; CI: Confidence interval.

observations, the timing was found to be 2-4 h or 12 h before elective PCI and was relatively fixed in other trials[9-12,14-17,19]. On the one hand, the regimen in ISCAP was more consistent with actual clinical practice. On the other hand, it was uncertain whether the timing of statin administration could affect the benefits of intensive statin therapy. Finally, the characteristics of patients enrolled in ISCAP were a higher proportion of multiple lesions, higher average number of stents, longer average length of stents and a higher incidence of MACE at 30 d following PCI; all indicated that the complexity of a coronary lesion might reduce the effectiveness of high-dose statin treatment.

The guidelines and consensus underwent a process of deeper understanding on whether the patients should receive preoperative intensive statin therapy in the

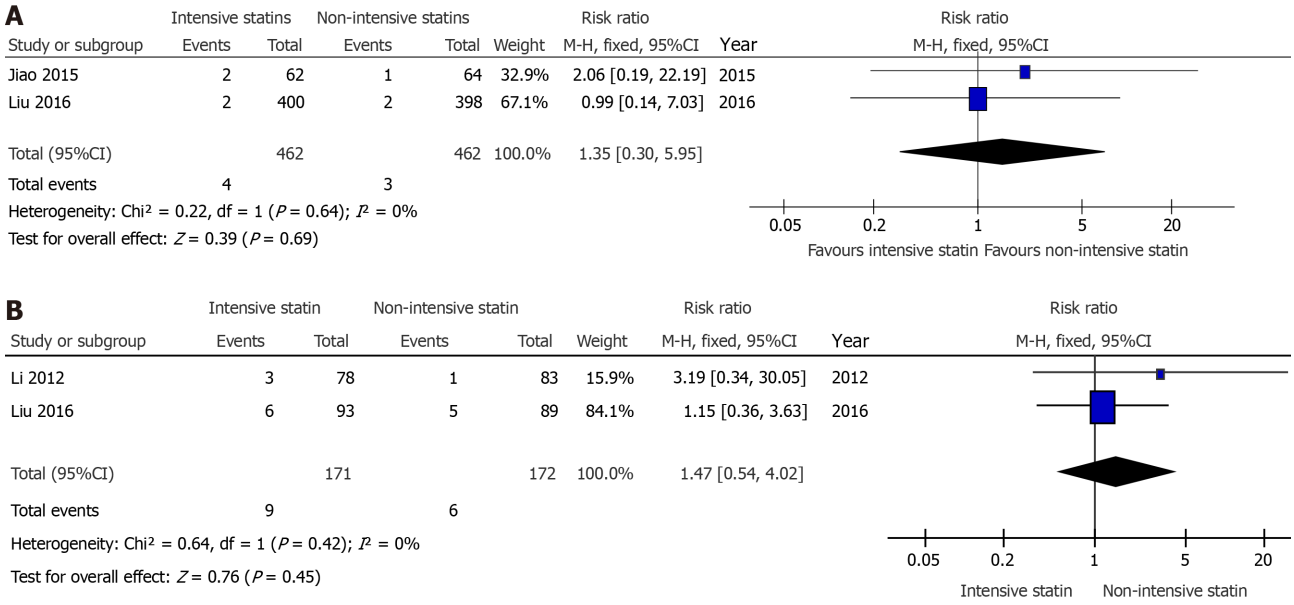

Figure 6 Forest plot. A forest plot of myalgia/myasthenia (A) and abnormal alanine aminotransferase (B) with preoperative intensive and non-intensive statin therapy in acute coronary syndrome patients. M-H: Mantel-Haenszel method; CI: Confidence interval.

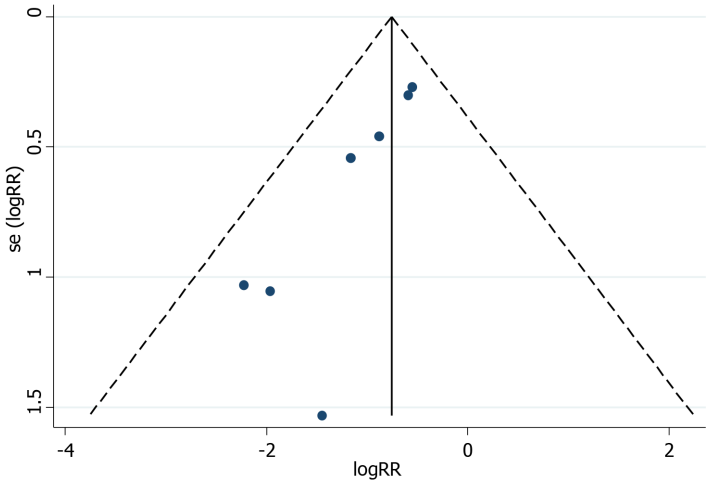

Figure 7 Funnel plot of major adverse cardiovascular events with preoperative high-intensity and placebo or no statin therapy in acute coronary syndrome patients.

Chinese population. Based on evidence from Western populations, expert consensus that was released in 2014 recommended that all patients with acute coronary syndrome undergoing PCI, including emergency and elective PCI, should initiate high-dose statin treatment immediately before PCI, such as treatment with atorvastatin 80 mg/d[27]. Furthermore, since ALPACS and ISCAP were published in succession, guidelines issued in 2016 concluded that in the absence of additional evidence of high-quality RCTs with hard endpoints, it was not recommended that acute coronary syndrome patients receive intensive statin therapy before PCI[28,29]. The results of this meta-analysis were consistent with the recommendations of the guidelines and further strengthened the foundations of evidence-based medicine.

Study limitations

This current article has the following limitations and deficiencies: (1) The quality of the included studies were generally not high, and the evidence was not sufficiently robust. The included RCTs were single-center studies and lacked rigorous trial design with the exception of ISCAP, which was not described in detail in randomization, blinding and data analysis. We also need to recognize that ISCAP was an open-label trial. Although it had all of the outcome events adjudicated by a blinded Clinical Event

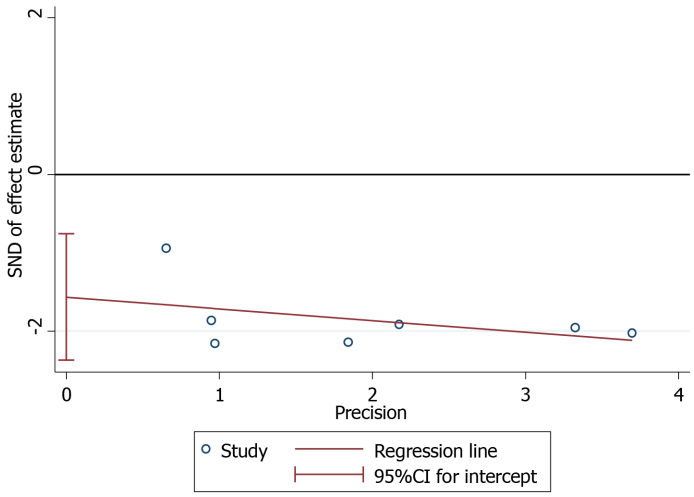

Figure 8 An Egger's plot of major adverse cardiovascular events with preoperative high-intensity and placebo or no statin therapy in acute coronary syndrome patients. CI: Confidence interval; SND: Standard normal deviation.

Committee group and all laboratory tests were done by blinded laboratory staff, the investigators and subjects were not blinded to the treatment arms of this trial. As such, both might tend to report more adverse events in the experiment arm, and this might subsequently lead to increased withdrawal from the study in this group. This trend could still have some undesirable effects on the results of the study. Hence, more studies with a sufficient level of statistical power are needed to investigate the effects of high-dose statin loading before PCI in the context of Chinese patients; (2) Subgroup analysis was not performed. Limited by the included literature, we did not implement subgroup analysis involving some factors, such as statin medication history (*i.e.* patients with chronic statin therapy or statin-naïve patients), categories of statin (*i.e.* atorvastatin or rosuvastatin), timing of statin administration (12 h before surgery or at other times) and the timing of revascularization (emergency PCI or elective PCI). It is also crucial to further explore the limitations by dividing the population into different subgroups as described above; and (3) Due to the lack of RCTs in Western populations, the influence of race could not be analyzed. Therefore, further studies are required to confirm whether or not high-intensity statin preloading before PCI might play a different role in Chinese and Western peoples, not only in terms of the incidence of MACE but also in terms of cholesterol levels and inflammatory markers levels[30].

CONCLUSION

Available evidence suggested that when compared with placebo or no statin pretreatment, Chinese patients receiving intensive statin therapy before PCI have a reduced incidence of MACE. However, there was no significant benefit on using high-intensity and moderate-intensity statin therapy. In addition, no significant difference was observed between intensive statin therapy and non-intensive statin therapy on the incidence ofTVR, myalgia/myasthenia and abnormal ALT except non-fatal MI. To summarize, our findings indicated that it may be reasonable for Chinese patients to receive at least moderate-intensity statin pretreatment before commencing PCI.

ARTICLE HIGHLIGHTS

Research background

At present, the burden of cardiovascular and cerebrovascular disease is very heavy in China. Despite the rapid development of percutaneous coronary intervention (PCI), the overall mortality rate of coronary heart disease and acute myocardial infarction in China is still on the rise. This suggests that there is room for optimizing perioperative therapy.

Research motivation

In China, patients with acute coronary syndrome regularly received intensive statin (such as atorvastatin 40 mg/d or rosuvastatin 20 mg/d) after PCI. Because of the very limited data, the guidelines do not give a positive recommendation for preoperative intensity statin therapy, which was inconsistent with Western people. As members of the medical team in a Coronary Care Unit, we are eager to know if intensive statin before PCI can benefit Chinese patients.

Research objectives

To evaluate the efficacy and safety of intensive statin therapy as compared to non-intensive statin pretreatment before PCI in the Chinese population through a meta-analysis investigation.

Research methods

Relevant studies were identified by searching the electronic databases of PubMed, Embase and Cochrane's Library to December 2019. The outcomes included an assessment of major adverse cardiovascular events, non-fatal myocardial infarction, cardiac death, target vessel revascularization, myalgia/myasthenia and abnormal alanine aminotransferase in all enrolled patients. Random effect model and fixed effect model were applied to combine the data, which were further analyzed by χ^2 test and I^2 test.

Research results

Compared with patients receiving placebo or no statin treatment before surgery, intensive statin treatment was associated with a clear reduction of risk of major adverse cardiovascular events [risk ratio (RR) = 0.44, 95% confidence interval (CI): 0.31-0.61, $P < 0.00001$]. However, compared with the patients receiving moderate-intensity statin before surgery, no advantage to intensive statin treatment was seen (RR = 1.04, 95%CI: 0.82-1.31, $P = 0.74$). In addition, no significant difference was observed between intensive statin therapy and non-intensive statin therapy on the incidence of target vessel revascularization (RR = 0.43, 95%CI: 0.18-1.02, $P = 0.06$) , myalgia/myasthenia (RR = 1.35, 95%CI: 0.30-5.95, $P = 0.69$) and abnormal alanine aminotransferase (RR = 1.47, 95%CI: 0.54-4.02, $P = 0.45$) except non-fatal myocardial infarction (RR = 0.54, 95%CI: 0.33-0.88, $P = 0.01$).

Research conclusions

Our finding was significant that when compared with placebo or no statin pretreatment, intensive statin before PCI displayed reduced incidence of major adverse cardiovascular events. However, there was no significant benefit between high and moderate-intensity statin.

Research perspectives

It is likely to promote at least the use of moderate-intensity statin before PCI instead of no statin pretreatment in Chinese patients.

REFERENCES

1 **Hu S**, Gao R, Liu L, Zhu M, Wang W, Wang Y, Wu Z, Li H, Gu D, Yang Y, Zheng Z, Chen W. Summary of the 2018 Report on Cardiovascular Diseases in China. *Zhongguo Faxing Qikan* 2019; **34**: 209-220 [DOI: 10.3969/j.issn.1000-3614.2019.03.001]

2 **Wu D**, Zhang Q. Current status and progress in the diagnosis and treatment of coronary heart disease in China. *Zhongguo Aizheng Yanjiu Zazhi* 2020; **7**: 159-169 [DOI: 10.19450/j.cnki.jcrh.2020.01.015]

3 **Di Sciascio G**, Patti G, Pasceri V, Gaspardone A, Colonna G, Montinaro A. Efficacy of atorvastatin reload in patients on chronic statin therapy undergoing percutaneous coronary intervention: results of the ARMYDA-RECAPTURE (Atorvastatin for Reduction of Myocardial Damage During Angioplasty) Randomized Trial. *J Am Coll Cardiol* 2009; **54**: 558-565 [PMID: 19643320 DOI: 10.1016/j.jacc.2009.05.028]

4 **Patti G**, Cannon CP, Murphy SA, Mega S, Pasceri V, Briguori C, Colombo A, Yun KH, Jeong MH, Kim JS, Choi D, Bozbas H, Kinoshita M, Fukuda K, Jia XW, Hara H, Cay S, Di Sciascio G. Clinical benefit of statin pretreatment in patients undergoing percutaneous coronary intervention: a collaborative patient-level meta-analysis of 13 randomized studies. *Circulation* 2011; **123**: 1622-1632 [PMID: 21464051 DOI: 10.1161/circulationaha.110.002451]

5 **Briguori C**, Visconti G, Focaccio A, Golia B, Chieffo A, Castelli A, Mussardo M, Montorfano M, Ricciardelli B, Colombo A. Novel approaches for preventing or limiting events (Naples) II trial:

impact of a single high loading dose of atorvastatin on periprocedural myocardial infarction. *J Am Coll Cardiol* 2009; **54**: 2157-2163 [PMID: 19664895 DOI: 10.1016/j.jacc.2009.07.005]

6 **Jang Y**, Zhu J, Ge J, Kim YJ, Ji C, Lam W. Preloading with atorvastatin before percutaneous coronary intervention in statin-naïve Asian patients with non-ST elevation acute coronary syndromes: A randomized study. *J Cardiol* 2014; **63**: 335-343 [PMID: 24216317 DOI: 10.1016/j.jjcc.2013.09.012]

7 **Zheng B**, Jiang J, Liu H, Zhang J, Li H, Su X, Wang H, Song Z, Han Y, Lei H. Efficacy and safety of serial atorvastatin load in Chinese patients undergoing elective percutaneous coronary intervention: results of the ISCAP (Intensive Statin Therapy for Chinese Patients with Coronary Artery Disease Undergoing Percutaneous Coronary Intervention) randomized controlled trial. *Eur Heart J* 2015; B47-B56 [DOI: 10.1093/eurheartj/suv021]

8 **Naito R**, Miyauchi K, Daida H. Racial Differences in the Cholesterol-Lowering Effect of Statin. *J Atheroscler Thromb* 2017; **24**: 19-25 [PMID: 27733728 DOI: 10.5551/jat.RV16004]

9 **Yong H**, Wang X, Mi L, Guo L, Gao W, Zhang Y, Cui M. Effects of atorvastatin loading prior to primary percutaneous coronary intervention on endothelial function and inflammatory factors in patients with ST-segment elevation myocardial infarction. *Exp Ther Med* 2014; **7**: 316-322 [PMID: 24396397 DOI: 10.3892/etm.2013.1432]

10 **Liu Z**, Joerg H, Hao H, Xu J, Hu S, Li B, Sang C, Xia J, Chu Y, Xu D. Efficacy of High-Intensity Atorvastatin for Asian Patients Undergoing Percutaneous Coronary Intervention. *Ann Pharmacother* 2016; **50**: 725-733 [PMID: 27307415 DOI: 10.1177/1060028016654722]

11 **Jiao Y**, Hu F, Zhang Z, Gong K, Sun X, Li A, Liu N. Effect of rosuvastatin dose-loading on serum sLox-1, hs-CRP, and postoperative prognosis in diabetic patients with acute coronary syndromes undergoing selected percutaneous coronary intervention (PCI). *Int J Clin Exp Med* 2015; **8**: 21565-21571 [PMID: 26885106]

12 **Jiao Y**, Hu F, Zhang Z, Gong K, Sun X, Li A, Liu N. Efficacy and Safety of Loading-Dose Rosuvastatin Therapy in Elderly Patients with Acute Coronary Syndromes Undergoing Elective Percutaneous Coronary Intervention. *Clin Drug Investig* 2015; **35**: 777-784 [PMID: 26387028 DOI: 10.1007/s40261-015-0335-1]

13 **Xie W**, Li P, Wang Z, Chen J, Lin Z, Liang X, Mo Y. Rosuvastatin may reduce the incidence of cardiovascular events in patients with acute coronary syndromes receiving percutaneous coronary intervention by suppressing miR-155/SHIP-1 signaling pathway. *Cardiovasc Ther* 2014; **32**: 276-282 [PMID: 25319951 DOI: 10.1111/1755-5922.12098]

14 **Luo J**, Li J, Shen X, Hu X, Fang Z, Lv X, Zhou S. The effects and mechanisms of high loading dose rosuvastatin therapy before percutaneous coronary intervention in patients with acute coronary syndrome. *Int J Cardiol* 2013; **167**: 2350-2353 [PMID: 23194788 DOI: 10.1016/j.ijcard.2012.11.032]

15 **Wang Z**, Dai H, Xing M, Yu Z, Lin X, Wang S, Zhang J, Hou F, Ma Y, Ren Y, Tan K, Wang Y, Ge Z. Effect of a single high loading dose of rosuvastatin on percutaneous coronary intervention for acute coronary syndromes. *J Cardiovasc Pharmacol Ther* 2013; **18**: 327-333 [PMID: 23364255 DOI: 10.1177/1074248412474346]

16 **Li Q**, Deng SB, Xia S, Du JL, She Q. Impact of intensive statin use on the level of inflammation and platelet activation in stable angina after percutaneous coronary intervention: a clinical study. *Med Clin (Barc)* 2013; **140**: 532-536 [PMID: 23177313 DOI: 10.1016/j.medcli.2012.05.042]

17 **Gao Y**, Jia ZM, Sun YJ, Zhang ZH, Ren LN, Qi GX. Effect of high-dose rosuvastatin loading before percutaneous coronary intervention in female patients with non-ST-segment elevation acute coronary syndrome. *Chin Med J (Engl)* 2012; **125**: 2250-2254 [PMID: 22882843 DOI: 10.3760/cma.j.issn.0366-6999.2012.13.002]

18 **Li W**, Fu X, Wang Y, Li X, Yang Z, Wang X, Geng W, Gu X, Hao G, Jiang Y, Fan W, Wu W, Li S. Beneficial effects of high-dose atorvastatin pretreatment on renal function in patients with acute ST-segment elevation myocardial infarction undergoing emergency percutaneous coronary intervention. *Cardiology* 2012; **122**: 195-202 [PMID: 22854323 DOI: 10.1159/000339472]

19 **Yu XL**, Zhang HJ, Ren SD, Geng J, Wu TT, Chen WQ, Ji XP, Zhong L, Ge ZM. Effects of loading dose of atorvastatin before percutaneous coronary intervention on periprocedural myocardial injury. *Coron Artery Dis* 2011; **22**: 87-91 [PMID: 21169815 DOI: 10.1097/MCA.0b013e328341baee]

20 **Guo X**. A meta-analysis of sequential therapy of statins on PCI patients in China. Shandong University, 2019. [cited 20 February 2021]. Available from: https://kns.cnki.net/kns8/defaultresult/index

21 **Ye Z**, Lu H, Su Q, Guo W, Dai W, Li H, Yang H, Li L. Effect of high-dose rosuvastatin loading before percutaneous coronary intervention in Chinese patients with acute coronary syndrome: A systematic review and meta-analysis. *PLoS One* 2017; **12**: e0171682 [PMID: 28231287 DOI: 10.1371/journal.pone.0171682]

22 **Cao A**, Qian J, Wang Z. Efficacy of high-dose statins administration before surgery on the reduction of cardiovascular events: A meta analysis. *Pharm Care Res* 2018; **18**: 282-287

23 **Birmingham BK**, Bujac SR, Elsby R, Azumaya CT, Zalikowski J, Chen Y, Kim K, Ambrose HJ. Rosuvastatin pharmacokinetics and pharmacogenetics in Caucasian and Asian subjects residing in the United States. *Eur J Clin Pharmacol* 2015; **71**: 329-340 [PMID: 25630984 DOI: 10.1007/s00228-014-1800-0]

24 **Lee E**, Ryan S, Birmingham B, Zalikowski J, March R, Ambrose H, Moore R, Lee C, Chen Y, Schneck D. Rosuvastatin pharmacokinetics and pharmacogenetics in white and Asian subjects

residing in the same environment. *Clin Pharmacol Ther* 2005; **78**: 330-341 [PMID: 16198652 DOI: 10.1016/j.clpt.2005.06.013]

25 **Birmingham BK**, Bujac SR, Elsby R, Azumaya CT, Wei C, Chen Y, Mosqueda-Garcia R, Ambrose HJ. Impact of ABCG2 and SLCO1B1 polymorphisms on pharmacokinetics of rosuvastatin, atorvastatin and simvastatin acid in Caucasian and Asian subjects: a class effect? *Eur J Clin Pharmacol* 2015; **71**: 341-355 [PMID: 25673568 DOI: 10.1007/s00228-014-1801-z]

26 **Tomlinson B**, Chan P, Liu ZM. Statin Responses in Chinese Patients. *J Atheroscler Thromb* 2018; **25**: 199-202 [PMID: 28740057 DOI: 10.5551/jat.40204]

27 **Huo Y**, Ge JB, Han YL. Expert consensus on intensive statin therapy for patients with acute coronary syndrome. *Zhongguo Jieru Xinzangbingxue Zazhi* 2014; **22**: 4-6 [DOI: 10.3969/j.issn.1004-8812.2014.01.002]

28 **Joint committee issued Chinese guideline for the management of dyslipidemia in adults**. Chinese guideline for the management of dyslipidemia in adults. *Zhongguo Faxing Qikan* 2016; **32**: 937-953

29 **Chinese Medical Association in cardiovascular disease branch interventional cardiology group**. Chinese Medical Doctor Association cardiovascular physician branch thrombus prevention and control Specialized Committee. Chinese Journal of cardiovascular disease editorial board. Guidelines for percutaneous coronary intervention in China (2016). *Zhongguo Xinxueguan Jibing Zazhi* 2016; **44**: 382-400

30 **Liu H**, Dong A, Wang H. Long-term benefits of high-intensity atorvastatin therapy in Chinese acute coronary syndrome patients undergoing percutaneous coronary intervention: A retrospective study. *Medicine (Baltimore)* 2018; **97**: e12687 [PMID: 30334951 DOI: 10.1097/md.0000000000012687]

World Journal of Clinical Cases

Submit a Manuscript: https://www.f6publishing.com

World J Clin Cases 2022 February 16; 10(5): 1572-1579

DOI: 10.12998/wjcc.v10.i5.1572

ISSN 2307-8960 (online)

CASE REPORT

Giant nodular fasciitis originating from the humeral periosteum: A case report

Shi-Li Yu, Ping-Li Sun, Jian Li, Meng Jia, Hong-Wen Gao

ORCID number: Shi-Li Yu 0000-0002-8741-6097; Ping-Li Sun 0000-0002-7511-3080; Jian Li 0000-0001-9510-4205; Meng Jia 0000-0001-9440-5110; Hong-Wen Gao 0000-0002-8974-4975.

Author contributions: Sun PL designed the review; Yu SL collected the data and prepared the draft; Li J and Jia M participated in data interpretation; Sun PL and Gao HW provided research fund; all authors read and approved the final manuscript.

Informed consent statement: Informed written consent was obtained from the patient for publication of this case report.

Conflict-of-interest statement: The authors declare that they have no competing interests to disclose.

CARE Checklist (2016) statement: The authors have read the CARE Checklist (2016), and the manuscript was prepared and revised according to the CARE Checklist (2016).

Supported by Jilin Province Department of Finance Project, No. 2019SCZT005, No. 2019SRCJ007 and No. 2020SCZT007; National Natural Science Foundation of China, No. 81902342; and Health Commission of Jilin Province, No. 2019Q002.

Shi-Li Yu, Ping-Li Sun, Jian Li, Meng Jia, Hong-Wen Gao, Department of Pathology, The Second Hospital of Jilin University, Changchun 130041, Jilin Province, China

Corresponding author: Hong-Wen Gao, MD, PhD, Chief Physician, Department of Pathology, The Second Hospital of Jilin University, No. 218 Ziqiang Road, Changchun 130041, Jilin Province, China. gaohongwen@jlu.edu.cn

Abstract

BACKGROUND

Nodular fasciitis (NF) is a self-limiting tumor that mostly occurs in the subcutaneous superficial fascia. NF originating from the appendicular periosteum is extremely rare. A large NF lesion of periosteal origin can be misdiagnosed as a malignant bone tumor and may cause overtreatment.

CASE SUMMARY

A right axillary mass was found in a 46-year-old man and was initially diagnosed intraoperatively as low-grade sarcoma, but later diagnosed as NF after post-resection histopathological evaluation. Furthermore, fluorescence *in situ* hybridization analysis revealed a *USP6* gene rearrangement that confirmed the diagnosis. To the best of our knowledge, this is the first case of NF in the humeral periosteum.

CONCLUSION

NF poses a diagnostic challenge as it is often mistaken for sarcoma. Postoperative histopathological examination of whole sections can be combined with immunohistochemical staining and, if necessary, the diagnosis can be confirmed by molecular detection, and thus help avoid overtreatment.

Key Words: Nodular fasciitis; Periosteum; Differential diagnosis; *USP6*; Fluorescence *in situ* hybridization; Case report

Core Tip: This article provides a comprehensive overview of the clinicopathological, immunohistochemical, and molecular features of nodular fasciitis originating from the humeral periosteum. To date, this is the first report of nodular fasciitis originating from

Country/Territory of origin: China

Specialty type: Medicine, research and experimental

Provenance and peer review: Unsolicited article; Externally peer reviewed.

Peer-review model: Single blind

Peer-review report's scientific quality classification
Grade A (Excellent): 0
Grade B (Very good): 0
Grade C (Good): C
Grade D (Fair): 0
Grade E (Poor): 0

Received: November 27, 2020
Peer-review started: November 30, 2020
First decision: September 28, 2021
Revised: October 9, 2021
Accepted: January 6, 2022
Article in press: January 6, 2022
Published online: February 16, 2022

P-Reviewer: Martínez-Pérez A
S-Editor: Gao CC
L-Editor: Wang TQ
P-Editor: Gao CC

the humeral periosteum and this type of research is critical to further our understanding of these lesions and advance pathological diagnoses.

Citation: Yu SL, Sun PL, Li J, Jia M, Gao HW. Giant nodular fasciitis originating from the humeral periosteum: A case report. *World J Clin Cases* 2022; 10(5): 1572-1579
URL: https://www.wjgnet.com/2307-8960/full/v10/i5/1572.htm
DOI: https://dx.doi.org/10.12998/wjcc.v10.i5.1572

INTRODUCTION

Nodular fasciitis (NF) was first described as a pseudosarcomatous fasciitis by Konwaler *et al*[1] in 1955. Similar to other soft-tissue sarcomas, NF is a rapidly growing, benign proliferation of fibroblasts and myofibroblasts displaying abundant, spindle-shaped cells and high mitotic activity. NF presents most typically in the upper extremities (46%), trunk (20%), and head and neck (18%)[2]. The peak incidences of NF are seen at ages 20 and 40, often presenting with tenderness, and it is a rare disease in children[3]. Most NF lesions are small, measuring less than 2 cm in diameter[2,4]. Periosteal fasciitis is considered a rare subtype of NF, with some case reports in the published literature and most of those were published over 20 years ago; only one case of periosteal fasciitis has been published recently, in 2017. The frequently reported sites of periosteal fasciitis are the maxilla and the hand; however, there are no reports of periosteal fasciitis in the limbs, and all reported cases described tumors that were smaller than 5 cm.

As NF has a nonspecific immunohistochemical profile[4], its histomorphological characteristics are the primary diagnostic criteria. Therefore, it remains a challenge to distinguish NF from other spindle cell lesions, particularly those of the myofibroblastic lineage.

In 2011, Erickson-Johnson *et al*[5] reported the rearrangement of the *USP6* gene on chromosome 17p13 as a recurrent and specific finding in NF. Subsequently in 2013, Amary *et al*[6] found *USP6* gene rearrangements in 91% of the 34 NF cases in their study, thereby making *USP6* fluorescence *in situ* hybridization (FISH) analysis a reliable and useful ancillary diagnostic test for NF.

This report presents findings from the first case of large-sized NF originating from the humeral periosteum. We emphasize the importance of highlighting this rare clinical entity, which usually represents a diagnostic dilemma.

CASE PRESENTATION

Chief complaints

Intermittent pain in the right axilla for 1 mo.

History of present illness

The patient had intermittent right axillary pain with no obvious cause of for 1 mo. And he found a lump under his axilla. Magnetic resonance imaging (MRI) showed a lesion measuring 62 mm × 58 mm × 44 mm, with relatively well-demarcated margins, and the lesion encircled the humerus, with localized thinning of the humeral cortex, and was closely related to the radial artery. The clinician recommended surgical treatment.

History of past illness

There was no history of past illness.

Personal and family history

There was no personal and family history.

Physical examination

A tough mass was locally palpable on the medial side of the upper right arm and was approximately 7 cm in size.

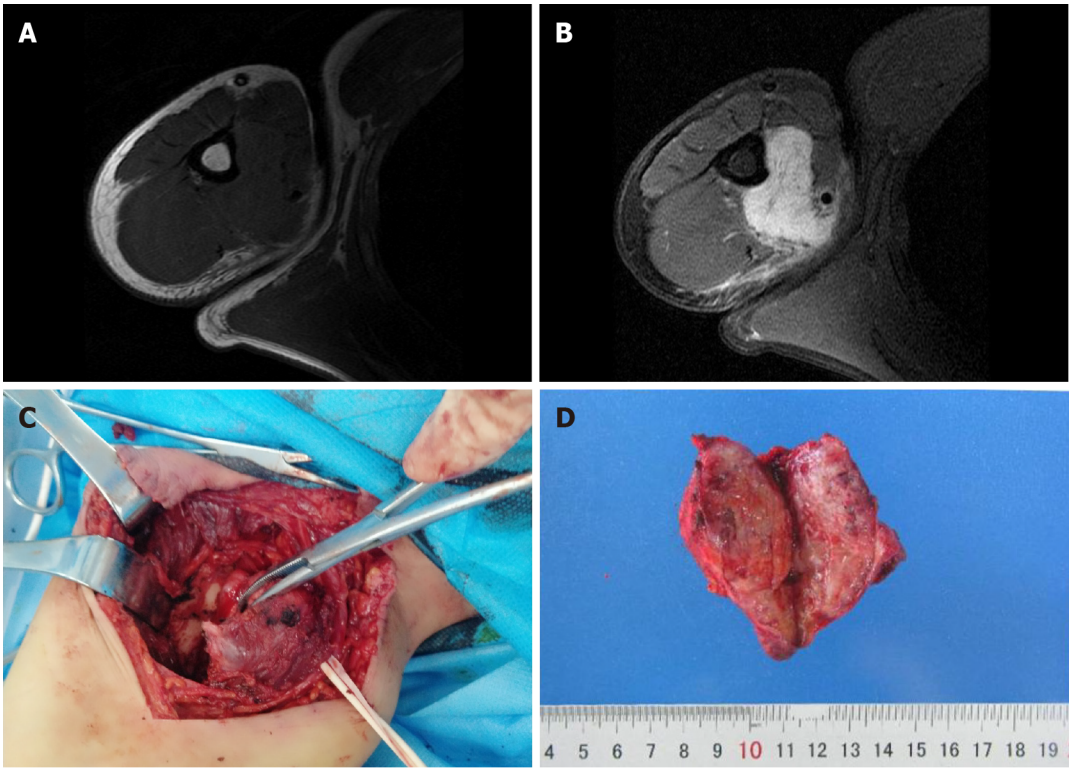

Figure 1 Imaging and gross examination. A: Magnetic resonance imaging showed patchy low signal in the medial humerus (T1WI); B: Magnetic resonance imaging showed a high signal intensity on the humerus, with local thinning of the humeral cortex (T2WI); C: The root of the mass extended laterally below the biceps brachii and was closely related to the humerus; D: The mass was nodular, with a diameter of 7.5 cm, a relatively clear boundary, and a reddish gray appearance on cross section.

Laboratory examinations

No abnormalities were found in routine laboratory tests.

Imaging examinations

An MRI scan showed a high signal intensity in the agglomerated pressure-fat phase near the right axillary region. The MRI images showed a lesion measuring 62 mm × 58 mm × 44 mm, with relatively well-demarcated margins. The lesion encircled the humerus, with localized thinning of the humeral cortex, and was closely related to the radial artery.

FINAL DIAGNOSIS

NF.

TREATMENT

Surgical tumor resection.

Diagnostic work-up

The differential diagnosis of sarcoma was made, and the patient underwent surgical tumor resection. Intraoperatively, we identified a mass with an approximate diameter of 7 cm that was closely related to the humerus, with a relatively clear boundary that separated it from the surrounding tissue. The tumor was completely separated from the periosteum. The surgical specimen was intraoperatively subjected to rapid histopathological examination. Gross examination revealed a gray nodule measuring 7.5 cm × 4 cm × 4 cm that had a reddish gray surface appearance on cross section and relatively tough texture (Figure 1). Microscopically, the lesion mainly comprised spindle-shaped fibroblast-like cells, with mucinous degeneration, mild atypia of some cells, and 3-4 mitotic figures per 10 high power fields. The intraoperative provisional

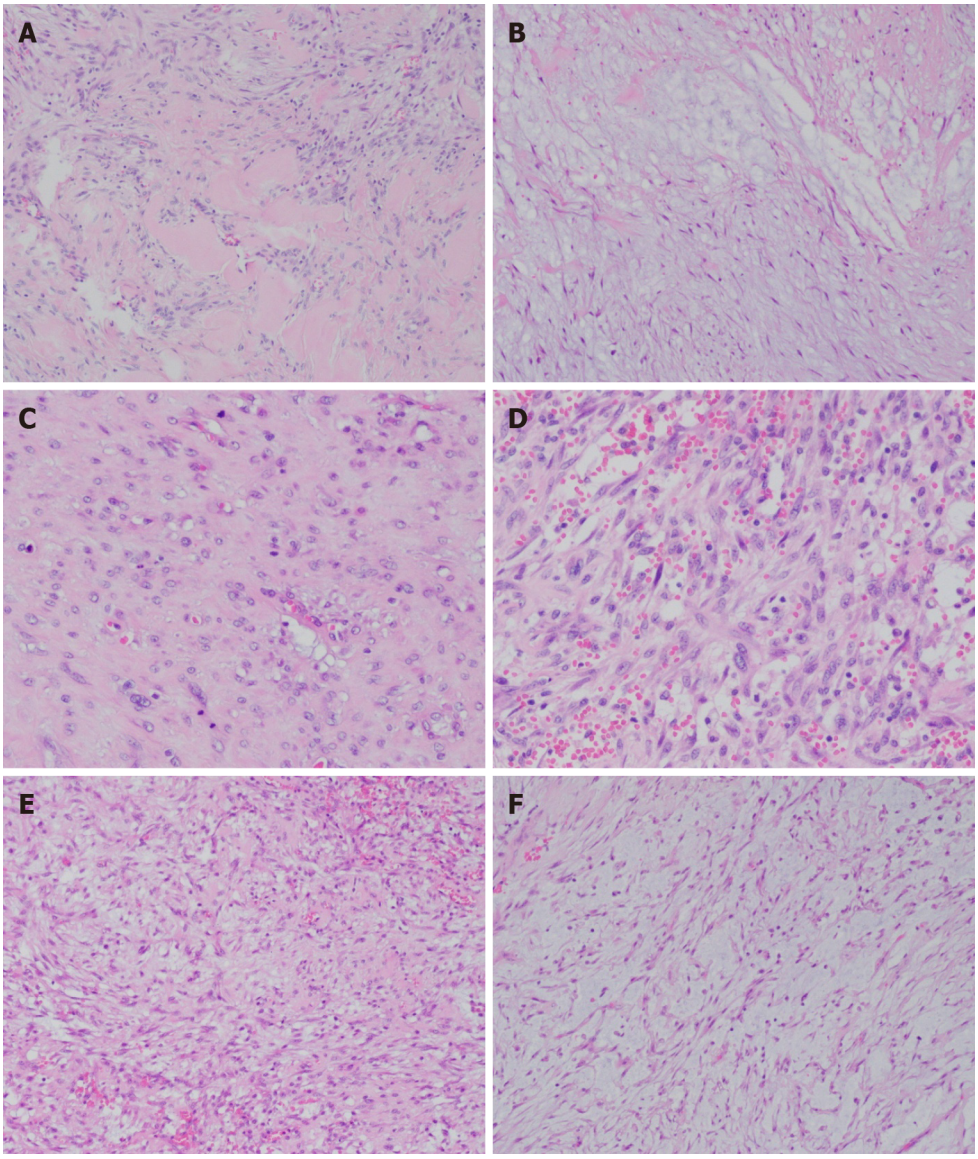

Figure 2 Hematoxylin-eosin staining. A: Localized fibrous tissue hyperplasia and hyaline degeneration [hematoxylin and eosin (HE), × 100]; B: Some areas showed extracellular mucoid matrix (HE, × 100); C: Mitotic figures (HE, × 200); D: Tumor cells are abundant and there is apparent extravasation of red blood cells (HE, × 200); E: Spindle-shaped and fibroblast-like tumor cells (HE, × 100); F: Spindle-shaped tumor cells with stromal mucous degeneration (HE, × 100).

pathological diagnosis was a mesenchymal neoplasm; the final diagnosis would be definitively based on the postoperative pathology. The postoperative histopathology of the lesions revealed spindle-shaped tumor cells with abundant extracellular mucoid matrix (Figure 2B and F); similarly, on examination of the frozen sections, some areas showed fibrous hyperplasia and hyaline degeneration (Figure 1A), whereas other areas had extravasation of red blood cells (Figure 2D). Tumor cells in areas with relatively high cellularity showed mild atypia (Figure 2C and D) and mitotic figures (Figure 2C). Immunohistochemistry showed that the specimen stained negative for CD34, S100, and β-catenin and positive for CD10 and SMA (Figure 3). FISH analysis revealed a *USP6* gene fracture rearrangement (Figure 4) with signal patterns as follows: 1G1R1F 16.5%, 1G1R 8.5%, 2F 35.5%, 1F 25.0%, 1G1F 7.0%, and 1R1F 7.5%.

OUTCOME AND FOLLOW-UP

The patient had an uneventful recovery after surgery and no further treatment was given. There was no recurrence during the 20-mo follow-up period.

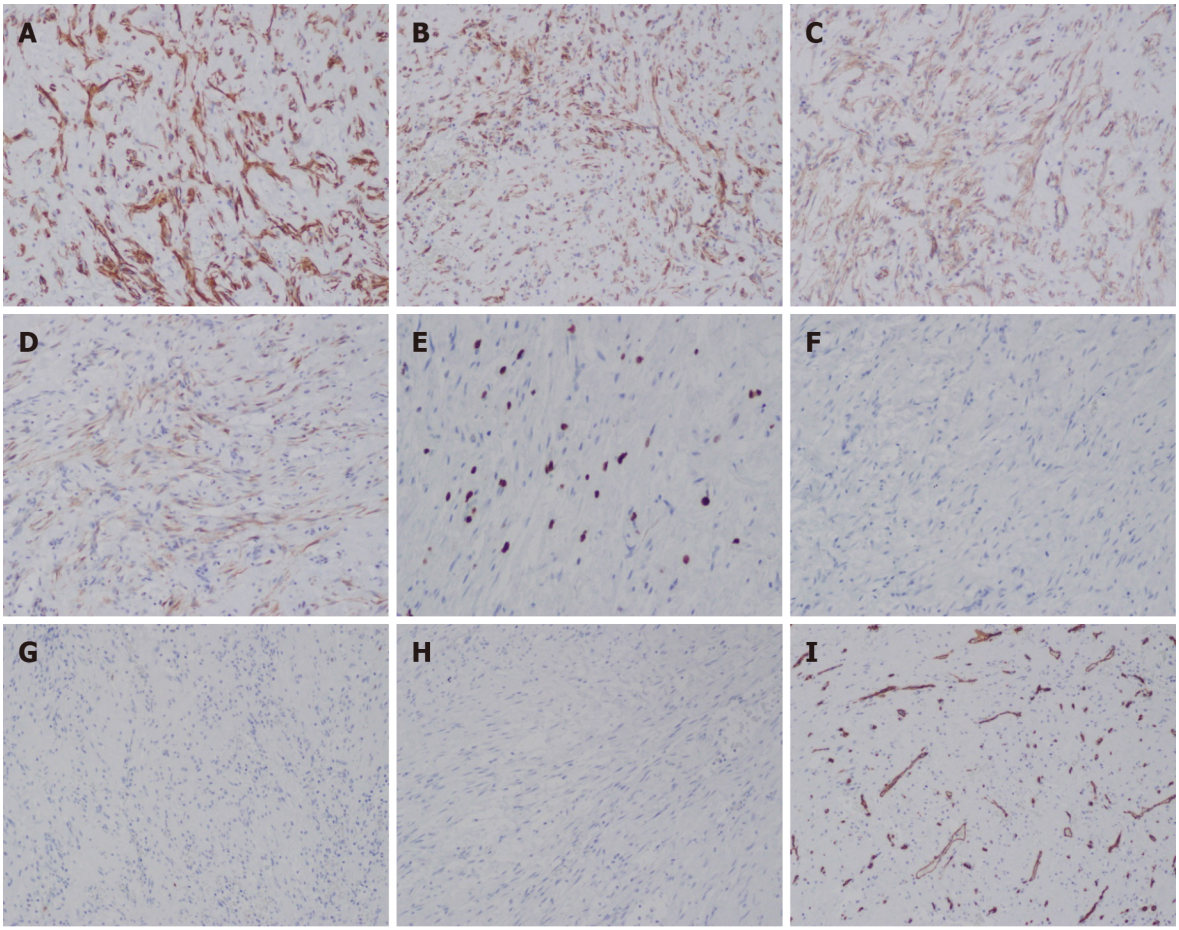

Figure 3 Immunohistochemical staining. A: Tumor cells stained positive for SMA; B: Tumor cells stained positive for CD10; C: The cytoplasm tested positive for β-catenin; D: Tumor cells stained positive for calponin; E: The Ki67 index was 10%; F: Tumor cells stained negative for desmin; G: Tumor cells stained negative for EMA; H: Tumor cells stained negative for S-100; I: Tumor cells stained negative for CD34 (EnVision, × 100).

DISCUSSION

The published literature describes NF as a benign myofibroblastic proliferation, which was initially reported in 1955 as a pseudosarcomatous fibromatosis or fasciitis[1]. The NF lesion typically develops in the subcutaneous superficial fascia of the upper limbs (46%), especially over the volar aspect of the forearm, followed by the head and neck (20%), trunk (18%), and lower extremities (16%). There are no gender differences in NF incidence, and all reported lesions measure less than 5 cm in diameter.

Periosteal fasciitis, a subtype of NF, is characterized by periosteal overgrowth and reactive new bone formation. There are only a few case reports (10 cases) of periosteal fasciitis in the literature, most of which were reported in the 1970s and 1980s, although one case was recently reported in 2017. Among those ten cases (four males; six females), four occurred in the jaw (one in the maxilla, three in the mandible) and six in the hand. The largest reported tumor diameter was approximately 5 cm. Most of the cases were diagnosed by histomorphological features, and FISH was undertaken in only one case in the recent literature and showed *USP6* gene-related heterotopia. All patients were followed, and there are no reports of recurrence (Table 1). In our case, NF was initially diagnosed by histomorphology and immunohistochemistry; however, because of the unusually large tumor and its periosteal origin, we undertook a *USP6* FISH examination. The results showed *USP6*-related ectopia, which further confirmed a diagnosis of NF. The patient has shown no recurrence on follow-up for 10 mo. This report presents a rare case of clinical NF of the humeral periosteum with a tumor diameter of 7.5 cm.

Due to its fast and infiltrative growth pattern, NF remains one of the most commonly misdiagnosed benign spindle cell neoplasms. A common differential diagnosis of NF is low-grade malignant myofibroblastic tumors because, despite their large size, the tumor cells are characterized by mild atypia; positive staining for actin, desmin, calponin, and CD34 (focal), and negative staining for S100 and nuclear β-

Table 1 Published studies reporting periosteal fasciitis

Ref.	Number of cases	Sex	Age (yr)	Symptom presence and duration	Location	Treatment	Size (cm)	*USP6* gene	Follow-up (mo)	Recurrence	Injury
Lääveri *et al* [11], 2017	1	Female	7	No	Mandible	Local resection	3	Yes	36	No	No
Rankin *et al* [12], 1991	1	Female	39	No	Hand	Local resection	5	NA	10	No	No
Mostofi *et al* [13], 1987	1	Male	46	No	Mandible	Local resection	3	NA	30	No	No
Sato *et al*[14], 1981	1	Male	31	Pain for 2 mo	Maxillary	Local resection	4	NA	8	No	No
McCarthy *et al* [15], 1976	1	Male	40	No	Ring finger	Amputation	NA	NA	12	No	No
Johnson and Lawrence[16], 1975	1	Male	38	Pain and swelling for 3 mo	Metacarpal and ring finger	Local resection	NA	NA	12	No	No
Goncalves[17], 1974	1	Female	23	Pain and swelling for 2 wk	Index finger	Amputation	NA	NA	60	No	No
Lumerman *et al* [18], 1972	1	Female	31	Pain for 3 d	Mandible	Local resection	2	NA	30	No	No
Carpenter and Lublin[19], 1967	1	Female	32	Pain and swelling for 7 mo	Proximal and middle phalanges, ring finger	Amputation	NA	NA	12	No	No
Mallory[20], 1933	1	Female	28	Pain, swelling for 4 wk	4th and 5th metacarpals	Incomplete local resection	NA	NA	12	No	No

NA: Not available.

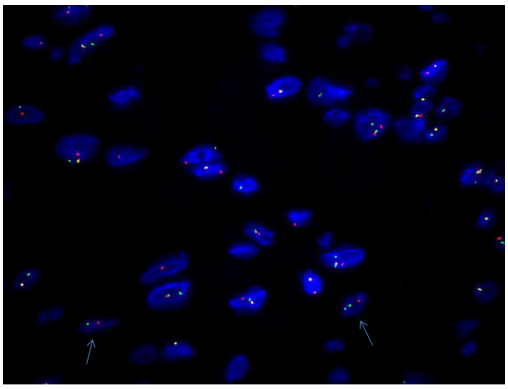

Figure 4 Fluorescence *in situ* hybridization analysis showing a *USP6* rearrangement as separated red and green signals.

catenin[7-9]. However, FISH shows no *USP6* gene-related ectopia, and myofibroblastic tumors have a high recurrence after surgical resection.

Sometimes, it may be difficult to distinguish low-grade myxofibrosarcoma from NF, especially in cases with small tumor volume and without specific immunohistochemical markers. Nonetheless, curvilinear thin-walled blood vessels and pseudolipoblasts suggest the possibility of a myxofibrosarcoma, and FISH examination shows no *USP6* gene-related ectopia.

Low-grade malignant fibromyxoid sarcoma is another differential diagnosis of NF. The identification can be comprehensively evaluated by immunohistochemical staining and molecular detection. Immunohistochemistry shows EMA positivity from focally to 80%, and MUC4 positivity has high sensitivity and specificity for the detection of fibromyxoid sarcoma[10]. Molecular genetics show *FUS-CREB3L2* or *FUS-CREB3L1* gene fusion (Table 2).

Table 2 Primary differential diagnosis

Tumor type	Epidemiology	Clinical features	Size	Histopathology	Immunophenotype	Genetics
Nodular fasciitis	Young adults, no gender difference	Grows rapidly, painless, recurrence is rare	Median size, ≤ 2 cm (always < 5 cm)	Spindle-shaped fibroblasts, growth in S- or C- shaped, interstitium is loose and myxoid, visible exosmosis of erythrocytes	Positive: SMA, Calponin, CD10; negative: S100, CD34, nuclear β-catenin	*MYH9–USP6* gene fusion
Low-grade fibromyxoid sarcoma	Typically affect young adults, no gender difference	Slow growth, no pain, easy recurrence	Median size, 5 cm (1-20 cm)	Original glue and myxoid region are mixed, spindle cell, small blood vessels, early formation of collagen rosettes	EMA positive from focally to 80%, MUC4 positive has high sensitivity and specificity	*FUS-CREB3L2* or *FUS-CREB3L1* gene fusion
Low-grade myofibroblastic sarcoma	Predominantly in adults, 40-50 yr see more, slight predominance in males	Enlarging mass, painless, easy recurrence	Median size, 4 cm (1.4-17 cm)	Diffusely infiltrative growth, spindle cells arranged in a storiform pattern or fascicles	Positive: actin, desmin, calponin, CD34 (focal); negative: S100, nuclear β-catenin	Only one showed a circular chromosome
Low-grade myxofibrosarcoma	Elderly patients, over 60 yr, slight predominance in males	Slowly enlarging, painless, easy recurrence	Larger volume (range variable)	Spindle cells, mild atypia, curvilinear thin-walled blood vessels, pseudolipoblasts	Positive: SMA, negative: Desmin and histiocyte-specific markers	No specific aberration

Immunohistochemical staining has no specific significance in the identification of NF; however, it can be used as an auxiliary and differential diagnostic tool because spindle cells in NF often diffusely express SMA, and are negative for desmin. Recent studies have shown that *USP6 in situ* hybridization has higher specificity and sensitivity in the diagnosis of NF[6], particularly in cases with uncharacteristic morphology.

Furthermore, NF can be accurately diagnosed by combining tumor morphological characteristics, immunohistochemical findings, and *USP6* detection, thereby avoiding misdiagnosis and overtreatment of patients.

CONCLUSION

NF poses a diagnostic challenge as it is often mistaken for a sarcoma, or easily misdiagnosed as a sarcomatous lesion such as malignant fibrous histiocytoma or fibrosarcoma, because of its rapid growth, rich cellularity, and poorly circumscribed nature. NF is a tumor with rapid growth and relatively clear boundary, but it is sometimes difficult to distinguish from low-grade sarcoma under the microscope. When the tumor location is atypical and volume is large, the possibility of the disease should also be considered, especially during the operation, which can avoid excessive treatment. Postoperative histopathological examination of whole sections can be combined with immunohistochemical staining and, if necessary, the diagnosis can be confirmed by molecular detection.

REFERENCES

1 **Konwaler BE**, Keasbey L, Kaplan L. Subcutaneous pseudosarcomatous fibromatosis (fasciitis). *Am J Clin Pathol* 1955; **25**: 241-252 [PMID: 14361319 DOI: 10.1093/ajcp/25.3.241]

2 **Meister P**, Bückmann FW, Konrad E. Nodular fasciitis (analysis of 100 cases and review of the literature). *Pathol Res Pract* 1978; **162**: 133-165 [PMID: 97640 DOI: 10.1016/S0344-0338(78)80001-6]

3 **Kayaselçuk F**, Demirhan B, Kayaselçuk U, Ozerdem OR, Tuncer I. Vimentin, smooth muscle actin, desmin, S-100 protein, p53, and estrogen receptor expression in elastofibroma and nodular fasciitis. *Ann Diagn Pathol* 2002; **6**: 94-99 [PMID: 12004356 DOI: 10.1053/adpa.2002.32377]

4 **Shimizu S**, Hashimoto H, Enjoji M. Nodular fasciitis: an analysis of 250 patients. *Pathology* 1984; **16**: 161-166 [PMID: 6462780 DOI: 10.3109/00313028409059097]

5 **Erickson-Johnson MR**, Chou MM, Evers BR, Roth CW, Seys AR, Jin L, Ye Y, Lau AW, Wang X, Oliveira AM. Nodular fasciitis: a novel model of transient neoplasia induced by MYH9-USP6 gene fusion. *Lab Invest* 2011; **91**: 1427-1433 [PMID: 21826056 DOI: 10.1038/labinvest.2011.118]

6 **Amary MF**, Ye H, Berisha F, Tirabosco R, Presneau N, Flanagan AM. Detection of USP6 gene

rearrangement in nodular fasciitis: an important diagnostic tool. *Virchows Arch* 2013; **463**: 97-98 [PMID: 23748914 DOI: 10.1007/s00428-013-1418-0]

7 **Sinhasan SP**, K V B, Bhat RV, Hartimath BC. Intra-muscular Nodular Fasciitis Presenting as Swelling in Neck: Challenging Entity for Diagnosis. *J Clin Diagn Res* 2014; **8**: 155-157 [PMID: 24596753 DOI: 10.7860/JCDR/2014/6424.3909]

8 **Mentzel T**, Dry S, Katenkamp D, Fletcher CD. Low-grade myofibroblastic sarcoma: analysis of 18 cases in the spectrum of myofibroblastic tumors. *Am J Surg Pathol* 1998; **22**: 1228-1238 [PMID: 9777985 DOI: 10.1097/00000478-199810000-00008]

9 **Qiu X**, Montgomery E, Sun B. Inflammatory myofibroblastic tumor and low-grade myofibroblastic sarcoma: a comparative study of clinicopathologic features and further observations on the immunohistochemical profile of myofibroblasts. *Hum Pathol* 2008; **39**: 846-856 [PMID: 18400254 DOI: 10.1016/j.humpath.2007.10.010]

10 **Doyle LA**, Wang WL, Dal Cin P, Lopez-Terrada D, Mertens F, Lazar AJ, Fletcher CD, Hornick JL. MUC4 is a sensitive and extremely useful marker for sclerosing epithelioid fibrosarcoma: association with FUS gene rearrangement. *Am J Surg Pathol* 2012; **36**: 1444-1451 [PMID: 22982887 DOI: 10.1097/PAS.0b013e3182562bf8]

11 **Lääveri M**, Heikinheimo K, Baumhoer D, Slootweg PJ, Happonen RP. Periosteal fasciitis in a 7-year old girl: a diagnostic dilemma. *Int J Oral Maxillofac Surg* 2017; **46**: 883-885 [PMID: 28262308 DOI: 10.1016/j.ijom.2017.02.005]

12 **Rankin G**, Kuschner SH, Gellman H. Nodular fasciitis: a rapidly growing tumor of the hand. *J Hand Surg Am* 1991; **16**: 791-795 [PMID: 1940154 DOI: 10.1016/s0363-5023(10)80137-6]

13 **Mostofi RS**, Soltani K, Beste L, Polak E, Benca P. Intraoral periosteal nodular fasciitis. *Int J Oral Maxillofac Surg* 1987; **16**: 505-509 [PMID: 3117929 DOI: 10.1016/s0901-5027(87)80094-2]

14 **Sato M**, Yanagawa T, Yoshida H, Yura Y, Shirasuna K, Miyazaki T. Submucosal nodular fasciitis arising within the buccal area. Report of case. *Int J Oral Surg* 1981; **10**: 210-213 [PMID: 6797976 DOI: 10.1016/s0300-9785(81)80055-5]

15 **McCarthy EF**, Ireland DC, Sprague BL, Bonfiglio M. Parosteal (nodular) fasciitis of the hand. A case report. *J Bone Joint Surg Am* 1976; **58**: 714-716 [PMID: 1064594]

16 **Johnson MK**, Lawrence JF. Metaplastic bone formation (myositis ossificans) in the soft tissues of the hand. Case report. *J Bone Joint Surg Am* 1975; **57**: 999-1000 [PMID: 1184654]

17 **Goncalves D**. Fast growing non-malignant tumour of a finger. *Hand* 1974; **6**: 95-97 [PMID: 4523580 DOI: 10.1016/0072-968x(74)90019-9]

18 **Lumerman H**, Bodner B, Zambito R. Intraoral (submucosal) pseudosarcomatous nodular fasciitis. Report of a case. *Oral Surg Oral Med Oral Pathol* 1972; **34**: 239-244 [PMID: 4504566 DOI: 10.1016/0030-4220(72)90414-8]

19 **Carpenter EB**, Lublin B. An unusual osteogenic lesion of a finger. *J Bone Joint Surg Am* 1967; **49**: 527-531 [PMID: 6022361]

20 **Mallory TB**. A Group of Metaplastic and Neoplastic Bone- and Cartilage-Containing Tumors of Soft Parts. *Am J Pathol* 1933; **9**: 765-776.3 [PMID: 19970111]

World Journal of Clinical Cases

Submit a Manuscript: https://www.f6publishing.com

World J Clin Cases 2022 February 16; 10(5): 1580-1585

DOI: 10.12998/wjcc.v10.i5.1580

ISSN 2307-8960 (online)

CASE REPORT

Tumor-related cytokine release syndrome in a treatment-naïve patient with lung adenocarcinoma: A case report

Peng-Bo Deng, Juan Jiang, Cheng-Ping Hu, Li-Ming Cao, Min Li

ORCID number: Peng-Bo Deng 0000-0002-8002-4904; Juan Jiang 0000-0002-5343-8335; Cheng-Ping Hu 0000-0002-1285-8579; Li-Ming Cao 0000-0001-9985-2972; Min Li 0000-0002-3578-2239.

Author contributions: Deng PB contributed to investigation and wrote the manuscript; Hu CP contributed to funding acquisition; Cao LM and Jiang J contributed to investigation; Li M contributed to review and editing; all authors have read and approve the final manuscript.

Informed consent statement: Informed written consent was obtained from the patient and her family for publication of this report and any accompanying images.

Conflict-of-interest statement: All authors declare no conflicts of interests.

CARE Checklist (2016) statement: The authors have read the CARE Checklist (2016), and the manuscript was prepared and revised according to the CARE Checklist (2016).

Supported by National Multidisciplinary Cooperative Diagnosis and Treatment Capacity Building Project for Major Diseases (Lung Cancer); National Key R&D Program of China, No.

Peng-Bo Deng, Juan Jiang, Cheng-Ping Hu, Li-Ming Cao, Min Li, Department of Respiratory Medicine, National Key Clinical Specialty, Branch of National Clinical Research Center for Respiratory Diseases, Xiangya Hospital, Central South University, Changsha 410008, Hunan Province, China

Peng-Bo Deng, Juan Jiang, Cheng-Ping Hu, Li-Ming Cao, Min Li, Xiangya Lung Cancer Center, Xiangya Hospital, Central South University, Changsha 410008, Hunan Province, China

Peng-Bo Deng, Juan Jiang, Cheng-Ping Hu, Li-Ming Cao, Min Li, Center of Respiratory Medicine, Xiangya Hospital, Central South University, Changsha 410008, Hunan Province, China

Peng-Bo Deng, Juan Jiang, Cheng-Ping Hu, Li-Ming Cao, Min Li, Clinical Research Center for Respiratory Diseases in Hunan Province, Changsha 410008, Hunan Province, China

Peng-Bo Deng, Juan Jiang, Cheng-Ping Hu, Li-Ming Cao, Min Li, National Clinical Research Center for Geriatric Disorders, Xiangya Hospital, Central South University, Changsha 410008, Hunan Province, China

Corresponding author: Min Li, MD, PhD, Chief Doctor, Department of Respiratory Medicine, National Key Clinical Specialty, Branch of National Clinical Research Center for Respiratory Diseases, Xiangya Hospital, Central South University, No. 87 Xiangya Road, Changsha 410008, Hunan Province, China. limin2050@csu.edu.cn

Abstract

BACKGROUND

Cytokine release syndrome (CRS) is defined as systemic inflammation that usually occurs following chimeric antigen receptor T-cell therapy administration; however, it has not been reported in patients with untreated non-small cell lung cancer to date.

CASE SUMMARY

A 44-year-old nonsmoking woman presented to the hospital due to fever, palpitation, nausea, and cough for 1 mo and was diagnosed with stage cT3N3M0 (IIIc) adenocarcinoma of the lung. Auxiliary examinations revealed elevated cytokine [tumor necrosis factor-α, interleukin (IL)-1β, and IL-6] and inflammatory factor levels, which decreased after treatment with corticosteroids and immunoglobulin and when tumor growth was controlled following chemotherapy, radiotherapy, and antiangiogenesis therapy. However, tumor recurrence was observed. After administration of nivolumab as third-line treatment, the patient's

2016YFC1303300; Xiangya Clinical Big Data Project of Central South University (Clinical big data project of lung cancer).

Country/Territory of origin: China

Specialty type: Medicine, research and experimental

Provenance and peer review: Unsolicited article; Externally peer reviewed.

Peer-review model: Single blind

Peer-review report's scientific quality classification

Grade A (Excellent): 0
Grade B (Very good): B
Grade C (Good): 0
Grade D (Fair): 0
Grade E (Poor): 0

Received: September 6, 2021
Peer-review started: September 6, 2021
First decision: December 1, 2021
Revised: December 7, 2021
Accepted: December 31, 2021
Article in press: December 31, 2021
Published online: February 16, 2022

P-Reviewer: Brat K
S-Editor: Fan JR
L-Editor: A
P-Editor: Fan JR

condition was transiently controlled; however, CRS-like symptoms suddenly emerged, which led to a resurgence of cytokines and inflammatory factors and rapid death.

CONCLUSION
CRS can develop in treatment-naïve lung cancer patients. Patients with tumor-related CRS may be at risk of CRS recurrence, aggravation, and onset of immune checkpoint inhibitor-related adverse events.

Key Words: Cytokine release syndrome; Non-small cell lung cancer; Immune checkpoint inhibitors; Nivolumab; Tumor necrosis factor α; Interleukin-1β; Interleukin-6; Case report

Core Tip: Cytokine release syndrome (CRS) is defined as systemic inflammation that usually occurs after chimeric antigen receptor T-cell therapy is administered. But the case we report suggests CRS can develop in treatment-naïve lung cancer patient. Patients with tumor-related CRS may be at risk of CRS recurrence, aggravation, and onset of immune checkpoint inhibitor (ICI)-related adverse events when ICIs are administered. Therefore, it is necessary to carefully evaluate whether the patient has CRS prior to the initiation of ICI treatment.

Citation: Deng PB, Jiang J, Hu CP, Cao LM, Li M. Tumor-related cytokine release syndrome in a treatment-naïve patient with lung adenocarcinoma: A case report. *World J Clin Cases* 2022; 10(5): 1580-1585
URL: https://www.wjgnet.com/2307-8960/full/v10/i5/1580.htm
DOI: https://dx.doi.org/10.12998/wjcc.v10.i5.1580

INTRODUCTION

Cytokine release syndrome (CRS) is defined as systemic inflammation that usually occurs after the initiation of chimeric antigen receptor (CAR) T-cell therapy[1]. Several case reports have shown that patients treated with immune checkpoint inhibitors (ICIs) such as pembrolizumab[2] and nivolumab[3] anti-programmed cell death-1 (antibody) can develop CRS. To our knowledge, CRS has not been previously reported in treatment-naïve patients with lung cancer. Based on the results of our follow-up on patients with non-small cell lung cancer, the present patient's primary CRS was attributed to lung cancer, which usually recurs due to the development of tumors and an increase in tumor burden. Moreover, the patient developed CRS after being administered nivolumab, which led to rapid death (Table 1). This finding suggests that tumor-related CRS may be associated with ICI-related adverse events (irAEs) and poor prognosis among patients treated with nivolumab.

CASE PRESENTATION

Chief complaints

A 44-year-old nonsmoking woman visited our hospital (Xiangya Hospital, Central South University, Changsha, Hunan Province, China) in October 2017 due to fever (maximum, 41 °C), palpitation, nausea, and cough for 1 mo.

History of present illness

The patient had fever (maximum, 41 °C), palpitation, nausea, and cough for 1 mo.

History of past illness

No special history of past illness.

Table 1 Timeline

Time	Syndrome or treatment	Oncologic response
October 2017	Fever (maximum 41 °C), palpitation, nausea and cough for 1 mo	
October 2017	Diagnosed as medium differentiated adenocarcinoma lung cancer with EGFR and ALK gene mutations negative by CT-guided puncture biopsy	
November 2017	Considered have primary CRS with related to lung cancer, and treated with DXM, gamma globulin and other supporting treatments. The patient stopped fever soon	
December 2017 to February 2018	Four cycles of chemotherapy with pemetrexed + cisplatin	PR
June 11, 2018	Recurrent fever for 10 d with CT showed tumor progressed again	PD
July 2018 to August 2018	Radiotherapy then stated to take	PR
August 2018	Anlotinib	PR
May 2019	Nivolumab for 5 cycles	PR
April 2019	Died	PD

EGFR: Epidermal growth factor receptor; ALK: Anaplastic lymphoma kinase; CT: Computed tomography; CRS: Cytokine release syndrome; DXM: Dexamethasone; PR: Partial remission; PD: Progressive disease.

Personal and family history

No special personal or family history was reported.

Physical examination

The patient had palpable right-sided supraclavicular lymph nodes, low breath sounds on the right lung, and the absence of rales.

Laboratory examinations

The patient was diagnosed with partially differentiated adenocarcinoma of the lung with negative epidermal growth factor receptor and anaplastic lymphoma kinase gene mutations based on the results of computed tomography (CT)-guided puncture biopsy. The patient exhibited characteristics similar to those of CRS based on her clinical manifestations (high fever, tachycardia, nausea, appetite loss, and malaise) and laboratory examination results (elevated cytokines [tumor necrosis factor α (TNFα) and interleukin (IL)-1β, IL-6, and IL-10 levels (Figure 1), organ dysfunction (liver), and elevated ferritin levels][4]. We excluded other conditions that may have caused similar symptoms, such as tumor lysis syndrome (no hyperkalemia, uric acidemia, *etc*.), infection, and hemophagocytic syndrome (absence of hematopoietic cells on bone marrow biopsy).

Imaging examinations

CT on October 9, 2017 revealed a thick-walled cavity in the upper right lobe (Figure 2A). Tumor stage was cT3N3M0 (IIIc).

FINAL DIAGNOSIS

Lung adenocarcinoma (stage T3N3M) and CRS.

TREATMENT

We speculated that the patient may have primary CRS related to lung cancer and administered a 10 mg intravenous infusion of dexamethasone qd for 7 d, 20 g intravenous infusion of gamma globulin for 3 d, and other supportive treatments. The patient's fever eventually subsided, her general condition improved, the levels of inflammatory factors and cytokines decreased (Figure 1), and the Eastern Cooperative

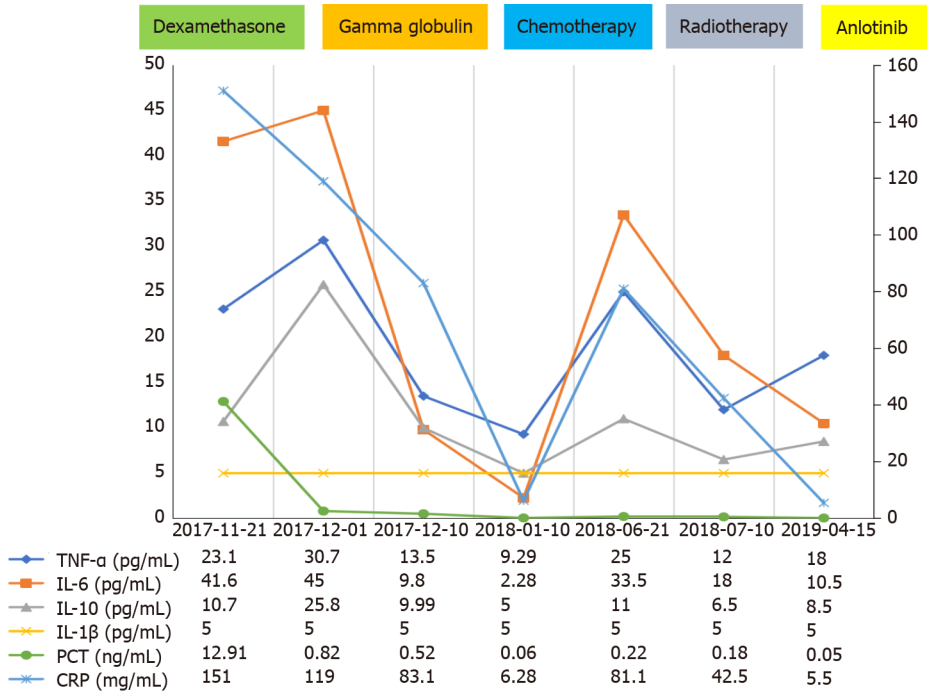

Figure 1 Curve showing the changes in the levels of cytokines and inflammatory factors. Curve showing the changes in the levels of cytokines and inflammatory factors. TNF-α: Tumor necrosis factor α; IL-1β: Interleukin-1β; IL-6: Interleukin-6; IL-10: Interleukin-10; PCT: Procalcitonin; CRP: C-reactive protein; WBC: White blood cell; N: Neutrophil; L: Lymphocyte; E: Eosinophil; M: Monocyte.

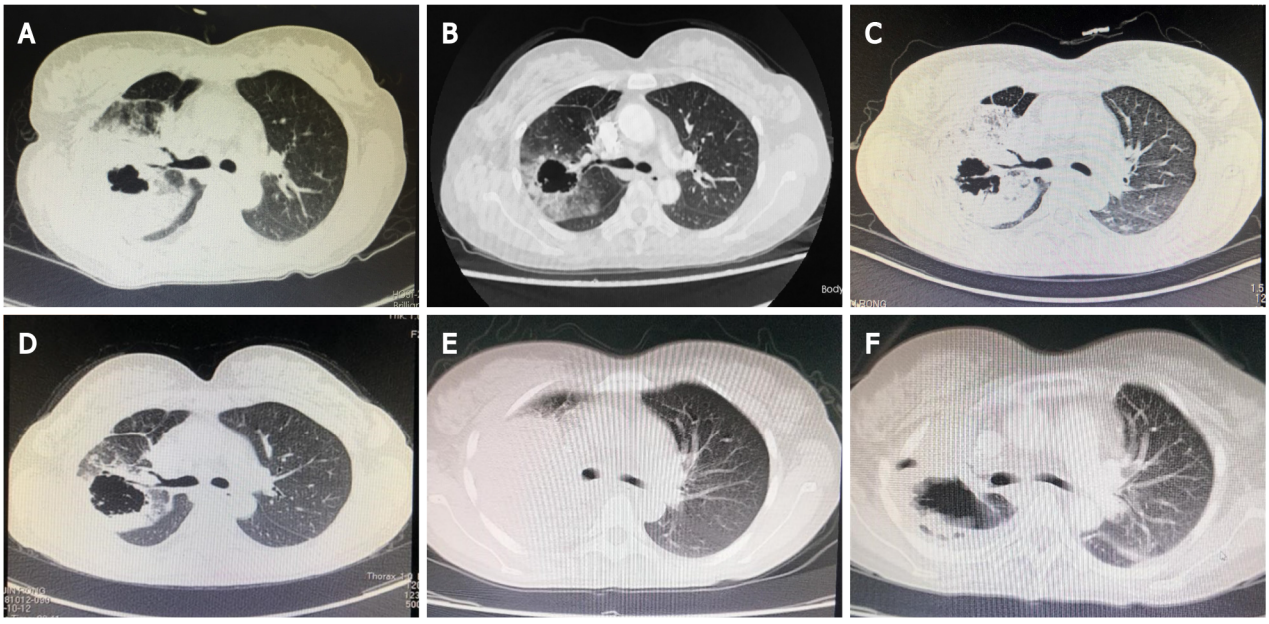

Figure 2 Computed tomography of the lung. A: First computed tomography (CT) scan showing thickening of the upper right lobe cavity (October 9, 2017); B: Figure showing reduction of the tumor and enlarged cavity after 4 cycles of chemotherapy (pemetrexed + cisplatin); C: Increase in tumor size 4 mo after the last chemotherapy session (June 11, 2018); D: After the patient had received radiotherapy, CT showed that the tumor began to shrink, (August 2, 2018) the tumor had reduced in size, and anlotinib was initiated (orally, 12 mg once daily from days 1 to 14 of a 21-d cycle); E: On May 1, 2019, the tumor started to enlarge but cavity enlargement was resolved; hence, nivolumab treatment was started (5 times, from May 6, 2019 to August 19, 2019); F: In August 12, 2019, the upper right lung mass was significantly smaller than that observed before the cavity enlarged.

Oncology Group (ECOG) score improved. Four cycles of chemotherapy with pemetrexed and cisplatin were initiated. The patient achieved partial remission (PR) at 1-mo follow-up according to the Response Evaluation Criteria in Solid Tumors, version 1.1 (Figure 2B). The patient had an ECOG score of 1, and her routine blood tests and cytokine and inflammatory factor levels had returned to normal (October 1, 2017) (Figure 1).

On June 11, 2018, she experienced recurrent fever for 10 d, and CT showed tumor progression (Figure 2C). The levels of cytokine and inflammatory factors began to increase (Figure 1), and we excluded the possibility of infectious fever and considered recurrent CRS. As the patient had stage IIIc adenocarcinoma, she was treated with radiotherapy from July 2018 to August 2018, and anlotinib therapy was initiated. The patient did not develop fever during this period. In October 2018, follow-up CT was performed, which revealed that the tumor had shrunk (Figure 2D); however, the size of the tumor started to increase in May 2019 (Figure 2E). Hence, five cycles of nivolumab treatment was administered. CT was performed in August 2019 and showed that the patient had achieved PR (Figure 2F).

OUTCOME AND FOLLOW-UP

Seventeen days after receiving the last dose of nivolumab, the patient was sent to the emergency department due to exacerbation of sudden dyspnea, high fever, respiratory failure, and sudden cardiac arrest. The patient eventually died on September 8, 2019, with laboratory tests showing elevated cytokine and inflammatory factor levels (Figure 1).

DISCUSSION

The exact mechanism of CRS has not been fully elucidated. Cytokines are released when the tumor interacts with immune effector cells, and they can originate not only from the CAR T cells but also from host immune cells, such as macrophages[5]. Previous studies have shown that lung cancer cells can directly release inflammatory cytokines, including IL-1, IL-6, TNFα, and interferon (IFN)[6]. Tumor necrosis can also release a large number of cytokines, such as TNF[7]. The patient had obvious necrotic cavities in her lungs which may have been the cause of cytokine release.

This clinical experience demonstrates that corticosteroids are an effective treatment for CRS, and steroids can be rapidly tapered within several days without CRS recurring. Another drug, tocilizumab, is a humanized immunoglobulin G1 + (IgG1 +) anti-human IL-6R monoclonal antibody which can usually resolve fever and hypotension within a few hours in patients with CRS and may induce a response more quickly than corticosteroids[8]. In the present case, corticosteroids and immunoglobulin were administered, and a significant therapeutic effect was achieved. With subsequent chemotherapy and other treatments to control lung cancer, CRS also improved, suggesting that antitumor therapy is also an important treatment for tumor-related CRS. Moreover, targeted immunosuppressive agents are also available to inhibit TNFα and IL-1, both of which may contribute to CRS, such as anti-TNFα monoclonal antibodies (infliximab), soluble TNFα receptor (etanercept), and IL-1R-based inhibitors (anakinra).

This patient was administered nivolumab as third-line treatment and experienced exacerbation of CRS-like symptoms and eventually passed away after showing an oncologic response following nivolumab administration. ICI-related CRS can develop 2 d to 4 mo after treatment, and before or after achieving a significant antitumor response to ICI therapy[2,3]; this type of CRS is related to tumor lysis through the induction of pyroptosis in target cells[9]. Based on the patient's symptoms and results of auxiliary examinations combined with her previous CRS, her disease progression may have been related to nivolumab treatment. A series of recent studies suggest inflammatory cytokines are potential biomarkers for irAEs, and one study found that patients treated with nivolumab who had a high level of soluble IL-2 measured at the initial tumor evaluation had a significantly increased risk of developing grade 3-4 nivolumab-related irAEs[10]. The above phenomena suggest that the use of ICIs in patients with tumor-associated CRS may induce the onset or aggravation of CRS or serious irAEs, which may be life-threatening.

CONCLUSION

We believe that CRS can occur in treatment-naïve patients with lung cancer. Corticosteroids, immunoglobulins, and subsequent antitumor treatments have played important roles in the control of tumor-related CRS. Patients with tumor-related CRS

may be at risk of CRS recurrence, aggravation, and onset of irAEs when treated with ICIs; therefore, it is necessary to carefully evaluate whether the patient has CRS prior to initiating ICI treatment.

REFERENCES

1 **Teachey DT**, Lacey SF, Shaw PA, Melenhorst JJ, Maude SL, Frey N, Pequignot E, Gonzalez VE, Chen F, Finklestein J, Barrett DM, Weiss SL, Fitzgerald JC, Berg RA, Aplenc R, Callahan C, Rheingold SR, Zheng Z, Rose-John S, White JC, Nazimuddin F, Wertheim G, Levine BL, June CH, Porter DL, Grupp SA. Identification of Predictive Biomarkers for Cytokine Release Syndrome after Chimeric Antigen Receptor T-cell Therapy for Acute Lymphoblastic Leukemia. *Cancer Discov* 2016; **6**: 664-679 [PMID: 27076371 DOI: 10.1158/2159-8290.CD-16-0040]

2 **Kogure Y**, Ishii Y, Oki M. Cytokine Release Syndrome with Pseudoprogression in a Patient with Advanced Non-Small Cell Lung Cancer Treated with Pembrolizumab. *J Thorac Oncol* 2019; **14**: e55-e57 [PMID: 30782385 DOI: 10.1016/j.jtho.2018.11.025]

3 **Honjo O**, Kubo T, Sugaya F, Nishizaka T, Kato K, Hirohashi Y, Takahashi H, Torigoe T. Severe cytokine release syndrome resulting in purpura fulminans despite successful response to nivolumab therapy in a patient with pleomorphic carcinoma of the lung: a case report. *J Immunother Cancer* 2019; **7**: 97 [PMID: 30944043 DOI: 10.1186/s40425-019-0582-4]

4 **Arkader R**, Troster EJ, Lopes MR, Júnior RR, Carcillo JA, Leone C, Okay TS. Procalcitonin does discriminate between sepsis and systemic inflammatory response syndrome. *Arch Dis Child* 2006; **91**: 117-120 [PMID: 16326799 DOI: 10.1136/adc.2005.077446]

5 **Gauthier J**, Turtle CJ. Insights into cytokine release syndrome and neurotoxicity after CD19-specific CAR-T cell therapy. *Curr Res Transl Med* 2018; **66**: 50-52 [PMID: 29625831 DOI: 10.1016/j.retram.2018.03.003]

6 **Dinarello CA**, Bunn PA Jr. Fever. *Semin Oncol* 1997; **24**: 288-298 [PMID: 9208885]

7 **Johnson M**. Neoplastic fever. *Palliat Med* 1996; **10**: 217-224 [PMID: 8817592 DOI: 10.1177/026921639601000306]

8 **Lee DW**, Gardner R, Porter DL, Louis CU, Ahmed N, Jensen M, Grupp SA, Mackall CL. Current concepts in the diagnosis and management of cytokine release syndrome. *Blood* 2014; **124**: 188-195 [PMID: 24876563 DOI: 10.1182/blood-2014-05-552729]

9 **Liu Y**, Fang Y, Chen X, Wang Z, Liang X, Zhang T, Liu M, Zhou N, Lv J, Tang K, Xie J, Gao Y, Cheng F, Zhou Y, Zhang Z, Hu Y, Zhang X, Gao Q, Zhang Y, Huang B. Gasdermin E-mediated target cell pyroptosis by CAR T cells triggers cytokine release syndrome. *Sci Immunol* 2020; **5** [PMID: 31953257 DOI: 10.1126/sciimmunol.aax7969]

10 **Costantini A**, Julie C, Dumenil C, Hélias-Rodzewicz Z, Tisserand J, Dumoulin J, Giraud V, Labrune S, Chinet T, Emile JF, Giroux Leprieur E. Predictive role of plasmatic biomarkers in advanced non-small cell lung cancer treated by nivolumab. *Oncoimmunology* 2018; **7**: e1452581 [PMID: 30221046 DOI: 10.1080/2162402X.2018.1452581]

World Journal of Clinical Cases

Submit a Manuscript: https://www.f6publishing.com

World J Clin Cases 2022 February 16; 10(5): 1586-1591

DOI: 10.12998/wjcc.v10.i5.1586

ISSN 2307-8960 (online)

CASE REPORT

Submucosal protuberance caused by a fish bone in the absence of preoperative positive signs: A case report

Wei-Wei Du, Tao Huang, Guo-Dong Yang, Jing Zhang, Jing Chen, Ying-Bang Wang

ORCID number: Wei-Wei Du 0000-0003-0149-6741; Tao Huang 0000-0003-4536-5022; Guo-Dong Yang 0000-0003-0992-5678; Jing Zhang 0000-0001-5339-4435; Jing Chen 0000-0002-4438-8882; Ying-Bang Wang 0000-0002-7553-0052.

Author contributions: Huang T was the patient's endoscopic surgeon; Du WW and Yang GD reviewed the literature and contributed to manuscript drafting; Zhang J and Wang YB collected the data; Chen J analyzed and interpreted the imaging findings; Huang T, Du WW, and Yang GD were responsible for the revision of the manuscript for important intellectual content; all authors issued final approval for the version to be submitted.

Informed consent statement: Informed written consent was obtained from the patient for the publication of this report and any accompanying images.

Conflict-of-interest statement: The authors declare that they have no conflict of interest to disclose.

CARE Checklist (2016) statement: The authors have read the CARE Checklist (2016), and the manuscript was prepared and revised according to the CARE Checklist (2016).

Wei-Wei Du, Department of Gastroenterology, The Third People's Hospital of Chengdu, The Affiliated Hospital of Southwest Jiaotong University, Chengdu, 610000, Sichuan Province, China

Tao Huang, Guo-Dong Yang, Jing Zhang, Ying-Bang Wang, Department of Gastroenterology and Hepatology, Affiliated Hospital of North Sichuan Medical College, Nanchong 637000, Sichuan Province, China

Jing Chen, Department of Radiology, Affiliated Hospital of North Sichuan Medical College, Nanchong 637000, Sichuan Province, China

Corresponding author: Tao Huang, MD, Doctor, Department of Gastroenterology and Hepatology, Affiliated Hospital of North Sichuan Medical College, No. 1 Maoyuan South Road, Shunqing District, Nanchong 637000, Sichuan Province, China. 514663870@qq.com

Abstract

BACKGROUND

Submucosal protuberance caused by fish bone insertion into the digestive tract has rarely been reported. These cases usually include patients with clear signs such as a history of fish intake, pain, and dysphagia, as well as positive findings on endoscopy and imaging. Here, we report a case of a fish bone hidden in the submucosal protuberance of the gastric antrum during endoscopic submucosal dissection without preoperative obvious positive signs.

CASE SUMMARY

A 58-year-old woman presented with epigastric pain for the past 20 d and a submucosal protuberance. Abdominal computed tomography and endoscopic ultrasonography did not indicate the presence of a fish bone. We assumed the cause to be an ordinary submucosal eminence and performed an endoscopic submucosal dissection to confirm its essence. During the operation, a fish bone approximately 20 mm in length was found incidentally.

CONCLUSION

Our report could potentially prevent the oversight of embedded fish bones and associated adverse effects in patients with similar presentation.

Key Words: Gastric submucosal protuberance; Endoscopic mucosal dissection; Computed tomography; Endoscopic ultrasonography; Case report

Country/Territory of origin: China

Specialty type: Gastroenterology and Hepatology

Provenance and peer review: Unsolicited article; Externally peer reviewed.

Peer-review model: Single blind

Peer-review report's scientific quality classification
Grade A (Excellent): 0
Grade B (Very good): 0
Grade C (Good): C
Grade D (Fair): 0
Grade E (Poor): 0

Received: August 13, 2021
Peer-review started: August 13, 2021
First decision: October 22, 2021
Revised: October 30, 2021
Accepted: December 31, 2021
Article in press: December 31, 2021
Published online: February 16, 2022

P-Reviewer: Okasha HH
S-Editor: Ma YJ
L-Editor: Wang TQ
P-Editor: Ma YJ

Core Tip: Ingested fish bones appear as high-density shadows and hyperechoic structures on computed tomography and endoscopic ultrasonography scans. Patients typically present with symptoms or positive findings on ancillary examinations. Herein, we present a case of a fish bone hidden in the submucosal protuberance of the gastric antrum without the usual positive signs. In this rare case, we identified the reasons for the fish bone being overlooked in the diagnosis process. This report could potentially prevent the future oversight of embedded fish bones and associated adverse effects.

Citation: Du WW, Huang T, Yang GD, Zhang J, Chen J, Wang YB. Submucosal protuberance caused by a fish bone in the absence of preoperative positive signs: A case report. *World J Clin Cases* 2022; 10(5): 1586-1591
URL: https://www.wjgnet.com/2307-8960/full/v10/i5/1586.htm
DOI: https://dx.doi.org/10.12998/wjcc.v10.i5.1586

INTRODUCTION

Ingestion of foreign bodies (FBs) in the upper digestive tract is a common cause of emergency hospital admissions. Usually, complications do not occur after the FB passes spontaneously through the digestive tract. However, approximately 20% of patients require non-surgical intervention, and less than 1% require surgery[1,2]. Accidental ingestion of fish bones is very common and accounts for 84% of accidental FB ingestions[3]. Cases of FBs embedding in various parts of the digestive tract causing submucosal protuberances are rarely reported. The diagnosis of accidental fish bone retention is usually based on a clear history of fish ingestion; typical symptoms such as pain and dysphagia; and a positive ancillary examination[4,5]. Ingested fish bones are visible as high-density shadows and hyperechoic structures on computed tomography (CT) and endoscopic ultrasonography (EUS), and are retrievable by ordinary endoscopy. Most previous reports of accidental fish bone ingestion describe patients presenting typical symptoms or positive findings on ancillary examination[6-8]. Herein, we present a case of a fish bone hidden in the submucosal protuberance of the gastric antrum without the usual positive signs.

CASE PRESENTATION

Chief complaints

A 56-year-old woman presented with epigastric pain without heartburn, acid reflux, or abdominal distension and in a good overall condition. Her diet, faeces, and urine were normal, and she had no recent changes in body weight.

History of present illness

The patient experienced epigastric pain for the past 20 d.

History of past illness

The patient had a history of cervical spondylosis and had undergone bilateral pterygium surgery in the past. There was no history of drinking or smoking.

Personal and family history

No special personal or family history.

Physical examination

The patient's vital signs were stable and physical examination was unremarkable.

Laboratory examinations

Preoperative blood tests, such as routine blood examination, liver function, and serum

tumour markers of the digestive system, showed no abnormalities.

Imaging examinations

Gastroscopy revealed a submucosal protuberance of the gastric antrum approximately 15 mm in diameter that had a smooth surface, scattered congestion, and an opening at the top (Figure 1A). EUS revealed a submucosal protuberance of approximately 1.19 cm × 0.89 cm (Figure 1B) on the posterior wall of the gastric antrum. The protuberance was round, similar to mixed echogenic masses, predominately hypoechoic with unclear boundaries, and originating from the submucosa. We considered the possibility of a heterotopic pancreas. An abdominal CT scan showed no obvious abnormal thickening or enhancement shadow of the gastric antrum (Figure 1C). Surgical contraindications were absent, and endoscopic submucosal dissection was performed with informed consent from the patient and her family. The lesion was located on the posterior wall of the gastric antrum. After marking and submucosal injection of methylene blue, glycerine fructose, adrenaline, and sodium hyaluronate, the lesion was cut with a dual knife (KD-650L; Olympus, Tokyo, Japan) and peeled off layer by layer. The recovered tissue was biopsied. While inspecting the wound, a strip of white foreign body was found under the wound that could not be pulled out using forceps (Figure 2A).

FINAL DIAGNOSIS

The final diagnosis of the present case was a fish bone submucosal protuberance of the gastric antrum.

TREATMENT

The fish bone, approximately 20 mm in length, was removed using a dual knife (Figure 2B), and the wound was clamped with a haemostatic clamp. No perforation or bleeding was observed, and the operation was concluded. Postoperatively, a gastric tube was placed for continuous gastrointestinal decompression. The patient underwent primary nursing, fasting, acid suppression (Esomeprazole Sodium 40mg ivgtt bid), haemostasis (Aminocaproic Acid and Sodium Chloride Injection 100 mL ivgtt qd), infection prevention (Cefuroxime Sodium 0.75 g ivgtt temporary twice), and fluid replacement. There were no changes in intervention and without other concurrent interventions.

OUTCOME AND FOLLOW-UP

Pathology results revealed hyperplastic polyps of the antral mucosa with irregular, dilated, hyperaemia of the vascular lumen in the lamina propria. Unexpected discovery of the fish bone prompted us to question the patient again for a more detailed history. The patient recollected having recurrent epigastric pain as early as 6 years after eating fish with no effective diagnosis or examination. We proceeded by inviting senior radiologists to review the patient's imaging studies. Upon careful review, the radiologists noticed a dot-like high-density shadow, which indicated a fish bone approximately 2.0 cm long on CT reconstruction (Figure 3). Finally, the patient improved and discharged.

DISCUSSION

The present case helps to highlight the importance of careful surgical wound inspection. In our case, the patient denied any recent ingestion of fish and diagnostic exams including endoscopy, CT, and EUS also showed no evidence of fish bones. A surgeon is most likely to think of a common submucosal protuberance as the likely aetiology given the present clinical scenario. Left unnoticed, the fish bone may form an inflammatory hyperplastic protuberance and cause recurring abdominal pain in the patient again. In more severe cases, delayed perforation, mediastinal abscess, or even severe fatal peritonitis can occur[9,10]. Therefore, careful inspection of the surgical

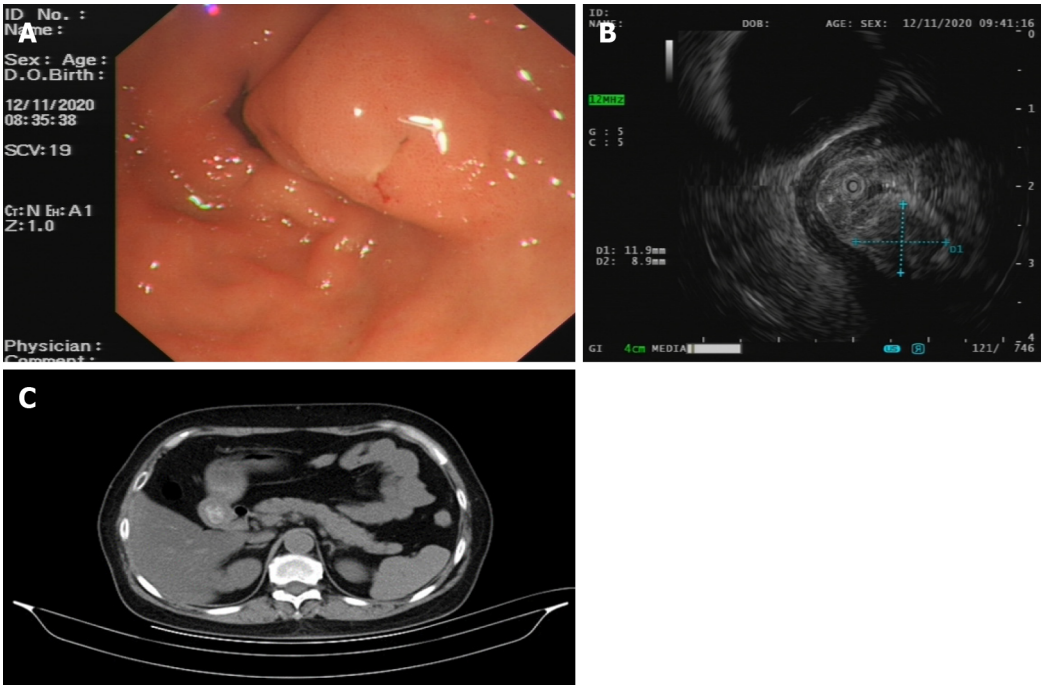

Figure 1 Preoperative imaging examinations. A: Gastroscopy revealing a submucosal protuberance of the gastric antrum; B: Endoscopic ultrasonography indicating a round mixed echogenic mass with a size of approximately 1.19 cm × 0.89 cm; C: Abdominal computed tomography scan showing no obvious abnormal thickening or enhancement shadow of the gastric antrum.

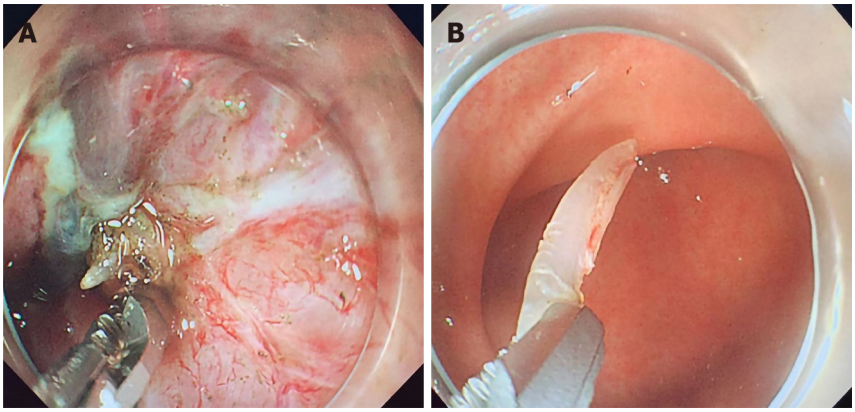

Figure 2 Surgical images. A: During the endoscopic submucosal dissection, a white strip of a foreign body was found under the wound; B: A fish bone approximately 20 mm in length was removed using a dual knife.

wound is a critical step in uncovering possible embedded fish bones or other FBs in the mucosa.

Gastric submucosal protuberances are often asymptomatic and are found accidently by gastroscopy due to other diseases. Acute abdominal pain, fever, or acute submucosal changes on gastroscopy, especially purulent changes, are signs that often alert clinicians to the possibility of FB ingestion. In our case, the patient presented with chronic abdominal pain, and the lesion seen on endoscopy had a smooth mucosa similar to the submucosal uplift caused by a stromal tumour, heterotopic pancreas, or leiomyoma. In view of these findings, the possibility of FB ingestion would rarely be considered. Few reported cases of digestive tract protuberances were caused by fishbone, and most were accompanied by abdominal pain[1,11]. Therefore, patients with chronic abdominal pain and submucosal protuberance must also be questioned regarding any intake of fish or FBs. Such questioning takes an extremely short time. When a patient's history is indicative of fishbone intake, surgeons need to be careful in peeling off the submucosal protuberance to avoid cutting the fishbone too short and thus requiring additional surgery, which will eventually bring burden and risk to the patients.

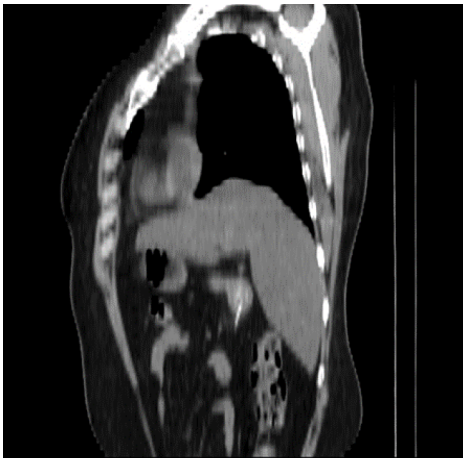

Figure 3 Computed tomography reconstruction of a fishbone-like (approximately 20 mm long) high-density image.

When hard FBs such as fish bones, jujube shells, or chicken bones enter the gastric cavity accidentally or are pushed into the open gastric space during endoscopy, they may be discharged from the body spontaneously through the peristaltic movements of the digestive tract[12]. In cases where the FB is sharp in nature, embedding into the gut can occur, which may lead to serious complications and unavoidable surgery. Thus, timely removal of the FB is perhaps more conducive to long-term patient prognosis.

There may be several reasons why the patient in our case did not show any obvious signs of fish bone ingestion upon ancillary examination. First, ingested fish bones are usually very small, and the superficial changes can easily be mistaken as calcifications and surgical suture[13], or ignored altogether due to the influence of gastric content. Second, if the fish bone was from a cartilaginous species of fish, it would have low density on CT and be hypoechogenic on EUS, thus making it difficult to differentiate it from surrounding soft tissue and hard to identify using CT imaging modalities. Third, when the length of the fish bone is perpendicular to the CT scan section, the punctuate changes seen would evade conclusive diagnosis. In one study, thoracic CT revealed an irregular high-density shadow in an oesophageal mucosal lesion[1], which was ultimately identified as a fish bone structure by three-dimensional CT reconstruction. Therefore, CT reconstruction is mandatory in scanning such lesions. Fourth, careful EUS examination of every gastrointestinal protuberance in all directions including longitudinal as well as transverse scanning during radial or linear echoendoscopic examination should be emphasized to avoid missing such fish bones.

CONCLUSION

Ingested fish bones appear as high-density shadows and hyperechoic structures on CT tomography and EUS, and patients typically present with symptoms or positive findings on ancillary examinations. Herein, we present a case of a fish bone hidden in the submucosal protuberance of the gastric antrum without the usual positive signs. Thus, the size, type, and course of the fish bone, as well as the diligence of the doctor, may all play a role and affect the patient's eventual outcome and clinical course.

REFERENCES

1 **Cao L**, Chen N, Chen Y, Zhang M, Guo Q, Chen Q, Cheng B. Foreign body embedded in the lower esophageal wall located by endoscopic ultrasonography: A case report. *Medicine (Baltimore)* 2018; **97**: e11275 [PMID: 29953004 DOI: 10.1097/MD.0000000000011275]

2 **Barkai O**, Kluger Y, Ben-Ishay O. Laparoscopic retrieval of a fishbone migrating from the stomach causing a liver abscess: Report of case and literature review. *J Minim Access Surg* 2020; **16**: 418-420 [PMID: 31793447 DOI: 10.4103/jmas.JMAS_196_19]

3 **Venkatesh SH**, Venkatanarasimha Karaddi NK. CT findings of accidental fish bone ingestion and its complications. *Diagn Interv Radiol* 2016; **22**: 156-160 [PMID: 26714057 DOI: 10.5152/dir.2015.15187]

4 **Erbil B**, Karaca MA, Aslaner MA, Ibrahimov Z, Kunt MM, Akpinar E, Özmen MM. Emergency admissions due to swallowed foreign bodies in adults. *World J Gastroenterol* 2013; **19**: 6447-6452 [PMID: 24151363 DOI: 10.3748/wjg.v19.i38.6447]

5 **Ambe P**, Weber SA, Schauer M, Knoefel WT. Swallowed foreign bodies in adults. *Dtsch Arztebl Int* 2012; **109**: 869-875 [PMID: 23293675 DOI: 10.3238/arztebl.2012.0869]

6 **Wang Z**, Du Z, Zhou X, Chen T, Li C. Misdiagnosis of peripheral abscess caused by duodenal foreign body: a case report and literature review. *BMC Gastroenterol* 2020; **20**: 236 [PMID: 32703254 DOI: 10.1186/s12876-020-01335-7]

7 **Xie R**, Tuo BG, Wu HC. Unexplained abdominal pain due to a fish bone penetrating the gastric antrum and migrating into the neck of the pancreas: A case report. *World J Clin Cases* 2019; **7**: 805-808 [PMID: 30968048 DOI: 10.12998/wjcc.v7.i6.805]

8 **Jimenez-Fuertes M**, Moreno-Posadas A, Ruíz-Tovar Polo J, Durán-Poveda M. Liver abscess secondary to duodenal perforation by fishbone: Report of a case. *Rev Esp Enferm Dig* 2016; **108**: 42 [PMID: 26765235]

9 **Geng C**, Li X, Luo R, Cai L, Lei X, Wang C. Endoscopic management of foreign bodies in the upper gastrointestinal tract: a retrospective study of 1294 cases. *Scand J Gastroenterol* 2017; **52**: 1286-1291 [PMID: 28691540 DOI: 10.1080/00365521.2017.1350284]

10 **Malick KJ**. Endoscopic management of ingested foreign bodies and food impactions. *Gastroenterol Nurs* 2013; **36**: 359-365 [PMID: 24084134 DOI: 10.1097/SGA.0b013e3182a71f92]

11 **Shan GD**, Chen ZP, Xu YS, Liu XQ, Gao Y, Hu FL, Fang Y, Xu CF, Xu GQ. Gastric foreign body granuloma caused by an embedded fishbone: a case report. *World J Gastroenterol* 2014; **20**: 3388-3390 [PMID: 24696619 DOI: 10.3748/wjg.v20.i12.3388]

12 **Kikuchi K**, Tsurumaru D, Hiraka K, Komori M, Fujita N, Honda H. Unusual presentation of an esophageal foreign body granuloma caused by a fish bone: usefulness of multidetector computed tomography. *Jpn J Radiol* 2011; **29**: 63-66 [PMID: 21264664 DOI: 10.1007/s11604-010-0495-0]

13 **Traynor P**, Stupalkowska W, Mohamed T, Godfrey E, Bennett JMH, Gourgiotis S. Fishbone perforation of the small bowel mimicking internal herniation and obstruction in a patient with previous gastric bypass surgery. *J Surg Case Rep* 2020; **2020**: rjaa369 [PMID: 33005325 DOI: 10.1093/jscr/rjaa369]

World Journal of Clinical Cases

Submit a Manuscript: https://www.f6publishing.com

World J Clin Cases 2022 February 16; 10(5): 1592-1597

DOI: 10.12998/wjcc.v10.i5.1592

ISSN 2307-8960 (online)

CASE REPORT

Misdiagnosis of unroofed coronary sinus syndrome as an ostium primum atrial septal defect by echocardiography: A case report

Jin-Ling Chen, Cai-Gui Yu, Dai-Jiao Wang, Hong-Bin Chen

ORCID number: Jin-Ling Chen 0000-0001-5997-131X; Cai-Gui Yu 0000-0003-2690-588X; Dai-Jiao Wang 0000-0003-1743-0130; Hong-Bin Chen 0000-0001-8021-8568.

Author contributions: Chen JL designed the study and wrote the paper; Chen HB collected the patient's clinical data; Yu CG and Wang DJ analyzed the data.

Informed consent statement: Informed written consent was obtained from the patient for publication of this report and any accompanying images.

Conflict-of-interest statement: The authors declare that they have no conflicts of interest.

CARE Checklist (2016) statement: The authors have read the CARE Checklist (2016), and the manuscript was prepared and revised according to the CARE Checklist (2016).

Country/Territory of origin: China

Specialty type: Medicine, research and experimental

Provenance and peer review: Unsolicited article; Externally peer reviewed

Peer-review model: Single blind

Peer-review report's scientific

Jin-Ling Chen, Cai-Gui Yu, Dai-Jiao Wang, Department of Echocardiography, Renmin Hospital of Wuhan University, Wuhan 430060, Hubei Province, China

Hong-Bin Chen, Department of Pulmonary and Critical Care Medicine, Renmin Hospital of Wuhan University, Wuhan 430060, Hubei Province, China

Corresponding author: Hong-Bin Chen, PhD, Chief Physician, Department of Pulmonary and Critical Care Medicine, Renmin Hospital of Wuhan University, No. 238 Jiefang Road, Wuchang District, Wuhan 430060, Hubei Province, China. rainman1974@yeah.net

Abstract

BACKGROUND

Unroofed coronary sinus syndrome (UCSS) is a rare congenital heart disease, which has variable morphologic features and is strongly associated with persistent left superior vena cava (PLSVC). However, it is often difficult to visualize the left-to-right shunt pathway through the CS by transthoracic echocardiography (TTE).

CASE SUMMARY

A 37-year-old female was admitted to the hepatological surgery department of a hospital with complaint of subxiphoid pain that had started 1 wk prior. Physical examination revealed a grade 3/6 systolic murmur at the left margin of the sternum, between the 2nd and 3rd intercostal cartilage. The patient underwent echocardiography and was diagnosed with ostium primum atrial septal defect (ASD); thus, she was subsequently transferred to the cardiovascular surgery department. A second TTE evaluation before surgery showed type IV UCSS with secundum ASD. Right-heart contrast echocardiography (RHCE) showed that the right atrium and right ventricle were immediately filled with microbubbles, but no microbubble was observed in the CS. Meanwhile, negative filling was observed at the right atrium orifice of the CS and right atrium side of the secundum atrial septal. RHCE identified UCSS combined with secundum ASD but without PLSVC in this patient.

CONCLUSION

This rare case of UCSS highlights the value of TTE combined with RHCE in confirming UCSS with ASD or PLSVC.

Key Words: Congenital heart disease; Coronary sinus; Atrial septal defect; Persistent left

quality classification
Grade A (Excellent): 0
Grade B (Very good): 0
Grade C (Good): C
Grade D (Fair): 0
Grade E (Poor): 0

Received: August 10, 2021
Peer-review started: August 10, 2021
First decision: October 16, 2021
Revised: October 24, 2021
Accepted: January 11, 2022
Article in press: January 11, 2022
Published online: February 16, 2022

P-Reviewer: Ong LT
S-Editor: Wang JJ
L-Editor: A
P-Editor: Wang JJ

superior vena cava; Echocardiography; Right heart contrast echocardiography; Case report

Core Tip: Unroofed coronary sinus syndrome (UCSS) is difficult to diagnose. Transthoracic echocardiography (TTE) of a 37-year-old female revealed ostium primum atrial septal defect (ASD). A second TTE showed type IV UCSS with secundum ASD. Right-heart contrast echocardiography (RHCE) confirmed UCSS and ASD with no persistent left superior vena cava (PLSVC). The patient was misdiagnosed because the defect location was near the endocardial cushions, which was mistaken for a defect of the ostium primum atrial septum. This case highlights the special value of TTE and RHCE for a rare case of type IV UCSS combined with ASD but without PLSVC.

Citation: Chen JL, Yu CG, Wang DJ, Chen HB. Misdiagnosis of unroofed coronary sinus syndrome as an ostium primum atrial septal defect by echocardiography: A case report. *World J Clin Cases* 2022; 10(5): 1592-1597
URL: https://www.wjgnet.com/2307-8960/full/v10/i5/1592.htm
DOI: https://dx.doi.org/10.12998/wjcc.v10.i5.1592

INTRODUCTION

Unroofed coronary sinus syndrome (UCSS) is a rare congenital heart disease, in which left atrial to right atrial shunt occurs through a partial or complete defect of the roof of the CS[1]. UCSS has variable morphologic features and the clinical syndrome of UCSS varies from symptomless to severe right heart failure, which is mainly determined by the size of the defect between the CS and other associated anomalies, such as persistent left superior vena cava (PLSVC) and atrial septal defect (ASD). UCSS is strongly associated with PLSVC in about 75% of cases[2], and UCSS in the terminal portion (Kirklin and Barratt-Boyes type IV) without PLSVC or other anomalies is classified as a type of ASD, which comprises less than 1% of all ASD cases[1]. However, it is often difficult to visualize the left-to-right shunt pathway through the CS by transthoracic echocardiography (TTE), which can lead to misdiagnosis or a missed diagnosis[3].

We present a rare case of UCSS combined with secundum ASD but without PLSVC, which was misdiagnosed as ostium primum ASD identified by TTE.

CASE PRESENTATION

Chief complaints

A 37-year-old female was admitted to the hepatological surgery department of the hospital with subxiphoid pain that had started 1 wk prior.

History of present illness

The patient's symptoms of intermittent subxiphoid pain began 5 years prior and had recurred and worsened over the past week. She also reported having experienced chest distress occasionally.

History of past illness

Five years ago, the patient began having intermittent subxiphoid pain and was hospitalized due to subxiphoid pain for 1 wk. Ultrasound examination showed a gallstone. Physical examination revealed grade 3/6 systolic murmur at the left margin of the sternum, between the 2nd and 3rd intercostal cartilage. Laboratory examination showed increased arterial partial pressure of oxygen (PaO_2; 146 mmHg) but normal partial pressure of carbon dioxide (PCO_2; 146 mmHg) and oxygen saturation (SaO_2; 99%).

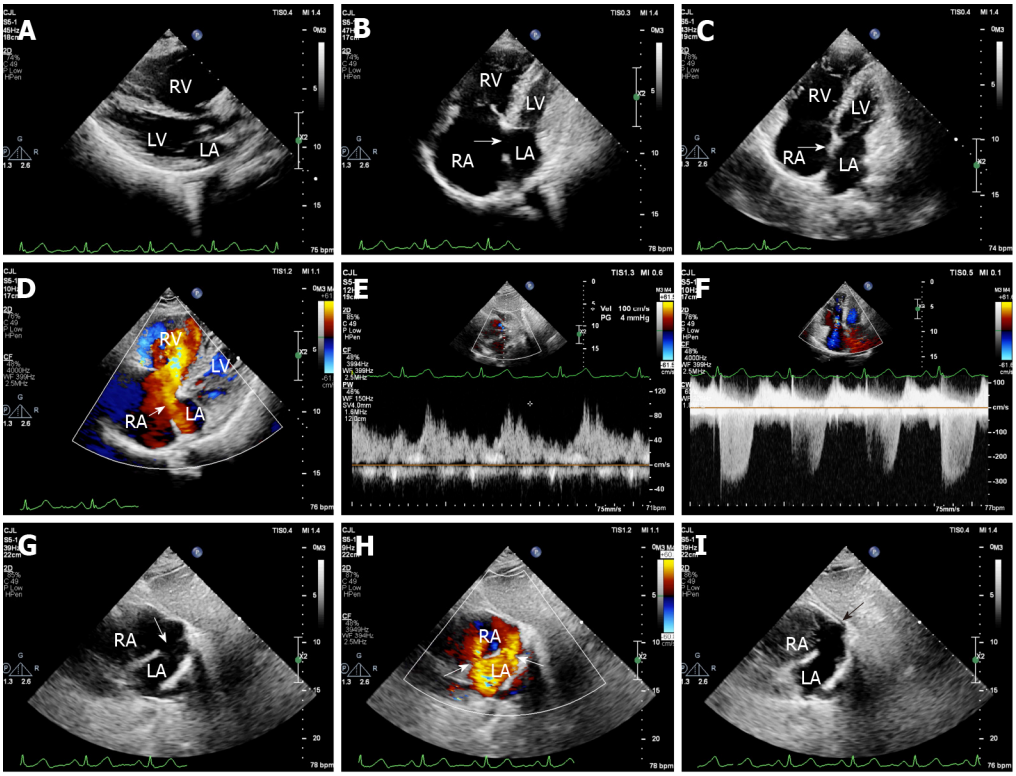

Figure 1 Transthoracic echocardiography before surgery. A: Significant enlargement of the right ventricle (anterior-posterior diameter = 43 mm); B: Location of the defect was near the endocardial cushions on apical four-chamber view, which was mistaken for a defect of the ostium primum atrial septal defect (ASD) (arrow); C: When detected on apical four-chamber view by scanning backward, a defect of the coronary sinus (CS) in the terminal portion and normal endocardial cushions were seen (arrow); D: A shunt through the defect of the CS in the terminal portion on apical four-chamber view (arrow); E: Pulse-wave Doppler spectrum showed a shunt during diastole through the defect of the CS in the terminal portion [Vmax = 100 cm/s, pressure gradient (PG) = 4 mmHg]; F: Moderate-to-severe tricuspid regurgitation (Vmax = 337cm/s, PG = 45 mmHg, pulmonary artery systolic pressure = 50 mmHg); G: The defect of the CS in the terminal portion and secundum ASD on subxiphorid biatrial view (arrow, 3.3 cm × 2.0 cm and 1.1 cm); H: Two shunts through the defect of the CS and secundum ASD on subxiphorid biatrial view (arrow); I: Negative filling was observed at the right atrium orifice of the CS and right atrium side of the secundum atrial septal by right-heart contrast echocardiography (arrow). RA: Right atrium; RV: Right ventricle; LA: Left atrium; LV: Left ventricle.

Personal and family history

The patient had no previous or family history of similar illnesses.

Physical examination

Physical examination revealed grade 3/6 systolic murmur at the left margin of the sternum, between the 2nd and 3rd intercostal cartilage.

Laboratory examinations

Blood analyses showed increased arterial PaO_2 (146 mmHg) but normal PCO_2 (146 mmHg) and SaO_2 (99%).

Imaging examinations

The patient underwent echocardiography and was diagnosed with ostium primum ASD; thus, she was subsequently transferred to the cardiovascular surgery department.

Before surgery, TTE was performed again. TTE showed: Enlargement of the right heart and pulmonary artery, with mildly increased systolic pulmonary arterial flow [velocity 177 cm/s, pressure gradient (PG) 12.5 mmHg]; moderate-to-severe tricuspid valve regurgitation; mild-to-moderate pulmonary hypertension [pulmonary arterial systolic pressure (PASP) 56 mmHg]; a secundum ASD (1.1 cm); and obvious broadening of the CS, with partial defect of the CS roof (3.3 cm × 2.0 cm), through which the left atrial to right atrial shunt occurred (velocity 100 cm/s, PG 4 mmHg) (Figures 1A-1H). There was no ectopic pulmonary vein drainage.

To find evidence of PLSVC, which is the most common associated anomaly, right-heart contrast echocardiography (RHCE) was performed. After agitated 50% glucose was injected into the left antecubital vein, the right atrium and right ventricle were immediately filled with microbubbles but no microbubble was observed in the CS.

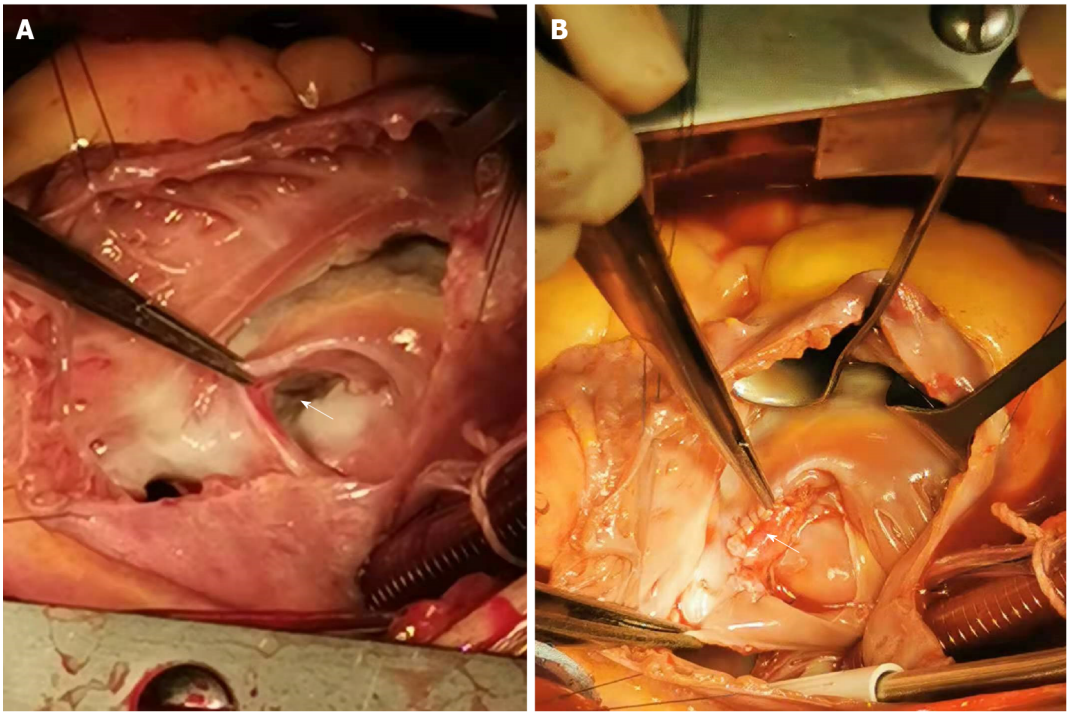

Figure 2 Imaging during the operation. A: Obvious broadening of the coronary sinus (CS) with a partial defect of the CS roof in the terminal portion (3.0 cm × 2.1 cm) was seen upon incision of the right atrium; B: The defect of the CS in the terminal portion was repaired.

Negative filling was observed at the right atrium orifice of the CS and right atrium side of the secundum atrial septum. The microbubbles were not observed in the left ventricle or the left atrium. RHCE did not identify PLSVC in this patient (Figure 1I).

Chest X-ray examination showed an increased heart shadow and no abnormality in the aorta, but the pulmonary artery segment showed extrusion.

RESPIRATORY EXAMINATIONS

Pulmonary function tests showed that the diffusing capacity of the lung for carbon monoxide was mildly decreased (78%), but the forced expiratory volume in 1 s and ratio of forced expiratory volume to forced vital capacity remained normal.

ELECTROCARDIOGRAM EXAMINATION

Electrocardiogram (ECG) examination showed that the patient had sinus rhythm, a normal ECG axis, and incomplete right bundle branch block.

GENETIC TESTING

No genetic testing was performed.

MULTIDISCIPLINARY EXPERT CONSULTATION

No multidisciplinary expert consultation was conducted.

FINAL DIAGNOSIS

Type IV UCSS combined with secundum ASD.

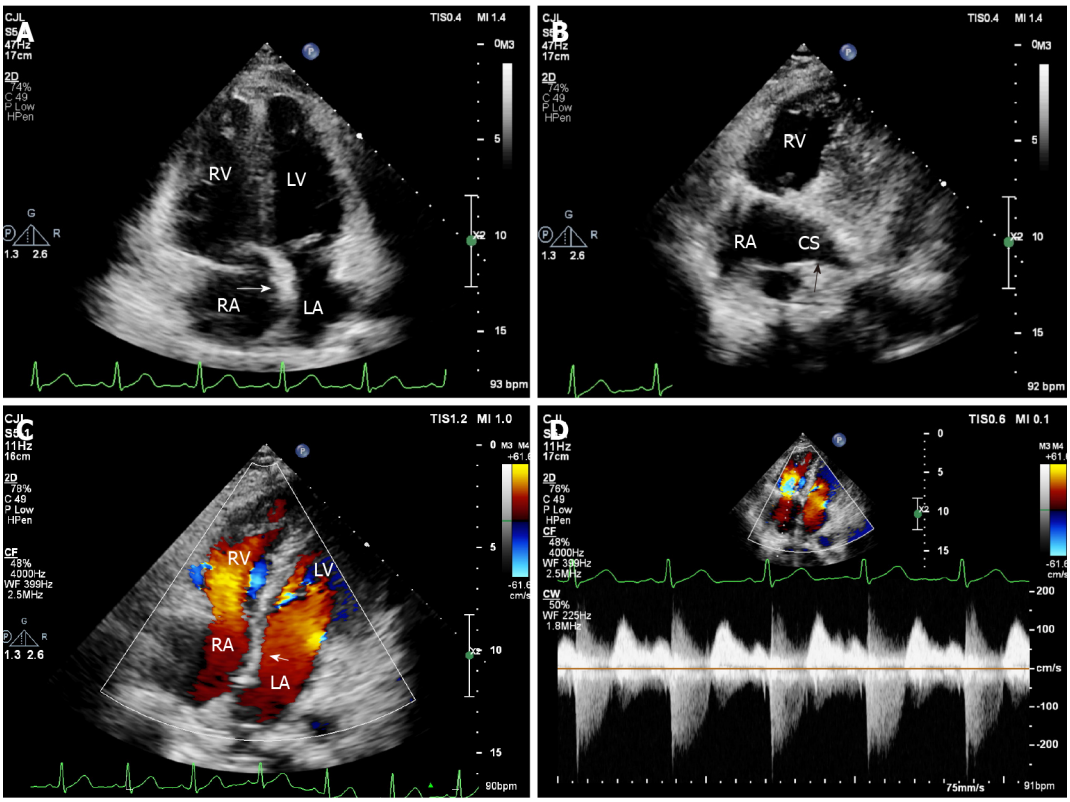

Figure 3 Transthoracic echocardiography at 1 wk after surgery. A: The repaired atrial septum was continuous and complete on apical four-chamber view (arrow); B: The repaired coronary sinus (CS) roof was continuous and complete on apical four-chamber view (arrow); C: There was no shunt from the left atrium to right atrium on apical four-chamber view (arrow); D: Trace tricuspid regurgitation (Vmax = 223 cm/s, pressure gradient = 20 mmHg, pulmonary artery systolic pressure = 25 mmHg). RA: Right atrium; RV: Right ventricle; LA: Left atrium; LV: Left ventricle; CS: Coronary sinus.

TREATMENT

The patient underwent repair surgery for the CS roof defect, secundum ASD closure, and tricuspid annuloplasty. During the operation, obvious broadening of the CS with partial defect of the roof of the CS (3.0 cm × 2.1 cm) and secundum ASD near the oval foramen (1.1 cm) were detected (Figures 2A and 2B). When perfused through the CS, the perfusate reflowed to both the left atrium and right atrium. The moderate-to-severe tricuspid valve regurgitation was due to a significantly dilated tricuspid annulus.

OUTCOME AND FOLLOW-UP

The patient was in good condition and no complications occurred after surgery. The patient was discharged from the hospital about 2 wk after surgery. TTE before discharge showed no shunt through the UCSS or ASD from the left atrium to right atrium, mild tricuspid valve regurgitation (velocity 223 cm/s, PG 20 mmHg), and normal PASP (25 mmHg) (Figures 3A-3D). At the 6-mo follow-up visit, the patient was in good condition.

DISCUSSION

UCSS is a rare congenital heart disease characterized by communication between the CS and the left atrium through the partial or complete absence of the CS roof. According to the location of the absence, UCSS is classified into the following four morphological types: Completely unroofed with PLSVC (type I); completely unroofed without PLSVC (type II); partially unroofed in the midsection (type III); and partially unroofed in the terminal portion (type IV)[1,4].

In general, UCSS is strongly associated with a PLSVC, which remains the most common association[2]. Moreover, it can also be associated with other congenital heart abnormalities, such as cor triatriatum, canal defects, tetralogy of Fallot, abnormal atrioventricular connection, pulmonary atresia or stenosis, and anomalous pulmonary venous return[5].

TTE is the most widely used noninvasive technique for the diagnosis of UCSS; although posterior structures such as the pulmonary veins or CS may not be seen well in some patients. RHCE using agitated saline or glucose injection through the left arm vein may help indicate PLSVC, the most common association which is characterized by microbubbles in the CS prior to its appearance in the right atrium.

However, it is not easy to determine the type of UCSS due to difficulties in detecting the exact location of the unroofed portion. In the present case, the defect of CS was partially unroofed in the terminal portion (type IV); this UCSS type was misdiagnosed at the first TTE because the location of the defect was near the endocardial cushions on apical four-chamber view, which was mistaken for a defect of the ostium primum ASD. On the second TTE, the defect of the CS in the terminal portion and normal endocardial cushions were detected on apical four-chamber view by scanning backward. Moreover, the CS was significantly dilated and the CS roof structure was not always seen while a shunt from the left atrium was passed through the dilated CS to the right atrium. All evidence led to the diagnosis of UCSS. Meanwhile, a small shunt through the secundum ASD was detected, with the exception of an atrial-level UCSS shunt.

In the present case, RHCE worked in two ways. When injected through the left arm vein, microbubbles first entered the right atrium but no microbubble appeared in the CS, indicating that there was no PLSVC. Moreover, negative filling was observed at the right atrium orifice of the CS and right atrium side of the secundum atrial septal during RHCE, confirming the diagnosis of UCSS and secundum ASD. Although TTE of suitable image sections is the first-line examination to evaluate UCSS, it should be more frequently used in combination with RHCE in these cases.

CONCLUSION

We highlight a rare case of type IV UCSS combined with secundum ASD but without PLSVC, which was misdiagnosed as ostium primum ASD identified by TTE. TTE combined with RHCE is of value in confirming UCSS with or without ASD and PLSVC.

REFERENCES

1 **Ootaki Y**, Yamaguchi M, Yoshimura N, Oka S, Yoshida M, Hasegawa T. Unroofed coronary sinus syndrome: diagnosis, classification, and surgical treatment. *J Thorac Cardiovasc Surg* 2003; **126**: 1655-1656 [PMID: 14666054 DOI: 10.1016/s0022-5223(03)01019-5]

2 **Kim H**, Choe YH, Park SW, Jun TG, Kang IS, Yang JH, Eo H, Lee HJ. Partially unroofed coronary sinus: MDCT and MRI findings. *AJR Am J Roentgenol* 2010; **195**: W331-W336 [PMID: 20966297 DOI: 10.2214/AJR.09.3689]

3 **Lee HS**, Song BG, Park MJ, Kim KH, Ok HS, Kim BK, Chun WJ, Oh JH. Rare case of an unroofed coronary sinus. *Heart Lung* 2012; **41**: 390-393 [PMID: 22197304 DOI: 10.1016/j.hrtlng.2011.12.001]

4 **Xie MX**, Yang YL, Cheng TO, Wang XF, Li K, Ren PP, Lü Q, Lin H, Li L. Coronary sinus septal defect (unroofed coronary sinus): echocardiographic diagnosis and surgical treatment. *Int J Cardiol* 2013; **168**: 1258-1263 [PMID: 23266300 DOI: 10.1016/j.ijcard.2012.11.113]

5 **Samuel W**, Robert EM. Atrial septal defect, unroofed coronary sinus surgical treatment, e-medicine Cardiothoracic surgery. 2009

World Journal of Clinical Cases

Submit a Manuscript: https://www.f6publishing.com

World J Clin Cases 2022 February 16; 10(5): 1598-1601

DOI: 10.12998/wjcc.v10.i5.1598

ISSN 2307-8960 (online)

CASE REPORT

Uncommon complication of nasoenteral feeding tube: A case report

Yong-Po Jiang, Sheng Zhang, Rong-Hai Lin

ORCID number: Yong-Po Jiang 0000-0002-5681-3663; Sheng Zhang 0000-0002-0164-7186; Rong-Hai Lin 0000-0002-1712-5438.

Author contributions: Lin RH helped to design the manuscript; Jiang YP helped to write the manuscript; Zhang S helped to revise the manuscript; all authors issued final approval for the version to be submitted.

Informed consent statement: Informed written consent was obtained from the patient for publication of this report and any accompanying images.

Conflict-of-interest statement: The authors declare that they have no conflict of interest.

CARE Checklist (2016) statement: The authors have read the CARE Checklist (2016), and the manuscript was prepared and revised according to the CARE Checklist (2016).

Supported by The Science and Technology Project of Taizhou, No.1902KY02.

Country/Territory of origin: China

Specialty type: Critical Care Medicine

Provenance and peer review: Unsolicited article; Externally peer reviewed.

Yong-Po Jiang, Sheng Zhang, Rong-Hai Lin, Department of Critical care medicine, Taizhou Hospital of Zhejiang Province affiliated to Wenzhou Medical University, Taizhou 317000, Zhejiang Province, China

Corresponding author: Rong-Hai Lin, MD, Chief Doctor, Depertment of Critical care medicine, Taizhou Hospital of Zhejiang Province Affiliated to Wenzhou Medical University, Taizhou Hospital of Zhejiang Province Affiliated to Wenzhou Medical University, No. 150, Ximen Street, Taizhou, China, Taizhou 317000, Zhejiang Province, China. tylinrh@163.com

Abstract

BACKGROUND

The jejunal nutrition tube has increasingly been used in clinical practice, and the results in frequent complications.

CASE SUMMARY

We present the case of a 74-year-old male patient who had been admitted to the intensive care unit for aspiration pneumonia and respiratory failure. When confirming the position of the jejunal tube by X-ray, we found that the feeding tube had been placed into the chest. The complications was a disaster, though the misplacement of jejunal feeding tube are uncommon.

CONCLUSION

We introduced a way of ultrasound-guided jejunum feeding tube placement to avert the disaster, which was convenient and economical.

Key Words: Nasoenteral feeding tube; Nutritional support; Complication; Ultrasound-guided; Feeding tube placement; Case report

Core Tip: We report a case of a patient who has a serious complication during the catheterization of the jejunal tube and introduce a way of using of bedside ultrasound to guide the placement of the jejunal tube to avert the disaster, which was convenient and economical.

Citation: Jiang YP, Zhang S, Lin RH. Uncommon complication of nasoenteral feeding tube: A case report. *World J Clin Cases* 2022; 10(5): 1598-1601

URL: https://www.wjgnet.com/2307-8960/full/v10/i5/1598.htm

Peer-review model: Single blind

Peer-review report's scientific quality classification

Grade A (Excellent): 0
Grade B (Very good): B
Grade C (Good): 0
Grade D (Fair): 0
Grade E (Poor): 0

Received: July 15, 2021
Peer-review started: July 15, 2021
First decision: October 18, 2021
Revised: January 7, 2022
Accepted: January 11, 2022
Article in press: January 11, 2022
Published online: February 16, 2022

P-Reviewer: Soares RLS
S-Editor: Li JH
L-Editor: A
P-Editor: Li JH

DOI: https://dx.doi.org/10.12998/wjcc.v10.i5.1598

INTRODUCTION

Early enteral nutrition in critically ill patients who cannot eat by mouth is widely recommended by the clinical practice guidelines of nutrition[1]. For patients at high risk of aspiration and who were intolerant of oral or gastric feeding the advice is to place a post-pyloric feeding tube[2,3]. Complication of jejunal feeding tubes are rare. A recent report revealed that a jejunal tube caused gastrointestinal perforation[4]. In this case report, we will present a case where a jejunal feeding tube was placed into the chest and provide a brief overview of a method to avoid the complication of placing a jejunal feeding tube. Written informed consent was obtained from the patient's family for publication of this manuscript and any accompanying images.

CASE PRESENTATION

Chief complaints

A 74-year-old male patient who with a history of chronic obstructive pulmonary disease (COPD) was admitted to the intensive care unit (ICU) for aspiration pneumonia and respiratory failure.

History of present illness

He had a prolonged course of treatment and a nasoduodenal feeding tube blind placed at the bedside.

Imaging examinations

A chest X-ray revealed that the position of the nasoduodenal feeding tube was in the chest (Figure 1A). An abdominal X-ray also made it clear that the nasoduodenal feeding tube was not placed in the abdomen (Figure 1B). Visual laryngoscopy revealed that the tube entered the airway together with the windpipe (Figure 2).

FINAL DIAGNOSIS

The patient suffered from pneumothorax due to tracheal pleura leakage, which occurred when the feeding tube was immediately removed.

TREATMENT

We administered chest drainage in the middle of the clavicle and second ribs.

OUTCOME AND FOLLOW-UP

However, the patient died as a result of the aggravation of the lung infection.

DISCUSSION

The most commonly used non-invasive method of enteral nutrition is a nasogastro-jejunal tube. The jejunal nutrition tube has increasingly been used in clinical practice, and the results in frequent complications[4,5]. The traditional method of intubation depends on the operator experience, X-ray, and gastroscope. Nasogastrojejunal tube insertion based on a minimally invasive catheterization procedure, combined with ultrasound guidance, is becoming more prevalent[6]. The use of bedside ultrasound to guide the placement of the jejunal tube is safe, convenient and economical. One of the common complications of indwelling jejunal tubes is the misplaced airway as reported in this case. How can we avoid it? When the cannula is about 30 cm, we need to

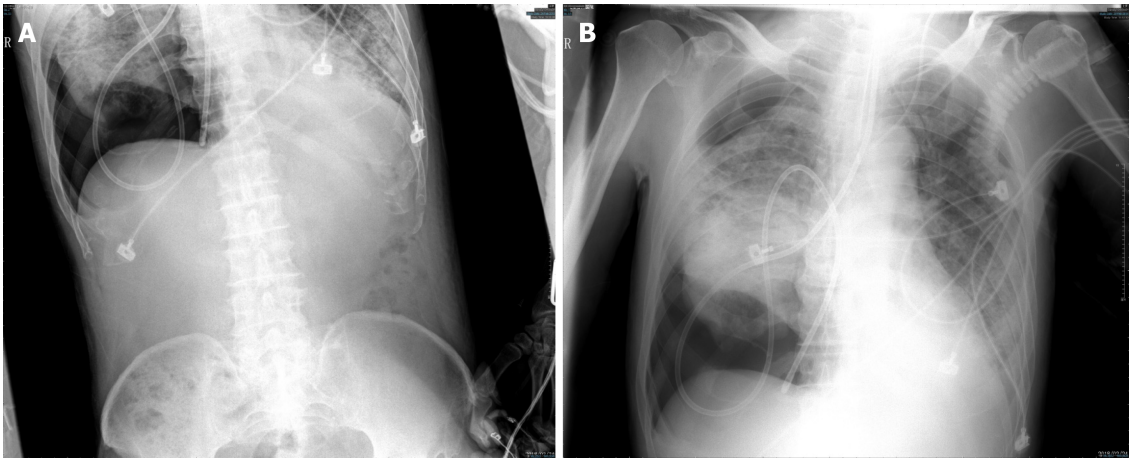

Figure 1 X-ray after placement of the feeding tube. A: Abdominal X-ray shows there is no jejunal tube in the abdomen, and the jejunal tube is on the diaphragm; B: Chest X-ray shows the jejunal tube is in the chest.

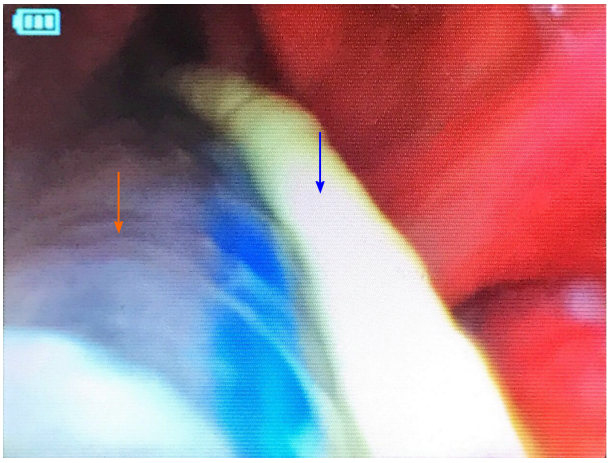

Figure 2 Visual laryngoscopy after placement of the feeding tube. The blue arrow is feeding tube and the orange arrow is windpipe.

observe the patient's response and ventilator condition. Even neck ultrasound determines access to the esophagus. If the patient has a severe cough response or a leak and a high pressure alarm, it may suggest that the tube has entered the airway. When the tube is placed around 50 cm, we need to complete a test of pumping. If you can hear the gas over water (bubble sound), then the catheter head has entered the stomach. If not, the patient should be reintubated.

CONCLUSION

The complication of blind bedside jejunal feeding tube placement was a disaster. Ultrasound guidance under visualization can avoid serious complications. Practitioners need to pay attention to patient response and the ventilator during catheterization.

REFERENCES

1 **Reintam Blaser A**, Starkopf J, Alhazzani W, Berger MM, Casaer MP, Deane AM, Fruhwald S, Hiesmayr M, Ichai C, Jakob SM, Loudet CI, Malbrain ML, Montejo González JC, Paugam-Burtz C, Poeze M, Preiser JC, Singer P, van Zanten AR, De Waele J, Wendon J, Wernerman J, Whitehouse T, Wilmer A, Oudemans-van Straaten HM; ESICM Working Group on Gastrointestinal Function. Early enteral nutrition in critically ill patients: ESICM clinical practice guidelines. *Intensive Care Med* 2017; **43**: 380-398 [PMID: 28168570 DOI: 10.1007/s00134-016-4665-0]

2 **Rhodes A**, Evans LE, Alhazzani W, Levy MM, Antonelli M, Ferrer R, Kumar A, Sevransky JE, Sprung CL, Nunnally ME, Rochwerg B, Rubenfeld GD, Angus DC, Annane D, Beale RJ, Bellinghan GJ, Bernard GR, Chiche JD, Coopersmith C, De Backer DP, French CJ, Fujishima S, Gerlach H, Hidalgo JL, Hollenberg SM, Jones AE, Karnad DR, Kleinpell RM, Koh Y, Lisboa TC, Machado FR, Marini JJ, Marshall JC, Mazuski JE, McIntyre LA, McLean AS, Mehta S, Moreno RP, Myburgh J, Navalesi P, Nishida O, Osborn TM, Perner A, Plunkett CM, Ranieri M, Schorr CA, Seckel MA, Seymour CW, Shieh L, Shukri KA, Simpson SQ, Singer M, Thompson BT, Townsend SR, Van der Poll T, Vincent JL, Wiersinga WJ, Zimmerman JL, Dellinger RP. Surviving Sepsis Campaign: International Guidelines for Management of Sepsis and Septic Shock: 2016. *Intensive Care Med* 2017; **43**: 304-377 [PMID: 28101605 DOI: 10.1007/s00134-017-4683-6]

3 **Taylor BE**, McClave SA, Martindale RG, Warren MM, Johnson DR, Braunschweig C, McCarthy MS, Davanos E, Rice TW, Cresci GA, Gervasio JM, Sacks GS, Roberts PR, Compher C; Society of Critical Care Medicine; American Society of Parenteral and Enteral Nutrition. Guidelines for the Provision and Assessment of Nutrition Support Therapy in the Adult Critically Ill Patient: Society of Critical Care Medicine (SCCM) and American Society for Parenteral and Enteral Nutrition (A.S.P.E.N.). *Crit Care Med* 2016; **44**: 390-438 [PMID: 26771786 DOI: 10.1097/CCM.0000000000001525]

4 **Fakih HAM**, Daouk S, Runnstrom M, Ataya A. A nasoenteral feeding tube barking up the wrong tree. *Intensive Care Med* 2017; **43**: 930-931 [PMID: 28124087 DOI: 10.1007/s00134-017-4686-3]

5 **Stefani A**, Ruggiero C, Aramini B, Scamporlino A. An unusual drain in the pleural cavity: iatrogenic pneumothorax due to pulmonary misplacement of a nasogastric tube. *Intensive Care Med* 2018; **44**: 2290-2291 [PMID: 29974170 DOI: 10.1007/s00134-018-5280-z]

6 **Li Y**, Ye Y, Mei Y, Ruan H, Yu Y. Semi-automated ultrasound guidance applied to nasogastrojejunal tube replacement for enteral nutrition in critically ill adults. *Biomed Eng Online* 2018; **17**: 21 [PMID: 29415733 DOI: 10.1186/s12938-018-0452-1]

World Journal of Clinical Cases

Submit a Manuscript: https://www.f6publishing.com

World J Clin Cases 2022 February 16; 10(5): 1602-1608

DOI: 10.12998/wjcc.v10.i5.1602

ISSN 2307-8960 (online)

CASE REPORT

Treatment of extracranial internal carotid artery dissecting aneurysm with SUPERA stent implantation: Two case reports

Min-Jian Qiu, Bao-Rong Zhang, Shui-Jiang Song

ORCID number: Min-Jian Qiu 0000-0001-5688-2485; Bao-Rong Zhang 0000-0002-8099-7407; Shui-Jiang Song 0000-0001-9155-6837.

Author contributions: Qiu MJ conceived and coordinated the study, performed and analyzed the experiments, wrote the paper; Zhang BR and Song SJ carried out the data collection, data analysis, and revised the paper; all authors have read and approve the final manuscript.

Informed consent statement: Informed written consent was obtained from the patient for publication of this report and any accompanying images.

Conflict-of-interest statement: The authors declare that they have no conflict of interest.

CARE Checklist (2016) statement: The authors have read the CARE Checklist (2016), and the manuscript was prepared and revised according to the CARE Checklist (2016).

Country/Territory of origin: China

Specialty type: Neurosciences

Provenance and peer review: Unsolicited article; Externally peer reviewed.

Peer-review model: Single blind

Min-Jian Qiu, Bao-Rong Zhang, Shui-Jiang Song, Department of Neurology, The Second Affiliated Hospital of Zhejiang University School of Medicine, Hangzhou 310009, Zhejiang Province, China

Corresponding author: Min-Jian Qiu, MD, Doctor, Department of Neurology, The Second Affiliated Hospital of Zhejiang University School of Medicine, Department of Neurology, Hangzhou 310009, Zhejiang Province, China. 3196011@zju.edu.cn

Abstract

BACKGROUND

There is no standard endovascular treatment for extracranial internal carotid artery dissecting aneurysms. In the past, stent-graft isolation and stent-assisted coil embolization were commonly used for wide-necked and fusiform aneurysms. Here, we present two cases of extracranial internal carotid artery dissecting aneurysms treated successfully using the SUPERA stent.

CASE SUMMARY

Case 1 was a 57-year-old male patient with sudden right limb weakness and vague speech and diagnosed with cerebral infarction in February 2019. Cervical computed tomographic angiography (CTA) revealed left internal carotid artery dissection with stenosis. CTA at 2 mo showed an eccentric wide-necked dissecting aneurysm (5 mm × 5 mm × 12 mm, 10-mm neck) that was enlarged at 4 mo (7 mm × 6 mm × 12 mm, 11-mm neck). The patient underwent SUPERA stent implantation. His condition was stable in July 2020. Case 2 was a 57-year-old man who suddenly felt dizzy and developed unsteady walking in November 2019. Cervical CTA suggested right internal carotid artery dissecting aneurysm (11 mm × 9 mm × 31 mm) complicated with severe lumen stenosis (95%). The patient underwent SUPERA stent implantation. The patient had no residual symptoms and was stable in December 2020.

CONCLUSION

SUPERA stent implantation might achieve good results in treating wide-necked or long fusiform internal carotid artery dissecting aneurysms.

Key Words: Extracranial; Internal carotid artery; Dissecting aneurysm; Stent; Case report

Peer-review report's scientific quality classification
Grade A (Excellent): A
Grade B (Very good): 0
Grade C (Good): 0
Grade D (Fair): 0
Grade E (Poor): 0

Received: July 16, 2021
Peer-review started: July 16, 2021
First decision: October 18, 2021
Revised: October 26, 2021
Accepted: January 8, 2022
Article in press: January 8, 2022
Published online: February 16, 2022

P-Reviewer: Ciccone MM
S-Editor: Li JH
L-Editor: A
P-Editor: Li JH

Core Tip: There is no standard endovascular treatment for extracranial internal carotid artery dissecting aneurysms. Stent-graft isolation and stent-assisted coil embolization are commonly used for wide-necked and fusiform aneurysms, but safety and effectiveness can be unsatisfactory. The SUPERA stent is a braided metal stent especially designed for arterial stenosis of the lower extremities. Here, we present two cases of extracranial internal carotid artery dissecting aneurysms treated successfully using the SUPERA stent. Hence, SUPERA stent implantation might achieve good results in treating wide-necked or long fusiform internal carotid artery dissecting aneurysms.

Citation: Qiu MJ, Zhang BR, Song SJ. Treatment of extracranial internal carotid artery dissecting aneurysm with SUPERA stent implantation: Two case reports. *World J Clin Cases* 2022; 10(5): 1602-1608
URL: https://www.wjgnet.com/2307-8960/full/v10/i5/1602.htm
DOI: https://dx.doi.org/10.12998/wjcc.v10.i5.1602

INTRODUCTION

Carotid artery dissections account for about 2.5% of all strokes[1], and the incidence of extracranial carotid dissection with dissecting aneurysms is about 9.1%[2]. About 10.7% of patients with extracranial carotid dissection develop a new dissecting aneurysm within 3 mo[2]. Patients under medical therapy for recurrent neurologic episodes and persistent high-grade stenosis or growing aneurysms are considered candidates for surgery or endovascular therapy[2].

There is no recognized endovascular treatment for extracranial internal carotid artery dissecting aneurysms. In the past, stent-graft isolation and stent-assisted coil embolization were commonly used for wide-necked and fusiform aneurysms[3-5]. New and more suitable endovascular treatment materials could possibly improve the safety and effectiveness of endovascular therapy. Inspired by the flow diverter for intracranial wide-necked aneurysms, we looked for a metal stent with a similar treatment mechanism to treat two complex internal carotid dissecting cases aneurysm, *i.e.*, wide-necked or long fusiform dissecting aneurysms. It is expected that through the implantation of a dense mesh stent to change the local hemodynamics, the aneurysm would shrink and disappear[6]. The SUPERA stent is a braided metal stent especially designed for arterial stenosis of the lower extremities[7]. When the stent is released, the wire density at the aneurysm is increased by the push-pull technique. In theory, it can change the aneurysm cavity's blood flow state like a flow diverter so that the aneurysm can be gradually reduced and cured.

Here we introduce for the first time two cases of extracranial internal carotid artery lesions treated successfully using the SUPERA stent system implantation.

CASE PRESENTATION

Chief complaints

Case 1: Weakness of right limb and vague speech for 4 mo.

Case 2: Dizziness and unsteady walking for 1 mo.

History of present illness

Case 1: A 57-year-old male patient with sudden right limb weakness and vague speech was diagnosed with cerebral infarction in February 2019 at the Department of Neurology of The Second Affiliated Hospital of Zhejiang University School of Medicine. Cervical computed tomographic angiography (CTA) revealed left internal carotid artery dissection with stenosis. Blood glucose, blood lipids, and routine blood and biochemistry examinations were all within the normal ranges. The patient received antiplatelet therapy with aspirin (100 mg) and clopidogrel (75 mg). In April 2019, *i.e.*, 2 mo after medical treatment, cervical CTA showed that the left internal carotid artery dissecting stenosis had disappeared but turned into an eccentric wide-necked dissecting aneurysm (Figure 1A and B). The size of the aneurysm was 5 mm ×

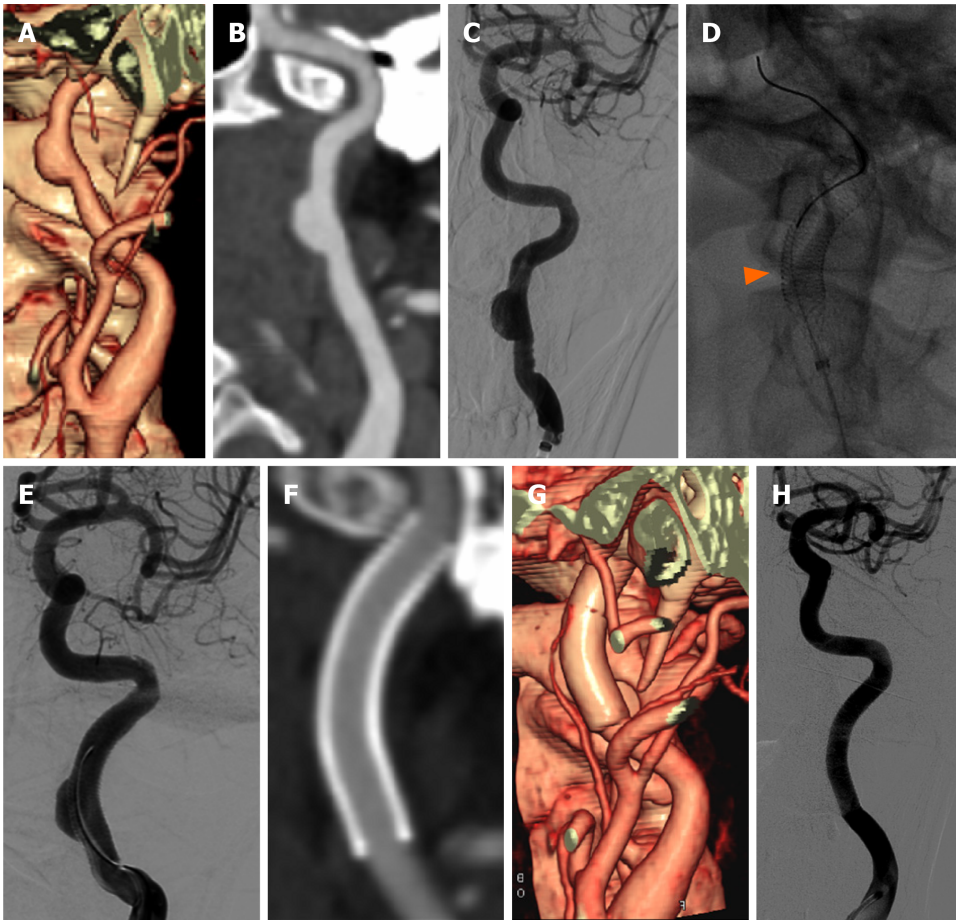

Figure 1 Case 1 was a 57-year-old male patient with sudden right limb weakness and vague speech and was diagnosed with cerebral infarction in February 2019. He was ultimately treated using a SUPERA stent. A: Cervical computed tomographic angiography (CTA) volume reconstruction; B: curved surface reconstruction show that the wide-necked dissecting aneurysm was situated on the upper segment of the left internal carotid artery; C: confirmed by digital subtraction angiography (DSA); D and E: The patient underwent SUPERA stent endovascular therapy, the arrow shows the dense stent mesh; F and G: Three months later, cervical CTA showed that the aneurysm had disappeared completely. H: One year later, DSA showed that the internal carotid artery was repaired perfectly.

5 mm × 12 mm, and its neck was 10 mm. In June 2019, *i.e.*, 4 mo after medical treatment, the aneurysm had enlarged to 7 mm × 6 mm × 12 mm, and its neck was 11 mm.

Case 2: The patient was a 57-year-old man who suddenly felt dizzy and developed unsteady walking in November 2019 and was admitted to the Department of Neurology of The Second Affiliated Hospital of Zhejiang University School of Medicine. MRI showed cerebral infarction in the right frontal lobe and parietal lobe. The left lower limb's muscle strength was grade 4, and the left Babinski sign was positive. Blood glucose, blood lipids, and routine blood and biochemistry examinations were all within the normal ranges. Cervical CTA suggested right internal carotid artery fusiform dissecting aneurysm complicated with severe lumen stenosis (Figure 2A). The size of the aneurysm was 11 mm × 9 mm × 31 mm, and the degree of stenosis was about 95%. The patient received antiplatelet therapy with aspirin (100 mg) and clopidogrel (75 mg).

FINAL DIAGNOSIS

Case 1: Wide-necked dissecting aneurysm of left internal carotid artery.

Case 2: Fusiform dissecting aneurysm of right internal carotid artery with severe lumen stenosis.

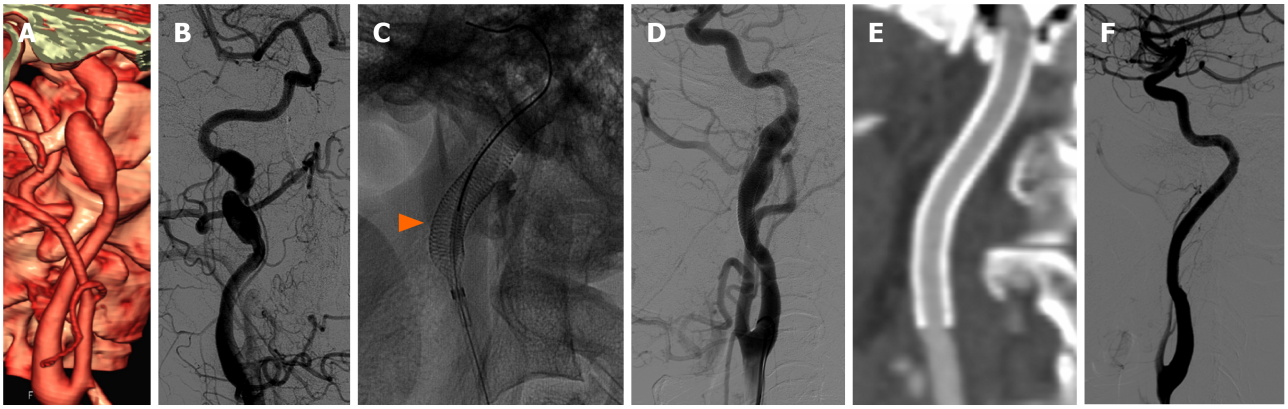

Figure 2 Case 2 was a 57-year-old man who suddenly felt dizzy and developed unsteady walking in November 2019. He was ultimately treated using a SUPERA stents. A: Cervical computed tomographic angiography (CTA) volume reconstruction; B: digital subtraction angiography (DSA) showed a fusiform dilated dissecting aneurysm with severe stenosis located in the upper segment of the right internal carotid artery, involving the petrous segment; C and D: It was treated with SUPERA stent endovascular treatment, the arrow shows the dense stent reticular wire; E: Three months later, cervical CTA showed that the aneurysm had disappeared completely, and the lumen of the internal carotid artery was unobstructed; F: One year later, DSA showed that the internal carotid artery was repaired perfectly.

TREATMENT

Case 1: Endovascular treatment was considered because of the enlarging aneurysm and the risk of rupture. Under local anesthesia, a 5F puncture sheath (Terumo Corporation, Hatagaya, Tokyo, Japan) was inserted into the right femoral artery. A 6F90cm sheath (Cook Medical, Bloomington, IN, United States) was exchanged and inserted into the left internal carotid artery. Intraoperative digital subtraction angiography (DSA) showed the wide-necked aneurysm in the carotid segment of the left internal carotid artery (Figure 1C), and the proximal artery wall was not smooth, which was considered to be fibromuscular dysplasia with dissecting aneurysm. Heparin (3000 IU) was injected intravenously. A 0.014 Synchro microwire (Stryker Neurovascular, West Valley City, CA, United States) and a Rebar27 microcatheter (Micro Therapeutics Inc, Irvine, CA, United States) were inserted to the cavernous sinus segment of the internal carotid artery through the guide catheter, followed by the exchange of an 0.018 Steelcore guidewire (Abbott, Santa Clara, CA, United States). A 6 mm × 40 mm SUPERA stent (Abbott Vascular, Santa Clara, CA, United States) was inserted along the guidewire and released at the appropriate position (Figure 1D-E). The stent was released by the push-pull technique, and the stent wire was compacted in the aneurysm segment. Repeated angiography showed that the contrast medium in the lumen was unobstructed, and the blood flow in the aneurysm was slowed down. There were no postoperative complications.

Case 2: Because the stroke in this patient was associated with severe internal carotid artery stenosis shown by CTA and ipsilateral cerebral infarction shown by MRI, SUPERA stent implantation was considered and performed in December 2019. Under local anesthesia, the right femoral artery was punctured, an 8F sheath (Terumo Corporation, Hatagaya, Tokyo, Japan) was placed, and an 8F guide catheter (Boston Scientific Corporation, Marlborough, MA, United States) was inserted into the right common carotid artery. Intraoperative DSA confirmed the severe stenosis and dissecting aneurysm of the right internal carotid artery (Figure 2B). Heparin (3000 IU) was injected intravenously. A 0.014 Synchro microwire (Stryker Neurovascular, West Valley City, CA, United States) and a Rebar27 microcatheter (Micro Therapeutics Inc, Irvine, CA, United States) were inserted across the stenosis to the cavernous sinus segment of the internal carotid artery through the guide catheter. After exchanging for an 0.018 Steelcore guidewire (Abbott Vascular, Santa Clara, CA, United States), a 5 mm × 20 mm fast exchange balloon catheter (Abbott Vascular, Santa Clara, CA, United States) was inserted along the guidewire to dilate the narrow segment. A 5 mm × 60 mm SUPERA stent was implanted by the same technique. Repeated DSA showed that the stenosis was significantly improved, the contrast medium in the lumen was unobstructed, and the blood flow in the aneurysm was slowed down (Figure 2C and D).

OUTCOME AND FOLLOW-UP

Case 1: Three months later, in September 2019, CTA showed that the dissecting aneurysm had disappeared completely (Figure 1F-G). The patient reported no new symptoms and was able to take care of himself. Muscle strength of the left limb remained decreased, and speech was slow. At 1 year after the operation, in July 2020, DSA showed that the lumen was completely repaired (Figure 1H). The symptoms remained the same.

Case 2: There were no postoperative complications, and the patient recovered well after the operation. Three months later, in April 2020, CTA showed that the dissecting aneurysm had disappeared completely (Figure 2E). DSA showed that the lumen was repaired entirely in December 2020 (Figure 2F). This patient had no residual abnormal symptoms during follow-up.

DISCUSSION

Endovascular treatment of extracranial cervical dissecting aneurysm is controversial because of the possible operative complications, and there is a possibility that the risks of treatment will be greater than the benefits to the patients[2,8]. Cothren *et al*[9] reported a 21% (4/19) complication rate and a documented occlusion rate of 45% (8/18) in the endovascular treatment of pseudoaneurysms from extracranial carotid dissections. They claim that the risks outweigh the benefits of stenting in the treatment of carotid dissecting pseudoaneurysms[9]. Nevertheless, there is no doubt that the incidence of complications is very low in the available case series of selective endovascular therapy reported in the literature, and the short- and long-term benefits are probably significant[4,5,10-12]. These previous studies highlighted the importance of selecting the right patients and using the right materials and tools in an individualized manner. In previous reports, endovascular treatment of extracranial cervical dissecting aneurysm included endovascular exclusion with a covered stent, stent-assisted coil embolization, and multi-stent overlap. A self-expanding covered stent is the first choice for treatment because of its immediate and long-term effect[4]. On the other hand, internal carotid artery dissections are usually located in the upper part of the extracranial internal carotid artery, and it is technically challenging to transport a covered stent for treating dissecting aneurysms near or involving the petrous segment. In contrast, balloon-dilated covered stents might be easier to transport, but there is a possible danger of acute closure after external force compression, and the adhesion of balloon stents is often not as good as that of self-expanding stents. Hence, it is suggested that balloon dilatation stents should not be used in extracranial carotid arteries, which are prone to external force compression. For wide-necked or fusiform dissecting aneurysms, bare carotid artery stents used alone often have difficulties eliminating the dissecting aneurysms. Balloon embolization is the only option for the treatment of this type of aneurysm. Later, it was found that coil-assisted embolization stent implantation can effectively eliminate dissecting aneurysm, but it is expensive and a residual space-occupying effect cannot be avoided.

The SUPERA stent is a braided metal stent specially designed for arterial stenosis of the lower extremities[7]. In theory, it can change the aneurysm cavity's blood flow state like a flow diverter so that the aneurysm can be gradually reduced and cured. We used this braided bare metal stent to treat two cases of extracranial internal carotid artery dissecting aneurysms, which were a wide-necked aneurysm and a long fusiform aneurysm with severe lumen stenosis. There were no postoperative complications in the two cases. The symptoms of cerebral ischemia disappeared, and there was no recurrence of stroke during the follow-up period. The lumen was anatomically repaired perfectly. The aneurysms had entirely disappeared at 3 mo, and there was no residual space-occupying effect. One year after the operation, DSA showed that the lumen was repaired well and there was no restenosis. Satisfactory results have been achieved. The literature presents studies of its use in femoropopliteal disease[13] and the subclavian artery[14]. Previous studies used different bare-metal stents (other than the SUPERA stent) to manage the carotid disease successfully[15,16]. The SUPERA stent might be easier to implant and have better outcomes, but the study is still necessary.

The SUPERA Stent System has moderate flexibility, convenient delivery, and uncomplicated release and can change the stent mesh size. We believe that it is a suitable choice to treat wide-necked dissecting aneurysms and long fusiform aneurysms. Nevertheless, several aspects must be mentioned. First, it is an over-to-

wire catheter system, and the inner core will move back and forth when the stent is released. If a distal protected device has been used, it will be challenging to maintain the system's stability. Therefore, we did not use remote embolization protection devices. Second, this stent system is best used in patients with straight parent arteries, and we have not tried it on very circuitous arteries. Only two cases were reported here. Additional studies with larger numbers of patients are necessary to determine the benefits of the SUPERA stent in managing extracranial internal carotid artery dissecting aneurysms.

CONCLUSION

In conclusion, according to the treatment and follow-up of these two cases, SUPERA stent implantation might achieve good results in treating a wide-necked or long fusiform internal carotid artery dissecting aneurysms. Still, additional studies are necessary to confirm these observations.

REFERENCES

1 **Goodfriend SD**, Tadi P, Koury R. Carotid Artery Dissection. StatPearls. Treasure Island (FL), 2020 [DOI: 10.32388/ivp1ee]

2 **Larsson SC**, King A, Madigan J, Levi C, Norris JW, Markus HS. Prognosis of carotid dissecting aneurysms: Results from CADISS and a systematic review. *Neurology* 2017; **88**: 646-652 [PMID: 28087823 DOI: 10.1212/WNL.0000000000003617]

3 **Saito R**, Ezura M, Takahashi A, Yoshimoto T. Combined neuroendovascular stenting and coil embolization for cervical carotid artery dissection causing symptomatic mass effect. *Surg Neurol* 2000; **53**: 318-322 [PMID: 10825514 DOI: 10.1016/s0090-3019(00)00206-8]

4 **Scavée V**, De Wispelaere JF, Mormont E, Coulier B, Trigaux JP, Schoevaerdts JC. Pseudoaneurysm of the internal carotid artery: treatment with a covered stent. *Cardiovasc Intervent Radiol* 2001; **24**: 283-285 [PMID: 11779022 DOI: 10.1007/s00270-001-0012-z]

5 **Feugier P**, Vulliez A, Bina N, Floccard B, Allaouchiche B. Urgent endovascular covered-stent treatment of internal carotid artery injury caused by a gunshot. *Eur J Vasc Endovasc Surg* 2007; **34**: 663-665 [PMID: 17681828 DOI: 10.1016/j.ejvs.2007.06.011]

6 **Turk AS 3rd**, Martin RH, Fiorella D, Mocco J, Siddiqui A, Bonafe A. Flow diversion *vs* traditional endovascular coiling therapy: design of the prospective LARGE aneurysm randomized trial. *AJNR Am J Neuroradiol* 2014; **35**: 1341-1345 [PMID: 24831596 DOI: 10.3174/ajnr.A3968]

7 **Scheinert D**, Grummt L, Piorkowski M, Sax J, Scheinert S, Ulrich M, Werner M, Bausback Y, Braunlich S, Schmidt A. A novel self-expanding interwoven nitinol stent for complex femoropopliteal lesions: 24-month results of the SUPERA SFA registry. *J Endovasc Ther* 2011; **18**: 745-752 [PMID: 22149221 DOI: 10.1583/11-3500.1]

8 **Markus HS**, Levi C, King A, Madigan J, Norris J; Cervical Artery Dissection in Stroke Study (CADISS) Investigators. Antiplatelet Therapy *vs* Anticoagulation Therapy in Cervical Artery Dissection: The Cervical Artery Dissection in Stroke Study (CADISS) Randomized Clinical Trial Final Results. *JAMA Neurol* 2019; **76**: 657-664 [PMID: 30801621 DOI: 10.1001/jamaneurol.2019.0072]

9 **Cothren CC**, Moore EE, Ray CE Jr, Ciesla DJ, Johnson JL, Moore JB, Burch JM. Carotid artery stents for blunt cerebrovascular injury: risks exceed benefits. *Arch Surg* 2005; **140**: 480-5; discussion 485 [PMID: 15897444 DOI: 10.1001/archsurg.140.5.480]

10 **Castellan L**, Casasco A, Toso V, Bernardi L. Stenting of the extracranial internal carotid artery for dissecting aneurysm. *Ital J Neurol Sci* 1999; **20**: 251-253 [PMID: 10551913 DOI: 10.1007/s100720050040]

11 **Cohen JE**, Leker RR, Gotkine M, Gomori M, Ben-Hur T. Emergent stenting to treat patients with carotid artery dissection: clinically and radiologically directed therapeutic decision making. *Stroke* 2003; **34**: e254-e257 [PMID: 14605318 DOI: 10.1161/01.STR.0000101915.11128.3D]

12 **Wilson MP**, Murad MH, Krings T, Pereira VM, O'Kelly C, Rempel J, Hilditch CA, Brinjikji W. Management of tandem occlusions in acute ischemic stroke - intracranial *vs* extracranial first and extracranial stenting *vs* angioplasty alone: a systematic review and meta-analysis. *J Neurointerv Surg* 2018; **10**: 721-728 [PMID: 29523749 DOI: 10.1136/neurintsurg-2017-013707]

13 **Bishu K**, Armstrong EJ. Supera self-expanding stents for endovascular treatment of femoropopliteal disease: a review of the clinical evidence. *Vasc Health Risk Manag* 2015; **11**: 387-395 [PMID: 26203255 DOI: 10.2147/VHRM.S70229]

14 **Vinayakumar D**, Sulaiman S, Govindan Sajeev C. Recurrent Spontaneous Stent Fracture in a Case of Takayasu Arteritis Treated Successfully with Supera Stent System. J Cardiol Cardiovasc Ther 2018; 10: 555778 [DOI: 10.19080/jocct.2018.10.555778]

15 **Ahlhelm F**, Kaufmann R, Ahlhelm D, Ong MF, Roth C, Reith W. Carotid artery stenting using a novel self-expanding braided nickel-titanium stent: feasibility and safety porcine trial. *Cardiovasc*

Intervent Radiol 2009; **32**: 1019-1027 [PMID: 19533229 DOI: 10.1007/s00270-009-9572-0]

16 **Cornwall JW**, Png CYM, Han DK, Tadros RO, Marin ML, Faries PL. Endovascular techniques in the treatment of extracranial carotid artery aneurysms. *J Vasc Surg* 2021; **73**: 2031-2035 [PMID: 33098945 DOI: 10.1016/j.jvs.2020.06.133]

World Journal of Clinical Cases

Submit a Manuscript: https://www.f6publishing.com

World J Clin Cases 2022 February 16; 10(5): 1609-1616

DOI: 10.12998/wjcc.v10.i5.1609

ISSN 2307-8960 (online)

CASE REPORT

Combination of atezolizumab and chidamide to maintain long-term remission in refractory metastatic extranodal natural killer/T-cell lymphoma: A case report

Juan Wang, Yong-Sheng Gao, Kun Xu, Xiao-Dong Li

ORCID number: Juan Wang 0000-0002-0508-8895; Yong-Sheng Gao 0000-0003-0095-8836; Kun Xu 0000-0003-2692-0107; Xiao-Dong Li 0000-0002-6934-2303.

Author contributions: Li XD designed the research study; Wang J collected data of the study; Gao YS advised on the pathological report; and Xu K wrote the manuscript; all authors have read and approve the final manuscript.

Informed consent statement: Informed written consent was obtained from the patient for publication of this report and any accompanying images.

Conflict-of-interest statement: The authors declare that they have no conflict of interest.

CARE Checklist (2016) statement: The authors have read the CARE Checklist (2016), and the manuscript was prepared and revised according to the CARE Checklist (2016).

Country/Territory of origin: China

Specialty type: Hematology

Provenance and peer review: Unsolicited manuscript; Externally peer reviewed.

Juan Wang, Xiao-Dong Li, Department of Radiation Oncology, Shandong Cancer Hospital and Institute, Shandong First Medical University and Shandong Academy of Medical Sciences, Jinan 250117, Shandong Province, China

Yong-Sheng Gao, Department of Pathology, Shandong Cancer Hospital and Institute, Shandong First Medical University and Shandong Academy of Medical Sciences, Jinan 250117, Shandong Province, China

Kun Xu, Department of Gastrointestinal Surgery, Shandong Cancer Hospital and Institute, Shandong First Medical University and Shandong Academy of Medical Sciences, Jinan 250117, Shandong Province, China

Corresponding author: Xiao-Dong Li, MD, PhD, Doctor, Professor, Department of Radiation Oncology, Shandong Cancer Hospital and Institute, Shandong First Medical University and Shandong Academy of Medical Sciences, No. 440 Jiyan Road, Jinan 250117, Shandong Province, China. sylxd1306@163.com

Abstract

BACKGROUND

The prognosis of refractory extranodal natural killer/T-cell lymphoma (ENKTL) is poor. Recent data have indicated that immune checkpoint blockade with a programmed cell death protein-1 (PD-1) antibody in combination with administration of histone deacetylase inhibitors represents a potentially effective treatment strategy. Compared with PD-1 antibodies, programmed death-ligand 1 antibodies have fewer side effects. Here, we present a rare case of a patient with refractory metastatic ENKTL who achieved sustained remission of approximately 10 mo with minor adverse effects after combination therapy with atezolizumab, chidamide, and radiotherapy.

CASE SUMMARY

A 56-year-old woman underwent resection of a tumour in her left nasal cavity and was diagnosed with ENKTL (nasal type). Medical examination revealed tumours observed in the bilateral nasal mucosa, the subcutaneous soft tissue of the inner side of the left eye, the soft tissue of the nasopharynx, the bilateral tonsils, and the left preauricular, right hilar, bilateral neck lymph nodes and bone marrow. However, tomography/computed tomography showed increased metabolism of

Peer-review model: Single blind

Peer-review report's scientific quality classification
Grade A (Excellent): 0
Grade B (Very good): 0
Grade C (Good): C
Grade D (Fair): 0
Grade E (Poor): 0

Received: July 30, 2021
Peer-review started: July 30, 2021
First decision: October 25, 2021
Revised: November 7, 2021
Accepted: January 6, 2022
Article in press: January 6, 2022
Published online: February 16, 2022

P-Reviewer: Shekouhi R
S-Editor: Wang LYT
L-Editor: A
P-Editor: Wang LYT

the bilateral nasal mucosa and subcutaneous soft tissue of the inner side of the left eye and newly increased metabolism of the left cervical lymph node after chemotherapy. Therefore, combination therapy with chidamide, atezolizumab, and radiotherapy was performed. Fortunately, the patient achieved a complete response following 10 mo of combination therapy.

CONCLUSION
The outcome in this case suggests that the combination of atezolizumab, chidamide, and radiotherapy is a promising regimen for treating refractory metastatic ENKTL following chemotherapy treatment failure.

Key Words: Long-term remission; Refractory metastatic extranodal natural killer/T-cell lymphoma; Histone deacetylase; Programmed death-ligand 1 antibody; Radiotherapy; Case report

Core Tip: extranodal natural killer/T-cell lymphoma (ENKTL) is a subtype of non-Hodgkin lymphoma with poor outcomes because ENKTL cells express high levels of P-glycoprotein that mediate tumour multidrug resistance. Furthermore, the standard treatment modality for chemotherapy-resistant ENKTL remains debated. We have experienced a patient with refractory metastatic ENKTL who was resistant to conventional DDGP chemotherapy. Following systemic therapy with atezolizumab and chidamide in combination with local radiotherapy, the patient achieved sustained remission of approximately 10 mo with minor adverse effects.

Citation: Wang J, Gao YS, Xu K, Li XD. Combination of atezolizumab and chidamide to maintain long-term remission in refractory metastatic extranodal natural killer/T-cell lymphoma: A case report. *World J Clin Cases* 2022; 10(5): 1609-1616
URL: https://www.wjgnet.com/2307-8960/full/v10/i5/1609.htm
DOI: https://dx.doi.org/10.12998/wjcc.v10.i5.1609

INTRODUCTION

Extranodal natural killer (NK)/T-cell lymphoma (ENKTL) is a distinct subtype of mature T-cell and NK-cell lymphoma that is prevalent in regions of East Asia and South America[1-3]. ENKTL progresses rapidly and has a poor prognosis. Although options for therapy continue to evolve, their curative effects remain unsatisfactory. Because ENKTL cells express high levels of P-glycoprotein that mediate tumour multidrug resistance, conventional chemotherapy regimens such as CHOP (cyclophosphamide, doxorubicin, vincristine, and prednisone) have poor outcomes. Thus, nonanthracycline-based chemotherapy has become the main therapeutic strategy. However, in patients for whom L-asparaginase-based regimens are ineffective, progression-free survival (PFS) after relapse or first progression was only 4.1 mo[4].

Recently, several studies have reported that HDAC inhibitors (HDACis) combined with anti-death protein-1 (PD-1) immunotherapy showed encouraging efficacy, thus representing a new treatment strategy for relapsed/refractory (r/r) ENKTL[5,6]. However, the combination of death-ligand 1 (PD-L1) antibody and HDACi for r/r ENKTL has not yet been investigated. Here, we report the case of a patient with refractory metastatic ENKTL who achieved a durable response following systemic therapy with PD-L1 antibody and chidamide in combination with local radiotherapy.

CASE PRESENTATION

Chief complaints

A 56-year-old woman had been diagnosed with ENKTL (nasal type) for one month.

History of present illness

The patient underwent resection of a tumour in her left nasal cavity and was diagnosed with ENKTL (nasal type). Before being transferred to our hospital, she accepted her first cycle chemotherapy with CHOPE (cyclophosphamide 1000 mg Day 1 + vincristine 2 mg Day 1 + epirubicin 100 mg Day 1 + etoposide 100 mg Days 1-3 + prednisone acetate 100 mg Days 1-5) and developed grade IV myelosuppression.

History of past illness

The patient had a free previous medical history.

Personal and family history

Personal and family history was non-contributory.

Physical examination

The patient's temperature was 36.4 °C, heart rate was 102 beats/min, respiratory rate was 25 breaths/min, and blood pressure was 122/95 mmHg. The clinical examination revealed facial strut and pain.

Laboratory examinations

The tumour cells stained positive for CD3, CD56, TIA-1, and Ki-67 (approximately 40%) but were negative for CD20 (Figure 1). Bone marrow examination was performed. Flow cytometry revealed 0.71% NK cells with the following abnormal immunophenotypes: CD2+, CD7+, CD56+, CD94+, CD161+, CD5-, CD16-, and CD8+/-.

Imaging examinations

Positron emission tomography/computed tomography (PET/CT) was performed for staging, and increased ^{18}F-fluorodeoxyglucose (FDG) uptake was observed in the bilateral nasal mucosa, the subcutaneous soft tissue of the inner side of the left eye, the soft tissue of nasopharynx, the bilateral tonsils, and the left preauricular, right hilar, and bilateral neck lymph nodes. These patterns were consistent with the infiltration of malignant lymphoma (Figure 2).

FINAL DIAGNOSIS

The patient was diagnosed with ENKTL (nasal type). Disease was evaluated as Ann Arbor stage IVE A, the prognostic index for NK/T-cell lymphoma, including Epstein-Barr virus DNA load (PINK-E), was calculated as 3, and disease was classified as high risk.

TREATMENT

Radiotherapy, chidamide, and nivolumab were concurrently administered. The target volume included the partial frontal sinus, the right maxillary sinus, all ethmoid sinuses, the sphenoid sinus, the left orbit and eye contents, the left maxillary sinus, the nasopharynx, the left preauricular lymphoid drainage area, and the bilateral neck level Ib, 2, 3, 4, and 5 Lymphatic drainage areas. The radiation dose was 50 Gy/25 fractions. The patient developed transient rash on the third day after nivolumab treatment and grade 4 thrombocytopenia following the first cycle of combination therapy. Therefore, the PD-1/PD-L1 inhibitor was changed to atezolizumab for subsequent immunotherapy after her haemogram recovered.

OUTCOME AND FOLLOW-UP

After four cycles of chidamide and atezolizumab, PET/CT showed slightly higher metabolism of the nasal cavity. Treatment was continued as planned. Fortunately, PET/CT showed no obvious FDG uptake after 11 cycles of combination therapy with chidamide and atezolizumab (Figure 2). Grade 3 adverse events, including neutropenia and thrombocytopenia, were manageable and resolved during maintenance treatment.

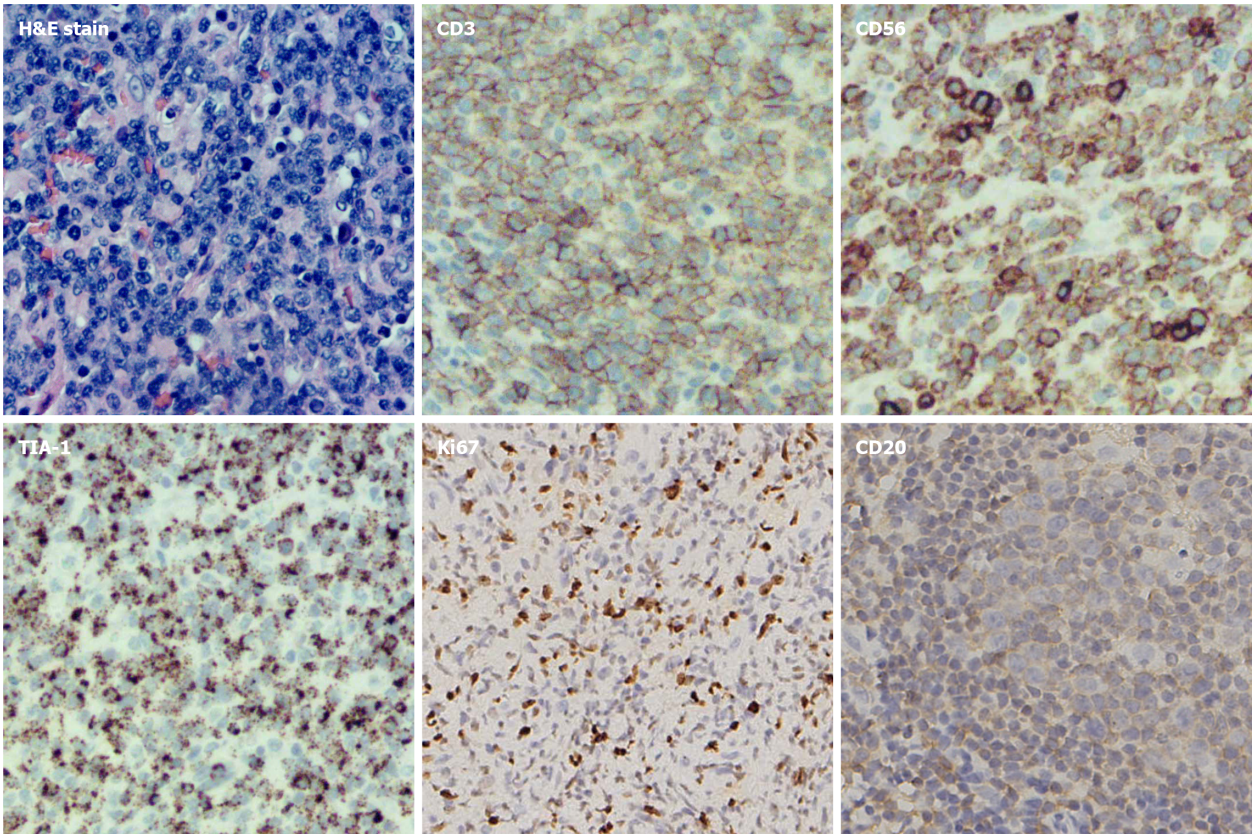

Figure 1 Photomicrographs of the left nasal cavity biopsy demonstrating extranodal natural killer/T-cell lymphoma. Immunohistochemical staining showed that the tissue of the left nasal cavity mass was positive for CD3, TIA-1, Ki67, and CD56 but negative for CD20.

DISCUSSION

ENKTL is a subtype of non-Hodgkin lymphoma with poor outcome. The standard treatment modality for refractory ENKTL is still debated, especially for chemotherapy-resistant tumours[4]. Here, we present the case of a patient with refractory metastatic ENKTL who was resistant to conventional DDGP chemotherapy. Following systemic therapy with a PD-L1 inhibitor and chidamide in combination with local radiotherapy, the patient achieved sustained remission of approximately 10 mo with minor adverse effects.

Previous studies suggested that NKTL was resistant to anthracycline[7]. Thus, pegaspargase, gemcitabine, or other non-anthracycline-based chemotherapy regimens are generally used for the first-line treatment of patients with newly diagnosed refractory NKTL[8,9]. Additionally, as described in previous reports, allogeneic stem cell transplantation (allo-SCT) may be beneficial for patients with ENKTL[10,11]. However, PFS in the subset of patients who maintained remission following allo-SCT was only approximately 10.0 mo. There has been no randomized, prospective study to evaluate the safety and efficacy of allo-SCT in ENKTL[12].

Recently, radiotherapy, PD-1 inhibitors, and HDACis (alone or in combination) have shown promising efficacy in treating r/r ENKTL. Chidamide is a novel benzamide-type HDACi that can selectively block HDAC1, 2, 3, and 10[13]. Recent data demonstrated that chidamide induced growth inhibition and apoptosis in NK/T lymphoma cells[14]. A phase II clinical trial of chidamide for r/r peripheral T-cell lymphoma showed median PFS and overall survival of 2.1 and 21.4 mo, respectively [15]. In this study, 16 ENKTL patients were enrolled and showed lower response rates compared with other studies: one patient achieved a complete response (CR), and two patients achieved partial responses (PRs).

PD-1/PD-L1 inhibitors are additional new agents for the treatment of r/r ENKTL. In previous reports (Table 1), combining PD-1 antibody with chemotherapy or chidamide obtained satisfactory results, and most of the cases achieved complete response and sustained curative effects[16-21]. The anti-PD-1 antibody (sintilimab) plus chidamide regimen was evaluated in a phase 1b/II clinical trial[22], where the CR rate was 44.4% in 41 r/r-NKTCL patients. A previous study demonstrated that anti-

Table 1 Reports regarding the application of death protein-1/death-ligand 1 inhibitors in refractory or relapsed extranodal natural killer/T-cell lymphoma

Ref.	Number of cases	Age mean year (range)	Gender	Treatment	Stage	Response	OS or PFS
McGehee *et al* [16] 2021	1	72	1 M	Pembrolizumab plus RT	IV	CR	33 mo, alive
Du *et al*[17] 2020	3	52 (51-54)	3 M	PD-1 antibody, plus Chidamide, etoposide, and thalidomide	1 (33.3%) IV; 1 (33.3%) III; 1 (33.3%) II	2 (66.7%) CR; 1 (33.3%) PD	-
Kwong *et al* [18] 2017	7	49 (31-68)	7 M	Pembrolizumab	5 (71.4%) IV; 2 (28.6%) IE	5 (71.4%) C; 2 (28.6%) PR	-
Li *et al*[19] 2018	7	47 (17-61)	4 M; 3 F	Pembrolizumab	2 (28.6%) IV; 3 (42.9%) II; 1 (14.3%) IIIE; 1 (14.3%) IE	2 (28.6%) CR; 2 (28.6%) PR	5 mo OS; 4.8 mo PFS
Diab *et al*[20] 2021	1	82	M	Pembrolizumab	IV	CR	21 mo, alive
Lai *et al*[21] 2017	1	37	F	Pembrolizumab	IV	CR	-
Gao *et al*[22] 2020	41	48 (20-72)	27 M; 14 F	Sintilimab plus chidamide	26 (70.3%) IV; 15 (29.7%) Non-IV	16 (44.4%) CR; 5 (13.9%) PR	-
Kim *et al*[24] 2020	21	≤ 60 16; > 60 5	13 M; 8F	Avelumab	-	5 (23.8%) CR; 3 (14.3%) PR	-

OS: Overall survival; PFS: Progression-free survival; M: Male; F: Female; Non-IV: Non-stage IV patients; RT: Radiotherapy.

PD-L1 antibodies have better efficacy and fewer adverse effects[23]. In particular, an open-label phase 2 study demonstrated that a PD-L1 antibody as a single agent induced tumour remission in a subset of patients. CRs were observed in 24% of patients, and the overall response rate was 38%; the study was terminated because of a lower than expected response rate[24]. Five responders in this study continued to show sustained responses, and the only adverse events observed were grades 1 or 2. However, to our knowledge, there have been no case reports evaluating the effects of PD-L1 antibody for r/r-ENKTL patients who could not tolerate previous treatment with PD-1 antibody.

Recently, multiple lines of evidence have demonstrated that HDACis could enhance the therapeutic effects of PD-1 antibodies[25,26]. Epigenetic modification could regulate T cell trafficking and reactivation, thus enhancing the efficacy of the PD-1 antibody. A few case reports suggested that the combination of PD-1 antibodies and HDACis might be effective in patients with refractory ENKTL[5,6]. However, the antitumour effect of combination therapy with PD-L1 antibody and chidamide has not been demonstrated for refractory ENKTL. The patient described here was successfully treated with local radiotherapy and systemic therapy with chidamide and PD-L1 antibodies. Evaluation 10 mofollowing the end of radiation therapy showed a sustained CR. We presume that the sustained therapeutic efficacy observed in this patient may result from synergistic effects of PD-L1 antibody, chidamide, and local radiotherapy. Studies with larger numbers of patients are needed to evaluate the efficacy and safety of this combination therapy regimen for refractory ENKTL.

CONCLUSION

We present a rare case of a patient with refractory ENKTL who was successfully treated with a combination of radiotherapy, chidamide, and PD-L1 antibody. Additional evidence is needed to evaluate the potential activity and safety of this regimen.

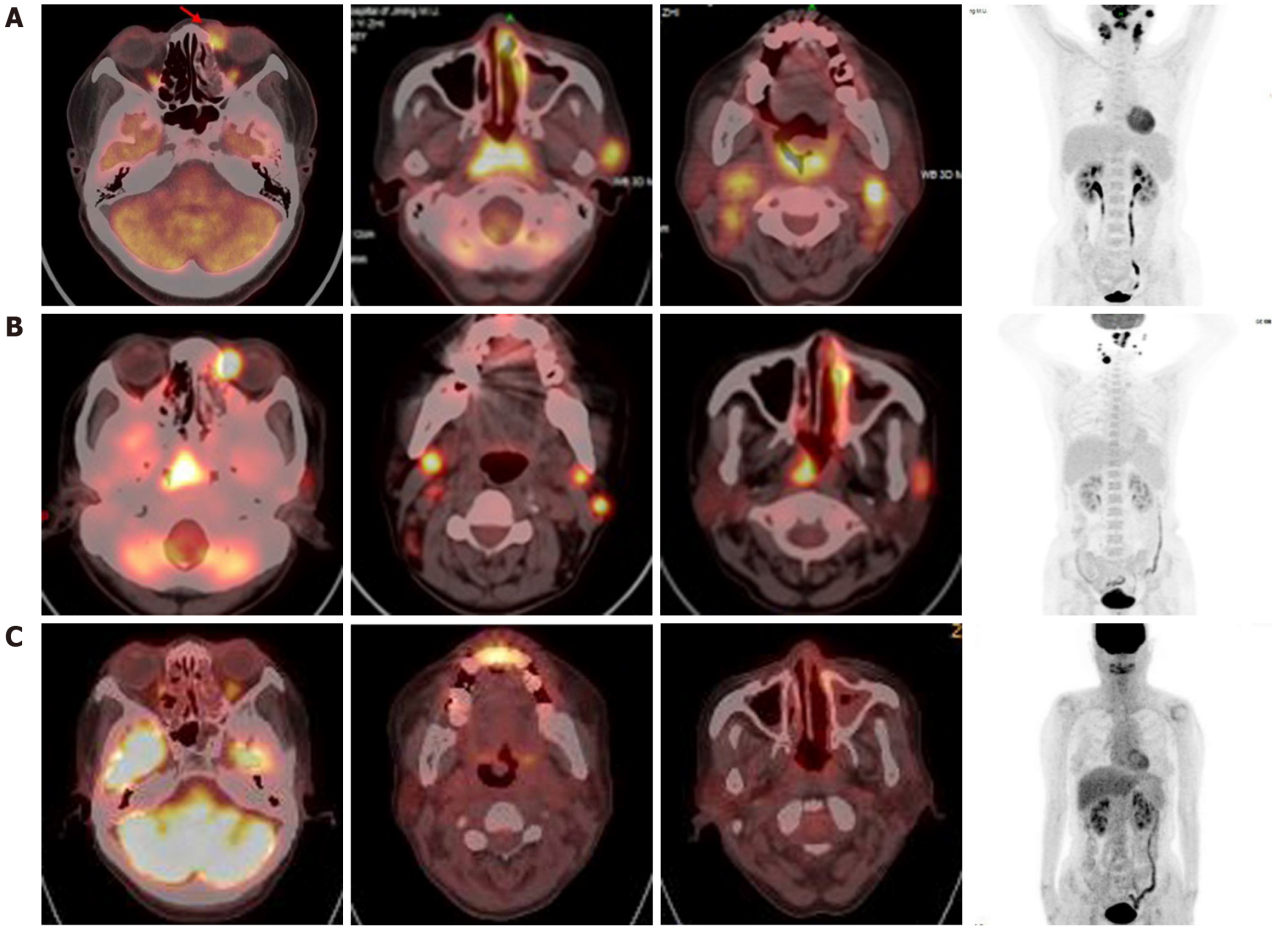

Figure 2 Imaging at diagnosis, after four cycles of chemotherapy with DDGP (cisplatin, dexamethasone, gemcitabine, and pegaspargase), and 10 mo posttreatment withdeath-ligand 1antibody and chidamide. A: Positron emission tomography showing hypermetabolism in the bilateral nasal mucosa, the subcutaneous soft tissue of the inner side of the left eye, the soft tissue of the nasopharynx, the bilateral tonsil, and the left preauricular, bilateral neck, and right hilar lymph nodes; B: After four cycles of DDGP chemotherapy, increased metabolism of the lesions was observed except in the right hilar lymph nodes; C: Patient achieved sustained remission for approximately 10 mo.

ACKNOWLEDGEMENTS

We thank the patient and her family for providing signed informed consent.

REFERENCES

1 **Shi Y**. Current status and progress of lymphoma management in China. *Int J Hematol* 2018; **107**: 405-412 [PMID: 29388166 DOI: 10.1007/s12185-018-2404-8]

2 **Haverkos BM**, Pan Z, Gru AA, Freud AG, Rabinovitch R, Xu-Welliver M, Otto B, Barrionuevo C, Baiocchi RA, Rochford R, Porcu P. Extranodal NK/T Cell Lymphoma, Nasal Type (ENKTL-NT): An Update on Epidemiology, Clinical Presentation, and Natural History in North American and European Cases. *Curr Hematol Malig Rep* 2016; **11**: 514-527 [PMID: 27778143 DOI: 10.1007/s11899-016-0355-9]

3 **Fox CP**, Civallero M, Ko YH, Manni M, Skrypets T, Pileri S, Kim SJ, Cabrera ME, Shustov AR, Chiattone CS, Horwitz SM, Dlouhy I, Spina M, Hitz F, Montoto S, Nagler A, Martinez V, De Souza CA, Fernandez-Alvarez R, Ballova V, Gabús R, Inghirami G, Federico M, Kim WS. Survival outcomes of patients with extranodal natural-killer T-cell lymphoma: a prospective cohort study from the international T-cell Project. *Lancet Haematol* 2020; **7**: e284-e294 [PMID: 32105608 DOI: 10.1016/S2352-3026(19)30283-2]

4 **Lim SH**, Hong JY, Lim ST, Hong H, Arnoud J, Zhao W, Yoon DH, Tang T, Cho J, Park S, Ko YH, Kim SJ, Suh C, Lin T, Kim WS. Beyond first-line non-anthracycline-based chemotherapy for extranodal NK/T-cell lymphoma: clinical outcome and current perspectives on salvage therapy for patients after first relapse and progression of disease. *Ann Oncol* 2017; **28**: 2199-2205 [PMID: 28911074 DOI: 10.1093/annonc/mdx316]

5 **Xu J**, Xu X, Chen J, Wang J, Jiang C, Lv C, Chen B. Sustained remission of multi-line relapsed extranodal NK/T-cell lymphoma, nasal type, following sintilimab and chidamide: A case report.

Medicine (Baltimore) 2021; **100**: e24824 [PMID: 33725836 DOI: 10.1097/MD.0000000000024824]

6 **Yan Z**, Yao S, Liu Y, Zhang J, Li P, Wang H, Chu J, Zhao S, Yao Z. Durable Response to Sintilimab and Chidamide in a Patient With Pegaspargase- and Immunotherapy-Resistant NK/T-Cell Lymphoma: Case Report and Literature Review. *Front Oncol* 2020; **10**: 608304 [PMID: 33363038 DOI: 10.3389/fonc.2020.608304]

7 **Yamaguchi M**, Kwong YL, Kim WS, Maeda Y, Hashimoto C, Suh C, Izutsu K, Ishida F, Isobe Y, Sueoka E, Suzumiya J, Kodama T, Kimura H, Hyo R, Nakamura S, Oshimi K, Suzuki R. Phase II study of SMILE chemotherapy for newly diagnosed stage IV, relapsed, or refractory extranodal natural killer (NK)/T-cell lymphoma, nasal type: the NK-Cell Tumor Study Group study. *J Clin Oncol* 2011; **29**: 4410-4416 [PMID: 21990393 DOI: 10.1200/JCO.2011.35.6287]

8 **Zhang L**, Wang Y, Li X, Li L, Wang X, Sun Z, Wu J, Fu X, Zhang X, Yu H, Wang G, Chang Y, Yan J, Zhou Z, Wu X, Nan F, Li W, Zhang M. Radiotherapy *vs* sequential pegaspargase, gemcitabine, cisplatin and dexamethasone and radiotherapy in newly diagnosed early natural killer/T-cell lymphoma: A randomized, controlled, open-label, multicenter study. *Int J Cancer* 2021; **148**: 1470-1477 [PMID: 33034052 DOI: 10.1002/ijc.33329]

9 **Wang JH**, Wang L, Liu CC, Xia ZJ, Huang HQ, Lin TY, Jiang WQ, Lu Y. Efficacy of combined gemcitabine, oxaliplatin and pegaspargase (P-gemox regimen) in patients with newly diagnosed advanced-stage or relapsed/refractory extranodal NK/T-cell lymphoma. *Oncotarget* 2016; **7**: 29092-29101 [PMID: 27093153 DOI: 10.18632/oncotarget.8647]

10 **Tse E**, Chan TS, Koh LP, Chng WJ, Kim WS, Tang T, Lim ST, Lie AK, Kwong YL. Allogeneic haematopoietic SCT for natural killer/T-cell lymphoma: a multicentre analysis from the Asia Lymphoma Study Group. *Bone Marrow Transplant* 2014; **49**: 902-906 [PMID: 24777195 DOI: 10.1038/bmt.2014.65]

11 **Ennishi D**, Maeda Y, Fujii N, Kondo E, Shinagawa K, Ikeda K, Ichimura K, Yoshino T, Tanimoto M. Allogeneic hematopoietic stem cell transplantation for advanced extranodal natural killer/T-cell lymphoma, nasal type. *Leuk Lymphoma* 2011; **52**: 1255-1261 [PMID: 21599584 DOI: 10.3109/10428194.2011.572322]

12 **Jeong SH**, Song HN, Park JS, Yang DH, Koh Y, Yoon SS, Lee HW, Eom HS, Won JH, Kim WS, Kim SJ. Allogeneic Stem Cell Transplantation for Patients with Natural Killer/T Cell Lymphoid Malignancy: A Multicenter Analysis Comparing Upfront and Salvage Transplantation. *Biol Blood Marrow Transplant* 2018; **24**: 2471-2478 [PMID: 30064012 DOI: 10.1016/j.bbmt.2018.07.034]

13 **Ning ZQ**, Li ZB, Newman MJ, Shan S, Wang XH, Pan DS, Zhang J, Dong M, Du X, Lu XP. Chidamide (CS055/HBI-8000): a new histone deacetylase inhibitor of the benzamide class with antitumor activity and the ability to enhance immune cell-mediated tumor cell cytotoxicity. *Cancer Chemother Pharmacol* 2012; **69**: 901-909 [PMID: 22080169 DOI: 10.1007/s00280-011-1766-x]

14 **Zhou J**, Zhang C, Sui X, Cao S, Tang F, Sun S, Wang S, Chen B. Histone deacetylase inhibitor chidamide induces growth inhibition and apoptosis in NK/T lymphoma cells through ATM-Chk2-p53-p21 signalling pathway. *Invest New Drugs* 2018; **36**: 571-580 [PMID: 29504068 DOI: 10.1007/s10637-017-0552-y]

15 **Shi Y**, Dong M, Hong X, Zhang W, Feng J, Zhu J, Yu L, Ke X, Huang H, Shen Z, Fan Y, Li W, Zhao X, Qi J, Zhou D, Ning Z, Lu X. Results from a multicenter, open-label, pivotal phase II study of chidamide in relapsed or refractory peripheral T-cell lymphoma. *Ann Oncol* 2015; **26**: 1766-1771 [PMID: 26105599 DOI: 10.1093/annonc/mdv237]

16 **McGehee E**, Patel H, Pearson C, Clements K, Jaso JM, Chen W, Callan A, Desai N, Ramakrishnan Geethakumari P. Combined immune checkpoint blockade and radiotherapy induces durable remission in relapsed natural killer/T-cell lymphoma: a case report and review of theliterature. *J Med Case Rep* 2021; **15**: 221 [PMID: 33926575 DOI: 10.1186/s13256-021-02798-2]

17 **Du L**, Zhang L, Li L, Li X, Yan J, Wang X, Fu X, Sun Z, Zhang X, Li Z, Wu J, Yu H, Chang Y, Zhou Z, Nan F, Wu X, Tian L, Zhang M. Effective Treatment with PD-1 Antibody, Chidamide, Etoposide, and Thalidomide (PCET) for Relapsed/Refractory Natural Killer/T-Cell Lymphoma: A Report of Three Cases. *Onco Targets Ther* 2020; **13**: 7189-7197 [PMID: 32801749 DOI: 10.2147/OTT.S262039]

18 **Kwong YL**, Chan TSY, Tan D, Kim SJ, Poon LM, Mow B, Khong PL, Loong F, Au-Yeung R, Iqbal J, Phipps C, Tse E. PD1 blockade with pembrolizumab is highly effective in relapsed or refractory NK/T-cell lymphoma failing l-asparaginase. *Blood* 2017; **129**: 2437-2442 [PMID: 28188133 DOI: 10.1182/blood-2016-12-756841]

19 **Li X**, Cheng Y, Zhang M, Yan J, Li L, Fu X, Zhang X, Chang Y, Sun Z, Yu H, Zhang L, Wang X, Wu J, Li Z, Nan F, Tian L, Li W, Young KH. Activity of pembrolizumab in relapsed/refractory NK/T-cell lymphoma. *J Hematol Oncol* 2018; **11**: 15 [PMID: 29386072 DOI: 10.1186/s13045-018-0559-7]

20 **Diab R**, Kamran S, Adcock B, Choucair K, Truong QV. Extra-Nodal, Nasal, Natural Killer T-Cell Lymphoma Treated With a Checkpoint Inhibitor: A Case Report of a Sustained Complete Response. *Cureus* 2021; **13**: e14654 [PMID: 34046285 DOI: 10.7759/cureus.14654]

21 **Lai J**, Xu P, Jiang X, Zhou S, Liu A. Successful treatment with anti-programmed-death-1 antibody in a relapsed natural killer/T-cell lymphoma patient with multi-line resistance: a case report. *BMC Cancer* 2017; **17**: 507 [PMID: 28754096 DOI: 10.1186/s12885-017-3501-4]

22 **Gao Y**, Huang H, Wang X, Bai B, Zhang L, Xiao Y, Liu X, Li W, Xu W, Feng R, Chen Y, Wu H, Li J, Wu X. Anti-PD-1 Antibody (Sintilimab) Plus Histone Deacetylase Inhibitor (Chidamide) for the Treatment of Refractory or Relapsed Extranodal Natural Killer/T Cell Lymphoma, Nasal Type (r/r-

ENKTL): Preliminary Results from a Prospective, Multicenter, Single-Arm, Phase Ib/II Trial (SCENT). *Blood* 2020; **136**: 39-40 [DOI: 10.1182/blood-2020-134665]

23 **Feng D**, Guan Y, Liu M, He S, Zhao W, Yin B, Liang J, Li Y, Wang J. Excellent Response to Atezolizumab After Clinically Defined Hyperprogression Upon Previous Treatment With Pembrolizumab in Metastatic Triple-Negative Breast Cancer: A Case Report and Review of the Literature. *Front Immunol* 2021; **12**: 608292 [PMID: 34135884 DOI: 10.3389/fimmu.2021.608292]

24 **Kim SJ**, Lim JQ, Laurensia Y, Cho J, Yoon SE, Lee JY, Ryu KJ, Ko YH, Koh Y, Cho D, Lim ST, Enemark MB, D'Amore F, Bjerre M, Ong CK, Kim WS. Avelumab for the treatment of relapsed or refractory extranodal NK/T-cell lymphoma: an open-label phase 2 study. *Blood* 2020; **136**: 2754-2763 [PMID: 32766875 DOI: 10.1182/blood.2020007247]

25 **Burke B**, Eden C, Perez C, Belshoff A, Hart S, Plaza-Rojas L, Delos Reyes M, Prajapati K, Voelkel-Johnson C, Henry E, Gupta G, Guevara-Patiño J. Inhibition of Histone Deacetylase (HDAC) Enhances Checkpoint Blockade Efficacy by Rendering Bladder Cancer Cells Visible for T Cell-Mediated Destruction. *Front Oncol* 2020; **10**: 699 [PMID: 32500025 DOI: 10.3389/fonc.2020.00699]

26 **Chen X**, Pan X, Zhang W, Guo H, Cheng S, He Q, Yang B, Ding L. Epigenetic strategies synergize with PD-L1/PD-1 targeted cancer immunotherapies to enhance antitumor responses. *Acta Pharm Sin B* 2020; **10**: 723-733 [PMID: 32528824 DOI: 10.1016/j.apsb.2019.09.006]

World Journal of Clinical Cases

Submit a Manuscript: https://www.f6publishing.com

World J Clin Cases 2022 February 16; 10(5): 1617-1622

DOI: 10.12998/wjcc.v10.i5.1617

ISSN 2307-8960 (online)

CASE REPORT

Hemangioma in the lower labial vestibule of an eleven-year-old girl: A case report

Ashwag Yagoub Aloyouny, Afrah Jaber Alfaifi, Shahad Mohammed Aladhyani, Ahad Ali Alshalan, Hadeel Mohammed Alfayadh, Hend Mahmoud Salem

ORCID number: Ashwag Yagoub Aloyouny 0000-0001-6759-2846; Afrah Jaber Alfaifi 0000-0002-9154-3806; Shahad Mohammed Aladhyani 0000-0003-1339-2747; Ahad Ali Alshalan 0000-0001-9934-4070; Hadeel Mohammed Alfayadh 0000-0003-1690-8470; Hend Mahmoud Salem 0000-0003-1126-80056.

Author contributions: Aloyouny AY contributed to data collection, reviewed the literature, interpreted the data, manuscript drafting and revision; Salem H prepared the specimen in the pathology laboratory and analysed it under the microscope; Alfaifi AJ, Aladhyani SM, Alshalan AA, and Alfayadh HM contributed to data collection, and manuscript drafting.

Informed consent statement: Informed written consent was obtained from the patient for publication of this case report and accompanying images.

Conflict-of-interest statement: The authors declare that they have no conflicts of interest.

CARE Checklist (2016) statement: The authors have read the CARE Checklist (2016) and have prepared and revised the manuscript accordingly.

Ashwag Yagoub Aloyouny, Afrah Jaber Alfaifi, Hend Mahmoud Salem, Department of Basic Dental Science, Princess Nourah Bint Abdulrahman University, Riyadh 11671, Saudi Arabia

Shahad Mohammed Aladhyani, Oral Medicine Special Care Dentistry, Prince Sultan Military Medical City, Riyadh 12211, Saudi Arabia

Ahad Ali Alshalan, Hadeel Mohammed Alfayadh, Department of Dentistry, Ministry of Health, Riyadh 11176, Saudi Arabia

Corresponding author: Ashwag Yagoub Aloyouny, DDS, Doctor, Department of Basic Dental Science, Princess Nourah Bint Abdulrahman University, King Khalid International Rd, Riyadh 11671, Saudi Arabia. ayaloyouny@pnu.edu.sa

Abstract

BACKGROUND

Hemangioma is a vascular benign tumour of endothelial origin. It appears commonly in the first decade of life with increases incidence in females. Hemangioma is not common to happen in the oral cavity and it is extremely rare to appear in the labial vestibule.

CASE SUMMARY

We present a case of an 11-year-old girl who complained of a painful, slowly growing mass which was consistent with the capillary hemangioma in the left mandibular vestibule. Vascular tumor such as hemangioma in the mandibular vestibule is extremely rare; hence, the clinical definitive diagnosis is very challenging. Therefore, radiographic imaging and histopathologic analysis are crucial to reach to the final diagnosis for proper management.

CONCLUSION

Comprehensive clinical evaluation, proper diagnostic imaging and microscopic analysis of the mass establish a precise diagnosis of the hemangioma for better management.

Key Words: Capillary hemangioma; Vascular malformation; Labial vestibule; Childhood; Case report

Supported by the Deanship of Scientific Research at Princess Nourah Bint Abdulrahman University Through the Fast-Track Research Funding Program.

Country/Territory of origin: Saudi Arabia

Specialty type: Dentistry, oral surgery and medicine

Provenance and peer review: Unsolicited article; Externally peer reviewed.

Peer-review model: Single blind

Peer-review report's scientific quality classification
Grade A (Excellent): 0
Grade B (Very good): 0
Grade C (Good): C, C
Grade D (Fair): 0
Grade E (Poor): 0

Received: July 31, 2021
Peer-review started: July 31, 2021
First decision: October 22, 2021
Revised: October 30, 2021
Accepted: December 31, 2021
Article in press: December 31, 2021
Published online: February 16, 2022

P-Reviewer: Feng J, Zhao GH
S-Editor: Liu JH
L-Editor: A
P-Editor: Liu JH

Core Tip: Although hemangioma rarely occurs in the oral cavity, it should be considered in the diagnosis of a red-bluish isolated mass. In this case report, the patient presented with a painful, slowly growing mass in the left labial vestibule which resulted in asymmetry and swelling of the lower lip. The final diagnosis of the mass was consistent with capillary hemangioma in the mandibular vestibule. Early detection and treatment of oral masses is essential to avoid any complications.

Citation: Aloyouny AY, Alfaifi AJ, Aladhyani SM, Alshalan AA, Alfayadh HM, Salem HM. Hemangioma in the lower labial vestibule of an eleven-year-old girl: A case report. *World J Clin Cases* 2022; 10(5): 1617-1622
URL: https://www.wjgnet.com/2307-8960/full/v10/i5/1617.htm
DOI: https://dx.doi.org/10.12998/wjcc.v10.i5.1617

INTRODUCTION

Hemangioma commonly appears early in life with increases incidence in females more than males. It usually gets smaller with time until it completely disappears. Mulliken *et al*[1] (1982) published the novel classification of vascular lesion and the International Society for the Study of Vascular Anomalies (2018) has provided updated guidelines for vascular anomalies classification. Accordingly, the vascular anomalies have been classified into vascular malformations and vascular tumors. Vascular tumors include non-harmful, locally destructive, and malignant lesions, whereas vascular malformations include simple and combined malformations.

Hemangiomas are vascular benign tumours of endothelial origin, presenting clinically with varying sizes and shapes. In some cases, hemangioma could cause functional disability and disfiguring appearance, which may lead to psychological issues. Histologically, hemangioma has another classification, into either cavernous or capillary types.

Hemangioma is uncommon to occur in the oral cavity and it is extremely rare to appear in the labial vestibule. To our knowledge and based on the review of English literature (PubMed), this case is the first report of capillary hemangioma in the mandibular vestibule. In this report, we present an 11-year-old girl patient complaining of a slowly growing mass that caused labial swelling and asymmetry. The diagnosis was consistent with capillary hemangioma in the mandibular vestibule.

CASE PRESENTATION

Chief complaints

An 11-year-old healthy girl was referred to the oral and maxillofacial surgery clinic for evaluation of labial asymmetry and swelling.

History of present illness

The patient had a two-month-history of a slowly growing lesion in the left side of the lower labial vestibule accompanied with persistent mild pain. The patient and her parents reported no history of trauma at the site of the mass.

History of past illness

The patient was healthy and did not undergo any surgeries.

Personal and family history

The parents revealed no significant family history and no genetic abnormalities.

Physical examination

Physical and systemic examination: The patient was healthy and had only taken Tylenol 15 mg as needed for fever.

Extraoral examination: Extraoral examination showed lower lip asymmetry and swelling in the left side.

Intraoral examination: Intraoral examination showed a 2.0-1.5 cm, solitary, fluctuant, bluish, smooth, palpable submucosal mass, rubbery in consistency, tender, and blanch on pressure (positive diascopy test). The submucosal mass located in the left mandibular vestibule opposite to tooth number 32 and 33 (23 and 33, according to the FDI World Dental Federation Notation) (Figure 1).

Imaging examinations

A panoramic radiograph showed normal structures with no significant pathologic findings. Additionally, Color-Doppler-ultrasound was performed to confirm the nature of the lesion. The imaging interpretation revealed a slow-flow vascular lesion in the left lower vestibule and attached to the lower orbicularis oris muscle.

FINAL DIAGNOSIS

The final diagnosis was based on histopathological analysis. The histopathological diagnosis was consistent with capillary hemangioma in the labial vestibule (Figure 2).

TREATMENT

Complete surgical removal of the lesion to reduce the risk of the recurrence.

OUTCOME AND FOLLOW-UP

At two-, four- and eight-week-follow up, the site of the surgery healed well with no sign of bleeding, infection, and swelling. At one- and three-year- follow up, there was no recurrence of the lesion or complications noted. Additionally, the patient was in a good health.

DISCUSSION

In 1982, vascular anomalies were categorised into two main categories: Vascular malformations and vascular tumors. Hemangiomas are true neoplasms represented by increased rate and proliferation of endothelial cell turnover. On the other hand, vascular malformations are localised abnormality and disorganisation of the blood vessel caused by defects in vascular development[1-3]. Simple vascular malformations are classified histologically, based on the vessel size, into capillary, venous, lymphatics, arteriovenous fistula, and arteriovenous malformations. Vascular lesions are further categorised into non-harmful, locally destructive, and malignant lesions[4]. Namely, hemangioma is a neoplasm of endothelial origin which is commonly found in the early years of life and then the neoplasm regresses gradually with age[5]. Intraoral and intramuscular hemangiomas are rare, dissimilar to cutaneous and subcutaneous hemangiomas. Oral hemangiomas could occur in more than 6% of infants and have high prevalence in female presenting 3:1 (female:male). Infants are more likely to develop oral hemangiomas if they fall in one of the following conditions; infants who are born to older mothers, twins or triplets, premature, or have low birth weight[6]. Hemangioma is a common vascular benign tumor which falls under the category of benign vascular tumors and it is further divided into capillary and cavernous hemangioma[2].

Capillary hemangioma is a common lesion, but it rarely occurs in the oral cavity. According to Matsumoto *et al*[7], 45.2% of capillary hemangiomas occur on buccal mucosa, 35.5% on the tongue, and only a small percentage occur in the lip, gingiva and palate. Capillary hemangiomas are firm in consistency and have a limited history of symptoms. Although the exact cause of oral hemangioma is not fully understood, hormonal changes, embolic phenomenon and genetic mutations are believed to play an important role in the tumor development[8].

Hemangiomas are hypothesised to develop because of both angiogenesis and vasculogenesis through three different stages, as follows: Endothelial cell proliferation stage, rapid growth stage and spontaneous disappearance. Endothelial cell proliferation is stimulated by many factors, such as basic fibroblast growth factor, vascular

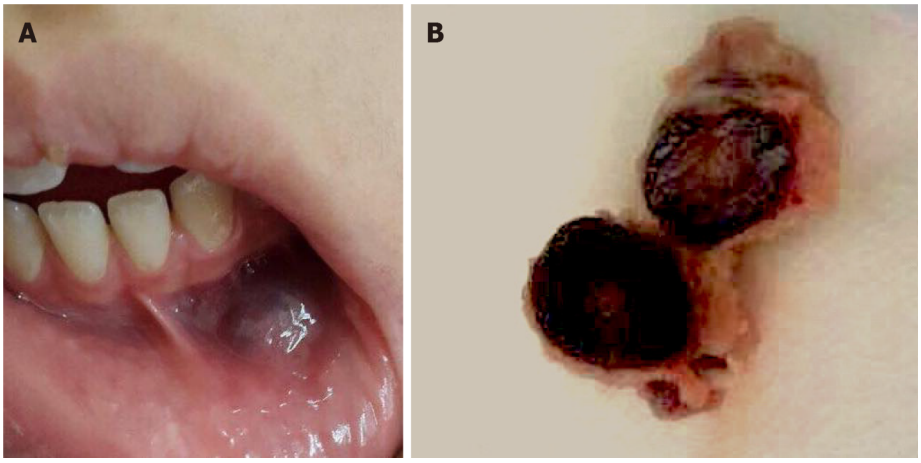

Figure 1 Intraoral examination and gross examination of the surgical specimen. A: Intraoral lesion measuring 2.0-1.5 cm, solitary, fluctuant, bluish, smooth, palpable submucosal mass located in the left mandibular vestibule; B: A single, solid mass, bluish in color, and rubbery in consistency.

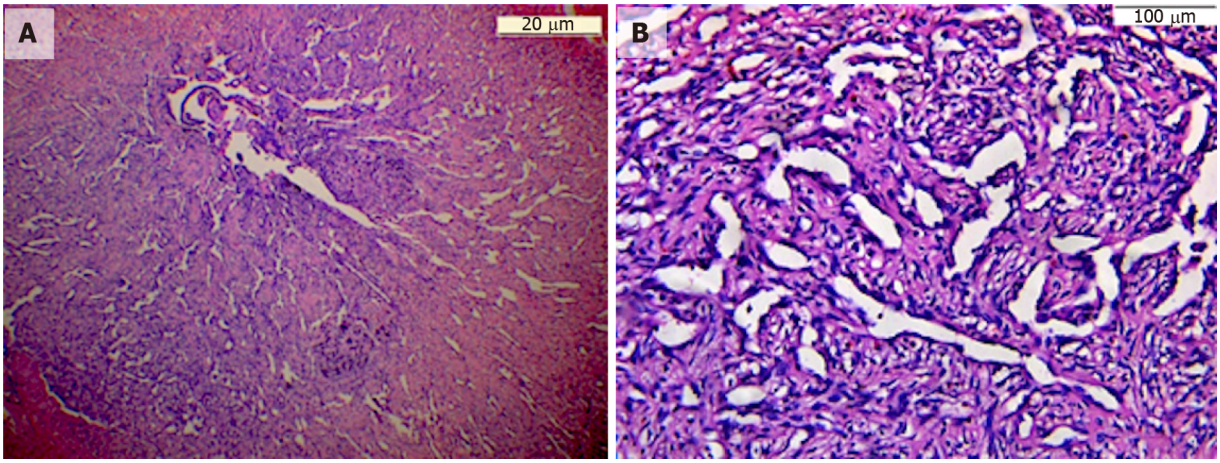

Figure 2 Histopathological analysis showed numerous thin-walled blood vessels with dilated blood vessel spaces, areas of hemorrhage and chronic inflammatory cell infiltrate which is consistent with capillary hemangioma in the labial vestibule. A: 20 µm; B: 100 µm.

endothelial growth factor and transforming growth factor-beta. Then, the quantity of endothelial cells is sustained, and each cell increases in size, leading to comprehensive enlargement of the structure size. At the end, spontaneous involution occurs when the endothelial cells are replaced by connective tissue, adipose, and fibroblast, and the number of small vessels decrease in quantity[9].

Hemangioma could be classified clinically as congenital or infantile (previously named strawberry or juvenile). Congenital hemangioma presents at birth and does not demonstrate proliferation stage. In contrast, infantile hemangioma may develop at the first months of the infant life and show a proliferative phase during the period of six to twelve months; then, most cases spontaneously regress between the age of six to nine years. High percentage of hemangiomas disappear completely in childhood, with < 20% carrying on to puberty[10,11]. Oral hemangioma presents as a solitary, soft, fluctuant, compressible, smooth, red, or bluish submucosal mass. Significant variations may present based on the depth and site of the mass. Superficial masses are easy to visualise and may present as pedunculated, sessile, or lobulated and reddish in colour. In contrast to deeper masses, they appear as a dark blue discolouration recognisable from surrounding normal colour mucosa. It also reveals tenderness on palpation and blanch on compression with glass slide (positive diascopy test)[12]. In this case, the differential diagnosis of the tumor was written down as vascular anomalies, including hemangioma, and vascular malformation, including venous, capillary, lymphatic and arterial malformations. Salivary gland tumor, mucocele and angioleiomyoma were also considered.

It is worth mentioning that vascular malformations, salivary gland tumor, mucocele and angioleiomyoma were all excluded because the lesion showed a slow-flow vascular lesion by using Colour-Doppler-ultrasound, which is highly consistent with hemangioma.

Histological analysis of vascular anomalies, including capillary hemangioma, is still the most acceptable and accurate method of diagnosis[3]. Microscopic description of capillary hemangioma illustrates several dilated capillaries lined by endothelial cells, filled with blood, and surrounded by inflammatory infiltrate.

Hemangioma is mostly characterised by its benign feature and has high tendency of involution by itself over time. However, sometimes hemangioma requires intervention, especially in case of impairment in breathing, swallowing and speech. The first line of evaluation and diagnosis would be by Color-Doppler ultrasound imaging. This imaging modality is non-invasive, cost-effective and has no risk of radiation. If intraosseous lesion is anticipated, other imaging modalities could be useful for the diagnosis, such as a contrast-enhanced magnetic resonance imaging (MRI), computed tomography (CT), and angiography[13]. A contrast-enhanced MRI and CT imaging identify the shape, size, and calcification of the tumor. The Color-Doppler ultrasound imaging modality was the suitable choice for the patient due to many factors, such as financial issues and the age of the patient[14].

Choosing a suitable method for managing hemangioma is based on multiple factors such as the aesthetic consideration, clinical nature, size, site, growth rate, accessibility, extent of the tumor, and age of the patient. Hemangioma could be managed by different ways; for instance, surgical excision of the tumor, embolization, electrosurgery, cryosurgery, laser, steroid injection, or sclerosing materials. In case of small oral hemangioma, the commonly used method is the total surgical excision of the whole mass to decrease the potential risk of recurrence[15]. However, if the lesion is large and located in a significant part of the mouth, such as the tongue, in this case the surgical excision of the lesion would not be preferred, so as to avoid post-surgical complications in swallowing and speech. Sclerotherapy is recommended to manage large hemangiomas in the oral cavity in which 3% sodium tetradecyl sulfate or ethanolamine oleate is injected into the main vessels of the lesion to destroy the endothelial cells, leading to lesion destruction. Precautionary measures should be taken to avoid bleeding during the surgical procedure or afterward during recovery phase. In the present case, the tumor was excised surgically with a thin rim of the attached orbicularis oris muscle to decrease the risk of recurrence[16,17].

CONCLUSION

Although hemangioma rarely appears in the oral cavity, it should be considered in the diagnosis of a red-bluish isolated mass. Comprehensive clinical evaluation, proper diagnostic imaging and microscopic analysis of the mass establish a precise diagnosis of the hemangioma for better treatment.

REFERENCES

1 **Mulliken JB**, Glowacki J. Hemangiomas and vascular malformations in infants and children: a classification based on endothelial characteristics. *Plast Reconstr Surg* 1982; **69**: 412-422 [PMID: 7063565 DOI: 10.1097/00006534-198203000-00002]

2 **Merrow AC**, Gupta A, Patel MN, Adams DM. 2014 Revised Classification of Vascular Lesions from the International Society for the Study of Vascular Anomalies: Radiologic-Pathologic Update. *Radiographics* 2016; **36**: 1494-1516 [PMID: 27517361 DOI: 10.1148/rg.2016150197]

3 **Larsen AK**, Damsgaard TE, Hedelund L. [Classification of vascular anomalies]. *Ugeskr Laeger* 2018; **180** [PMID: 30187855]

4 **Allen PW**, Enzinger FM. Hemangioma of skeletal muscle. An analysis of 89 cases. *Cancer* 1972; **29**: 8-22 [PMID: 5061701 DOI: 10.1002/1097-0142(197201)29:1<8::aid-cncr2820290103>3.0.co;2-a]

5 **Kale US**, Ruckley RW, Edge CJ. Cavernous haemangioma of the parapharyngeal space. *Indian J Otolaryngol Head Neck Surg* 2006; **58**: 77-80 [PMID: 23120244 DOI: 10.1007/BF02907748]

6 **Corrêa PH**, Nunes LC, Johann AC, Aguiar MC, Gomez RS, Mesquita RA. Prevalence of oral hemangioma, vascular malformation and varix in a Brazilian population. *Braz Oral Res* 2007; **21**: 40-45 [PMID: 17384854 DOI: 10.1590/s1806-83242007000100007]

7 **Matsumoto N**, Tsuchiya M, Nomoto S, Matsue Y, Nishikawa Y, Takamura T, Oki H, Komiyama K. CD105 expression in oral capillary hemangiomas and cavernous hemangiomas. *J Oral Sci* 2015; **57**: 45-53 [PMID: 25807908 DOI: 10.2334/josnusd.57.45]

8 **Marchuk DA**. Pathogenesis of hemangioma. *J Clin Invest* 2001; **107**: 665-666 [PMID: 11254664 DOI: 10.1172/JCI12470]

9 **Greenberger S**, Bischoff J. Pathogenesis of infantile haemangioma. *Br J Dermatol* 2013; **169**: 12-19 [PMID: 23668474 DOI: 10.1111/bjd.12435]

10 **George A**, Mani V, Noufal A. Update on the classification of hemangioma. *J Oral Maxillofac Pathol* 2014; **18**: S117-S120 [PMID: 25364160 DOI: 10.4103/0973-029X.141321]

11 **Nayak SK**, Nayak P. Intramuscular hemangioma of the oral cavity - a case report. *J Clin Diagn Res* 2014; **8**: ZD41-ZD42 [PMID: 25302283 DOI: 10.7860/JCDR/2014/8305.4756]

12 **da Silva WB**, Ribeiro AL, de Menezes SA, de Jesus Viana Pinheiro J, de Melo Alves-Junior S. Oral capillary hemangioma: a clinical protocol of diagnosis and treatment in adults. *Oral Maxillofac Surg* 2014; **18**: 431-437 [PMID: 24263242 DOI: 10.1007/s10006-013-0436-z]

13 **Gianfranco G**, Eloisa F, Vito C, Raffaele G, Gianluca T, Umberto R. Color-Doppler ultrasound in the diagnosis of oral vascular anomalies. *N Am J Med Sci* 2014; **6**: 1-5 [PMID: 24678469 DOI: 10.4103/1947-2714.125852]

14 **Ghanem AA**, El Hadidi YN. Management of a Life Threatening Bleeding Following Extraction of Deciduous Second Molar Related to a Capillary Haemangioma. *Craniomaxillofac Trauma Reconstr* 2017; **10**: 166-170 [PMID: 28523092 DOI: 10.1055/s-0037-1598102]

15 **Barrón-Peña A**, Martínez-Borras MA, Benítez-Cárdenas O, Pozos-Guillén A, Garrocho-Rangel A. Management of the oral hemangiomas in infants and children: Scoping review. *Med Oral Patol Oral Cir Bucal* 2020; **25**: e252-e261 [PMID: 31967983 DOI: 10.4317/medoral.23329]

16 **Bonet-Coloma C**, Mínguez-Martínez I, Palma-Carrió C, Galán-Gil S, Peñarrocha-Diago M, Mínguez-Sanz JM. Clinical characteristics, treatment and outcome of 28 oral haemangiomas in pediatric patients. *Med Oral Patol Oral Cir Bucal* 2011; **16**: e19-e22 [PMID: 20711165 DOI: 10.4317/medoral.16.e19]

17 **Stuepp RT**, Scotti FM, Melo G, Munhoz EA, Modolo F. Effects of sclerosing agents on head and neck hemangiomas: A systematic review. *J Clin Exp Dent* 2019; **11**: e1033-e1044 [PMID: 31700578 DOI: 10.4317/jced.56143]

World Journal of Clinical Cases

Submit a Manuscript: https://www.f6publishing.com

World J Clin Cases 2022 February 16; 10(5): 1623-1629

DOI: 10.12998/wjcc.v10.i5.1623

ISSN 2307-8960 (online)

CASE REPORT

Primary orbital monophasic synovial sarcoma with calcification: A case report

Ming-Yu Ren, Jing Li, Rui-Miao Li, Yi-Xiang Wu, Rui-Juan Han, Chi Zhang

ORCID number: Ming-Yu Ren 0000-0002-8270-0523; Jing Li 0000-0002-0769-5891; Rui-Miao Li 0000-0002-9146-1624; Yi-Xiang Wu 0000-0002-1175-2609; Rui-Juan Han 0000-0003-0017-0483; Chi Zhang 0000-0002-4641-9830.

Author contributions: Ren MY conceptualized this study, made the literature review and wrote the first draft of this paper; Li J, Li RM, Wu YX, Han RJ, and Zhang C made the literature review; all authors revised the paper and approved the final version for submission.

Informed consent statement: Informed written consent was obtained from the patient for publication of this report and any accompanying images.

Conflict-of-interest statement: The authors declare that they have no conflict of interest.

CARE Checklist (2016) statement: The authors have read the CARE Checklist (2016), and the manuscript was prepared and revised according to the CARE Checklist (2016).

Supported by the Science and Technology Planning Project of Xingtai, No.2019ZC246.

Country/Territory of origin: China

Ming-Yu Ren, Rui-Miao Li, Yi-Xiang Wu, Rui-Juan Han, Chi Zhang, Department of Orbital Disease and Ocular Tumor, Hebei Eye Hospital, Xingtai 054001, Hebei Province, China

Jing Li, Intensive Care Unit, Xingtai Third Hospital, Xingtai 054001, Hebei Province, China

Corresponding author: Ming-Yu Ren, MMed, Associate Chief Physician, Department of Orbital Disease and Ocular Tumor, Hebei Eye Hospital, No. 399 Quanbeidong, Xingtai 054001, Hebei Province, China. 147237583@qq.com

Abstract

BACKGROUND

Synovial sarcoma is a malignant mesenchymal neoplasm with variable epithelial differentiation. Most synovial sarcoma cases are reported in young adults and can arise in any body site. Notably, primary orbital synovial sarcoma is rare.

CASE SUMMARY

An 8-year-old east Asian girl with 1-month history of gradual painless proptosis and lacrimation of the right eye was admitted. The patient presented with painless proptosis, downward eyeball displacement, and upward movement disorders. According to clinical manifestations, imaging examinations and postoperative immunohistochemical examinations, the diagnosis was monophasic synovial sarcoma with calcification. The patient underwent anterior orbitotomy procedure for removal of the right orbital mass under general anesthesia. The diagnosis of monophasic synovial sarcoma with calcification was confirmed finally through histological and immunohistochemical exam. The follow-up period was 6 mo, and no recurrence was observed during this period.

CONCLUSION

Primary orbital monophasic synovial sarcoma with calcification is a rare sarcoma, and clinical manifestations and imaging results are not specific. The tumor may present similar features as a benign tumor. Comprehensive analysis of clinical, radiological, and pathological findings is critically important for making the right diagnosis. Conventional treatment approach for synovial sarcoma is surgical resection with adjuvant or neoadjuvant radiotherapy, which is highly effective for localized tumors.

Key Words: Orbital tumor; Synovial sarcoma; Calcification; Histological; Case report

Specialty type: Ophthalmology

Provenance and peer review: Unsolicited article; Externally peer reviewed.

Peer-review model: Single blind

Peer-review report's scientific quality classification
Grade A (Excellent): A
Grade B (Very good): 0
Grade C (Good): 0
Grade D (Fair): 0
Grade E (Poor): 0

Received: July 31, 2021
Peer-review started: July 31, 2021
First decision: October 25, 2021
Revised: October 28, 2021
Accepted: December 28, 2021
Article in press: December 28, 2021
Published online: February 16, 2022

P-Reviewer: Maglangit SACA
S-Editor: Guo X
L-Editor: Kerr C
P-Editor: Guo X

Core Tip: We describe a patient with 1-month history of gradual painless proptosis and lacrimation of the right eye. The patient underwent anterior orbitotomy procedure for removal of the right orbital mass under general anesthesia. The diagnosis of monophasic synovial sarcoma with calcification was confirmed finally through histological and immunohistochemical exam. The follow-up period was 6 mo, and no recurrence was observed during this period. This case illustrates the tumor may present similar features as a benign tumor. Comprehensive analysis of clinical, radiological, and pathological findings is critically important for making the right diagnosis.

Citation: Ren MY, Li J, Li RM, Wu YX, Han RJ, Zhang C. Primary orbital monophasic synovial sarcoma with calcification: A case report. *World J Clin Cases* 2022; 10(5): 1623-1629
URL: https://www.wjgnet.com/2307-8960/full/v10/i5/1623.htm
DOI: https://dx.doi.org/10.12998/wjcc.v10.i5.1623

INTRODUCTION

Synovial sarcoma is a malignant mesenchymal neoplasm with variable epithelial differentiation. It mainly occurs in young adults and can arise at several sites[1]. It mainly commonly occurs in deep soft tissue of the extremities in adolescents and young adults[2]. Synovial sarcoma of the head and neck region is very rare, and only a few cases of sarcoma arising from the orbit have been reported[3,4]. The current study reports a case of primary orbital monophasic synovial sarcoma which was characterized by calcification in an 8-year old patient.

CASE PRESENTATION

Chief complaints

An 8-year-old east Asian girl with 1-mo history of gradual painless proptosis and lacrimation of the right eye was admitted to our hospital.

History of present illness

The patient presented with gradual painless proptosis and lacrimation of the right eye for 1 mo. The proptosis was gradual and painless. No special treatment was performed, and there was no other significant change in ocular symptoms.

History of past illness

The patient had no history of any previous disease.

Personal and family history

There was no family history of malignant neoplasm.

Physical examination

Physical examination showed no neurological signs. The patient presented with painless proptosis, downward eyeball displacement, and upward movement disorders. Ocular examination showed that the binocular best-corrected visual acuity was 20/20. Eye examination did not show any significant eyelid, conjunctival, corneal and lenticular abnormalities, and fundus examination did not show any abnormalities. Hertel exophthalmometry analysis showed that the right eye was 18 mm and whereas the left eye was 13 mm, and the interorbital distance was 91 mm. Intraocular pressure of the right eye was 13 mmHg and 11 mmHg in the left eye.

Laboratory examinations

Blood and urine tests were normal.

Imaging examinations

A/B-scan showed moderate echogenic lesions in the right eye orbital. Echoes were uneven, well-distributed and sound transmission normal. Patchy strong echoes and sound shadows were detected (Figure 1). Orbital CT scan showed a well-defined soft tissue density mass in the right orbit, with flaky high-density shadows observed inside the right orbital. The size of the mass was approximately 20 mm × 20 mm × 19 mm, and exophthalmos; extraocular muscles and optic nerve were compressed (Figure 2). Orbital magnetic resonance imaging showed a circular-like mass in the right orbital. T1-weighted images (T1WI) showed moderate signals, whereas T2-weighted images (T2WI) showed mixed signals, with high number of moderately high signals. T1WI and T2WI were characterized by low-signal regions. Most part of the lesion was significantly and unevenly enhanced, whereas local lesions did not exhibit any enhancement (Figure 3).

Primary diagnosis

Based on the findings described above, the preliminary diagnosis was rhabdomyosarcoma or other malignant neoplasm.

FINAL DIAGNOSIS

Histological examination showed that the tumor was monophasic synovial sarcoma with calcification. Immunohistochemical analysis showed positive staining for CD34, CD99, Bcl-2, CKpan, TLE1, INI-1 and Ki-67 (25%), and negative staining for SMA, Vimentin, Myogenin, Myoglobin, Syn, CgA, NSE, S-100, PGP9.5, EMA, CK7, CK (AE1/AE3), CD65, Calretinin, TTF1 and MUC-4 (Figure 4).

TREATMENT

After preoperative examination, the patient underwent anterior orbitotomy procedure for removal of the right orbital mass under general anesthesia. The operation showed an oval tumor above the optic nerve in the right orbit. The tumor margins were well defined, however, it was significantly large, reddish, unmovable, and adhesive to the levator palpebrae muscle (Figure 5). The levator palpebrae muscle was cut along its path, the tumor was carefully separated from the muscle and removed. The levator palpebrae muscle was sutured before the end of the operation. After treatment, the patient was transferred to the tumor hospital and underwent systemic chemotherapy.

OUTCOME AND FOLLOW-UP

The follow-up period was 6 mo, and no recurrence was observed during this period.

DISCUSSION

Synovial sarcoma accounts for 10%-20% of soft tissue sarcomas. It is a high-grade soft-tissue sarcoma occurring mainly in older children and young adults. Approximately 7% of soft tissue sarcoma cases occur in the head and neck region, and synovial sarcoma represents less than 0.1% of all head and neck cancers[5,6]. Orbital synovial sarcoma is a rare kind of malignancy. Therefore, diagnosis of orbital synovial sarcoma in clinical practice is challenging, and required an integrated approach that incorporates specific clinical, histological, immunohistochemical, and molecular analyses.

Synovial sarcoma is a rare kind of orbital tumor and the clinical characteristics have not been fully elucidated. Clinical manifestations include gradual painless proptosis, eyelid swelling, a palpable painless mass, epiphora, ptosis, and periorbital spontaneous pain or tenderness. However, these clinical manifestations are not unique to synovial sarcoma. Characteristic findings are not reported in current imaging studies due to the small number of cases. A case of monophasic synovial sarcoma primarily arising in the left supero-nasal orbital region was reported in a 24-year-old woman, which was clinically mistaken for a periocular cyst[6]. However, the lesion

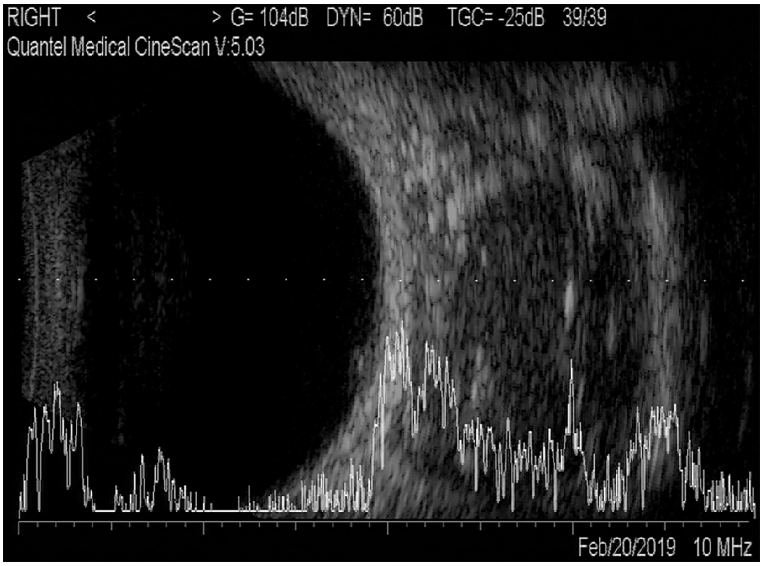

Figure 1 A/B-scan showed moderate echogenic lesions in the right eye orbital.

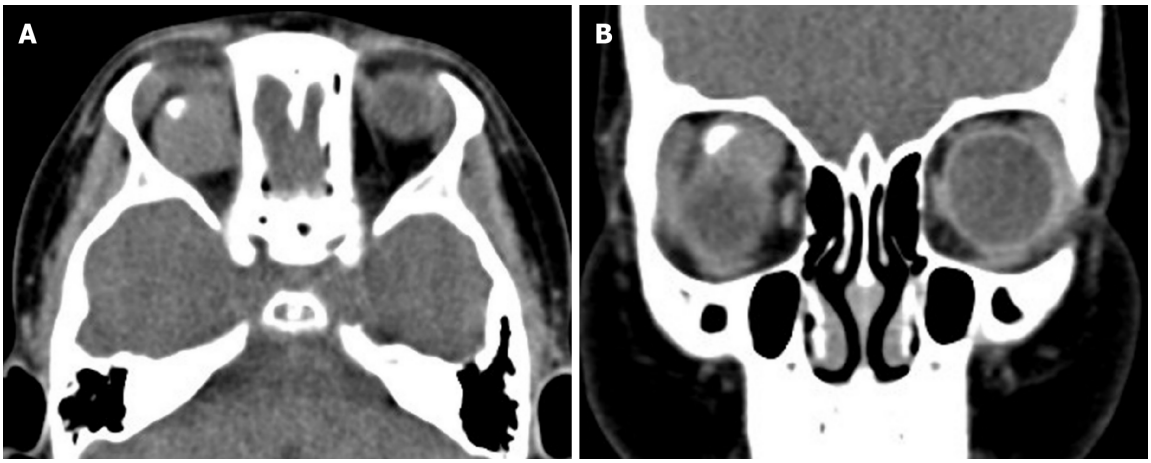

Figure 2 Orbital computed tomography scan showed a well-defined soft tissue density mass in the right orbit, with a hyperdense speck suggestive of coarse calcification. A: Axial computed tomography (CT) scans; B: Coronal CT scans.

was characterized by calcification similar to the current case.

The calcification can be pathologically divided into dystrophic calcification and metastatic calcification. In the current case, the growth of the lesion was relatively rapid, resulting in ischemia and necrosis of the tumor. Significant calcification of the lesion may be caused by dystrophic calcification. Occurrence of a lesion with calcification in orbit of a pediatric patient, orbital tumor such as vascular lesions or malformations, and orbital malignancies should be explored when carrying out diagnosis. Irregular calcification is common in malignant tumors and partially benign tumors. Cases of orbital tumors, in children are associated with higher incidence of rhabdomyosarcoma[7]. In addition, most common soft-tissue sarcoma cases in children are reported in the head and neck with 10% of all cases occurring in the orbit. Notably, a detailed history is essential if a child is suspected to have rhabdomyosarcoma[8]. A case of recurrent primary orbital calcified synovial sarcoma in a young lady was previously reported[4]. In addition, diagnosis should distinguish the primary lesion from metastatic lesion, as metastatic synovial sarcomas are characterized by poor prognosis[9]. Notably, the case reported in the current study showed no other systemic lesions, was primary tumor, and not a recurrent case.

Orbital tumor such as vascular lesions, vascular malformations, other benign lesions and orbital malignancies should be considered when there is a lesion characterized by calcification in the orbit during childhood. Irregular calcification is common in malignant tumors and partially benign lesions. In the current case, orbital computed

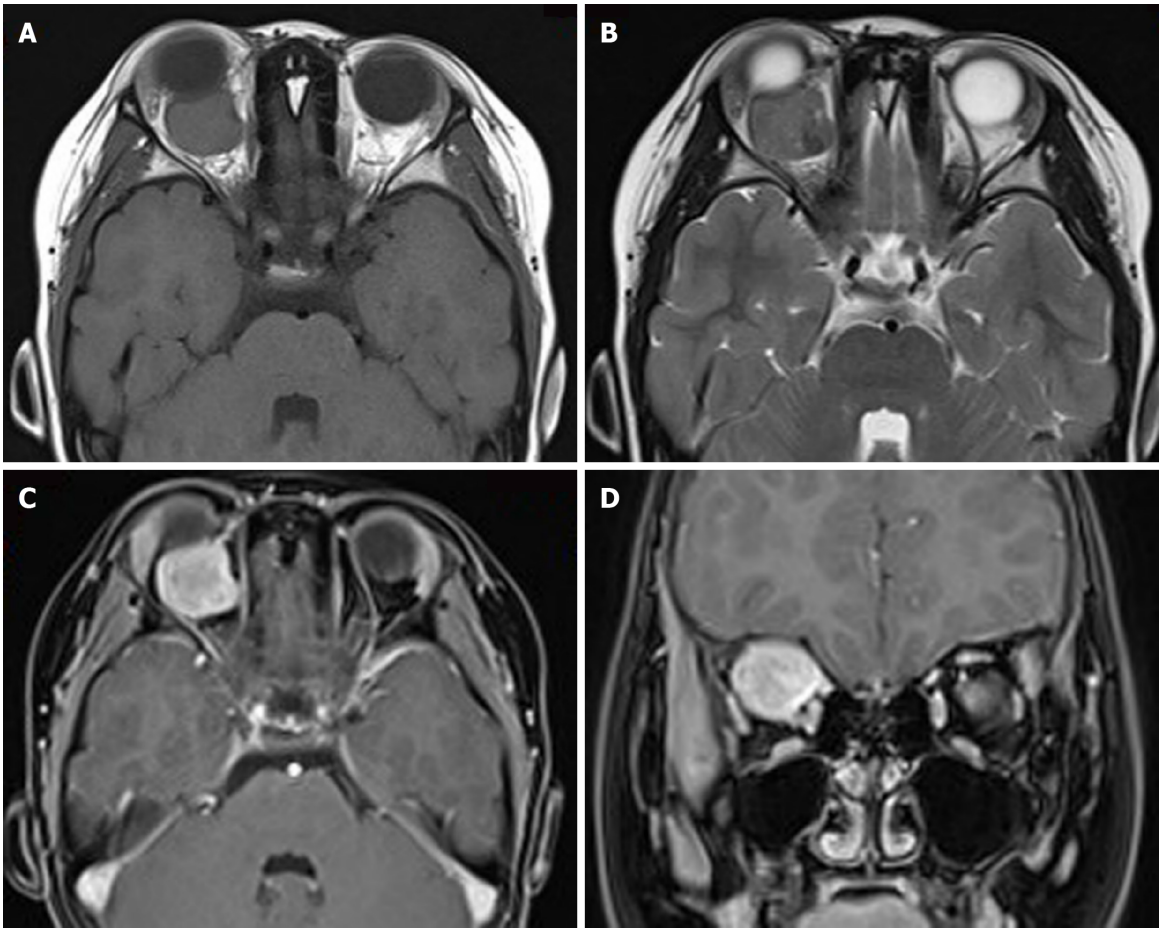

Figure 3 Orbital magnetic resonance imaging showed a circular-like mass in the right orbital. A: T1-weighted images showed moderate signals, mixed with low-signal regions; B: T2-weighted images showed mixed signals, with high number of moderately high signals, and mixed with low-signal regions; C and D: Most part of the lesion was significantly and unevenly enhanced, whereas local lesions did not exhibit any enhancement.

tomography and magnetic resonance imaging scans showed a well-defined soft tissue density mass in the right orbital. The tumor may present similar features as benign tumors. Differential diagnosis may identify findings that do not perfectly fit preliminary diagnosis of benign tumors. In such cases comprehensive consideration of clinical, radiological, and pathological findings is critically important[10].

Synovial sarcoma is a type of highly malignant soft tissue sarcoma, with poor survival of patients. Conventional treatment approach is surgical resection with adjuvant or neoadjuvant radiotherapy, which are highly effective for localized tumors. Synovial sarcoma is relatively sensitive to chemotherapy. Ifosfamide and ifosfamide combinations are effective for treatment of synovial sarcoma[5,11,12]. A combinatory treatment of doxorubicin and ifosfamide is the preferred first-line therapy for patients with metastatic cases. On the other hand, sequential doxorubicin and ifosfamide can be considered for localized tumors. Pazopanib and trabectedin are effective as second-line therapies and for subsequent treatment[11].

A previous study reported high local recurrence rates despite surgical and postoperative radiotherapy, adjuvant chemotherapy and distant metastasis rates were not reduced by these approaches[2]. The disease is characterized by early and late recurrences, and the 10-year disease-free survival is approximately 50%[5]. Several new approaches for treatment of metastatic synovial sarcoma are currently under investigation, both at preclinical and clinical levels, including receptor tyrosine kinase inhibitors, epigenetic modulators, compounds interfering with DNA damage response (DDR), and immunotherapy[11].

Histological analysis shows that synovial sarcoma is monophasic, biphasic, or poorly differentiated and exhibits a specific chromosomal translocation t (X; 18) (p11.2; q11.2) in > 95% of cases[6]. Genetic analysis shows that synovial sarcoma tumors have a characteristic fusion protein, SS18-SSX, implicated in promoting disease development. BRD9 is a component of SS18-SSX containing BAF complexes in synovial sarcoma cells. Studies report that BRD9 is implicated in oncogenic

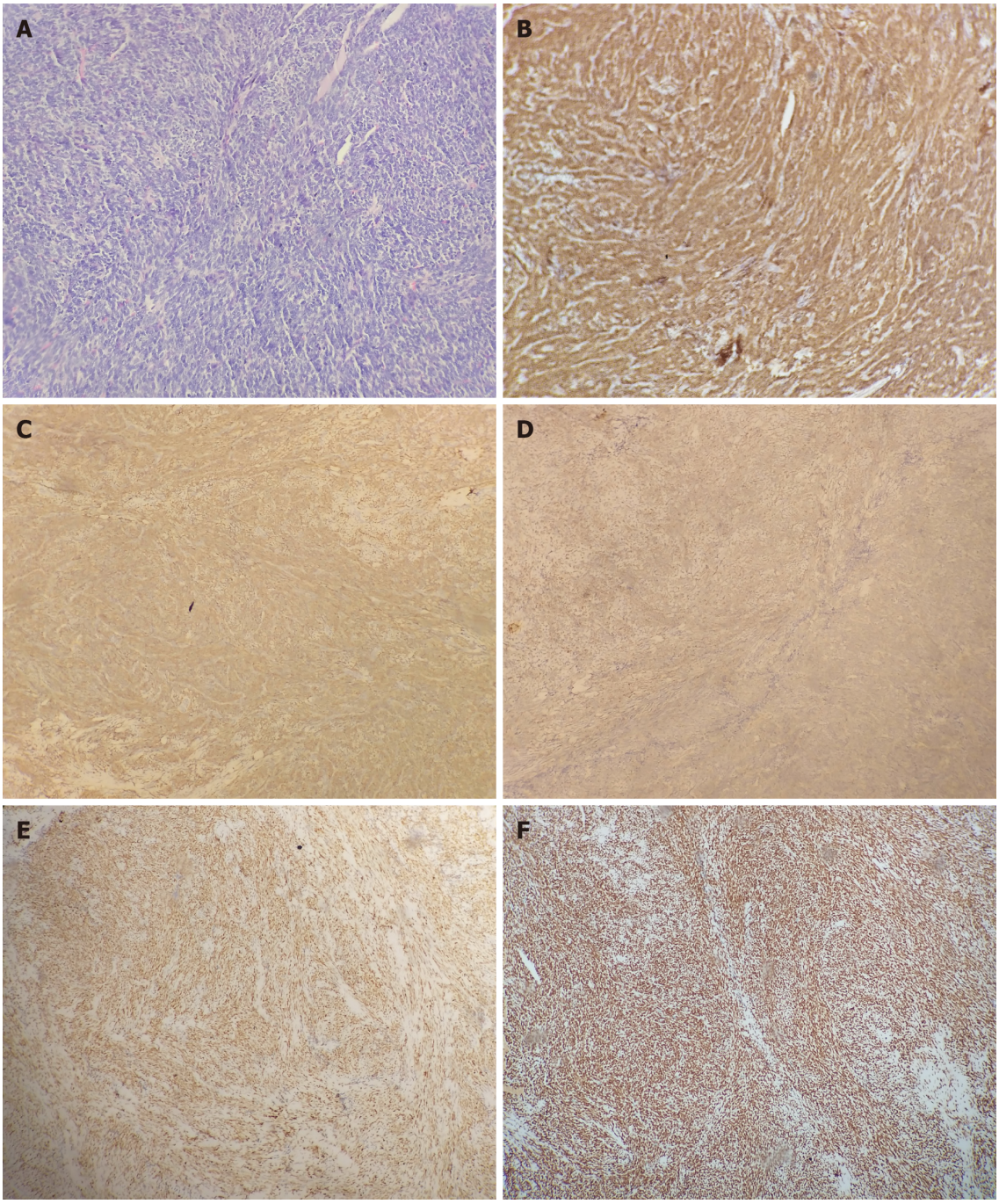

Figure 4 Histological and immunohistochemical examination. A: The tumor was confirmed as monophasic synovial sarcoma with calcification based on histological analysis (HE, × 200); B-F: Immunohistochemical study revealed positive staining for Bcl-2 (B), CD99 (C), CKpan (D), TLE1 (E), and INI-1 (F) (× 100).

mechanisms underlying the SS18-SSX fusion in synovial sarcoma and targeted degradation of BRD9 is a potential therapeutic approach for treatment of synovial sarcoma[13].

CONCLUSION

These findings show that primary orbital synovial sarcoma cases with calcification are rare, and clinical manifestations and imaging results are not specific. The tumor may exhibit similar features as a benign tumor. Therefore, these cases require comprehensive clinical, radiological, and pathological analysis to achieve the right diagnosis. The conventional treatment approach for surgical resection with adjuvant or neoadjuvant radiotherapy, which are highly effective for localized tumors. However, a longer follow-up time is required to determine effectiveness of the treatment.

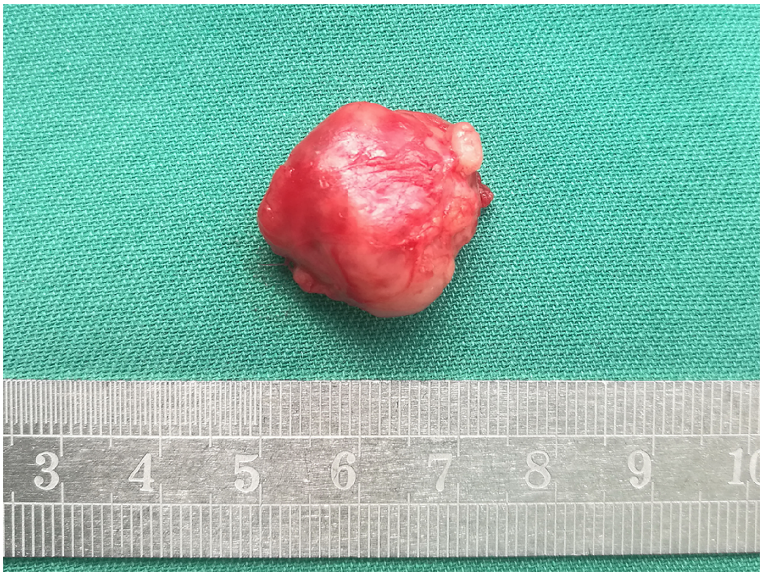

Figure 5 It presented as a well-defined, reddish, with irregularly shaped soft tissue density mass.

REFERENCES

1 **Thway K**, Fisher C. Synovial sarcoma: defining features and diagnostic evolution. *Ann Diagn Pathol* 2014; **18**: 369-380 [PMID: 25438927 DOI: 10.1016/j.anndiagpath.2014.09.002]

2 **Gervasio KA**, Ramesh S, Sivalingam MD, Markovitz M, Milman T. Primary Synovial Sarcoma of the Orbit: A Case Report and Update on Diagnostic Techniques. *Ophthalmic Plast Reconstr Surg* 2021; **37**: e155-e157 [PMID: 33587418 DOI: 10.1097/IOP.0000000000001937]

3 **Xu P**, Chen J. Primary Synovial Sarcoma of the Orbit. *Ophthalmol Eye Dis* 2017; **9**: 1179172117701732 [PMID: 28469480 DOI: 10.1177/1179172117701732]

4 **Shukla PN**, Pathy S, Sen S, Purohit A, Julka PK, Rath GK. Primary orbital calcified synovial sarcoma: a case report. *Orbit* 2003; **22**: 299-303 [PMID: 14685906 DOI: 10.1076/orbi.22.4.299.17246]

5 **Nielsen TO**, Poulin NM, Ladanyi M. Synovial sarcoma: recent discoveries as a roadmap to new avenues for therapy. *Cancer Discov* 2015; **5**: 124-134 [PMID: 25614489 DOI: 10.1158/2159-8290.CD-14-1246]

6 **Portelli F**, Pieretti G, Santoro N, Gorelli G, De Giorgi V, Massi D, Dei Tos AP, Mazzini C. Primary Orbital Synovial Sarcoma Mimicking a Periocular Cyst. *Am J Dermatopathol* 2019; **41**: 655-660 [PMID: 30624245 DOI: 10.1097/DAD.0000000000001351]

7 **Dai XZ**, Wang LY, Shan Y, Qian J, Xue K, Ye J. Clinicopathological analysis of 719 pediatric and adolescents' ocular tumors and tumor-like lesions: a retrospective study from 2000 to 2018 in China. *Int J Ophthalmol* 2020; **13**: 1961-1967 [PMID: 33344197 DOI: 10.18240/ijo.2020.12.18]

8 **Jurdy L**, Merks JH, Pieters BR, Mourits MP, Kloos RJ, Strackee SD, Saeed P. Orbital rhabdomyosarcomas: A review. *Saudi J Ophthalmol* 2013; **27**: 167-175 [PMID: 24227982 DOI: 10.1016/j.sjopt.2013.06.004]

9 **Wladis EJ**, Farber MG, Nepo AG. Metastatic synovial sarcoma to the orbit. *Ophthalmic Plast Reconstr Surg* 2012; **28**: e131-e132 [PMID: 22743696 DOI: 10.1097/IOP.0b013e3182467e11]

10 **Fujibuchi T**, Miyawaki J, Kidani T, Imai H, Kiyomatsu H, Kitazawa R, Miura H. Intraosseous synovial sarcoma of the distal ulna: a case report and review of the literature. *BMC Cancer* 2019; **19**: 116 [PMID: 30709383 DOI: 10.1186/s12885-019-5325-x]

11 **Desar IME**, Fleuren EDG, van der Graaf WTA. Systemic Treatment for Adults with Synovial Sarcoma. *Curr Treat Options Oncol* 2018; **19**: 13 [PMID: 29516254 DOI: 10.1007/s11864-018-0525-1]

12 **Ferrari A**, De Salvo GL, Brennan B, van Noesel MM, De Paoli A, Casanova M, Francotte N, Kelsey A, Alaggio R, Oberlin O, Carli M, Ben-Arush M, Bergeron C, Merks JH, Jenney M, Stevens MC, Bisogno G, Orbach D. Synovial sarcoma in children and adolescents: the European Pediatric Soft Tissue Sarcoma Study Group prospective trial (EpSSG NRSTS 2005). *Ann Oncol* 2015; **26**: 567-572 [PMID: 25488687 DOI: 10.1093/annonc/mdu562]

13 **Brien GL**, Remillard D, Shi J, Hemming ML, Chabon J, Wynne K, Dillon ET, Cagney G, Van Mierlo G, Baltissen MP, Vermeulen M, Qi J, Fröhling S, Gray NS, Bradner JE, Vakoc CR, Armstrong SA. Targeted degradation of BRD9 reverses oncogenic gene expression in synovial sarcoma. *Elife* 2018; **7** [PMID: 30431433 DOI: 10.7554/eLife.41305]

World Journal of Clinical Cases

Submit a Manuscript: https://www.f6publishing.com

World J Clin Cases 2022 February 16; 10(5): 1630-1638

DOI: 10.12998/wjcc.v10.i5.1630

ISSN 2307-8960 (online)

CASE REPORT

Small-cell carcinoma of the prostate with negative CD56, NSE, Syn, and CgA indicators: A case report

Hong-Jin Shi, Zhi-Nan Fan, Jin-Song Zhang, Bo-Bo Xiong, Hai-Feng Wang, Jian-Song Wang

ORCID number: Hong-Jin Shi 0000-0001-9883-270X; Zhi-Nan Fan 0000-0003-4547-4202; Jin-Song Zhang 0000-0003-3271-3454; Bo-Bo Xiong 0000-0001-6121-9565; Hai-Feng Wang 0000-0003-0360-1402; Jian-Song Wang 0000-0002-2140-1618.

Author contributions: Shi HJ and Fan ZN collected the data, reviewed the literature, and contributed to manuscript drafting; Xiong BB performed the histological analyses and interpretation; Zhang JS and Wang HF was responsible for the revision of the manuscript for important intellectual content; all authors issued final approval for the version to be submitted.

Informed consent statement: Informed written consent was obtained from the patient for publication of this report and any accompanying images.

Conflict-of-interest statement: The authors declare that they have no conflict of interest.

CARE Checklist (2016) statement: The authors have read the CARE Checklist (2016), and the manuscript was prepared and revised according to the CARE Checklist (2016).

Supported by the National Natural Science Foundation of China, No.

Hong-Jin Shi, Zhi-Nan Fan, Jin-Song Zhang, Bo-Bo Xiong, Hai-Feng Wang, Jian-Song Wang, Department of Urology, The Second Affiliated Hospital, Kunming Medical University, Kunming 650000, Yunnan Province, China

Corresponding author: Jin-Song Zhang, Doctor, Doctor, Department of Urology, The Second Affiliated Hospital, Kunming Medical University, No. 374 Dianmian Road, Kunming 650000, Yunnan Province, China. 945933392zjs@sina.com

Abstract

BACKGROUND

Small-cell carcinoma of the prostate (SCCP) is a clinically rare malignant tumor, accounting for < 1% of all prostate tumors. However, negativity for all SCCP neuroendocrine markers is rare. Herein, we report a case of SCCP with completely negative neuroendocrine markers and explore its clinicopathologic features, thus improving the understanding of its clinical diagnosis and management.

CASE SUMMARY

We report the case of a 48-year-old patient with SCCP negative for common sensitive neuroendocrine-staining indicators. Dysuria was the first symptom, and rectal examination revealed a hard prostate, palpable nodules, diffuse prostate enlargement, no pressure pain, no blood staining in the finger sleeve, 1.33 ng/mL total prostate-specific antigen level, and a free-to-total prostate-specific antigen ratio of 0.21 ng/mL. Ultrasound suggested a prostate size of 5.3 cm × 5.8 cm × 5.6 cm, and magnetic resonance imaging suggested prostate cancer. The lower posterior bladder wall, rectal mesentery, and bilateral seminal vesicles were invaded, with multiple lymph node metastases in the pelvis. A whole-body bone scan suggested an abnormally active multiple bone metabolism and possible bone metastases. Head and lungs computed tomography revealed no significant nodal shadow. Following a pathological diagnosis of SCCP after a prostate puncture, with negative indicators of common sensitive neuroendocrine staining, chemotherapy was administered; the patient died 4-5 mo after SCCP diagnosis.

CONCLUSION

SCCP is a rare disease characterized by atypical clinical symptoms, limited treatment options, a short survival period, and a poor prognosis.

Key Words: Prostate cancer; Small cell carcinoma; Neuroendocrine tumor; Therapeutics; Diagnosis; Case report

81972395, and No. 82060464.

Country/Territory of origin: China

Specialty type: Urology and nephrology

Provenance and peer review: Unsolicited article; Externally peer reviewed.

Peer-review model: Single blind

Peer-review report's scientific quality classification
Grade A (Excellent): 0
Grade B (Very good): B
Grade C (Good): C
Grade D (Fair): 0
Grade E (Poor): 0

Received: August 1, 2021
Peer-review started: August 1, 2021
First decision: November 7, 2021
Revised: November 14, 2021
Accepted: December 31, 2021
Article in press: December 31, 2021
Published online: February 16, 2022

P-Reviewer: Dadgar H
S-Editor: Liu JH
L-Editor: A
P-Editor: Liu JH

Core Tip: Small cell carcinoma of the prostate (SCCP) is a very rare type of prostate tumor, generally characterized by low differentiation, high malignancy, rapid growth, easy diffusion, and poor prognosis. Among SCCP types, mixed SCCP is relatively common, completely simple SCCP is rarely reported, and SCCP with negative neuroendocrine markers is even rarer. This study reports a rare case of SCCP with completely negative neuroendocrine markers, and it found SCCP to be characterized by atypical clinical symptoms, limited treatment options, a short survival period, and a poor prognosis, requiring pathological examination to confirm its diagnosis.

Citation: Shi HJ, Fan ZN, Zhang JS, Xiong BB, Wang HF, Wang JS. Small-cell carcinoma of the prostate with negative CD56, NSE, Syn, and CgA indicators: A case report. *World J Clin Cases* 2022; 10(5): 1630-1638
URL: https://www.wjgnet.com/2307-8960/full/v10/i5/1630.htm
DOI: https://dx.doi.org/10.12998/wjcc.v10.i5.1630

INTRODUCTION

Small-cell carcinoma of the prostate (SCCP) is one of the rarest types of prostate tumors. It is generally characterized by low differentiation, high malignancy, rapid growth, easy spread, and poor prognosis[1]. It has been reported on a case-by-case basis in both domestic and international literature, with more cases of mixed SCCP than those of completely simple SCCP being reported[2]. SCCP is generally characterized by neuroendocrine granules in the cytoplasm, and immunohistochemistry suggests at least one positive neuroendocrine marker, predominantly in small-cell neuroendocrine carcinoma of the prostate[3], whereas SCCP negativity for almost all neuroendocrine markers is even rarer. SCCP diagnosis and treatment have not yet been standardized internationally and are still being explored. Herein, we report the treatment of a patient with SCCP who was negative for almost all neuroendocrine markers. By reviewing the relevant literature from recent years, we analyzed and summarized SCCP diagnosis and treatment, aiming to deepen the understanding of this disease.

CASE PRESENTATION

Chief complaints

A 48-year-old man was admitted to our hospital on January 7, 2019, due to dysuria that lasted for 10 d.

History of present illness

A 48-year-old man was admitted to our hospital on January 7, 2019, due to dysuria that lasted for 10 d. No gross hematuria or acute urinary retention, and no treatment in other hospitals.

History of past illness

The patient had no history of surgery, trauma, or other diseases.

Personal and family history

There was no history of hereditary diseases. No family members had similar symptoms.

Physical examination

On rectal examination, the prostate was hard and diffusely enlarged, the nodules were palpable, no pressure pain was experienced, and the finger sleeve was not stained with blood.

Laboratory examinations

Laboratory tests revealed that the total prostate-specific antigen level and free-to-total prostate-specific antigen ratio were 1.33 ng/mL (reference range: 0-4 ng/mL) and 0.21 ng/mL (reference range: 0-0.944 ng/mL), respectively. Liver and kidney function was normal. Serum tumor markers were in the normal range.

Imaging examinations

B-mode ultrasound revealed a prostate size of 5.3 cm × 5.8 cm × 5.6 cm, echogenicity in the prostate was heterogeneous, and the envelope was not smooth.

Computed tomography (CT) imaging of the abdomen exhibited heterogeneous density within the prostate and heterogeneous enhancement after enhancement, suggesting possible prostate cancer, possible pelvic lymph node metastasis, pelvic floor fascia, and rectal wall and seminal vesicle invasion (Figure 1A).

Prostate magnetic resonance imaging confirmed mixed signals in the prostate, with possible prostate tumor invasion of the lower posterior bladder wall, rectal mesentery and bilateral seminal vesicles, and multiple lymph node metastases in the pelvis (Figure 1B-D).

Whole-body bone scan revealed multiple abnormalities in bone metabolism, with possible bone metastases (Figure 2), and CT of the head and lung suggested no obvious nodal shadow.

We strongly recommend that the patient use ^{68}Ga-PSMA PET/CT to look for small lesions around the prostate bed or extra-prostatic lymph node metastases. However, the patient and his family declined our offer due to the high cost.

Further diagnostic work-up

The patient was advised to initially undergo prostate puncture biopsy. The tumor cells appeared oval to spindle-shaped, with obvious heterogeneity and a mixture of oval and spindle-shaped cells (Figure 3). The immunophenotypes were as follows: CKPAN (foci +), KI67 (60%), AR (-), PSA (-), PSAP (-), P504S (-), CK5/6 (-), CKH (-), GATA3 (-), Vimentin (-), CEA (-), CK7 (-), CK20 (-), villin (-), NSE (-), Syn (-), CD56 (-), CgA (-), P40 (-), P63 (-), LCA (-), CD38 (-), CD138 (-), EMA (-), MUM1 (-), CD30 (-), Desmin (-), HMB45 (-), Melan-A (-), S100 (-), and MyoD1 (-) (Figure 4A and B). Hence, the initial diagnosis was small cell malignancy.

FINAL DIAGNOSIS

On combining the initial diagnosis with immunohistochemical markers, undifferentiated carcinoma was considered. On further combining with the adjuvant examination and clinical manifestations, the patient was finally diagnosed with advanced SCCP.

TREATMENT

The current treatment modality recommended radiotherapy; however, the patient and family declined radiotherapy and finally selected the etoposide combined with cisplatin (EP) chemotherapy regimen as follows: Cisplatin 80 mg on day 1 of chemotherapy as well as etoposide 100 mg on days 1-3 and 21-28 for one cycle, in a course of 6 cycles.

OUTCOME AND FOLLOW-UP

A repeat of CT imaging of the lung on February 14, 2019, revealed the following: Multiple nodal shadows, suggesting possible SCCP metastasis (Figure 5A and B). Further CT imaging of the abdomen on March 17, 2019, suggested an irregular enlargement of SCCP, exhibiting a tendency to infiltrate, bilateral involvement of the inner segment of the ureteral bladder wall, dilatation and fluid retention in the urinary tract, multiple bone destruction in the pelvis (Figure 5C and D), and creatinine increase to 301 μmol/L, and the patient was treated with bilateral nephrostomy.

As the patient developed insensitivity to the EP regimen, EP was replaced with the gemcitabine combined with oxaliplatin (GEMOX) regimen, which was administered as

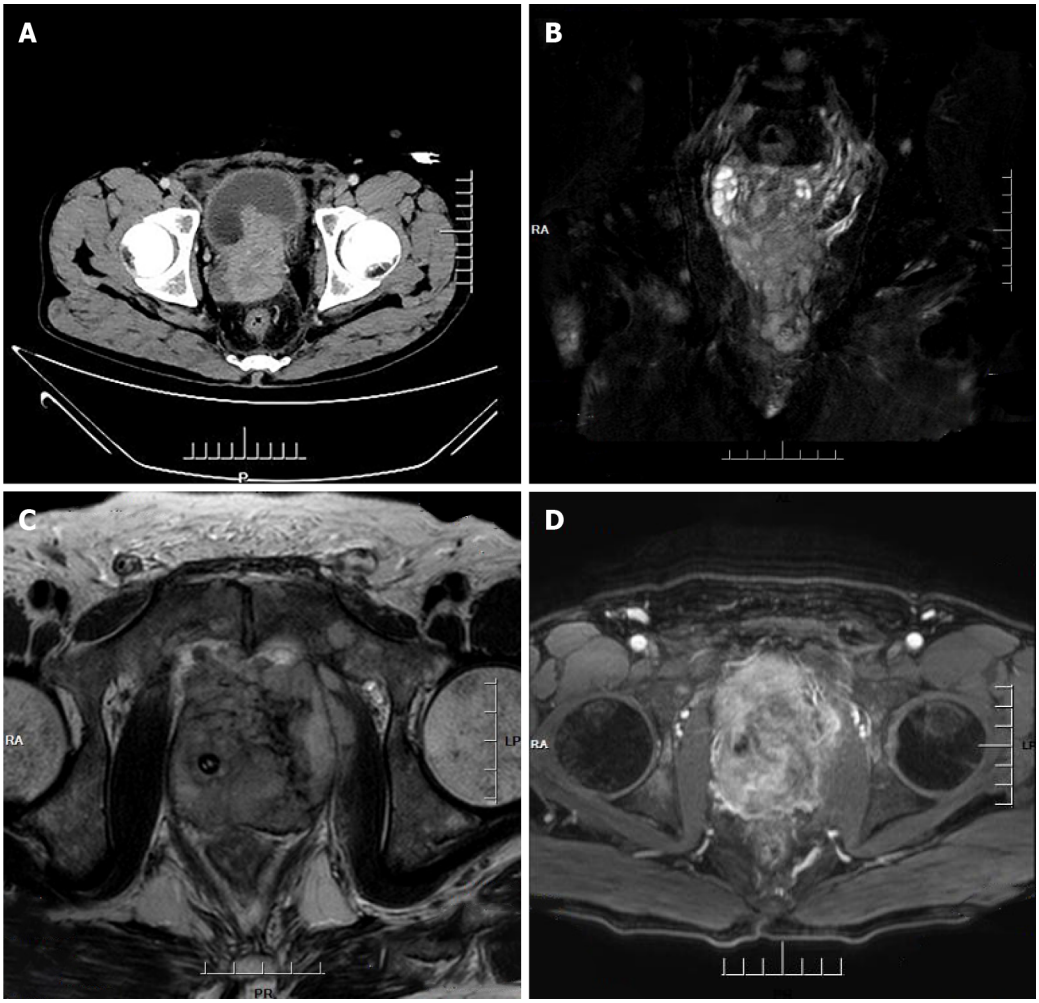

Figure 1 Computed tomography imaging and magnetic resonance imagining. A: Computed tomography imaging of the abdomen: Heterogeneous density within the prostate and heterogeneous enhancement after enhancement, suggesting possible prostate cancer, possible pelvic lymph node metastasis, pelvic floor fascia, and rectal wall and seminal vesicle invasion; B-D: Prostate magnetic resonance imagining: Mixed signals in the prostate, with possible prostate tumor invasion of the lower posterior bladder wall, rectal mesentery, and bilateral seminal vesicles, with multiple lymph node metastases in the pelvis.

follows: Gemcitabine 1 g on day 1 of chemotherapy as well as oxaliplatin 60 mg on days 1-5 and 21-28 in a course of 6 cycles. On April 25, 2019, the patient was admitted to the hospital for further chemotherapy, with routine blood work suggesting normal hemoglobin and central granulocytes, normal platelets, hemoglobin level of 48 g/L, and creatinine concentration of 156 μmol/L. After a blood transfusion, hemoglobin concentration rose to 110 g/L. The patient's general condition was extremely poor (dyspnea, intolerable bone pain, and extreme wasting), and they could not tolerate further chemotherapy. The family decided to abandon the treatment, and the patient died of respiratory failure on May 20, 2019.

DISCUSSION

The lung is the most common site of small-cell carcinoma, and its most common site outside the lung is the prostate, accounting for approximately 3% of cases[4]. SCCP is a rare malignancy in clinical practice, accounting for less than 1% of all prostate tumors [4]. Despite having a low incidence, SCCP exhibits high malignancy and poor prognosis[5], and often metastasizes to tissues and organs, such as the brain, lung, liver, and bone *via* blood circulation[6]. At present, three hypotheses regarding the origin of SCCP exist: (1) The abnormal differentiation of prostatic adenocarcinoma into small-cell carcinoma after endocrine therapy[7]; (2) Derivation of the different types of adenocarcinoma and small-cell carcinoma of prostatic epithelium from pluripotent stem cells; and (3) Neuroendocrine cells in the prostatic epithelium. Prostatic neuroendocrine carcinoma includes prostate cancer with neuroendocrine differentiation,

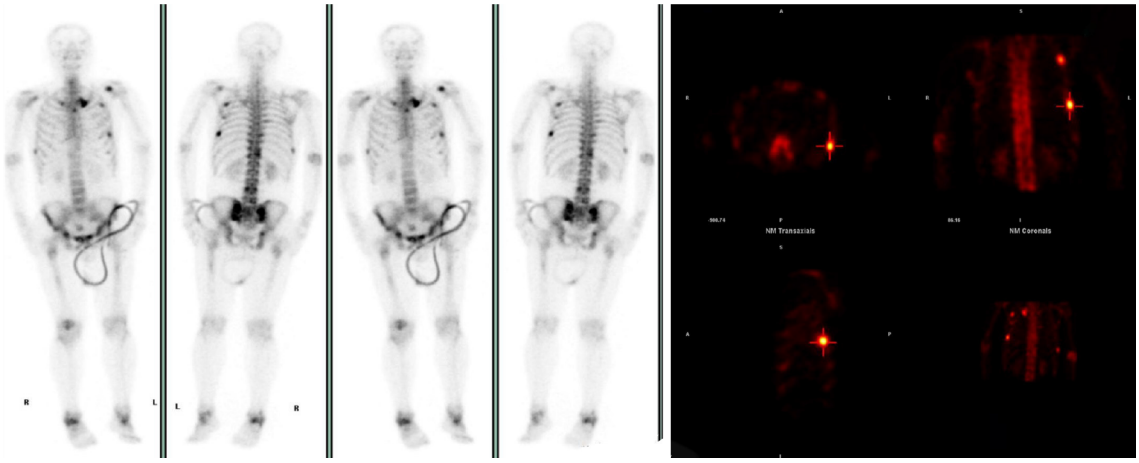

Figure 2 Whole-body bone scan: Abnormally active bone metabolism in the left sternoclavicular joint, multiple ribs, T12, L4, L5 vertebrae, and right acetabulum.

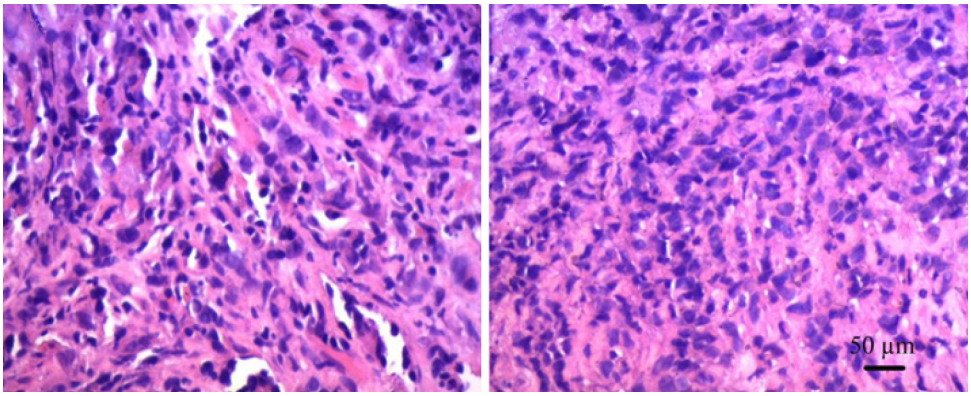

Figure 3 HE × 200 ×; tumor cells arranged in strips and sheets; tumor cells appear oval or spindle-shaped.

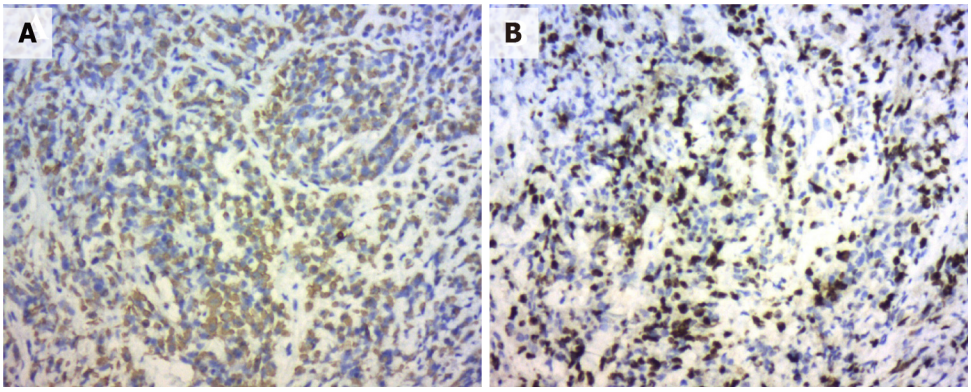

Figure 4 Immunohistochemical. A: SP method immunohistochemical staining for CK broadly focally positive; B: SP method immunohistochemical staining for Ki67 (50%+).

prostate carcinoid, prostatic small-cell neuroendocrine carcinoma, and prostatic large-cell neuroendocrine carcinoma, among others[1]. The above hypotheses have a certain degree of validity, and additional molecular genetic studies have identified multiple mechanisms involved in the pathogenesis of SCCP[8], including *TMPRSS2-ERG* gene rearrangement; *RB1* gene deletion; *MYCN* and *AURK4* gene overexpression and amplification; *Akt*, *β-catenin*, and *P13k* gene inactivation; P53 signaling pathway inactivation; upregulation of the *EZH2* gene; and down-regulation of *DUSP1* expression, among others[9,10].

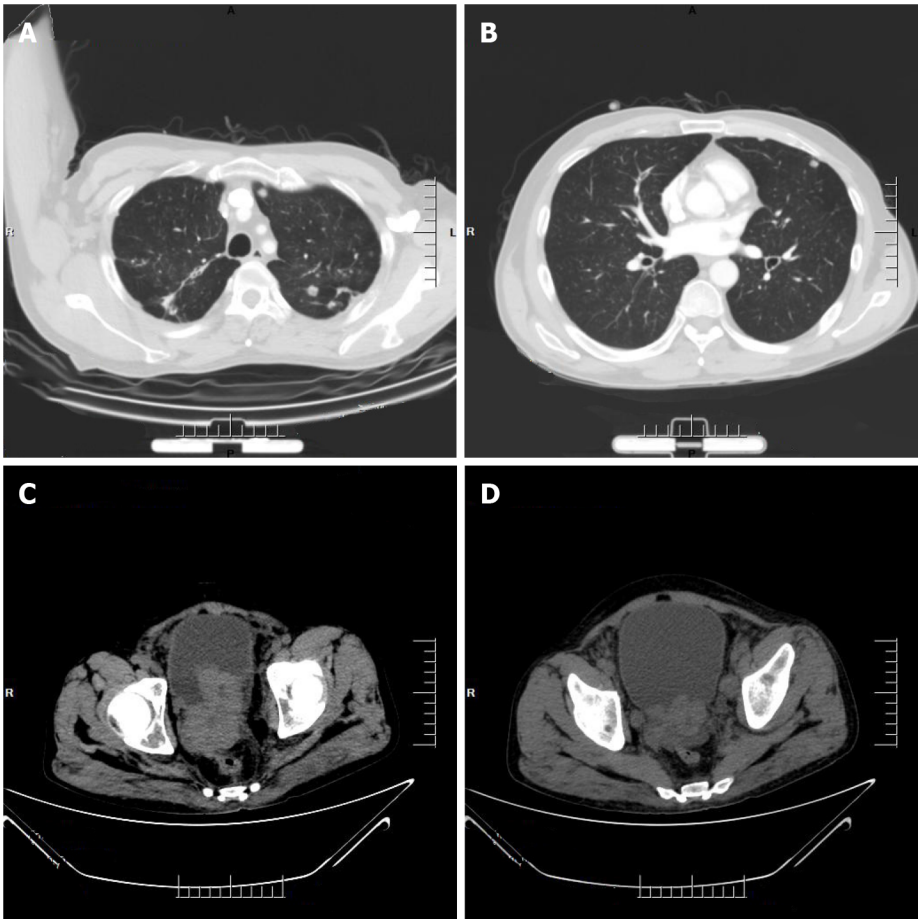

Figure 5 Computed tomography. A and B: Computed tomography (CT) imaging of the lung: Multiple nodular shadows in both lungs, with possible Small-cell carcinoma of the prostate metastases; C and D: CT imaging of the abdomen: An irregular enlargement of Small-cell carcinoma of the prostate showing a tendency to infiltrate, bilateral involvement of the inner segment of the ureteral bladder wall, dilatation and fluid retention in the urinary tract, and multiple bone destruction in the pelvis.

The early stage of SCCP is typical without specific clinical symptoms. As the tumor progresses, it may invade the bladder and rectum, potentially causing difficult urination, hematuria, and perineal discomfort. In addition, signs of metastases may appear, involving the brain, lung, bone, and lymph nodes[11]. Very few patients produce ectopic endocrine hormones and exhibit paraneoplastic syndrome[2], including Cushing's syndrome, neurological symptoms, and hypercalcemia, among others[12]. In this case, the patient was 48 years old and predominantly exhibited lower urinary tract obstruction symptoms; therefore, it is necessary to maintain a suspicious mindset and perform a rectal examination in middle-aged men with combined lower urinary tract obstruction symptoms.

SCCP diagnosis relies mainly on pathological examination. Microscopically, cells are observed as small round shapes, arranged in sheets or nests, with little cytoplasm, and the nucleoli are unclear with visible nuclear fission[13]. Immunohistochemistry is the main method of confirming SCCP diagnosis, and the typical sensitive neuroendocrine staining markers are NSE, Syn, CD56, and CgA[14], in addition to TTF-1, insulinoma-associated protein 1 (INSM1)[14], and FOXA2[15], among others. SCCP is a type of prostate neuroendocrine tumor that can be diagnosed provided one or more of the following indicators are positive: NSE, Syn, CD56, CgA, TTF-1, INSM1, and FOXA2. AR, PSA, PSAP, P504S, and other classical immune indicators of prostate adenocarcinoma are also widely expressed in poorly differentiated adenocarcinoma, whereas in SCCP, they are almost not expressed; therefore, they can be used to distinguish SCCP from poorly differentiated adenocarcinoma[16]. The patient described in this paper exhibited negative NSE, Syn, CD56, CgA, AR, PSA, PSAP, and P504S indexes, and due to equipment limitations in the hospital pathology department, TTF-1, INSM1, and FOXA2 immune indexes were not assessed, rendering the final diagnosis rather limited. While the final diagnosis was SCCP (undifferentiated carcinoma), the author still considered neuroendocrine small-cell carcinoma based on current relevant tests and related examinations. Overall, the probability that

the most sensitive immune indicators, such as NSE, Syn, CD56, and CgA, would be simultaneously negative in prostate neuroendocrine small-cell carcinoma was considerably low.

Currently, there is no unified standard treatment for SCCP. Clinically, the treatment plan of lung small-cell carcinoma is generally referred to, which is mainly combined with chemotherapy, supplemented by surgery and radiotherapy[3]. Surgery is suitable for early-stage SCCP without metastasis or local progression. Relevant studies have concluded that for early-stage or locally progressive SCCP, early surgery and postoperative combined chemotherapy can effectively improve patient survival or even cure[17]. However, SCCP progresses rapidly, and most patients are at an advanced stage, losing the opportunity for surgery, and palliative surgery potentially improves patients' quality of life. Chemotherapy is based on the EP regimen, with an efficiency of up to 61.0%[18]. If ineffective, other regimens can alternatively be used. In this case, the patient was not sensitive to the EP regimen; thus, it was subsequently replaced with the GEMOX regimen, which was unsatisfactory. Hence, the chemotherapy regimen for SCCP is still currently being explored. Radiotherapy combined with chemotherapy may improve the patient's prognosis. Radiotherapy alone is ineffective and is generally used in patients with bone metastases to control pain symptoms caused by these metastases[19]. In this case, the patient declined radiotherapy, and the patient and family accepted chemotherapy in consideration of the toxic reactions in the urinary tract and rectum caused by radiotherapy.

The application of ^{68}Ga-PSMA PET/CT in the whole diagnosis of prostate cancer has developed rapidly, which plays a vital role in assisting clinical tumor staging. It can accurately detect local lesions, lymph node metastasis, and distant metastasis in prostate cancer, with high sensitivity and specificity. It can be found that the advantage is especially significant at a low PSA value (< 0.5 ng/mL)[20]. The patient described in this article refuses to undergo ^{68}Ga-PSMA PET/CT examination, when the patient's CT scan finds the lesions in the lung as a metastatic site, but we do not know about the function of the lesion. Parghane and Basu[21] used Dual-tracer (^{68}Ga-PSMA and ^{18}F-FDG) PET/CT in the case of metastatic SCCP, Interestingly, whereas metastatic SCCP transformed pelvic and penile lesions were nonavid with ^{68}Ga-PSMA but avid with ^{18}F-FDG. Therefore, the role of new tracer ^{18}F-FDG in metastatic SCCP should not be underestimated. The bone and pelvic lesions demonstrated a favorable response to a multimodal therapeutic approach (^{177}Lu-PSMA radioligand therapy and radiotherapy), a trend toward a decrease in PSA level[21]. ^{177}Lu-PSMA radioligand therapy shows promising prospects for metastatic SCCP patients who progress after conventional therapy. For patients with metastatic SCCP patients that progress after chemotherapy, ^{177}Lu-PSMA radioligand therapy is expected to change the status quo of patients with short survival and poor quality of life[22]. ^{68}GA-PSMA PET/CT is used to screen patients suitable for ^{177}Lu-PSMA radioligand therapy, and then ^{177}Lu-PSMA radioligand therapy for the suitable patients for targeted therapy, can intuitively and visually dynamic evaluation of efficacy. Tumor staging is carried out to realize the integration of diagnosis and treatment, which embodies the precision and personalized diagnosis and treatment concept of nuclear medicine. Despite urgent clinical needs, ^{177}Lu-PSMA radioligand therapy for metastatic SCCP has yet to be approved by FDA and the European Medicines Agency. However, with the accumulation of global research data, it is expected to become an extension and complement to the clinical routine treatment of metastatic SCCP.

In recent years, targeted therapies have emerged through continued research into the molecular mechanisms of SCCP. AURKA plays an important role in the treatment development of SCCP, and AURKA inhibitors (danusertib, CD532, and MLN8237) improve patient outcomes[6]. Fifty percent of SCCP samples have been found to have fusion rearrangements of *TMPRSS2-ERG*. PARP1 inhibitor (olaparib) potentially improves the sensitivity of tumor cells to radiotherapy, thus improving the effect of chemoradiotherapy on SCCP[23]. Researchers have continued to explore the molecular mechanisms of SCCP to establish a pathway for precision therapy.

The current patient was 48 years old and was admitted to the hospital with symptoms of dysuria. On combining the initial diagnosis with the medical history and relevant investigations, the patient was considered to have advanced primary SCCP, with negative CD56, NSE, Syn, and CgA indicators, which is a rare phenomenon. The treatment strategy was to consider the patient's young age and use preoperative chemotherapy, await tumor shrinkage before surgery, and subsequently combine radiotherapy after surgery to improve the patient's survival; however, the patient's preoperative chemotherapy was not effective and failed to control tumor progression. A few studies have investigated SCCP with negative CD56, NSE, Syn, and CgA indicators, and whether it is insensitive to EP chemotherapy and effective with

targeted therapy warrants full elucidation.

CONCLUSION

In summary, SCCP is a rare malignant tumor, and SCCP with negative CD56, NSE, Syn, and CgA indexes is even rarer, with no specific symptoms in the early stage. Further, it is often detected in its advanced stage, with diagnosis relying on pathological examination. An in-depth study of the molecular mechanism of SCCP may provide a new basis for the diagnosis and treatment of SCCP.

REFERENCES

1 **Nadal R**, Schweizer M, Kryvenko ON, Epstein JI, Eisenberger MA. Small cell carcinoma of the prostate. *Nat Rev Urol* 2014; **11**: 213-219 [PMID: 24535589 DOI: 10.1038/nrurol.2014.21]

2 **Rueda-Camino JA**, Losada-Vila B, De Ancos-Aracil CL, Rodríguez-Lajusticia L, Tardío JC, Zapatero-Gaviria A. Small cell carcinoma of the prostate presenting with Cushing Syndrome. A narrative review of an uncommon condition. *Ann Med* 2016; **48**: 293-299 [PMID: 27068390 DOI: 10.3109/07853890.2016.1168936]

3 **Puca L**, Vlachostergios PJ, Beltran H. Neuroendocrine Differentiation in Prostate Cancer: Emerging Biology, Models, and Therapies. *Cold Spring Harb Perspect Med* 2019; **9** [PMID: 29844220 DOI: 10.1101/cshperspect.a030593]

4 **Hingorani R**, Young J, Alweis R. Mixed adenocarcinoma and neuroendocrine prostate cancer: a case report. *J Community Hosp Intern Med Perspect* 2014; **4**: 25176 [PMID: 25432647 DOI: 10.3402/jchimp.v4.25176]

5 **Lopez-Barcons LA**. Small-cell neuroendocrine carcinoma of the prostate: are heterotransplants a better experimental model? *Asian J Androl* 2010; **12**: 308-314 [PMID: 20023690 DOI: 10.1038/aja.2009.68]

6 **Monn MF**, Cheng L. Emerging trends in the evaluation and management of small cell prostate cancer: a clinical and molecular perspective. *Expert Rev Anticancer Ther* 2016; **16**: 1029-1037 [PMID: 27534689 DOI: 10.1080/14737140.2016.1226137]

7 **Lotan TL**, Gupta NS, Wang W, Toubaji A, Haffner MC, Chaux A, Hicks JL, Meeker AK, Bieberich CJ, De Marzo AM, Epstein JI, Netto GJ. ERG gene rearrangements are common in prostatic small cell carcinomas. *Mod Pathol* 2011; **24**: 820-828 [PMID: 21336263 DOI: 10.1038/modpathol.2011.7]

8 **Carneiro BA**, Pamarthy S, Shah AN, Sagar V, Unno K, Han H, Yang XJ, Costa RB, Nagy RJ, Lanman RB, Kuzel TM, Ross JS, Gay L, Elvin JA, Ali SM, Cristofanilli M, Chae YK, Giles FJ, Abdulkadir SA. Anaplastic Lymphoma Kinase Mutation (*ALK* F1174C) in Small Cell Carcinoma of the Prostate and Molecular Response to Alectinib. *Clin Cancer Res* 2018; **24**: 2732-2739 [PMID: 29559559 DOI: 10.1158/1078-0432.CCR-18-0332]

9 **Kumar K**, Ahmed R, Chukwunonso C, Tariq H, Niazi M, Makker J, Ihimoyan A. Poorly Differentiated Small-Cell-Type Neuroendocrine Carcinoma of the Prostate: A Case Report and Literature Review. *Case Rep Oncol* 2018; **11**: 676-681 [PMID: 30483097 DOI: 10.1159/000493255]

10 **Zhang Y**, Zhang Y, Chen M, Liu C, Xiang C. DUSP1 is involved in the progression of small cell carcinoma of the prostate. *Saudi J Biol Sci* 2018; **25**: 858-862 [PMID: 30108432 DOI: 10.1016/j.sjbs.2017.09.015]

11 **Priemer DS**, Montironi R, Wang L, Williamson SR, Lopez-Beltran A, Cheng L. Neuroendocrine Tumors of the Prostate: Emerging Insights from Molecular Data and Updates to the 2016 World Health Organization Classification. *Endocr Pathol* 2016; **27**: 123-135 [PMID: 26885643 DOI: 10.1007/s12022-016-9421-z]

12 **Elston MS**, Crawford VB, Swarbrick M, Dray MS, Head M, Conaglen JV. Severe Cushing's syndrome due to small cell prostate carcinoma: a case and review of literature. *Endocr Connect* 2017; **6**: R80-R86 [PMID: 28584167 DOI: 10.1530/EC-17-0081]

13 **Weprin S**, Yonover P. Small Cell Carcinoma of the Prostate: A Case Report and Brief Review of the Literature. *Urol Case Rep* 2017; **13**: 61-62 [PMID: 28462157 DOI: 10.1016/j.eucr.2016.10.010]

14 **Xin Z**, Zhang Y, Jiang Z, Zhao L, Fan L, Wang Y, Xie S, Shangguan X, Zhu Y, Pan J, Liu Q, Huang Y, Dong B, Xue W. Insulinoma-associated protein 1 is a novel sensitive and specific marker for small cell carcinoma of the prostate. *Hum Pathol* 2018; **79**: 151-159 [PMID: 29885405 DOI: 10.1016/j.humpath.2018.05.014]

15 **Park JW**, Lee JK, Witte ON, Huang J. FOXA2 is a sensitive and specific marker for small cell neuroendocrine carcinoma of the prostate. *Mod Pathol* 2017; **30**: 1262-1272 [PMID: 28621319 DOI: 10.1038/modpathol.2017.44]

16 **Wang W**, Epstein JI. Small cell carcinoma of the prostate. A morphologic and immunohistochemical study of 95 cases. *Am J Surg Pathol* 2008; **32**: 65-71 [PMID: 18162772 DOI: 10.1097/PAS.0b013e318058a96b]

17 **Guo A**, Wen S, Ma Y, Wei L, Liu A. Clinicopathological analysis on small cell carcinoma of the prostate in chinese patients. *J Cancer* 2014; **5**: 797-803 [PMID: 25520757 DOI: 10.7150/jca.9388]

18 **Papandreou CN**, Daliani DD, Thall PF, Tu SM, Wang X, Reyes A, Troncoso P, Logothetis CJ. Results of a phase II study with doxorubicin, etoposide, and cisplatin in patients with fully characterized small-cell carcinoma of the prostate. *J Clin Oncol* 2002; **20**: 3072-3080 [PMID: 12118020 DOI: 10.1200/JCO.2002.12.065]

19 **Palmgren JS**, Karavadia SS, Wakefield MR. Unusual and underappreciated: small cell carcinoma of the prostate. *Semin Oncol* 2007; **34**: 22-29 [PMID: 17270662 DOI: 10.1053/j.seminoncol.2006.10.026]

20 **Treglia G**, Pereira Mestre R, Ferrari M, Bosetti DG, Pascale M, Oikonomou E, De Dosso S, Jermini F, Prior JO, Roggero E, Giovanella L. Radiolabelled choline versus PSMA PET/CT in prostate cancer restaging: a meta-analysis. *Am J Nucl Med Mol Imaging* 2019; **9**: 127-139 [PMID: 31139496]

21 **Parghane R**, Basu S. Small Cell Transformation of Metastatic Prostate Adenocarcinoma Diagnosed by Dual-Tracer PET/CT (^{68}Ga-PSMA and ^{18}F-FDG): Potential Clinical Utility in Therapeutic Decision Making and Treatment Monitoring. *J Nucl Med Technol* 2019; **47**: 85-87 [PMID: 30139889 DOI: 10.2967/jnmt.118.215582]

22 **Ahmadzadehfar H**, Rahbar K, Kürpig S, Bögemann M, Claesener M, Eppard E, Gärtner F, Rogenhofer S, Schäfers M, Essler M. Early side effects and first results of radioligand therapy with (177)Lu-DKFZ-617 PSMA of castrate-resistant metastatic prostate cancer: a two-centre study. *EJNMMI Res* 2015; **5**: 114 [PMID: 26099227 DOI: 10.1186/s13550-015-0114-2]

23 **Chedgy EC**, Vandekerkhove G, Herberts C, Annala M, Donoghue AJ, Sigouros M, Ritch E, Struss W, Konomura S, Liew J, Parimi S, Vergidis J, Hurtado-Coll A, Sboner A, Fazli L, Beltran H, Chi KN, Wyatt AW. Biallelic tumour suppressor loss and DNA repair defects in de novo small-cell prostate carcinoma. *J Pathol* 2018; **246**: 244-253 [PMID: 30015382 DOI: 10.1002/path.5137]

World Journal of Clinical Cases

Submit a Manuscript: https://www.f6publishing.com

World J Clin Cases 2022 February 16; 10(5): 1639-1644

DOI: 10.12998/wjcc.v10.i5.1639

ISSN 2307-8960 (online)

CASE REPORT

Disseminated peritoneal leiomyomatosis with malignant transformation involving right ureter: A case report

Chen-Yueh Wen, Herng-Sheng Lee, Jen-Tai Lin, Chia-Cheng Yu

ORCID number: Chen-Yueh Wen 0000-0002-1256-698X; Herng-Sheng Lee 0000-0002-1596-2304; Jen-Tai Lin 0000-0001-7702-5562; Chia-Cheng Yu 0000-0002-2620-1914.

Author contributions: Wen CY and Yu CC were involved in case management; Lee HS helped with the pathological interpretation; The images were collected and the main text was written by Wen CY; and all authors helped with data collection and preparation for submission of the final article.

Informed consent statement: Informed written consent was obtained from the patient for publication of this report and any accompanying images.

Conflict-of-interest statement: The authors declare that they have no conflict of interest.

CARE Checklist (2016) statement: The authors have read the CARE Checklist (2016), and the manuscript was prepared and revised according to the CARE Checklist (2016).

Country/Territory of origin: Taiwan

Specialty type: Medicine, research and experimental

Provenance and peer review: Unsolicited article; Externally peer

Chen-Yueh Wen, Jen-Tai Lin, Chia-Cheng Yu, Division of Urology, Department of Surgery, Kaohsiung Veterans General Hospital, Kaohsiung 81346, Taiwan

Herng-Sheng Lee, Department of Pathology and Laboratory Medicine, Kaohsiung Veterans General Hospital, Kaohsiung 81346, Taiwan

Chia-Cheng Yu, School of Medicine, National Yang-Ming University, Taipei 814, Taiwan

Chia-Cheng Yu, Department of Pharmacy, Tajen University, Pingtung 900, Taiwan

Corresponding author: Chia-Cheng Yu, Doctor, Professor, Division of Urology, Department of Surgery, Kaohsiung Veterans General Hospital, 386 Ta-Chung 1st Rd, Kaohsiung 81346, Taiwan. mlee0857@gmail.com

Abstract

BACKGROUND

Disseminated peritoneal leiomyomatosis (DPL) with myxoid leiomyosarcoma is a rare variant of leiomysosarcoma, and hematuria as a presenting symptom has never been reported. Through this case report, we emphasize the investigation of the etiology, clinical presentation, diagnosis, treatment, and prognosis of DPL with malignant changes mimicking metastatic urinary tract cancer and to help develop further clinical management.

CASE SUMMARY

We describe a case of DPL with malignant transformation involving the right ureter after laparoscopic hysterectomy. An exploratory laparotomy was performed and all visible nodules were surgically removed. DPL with focal malignant transformation to myxoid leiomyosarcoma was confirmed based on pathology results.

CONCLUSION

Professionals who preoperatively diagnose DPL with malignant change to myxoid leiomyosarcoma involving the genitourinary tract should consider symptoms of abdominal pain, hematuria, and imaging of disseminated pelvic tumors in women, especially those with prior history of laparoscopic hysterectomy. Early complete removal of all tumors is the cornerstone to prevent DPL from malignant changes.

Key Words: Disseminated peritoneal leiomyomatosis; Leiomyosarcoma; Laparoscopic

reviewed.

Peer-review model: Single blind

Peer-review report's scientific quality classification
Grade A (Excellent): 0
Grade B (Very good): 0
Grade C (Good): C, C
Grade D (Fair): 0
Grade E (Poor): 0

Received: August 7, 2021
Peer-review started: August 7, 2021
First decision: November 6, 2021
Revised: November 14, 2021
Accepted: January 11, 2022
Article in press: January 11, 2022
Published online: February 16, 2022

P-Reviewer: Govindarajan KK, Park SB
S-Editor: Wang JJ
L-Editor: A
P-Editor: Wang JJ

hysterectomy; Hematuria; Ureteroneocystostomy; Case report

Core Tip: Disseminated peritoneal leiomyomatosis (DPL) is a rare disease characterized by the presence of multiple nodules composed of smooth muscle cells located in both peritoneal and extraperitoneal spaces of the abdomen. Malignant changes in DPL correspond to a rare variant of leiomyosarcoma characterized by aggressive behavior. We describe a case of DPL with malignant transformation involving the right ureter after laparoscopic hysterectomy, mimicking urothelial carcinoma with peritoneal carcinomatosis. The aim of our case report is to investigate the etiology, clinical presentation, diagnosis, treatment, and prognosis of DPL and to help develop further clinical management of this disease.

Citation: Wen CY, Lee HS, Lin JT, Yu CC. Disseminated peritoneal leiomyomatosis with malignant transformation involving right ureter: A case report. *World J Clin Cases* 2022; 10(5): 1639-1644
URL: https://www.wjgnet.com/2307-8960/full/v10/i5/1639.htm
DOI: https://dx.doi.org/10.12998/wjcc.v10.i5.1639

INTRODUCTION

Disseminated peritoneal leiomyomatosis (DPL) is a rare disease characterized by the presence of multiple nodules composed of smooth muscle cells located in both the peritoneal and extraperitoneal spaces of the abdomen[1]. This disease is usually observed in women of reproductive age. To date, hundreds of cases have been reported[2,3]. However, malignant changes in DPL with myxoid leiomyosarcoma are rare, and hematuria as a presenting symptom has never been reported[4,5]. Herein, we present a case of DPL with malignant transformation involving the right ureter after laparoscopic hysterectomy. The aim of our case report is to investigate the etiology, clinical presentation, diagnosis, treatment, and prognosis of DPL with malignant changes mimicking metastatic urinary tract cancer and to help develop further clinical management.

CASE PRESENTATION

Chief complaints

A 72-year-old woman presented with gross hematuria one month before visiting our hospital.

History of present illness

This patient also noted intermittent abdominal cramping pain for half a year. The patient reported no urinary urgency, dysuria, flank pain, or fever.

History of past illness

The patient had undergone laparoscopic hysterectomy for uterine leiomyoma at another institution 2 years ago prior to her visit. Prior medical histories of hypertension, diabetes mellitus, and gout were noted.

Personal and family history

The patient had no relevant personal or family history.

Physical examination

Physical examination revealed multiple painful hard subcutaneous nodules in the lower abdomen.

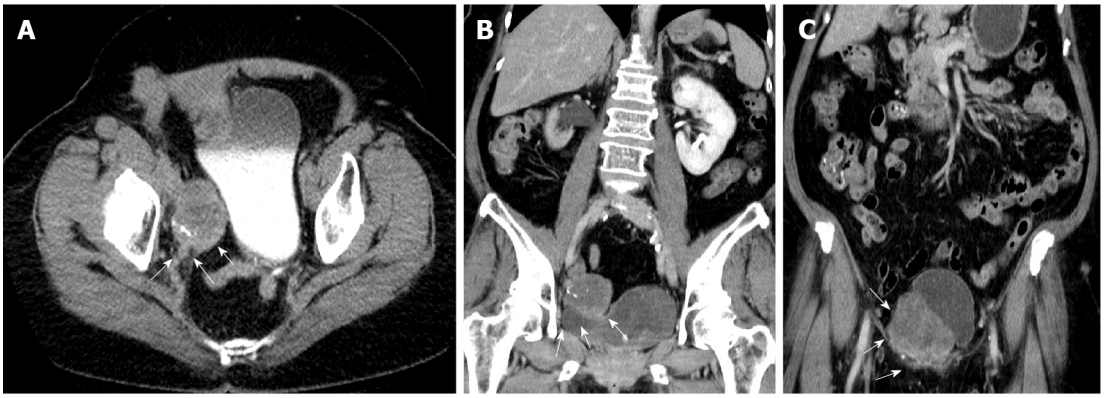

Figure 1 Abdominal computed tomography demonstrated that the tumor extended from the right distal third ureter to the ureterovesical junction. A: White arrowhead in the axial view; B and C: Coronal view.

Laboratory examinations

Laboratory examination revealed an elevated leukocyte count of 15109/mL, hemoglobin count of 12.9 g/dL, and C-reactive protein count of 3.72 mg/dL. Urine cytology, urinalysis, blood coagulation, kidney function, and liver function were all within normal range.

Imaging examinations

Abdominal computed tomography (CT) suggested urothelial carcinoma of the right lower third ureter with hydronephrosis and multiple seeding lesions at the anterior abdominal wall, subcutaneous fat, and bilateral inguinal areas (Figure 1).

FINAL DIAGNOSIS

Percutaneous ultrasound-guided biopsy of the most superficial lesion in the right lower quadrant of the abdomen was performed first. The tumor cells showed smooth muscle cell differentiation, which was compatible with leiomyoma as evidenced by pathology results.

TREATMENT

Because of persistent lower abdominal pain, the patient requested all tumors to be removed. An exploratory laparotomy was conducted with a lower midline incision, and multiple tumors of different sizes were found attached to the rectus muscle, bilateral inguinal areas, right ureter, and sigmoid colon (Figure 2). All nodules were meticulously dissected and resected with margins. Segmental resection of the right ureter, ureteroneocystostomy, partial resection of the sigmoid colon wall with primary closure, and transverse colostomy were also performed. The postoperative convalescence was uneventful. Final pathology revealed DPL with focal malignant transformation to myxoid leiomyosarcoma. Microscopically, the tumor was composed of malignant spindle cells with moderate to abundant eosinophilic cytoplasm arranged in interlacing fascicles (Figure 3).

OUTCOME AND FOLLOW-UP

Abdominal discomfort and pain improved significantly postoperatively. The transverse colostomy was closed after 3 mo. Adjuvant systemic chemotherapy was recommended, with periodic follow-up imaging; however, the patient opted for active surveillance only. The patient was doing well without evidence of recurrence 24 mo after the operation.

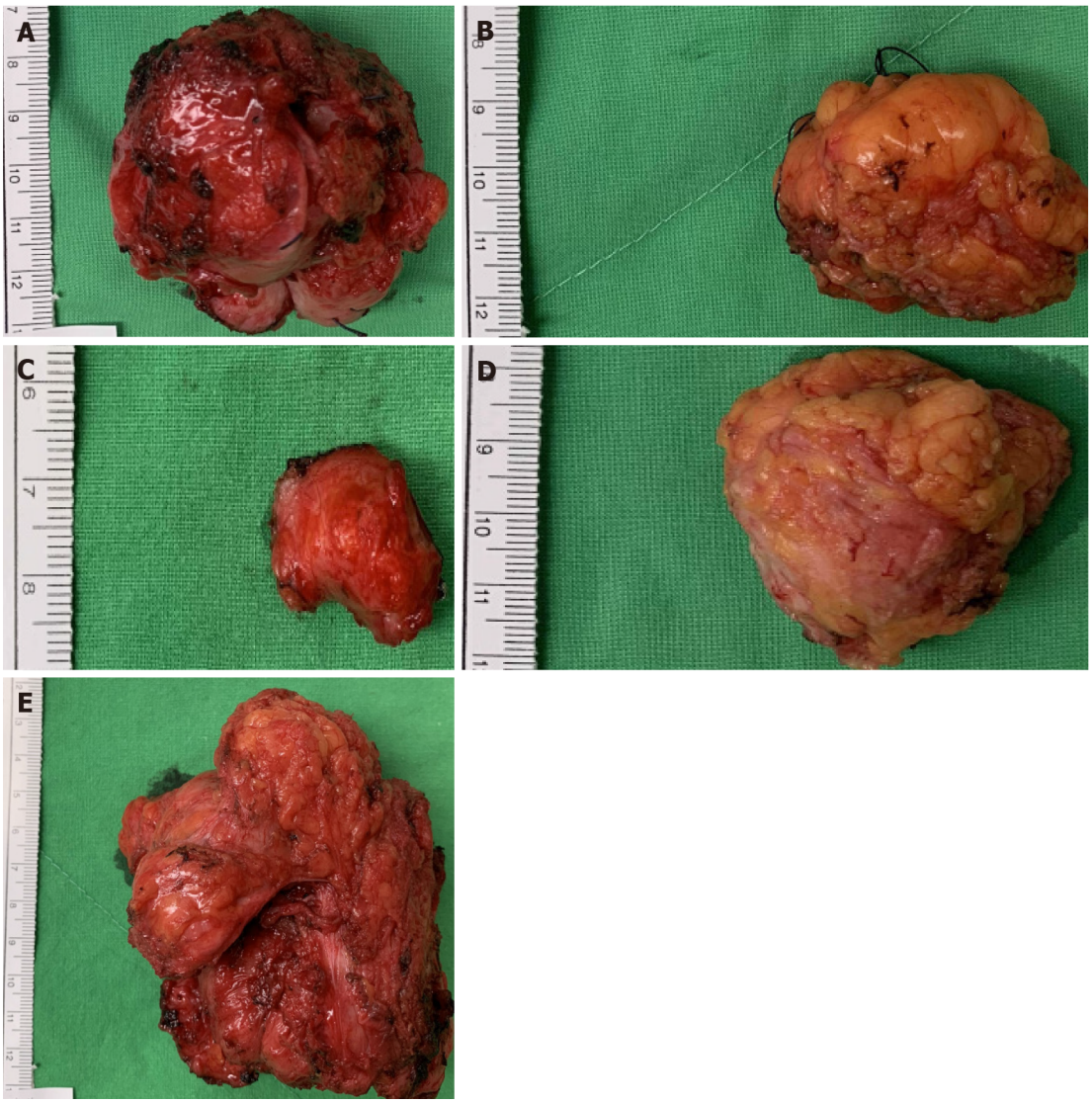

Figure 2 Intraoperative images of firm gray-whitish tumors. A: Located at right distal ureter; B: Located at right inguinal area; C: Located at left inguinal area; D: Located at abdominal wall; E: Located at sigmoid colon.

DISCUSSION

The etiology and pathophysiology of DPL are not yet well-established. Most reported cases are related to a history of laparoscopic hysterectomy or uterine myomectomy. Iatrogenic contamination after morcellation of myoma during laparoscopic surgery is considered to be a possible cause of DPL[1]. In the current case, the patient underwent laparoscopic hysterectomy 2 years ago; the use of a power morcellator may enhance potential for tumor implantation and dissemination[6,7].

Most patients with DPL are asymptomatic. In these patients, DPL is found incidentally through imaging. Several non-specific symptoms, including abdominal pain, distension, menostaxis, and bleeding from the rectum or vagina have been reported[7-9]. In the present case, the patient reported abdominal pain for one month, which is the most common manifestation of DPL. In addition, she first complained of gross hematuria and was referred to our urology outpatient department. To the best of our knowledge, this is the first report of DPL with hematuria as an initial presentation that could mimic urothelial cancer with peritoneal carcinomatosis[10,11]. Preoperative diagnosis of DPL is challenging, and only histopathologic examination can discriminate DPL from peritoneal metastatic malignancies or benign metastasizing leiomyoma[9,12]. Hence, we performed percutaneous ultrasound-guided biopsy of the abdominal wall lesion to delineate the nature of these tumors, and pathology showed a smooth muscle tumor compatible with leiomyoma.

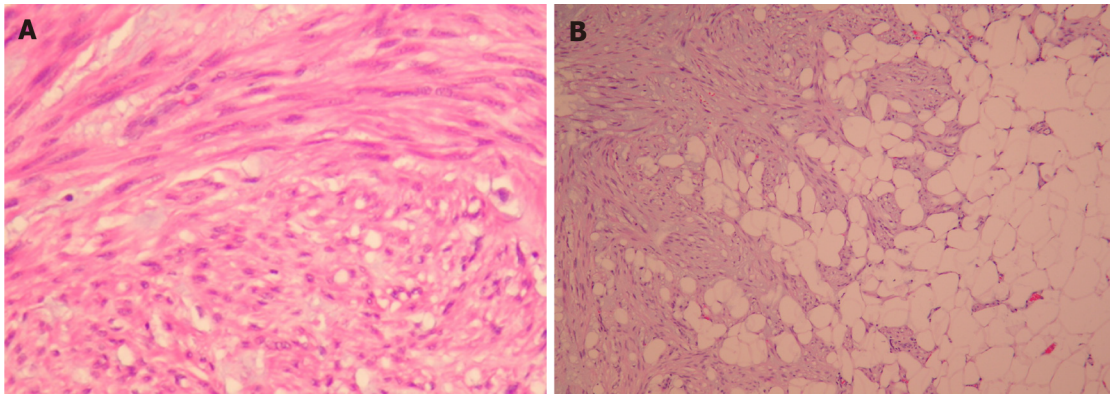

Figure 3 Histological appearance of disseminated peritoneal leiomyomatosis tumor. A: The tumor has hypercellular areas with focal myxoid matrix, composed of spindled-shape neoplastic cells arranged in interlacing fascicles and storiform growth pattern (original magnification, 200 ×); B: Myxoid matrix infiltrated into adipose tissue (original magnification, 100 ×).

DPL is histologically benign but can transform into a malignant leiomyosarcoma. The duration between the initial diagnosis of DPL and malignant changes varies from 1 mo to 8 years[4,13]. This duration can be under- or overestimated because malignant change may occur focally and insidiously, which makes histological sampling difficult. In the current case, the duration of malignant transformation was speculated to be less than 2 years according to the patient's operative history. Nevertheless, the focal tumor specimen involving the right ureter revealed a smooth muscle tumor with infiltrative borders, rich myxoid matrix, spindled neoplastic cells arranged in interlacing fascicles, mitotic activity up to 4 mitoses in 10 high-power fields, and foci of tumor necrosis. These findings are compatible with DPL with focal malignant transformation to myxoid leiomyosarcoma.

Standard treatment for DPL is debated. Since most DPLs are found in women of reproductive age, conservative treatment should be considered. Treatment of DPL includes a variety of treatments, such as active surveillance, hormone therapy, debulking surgery, chemotherapy, and radiation therapy, while surgical removal remains the mainstay because of its malignant potential[13,14]. In our case, no adjuvant chemotherapy or radiotherapy was administered.

CONCLUSION

In conclusion, we present a case of DPL with focal malignant transformation involving the right ureter, mimicking urothelial carcinoma with peritoneal carcinomatosis. Preoperative diagnosis of malignancy is usually challenging. DPL with malignant change to myxoid leiomyosarcoma involving the genitourinary tract should be weighed against differential diagnoses in women presenting with abdominal pain and hematuria with imaging of disseminated pelvic tumors, especially those with prior history of laparoscopic hysterectomy. Early complete surgical resection of all tumors is the most important factor in preventing malignant transformation of DPL, even though it has a relatively favorable outcome.

REFERENCES

1 **Al-Talib A**, Tulandi T. Pathophysiology and possible iatrogenic cause of leiomyomatosis peritonealis disseminata. *Gynecol Obstet Invest* 2010; **69**: 239-244 [PMID: 20068330 DOI: 10.1159/000274487]
2 **Bekkers RL**, Willemsen WN, Schijf CP, Massuger LF, Bulten J, Merkus JM. Leiomyomatosis peritonealis disseminata: does malignant transformation occur? *Gynecol Oncol* 1999; **75**: 158-163 [PMID: 10502446 DOI: 10.1006/gyno.1999.5490]
3 **Nappi L**, Sorrentino F, Angioni S, Pontis A, Barone I, Greco P. Leiomyomatosis Peritonealis Disseminata (LPD) ten years after laparoscopic myomectomy associated with ascites and lymph nodes enlargement: a case report. *Int J Surg Case Rep* 2016; **25**: 1-3 [PMID: 27280492 DOI: 10.1016/j.ijscr.2016.05.017]
4 **Sharma P**, Chaturvedi KU, Gupta R, Nigam S. Leiomyomatosis peritonealis disseminata with malignant change in a post-menopausal woman. *Gynecol Oncol* 2004; **95**: 742-745 [PMID: 15581996 DOI: 10.1016/j.ygyno.2004.09.007]

5 **Raspagliesi F**, Quattrone P, Grosso G, Cobellis L, Di Re E. Malignant degeneration in leiomyomatosis peritonealis disseminata. *Gynecol Oncol* 1996; **61**: 272-274 [PMID: 8626146 DOI: 10.1006/gyno.1996.0138]

6 **Lu B**, Xu J, Pan Z. Iatrogenic parasitic leiomyoma and leiomyomatosis peritonealis disseminata following uterine morcellation. *J Obstet Gynaecol Res* 2016; **42**: 990-999 [PMID: 27125448 DOI: 10.1111/jog.13011]

7 **Psathas G**, Zarokosta M, Zoulamoglou M, Chrysikos D, Thivaios I, Kaklamanos I, Birbas K, Mariolis-Sapsakos T. Leiomyomatosis peritonealis disseminata: A case report and meticulous review of the literature. *Int J Surg Case Rep* 2017; **40**: 105-108 [PMID: 28965085 DOI: 10.1016/j.ijscr.2017.09.016]

8 **Huang SF**, Wen CY, Liao CI, Lin JC, Tsai CC. Leiomyomatosis peritonealis disseminata mimicking peritoneal carcinomatosis 13 years after laparoscopic uterine myomectomy: A case report. *Int J Surg Case Rep* 2021; **81**: 105745 [PMID: 33743252 DOI: 10.1016/j.ijscr.2021.105745]

9 **Li J**, Dai S. Leiomyomatosis Peritonealis Disseminata: A Clinical Analysis of 13 Cases and Literature Review. *Int J Surg Pathol* 2020; **28**: 163-168 [PMID: 31615319 DOI: 10.1177/1066896919880962]

10 **Morita J**, Naoe M, Fuji K, Hiramatsu A, Unoki T, Matsui Y, Shimoyama H, Nakasato T, Oshinomi K, Saito K, Maeda Y, Ogawa Y. Indications for ureteropyeloscopy in the detection of upper urinary tract tumors. *Urol Sci* 2018; **29**: 186-192 [DOI: 10.4103/UROS.UROS_55_18]

11 **Sharma S**, Ksheersagar P, Sharma P. Diagnosis and treatment of bladder cancer. *Am Fam Physician* 2009; **80**: 717-723 [PMID: 19817342]

12 **Patton KT**, Cheng L, Papavero V, Blum MG, Yeldandi AV, Adley BP, Luan C, Diaz LK, Hui P, Yang XJ. Benign metastasizing leiomyoma: clonality, telomere length and clinicopathologic analysis. *Mod Pathol* 2006; **19**: 130-140 [PMID: 16357844 DOI: 10.1038/modpathol.3800504]

13 **Yamaguchi T**, Imamura Y, Yamamoto T, Fukuda M. Leiomyomatosis peritonealis disseminata with malignant change in a man. *Pathol Int* 2003; **53**: 179-185 [PMID: 12608900 DOI: 10.1046/j.1440-1827.2003.01452.x]

14 **Grimer R**, Judson I, Peake D, Seddon B. Guidelines for the management of soft tissue sarcomas. *Sarcoma* 2010; **2010**: 506182 [PMID: 20634933 DOI: 10.1155/2010/506182]

World Journal of Clinical Cases

Submit a Manuscript: https://www.f6publishing.com

World J Clin Cases 2022 February 16; 10(5): 1645-1653

DOI: 10.12998/wjcc.v10.i5.1645

ISSN 2307-8960 (online)

CASE REPORT

Arthroscopic surgery for synovial chondroma of the subacromial bursa with non-traumatic shoulder subluxation complications: Two case reports

Xiong-Feng Tang, Yan-Guo Qin, Xian-Yue Shen, Bo Chen, Ying-Zhi Li

ORCID number: Xiong-Feng Tang 0000-0002-0424-7946; Yan-Guo Qin 0000-0003-3296-3779; Xian-Yue Shen 0000-0002-3623-201X; Bo Chen 0000-0002-5591-9597; Ying-Zhi Li 0000-0002-8525-6472.

Author contributions: Tang XF, Shen XY, Chen B, and Li YZ were the clinicians involved in the diagnosis, management, therapy, and follow-up of the patients; Tang XF reviewed the literature and wrote the draft; Qin YG and Li YZ were responsible for the critical revision of the manuscript for relevant intellectual content. All of the authors approved the final version of the paper prior to submissions.

Informed consent statement: The patients were informed and agreed to participate in this study.

Conflict-of-interest statement: All the authors declare no conflicts of interest for this article.

CARE Checklist (2016) statement: The authors have read the CARE Checklist (2016), and the manuscript was prepared revised according to the CARE Checklist.

Supported by the Natural Science Foundation of Jilin Province, No. 20200201536JC.

Xiong-Feng Tang, Yan-Guo Qin, Xian-Yue Shen, Bo Chen, Ying-Zhi Li, Orthpoeadic Medical Center, Jilin University Second Hospital, Changchun 130041, Jilin Province, China

Corresponding author: Ying-Zhi Li, MD, Associate Professor, Surgeon, Orthpoeadic Medical Center, Jilin University Second Hospital, Nanguan Road, No. 218 Ziqiang Street, Changchun 130041, Jilin Province, China. dlyz2005@jlu.edu.cn

Abstract

BACKGROUND

Synovial chondromatosis is a disease originating from the synovium and characterized by the presence of metaplastic cartilaginous nodules in synovial cavities. The exact prevalence of synovial chondromatosis remains unknown, and the involvement of the shoulder joint is very rare. Synovial chondromatosis accompanied by subluxation of the humeral head without a history of trauma is rarely encountered, and to our knowledge, no published reports describe this condition.

CASE SUMMARY

We present two cases of synovial chondromatosis in the shoulder joint, accompanied by subluxation of the humeral head, in two arthroscopically managed adult patients. We performed arthroscopic labrum fixation and removal of the loose body from the shoulder joint. To identify primary and secondary categories, pathological analysis was arranged. Clinical and radiographic evaluations at the 1-mo follow-up were satisfactory.

CONCLUSION

The biomechanical function of the shoulder joint requires attention, especially following the detection of loose bodies, as observed with synovial chondroma occurring in rare sites. Arthroscopic management is successful in patients with synovial chondromatosis combined with shoulder subluxation.

Key Words: Synovial chondromatosis; Shoulder; Subluxation; Arthroscopic surgery; Case report

Country/Territory of origin: China

Specialty type: Orthopedics

Provenance and peer review: Unsolicited article; Externally peer reviewed

Peer-review model: Single blind

Peer-review report's scientific quality classification
Grade A (Excellent): 0
Grade B (Very good): 0
Grade C (Good): C
Grade D (Fair): 0
Grade E (Poor): 0

Received: August 23, 2021
Peer-review started: August 23, 2021
First decision: October 22, 2021
Revised: November 4, 2021
Accepted: January 11, 2022
Article in press: January 11, 2022
Published online: February 16, 2022

P-Reviewer: Akbulut S
S-Editor: Zhang H
L-Editor: Wang TQ
P-Editor: Zhang H

Core Tip: Synovial chondromatosis accompanied with subluxation of the humeral head without a history of trauma is rarely encountered and, to our knowledge, there are no reports yet of this condition. We report two cases that had synovial chondromatosis accompanied with subluxation of the humeral head and it is the first to describe. Arthroscopic management was successful in patients with synovial chondromatosis combined with subluxation of the shoulder. Biomechanical working of the shoulder joint should not be ignored in synovial chondromatosis diagnosis, especially with the emergence of loose bodies such as in synovial chondroma occurring in rare sites.

Citation: Tang XF, Qin YG, Shen XY, Chen B, Li YZ. Arthroscopic surgery for synovial chondroma of the subacromial bursa with non-traumatic shoulder subluxation complications: Two case reports. *World J Clin Cases* 2022; 10(5): 1645-1653
URL: https://www.wjgnet.com/2307-8960/full/v10/i5/1645.htm
DOI: https://dx.doi.org/10.12998/wjcc.v10.i5.1645

INTRODUCTION

Synovial chondromatosis is a disease of unknown etiology, originating from the synovium and characterized by the presence of metaplastic cartilaginous nodules in synovial cavities, bursa, or tendon sheaths[1-3]. Synovial chondromatosis commonly presents in young to middle-aged men[4], and usually involves large joints, including the knee, hip, and elbow, but can occur in any synovial joint throughout the body. The disease most commonly affects the knee joint, followed by the hip and elbow; however, the occurrence of synovial chondromatosis in either the shoulder or ankle joints is extremely rare[3,5,6].

A diagnosis of synovial chondromatosis is often delayed due to initially mild and nonspecific symptoms[7]. If the intra-articular fragments are not adequately calcified, synovial chondromatosis can go undetected for years[8]. The complaints associated with synovial chondromatosis typically include joint pain, joint swelling, decreased mobility, and loose bodies[9]. However, synovial chondromatosis accompanied by subluxation of the humeral head in the absence of any history of trauma is rare and, to our knowledge, has not yet been reported in the literature, and the mechanism of subluxation has not ever been analyzed.

The most commonly recommended treatment for synovial chondromatosis is the surgical removal of loose bodies to ameliorate the associated symptoms. Currently, an arthroscopic approach is recommended for most shoulder pathologies[10,11]. The primary advantages of using arthroscopic approaches include decreased morbidity, synchronous visualization, and the ability to treat both intra- and extra-articular pathologies. Hypertrophic synovia and multiple loose bodies are typical arthroscopic findings[12,13].

In this report, we present two cases of synovial chondromatosis in the shoulder joint accompanied by subluxation of the humeral head treated with arthroscopic management in adult patients and discuss the potential underlying mechanisms involved in disease development.

CASE PRESENTATION

Chief complaints

Case one: A 56-year-old woman experienced severe right shoulder pain and decreased range of motion for 3 d without any history of trauma.

Case two: A 56-year-old woman experienced severe left shoulder pain with limited mobility for 3 mo, which worsened over the past 4 d, without any history of trauma prior to presence at our hospital.

History of present illness

Case one: As reported by the patient, the right shoulder pain was accompanied by limited mobility and significant swelling due to slight external force over the previous

3 d. The pain and swelling continued to increase without systemic treatment, and the patient was referred to our hospital for further treatment. After physical examination, imaging examinations, and a review of the patient's medical history, the patient was diagnosed with right shoulder joint dislocation.

Case two: The patient described left shoulder joint pain without an obvious cause and limited joint movement, which started 3 mo prior to presentation. Conservative treatments, such as acupuncture and therapeutic massage at a local hospital, did not provide symptom relief, and the pain had become aggravated over the past 4 d without any trauma.

History of past illness

Case one: The patient's medical history was unremarkable, and she was in generally good health.

Case two: The patient's medical history showed a 3-year history of hypertension, reaching as high as 160/100 mmHg, without regular oral antihypertensive medication, resulting in poorly controlled hypertension.

Physical examination

Case one: The physical examination revealed obvious swelling in the right shoulder, with an empty glenoid cavity and obvious deformity. Tenderness was detected in the spinous process of the cervical spine and in front of and above the right shoulder. Mobility was limited, and the Dugas sign was positive.

Case two: Physical examination revealed obvious swelling of the left shoulder joint, mild atrophy of surrounding muscles, positive tenderness in front of and above the left shoulder joint, positive Jobe sign, positive arm drop test, positive pain arc sign, and positive Dugas sign.

Imaging examinations

Case one: Radiographs showed subluxation of the shoulder joint (Figure 1A). Computed tomography (CT) indicated that the right humerus head was dislocated anteriorly and inferiorly. The joint space was narrowed, the shadow of the surrounding tissue was thick, and the shadow of the fluid density was visible within the joint cavity. A point-striped bone density shadow was observed near the pelvis of the right shoulder. Magnetic resonance imaging (MRI) examination of the shoulder joint indicated a quasi-circular, short T2 weighted signal in the shoulder cavity, with a large area of long T1 and long T2 liquid signals observed in the subacromial bursa (Figure 1B).

Case two: Radiography of the shoulder joint showed a dislocated left shoulder joint and the presence of multiple bone-like loose bodies within the glenohumeral joint space (Figure 2A). On three-dimensional CT, the left humeral head could be observed surrounded by sheet-like, low-density shadows. The CT value was approximately 25 HU, and the surrounding lipolysis remained clear, with multiple sheet-like, bone-like dense shadows visible. The head position was slightly lower than the normal anatomical relationship of the left humerus (Figure 2B and C). MRI examination of the shoulder joint showed a round, short T2-weighted signal, an irregular shape for the supraspinatus muscle, and patchy proton density–weighted image hyperintensity at the attachment point of the supraspinatus tendon in the joint cavity. Sheet-like long T1 and long T2 fluid signals in the subacromial space of the deltoid synovial sac were observed (Figure 3).

Pathological diagnosis

Case one: The pathological analysis showed right shoulder joint disease of the synovium and exfoliated cartilage. Hyperplastic cartilage tissue was submitted for inspection, which revealed degenerative local necrosis and ossification in some areas; the subacromial lesion synovium and loose bodies were submitted for inspection as suspected hyperplastic cartilage. The surface of the tissue was covered in a small amount of synovial membrane, consistent with synovial chondroma (Figure 4).

Case two: Upon pathological examination, the specimen was identified as a cartilaginous nodule surrounded by fibrous tissue with local calcification. Fragments of articular cartilage or subchondral lamellar bone were observed (Figure 5).

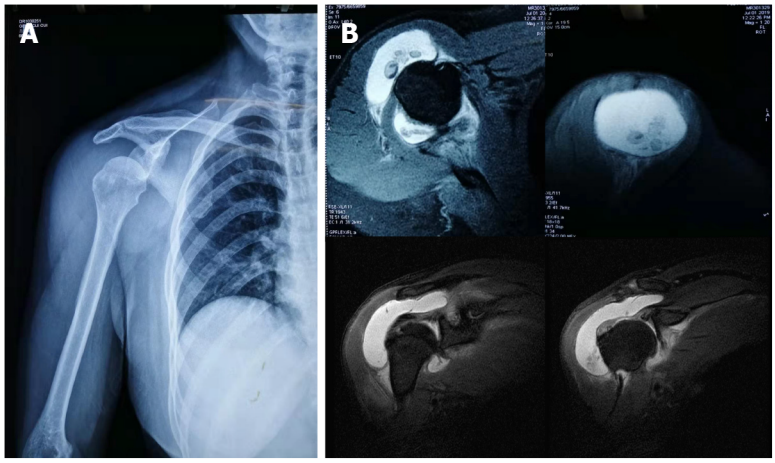

Figure 1 Imaging examinations of case one. A: Plain radiograph in anteroposterior view of the right shoulder, showing subluxation of the humeral head; B: Magnetic resonance imaging examination of the shoulder joint, showing multiple intra-articular loose bodies and joint effusion.

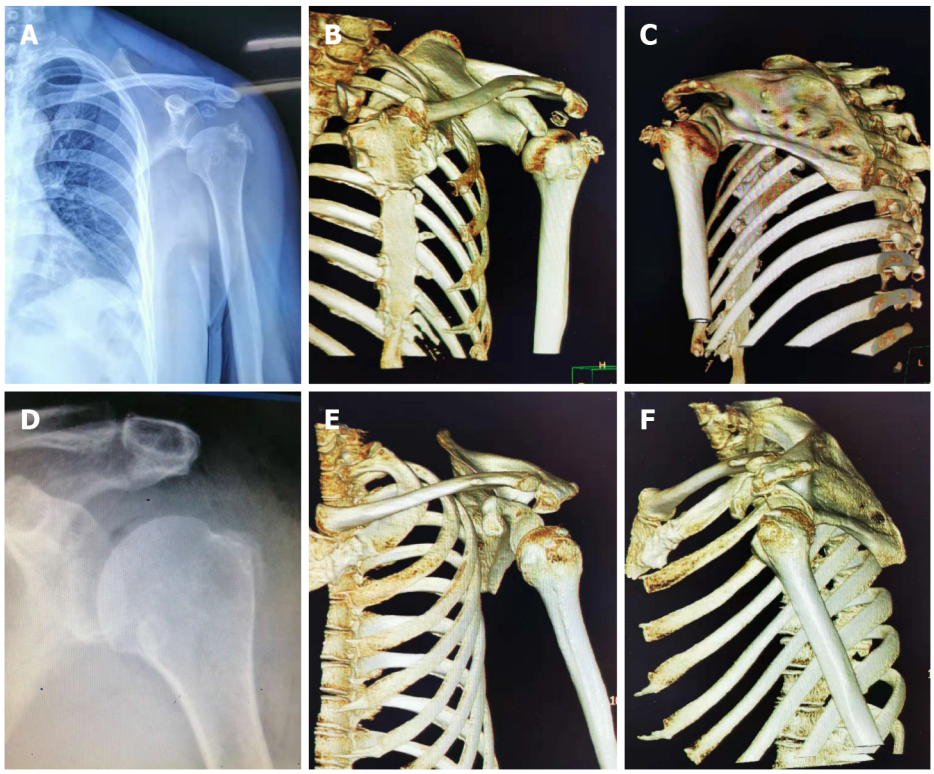

Figure 2 Imaging examinations of case two. A–C: Plain radiographs and three-dimensional computed tomography (3D-CT) reconstruction of the left shoulder, showing multiple intra-articular loose bodies and the subluxation of the humeral head; D–F: Postoperative radiographic re-examination and 3D-CT reconstruction showed no loose bodies in the subacromial space. The humeral head returned to a normal anatomical relationship.

FINAL DIAGNOSIS

Case one: The final diagnosis was subluxation and synovial chondroma of the right shoulder joint.

Case two: Subluxation and synovial chondroma, along with calcified tendinitis of the left shoulder joint.

TREATMENT

Case one: We performed arthroscopic labrum fixation and removal of the loose body

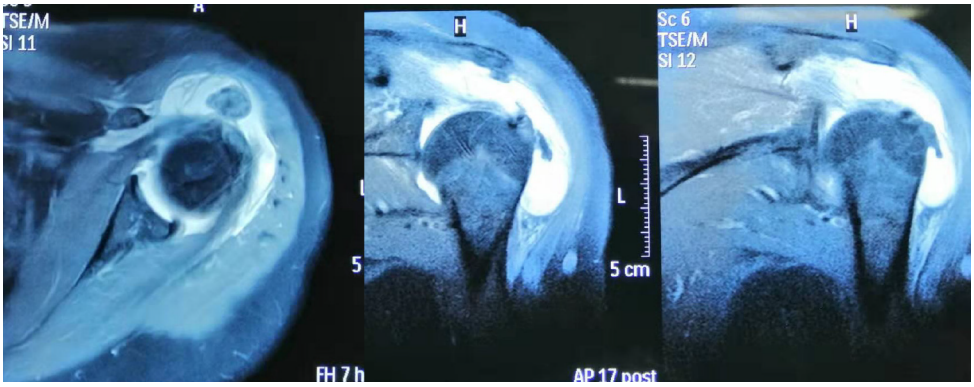

Figure 3 Magnetic resonance imaging of the shoulder joint showed multiple intra-articular loose bodies and joint effusion.

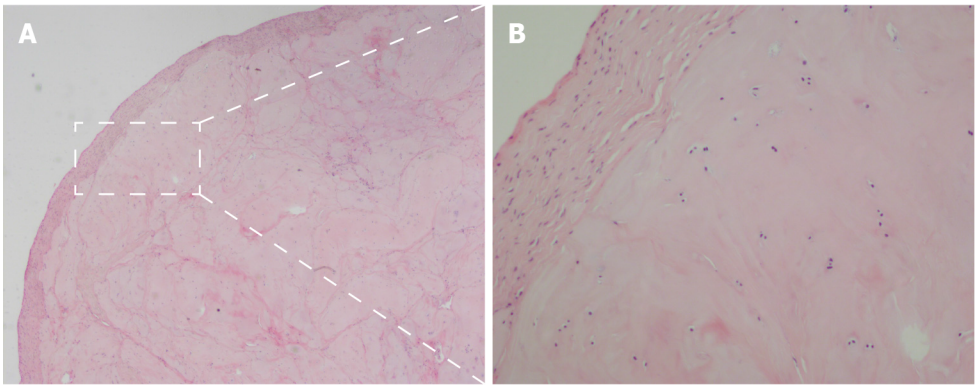

Figure 4 Pathological examination of case one. A: Lobulated areas of hyaline cartilage just below the synovial surface were easily identified by hematoxylin-eosin staining (magnification: 20 ×); B: Chondrocytes were found clustered together and were not uniformly distributed throughout the ground substance (magnification: 100 ×).

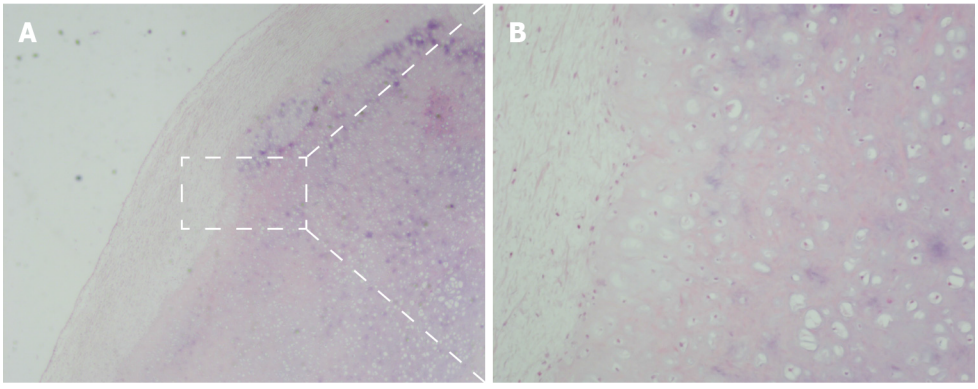

Figure 5 Pathological examination of case two. A: Fragments of articular cartilage or subchondral lamellar bone were present in loose bodies identified by hematoxylin-eosin staining (magnification: 20 ×); B: Chondrocytes were found in the zonal and ring-like units together and were uniformly distributed throughout the ground substance (magnification: 100 ×).

from the shoulder joint. After successful anesthesia induction, the patient was placed in a left-sided lying position, the right limb was placed in an abduction position, and a traction weight of 4 kg was applied. The standard posterior approach was used for glenohumeral arthroscopy, which showed a large quantity of cartilaginous debris in the joint cavity (Figure 6). Arthroscopy revealed a free cartilage sheet, obvious synovial hyperplasia, massive exfoliation of the articular surface of the humeral head, scapular glenoid cartilage, degeneration of the long head of the biceps, an inferior anterior labrum, and separation of the joint capsule from the glenoid. During arthroscopy, both superior and anterior approaches were used to remove all free cartilage and exfoliate the cartilage from the articular head to proliferate the synovium.

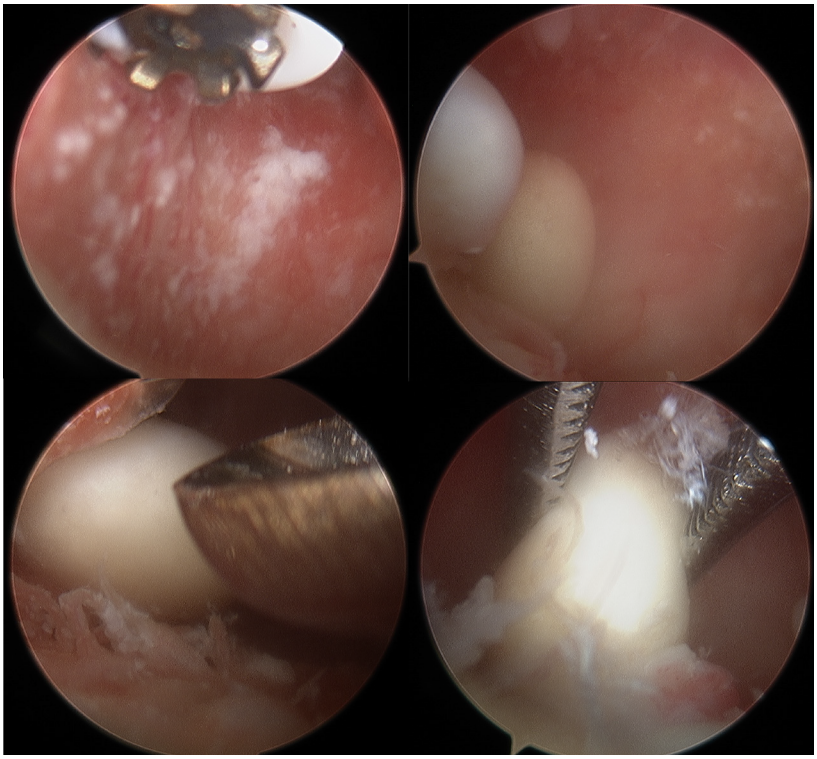

Figure 6 From the standard posterior portal, the arthroscopic view revealed a large number of cartilaginous loose bodies in the region of the subscapularis.

The anterior inferior joint capsule and labrum were loosened, and 2.9 mm anchors were implanted at the 5:30, 4:30, and 3:00 o'clock positions. The anterior inferior joint capsule and labrum were sutured by lifting and repositioning. The humeral head was located in the center of the joint, and the glenoid labrum was reset. The arthroscope was then moved to the subacromial space, which showed large amounts of synovial hyperplasia under the acromion, accompanied by cartilaginous fragments and free loose bodies, the proliferation of the subacromial capsule, and inflammatory changes. The proliferative synovial membrane, cartilage debris, and loose bodies were removed and sent for pathological examination. The joint cavity and subacromial space were washed with a large volume of normal saline. After checking the gauze and instruments, the incision was sutured, and the affected limb was suspended. After hanging and fixation, the operation was complete.

Case two: The loose bodies were removed from the shoulder joint under arthroscopic guidance through the following steps. After successful anesthesia induction, the patient was placed in the right decubitus and left limb abduction position, and a traction weight of 4 kg was applied. A standard posterior approach was utilized for glenohumeral arthroscopy after routine disinfection and draping were performed. Under arthroscopic guidance (Figure 7), the synovia of the joints were observed, featuring hyperplasia, with degeneration of the articular surface of the humeral head, scapula, biceps, and long head muscles; intact subscapularis, supraspinatus, and small round muscles; and degenerative lesions detected on the subspinal muscles. Two loose bodies were observed in the joint space, which were removed using nucleus pulposus forceps. An arthroscopic anterior approach was established to remove the synovial hyperplasia. The arthroscope was repositioned to the subacromial space, which revealed the hyperplasia of the outer edge of the front shoulder bone and subacromial bursa and inflammatory changes. After establishing a posterolateral approach, a synovial resection line was determined, and acromioplasty was performed. The joint cavity was washed with a large volume of physiological saline. After checking the gauze and instrument inventory, the incisions were sutured, covered with sterile dressing, and the limb was suspended.

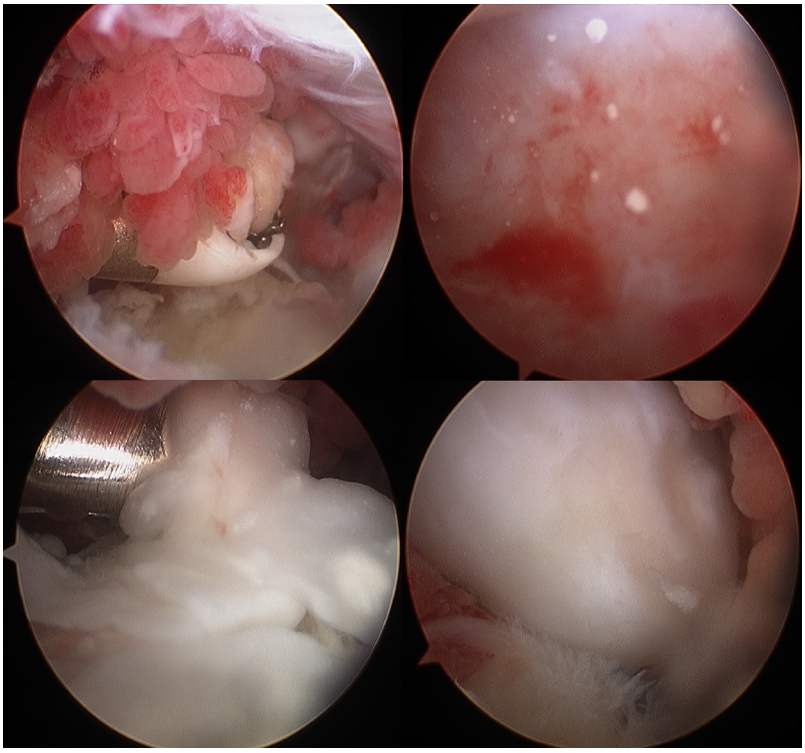

Figure 7 From the standard posterior portal, the arthroscopic view revealed a large number of cartilaginous loose bodies and synovial capsule hyperplasia, with inflammatory changes in the region of the subscapularis.

OUTCOME AND FOLLOW-UP

Case one: Re-examination by postoperative radiography showed no loose bodies in the subacromial space. The humeral head returned to a normal anatomical relationship. The swelling and pain of the shoulder joint gradually disappeared, and shoulder joint function returned to normal. Range of movement exercises were started as soon as the patient was comfortable. At the 1-mo follow-up, the patient had pain-free range of movement in the right shoulder that was comparable to that in the left shoulder, with no remaining preoperative symptoms.

Case two: Postoperative radiographic re-examination showed no loose bodies in the subacromial space. The humeral head returned to its normal anatomical relationship (Figure 2D–F). The swelling and pain of the shoulder joint gradually disappeared, and shoulder joint function generally returned to normal. At the 1 mo follow-up, normal shoulder function was restored.

DISCUSSION

Synovial chondromatosis of the joints is a rare clinical condition with an unclear definition and diagnostic criteria[14], resulting in limited available knowledge regarding this condition. Synovial chondromatosis can be divided into primary and secondary categories[15]. Primary synovial chondromatosis involves no prior basic bone or joint lesions and is generally regarded as a benign neoplastic disease rather than synovial metaplasia, with a reported incidence of approximately 5%[16]. By contrast, secondary membrane chondromatosis typically occurs secondary to trauma, osteoarthritis, or rheumatoid arthritis[17,18]. Clinically, the signs and symptoms are nonspecific and may be suggestive of several pathological conditions. In most cases, the symptoms comprise pain or range of motion loss. Shoulder pain is one of the first symptoms, followed by the locking of the joint in some cases[18,19]. However, dislocation is not a typical feature. Both of our patients experienced a painful range of motion, with signs and symptoms typical of shoulder joint subluxation.

Most previously reported investigations have not described synovial chondromatosis accompanied by subluxation, and no previous literature reports have reported any clinical manifestations of joint subluxation; despite the presence of many loose

bodies, no cases of joint dislocation have been reported. Koichi *et al* retrieved more than 200 loose bodies from a young female patient with a rare condition of secondary synovial chondromatosis in her right shoulder[20]. Hiroyuki extracted 17 free bodies from the subscapularis bursa of a confirmed case of synovial chondromatosis in a 12-year-old boy[21]. Therefore, we questioned the occurrence of shoulder dislocation in our patients, who were characterized by the presence of relatively few loose bodies. To our knowledge, previous case reports and studies have focused on the characteristic symptoms caused by loose bodies, such as joint pain, swelling, and limited mobility, without examining the biomechanical function of the shoulder joint. The emergence of loose bodies, such as those observed with synovial chondroma in unusual locations, disrupts the stabilization mechanism of the shoulder joint. The lever effect occurs during specific movements, resulting in shoulder joint dislocation.

The biomechanics of the glenohumeral joints depend on interactions between both static and dynamic stabilizing structures[22]. Static stabilizers include the bony anatomy, negative intra-articular pressure, glenoid labrum, and the glenohumeral ligaments, along with the joint capsule. The dynamic stabilizing structures include the rotator cuff muscles and other muscular structures surrounding the shoulder joint. The combined functions of these stabilizers serve to support multiple degrees of motion within the glenohumeral joint. When any one of these mechanisms fails, shoulder joint pathology, such as subluxation or dislocation, can occur[22,23].

Whether the observed synovial cartilage tumors observed in our patients represent primary or secondary hyperplasias and the order in which dislocation and synovial chondroma developed are other concerns. Histopathological identification is needed to differentiate between primary and secondary synovial chondromatosis[18]. According to Villacin *et al*[24], who delineated the histologic criteria for differentiating between primary and secondary synovial chondromatosis, in primary lesions, the chondro-metaplasia foci in the synovium and loose bodies are characterized by a markedly disorganized pattern, with many binucleate, plump chondrocytes, and patchy, diffuse calcification. By contrast, in secondary lesions, fragments of articular cartilage or subchondral lamellar bone may be present in the loose bodies, and the pattern of calcification is zonal and ring-like, with uniform, evenly distributed chondrocytes[20, 24]. Milgram suggested that primary synovial chondromatosis has three phases: (1) Active intrasynovial disease, without loose bodies; (2) transitional lesions, characterized by both active intrasynovial proliferation and loose bodies; and (3) multiple free bodies, without intrasynovial disease[25]. Combined with the operative findings of multiple loose bodies and the histologic absence of intrasynovial disease, patient 1 in our case report may have had phase 3 primary synovial chondromatosis, whereas patient 2 may have had a secondary synovial chondromatosis.

The treatment decision is made according to the patient's age, symptoms, and the disease stage[6]. Preventing missed diagnoses and misdiagnoses and performing a differential diagnosis when loose bodies are detected are important concerns, especially when rotator cuff injuries are suspected. The differentiation between a loose body and an avulsion fracture is also necessary. If the intra-articular fragments are not adequately calcified, synovial chondromatosis can go undetected for years[26]. Obtaining a detailed medical history and performing complete physical examinations and MRI scans can contribute to the accurate diagnosis and treatment of synovial chondromatosis.

CONCLUSION

We believe that the biomechanical function of the shoulder joint should be considered, especially when loose bodies are detected, as observed with synovial chondroma occurring in rare sites. Arthroscopic management was successful in two patients with synovial chondromatosis combined with shoulder subluxation. In such conditions, subluxation is usually transient, and the humeral head returns spontaneously to its normal position after the operation.

REFERENCES

1 **Blümlein H**, Puls P, Schneider HM, Wunderlich T. [Benign and malignant chondromatosis of the joints. A contribution to the clinical aspects and histology of the disease]. *Z Orthop Ihre Grenzgeb* 1980; **118**: 8-14 [PMID: 7424110 DOI: 10.1055/s-2008-1051448]

2 **McFarland EG**, Neira CA. Synovial chondromatosis of the shoulder associated with osteoarthritis:

conservative treatment in two cases and review of the literature. *Am J Orthop (Belle Mead NJ)* 2000; **29**: 785-787 [PMID: 11043962]

3 **Wiedemann NA**, Friederichs J, Richter U, Bühren V. [Secondary synovial chondromatosis of the ankle joint]. *Orthopade* 2011; **40**: 807-811 [PMID: 21104226 DOI: 10.1007/s00132-010-1706-1]

4 **Davis RI**, Hamilton A, Biggart JD. Primary synovial chondromatosis: a clinicopathologic review and assessment of malignant potential. *Hum Pathol* 1998; **29**: 683-688 [PMID: 9670824 DOI: 10.1016/s0046-8177(98)90276-3]

5 **Aydogan NH**, Kocadal O, Ozmeric A, Aktekin CN. Arthroscopic treatment of a case with concomitant subacromial and subdeltoid synovial chondromatosis and labrum tear. *Case Rep Orthop* 2013; **2013**: 636747 [PMID: 24383030 DOI: 10.1155/2013/636747]

6 **Fukuda A**, Uemura T, Nishimura A, Kato K, Sudo A. Arthroscopic Treatment of Primary Synovial Chondromatosis of the Subscapular Bursa: A Case Report. *J Orthop Case Rep* 2020; **9**: 40-43 [PMID: 32548026 DOI: 10.13107/jocr.2019.v09.i06.1580]

7 **Sinikumpu JJ**, Sinikumpu SP, Sirniö K, Näpänkangas J, Blanco Sequeiros R. Pediatric primary synovial chondromatosis of the shoulder, biceps tendon sheath and subcoracoid bursa. *J Clin Orthop Trauma* 2020; **11**: 317-320 [PMID: 32099303 DOI: 10.1016/j.jcot.2019.12.005]

8 **Miranda JJ**, Hooker S, Baechler MF, Burkhalter W. Synovial chondromatosis of the shoulder and biceps tendon sheath in a 10-year-old child. *Orthopedics* 2004; **27**: 321-323 [PMID: 15058455 DOI: 10.3928/0147-7447-20040301-17]

9 **Covall DJ**, Fowble CD. Synovial chondromatosis of the biceps tendon sheath. *Orthop Rev* 1994; **23**: 902-905 [PMID: 7677824]

10 **Jiménez-Martín A**, Zurera-Carmona M, Santos-Yubero FJ, Pérez-Hidalgo S. Arthroscopic treatment of synovial chondromatosis, an unusual cause of shoulder pain. *Reumatol Clin* 2014; **10**: 416-417 [PMID: 24529638 DOI: 10.1016/j.reuma.2013.12.008]

11 **Ranalletta M**, Bongiovanni S, Calvo JM, Gallucci G, Maignon G. Arthroscopic treatment of synovial chondromatosis of the shoulder: report of three patients. *J Shoulder Elbow Surg* 2009; **18**: e4-e8 [PMID: 19213576 DOI: 10.1016/j.jse.2008.12.003]

12 **Duymus TM**, Yucel B, Mutlu S, Tuna S, Mutlu H, Komur B. Arthroscopic treatment of synovial chondromatosis of the shoulder: A case report. *Ann Med Surg (Lond)* 2015; **4**: 179-182 [PMID: 26005571 DOI: 10.1016/j.amsu.2015.05.001]

13 **Urbach D**, McGuigan FX, John M, Neumann W, Ender SA. Long-term results after arthroscopic treatment of synovial chondromatosis of the shoulder. *Arthroscopy* 2008; **24**: 318-323 [PMID: 18308184 DOI: 10.1016/j.arthro.2007.08.034]

14 **Neumann JA**, Garrigues GE, Brigman BE, Eward WC. Synovial Chondromatosis. *JBJS Rev* 2016; **4** [PMID: 27490219 DOI: 10.2106/JBJS.RVW.O.00054]

15 **Poyser E**, Morris R, Mehta H. Primary synovial osteochondromatosis of the shoulder: a rare cause of shoulder pain. *BMJ Case Rep* 2018; **11** [PMID: 30567134 DOI: 10.1136/bcr-2018-227281]

16 **Raval P**, Vijayan A, Jariwala A. Arthroscopic Retrieval of over 100 Loose Bodies in Shoulder Synovial Chondromatosis: A Case Report and Review of Literature. *Orthop Surg* 2016; **8**: 511-515 [PMID: 28032713 DOI: 10.1111/os.12294]

17 **Díaz Fernández JF**, Peraza Mc Liberty RA. Synovial osteochondromatosis of the shoulder: Case report and literature review. *Reumatol Clin (Engl Ed)* 2018; **14**: 56-58 [PMID: 27613313 DOI: 10.1016/j.reuma.2016.07.009]

18 **Utashima D**, Matsumura N, Suzuki T, Iwamoto T, Ogawa K. Clinical Results of Surgical Resection and Histopathological Evaluation of Synovial Chondromatosis in the Shoulder: A Retrospective Study and Literature Review. *Clin Orthop Surg* 2020; **12**: 68-75 [PMID: 32117541 DOI: 10.4055/cios.2020.12.1.68]

19 **Shearer H**, Stern P, Brubacher A, Pringle T. A case report of bilateral synovial chondromatosis of the ankle. *Chiropr Osteopat* 2007; **15**: 18 [PMID: 18036237 DOI: 10.1186/1746-1340-15-18]

20 **Hamada J**, Tamai K, Koguchi Y, Ono W, Saotome K. Case report: A rare condition of secondary synovial osteochondromatosis of the shoulder joint in a young female patient. *J Shoulder Elbow Surg* 2005; **14**: 653-656 [PMID: 16337537 DOI: 10.1016/j.jse.2004.12.004]

21 **Katoh H**, Ogawa K, Ikegami H, Inokuchi W, Toyama Y. Osteochondromatosis of the shoulder in a twelve-year-old boy. *J Shoulder Elbow Surg* 2007; **16**: e15-e19 [PMID: 17056280 DOI: 10.1016/j.jse.2006.02.005]

22 **Lugo R**, Kung P, Ma CB. Shoulder biomechanics. *Eur J Radiol* 2008; **68**: 16-24 [PMID: 18511227 DOI: 10.1016/j.ejrad.2008.02.051]

23 **Ahmad CS**, Wang VM, Sugalski MT, Levine WN, Bigliani LU. Biomechanics of shoulder capsulorrhaphy procedures. *J Shoulder Elbow Surg* 2005; **14**: 12S-18S [PMID: 15726071 DOI: 10.1016/j.jse.2004.09.015]

24 **Villacin AB**, Brigham LN, Bullough PG. Primary and secondary synovial chondrometaplasia: histopathologic and clinicoradiologic differences. *Hum Pathol* 1979; **10**: 439-451 [PMID: 468226 DOI: 10.1016/s0046-8177(79)80050-7]

25 **Milgram JW**. Synovial osteochondromatosis: a histopathological study of thirty cases. *J Bone Joint Surg Am* 1977; **59**: 792-801 [PMID: 908703]

26 **Isbell JA**, Morris AC, Araoye I, Naranje S, Shah AB. Recurrent Extra- and Intra-articular Synovial Chondromatosis of the Ankle with Tarsal Tunnel Syndrome: A Rare Case Report. *J Orthop Case Rep* 2017; **7**: 62-65 [PMID: 28819605 DOI: 10.13107/jocr.2250-0685.752]

World Journal of Clinical Cases

Submit a Manuscript: https://www.f6publishing.com

World J Clin Cases 2022 February 16; 10(5): 1654-1666

DOI: 10.12998/wjcc.v10.i5.1654

ISSN 2307-8960 (online)

CASE REPORT

Wilkie's syndrome as a cause of anxiety-depressive disorder: A case report and review of literature

Raluca Cristina Apostu, Lucian Chira, Doina Colcear, Andrei Lebovici, Georgiana Nagy, Radu Razvan Scurtu, Radu Drasovean

ORCID number: Raluca Cristina Apostu 0000-0001-8646-4241; Lucian Chira 0000-0003-1028-0803; Doina Colcear 0000-0001-6067-5307; Andrei Lebovici 0000-0002-2815-2132; Georgiana Nagy 0000-0002-6134-9762; Radu Razvan Scurtu 0000-0002-7204-3988; Radu Drasovean 0000-0001-8005-0988.

Author contributions: Apostu RC, Scurtu RR, and Drasovean R contributed equally to this work; designed research, analyzed data and wrote the paper; Colcear D, Lebovici A and Nagy G contributed with expert opinions about the case; Apostu RC, Drasovean R, Scurtu RR, and Chira L performed the research and analyzed data; all authors contributed equally to this work.

Informed consent statement: Informed written consent for publication was obtained from the patient in accordance with institutional guidelines.

Conflict-of-interest statement: The authors declare that they have no conflicts of interest.

CARE Checklist (2016) statement: The authors have read the CARE Checklist (2016), and the manuscript was prepared and revised according to the CARE Checklist (2016).

Raluca Cristina Apostu, Lucian Chira, Radu Razvan Scurtu, Radu Drasovean, Department of Surgery, "Iuliu Hatieganu" University of Medicine and Pharmacy, Cluj-Napoca 400001, Romania

Doina Colcear, Department of Psychiatry, Clinical Infectious Disease Hospital, Cluj-Napoca 400000, Romania

Andrei Lebovici, Department of Radiology, "Iuliu Hatieganu" University of Medicine and Pharmacy, Cluj-Napoca 400006, Romania

Georgiana Nagy, Department of Internal Medicine, "Iuliu Hatieganu" University of Medicine and Pharmacy Cluj-Napoca, 400006, Romania

Corresponding author: Radu Razvan Scurtu, MD, PhD, Assistant Professor, Department of Surgery, "Iuliu Hatieganu" University of Medicine and Pharmacy, 8 Victor Babes st, Cluj-Napoca 400006, Romania. razvan.scurtu@umfcluj.ro

Abstract

BACKGROUND

Superior mesenteric artery syndrome is a disease with a complex diagnosis, and it is associated with complications that make it even harder to identify. Currently, a frequent association with psychiatric disorders has been noted. Despite numerous case reports and case series, the variability of the disease has not allowed the development of protocols regarding diagnosis and management.

CASE SUMMARY

A 33-year-old woman presented with abdominal pain, nausea, and bile vomiting over the last 15 mo, associated with a 15-kg weight loss over the last three months. After the onset of the symptoms, the patient was diagnosed with anxiety-depressive disorder and treated appropriately. Standard examinations excluded an organic cause, and the cause of the symptoms was considered psychogenic. The persistence of symptoms, even under treatment, prompted a computer tomography angiography examination of the abdomen and pelvis. The examination identified emergence at a sharp angle of 13.7° of the superior mesenteric artery, with a reduced distance between the artery and the anterior wall of the aorta up to a maximum of 8 mm. A diagnosis of aortomesenteric clamp was established. Surgical treatment by laparoscopic duodenojejunostomy was performed. Postoperative evolution was marked by a patent anastomosis at 1 mo,

Country/Territory of origin: Romania

Specialty type: Surgery

Provenance and peer review: Unsolicited article; Externally peer reviewed.

Peer-review model: Single blind

Peer-review report's scientific quality classification
Grade A (Excellent): 0
Grade B (Very good): 0
Grade C (Good): C
Grade D (Fair): 0
Grade E (Poor): 0

Received: August 13, 2021
Peer-review started: August 13, 2021
First decision: October 20, 2021
Revised: November 5, 2021
Accepted: December 31, 2021
Article in press: December 31, 2021
Published online: February 16, 2022

P-Reviewer: Peltrini R
S-Editor: Ma YJ
L-Editor: A
P-Editor: Ma YJ

with a 10-kg weight gain and improvement of the associated anxiety.

CONCLUSION
This case report underlines two major aspects. One aspect refers to the predisposition of patients with superior mesenteric artery syndrome to develop psychiatric disorders, with an excellent outcome when proper treatment is administered. The second aspect underlines the key role of a multidisciplinary approach and follow-up.

Key Words: Wilkie's syndrome; Weight loss; Anxiety-depressive disorder; Duodenojejunostomy; Laparoscopy; Case report

Core Tip: Wilkie's syndrome is a rare vasculo-intestinal obstructive pathology that is difficult to diagnose due to nonspecific symptoms and the ability to mimic or coexist with other functional disorders. Its association with psychiatric eating disorders makes its differential diagnosis even more complex, allowing it to progress toward late, chronic stages. Untreated disease is associated with significant morbidity and mortality due to complications. It is important to consider its impact on psychosocial status and the appropriate approach to make an exclusion diagnosis.

Citation: Apostu RC, Chira L, Colcear D, Lebovici A, Nagy G, Scurtu RR, Drasovean R. Wilkie's syndrome as a cause of anxiety-depressive disorder: A case report and review of literature. *World J Clin Cases* 2022; 10(5): 1654-1666
URL: https://www.wjgnet.com/2307-8960/full/v10/i5/1654.htm
DOI: https://dx.doi.org/10.12998/wjcc.v10.i5.1654

INTRODUCTION

Superior mesenteric artery (SMA) syndrome is a rare cause of proximal small bowel obstruction, defined as compression of the third part of the duodenum between the aorta and superior mesenteric artery[1]. The syndrome has been given many names, including chronic duodenal ileus, Wilkie's syndrome, arteriomesenteric duodenal compression syndrome, and cast syndrome[1,2].

Its incidence ranges between 0.005 and 0.3%[1,3-7]. In fluoroscopic studies, the reported incidence is 0.01%[8]. A reported incidence of 0.8% was reported by Neri *et al* [9] in a prospective study, while other reports mention a frequency of up to 2.4%[10]. In patients with gastric bypass surgery, the reported prevalence is 0.6%[11].

There are approximately 400 cases reported in the literature. SMA syndrome diagnosed after Roux-en-Y gastric bypass has been reported for 14 cases, while one case was reported after sleeve gastrectomy[12].

Despite numerous case reports, no large trials have been published, the diagnosis is often delayed, and patients are treated with ineffective symptomatic therapies[1,13].

The importance of this pathology is derived from its association with significant morbidity and mortality due to a delayed diagnosis. This is why it is considered an important differential diagnosis, especially in a setting of recent weight loss[1]. Additionally, the choice of treatment requires individual evaluation.

We present the case of a 33-year-old female patient diagnosed with Wilkie's syndrome 15 mo after the onset of symptoms, initially assumed to be anxiety-depressive disorder.

CASE PRESENTATION

Chief complaints

A 33-year-old female patient presented to the emergency department for diffuse, progressive abdominal pain, nausea, bile vomiting, loss of appetite, and weight loss of

15 kg in the last three months. The pain was characteristically located in the epigastrium, with diffuse extension in the rest of the abdomen, after food ingestion.

History of present illness

The symptoms began in the last year, after the initiation of a planned weight loss diet. Over time, her food tolerance gradually decreased, accentuating the symptoms. She presented multiple times to the emergency department with the same symptoms. At every evaluation, an organic cause was excluded, fluid resuscitation was performed, and a psychogenic origin of the symptoms was suspected, given her past medical history.

History of past illness

She was previously diagnosed with Hashimoto thyroiditis and was under levothyroxine replacement therapy at 125 μg/d. After the onset of her symptoms, she was diagnosed with major anxiety-depressive disorder and placed under treatment with alprazolam 0.5 mg, 1 mg/24 h, and escitalopram 10 mg, 25 mg/24 h.

Personal and family history

The patient had a history of irregular diets, with attempts to lose weight under normal weight conditions. Her history included surgical repair of bilateral inguinal hernia and an episode of acute pancreatitis of unknown cause.

Physical examination

Physical examination revealed a cachectic patient with an anxious face and a body mass index (BMI) of 17.8 kg/m^2 (normal level 18.5-24.9 kg/m^2) at 45 kg and 159 cm height, with tenderness in the epigastrium.

Laboratory examinations

Laboratory results showed an elevated hemoconcentration [hemoglobin 16.8 g/dL (n.v. 12-15.5 g/dL), hematocrit 48.8% (n.v. 37%-47%)], with hyposodemia [131 mmol/L (n.v. 136-146 mmol/L)], and hypocloremia [91 mmol/L (n.v. 101-109 mmol/L)], which were easily corrected with fluid resuscitation.

Imaging examinations

Upper digestive endoscopy: Given her symptoms in the superior abdomen, upper digestive endoscopy was performed, and esophagitis and gastritis secondary to bile reflux in the gastric antrum were detected. The first and second parts of the duodenum also had acute erosion and flattened folds. Biopsies were performed to exclude celiac disease and confirm chronic duodenitis. Treatment was initiated with proton pump inhibitor 40 mg, 80 mg/24 h, sucralfate 2 tb/12 h, and prokinetic domperidone 10 mg, 30 mg/24 h. Vitamins were prescribed.

Angio-computed tomography: After one month, given the persistence of the symptoms, computer tomography angiography (Angio-CT) of the abdomen and pelvis was performed. The results revealed emergence at a sharp angle of 13.7° of the superior mesenteric artery, with a reduced distance between the SMA and the anterior wall of the aorta up to a maximum of 8 mm (Figure 1). In this clinical-biological context, a diagnosis of aortomesenteric clamp was established.

Further diagnostic work-up

A psychiatric consultation was performed, and the diagnosis of major anxiety-depressive disorder was confirmed. Treatment was continued with alprazolam 0.5 mg, 1 mg/24 h and escitalopram 10 mg, 25 mg/24 h, and regular evaluations were scheduled.

MULTIDISCIPLINARY EXPERT CONSULTATION

Georgiana Nagy, MD, PhD, Assistant Professor of Gastroenterology, Department of Gastroenterology, "Iuliu Hatieganu" University of Medicine and Pharmacy

The patient presented with a long history (over 1 year) of vomiting, bloating and abdominal pain, symptoms that worsened over the last 3 mo, leading to severe weight loss and the development of a mixed anxiety-depressive disorder. Considering the symptoms, radiologic criteria and failed conservative therapy, we concluded that a

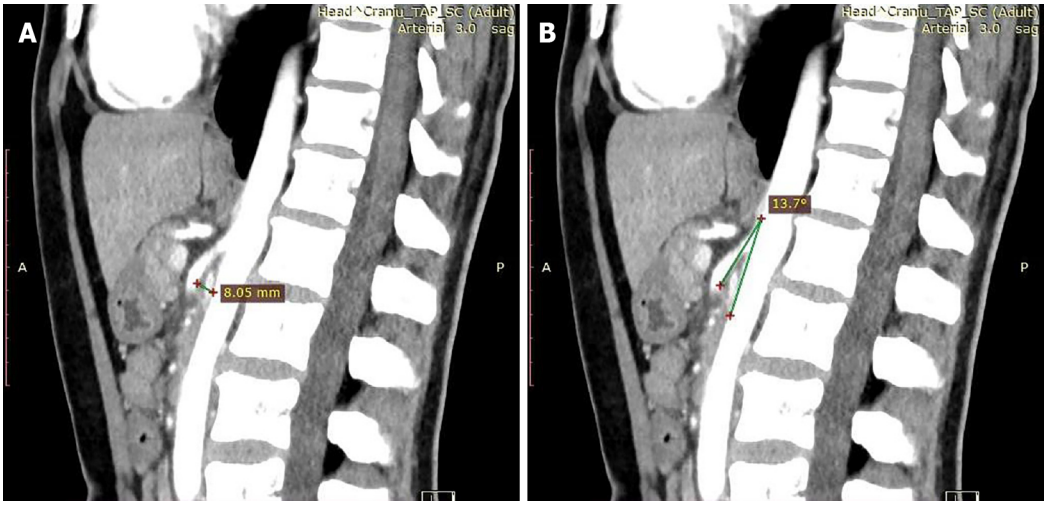

Figure 1 Angio-computed tomography images. A: Reduced distance between the superior mesenteric artery (SMA) and the anterior wall of the aorta up to a maximum of 8.05 mm; B: Emergence at a sharp angle of 13.7° of the SMA.

surgical approach was the only appropriate treatment.

Radu Drasovean, MD, PhD, Assistant Professor of General Surgery, Department of Surgery, "Iuliu Hatieganu" University of Medicine and Pharmacy

Given the long period of persisting symptoms, the severity of the weight loss and the absence of major dehydration or electrolyte abnormalities upon admission, due to fluid resuscitation, nutritional and vitamin supplements used in the period before the diagnosis, the patient shows an indication for surgical treatment with laparoscopic duodenojejunostomy.

Andrei Lebovici, MD, PhD, University Lecturer, Department of Radiology, "Iuliu Hatieganu" University of Medicine and Pharmacy

The angio-CT images helped narrow the differential diagnosis by showing some characteristic features of aortomesenteric clamp without any other morphological changes on CT to suggest other pathological conditions.

Doina Colcear, MD, PhD, Psychiatrist, Clinical Infectious Disease Hospital, Cluj-Napoca, Romania

Repeated psychiatric evaluations prior to the diagnosis of Wilkie's syndrome revealed the presence of an anxiety-depressive disorder that was attributed to somatic symptoms. These psychiatric symptoms persisted after the somatic disease was clarified. Pre- and postoperative antidepressant and anxiolytic treatment with 10 mg/d escitalopramum and 0.5 mg/d alprazolamum helped to relieve the symptoms. Specialized monitoring of the progression of her emotional state after discharge with re-evaluation of treatment is recommended.

FINAL DIAGNOSIS

The final preoperative diagnosis of the presented case was Wilkie's syndrome in a 33-year-old female patient with a secondary anxiety-depressive disorder.

TREATMENT

Laparoscopic duodenojejunostomy was performed. A standard surgical technique was followed. After pneumoperitoneum was induced, four ports were placed: A periombilical 10 mm optic port, 5 mm port in the right lower quadrant, 12 mm working port in the left quadrant, midclavicular line, at the level of the umbilicus, and a 5 mm port in the left upper quadrant, below the costal margin. During exploration, a dilated duodenum in the first and second parts was noticed, with a collapsed third part,

without ascites or other pathological changes (Figure 2). The second portion of the duodenum was mobilized by a partial Kocher maneuver. At 25 cm distal to the ligament of Treitz, a jejunal loop was prepared and positioned near the duodenum. A side-to-side duodenojejunostomy was performed using a -60 mm endoscopic liner articulated stapler (Figure 3). The common enterotomy was closed with 3-0 polydioxanone absorbable sutures (Figure 4).

OUTCOME AND FOLLOW-UP

The postoperative course was uneventful, and the patient was discharged home. Nutritional and gastroenterological monitoring was initiated, while psychiatric monitoring was continued. At the 1-mo evaluation, the patient presented a 10 kg weight gain, with complete remission of symptoms (Figure 5). A barium study was conducted showing a free passage of the contrast through the anastomosis (Figure 6).

At the 5-mo follow-up, the patient was asymptomatic, with a 15 kg weight gain. Considering the favorable postoperative outcome and the degree of weight recovery, the patient continued nutritional and psychiatric monitoring, and psychiatric treatment ceased. Long-term evaluation will establish the degree of involvement of psychiatric pathology in the clinical picture, and final conclusions will be drawn.

DISCUSSION

Superior mesenteric artery syndrome occurs preferentially in young adults and adolescents, with an age range of 10 to 39 years, but cases in 88-year-old patients have also been reported[14]. It occurs more commonly in women, with a 3:2 ratio compared to men[1,4,13].

The primary reported cause of this disease is the loss of the fat pad between the aorta and SMA, resulting in a narrower angle between the vessels and compression of the duodenum[1,12]. This syndrome can be congenital or acquired[1]. Based on this fact, two types of SMA syndrome have been described. The irreversible one (either repeated or permanent) is caused by congenital or developmental factors, such as high insertion of the ligament of Treitz, a low origin of the SMA[5], a short ligament of Treitz, abnormal rotation of the intestines, adhesions due to surgery or duodenal stenosis due to inflammation. Abdominal aortic aneurysms or mesenteric root neoplasms have also been reported to be linked[1,15]. For this type, surgery has been reported as essential for treatment. The reversible type (transient), caused by gravity, for example, can be treated with a conservative approach, including positional changes, intestinal tract decompression and improved nutrition[15]. Furthermore, there might be a genetic component, as suggested by Castro *et al*[16], while 40% of cases have no identifiable risk factors[10].

A rare association has been reported after inferior vena cava (IVC) filter placement with a local inflammatory response and compression of the duodenum between the IVC and the SMA[17].

The main difficulty in establishing the diagnosis of SMA syndrome resides in the fact that patients tend to be asymptomatic until significant weight loss is registered, secondary to intentional dieting or illness. The most frequently reported cause used to be the corrective treatment of scoliosis, where a relative lengthening of the spine increases the tension on the mesentery and narrows the angle between the vessels[13]. Today, things tend to be different, with the majority of published reports suggesting a very common association with a psychiatric disease[4,13]. SMA syndrome can appear secondary to the disease but can also cause psychological and social problems, including depression and anorexia, due to the severity of the disease[2].

This case report is an example of SMA syndrome as a cause of anxiety-depressive disorder. In this patient, the persistence of symptoms for a long period of time, without identifying an organic cause, led to the development of an anxiety-depressive disorder that was interpreted as the source of the symptoms. The condition's progression, with the persistence of symptoms despite treatment of the anxiety, triggered extension of the investigations, with the establishment of a final diagnosis.

A characteristic of this disease is significant weight loss, described in different situations as cachexia (AIDS, malabsorption, cancer, paraplegia), hypermetabolism or dietary conditions (anorexia nervosa, drug use). Patients usually register a marked weight loss of > 5 kg[7]. Less frequent reports are incriminating weight loss following surgery, secondary to bariatric surgery, esophagectomy or abdominal trauma, in its

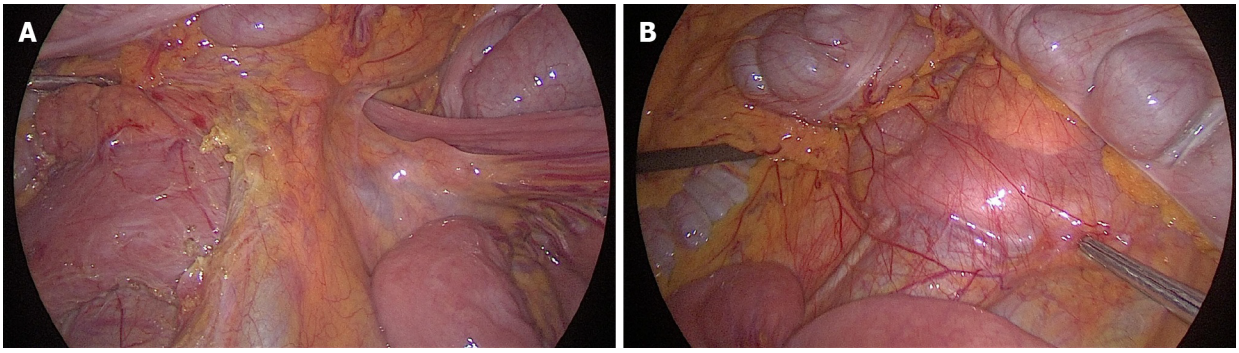

Figure 2 Exploratory laparoscopy. A: Dilated duodenum in the first and second parts; B: A collapsed third part beyond the mesenteric pedicle.

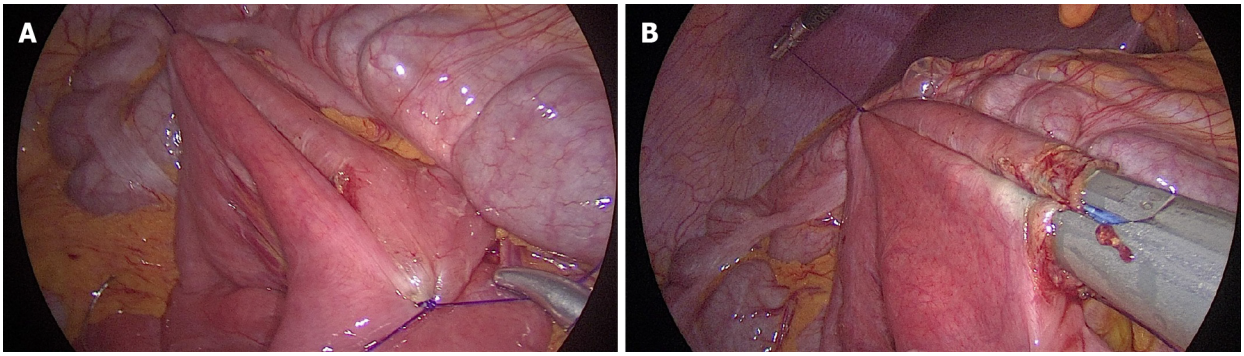

Figure 3 Laparoscopic duodenojejunostomy. A: Threaded spotting of the two enteral segments for the anastomosis; B: Side-to-side duodenojejunostomy using a 60 mm endoscopic liner articulated stapler.

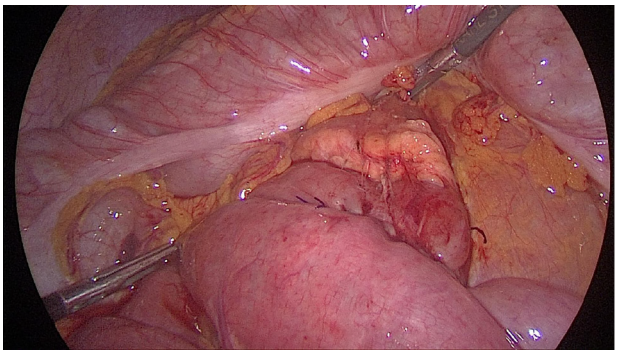

Figure 4 Final aspect of the anastomosis after closing the common enterotomy.

etiology[1,12,13,18,19].

The diagnosis is based on symptoms and radiological testing[1]. It needs a high index of suspicion because of its vague and nonspecific symptoms[12]. Additionally, the measurements performed on imaging investigations must also be correlated with the clinical complaints[8], and even this diagnostic approach cannot exclude all motility disorder cases[4]. Thus, a realistic diagnosis can only be established with a comprehensive panel of investigations, a specific history of symptoms and characteristic imaging changes.

The most frequently reported symptoms are abdominal pain (92%), nausea, vomiting (77%), and weight loss (69.2%)[1,4,13,20,21], while in some cases, a predominance of vomiting (70%), nausea (66.3%), abdominal pain (65%), anorexia (33.8%), postprandial fullness (33.8%), and early satiety (12.5%) was reported[3,22]. Another reported characteristic is epigastric pain, which worsens in the supine position[1,4,10]. A sign that can help suggest the diagnosis is the relief of the patient's symptoms when leaning forward[12] or in the left lateral decubitus position[13]. In our case, weight loss was followed by abdominal pain, nausea, and vomiting, a vicious cycle followed by a

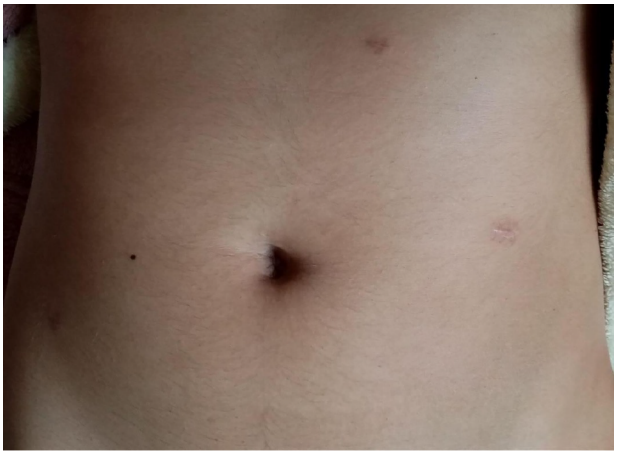

Figure 5 Postoperative aspect of the abdomen at 1 mo evaluation, with 10 kg weight gain.

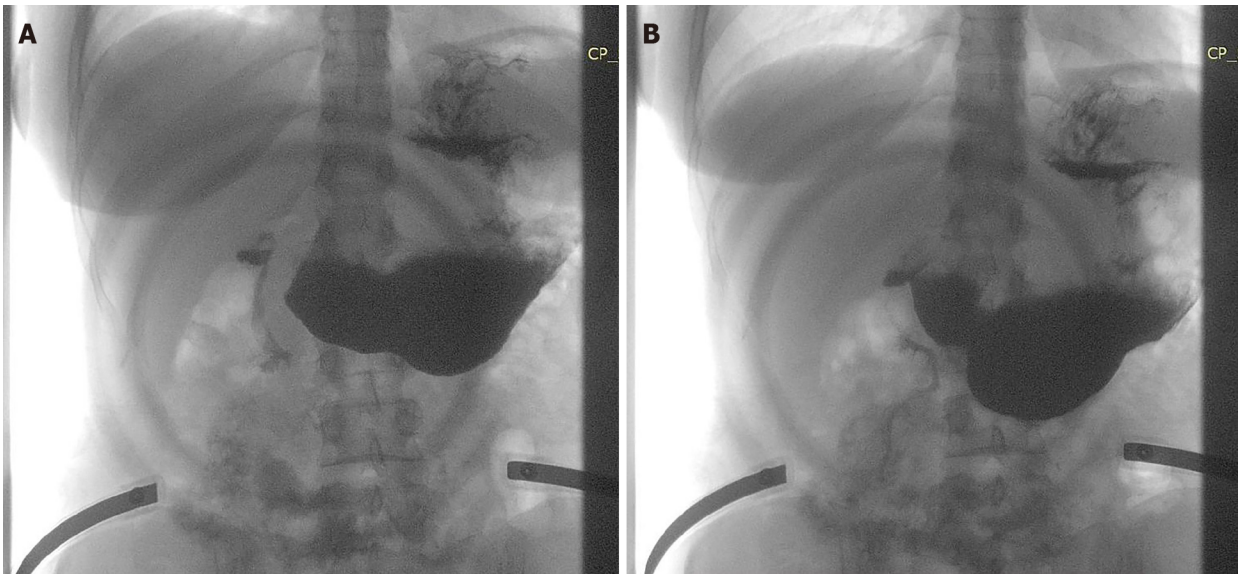

Figure 6 Oral gastrografin study. A: Free passage of the contrast through the anastomosis in the small bowel; B: Contraction of the stomach and duodenum.

marked reduction in weight.

The heterogeneous presentation is aggravated by the presence of comorbidities, such as mental and behavioral disorders (21.3%), infectious disorders (12.5%), and disorders of the nervous system (11.3%)[6].

An acute course of the disease has been described with life-threatening dilatation of the stomach[1]. Despite that, a long-standing onset seems to be more characteristic, with symptom persistence between 6 and 24 mo[7,13], while a time lag of 1 to 51 mo until diagnosis is often described[4,6].

Usually, physical examination and laboratory findings are nonspecific[3]. Despite the marked weight loss, patients have serum albumin and serum proteins within normal limits, while frequent electrolyte abnormalities are encountered[13].

The most commonly used imaging modalities are contrast-enhanced computed tomography and MRA[23]. Computed tomography (CT) angiography is a more specific investigation, while endoscopy and ultrasound are adjunctive diagnostic methods[6].

CT angiography measures the aortomesenteric angle and the distance between the two vessels. A normal aortomesenteric angle is between 25° and 87° with different subintervals in different reports[1-4,8,10,13,17]. The normal reported distance between the two vessels is 10 mm-34 mm[2,3,8,21], confirmed by imaging studies[8]. The mean reported angle measurements are 12°[13] and 13.5°[8], with a mean measured distance of 4.4 mm[8]. However, there are variations regarding the angle dimensions, between 6°-22° in different reports[1,3,4,8,10,13,21], while reported variations regarding

distance are between 2 mm and < 10 mm[1-4,8,10,13,21]. It has been suggested that the distance is more accurate for SMA diagnosis than the angle[7].

Cases with SMA syndrome with an angle and distance overlapping the normal range have also been reported. An aorto-mesenteric angle < 8°-46° and a distance < 8 mm have been specifically reported, compared to 25°-87° and 10-34 mm identified in control groups as normal values. In these cases, other diagnostic methods must be considered, such as gastric-emptying scintigraphy[23].

Reports suggest an association of the degree of angulation with (BMI)[10,24]. Alzervi found a significant reduction in the aortomesenteric angle and distance in patients with SMA syndrome compared to other patients with acute or chronic abdominal pain, while BMI was positively correlated with the aortomesenteric angle and distance. Thus, BMI could be used as a screening factor for SMA syndrome[21].

Characteristic CT findings are not just numerical cutoff but also distension of the stomach and proximal duodenum or narrowing of the duodenum at the SMA level. Association with compression of the left renal vein, isolated left renal vein thrombosis, enlargement of the left gonadal vein, or left-sided venous collaterals are additional elements to consider for a positive diagnosis[8].

Rotational CT from the supine to prone position can demonstrate improved outflow passing the SMA[12]. Additionally, CT has replaced magnetic resonance enterography (MRE) as a standard investigation[1,21]. The advantage of showing anatomical variants and consequences, such as delayed transit and obstruction, is highlighted in limited reports using MRE[25].

Diagnosis can also be confirmed by mesenteric artery ultrasonography[12]. Color Doppler ultrasound can also measure the aortomesenteric angle[23].

Endoscopy is useful to diagnose complications, such as esophagitis, reflux gastritis, stasis, and chronic duodenal obstruction[1,13,21]. However, a suspicion of obstruction of the third part of the duodenum is raised only in some cases during endoscopy[13]. A more specific finding for the diagnosis is pulsatile extrinsic compression of the duodenum, excluding other diseases of the superior digestive tract[23].

Barium or gastrografin contrast studies are classic diagnostic procedures, and specific findings are dilatation of the stomach and the first and second parts of the duodenum and the failure of contrast passage in the third part of the duodenum, with antiperistaltic flow[13,23,26]. However, these changes are not specific to SMA syndrome[23].

Gastric-emptying scintigraphy is a known imaging modality to evaluate gastroparesis and gastric motility, and it might be of great value for a differential diagnosis between SMA syndrome and gastric motility disorders, especially in patients with diabetes. This investigation provides a qualitative and quantitative analysis of gastric motility, which might allow differential diagnosis of similar diseases and an assessment of the degree of obstruction or stenosis[23]. Other differentials include internal hernia, adhesive disease, intussusception[12], and megaduodenum[13].

Another difficult situation occurs in cases associated with systemic sclerosis, in which gastrointestinal involvement creates a clinical picture similar to SMA syndrome, with progression toward malnutrition[27]. Another rare condition that has to be differentiated is aortoduodenal syndrome, namely, obstruction of the third portion of the duodenum by a large abdominal aortic aneurysm[28].

If the disease is unrecognized and left untreated, severe complications may occur, such as malnutrition, dehydration, electrolyte abnormalities, gastric pneumatosis and portal venous gas, gastric perforation, duodenal compromise, ischemia, necrosis[1,17], or gastrointestinal hemorrhage[1]. Patients with severe hypokalemia, metabolic alkalosis, and acute kidney injury resulting in cardiorespiratory arrest have also been described[29]. Recognition of the condition, even in advanced stages with massive gastric dilatation and gastric ischemia lesions, can lead to remission of the pathological changes with decompression and endoscopic surveillance[15,30], without the need for surgery.

The management of SMA syndrome is individualized, with either conservative treatment and nutritional support or invasive treatment[3]. Multidisciplinary management is necessary[1]. Given that there is a common association with psychiatric disease or dietary conditions[1,4,13], psychotherapy is an important part of treatment [31], while patients should also be educated on lifestyle changes. Most patients require a dietary consultation for their significant weight loss[1] and a close clinical follow-up by a gastroenterologist and a nutritionist[23].

In the conservative approach, the primary focus should be on weight regain with mass restoration while monitoring the caloric needs with care to avoid refeeding syndrome and recovery of the electrolyte balance[2,5]. Treatment includes nasogastric decompression, prokinetic agents, fluid resuscitation, electrolyte correction, parenteral

nutrition, nasogastric tube insertion, nutritional support through hyperalimentation [1], and the removal of precipitating factors. Nutrition may be provided by small, frequent meals or nasojejunal feeding, with the aim of providing a high-calorie diet to increase the mesenteric fat and expand the angle[26]. Positional changes and different maneuvers have also been reported as aids in tolerating enteral feeds, such as the prone position, left lateral decubitus, knee-chest maneuver, or Hayes maneuver. In cases of failure, parenteral nutrition should be considered[5].

Retrospective studies have reported successful treatment of SMA syndrome in short-term follow-up with enteral nutrition[15,17,26,30-34]. After a mean period of 10 mo with enteral therapy, 65% of patients were without symptoms, while in 15%, their symptoms had improved. Nutrition was administered *via* a nasal jejunal tube and percutaneous endoscopic gastrostomy with a jejunal extension tube. The reported complications were all catheter-related[35].

The success rates for medical management are reported to be between 14% and 83% [6,10], with a 71.3% success rate at a 5-mo follow-up[35]. Predictors of a poor response are a chronic course of disease, prolonged medical treatment, or associated psychosocial disorders[6].

In children, successful treatment was in most reports obtained by the medical approach, with a decline in the need for surgery from 70% to 14%. An acute presentation was most often registered, while weight loss was not a necessary condition. The expected outcome in these cases was excellent[36].

However, as the syndrome progresses, nutritional support becomes less successful, and surgical correction is necessary[17]. Recently, many studies have suggested an earlier surgical approach, since prolonged medical therapy is associated with multiple admissions, a lower success rate, and increased disease recurrence. They recommended no more than 3 mo for a trial of conservative management[6,22].

More than 75% of patients with SMA syndrome require surgical intervention[24]. Surgery usually follows a period of refeeding and the correction of electrolyte disorders. Although significant preoperative weight loss is a known risk factor for postoperative complications, there are no data about an optimal period for nutritional support, either enteral or parenteral, or indications for its use. According to some reports, surgery may be safely performed in the presence of normal serum proteins using preoperative nutritional supplementation on an individual basis. Other reports suggest nasogastric decompression and total parenteral nutrition for 7 d before surgery[2].

Several procedures have been described as a possible surgical treatment for SMA syndrome: duodenal circular drainage, derotation procedure, transposition of the SMA to the infrarenal aorta, anterior transposition of the third part of the duodenum, Billroth II gastrectomy, gastrojejunostomy, Ladd's procedure, Strong's operation and transabdominal or laparoscopic duodenojejunostomy[1,6,13]. All of these procedures are associated with nutritional loss, blind loop syndrome, gastric bile reflux[2,5] or a risk of duodenal entrapment between the pancreaticoduodenal arteries and a persistence of the symptoms in 25% of cases after the Strong procedure[5,10,13]. Based on their possible complications, these procedures have all been abandoned, except for duodenojejunostomy[6]. Duodenojejunostomy can significantly improve symptoms, physical activity, emotional well-being, and social functioning[12]. Laparoscopic duodenojejunostomy has the advantages of an acceptable operating time, a faster recovery, reduced postoperative pain, shorter hospitalization, reduced risk of incisional hernia, and a good cosmetic outcome[1,4,6,10,16,26], which makes it important in young patients with associated psychosocial symptoms secondary to the severity of their disease[2]. Blind loop syndrome is the most common complication after this type of procedure[13].

To close the common enterotomy, a mini laparotomy and a manual suture were performed in most of the reported cases to avoid a narrowed anastomosis. An alternative to this approach is to close the enterotomy with a laparoscopic suture or a linear stapler in a complete laparoscopic maneuver[26], as was done in our patient.

The success rate of surgical treatment is reported to be as high as 75%-100%[1,4,8,10, 16]. Minimally invasive procedures, including robotic and single-port approaches[37], have reported a success rate of more than 90% with a 7% complication rate[6], while laparoscopic duodenojejunostomy alone has a success rate of 96%[1,10].

In Lee *et al*[22]'s case series, where half of the patients presented with associated diseases, a medical treatment success rate of 71.3%, with a 15.8% recurrence rate, was reported, while surgical management had a 92.9% success rate.

The postoperative course is marked by a major weight gain, usually registered during the first postoperative 6 mo with a mean gain between 5 and 15 kg[13].

Intermediate follow-up results were reported by Chang *et al*[4] for 26 patients treated with laparoscopic or robotic duodenojejunostomy, with the majority of cases secondary to psychiatric disease. Only 33.3% declared resolution or improvement of their symptoms, while 30% of patients were still severely symptomatic, with 19% of patients still requiring nutritional supplementation. Recurrence was associated with a patent anastomosis and the concomitant presence of dysmotility disorders, such as gastroparesis or global intestinal dysmotility, with an indication for intestinal transplant[4]. An important conclusion was that radiographic findings of SMA syndrome should not automatically be assumed to exclude intestinal dysmotility syndrome[4,20]. Given the overlapping symptomatology, gastrointestinal transit studies should always be included in the preoperative workup[4].

Although there are several reports of SMA syndrome, diagnosed as a complication of anorexia nervosa, only a few of them emphasize the evolution of psychiatric disease. Kurisu *et al*[38] pointed out that surgical treatment must be cautiously considered in cases of anorexia nervosa, as the long-term results are unclear. They also reported the case of a patient with anorexia nervosa and SMA syndrome treated with surgery, without postoperative improvement. In this case, a psychological approach was necessary to be continued[38]. On the other hand, Kornmehl *et al*[39] emphasized the overdiagnosis of anorexia nervosa, while SMA syndrome should be considered in these cases. The novelty of our case is represented by the absence of a history of psychiatric diseases, a diagnosis of the disorder after the onset of symptoms, while a restoration of her body weight was registered postoperatively, and psychiatric treatment was stopped.

In their case series, Sun *et al*[4] reported a mean weight gain of 3.8 kg at mid-term follow-up, with reported complications such as infection and dumping syndrome.

Cienfuegos *et al*[20] presented long-term results (median follow-up of 94 mo) after laparoscopic latero-lateral duodenojejunostomy, with excellent results in 61.5% of cases. Long-term results were also evaluated by Jain *et al*[6] with weight gain, complete symptom remission, and no recurrence.

Even though this pathology is rarely described in elderly patients, for this category and in those with significant comorbidities, endoscopic ultrasound-guided gastroenterostomy (EUS-GE) was reported as an appropriate procedure[14,40]. EUS-GE using lumen-apposing metal stents seems to be a safe and effective option[40], with a success rate of 90%, adverse events in 5% of patients and a reintervention rate of 11%[41]. A rate of 83% in preventing surgery was reported, with a mean period of 8.5 mo until symptom resolution and removal of the LAMS and a 5.6% rate of recurrent symptoms [42]. A comparison between EUS gastrojejunostomy and laparoscopic gastrojejunostomy was performed, showing a similar success rate and a significantly higher rate of complications for the surgical procedure[43-45].

In addition to the specificity of this complex pathology, some rare associations have been reported in the literature. One of them is the nutcracker syndrome[13,31]. The most commonly reported causes of this rare syndrome are anatomical variants such as posterior renal ptosis, a high course of the left renal vein and abnormal SMA branching, but the two syndromes can coexist in the context of major weight loss. Treatment for nutcracker syndrome varies from conservative management to different surgical procedures, with the best results reported after laparoscopic extravascular titanium stent placement[5].

In a small number of cases, an association with cystic fibrosis has been reported. In these cases, BMI below the 5th percentile is the best predictor of SMA syndrome. The diagnosis is difficult because of the risk of cystic fibrosis enteropathy[24]. Other rare associations are hyperthyroidism-related sympathetic hyperstimulation, vasculopathy and cerebellar infarction[46] and diabetic patients with excessive body weight loss and associated ketoacidosis after using sodium-glucose cotransporter 2 inhibitors[47]. Rare associations with rheumatoid arthritis and rheumatoid cachexia have also been reported[48].

This case report highlights the importance of SMA syndrome, especially regarding the consequences when left undiagnosed and untreated for a long period of time, as well as the numerous possibilities of its overlapping with other functional diseases or even being the cause of their onset.

The major limitation of this case report is the short follow-up, which allowed us to register the resolution of the anxiety disorder. Only a long-term follow-up will confirm that the syndrome can be a cause for the psychiatric disorder and not the other way around.

CONCLUSION

SMA syndrome is a rare occlusive pathology that needs an extensive diagnostic workup since it is hampered by a specific mimicry of psychiatric or motility disorders. The vicious cycle of its progression can be interrupted by knowing and considering the large number of differential diagnostic possibilities while individualizing the treatment. Since favorable results depend on the treatment of multiple systems, multidisciplinary management is mandatory.

REFERENCES

1 **Van Horne N**, Jackson JP. Superior mesenteric artery syndrome. In: StatPearls [Internet]. Treasure Island (FL): StatPearls Publishing; 2021 Jul 21 [PMID: 29489172]
2 **Barkhatov L**, Tyukina N, Fretland ÅA, Røsok BI, Kazaryan AM, Riis R, Edwin B. Superior mesenteric artery syndrome: quality of life after laparoscopic duodenojejunostomy. *Clin Case Rep* 2018; **6**: 323-329 [PMID: 29445471 DOI: 10.1002/ccr3.1242]
3 **Lima Silva A**, Antunes D, Cordeiro E Cunha J, Nogueira R, Fernandes D, Salazar T, Madureira Pinto C. Epigastric Pain and Weight Loss - A Case of Wilkie's Syndrome. *Eur J Case Rep Intern Med* 2020; **7**: 001557 [PMID: 32399444 DOI: 10.12890/2020_001557]
4 **Chang J**, Boules M, Rodriguez J, Walsh M, Rosenthal R, Kroh M. Laparoscopic duodenojejunostomy for superior mesenteric artery syndrome: intermediate follow-up results and a review of the literature. *Surg Endosc* 2017; **31**: 1180-1185 [PMID: 27405482 DOI: 10.1007/s00464-016-5088-2]
5 **Diab S**, Hayek F. Combined Superior Mesenteric Artery Syndrome and Nutcracker Syndrome in a Young Patient: A Case Report and Review of the Literature. *Am J Case Rep* 2020; **21**: e922619 [PMID: 32772039 DOI: 10.12659/AJCR.922619]
6 **Jain N**, Chopde A, Soni B, Sharma B, Saini S, Mishra S, Gupta R, Bhojwani R. SMA syndrome: management perspective with laparoscopic duodenojejunostomy and long-term results. *Surg Endosc* 2021; **35**: 2029-2038 [PMID: 32342220 DOI: 10.1007/s00464-020-07598-1]
7 **Sinagra E**, Raimondo D, Albano D, Guarnotta V, Blasco M, Testai S, Marasà M, Mastrella V, Alaimo V, Bova V, Albano G, Sorrentino D, Tomasello G, Cappello F, Leone A, Rossi F, Galia M, Lagalla R, Midiri F, Morreale GC, Amvrosiadis G, Martorana G, Spampinato MG, Virgilio V, Midiri M. Superior Mesenteric Artery Syndrome: Clinical, Endoscopic, and Radiological Findings. *Gastroenterol Res Pract* 2018; **2018**: 1937416 [PMID: 30224915 DOI: 10.1155/2018/1937416]
8 **Raman SP**, Neyman EG, Horton KM, Eckhauser FE, Fishman EK. Superior mesenteric artery syndrome: spectrum of CT findings with multiplanar reconstructions and 3-D imaging. *Abdom Imaging* 2012; **37**: 1079-1088 [PMID: 22327421 DOI: 10.1007/s00261-012-9852-z]
9 **Neri S**, Signorelli SS, Mondati E, Pulvirenti D, Campanile E, Di Pino L, Scuderi M, Giustolisi N, Di Prima P, Mauceri B, Abate G, Cilio D, Misseri M, Scuderi R. Ultrasound imaging in diagnosis of superior mesenteric artery syndrome. *J Intern Med* 2005; **257**: 346-351 [PMID: 15788004 DOI: 10.1111/j.1365-2796.2005.01456.x]
10 **Martínez H**, Martínez S, Sánchez-Ussa S, Pedraza M, Cabrera LF. Laparoscopic management for Wilkie´s syndrome. *Cir Cir* 2019; **87**: 22-27 [PMID: 31501628 DOI: 10.24875/CIRU.18000571]
11 **Chrysikos D**, Troupis T, Tsiaoussis J, Sgantzos M, Bonatsos V, Karampelias V, Piperos T, Kalles V, Theodoropoulos P, Kakaviatos D, Flessas I, Nikou E, Mariolis-Sapsakos T. Superior mesenteric artery syndrome: a rare case of upper gastrointestinal obstruction. *J Surg Case Rep* 2019; **2019**: rjz054 [PMID: 30886692 DOI: 10.1093/jscr/rjz054]
12 **Andrew BD**, Hamed AB, Gourash W, Ahmed BH. Laparoscopic duodenojejunostomy to manage small bowel obstruction due to superior mesenteric artery syndrome after Roux-en-Y gastric bypass. *Surg Obes Relat Dis* 2021; **17**: 242-244 [PMID: 33172702 DOI: 10.1016/j.soard.2020.09.038]
13 **Merrett ND**, Wilson RB, Cosman P, Biankin AV. Superior mesenteric artery syndrome: diagnosis and treatment strategies. *J Gastrointest Surg* 2009; **13**: 287-292 [PMID: 18810558 DOI: 10.1007/s11605-008-0695-4]
14 **Bronswijk M**, Fransen L, Vanella G, Hiele M, van der Merwe S. Successful treatment of superior mesenteric artery syndrome by endoscopic ultrasound-guided gastrojejunostomy. *Endoscopy* 2021; **53**: 204-205 [PMID: 32559775 DOI: 10.1055/a-1190-3228]
15 **Furuya Y**, Wakahara T, Furuya A, Yanagie H, Yasuhara H. Rare bowel emphysema with superior mesenteric artery syndrome after surgery. *Ann R Coll Surg Engl* 2020; **102**: e26-e28 [PMID: 31418283 DOI: 10.1308/rcsann.2019.0114]
16 **Aneiros Castro B**, Cano Novillo I, García Vázquez A, Martín Alelu R, Gómez Fraile A. Wilkie's syndrome in monozygotic twins treated by 3-D laparoscopic duodenojejunostomy. *Asian J Endosc Surg* 2019; **12**: 125-127 [PMID: 29673098 DOI: 10.1111/ases.12489]
17 **Haidar A**, Davies A, Hussain A, Gregerson S, Thammineni D, Markus J. Wilkie's Weight Loss Wonder, A Case Series. *Spartan Med Res J* 2020; **5**: 13485 [PMID: 33655184 DOI: 10.51894/001c.13485]
18 **Haider A**, Sharma M, Siddiqa A. Superior Mesenteric Artery Syndrome: A Forgotten Cause of Duodenal Obstruction. *Cureus* 2020; **12**: e10710 [PMID: 33133874 DOI: 10.7759/cureus.10710]

19 **Wong LH**, Sutton TL, Spurrier RG, Zigman AF, Mayo SC. Post-Operative Superior Mesenteric Artery Syndrome Following Retroperitoneal Sarcoma Resection. *Clin Pract* 2020; **11**: 2-7 [PMID: 33599214 DOI: 10.3390/clinpract11010002]

20 **Cienfuegos JA**, Hurtado-Pardo L, Valentí V, Landecho MF, Vivas I, Estévez MG, Diez-Caballero A, Hernández-Lizoáin JL, Rotellar F. Minimally Invasive Surgical Approach for the Treatment of Superior Mesenteric Artery Syndrome: Long-Term Outcomes. *World J Surg* 2020; **44**: 1798-1806 [PMID: 32030438 DOI: 10.1007/s00268-020-05413-5]

21 **Alzerwi NAN**. Predictors of Superior Mesenteric Artery Syndrome: Evidence from a Case-Control Study. *Cureus* 2020; **12**: e9715 [PMID: 32821627 DOI: 10.7759/cureus.9715]

22 **Lee TH**, Lee JS, Jo Y, Park KS, Cheon JH, Kim YS, Jang JY, Kang YW. Superior mesenteric artery syndrome: where do we stand today? *J Gastrointest Surg* 2012; **16**: 2203-2211 [PMID: 23076975 DOI: 10.1007/s11605-012-2049-5]

23 **Kang S**, Choi BW. Clinical Usefulness of Gastric-emptying Scintigraphy in Superior Mesenteric Artery Syndrome: A Case Report. *Nuklearmedizin* 2020; **59**: 335-337 [PMID: 32227314 DOI: 10.1055/a-1140-5430]

24 **Schwarz J**, Sýkora J, Pomahačová R, Sýkorová A, Fremuth J, Šašek L, Vondráková R, Kreslová M. Rare cause of upper bowel obstruction arising in a 17-year-old boy with cystic fibrosis: Superior mesenteric artery (Wilkie's) syndrome. *J Paediatr Child Health* 2020; **56**: 1827-1829 [PMID: 32364286 DOI: 10.1111/jpc.14904]

25 **Cicero G**, D'Angelo T, Bottari A, Costantino G, Visalli C, Racchiusa S, Marino MA, Cavallaro M, Frosina L, Blandino A, Mazziotti S. Superior Mesenteric Artery Syndrome in Patients with Crohn's Disease: A Description of 2 Cases Studied with a Novel Magnetic Resonance Enterography (MRE) Procedure. *Am J Case Rep* 2018; **19**: 431-437 [PMID: 29643328 DOI: 10.12659/ajcr.908273]

26 **Yoneda A**, Kanetaka K, Yamaguchi S, Koga Y, Isagawa Y, Maruya Y, Inoue Y, Torashima Y, Adachi T, Hidaka M, Kobayashi K, Ito S, Eguchi S. Complete laparoscopic duodenojejunostomy for superior mesenteric artery syndrome: Linear stapled closure of the common enterotomy. *Asian J Endosc Surg* 2020; **13**: 552-555 [PMID: 31845494 DOI: 10.1111/ases.12773]

27 **Chua CG**, Wansaicheong GK, Lim WC, Thong BY. Superior Mesenteric Artery Syndrome: A Potentially Fatal but Reversible Gastrointestinal Manifestation of Systemic Sclerosis. *Case Rep Rheumatol* 2020; **2020**: 8831417 [PMID: 32695548 DOI: 10.1155/2020/8831417]

28 **Parashar K**, Gandhi D, Nepal P, Sapire J, Ahuja K, Siddiqui I. Abdominal aortic aneurysm and its association with duodenal obstruction: aortoduodenal syndrome. *BJR Case Rep* 2020; **6**: 20200040 [PMID: 33299591 DOI: 10.1259/bjrcr.20200040]

29 **Mohammad Kazmin NE**, Kamaruzaman L, Wong Z, Fong VK, Mohd R, Mustafar R. Acute Kidney Injury Caused by Superior Mesenteric Artery Syndrome. *Case Rep Nephrol* 2020; **2020**: 8364176 [PMID: 32328326 DOI: 10.1155/2020/8364176]

30 **Sakurai Y**, Hirai F, Abe M, Okaya T, Suzuki H, Sugano I. A case of gastric ischemia caused by massive gastric dilatation due to superior mesenteric artery syndrome. *Clin J Gastroenterol* 2020; **13**: 1066-1069 [PMID: 32720221 DOI: 10.1007/s12328-020-01192-7]

31 **Lin TH**, Lin CC, Tsai JD. Superior mesenteric artery syndrome and nutcracker syndrome. *Pediatr Neonatol* 2020; **61**: 351-352 [PMID: 31902598 DOI: 10.1016/j.pedneo.2019.12.003]

32 **Russell EA**, Braverman RM, Vasudevan SA, Patel B. A Traumatic Quinceañera: Acute Superior Mesenteric Artery Syndrome in an Adolescent Girl. *Pediatr Emerg Care* 2021; **37**: e203-e205 [PMID: 30130339 DOI: 10.1097/PEC.0000000000001563]

33 **Ren PLJ**, Gupta A. Adolescent with Superior Mesenteric Artery Syndrome. *J Radiol Case Rep* 2020; **14**: 14-23 [PMID: 33082917 DOI: 10.3941/jrcr.v14i3.3830]

34 **Dimopoulou A**, Zavras N, Alexopoulou E, Fessatou S, Dimopoulou D, Attilakos A. Superior mesenteric artery syndrome mimicking cyclic vomiting syndrome in a healthy 12-year-old boy. *J Paediatr Child Health* 2020; **56**: 168-170 [PMID: 31408239 DOI: 10.1111/jpc.14592]

35 **Wan S**, Zhang L, Yang J, Gao X, Wang X. Superior Mesenteric Artery Syndrome Improved by Enteral Nutritional Therapy: A Retrospective Case-Series Study in a Single Institution. *Ann Nutr Metab* 2020; **76**: 37-43 [PMID: 32172254 DOI: 10.1159/000506620]

36 **Biank V**, Werlin S. Superior mesenteric artery syndrome in children: a 20-year experience. *J Pediatr Gastroenterol Nutr* 2006; **42**: 522-525 [PMID: 16707974 DOI: 10.1097/01.mpg.0000221888.36501.f2]

37 **Konstantinidis H**, Charisis C, Kottos P. Robotic Strong's procedure for the treatment of superior mesenteric artery syndrome. Description of surgical technique on occasion of the first reported case in the literature. *Int J Med Robot* 2018; **14** [PMID: 29168288 DOI: 10.1002/rcs.1876]

38 **Kurisu K**, Yamanaka Y, Yamazaki T, Yoneda R, Otani M, Takimoto Y, Yoshiuchi K. A clinical course of a patient with anorexia nervosa receiving surgery for superior mesenteric artery syndrome. *J Eat Disord* 2021; **9**: 79 [PMID: 34193279 DOI: 10.1186/s40337-021-00436-2]

39 **Kornmehl P**, Weizman Z, Liss Z, Bar-Ziv J, Joseph A. Superior mesenteric artery syndrome presenting as an anorexia nervosa-like illness. *J Adolesc Health Care* 1988; **9**: 340-343 [PMID: 3417512 DOI: 10.1016/0197-0070(88)90263-x]

40 **Kouanda A**, Watson R, Binmoeller KF, Nett A, Hamerski C. EUS-guided gastroenterostomy for duodenal obstruction secondary to superior mesenteric artery syndrome. *VideoGIE* 2021; **6**: 14-15 [PMID: 33490746 DOI: 10.1016/j.vgie.2020.09.008]

41 **McCarty TR**, Garg R, Thompson CC, Rustagi T. Efficacy and safety of EUS-guided gastroenterostomy for benign and malignant gastric outlet obstruction: a systematic review and meta-

analysis. *Endosc Int Open* 2019; **7**: E1474-E1482 [PMID: 31673620 DOI: 10.1055/a-0996-8178]

42 **James TW**, Greenberg S, Grimm IS, Baron TH. EUS-guided gastroenteric anastomosis as a bridge to definitive treatment in benign gastric outlet obstruction. *Gastrointest Endosc* 2020; **91**: 537-542 [PMID: 31759034 DOI: 10.1016/j.gie.2019.11.017]

43 **Tyberg A**, Perez-Miranda M, Sanchez-Ocaña R, Peñas I, de la Serna C, Shah J, Binmoeller K, Gaidhane M, Grimm I, Baron T, Kahaleh M. Endoscopic ultrasound-guided gastrojejunostomy with a lumen-apposing metal stent: a multicenter, international experience. *Endosc Int Open* 2016; **4**: E276-E281 [PMID: 27004243 DOI: 10.1055/s-0042-101789]

44 **Perez-Miranda M**, Tyberg A, Poletto D, Toscano E, Gaidhane M, Desai AP, Kumta NA, Fayad L, Nieto J, Barthet M, Shah R, Brauer BC, Sharaiha RZ, Kahaleh M. EUS-guided Gastrojejunostomy Versus Laparoscopic Gastrojejunostomy: An International Collaborative Study. *J Clin Gastroenterol* 2017; **51**: 896-899 [PMID: 28697151 DOI: 10.1097/MCG.0000000000000887]

45 **Xu MM**, Dawod E, Gaidhane M, Tyberg A, Kahaleh M. Reverse Endoscopic Ultrasound-Guided Gastrojejunostomy for the Treatment of Superior Mesenteric Artery Syndrome: A New Concept. *Clin Endosc* 2020; **53**: 94-96 [PMID: 31794656 DOI: 10.5946/ce.2018.196]

46 **Wang HK**, Huang WH, Chen KT. An extensive posterior circulation infarction secondary to primary hyperthyroidism accompanied with superior mesenteric artery syndrome: A case report and description of patho-physiological association. *Medicine (Baltimore)* 2020; **99**: e22664 [PMID: 33181647 DOI: 10.1097/MD.0000000000022664]

47 **Hirai T**, Kitada M, Hayashi Y, Monno I, Takagaki Y, Shimada K, Ogura Y, Fujii M, Konishi K, Nakagawa A, Koya D. Case report of superior mesenteric artery syndrome that developed in a lean type 2 diabetes patient and was associated with rapid body weight loss after sodium-glucose cotransporter 2 inhibitor administration. *J Diabetes Investig* 2020; **11**: 1359-1362 [PMID: 32020751 DOI: 10.1111/jdi.13228]

48 **Galarza-Delgado DÁ**, Flores-Alvarado DE, Compeán-Villegas JE. Superior mesenteric artery syndrome in a patient with rheumatoid arthritis and rheumatoid cachexia during the COVID-19 pandemic. *Clin Rheumatol* 2021; **40**: 2095-2096 [PMID: 33428099 DOI: 10.1007/s10067-020-05570-x]

World Journal of Clinical Cases

Submit a Manuscript: https://www.f6publishing.com

World J Clin Cases 2022 February 16; 10(5): 1667-1674

DOI: 10.12998/wjcc.v10.i5.1667

ISSN 2307-8960 (online)

CASE REPORT

Gastric schwannoma misdiagnosed as gastrointestinal stromal tumor by ultrasonography before surgery: A case report

Qing-Qing Li, Dong Liu

ORCID number: Qing-Qing Li 0000-0002-3166-3195; Dong Liu 0000-0001-8285-2394.

Author contributions: Li QQ reviewed the literature and helped draft the manuscript; Liu D revised the manuscript for important intellectual content and analyzed and interpreted the imaging findings; All authors approved the submitted manuscript.

Informed consent statement: Informed written consent was obtained from the patient for publication of this report and any accompanying images.

Conflict-of-interest statement: The authors declare that they have no conflict of interest.

CARE Checklist (2016) statement: The authors have read the CARE Checklist (2016), and the manuscript was prepared and revised according to the CARE Checklist (2016).

Supported by the National Natural Science Foundation of China, No. 82001819.

Country/Territory of origin: China

Specialty type: Radiology, nuclear medicine and medical imaging

Provenance and peer review:

Qing-Qing Li, Dong Liu, Department of Ultrasound, Beijing Friendship Hospital, Capital Medical University, Beijing 100050, China

Corresponding author: Dong Liu, Doctor, PhD, Associate Chief Physician, Department of Ultrasound, Beijing Friendship Hospital, Capital Medical University, No. 95 Yongan Road, Xicheng District, Beijing 100050, China. winterwenny@126.com

Abstract

BACKGROUND

Gastric origin tumors were diagnosed and evaluated preoperatively by gastroscopy, endoscopic ultrasonography, computed tomography (CT) or magnetic resonance imaging. Currently, transabdominal high-resolution ultrasound combined with gastrointestinal contrast agent can be used to diagnose stomach tumors effectively and without invasive procedures or radiation. However, although an appreciable number of cases of gastric schwannoma (GS) have been reported since the first description of such in 1988, the ongoing lack of a comprehensive list of ultrasonic characteristics has limited the accuracy of preoperative ultrasound diagnosis.

CASE SUMMARY

A 64-year-old female patient presented to our hospital with dizziness and head discomfort. During an abdominal ultrasound, a hypoechoic gastric mass was found, having clear and regular boundaries and no observable blood flow. Based on these characteristics, a gastrointestinal stromal tumor was suspected. Results from an endoscopic ultrasound biopsy and accompanying immunohistochemical analysis, coupled with abdominal CT findings indicating lymph node enlargement around the stomach, led to diagnosis of GS but did not exclude malignancy. After surgical resection of the tumor, the final diagnosis of GS without lymph node metastasis was made. No recurrence has occurred in the 6 years of follow-up.

CONCLUSION

A clearly defined ultrasonic characteristic profile of GS is important to improve diagnostic accuracy.

Key Words: Gastric schwannoma; Gastrointestinal stromal tumor; Gastrointestinal ultrasound; Endoscopic ultrasonography; Computed tomography; Case report

Unsolicited article; Externally peer reviewed.

Peer-review model: Single blind

Peer-review report's scientific quality classification
Grade A (Excellent): 0
Grade B (Very good): B
Grade C (Good): C
Grade D (Fair): 0
Grade E (Poor): 0

Received: August 26, 2021
Peer-review started: August 26, 2021
First decision: October 22, 2021
Revised: October 31, 2021
Accepted: December 31, 2021
Article in press: December 31, 2021
Published online: February 16, 2022

P-Reviewer: Govindarajan KK, Gunay S
S-Editor: Zhang H
L-Editor: A
P-Editor: Zhang H

Core Tip: Gastrointestinal stromal tumor (GIST) is the most common gastrointestinal mesenchymal tumor. Since the concept of gastric schwannoma (GS) was proposed in 1988, the incidence of cases has amassed. Transabdominal high-resolution ultrasound combined with abdominal gastrointestinal contrast agent has a unique advantage in gastrointestinal disease diagnosis as it can effectively diagnose tumors non-invasively without radiation. Although ultrasonographic characteristics of GIST have been reported, the literature lacks series of cases of GS and a clear summary of the ultrasonographic characteristics. A summarized ultrasonographic characteristic profile of GS will improve accuracy of differential diagnosis from to other types of gastrointestinal mesenchymal tumor.

Citation: Li QQ, Liu D. Gastric schwannoma misdiagnosed as gastrointestinal stromal tumor by ultrasonography before surgery: A case report. *World J Clin Cases* 2022; 10(5): 1667-1674
URL: https://www.wjgnet.com/2307-8960/full/v10/i5/1667.htm
DOI: https://dx.doi.org/10.12998/wjcc.v10.i5.1667

INTRODUCTION

In the past, gastric tumors were diagnosed by gastroscopy, computed tomography (CT), or magnetic resonance imaging (MRI). However, with the development of gastrointestinal ultrasound and the use of gastrointestinal contrast agent[1,2], transabdominal high-resolution ultrasound has attracted more clinical attention in the diagnosis of gastrointestinal diseases. Transabdominal high-resolution ultrasound can provide overall information on the lesions, is non-invasive, and does not expose the patient to radiation. In this paper, a patient with a gastric schwannoma was misdiagnosed as gastrointestinal stromal tumor (GIST) by ultrasound before surgery, due in part to a lack of compiled information on the ultrasonic characteristics of GS. As such, we have provided a summarization of the clinical and imaging characteristics of GIST and GS in order to improve the diagnostic accuracy of GS.

CASE PRESENTATION

Chief complaints

A 64-year-old female of Han nationality visited the outpatient clinic on January 19, 2015, after experiencing dizziness and head discomfort for 3 d. The patient had been diagnosed with hypertension for more than 20 years, and at the time of this visit, her blood pressure was 190/100 mmHg.

History of present illness

The outpatient doctor performed relevant examinations and advised her to take medication regularly to control blood pressure. The patient also underwent an abdominal ultrasound, which identified a hypoechoic lesion between the upper pole of the spleen and the abdominal aorta that measured 4.7 cm × 4.4 cm, with a clear and regular boundary and no evident blood flow (Figure 1). The ultrasound findings indicated that the lesion had possibly originated from the stomach and was a GIST. The patient presented no abdominal distention, abdominal pain, hematemesis, melena, or dysphagia.

History of past illness

Hypertension for more than 20 years. She took oral nifedipine controlled release tablet 60 mg daily, bisoprolol fumarate tablet 10 mg daily, and indapamide tablet 1.25 mg daily. The patient had no hepatitis B, hepatitis and other infectious diseases.

Personal and family history

The patient had no family history of gastrointestinal cancer.

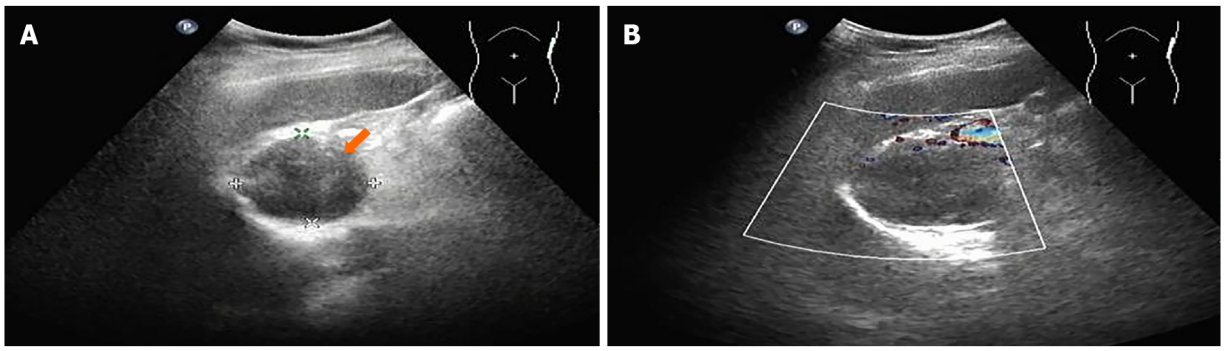

Figure 1 Conventional abdominal ultrasound examination. A: Gray-scale sonography showed a hypoechoic lesion (orange arrow), size 4.7 cm × 4.4 cm, with clear and regular boundary, between the upper pole of the spleen and the abdominal aorta; B: Color Doppler showed no evident blood flow.

Physical examination

After the patient's blood pressure was stabilized, she was admitted to the general surgery department for treatment of the gastric tumor. At the time of admittance, her temperature was 36.4 °C, heart rate was 60 beats/min, respiration was 18 breaths/min, and blood pressure was 130/75 mmHg. No enlarged lymph nodes were palpable on either clavicle. The abdomen appeared flat, and no peristaltic waves (in esophagus or stomach) were observed. Upon palpation, the abdomen was soft, with no tenderness, muscle tension, or rebound pain.

Laboratory examinations

Results from routine blood and fecal tests, occult blood test, and blood biochemistry panels were all within normal limits. Tumor marker tests did not reveal any obvious abnormalities.

Imaging examinations

February 5, 2015: Abdominal CT plain and contrast-enhanced scans showed a local soft tissue density mass in the gastric wall with a smooth boundary, sized 5.5 cm × 4.3 cm. There was local protrusion observed outside the contour of the stomach, with obvious enhancement. The surrounding lymph nodes were enlarged, with the larger ones measuring 1.0 cm in diameter. CT did not exclude malignancy (*i.e.* GIST with peripheral lymph node metastasis) (Figures 2 and 3).

February 10, 2015: Endoscopy confirmed a hemispherical eminence on the fundus of the stomach, with a smooth surface. Endoscopic ultrasonography showed a hypoechoic and heterogeneous mass, sized 3.7 cm × 4.4 cm, derived from the mucous muscularis. Color Doppler showed no evident blood flow. Gastroscopy and endoscopic ultrasonography suggested the possibility of GIST (Figure 4A and B).

February 10, 2015: Fine needle aspiration (FNA) under endoscopic ultrasound guidance (Figure 4C) primarily showed coagulation and calcification, with a small amount of gastric mucosal tissue and few spindle cells, suggesting that spindle cell tumor should be excluded (Table 1).

March 4, 2015: Since the pathological diagnosis was unclear, the FNA was repeated (again under endoscopic ultrasound guidance). Subsequent immunohistochemical examination was performed and indicated GS (Table 1).

FINAL DIAGNOSIS

Benign GS.

TREATMENT

Given the very few malignant cases of GS reported in the literature[3], and the presence of peripheral lymph nodes indicated by CT in this case, malignant GS was not excluded. Therefore, the patient was admitted to the hospital for elective surgery. An upper abdominal midline incision was made, with a length of about 20 cm. The organs around the lesion were explored. No other abnormality was found in the

Table 1 Results of two endoscopic and endoscopic puncture biopsies

Date	Where	Endoscopic ultrasound					FNA pathological
		Echo	Cumulative level	Homogeneity or not	Border	Blood supply	
February 10, 2015	Inpatient	Low	Mucosal muscularis	Heterogeneous, with calcification	Smooth	No	Few spindle cells
March 4, 2015	Outpatient	Low	Mucosal muscularis	Heterogeneous, with calcification	Smooth	No	Immunohistochemical examination indicated GS

FNA: Fine needle aspiration; GS: Gastric schwannoma.

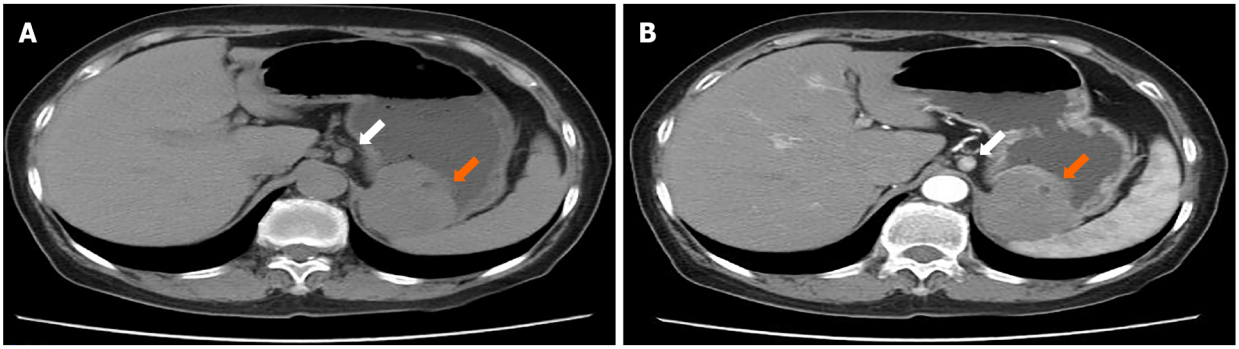

Figure 2 Abdominal computed tomography plain scan and enhancement. A: Plain computed tomography (CT) showed a local soft tissue density mass in gastric wall (orange arrow), smooth boundary, local protrusion outside the contour of the stomach, with surrounding enlarged lymph nodes (white arrow); B: Enhanced CT showed a markedly enhanced mass (orange arrow), with surrounding enlarged lymph nodes (white arrow).

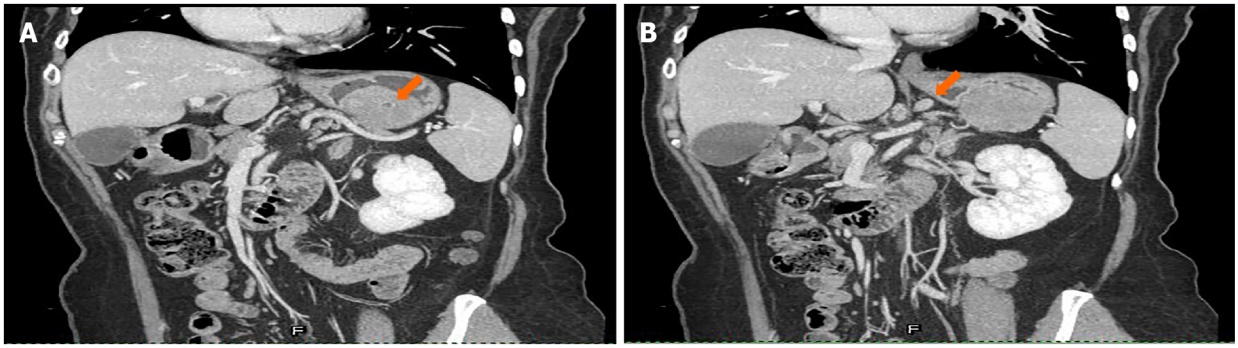

Figure 3 Coronal computed tomography. A: Computed tomography (CT) showed a mass on the fundus of the stomach (orange arrow); B: CT showed enlarged lymph nodes around the mass (orange arrow).

peritoneum, and no ascites were found. However, a lesion of 4 cm diameter was identified in the anterior wall of the fundus near the greater curvature of the gastric body, with no obvious infiltration of the serous layer. In addition, enlarged lymph nodes were felt around the stomach. As treatment, a radical proximal subtotal gastrectomy was performed (proximal subtotal gastrectomy + radical abdominal lymph node dissection + esophagogastric end-to-end anastomosis) yielding status of R0 (no microscopic residue after resection) and D2 (lymph nodes at the second station completely cleared).

OUTCOME AND FOLLOW-UP

The tumor observed intraoperatively on the anterior wall of the greater curvature of the gastric fundus was a swollen mass, of 6.0 cm × 5.0 cm × 4.5 cm in size, protruding into the serosal side and having a complete capsule and a grayish and yellowish

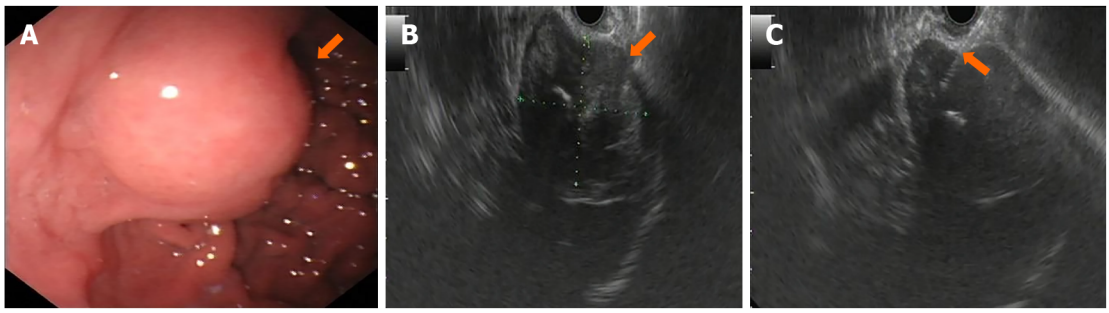

Figure 4 Mass was observed on the fundus of the stomach by endoscopy and endoscopic ultrasound. A: Endoscopy showed a smooth surface of the mass (orange arrow); B: Endoscopic ultrasonography showed a hypoechoic and heterogeneous mass, derived from mucous muscularis, with hyperechoic area (orange arrow); C: Endoscopic ultrasound guided fine needle aspiration. The bright line is the puncture needle (orange arrow).

section. Subsequent histological examination defined it as a gastric submucosal spindle cell tumor, with nuclear division of < 5/50 per high power field and immunohistochemistry marker signature of CD117 (-), CD34 (-), DOG-1 (-), S-100 (+), actin (-), and desmin (-). These findings were consistent with GS (Figure 5). A total of 12 large, curved lymph nodes and four small, curved lymph nodes were observed, all of which showed reactive hyperplasia. According to the 2010 World Health Organization (WHO) Clinicopathological Classification Guidelines for gastric neoplasms, the clinicopathological stage was T0N0M0. All annual CT re-examinations have shown no recurrence over the 6-year period of follow-up.

DISCUSSION

GS was first reported by Daimaru *et al*[4] in 1988. It is a rare tumor of gastric stromal origin, accounting for 0.2% of all gastric tumors and 6.3% of all gastric stromal tumors. GS has a good prognosis and rarely relapses, but malignant lesions have been reported [3,5,6]. GIST is the most common gastric tumor, accounting for about 80% of all[7], followed by gastric leiomyoma, lymphoma, etc. In clinical practice, gastric stromal tumors are generally classified as GIST. Clinically, only 10%-30% of GISTs are malignant, but all GISTs have malignant potential[8,9]. Preoperative differential diagnosis of GS and GIST is difficult, and the auxiliary examinations lack specificity. So far, only pathological and immunohistochemical results are reliable, and genetic tests can be performed when necessary[5].

Upper gastrointestinal angiography, gastroscopy, endoscopic ultrasonography, abdominal CT, abdominal MRI, and other examinations were previously used to diagnose gastric tumors. At present, transabdominal high-resolution ultrasound and gastric contrast agent is routinely applied for the diagnosis of gastric diseases[1,2]. This type of imaging is non-invasive, non-radiative, convenient, fast, repeatable, and safe for the preliminary screening of gastric diseases. Under optimal conditions, it can identify the layered structure of the gastric wall from which the lesions originate. However, to date, transabdominal ultrasound examinations of GS have only been reported in individual case reports, and its ultrasonic characteristics have not yet been clearly summarized.

According to literature reports, a small number of patients have symptoms, such as upper abdominal pain or discomfort, melena, hematemesis, anemia, weight loss, etc., which are mostly seen in female patients aged 50-60 years[5,6,10]. However, most GS patients have no obvious complaints of discomfort. GS is occasionally identified in abdominal ultrasound, abdominal CT, upper gastrointestinal angiography, and gastroscopy. In abdominal ultrasound, the characteristics of GS are local hypoechoic lesion in the gastric wall, with complete mucosal and serous layers and clear boundaries. The lesions are regular or lobulated in shape and lack a blood supply[11]. On CT, GS is characterized by local low-density lesions in the gastric wall, with clear boundaries. The lesions are regular or lobulated and can be enhanced. CT can also provide information about the enlargement of lymph nodes around the lesion. This enlargement is unique to GS but can easily be confused for gastric malignant tumors with peripheral lymph node enlargement[12,13]. Diagnosis of GS is based on immunohistochemical pathology; the tumors are positive for S-100 protein and negative for c-kit, CD34, CD117, actin, desmin, SMA, and DOG-1. Pathological features of GS include

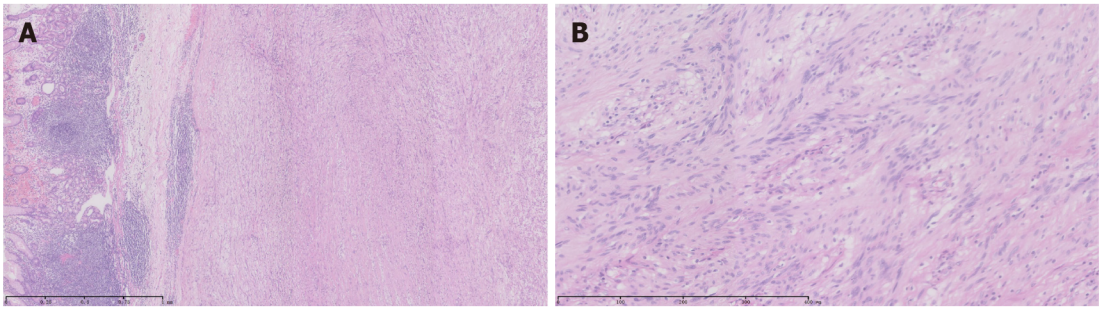

Figure 5 Postoperative pathology. Hematoxylin and eosin staining. A: A large number of lymphocyte aggregates and lymphoid tissue hyperplasia (40 × magnification) was observed; B: A large number of spindle cells (200 × magnification) was observed.

spindle cells arranged in bundles in the tumor center and the surrounding lymphocyte sleeve[14]. The lymphocyte sleeve is a characteristic manifestation of GS, and the formation of a lymphocyte mantle may be caused by lymphocyte chemotaxis due to cytokines secreted by tumor cells. This mechanism can also be used to explain why GS is often accompanied by peripheral lymph node enlargement[13].

GIST can occur in any part of the digestive tract but most commonly are found in the stomach (60%-70% of the cases), followed by the small intestine (25%-35%), and the colorectum (5%-10%). Less than 2% of GISTs occur in the esophagus, and a few are found in the mesentery, omentum, and retroperitoneum[15]. On ultrasound, GIST is characterized by irregular thickening of the gastrointestinal wall. It can present as either isoechoic or hypoechoic and the mass can be spherical, lobulated or irregular, with a clear boundary. The internal echo can be either uniform or uneven, accompanied by anechoic necrosis and have either a rich or poor blood supply[16]. The concept of GIST was proposed by Mazur *et a]*[17] in 1983 based on the differentiation characteristics of tumors. In the past, due to the limitations of pathological techniques and the presence of smooth muscle or nerve bundles in many spindle cell tumors of the gastrointestinal tract, which were similar to other types of tumors in histological morphology, they were considered as smooth muscle or neurogenic tumors and were classified as leiomyoma, leiomyoblastoma, or leiomyosarcoma.

Recent clinical and pathological studies have shown that GIST may originate from astrocytes of the gastrointestinal interstitial region, with special immunophenotype and histological characteristics, and is characterized by multidirectional differentiation, which can differentiate or disorient toward smooth muscle and nerve[18]. Its biological characteristics are difficult to predict. It is, however, classified as a type of gastrointestinal submucosal tumor with malignant potential[8,9]. GIST pathology indicates that cell morphology can be divided into spindle type, epithelioid type, or mixed type, of which spindle cells are the most common[19], but there is no lymphocyte sleeve. Immunohistochemical findings include cells that are positive for CD117, CD34, DOG-1, Ki-67, and succinate dehydrogenase B. C-kit proto-oncogene mutations are common in GIST, mainly in exons 9, 11, 13, and 17. In addition, the PDGFRA gene is also frequently mutated in GIST, mainly in exons 12 and 18[19-21]. GS does not exhibit c-kit proto-oncogene and PDGFRA gene mutations[10].

The gastric wall is divided into five layers under transabdominal high-resolution ultrasound, and the echo from inside to outside is in the order of high-low-high-low-high, corresponding to the interface of the gastric wall and the mucosal epithelium, muscularis mucosa, submucosa, muscularis propria, and serosal layer, respectively. The origin and level of involvement were determined according to the continuous relationship between the lesion and the five-layer structure of the gastric wall[22]. GS may originate from mucosa or muscularis propria. Gastric cancer primarily includes mucosal neoplasms, originating from the mucosal layer. Other gastric parietal layers are not involved in the early stage, while the whole gastric wall is involved in the late stage. Most GISTs originate from the muscularis propria. Gastric primary lymphoma mainly originates from the mucosa. Gastric nerve fibroma can be isolated nerve fibroma or nerve fibroma disease, and typically involves isolated nerve fibroma from the lower mucosal layer. By identifying the layer of origin, GS may be better distinguished from GIST and other gastric tumors.

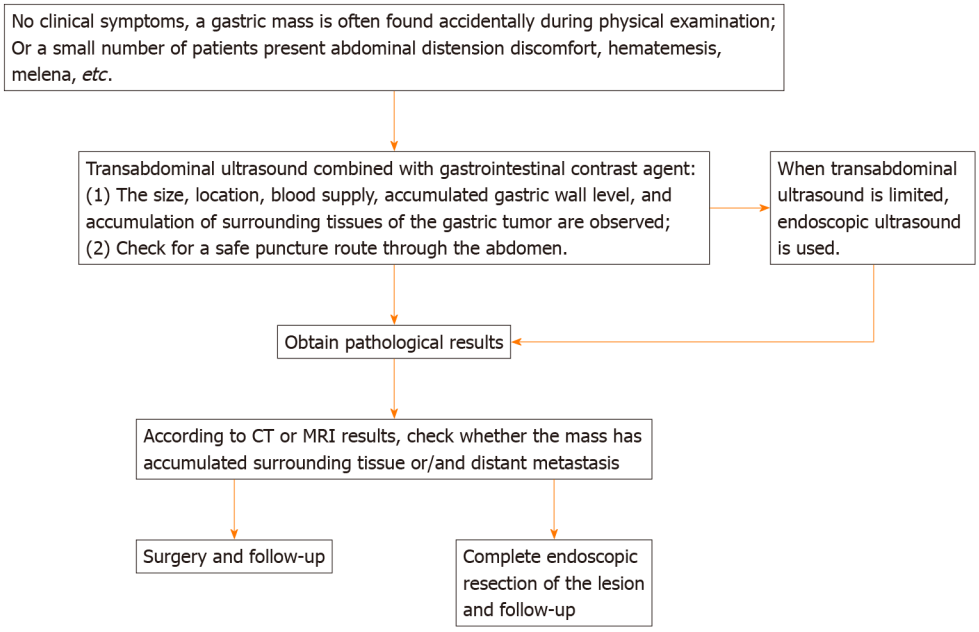

Figure 6 Procedure for diagnosis and treatment of gastrointestinal stromal tumors. The characteristics and accumulation levels of the mass were observed under transabdominal ultrasonography or endoscopic ultrasonography. CT: Computed tomography; MRI: Magnetic resonance imaging.

CONCLUSION

The characteristics of gastric wall tumors can be observed by transabdominal high-resolution and endoscopic ultrasonography (Figure 6), with two-dimensional and color Doppler ultrasound. The wall layer that the tumor involves can help to preoperatively determine whether the gastric wall tumor originates from the epithelium or the stroma. If the tumor originates from gastric stroma, GIST should be considered first, and then the possibility of GS should be considered. The reported rate of GS is not very low but the actual incidence remains to be confirmed by large-scale studies. The ultrasound and clinical characteristics of GIST and GS should be actively summarized in future work, in order to provide guidance for the preoperative diagnosis of gastric stromal tumors.

GS are generally benign tumors, and only a few malignant cases have been reported. GS is often accompanied by peripheral lymph node enlargement, which is not an indication of malignancy. In our case, lymph nodes around the lesion were confirmed as reactive hyperplasia, and there was no recurrence during the 6-year follow-up. After the preliminary diagnosis of GS but before confirmation from histopathological tests after surgery, the treatment is as follows: (1) Complete surgical resection is recommended, which can be performed under endoscopy or laparotomy according to the tumor size, location, and relationship with surrounding organs; and (2) Simultaneous resection is recommended for patients with locally enlarged lymph nodes.

ACKNOWLEDGEMENTS

We greatly appreciate the patient for allowing us to use the medical documents and information.

REFERENCES

1 **Liu G**, Zhong JM, Song PL, Li Y, Zhu JB, Kang HQ, Xu RX. The clinical value of gastrointestinal ultrasound filling combined with contrast-enhanced ultrasound in the diagnosis of gastrointestinal diseases. China Health and Nutrition Survey 2016; 8: 32-33

2 **Zhang Y**. A clinical study on the diagnosis of gastric lesions with and without gastrointestinal contrast agent. *Shijie Zuixin Yixue Xinxi Wenzhai* 2019; **19**: 147, 169 [DOI: 10.19613/j.cnki.1671-3141.2019.49.096]

3 **Takemura M**, Yoshida K, Takii M, Sakurai K, Kanazawa A. Gastric malignant schwannoma presenting with upper gastrointestinal bleeding: a case report. *J Med Case Rep* 2012; **6**: 37 [PMID: 22277785 DOI: 10.1186/1752-1947-6-37]

4 **Daimaru Y**, Kido H, Hashimoto H, Enjoji M. Benign schwannoma of the gastrointestinal tract: a clinicopathologic and immunohistochemical study. *Hum Pathol* 1988; **19**: 257-264 [PMID: 3126126 DOI: 10.1016/S0046-8177(88)80518-5]

5 **Yanagawa S**, Kagemoto K, Tanji H, Kodama S, Takeshima Y, Sumimoto K. A Rare Case of Gastric Schwannoma: A Case Report and Literature Review. *Case Rep Oncol* 2020; **13**: 330-335 [PMID: 32308600 DOI: 10.1159/000506450]

6 **Mekras A**, Krenn V, Perrakis A, Croner RS, Kalles V, Atamer C, Grützmann R, Vassos N. Gastrointestinal schwannomas: a rare but important differential diagnosis of mesenchymal tumors of gastrointestinal tract. *BMC Surg* 2018; **18**: 47 [PMID: 30045739 DOI: 10.1186/s12893-018-0379-2]

7 **Hirota S**. Differential diagnosis of gastrointestinal stromal tumor by histopathology and immunohistochemistry. *Transl Gastroenterol Hepatol* 2018; **3**: 27 [PMID: 29971258 DOI: 10.21037/tgh.2018.04.01]

8 **Miettinen M**, Sobin LH, Lasota J. Gastrointestinal stromal tumors of the stomach: a clinicopathologic, immunohistochemical, and molecular genetic study of 1765 cases with long-term follow-up. *Am J Surg Pathol* 2005; **29**: 52-68 [PMID: 15613856 DOI: 10.1097/01.pas.0000146010.92933.de]

9 **Kim GH**, Ahn JY, Gong CS, Kim M, Na HK, Lee JH, Jung KW, Kim DH, Choi KD, Song HJ, Lee GH, Jung HY. Efficacy of Endoscopic Ultrasound-Guided Fine-Needle Biopsy in Gastric Subepithelial Tumors Located in the Cardia. *Dig Dis Sci* 2020; **65**: 583-590 [PMID: 31410755 DOI: 10.1007/s10620-019-05774-5]

10 **Voltaggio L**, Murray R, Lasota J, Miettinen M. Gastric schwannoma: a clinicopathologic study of 51 cases and critical review of the literature. *Hum Pathol* 2012; **43**: 650-659 [PMID: 22137423 DOI: 10.1016/j.humpath.2011.07.006]

11 **Xu CM**, Wang ZG, Li F, Zhong H, Zhang N, Zhou F, Zhu JC, Chen P. Ultrasonographic findings of gastrointestinal schwannoma: 2 cases. *Zhongguo Chaosheng Yingxiangxue Zazhi* 2012; **21**: 640-641 [DOI: 10.3760/cma.j.issn.1004-4477.2012.07.032]

12 **Ji JS**, Lu CY, Mao WB, Wang ZF, Xu M. Gastric schwannoma: CT findings and clinicopathologic correlation. *Abdom Imaging* 2015; **40**: 1164-1169 [PMID: 25316564 DOI: 10.1007/s00261-014-0260-4]

13 **Wadhawan A**, Brady M, LeVea C, Hochwald S, Kukar M. Case reports on a gastric mass presenting with regional lymphadenopathy: A differential diagnosis is gastric schwannoma. *Int J Surg Case Rep* 2020; **72**: 369-372 [PMID: 32563823 DOI: 10.1016/j.ijscr.2020.05.098]

14 **Peltrini R**, Greco PA, Nasto RA, D'Alessandro A, Iacobelli A, Insabato L, Bucci L. Gastric schwannoma misdiagnosed as a GIST. *Acta Chir Belg* 2019; **119**: 411-413 [PMID: 31311458 DOI: 10.1080/00015458.2019.1642597]

15 **Miettinen M**, Majidi M, Lasota J. Pathology and diagnostic criteria of gastrointestinal stromal tumors (GISTs): a review. *Eur J Cancer* 2002; **38** Suppl 5: S39-S51 [PMID: 12528772 DOI: 10.1016/s0959-8049(02)80602-5]

16 **Xie C**, Bo G, Zhang WJ, Wang DW, Wang ZP. Ultrasonography and CT analysis of 32 cases of gastrointestinal stromal tumor. *Shandong Yiyao* 2015; **55**: 57-59 [DOI: 10.3969/j.issn.1002-266X.2015.22.022]

17 **Mazur MT**, Clark HB. Gastric stromal tumors. Reappraisal of histogenesis. *Am J Surg Pathol* 1983; **7**: 507-519 [PMID: 6625048 DOI: 10.1097/00000478-198309000-00001]

18 **Jiang YN**, Cai X. Research progress in the origin of gastrointestinal stromal tumor. *Zhongguo Aizheng Zazhi* 2011; **21**: 893-897 [DOI: 10.3969/j.issn.1007-3969.2011.11.014]

19 **Li Y**, Teng Y, Wei X, Tian Z, Cao Y, Liu X, Duan X. A rare simultaneous coexistence of epithelioid gastrointestinal stromal tumors and schwannoma in the stomach: a case report. *Diagn Pathol* 2019; **14**: 116 [PMID: 31647020 DOI: 10.1186/s13000-019-0898-x]

20 **Gopie P**, Mei L, Faber AC, Grossman SR, Smith SC, Boikos SA. Classification of gastrointestinal stromal tumor syndromes. *Endocr Relat Cancer* 2018; **25**: R49-R58 [PMID: 29170162 DOI: 10.1530/ERC-17-0329]

21 **Madhala D**, Sundaram S, Chinambedudandapani M, Balasubramanian A. Analysis of C-Kit Exon 9, Exon 11 and BRAFV600E Mutations Using Sangers Sequencing in Gastrointestinal Stromal Tumours. *Cureus* 2020; **12**: e7369 [PMID: 32328381 DOI: 10.7759/cureus.7369]

22 **Cao YD**, Wen LM. Endoscopic ultrasonography for differential diagnosis and treatment of gastric muscularis propria lesions. M.Sc. Thesis, Southwest Medical University 2018. [cited 26 Aug 2021]. Available from: https://kns.cnki.net/kcms/detail/detail.aspx?dbcode=CMFD&dbname=CMFD201802&filename=1018178824.nh&uniplatform=NZKPT&v=fvHjXYk4w5lN-ld6kFmUKWvjsOuNI9xpOiKuVstLvtLuYX3bN2iPtyqlnSeZu94j

World Journal of Clinical Cases

Submit a Manuscript: https://www.f6publishing.com

World J Clin Cases 2022 February 16; 10(5): 1675-1683

DOI: 10.12998/wjcc.v10.i5.1675

ISSN 2307-8960 (online)

CASE REPORT

Giant retroperitoneal lipoma presenting with abdominal distention: A case report and review of the literature

Zhi-Yan Chen, Xian-Long Chen, Qi Yu, Qing-Bo Fan

ORCID number: Zhi-Yan Chen 0000-0002-1695-1455; Xian-Long Chen 0000-0002-3677-4281; Qi Yu 0000-0001-9737-5957; Qing-Bo Fan 0000-0002-8745-1132.

Author contributions: Chen ZY wrote and revised the manuscript; Chen ZY and Fan QB were part of the clinical team that treated the patient; Chen XL participated in the review of the pathology; Yu Q and Fan QB revised the manuscript and supervised the study.

Informed consent statement: Informed written consent was obtained from the patient for publication of this case report and any accompanying images.

Conflict-of-interest statement: No conflict of interests exists to any of the authors.

CARE Checklist (2016) statement: The authors have read the CARE Checklist (2016), and the manuscript was prepared and revised according to the CARE Checklist (2016).

Supported by the National Key Research and Development Program, No. 2018YFC1002105.

Country/Territory of origin: China

Specialty type: Obstetrics and gynecology

Zhi-Yan Chen, Qi Yu, Qing-Bo Fan, Department of Obstetrics and Gynecology, Peking Union Medical College Hospital, Beijing 100730, China

Xian-Long Chen, Department of Pathology, Peking Union Medical College Hospital, Beijing 100730, China

Corresponding author: Qing-Bo Fan, MD, Professor, Department of Obstetrics and Gynecology, Peking Union Medical College Hospital, No. 1 Shuaifuyuan, Wangfujing, Dongcheng District, Beijing 100730, China. qbfan@sohu.com

Abstract

BACKGROUND

Retroperitoneal lipomas are extremely rare tumors and tend to be large in size (> 10 cm) when diagnosed, causing various clinical manifestations. Preoperative diagnosis of retroperitoneal lipomas is difficult. There is a lack of relevant information about the management and prognosis of these benign tumors due to limited reports.

CASE SUMMARY

A 53-year-old woman who complained about progressive abdominal distention and aggravating satiety was referred to the gynecological outpatient department of Peking Union Medical College Hospital. Computerized tomography (CT) revealed an immense mass with fat density, measuring 28.6 cm× 16.6 cm in size. Adjacent organs, including the intestinal tract and uterus, were squeezed to the right side of the abdomen. An exploratory laparotomy was performed with suspicion of liposarcoma. Intraoperatively, a giant yellowish lobulated mass was found occupying the retroperitoneum and it was removed by tumor debulking. Postoperative histopathological results confirmed the diagnosis of retroperitoneal lipoma.

CONCLUSION

Retroperitoneal lipoma is a very rare condition and is difficult to differentiate from well-differentiated liposarcoma. Radiographic investigations, especially CT and magnetic resonance imaging, are important for preoperative diagnosis. Surgical resection is the fundamental treatment, which is difficult due to its size and relation to neighboring structures.

Key Words: Retroperitoneal lipoma; Well-differentiated liposarcoma; Retroperitoneal

Provenance and peer review: Unsolicited article; Externally peer reviewed.

Peer-review model: Single blind

Peer-review report's scientific quality classification
Grade A (Excellent): 0
Grade B (Very good): B
Grade C (Good): C
Grade D (Fair): 0
Grade E (Poor): 0

Received: August 21, 2021
Peer-review started: August 21, 2021
First decision: November 17, 2021
Revised: December 8, 2021
Accepted: January 8, 2022
Article in press: January 8, 2022
Published online: February 16, 2022

P-Reviewer: Dhali A, Meglio LD
S-Editor: Wang JL
L-Editor: Wang TQ
P-Editor: Wang JL

tumors; Treatment; Prognosis; Case report

Core Tip: Retroperitoneal lipomas are rare benign tumors originating from adipose tissues and they tend to have large sizes. Imaging examinations, especially computerized tomography and magnetic resonance imaging, are fundamental diagnostic tools for these tumors. Surgical resection is the main treatment method. *En bloc* resection is commonly required. Postoperative histopathology determines the final diagnosis, and immunohistochemical analysis could be useful in the differentiation of liposarcomas. Regular follow-ups are also required for the patients.

Citation: Chen ZY, Chen XL, Yu Q, Fan QB. Giant retroperitoneal lipoma presenting with abdominal distention: A case report and review of the literature. *World J Clin Cases* 2022; 10(5): 1675-1683
URL: https://www.wjgnet.com/2307-8960/full/v10/i5/1675.htm
DOI: https://dx.doi.org/10.12998/wjcc.v10.i5.1675

INTRODUCTION

Lipomas are a category of benign tumors originating from well-differentiated adipocytes. Their predilection sites are subdermal tissues of the trunk and extremities [1,2]. Retroperitoneal lipomas are a rare condition, with just 22 case reports describing the tumour in adults in the previous literature of PubMed since 1970[3-22]. They account for 2.9% of primary retroperitoneal tumors, approximately 80% of which are known as malignant[6,23,24]. Unlike subcutaneous lipomas, which are related to obesity, hyperlipidaemia, and injuries, retroperitoneal lipomas have an unknown aetiology[5,25-27]. On account of the rarity and limited knowledge of these tumors, further reports and investigations are necessary. In this report, we describe the case of a 53-year-old postmenopausal woman who presented with a massive fatty retroperitoneal mass measuring 28.6 cm× 16.6 cm and weighing 7.126 kg.

CASE PRESENTATION

Chief complaints

A 53-year-old postmenopausal woman who complained about progressive abdominal distention and aggravating satiety was referred to the department of gynaecology in our center.

History of present illness

The patient started to feel intensifying abdominal distention and satiety for the last 2 mo. She also found a significant increase in abdominal circumference and thinning of the limbs. The patient denied other discomforts, including fever, abdominal pain, nausea, and vomiting. The patient had been postmenopausal for 5 years and did not report abnormal vaginal bleeding.

History of past illness

The patient had a 10-year history of hypertension and took Loxone once per day, with stable control of blood pressure. The patient denied any history of diabetes, coronary heart disease, or malignancy. She also reported no drug allergy or other physical impairment. Additionally, the patient did not receive regular physical examinations, and the last medical examination had occurred more than 10 years prior.

Personal and family history

No noteworthy personal or family history was reported by the patient.

Physical examination

The patient's height was 161 cm, and her weight was 60 kg (body mass index: 23.3, within the normal range). The physical examination revealed a palpable giant abdominal mass reaching the xiphisternum with a rubbery consistency. Other clinical symptoms, including tenderness, rebound tenderness, and mobile turbid sounds, were found.

Laboratory examinations

After hospitalization, the patient received a series of laboratory examinations for testing liver and kidney function, faecal occult blood, blood coagulation factors, electrolyte panel, and tumor biomarkers. The laboratory findings fell within the normal range.

Imaging examinations

The patient had received a computed tomography (CT) plain scan at another hospital, and was re-evaluated by ultrasonography at our hospital. A massive hyperechoic mass, approximately 30 cm × 17 cm in size, was visualized *via* ultrasound. The mass was clearly defined and had internal echogenicity, filled with stripe-like structures. Minimal blood signals were detected by colour Doppler ultrasound (Figure 1). A CT plain scan demonstrated a giant homogeneous mass mainly consisting of fatty tissue and thin septa. It measured 16.6 cm × 28.6 cm in volume and pushed the peritoneal contents, such as the bowel loops and uterus, to the right part of the abdomen (Figure 2).

FINAL DIAGNOSIS

Based on the clinical manifestations, normal laboratory examinations, and imaging examinations indicating its adipose origin, the clinicians considered the mass to be a giant retroperitoneal lipoma. However, the possibility of malignancy cannot be overlooked due to its large size.

TREATMENT

After completing the examinations and preoperative assessments, the patient underwent an exploratory laparotomy with the suspicion of malignancy, most likely retroperitoneal liposarcoma. During the operation, a bulky yellowish tumor originating from perirenal fatty tissues in the left retroperitoneal region was found to occupy the retroperitoneum. The uterus and adnexa were displaced by the mass. The mass adhered to the left psoas major muscle and wrapped around the left ureter, making it unfeasible to perform *en bloc* resection. After carefully separating the left ureter, we performed tumor debulking and resection of the left adnexa, which was also tightly adhered to the tumor. The total weight of the mass was 7.126 kg (Figure 3). The frozen pathological results suggested that the mass mainly consisted of adipose tissues, and a retroperitoneal lipomatous tumor was considered.

After 1 wk of uneventful hospitalization, the patient was discharged from the hospital with full recovery from her clinical symptoms. The final paraffin pathology showed that the tumor was composed of mature adipose tissues and hematopoietic cells, without cytologic atypia, and confirmed the diagnosis of multiple lipomas and multiple myelolipomas (Figure 4).

OUTCOME AND FOLLOW-UP

The patient reported no relevant clinical symptoms after the operation. During a series of follow-ups for 18 mo, the laboratory tests and imaging examinations were normal and indicated no signs of relapse.

DISCUSSION

We herein report a massive retroperitoneal lipoma, which consisted of multiple

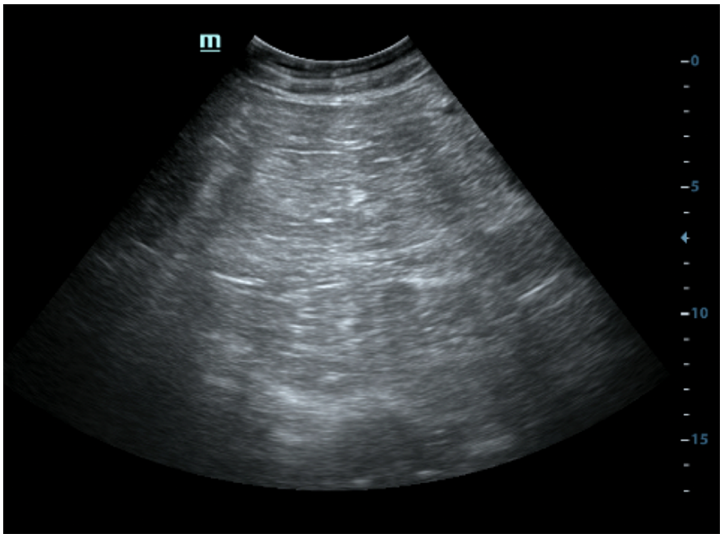

Figure 1 Abdominal ultrasonography of the mass. A giant hyperechoic mass filling the abdomen was presented on grey-scale ultrasound. The mass had a relative clear margin and internal septas.

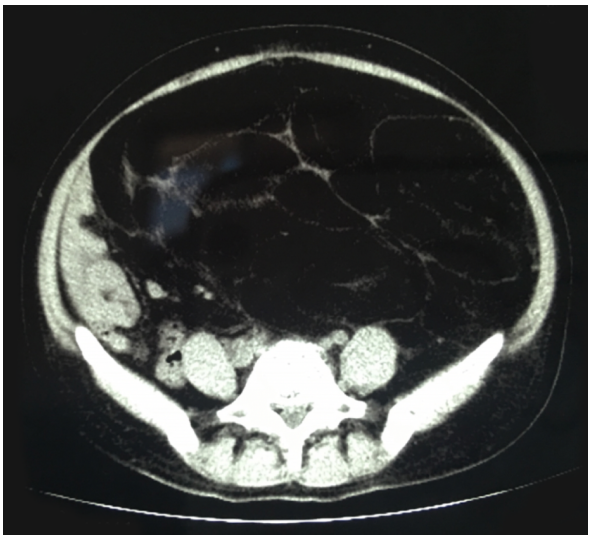

Figure 2 Abdominal computed tomography in the axial plane. Computed tomography imaging showed a giant homogenous mass, mainly consisting of fatty tissue measuring 16.6 cm × 28.6 cm with thin septa, pushing the peritoneal containing such as bowel loops and uterus to the right part of abdomen.

conventional lipomas and multiple myelolipomas. Retroperitoneal lipomas are rare mesenchymal-originated tumors. It was first reported in 1947[22], and since then, a total of 22 cases have been reported in adults sporadically (Table 1). The peak incidence of adult retroperitoneal lipomas occurs between the ages of 40 and 60, with no discernible gender predisposition. According to the morphologic characteristics, lipomas can be subdivided into conventional lipoma, fibrolipoma, angiolipoma, spindle cell lipoma, pleomorphic lipoma, and myelolipoma[7], of which, almost all myelolipomas have been identified inside the adrenal gland, with just about 50 cases of myelolipomas being identified in extra-adrenal locations, such as the retroperinoneum[28]. The exact underlying aetiology of retroperitoneal lipomas is not well understood. Seeding after fibroid excision, exogenous hormone treatment, or chronic abnormalities in glucose homeostasis have all been blamed for these benign tumors. And genetic factors are thought to have an important role in adipocyte proliferation[5].

Retroperitoneal tumors are often asymptomatic for a long period of time throughout their early clinical course, owing to the vast potential spaces in the retroperitoneum. Local compression of surrounding organs and tissues, which can manifest obstructive urinary/bowel symptoms such as stomach pain, fullness, early satiety, or lower extremity oedema, may occur once the tumors have grown to gigantic sizes. The

Table 1 Summary of all case reports describing retroperitoneal lipomas resected in adults

Ref.	Age	Sex	Symptoms	Imaging methods	Tumor size (cm)	Tumor weight	Follow-up
Cattell *et al*[22], 1947	55	Female			10 cm in diameter		
Cattell *et al*[22], 1947	61	Female	Epigastric distress and bloating			12700 g	
Deppe *et al*[21], 1985	24	Female		Barium enema, CT	11 × 8 × 3	NA	
Zhang *et al*[20], 1987	65	Male	Weight gain, leg edema	NA	50 cm in diameter	19500 g	4 yr
Acheson *et al*[19], 1997	76	Female	Swollen leg	CT, MRI	20 × 20× 12	576 g	
Matsubara *et al*[18], 2000	65	Male		NA	12 × 13	NA	
Marshall *et al*[17], 2001	47	Male		CT	NA	4990 g	
Forte *et al*[15], 2002	61	Male	Urinary frequency, urgency and nocturia	CT			
Foa *et al*[16], 2002	52	Male			10.5 × 9.5 × 2	145 g	
Raftopoulos *et al*[14], 2002	62	Male	Abdominal pain	CT	20 × 15 × 10	790 g	
Martinez *et al*[12], 2003	32	Female	Abdominal pain	US, barium enema	20 × 13 × 10	3400 g	17 yr
Drop *et al*[13], 2003	60	Female	Abdominal pain, gastrointestinal symptoms	US, CT	13 × 12		
Drop *et al*[13], 2003	72	Female	Abdominal pain, sickness	US, CT	12 × 9 × 4		
Ida *et al*[11], 2008	65	Male	Painless swelling in left inguinal region		22 × 14 × 5		18 mo
Ukita *et al*[10], 2009	61	Female	Gluteal pain	MRI	25 × 15		
Singh *et al*[9], 2011	65	Male	Inguinal pain		15.6 cm in diameter	NA	
Chander *et al*[8], 2012	36	Female			13.6 × 11.2 × 9.1	1300 g	
Wei *et al*[6], 2013	25	Female		US	20 × 12 × 10	1650 g	6 mo
Saito *et al*[7], 2013	65	Male	Flank pain	US, CT	30 cm in diameter	NA	
Weniger *et al*[5], 2015	73	Female	Abdominal swelling, pain, and obstipation	CT	55 × 40 × 10	8950 g	
Al-Ali *et al*[4], 2019	34	Female	Abdominal distention and back pain	US, CT	45 × 48 × 13	1200 g	6 mo
Mitchell *et al*[3], 2020	29	Female	Abdominal pain, distention, orthopnea	MRI	28 × 14 × 6		

CT: Computerized tomography; MRI: Magnetic resonance imaging; US: Ultrasonography; NA: Not available.

clinical presentations tend to be variable and nonspecific[4]. Hence, imaging examinations play an essential role in the diagnosis of these lesions.

Ultrasound is generally used for the initial diagnosis and screening of abdominal masses. Radiography, especially CT and magnetic resonance imaging (MRI), is a crucial diagnostic tool for further evaluation of retroperitoneal tumors. The characteristics of adipose tissues are consistent on CT and MRI, but they differ on ultrasonography depending on the physical properties and histologic types. The fatty content is the fundamental feature to identify fat-containing retroperitoneal tumors during imaging examinations. Typical lipomas appear as extensive hyperechoic lesions on ultrasound, while they appear as homogeneous fat-containing masses with thin septa on CT and MRI. Retroperitoneal lipomas are difficult to identify preoperatively since they mimic liposarcomas, which account for the majority of fat-containing retroperitoneal tumors. Liposarcomas present heterogeneous signal intensity and variable appearances on MRI and CT due to the varying subtypes, which included well-differentiated liposarcoma (WDLPS), dedifferentiated liposarcoma, myxoid/round cell liposarcoma, pleomorphic liposarcoma, and mixed liposarcoma. The increased vascularity in liposarcomas that present as low-intensity signals on T1-weighted images can be used for differentiation. However, both lipomas and WDLPS are accompanied by a large amount of fat and minimal soft tissue and have identical appearances on CT and MRI, making it hard to distinguish lipomas from well-differentiated liposarcomas preoperatively.

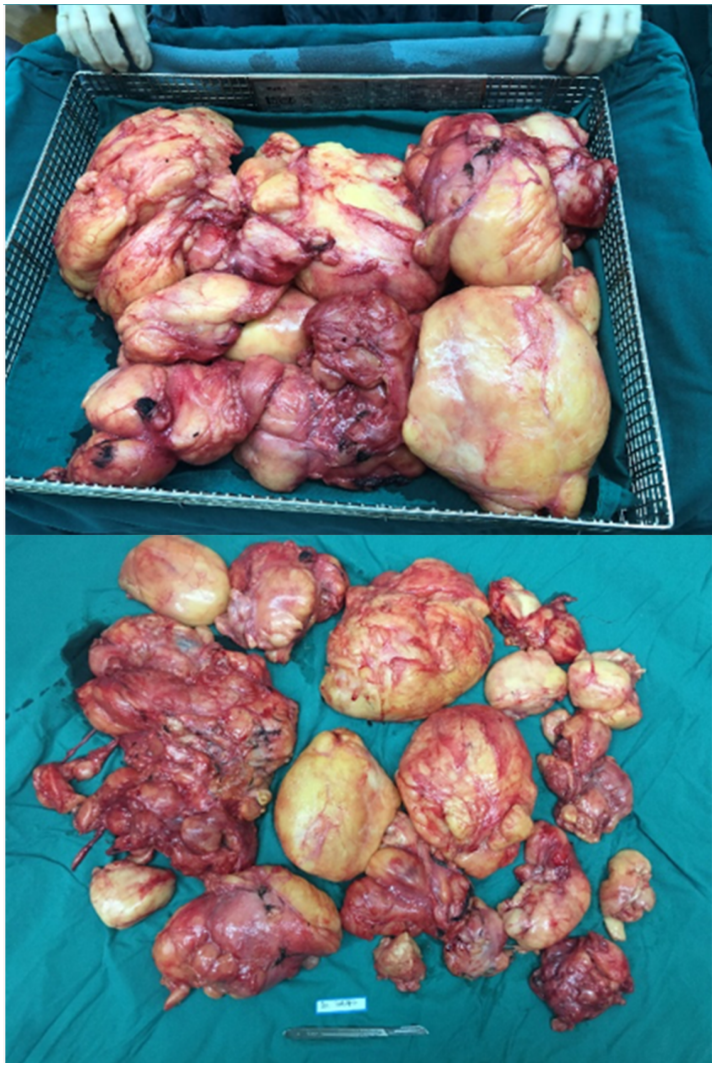

Figure 3 Macroscopic view of extracted retroperitoneal lipoma. During the operation, a bulky yellowish tumor, originating from the left retroperitoneal region, was found to occupy the retroperitoneum. The mass weighted 7.126 kg.

Due to the large size, the measurement of retroperitoneal tumors by preoperative imaging examinations can be inaccurate. Despite their typical presentations on CT and MRI, both imaging modalities may not rule out the possibility of WDLPS[29]. Approximately 80% of retroperitoneal tumors appear to be malignant, most of which are soft-tissue sarcomas, a category of very uncommon neoplasms, with an overall incidence of 0.3% to 0.4% per 100000 people[10]. Liposarcomas account for 41% of sarcomas, and the majority of the cases are malignant from the start. A few outliers arise from benign lipomas in the early stages[30]. The final diagnosis of lipomas depends on histopathology. Tissue for pathology can be acquired by fine-needle aspiration or core-needle biopsy, but it is nearly impossible to distinguish lipoma-like WDLPS and lipomas due to the limited tissue sample obtained by these methods for detecting atypia and hyperchromatic cells. Postoperative histopathology remains the gold standard for diagnosis. Histologic characteristics for WDLPS include mature adipocytes punctuated with big atypical hyperchromatic cells. However, WDLPS are likely to be misdiagnosed, because atypia may be localized, especially in deep lesions with tiny samples. Murine double minute (*MDM2*, located at 12q14-15) and cyclin-dependent kinase 4 gene are regularly amplified in WDLPS, which cannot be observed in benign lipomas. Hence, fluorescence *in situ* hybridization has emerged as a promising method for differential diagnosis[11,16,18].

It is of great importance to discern tumor characteristics intraoperatively and make decisions about the resection extent subsequently. In cases of the pathological diagnosis of liposarcoma, resection with negative margins (R0) is crucial. If infiltrative growth is detected by frozen pathology, a broad excision should be performed. Surgeons should also tailor personalized surgical strategies for patients with important involved adjacent structures who are unsuitable for an entire resection. Commonly, *en*

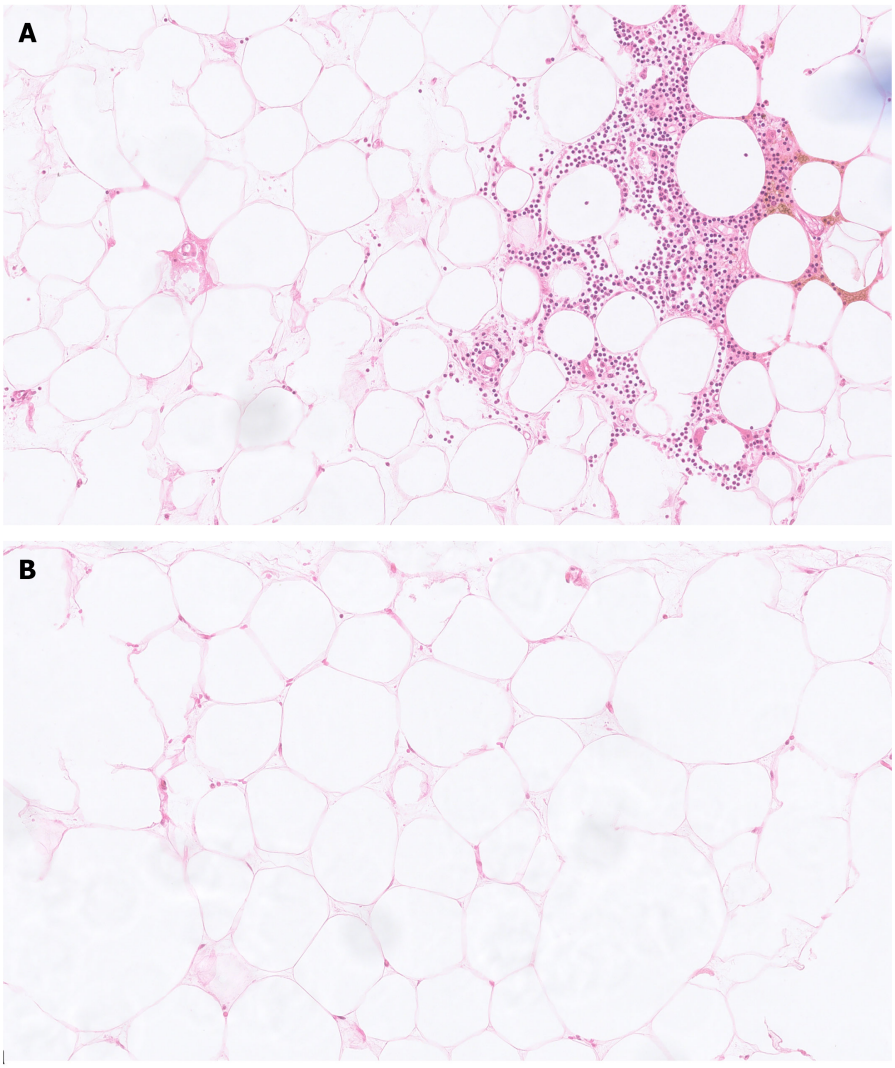

Figure 4 Microscopical picture of the extracted tumors (H&E, 20 ×). A: Myelolipoma was composed of mature adipose adipocytes and hematopoietic cells, without necrosis, atypia, and hyperchromatic cells; B: Conventional lipoma was composed of mature adipocytes.

bloc removal of the involved structures is required[3,5]. The prognosis and recurrence risk for patients with benign retroperitoneal lipomas are unclear due to the limited number of case reports. Patients are often recommended to receive regular clinical and radiologic follow-ups.

CONCLUSION

Retroperitoneal lipomas are rare benign tumors originating from adipose tissues and they tend to have large sizes. Imaging examinations, especially CT and MRI, are fundamental diagnostic tools for these tumors. Surgical resection is the main treatment method. *En bloc* resection is commonly required. Postoperative histopathology determines the final diagnosis, and immunohistochemical analysis could be useful in the differentiation of liposarcomas. Regular follow-ups are also required for the patients.

ACKNOWLEDGEMENTS

The authors are deeply grateful to Dr. Zhao H and Dr. Shi J for their help in reviewing the postoperative pathology.

REFERENCES

1 **Terada T**. Giant fibrolipoma of the spermatic cord. *Pathol Int* 2010; **60**: 330-332 [PMID: 20403037 DOI: 10.1111/j.1440-1827.2010.02521.x]
2 **Johnson CN**, Ha AS, Chen E, Davidson D. Lipomatous Soft-tissue Tumors. *J Am Acad Orthop Surg* 2018; **26**: 779-788 [PMID: 30192249 DOI: 10.5435/JAAOS-D-17-00045]
3 **Mitchell K**, Fuller K, Thomay A, Shapiro R. Diagnosis and Surgical Management of a Retroperitoneal Lipoma in Pregnancy. *Case Rep Obstet Gynecol* 2020; **2020**: 6309417 [PMID: 32724687 DOI: 10.1155/2020/6309417]
4 **Al-Ali MHM**, Salih AM, Ahmed OF, Kakamad FH, Mohammed SH, Hassan MN, Sidiq SH, Mustafa MQ, Najar KA, Abdullah IY. Retroperitoneal lipoma; a benign condition with frightening presentation. *Int J Surg Case Rep* 2019; **57**: 63-66 [PMID: 30904820 DOI: 10.1016/j.ijscr.2019.02.044]
5 **Weniger M**, D'Haese JG, Kunz W, Pratschke S, Guba M, Werner J, Angele MK. En-bloc resection of a giant retroperitoneal lipoma: a case report and review of the literature. *BMC Res Notes* 2015; **8**: 75 [PMID: 25890295 DOI: 10.1186/s13104-015-1038-7]
6 **Wei D**, Shen L, Yang K, Fang F. Giant retroperitoneal lipoma in a pregnant patient. *J Obstet Gynaecol* 2013; **33**: 522 [PMID: 23815212 DOI: 10.3109/01443615.2013.788621]
7 **Saito S**. Retroperitoneal lipoma presenting with nutcracker-like phenomenon. *Case Rep Urol* 2013; **2013**: 893242 [PMID: 24349819 DOI: 10.1155/2013/893242]
8 **Chander B**, Krishna M, Thakur S, Mahajan N, Vij A, Diwakaran J. Extremely rare giant retroperitoneal fibrolipoma: a case report. *J Cancer Res Ther* 2012; **8**: 314-316 [PMID: 22842386 DOI: 10.4103/0973-1482.99002]
9 **Singh G**, Bharadwaj RN, Purandare SN, Gore CR, Dubhashi SP, Vaidya S, Patil A, Kompally GR. Giant retroperitoneal lipoma presenting as inguinal hernia. *Indian J Surg* 2011; **73**: 187-189 [PMID: 22654328 DOI: 10.1007/s12262-010-0210-5]
10 **Ukita S**, Koshiyama M, Ohnaka M, Miyagawa N, Yamanishi Y, Nishimura F, Nagura M, Kim T, Hirose M, Shirase T, Kobayashi H, Ozasa H. Retroperitoneal lipoma arising from the urinary bladder. *Rare Tumors* 2009; **1**: e13 [PMID: 21139884 DOI: 10.4081/rt.2009.e13]
11 **Ida CM**, Wang X, Erickson-Johnson MR, Wenger DE, Blute ML, Nascimento AG, Oliveira AM. Primary retroperitoneal lipoma: a soft tissue pathology heresy? *Am J Surg Pathol* 2008; **32**: 951-954 [PMID: 18551755 DOI: 10.1097/pas.0b013e318160cfbf]
12 **Martinez CA**, Palma RT, Waisberg J. Giant retroperitoneal lipoma: a case report. *Arq Gastroenterol* 2003; **40**: 251-255 [PMID: 15264048 DOI: 10.1590/s0004-28032003000400010]
13 **Drop A**, Czekajska-Chehab E, Maciejewski R. Giant retroperitoneal lipomas--radiological case report. *Ann Univ Mariae Curie Sklodowska Med* 2003; **58**: 142-146 [PMID: 15323181]
14 **Raftopoulos I**, Lee T, Byrne MP. Image of the month: retroperitoneal lipoma. *Arch Surg* 2002; **137**: 865-866 [PMID: 12093348 DOI: 10.1001/archsurg.137.7.865]
15 **Forte F**, Maturo G, Catania A, Sorrenti S, Gemma D, Foti N, Vanni B, Virgili G, Vespasiani G, De Antoni E. Retroperitoneal lipoma. Unusual presentation with detrusor instability. *Minerva Urol Nefrol* 2002; **54**: 131-133 [PMID: 12070462]
16 **Foa C**, Mainguené C, Dupré F, Coindre JM, Huguet C, Kober C, Pedeutour F. Rearrangement involving chromosomes 1 and 8 in a retroperitoneal lipoma. *Cancer Genet Cytogenet* 2002; **133**: 156-159. [PMID: 11943344 DOI: 10.1016/s0165-4608(01)00573-8]
17 **Marshall MT**, Rosen P, Berlin R, Greenson N. Appendicitis masquerading as tumor: a case of two diagnoses. *J Emerg Med* 2001; **21**: 397-399 [PMID: 11728767 DOI: 10.1016/s0736-4679(01)00422-x]
18 **Matsubara N**, Yoshitaka T, Matsuno T, Ikeda M, Isozaki H, Tanaka N, Shimizu K. Multiple tumors and a novel E2F-4 mutation. A case report. *Digestion* 2000; **62**: 213-216 [PMID: 11025371 DOI: 10.1159/000007816]
19 **Acheson A**, McIlrath E, Barros D'Sa AA. Pelvic lipoma causing venous obstruction syndrome. *Eur J Vasc Endovasc Surg* 1997; **14**: 149-150 [PMID: 9314859 DOI: 10.1016/s1078-5884(97)80213-4]
20 **Zhang SZ**, Yue XH, Liu XM, Lo SL, Wang XZ. Giant retroperitoneal pleomorphic lipoma. *Am J Surg Pathol* 1987; **11**: 557-562 [PMID: 3605490]
21 **Deppe G**, Malviya VK, Hercule J, Gleicher N. Retroperitoneal pelvic lipoma. *J Natl Med Assoc* 1985; **77**: 574-576 [PMID: 4046056]
22 **Cattell RB**, Warren KW. Retroperitoneal lipoma. *Surg Clin North Am* 1947; **27**: 659-665 [PMID: 20242255 DOI: 10.1016/s0039-6109(16)32148-x]
23 **Pai MR**, Naik R, Raghuveer CV. Primary retroperitoneal tumors a 25 year study. *Indian J Med Sci* 1995; **49**: 139-141 [DOI: 10.1111/j.1744-1633.2010.00485.x]
24 **Armstrong JR**, Cohn I. Primary malignant retroperitoneal tumors. *Am J Surg* 1965; **110**: 937-943 [DOI: 10.1016/0002-9610(65)90181-9]
25 **Rubinstein A**, Goor Y, Gazit E, Cabili S. Non-symmetric subcutaneous lipomatosis associated with familial combined hyperlipidaemia. *Br J Dermatol* 1989; **120**: 689-694 [PMID: 2757931 DOI: 10.1111/j.1365-2133.1989.tb01357.x]
26 **Self TH**, Akins D. Dramatic reduction in lipoma associated with statin therapy. *J Am Acad Dermatol* 2008; **58**: S30-S31 [PMID: 18191694 DOI: 10.1016/j.jaad.2007.08.034]
27 **Pires Botelho da Costa JS**, Reis JC, Valença-Filipe R. Giant atypical lipoma of the thigh. *Dermatol*

Surg 2014; **40**: 213-214 [PMID: 24354663 DOI: 10.1111/dsu.12397]

28 **Cho J**, Kinsey D, Kimchi ET, O'Carroll KS, Nguyen V, Alsabbagh M, Gaballah A. Retroperitoneal extra-adrenal myelolipoma misdiagnosed as liposarcoma: A case report. *Radiol Case Rep* 2021; **16**: 364-368 [PMID: 33532014 DOI: 10.1016/j.radcr.2020.11.045]

29 **Shaaban AM**, Rezvani M, Tubay M, Elsayes KM, Woodward PJ, Menias CO. Fat-containing Retroperitoneal Lesions: Imaging Characteristics, Localization, and Differential Diagnosis. *Radiographics* 2016; **36**: 710-734 [PMID: 27163589 DOI: 10.1148/rg.2016150149]

30 **Vijay A**, Ram L. Retroperitoneal liposarcoma: a comprehensive review. *Am J Clin Oncol* 2015; **38**: 213-219 [PMID: 24136142 DOI: 10.1097/COC.0b013e31829b5667]

World Journal of Clinical Cases

Submit a Manuscript: https://www.f6publishing.com

World J Clin Cases 2022 February 16; 10(5): 1684-1688

DOI: 10.12998/wjcc.v10.i5.1684

ISSN 2307-8960 (online)

CASE REPORT

Pneumothorax during retroperitoneal laparoscopic partial nephrectomy in a lupus nephritis patient: A case report

Yi Zhao, Xiao-Qiang Xue, Di Xia, Wei-Feng Xu, Guang-Hua Liu, Yi Xie, Zhi-Gang Ji

ORCID number: Yi Zhao 0000-0002-4569-1349; Xiao-Qiang Xue 0000-0003-1954-8271; Di Xia 0000-0002-1984-8576; Wei-Feng Xu 0000-0002-7347-8748; Guang-Hua Liu 0000-0002-6581-4692; Yi Xie 0000-0002-1455-7534; Zhi-Gang Ji 0000-0003-3834-6579.

Author contributions: Zhao Y and Xue XQ are co-first authors who contributed equally to this work; Zhao Y and Xue XQ reviewed the literature, acquired the data, and contributed to manuscript drafting; Xu WF, Liu GH, Xia D, and Xie Y contributed to manuscript revision; Xia D provided further interpretation of the figures and data; Ji ZG managed the patient, performed the operation, and was responsible for the revision of the manuscript for important intellectual content. All authors issued final approval for the version to be submitted.

Informed consent statement: Informed written consent was obtained from the patient for publication of this report and any accompanying images.

Conflict-of-interest statement: The authors declare that they have no conflict of interest to disclose.

CARE Checklist (2016) statement: The authors have read the CARE Checklist (2016), and the

Yi Zhao, Xiao-Qiang Xue, Wei-Feng Xu, Guang-Hua Liu, Yi Xie, Zhi-Gang Ji, Department of Urology, Peking Union Medical College Hospital, Beijing 100730, China

Di Xia, Department of Anesthesiology, Peking Union Medical College Hospital, Beijing 100730, China

Corresponding author: Zhi-Gang Ji, MD, Chief Doctor, Professor, Department of Urology, Peking Union Medical College Hospital, No. 1 Shuaifuyuan Road, Dongcheng District, Beijing 100730, China. jizhiganguro@126.com

Abstract

BACKGROUND

Downgrading target treatment and laparoscopic partial nephrectomy have become increasingly popular in patients with renal cell carcinomas. Rare as it is, pneumothorax is one of the most severe intraoperative complications which needs immediate recognition. On the other hand, as a rheumatological disease, lupus nephritis requires a long period of hormone therapy. Cases of pneumothorax in hormone-consuming renal cancer patients are even fewer.

CASE SUMMARY

A 39-year-old woman was admitted to our department to take a laparoscopic partial nephrectomy. The patient had a medical history of lupus nephritis and renal clear cell carcinoma with hormone and target treatment. Her blood oxygen saturation dropped to 92% during the operation, and pneumothorax was detected by ultrasound. O_2 inhalation and lung dilation were performed. Her vital signs were monitored closely throughout the operation. The operation was accomplished, and she regained consciousness smoothly. A postoperative bedside chest X-ray was conducted after she was transferred to the urosurgery ward, while no evidence of further pneumothorax or lib injury was observed.

CONCLUSION

Pneumothorax is a severe complication in laparoscopic or robotic-assisted laparoscopic operations, especially in retroperitoneal ones. It is easily neglected unless the injury of the diaphragm is found. Low insufflation pressure and shorter operation time are necessary for patients with a history of long-term hormone consumption or chronic immune system disease.

Key Words: Pneumothorax; Laparoscopic partial nephrectomy; Lupus nephritis; Case

manuscript was prepared and revised according to the CARE Checklist (2016).

Country/Territory of origin: China

Specialty type: Urology and nephrology

Provenance and peer review: Unsolicited article; Externally peer reviewed

Peer-review model: Single blind

Peer-review report's scientific quality classification

Grade A (Excellent): 0
Grade B (Very good): 0
Grade C (Good): C
Grade D (Fair): 0
Grade E (Poor): 0

Received: August 26, 2021
Peer-review started: August 26, 2021
First decision: October 22, 2021
Revised: October 24, 2021
Accepted: January 5, 2022
Article in press: January 5, 2022
Published online: February 16, 2022

P-Reviewer: Surani S
S-Editor: Zhang H
L-Editor: Wang TQ
P-Editor: Zhang H

report

Core Tip: Controlling the gas pressure in the abdomen or retroperitoneum is an essential issue in laparoscopic operations. High gas pressure may lead to the injury of the diaphragm and, thereafter, pneumothorax. This article presents a case with accidental pneumothorax during the operation. The novelties are: First, this patient may be at high risk of pneumothorax due to long-term hormone application, and this article could arouse everyone's attention to this issue by sharing a clinical example; second, our early recognition and quick reaction to the pneumothorax could provide precious data for peers. Overall, this case should have enlightening significance for managing surgical patients with long-term application of hormones.

Citation: Zhao Y, Xue XQ, Xia D, Xu WF, Liu GH, Xie Y, Ji ZG. Pneumothorax during retroperitoneal laparoscopic partial nephrectomy in a lupus nephritis patient: A case report. *World J Clin Cases* 2022; 10(5): 1684-1688
URL: https://www.wjgnet.com/2307-8960/full/v10/i5/1684.htm
DOI: https://dx.doi.org/10.12998/wjcc.v10.i5.1684

INTRODUCTION

Laparoscopic partial nephrectomy and robotic-assisted laparoscopic partial nephrectomy have been widely used with features of less invasiveness and quicker recovery. However, some complications such as pneumothorax or potential bleeding are uncommon but lethal. The approximate incidence rate of pneumothorax was 1%. Moreover, it could be detected in almost all laparoscopic or robotic operations and calls for prompt treatment[1]. There are many reasons for pneumothorax, amongst which spontaneous diaphragm injury is one of the most difficult to discover. We present a lupus nephritis case with a long-term target treatment and hormone therapy who developed a pneumothorax during the operation.

CASE PRESENTATION

Chief complaints

A 39-year-old woman demanded the resection of her primary renal carcinoma after receiving 6-mo target therapy.

History of present illness

The patient was diagnosed with renal clear cell carcinoma with bone metastasis half a year ago. After receiving 6-mo target therapy, manifestations of bone lesions disappeared while the size of the renal mass increased. A partial nephrectomy was recommended for the treatment of her primary renal tumor.

History of past illness

The patient had been on hormone for lupus nephritis treatment for 17 years.

Personal and family history

The patient had no markable personal and family history.

Physical examination

On arrival at the urosurgery ward, the patient's blood pressure (BP) was 128/76 mmHg, and her pulse rate was 77 beats per minute (bpm). No percussion pain was detected alongside her urinary system.

Laboratory examinations

Nothing abnormal was shown in the laboratory examinations.

Imaging examinations

A mass with mixing density was found on her left kidney on the enhanced computed tomography (CT). Its size was about 5.6 × 4.4 × 4.8 cm.

INTRAOPERATIVE PNEUMOTHORAX

Hydrocortisone was prescribed as a premedication preoperatively. The patient's electrocardiogram, blood oxygen saturation (SpO_2), heart rate (HR), BP, body temperature, and end-tidal carbon dioxide (EtCO2) were monitored. Anesthesia was induced with 150 mg of propofol, 10 mg of oxycodone, and 40 mg of rocuronium. The endotracheal intubation depth was 21 cm from the incisors. The anesthesia was maintained by inhaled sevoflurane and intravenous remifentanil. Ventilation parameters were set to volume-controlled mode (tidal volume at 6-8 mL/kg, respiratory rate at 10-12 times/min). As a result, the $EtCO_2$ partial pressure was about 31-44 mmHg, and airway pressure was maintained between 20-25 mmHg.

The patient was set to the right lateral position for laparoscopic partial nephrectomy. After establishing the retroperitoneal space, continuous CO_2 insufflation was adopted to maintain the pneumoperitoneal pressure at 14 mmHg. The operation went on smoothly for half an hour, then suddenly, the patient's SpO_2 dropped to 92%, while her HR increased to 106 bpm, and her BP increased from 80-90/60-65 mmHg to 106/80 mmHg. We paused the operation to recheck all equipment to make sure they were working well. Minutes later, her SpO_2 decreased to 85%-88%, and BP dropped to 80-85/50-60 mmHg like in a roller coaster. On the contrary, her HR increased to 116-125 bpm. The auscultation revealed that no breath sound of her right lung could be heard. Intraoperative pneumothorax was suspected, whereas pulmonary embolism could not be excluded, either.

The operation had to be ceased temporarily to set the patient's body position to supine. The anesthetist withdrew all intravenous medications and maximized the O_2 supply to 100%. Lung dilation was also conducted. However, after a 5-min resuscitation, her highest SpO_2 could only reach 92%. Arterial blood gas analysis showed that her partial CO_2 pressure was 47.5 mmHg, and blood lactic acid was 1.0 mmol/L. Due to the shielding of the metal part of the operating table, intraoperative X-ray was not feasible in this case. Intraoperative ultrasound of the right lung was conducted, and the result showed an advection requisition on M-mode (Figure 1). With this evidence, intraoperative pneumothorax was diagnosed. Residual retroperitoneal CO_2 was released immediately. The patient's SpO_2 could be maintained at 94%-98%, and intraarterial pressure was controlled at 90-100/60-70 mmHg after 30 min of pure O_2 flow and lung dilation. Finally, her breath sound of the right lung could be heard again.

After careful evaluation, the patient was again set to the right lateral position, and the retroperitoneal CO_2 pressure was lowered to 10-12 mmHg. Laparoscopic exploration proved the integrity of the diaphragm: No injury or damage was found. The surgery was finished within the next hour, and the patient's SpO_2 could still be around 90%-94% after turning her back to a supine position. An extra 30-min pure O_2 insufflation and lung dilation were performed until her SpO_2 reached 100%. We transferred the patient to the post-anesthesia care unit and monitored her vital signs for more than 1 h. The patient claimed mild pain in her right chest during the monitoring. She was sent back to the urosurgery ward after her SpO_2 was sustained at 100% and all other vital signs were steady.

As soon as she entered the ward, she received low-flow oxygen support with a nasal cannula, and her SpO_2 was maintained at 100%. A bedside chest X-ray (Figure 2) was ordered, whereas no evidence of pneumothorax or lib injury was found. Her spontaneous breathing SpO_2 was about 96%-98% on the first day after surgery. There were no other complications till the patient was discharged.

FINAL DIAGNOSIS

The final diagnosis of the presented case was left renal cell carcinoma with a history of bone metastasis. Intraoperative pneumothorax was diagnosed in this patient.

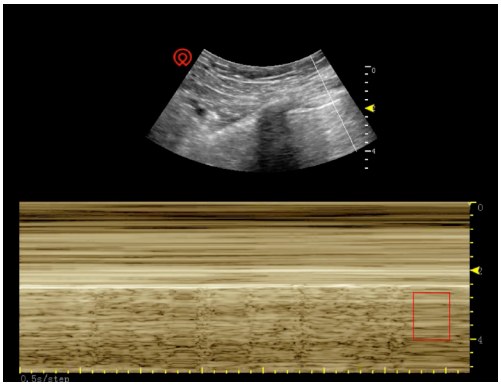

Figure 1 Ultrasound showed an advection level sign on M-mode during the operation. Red square indicates the advection level sign on M-mode, whereas no B line could be detected on ultrasonography.

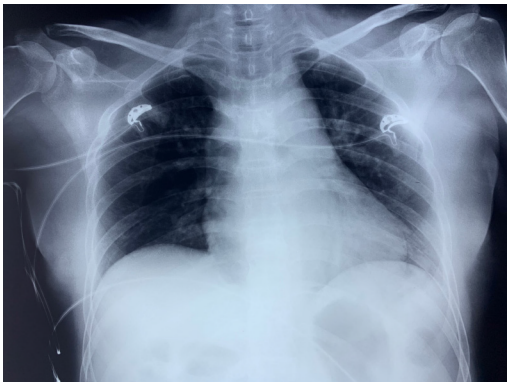

Figure 2 Bedside chest X-ray result after the patient had been transferred to the urosurgery ward. No evidence of pneumothorax or lib injury was found after the lung dilation.

TREATMENT

After pure O_2 flowing, lung dilation, and lowering the retroperitoneal CO_2 pressure, the patient's breath sound of the right lung could be heard again. Laparoscopic partial nephrectomy was performed successfully for this patient.

OUTCOME AND FOLLOW-UP

The patient reported no shortness of breath or chest pain at her first and second postoperative outpatient visits.

DISCUSSION

Pneumothorax is one of the most dangerous complications during laparoscopic or robot-assisted laparoscopic operations. The literature review showed 11 cases of intraoperative pneumothorax that happened[2-3]. The diagnosis of a pneumothorax always depends on ultrasound, X-ray, or chest CT scanning. Chest X-ray is usually the initial tool to detect potential cases. However, its application is limited in the operation room due to the inconvenience of fetching the equipment and low accuracy.

In contrast, transthoracic ultrasound has been reported to be a cheaper, more efficient, and more accurate source of evidence than chest X-ray with an 81% sensitivity and 100% specificity[4]. The typical manifestation of pneumothorax under ultrasound is the multiple advection levels on M-mode, and the pleura moves without line B. X-ray or CT scan reveals the compression or atrophy of the lung. Intraoperative pneumothorax may result from: (1) Intraoperative diaphragm injury, including sharp instrument puncturing or thermal burning; (2) the congenital defection of the

diaphragm, which was not discovered before the operation[5]; and (3) high insufflation pressure and long surgery time[6].

Pneumothorax is sometimes misdiagnosed or confused with pulmonary embolism. In this case, we performed the arterial blood gas analysis to assess the patient's condition and exclude pulmonary embolism. An intraoperative ultrasound examination of the lung was also performed to seek more evidence of the pneumothorax. In this case, no injury or damage to the diaphragm was found before or during the operation. However, intraoperative exploration showed that her connective tissues and vessels were extremely fragile. Considering that cases had been sporadically reported, a 12-15 mmHg pneumoperitoneum pressure might cause intraoperative pneumothorax[3,7], while the insufflation pressure was set to 14 mmHg in this case. Given that this patient had a medical history of lupus nephritis and had been on hormone therapy for more than 10 years, we supposed that this might be the reason for the development of the pneumothorax, as CO_2 could transfer from the retroperitoneal space to the chest under a higher insufflation pressure and a longer operation time.

The treatment of the pneumothorax should be adjusted dynamically according to its cause and severity. Regardless, the CO_2 insufflation should be discontinued, whereas endotracheal intubation, hyperventilation, and higher positive end-expiratory pressure should be maintained for lung dilation[8]. In this patient, an insufflation pressure of 10-12 mmHg might be feasible as her renal tumor was located in the middle to lower kidney, where there was a relatively wider retroperitoneal space. However, in those where the tumors are particularly close to the diaphragm, lowering the retroperitoneal CO_2 pressure might interfere with the operation.

CONCLUSION

Pneumothorax is a rare but severe complication in laparoscopic or robot-assisted laparoscopic operations. It is sometimes neglected unless the injury or damage of the diaphragm is found. Intraoperative ultrasound is a convenient method for diagnosis. Low insufflation pressure and shorter operation time might be necessary for patients with a long-term hormone treatment history or chronic immune systematic disease.

REFERENCES

1 **Del Pizzo JJ**, Jacobs SC, Bishoff JT, Kavoussi LR, Jarrett TW. Pleural injury during laparoscopic renal surgery: early recognition and management. *J Urol* 2003; **169**: 41-44 [PMID: 12478098 DOI: 10.1097/01.ju.0000035357.98762.cc]

2 **Wu Q**, Zhang H. Carbon dioxide pneumothorax following retroperitoneal laparoscopic partial nephrectomy: a case report and literature review. *BMC Anesthesiol* 2018; **18**: 202 [PMID: 30579345 DOI: 10.1186/s12871-018-0662-x]

3 **Mamić I**, Danolić D, Puljiz M, Kasum M, Alvir I, Kostić L, Milas I, Šoštar A, Pedišić I, Bečejac T. Pneumothorax and Pneumomediastinum as a Rare Complication of Laparoscopic Surgery. *Acta Clin Croat* 2016; **55**: 501-504 [PMID: 29046017 DOI: 10.20471/acc.2016.55.03.22]

4 **Lichtenstein DA**, Mezière GA. Relevance of lung ultrasound in the diagnosis of acute respiratory failure: the BLUE protocol. *Chest* 2008; **134**: 117-125 [PMID: 18403664 DOI: 10.1378/chest.07-2800]

5 **Park HJ**, Kim DK, Yang MK, Seo JE, Kwon JH. Carbon dioxide pneumothorax occurring during laparoscopy-assisted gastrectomy due to a congenital diaphragmatic defect: a case report. *Korean J Anesthesiol* 2016; **69**: 88-92 [PMID: 26885310 DOI: 10.4097/kjae.2016.69.1.88]

6 **Murdock CM**, Wolff AJ, Van Geem T. Risk factors for hypercarbia, subcutaneous emphysema, pneumothorax, and pneumomediastinum during laparoscopy. *Obstet Gynecol* 2000; **95**: 704-709 [PMID: 10775733 DOI: 10.1016/s0029-7844(00)00781-x]

7 **Aravind A**, Shroff P, Dewoolkar L. Epigastric pain caused by pneumothorax following extubation in a case of transperitoneal laparoscopic nephrectomy. *Intern J Anesthesiol* 2006; **13** [DOI: 10.5580/1ca1]

8 **Joris JL**, Chiche JD, Lamy ML. Pneumothorax during laparoscopic fundoplication: diagnosis and treatment with positive end-expiratory pressure. *Anesth Analg* 1995; **81**: 993-1000 [PMID: 7486090 DOI: 10.1097/00000539-199511000-00017]

World Journal of Clinical Cases

Submit a Manuscript: https://www.f6publishing.com

World J Clin Cases 2022 February 16; 10(5): 1689-1696

DOI: 10.12998/wjcc.v10.i5.1689

ISSN 2307-8960 (online)

CASE REPORT

Bulbar conjunctival vascular lesion combined with spontaneous retrobulbar hematoma: A case report

Jia-Ying Lei, Hong Wang

ORCID number: Jia-Ying Lei 0000-0001-9972-0988; Hong Wang 0000-0001-8460-0529.

Author contributions: Lei JY presented the idea, learned about optic neuritis, hepatitis B virus, and immune complex disease, she also wrote the manuscript; Wang H reviewed and corrected the manuscript; and all authors have approved the manuscript and agree with submission to journal.

Informed consent statement: Written informed consent was obtained from the patient for publication of this report and any accompanying images.

Conflict-of-interest statement: The authors declare that they have no conflicts of interest.

CARE Checklist (2016) statement: The authors have read the CARE Checklist (2016), and the manuscript was prepared and revised according to the CARE Checklist (2016).

Country/Territory of origin: China

Specialty type: Ophthalmology

Provenance and peer review: Unsolicited article; Externally peer reviewed.

Peer-review model: Single blind

Jia-Ying Lei, Hong Wang, Department of Ophthalmology, Qilu Hospital of Shandong University, Jinan 250012, Shandong Province, China

Corresponding author: Hong Wang, BMed, Chief Physician, Professor, Department of Ophthalmology, Qilu Hospital of Shandong University, Wenhua West Road, Jinan 250012, Shandong Province, China. dr.wanghong@163.com

Abstract

BACKGROUND

Orbital hemorrhage can be classified as traumatic or spontaneous depending on its cause. Spontaneous orbital hemorrhage refers to an internal orbital hemorrhage without apparent cause. Therefore, we aimed to describe a case of an orbital hematoma after a severe cough the night before due to inhalation of cooking oil fumes.

CASE SUMMARY

A 46-year-old woman was referred to our hospital with a complaint of exophthalmos accompanied with blurred vision, pain, binocular diplopia, and dizziness lasting for 5 h noted on waking in the morning. She also experienced nausea and vomiting due to high pressure of orbit and dizziness. Based on the auxiliary examination and her medical history, the patient was finally diagnosed with bulbar conjunctival vascular lesion combined with spontaneous retrobulbar hematoma. The patient was administered tobramycin and dexamethasone eye ointment, and applied pressure dressing on the left eye to stop the bleeding. Simultaneously, we administered intravenous etamsylate, oral Yunnan Baiyao capsule, intravenous mannitol to reduce orbital pressure, and intravenous dexamethasone injection at 10 mg/dL combined with neurotrophic therapy to reduce tissue edema. Among them, the Yunnan Baiyao capsule is a traditional Chinese herbal medicine to remove stasis and stop bleeding; thus, it promotes blood circulation and relieves pain resulting in reduced edema of the lesion site. The symptoms did not improve significantly during the first 2 d of treatment. We speculate that high orbital pressure and binocular diplopia induced frequent nausea and vomiting in the patient, causing increased pressure on the superior vena cava and leading to repeated orbital bleeding. After the second day, the symptoms started gradually improving.

CONCLUSION

This case further emphasizes the importance of comprehensive, detailed medical

Peer-review report's scientific quality classification
Grade A (Excellent): 0
Grade B (Very good): 0
Grade C (Good): C
Grade D (Fair): 0
Grade E (Poor): 0

Received: August 31, 2021
Peer-review started: August 31, 2021
First decision: November 17, 2021
Revised: November 22, 2021
Accepted: January 8, 2022
Article in press: January 8, 2022
Published online: February 16, 2022

P-Reviewer: Nuño JSZ
S-Editor: Wang JL
L-Editor: A
P-Editor: Wang JL

history and careful ophthalmic examination of the patient.

Key Words: Bulbar conjunctival vascular lesion; Spontaneous retrobulbar hematoma; Intraorbital hemorrhage; Nontraumatic orbital hemorrhage; Case report

Core Tip: Orbital hemorrhage can be classified as traumatic or spontaneous according to its cause. Spontaneous orbital hemorrhage is an extremely rare and vision-threatening condition that may occur due to a variety of systemic predisposing factors. This case report suggests that patients with malformed periorbital vasculature should be alert for the risk of spontaneous intraorbital hemorrhage. In previous literature, we found reports of retrobulbar hematomas caused by sneezing or vomiting. However, to our knowledge, this is the first reported case of apparent bulbar conjunctival vascular malformation combined with retrobulbar hematoma caused by severe coughing.

Citation: Lei JY, Wang H. Bulbar conjunctival vascular lesion combined with spontaneous retrobulbar hematoma: A case report. *World J Clin Cases* 2022; 10(5): 1689-1696
URL: https://www.wjgnet.com/2307-8960/full/v10/i5/1689.htm
DOI: https://dx.doi.org/10.12998/wjcc.v10.i5.1689

INTRODUCTION

Orbital hemorrhage can be classified as traumatic or spontaneous depending on its cause. Spontaneous orbital hemorrhage refers to internal orbital hemorrhage without apparent cause with sudden onset, manifesting as proptosis, ophthalmoplegia, ocular distension, pain, increased intraocular pressure, vision loss, diplopia, loss of pupillary reflexes, and optic disc or retinal pallor[1]. Spontaneous orbital hemorrhage is an extremely rare and vision-threatening condition. It may occur due to various systemic predisposing factors such as hypertension, atherosclerosis, intraorbital vascular malformation, and hematologic diseases (abnormal platelet aggregation, hemophilia, and deficiency of human coagulation factor IX). Hass *et al*[2] reported that the Valsalva maneuver (when caused by vomiting and coughing) is another uncommon etiologic factor. Orbital hemangioma is the most common benign orbital tumor involving one eye, accounting for 24% of orbital tumors. It usually occurs in the muscle cone and is caused by congenital vascular anomalies and can be diagnosed using magnetic resonance imaging (MRI) or computed tomography (CT). Treatment aims to lower the intraorbital pressure and protect the optic nerve from damage. Pharmacotherapy may be considered in cases with minor retrobulbar hemorrhage; however, if the pain in the patient's eye or head is intolerable, or corneal function and vision are significantly affected, surgery is required[1].

Therefore, we report a patient with bulbar conjunctival vascular malformation combined with a spontaneous retrobulbar hematoma that was mistaken for anemia when admitted to a local hospital.

CASE PRESENTATION

Chief complaints

A 46-year-old woman was referred to our hospital on February 16, 2021, for left eye protrusion combined with blurred vision, pain, binocular diplopia, and dizziness lasting for 5 h noted on waking in the morning. She also experienced nausea and vomiting due to high intraocular pressure and dizziness.

History of present illness

The patient recalled having a severe cough the night before the hospital visit, due to inhalation of cooking oil fumes. Upon initial admission to a local hospital, her complete blood count suggested anemia, and her left eye subconjunctival vascular

malformation was mistaken as being caused by a hemorrhage. The local hospital discovered a retrobulbar hematoma and suspected that it was caused by a blood system disease; therefore, she was referred to our hospital for a systematic examination.

History of past illness

The patient had a history of heavy menstrual bleeding, lasting approximately 15 d. She denied other medical and surgical histories.

Personal and family history

The patient's personal and family histories were negative.

Physical examination

The visual acuity of the right eye was 0.04 (-7.00/-0.75 × 100 = 0.8), the left eye was 0.08 (-7.50/-2.00 × 65 = 0.3). The bilateral intraocular pressure was 19 mmHg and 21 mmHg, respectively. There was no redness or swelling in the left eyelid, but the lift was limited, and the upper eyelid covered the upper half of the pupil. The left eyeball protruded forward and was lowered (Figure 1A), the eye movements were limited to up gaze. Slit-lamp examination revealed that her left conjunctiva was not congestible, and curled blood vessels were seen under the conjunctiva on the temporal side, with a dark purple color and a range of approximately 1 cm × 1 cm (Figure 1B). Pupillary reflexes were insensitive, and no obvious abnormalities were observed in the fundus. The exophthalmos of the right and left eye were 14.5 mm and 23 mm, respectively, and the distance between the lateral margin of both orbitals was 100 mm.

Laboratory examinations

Screening showed a hemoglobin concentration of 76 g/L, hematocrit of 29.1%, mean erythrocyte volume of 67.2 fL, a ferritin level of 4.69 ng/mL, and coagulation profile was within normal limits.

Imaging examinations

Gynecological B-ultrasound examination revealed multiple uterine fibroids.

A CT scan indicated left eye protrusion, and orbital near the bottom side showed a clumpy high-density mass (88 HU); the cross-section of this shadow was approximately 2.3 cm × 1.5 cm. No obvious disruption of the orbital wall bone structure was observed.

MRI scans of the orbits showed protrusion of the left eye and an elliptical long-short T1 Long-short T2 signal focus was observed in the lateral optic nerve of the left orbital muscle cone, with smooth edges and low signal on diffusion-weighted imaging. The left hyperdense retrobulbar mass displaced the optic nerve superomedially (Figure 2).

Ocular ultrasound showed uneven echo of the posterior eyeball mass of the left eye that disappeared while the gain reduced, suggestive of goiter of the left orbit (Figure 3).

FINAL DIAGNOSIS

Based on the auxiliary examination and medical history, the diagnoses were as follows: (1) Spontaneous retrobulbar hematoma; (2) Bulbar conjunctival vascular lesion; (3) Anemia; (4) Myopia of both eyes; and (5) Multiple uterine fibroids.

TREATMENT

The patient received tobramycin and dexamethasone eye ointment, and the left eye was bandaged with pressure. Simultaneously, intravenous etamsylate, oral Yunnan Baiyao capsule, intravenous mannitol to reduce orbital pressure, and intravenous dexamethasone injection at 10 mg/dL combined with neurotrophic therapy to reduce tissue edema, were administered.

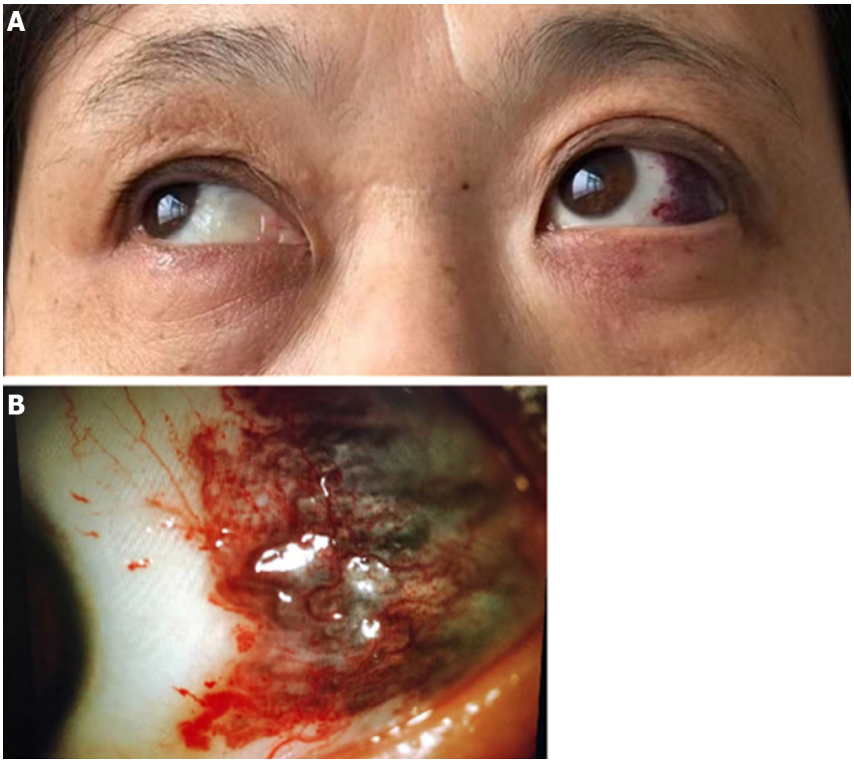

Figure 1 The slit-lamp examination of left eye. A: The left eyeball protruded forward; B: The slit-lamp examination found that her left conjunctiva was not congestible and curled blood vessels were seen under the conjunctiva in the temporal side, which color was dark purple, with a range of about 1 cm × 1 cm.

OUTCOME AND FOLLOW-UP

Two days after the initial treatment, symptoms had not improved significantly. The high orbital pressure was suspected of having induced frequent nausea and vomiting of the patient, increasing the pressure on the superior vena cava, leading to repeated orbital bleeding. However, her symptoms started to improve after the second day gradually. Considering that the visual acuity and corneal function were not significantly affected and the high risk of surgical treatment, we continued with a conservative (wait and see) treatment. After seven days, the visual acuity of the left eye was 0.08 (-5.25/-2.00 × 80 = 0.8), and the intraocular pressure in both eyes was 19 mmHg and 20 mmHg, respectively. The exophthalmos of the left eye was less severe than at the beginning of hospitalization; the right eye was 14.5 mm, and the left was 18 mm, and the distance between the lateral margin of both orbitals was 100 mm. Visual field examination revealed a visual field defect below the temporal of the left eye (Figure 4). MRI revealed a small reduction in the size of the lesion (1.8 cm × 1.3 cm). Prior to discharge, improvements were observed in the patient's visual acuity and exophthalmos.

DISCUSSION

Orbital hemorrhage can be classified as traumatic or spontaneous according to its cause. In 2000, Sullivan *et al*[3] reviewed the records of 115 patients diagnosed with non-traumatic orbital hemorrhage and found that underlying vascular anomalies were present in 104 (90%), usually younger patients. Acute onset painful proptosis, associated with lid swelling or mass, was the most common presentation. Among these patients, only 7% underwent surgery for optic nerve compression, while 89% had complete or partial spontaneous resolution of the hemorrhage.

When the patient was first admitted to a local hospital, laboratory findings suggested anemia. Furthermore, the left eye subconjunctival vascular malformation was mistaken as being caused by the hemorrhage, supported by the orbital CT, which revealed an orbital hematoma in the left eye. Therefore, a spontaneous retrobulbar hematoma was suspected caused by a blood system disease and was then referred to our hospital for a systematic examination to determine the cause. When referred to our

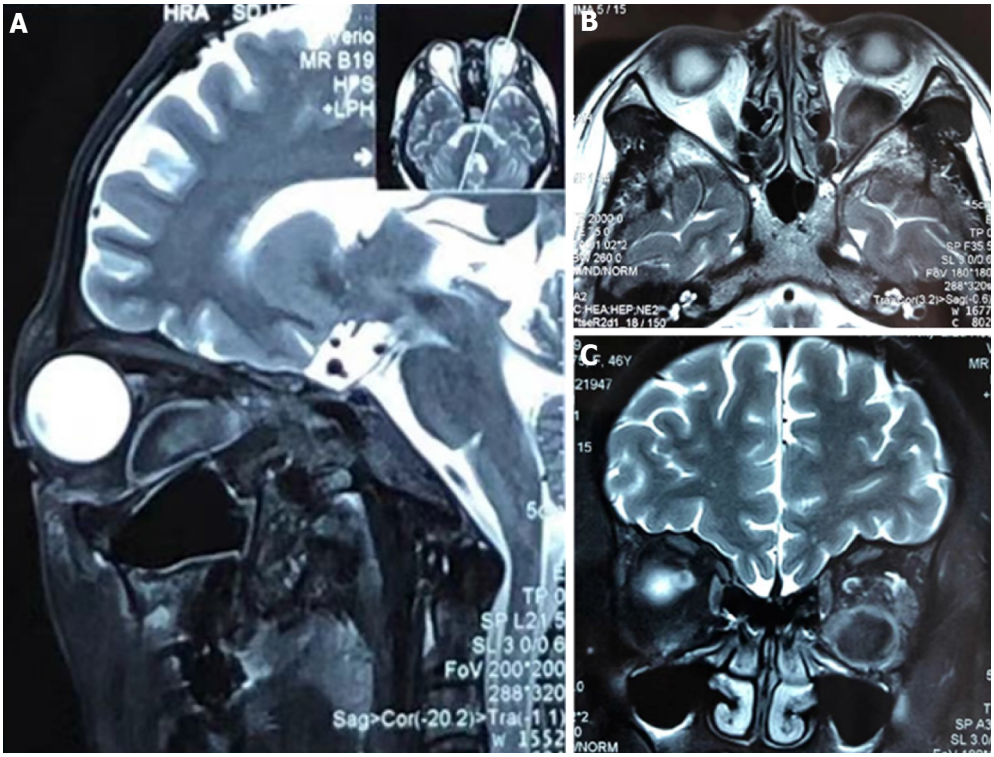

Figure 2 Magnetic resonance imaging scans of orbits. A-C: Magnetic resonance imaging scans of orbits showed that the left eye was protruding, and an elliptical long-short T1 long-short T2 signal focus was observed in the lateral optic nerve of the left orbital muscle cone, with smooth edges and low signal on DWI. The left hyperdense retrobulbar mass displaced optic nerve superomedial.

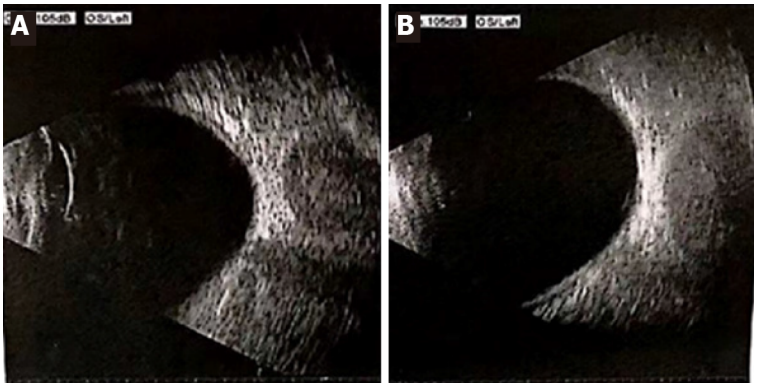

Figure 3 Ocular ultrasound of the left eye. A, B: Ocular Ultrasound showed that the echo of the posterior eyeball mass of the left eye is uneven, and it disappears while the gain reduced, suggesting there was a goitre of the left orbit.

hospital, careful eye examination and comprehensive auxiliary examination revealed that the abnormal change under the conjunctiva of the left eye was a vascular malformation. In addition, we found that her anemia was due to multiple uterine fibroids; therefore, we concluded that the orbital hematoma was related to the malformed subconjunctival vessels and that there might have been similar malformed vessels in the intraorbital area before bleeding.

In this case, we found that the patient had a congenital venous vascular mass of the temporal bulbar subconjunctival malformation of the left eye. She recalled having a severe cough the night before due to the inhalation of cooking oil fumes. Therefore, it was considered more likely that the orbital hematoma was caused by rupture of the malformed intraorbital vessels rather than anemia. Due to the abnormal congenital development of these malformed vessels, the structure of their walls is defective; hence, they become weaker after luminal congestion. Any factor that causes increased internal jugular venous pressure may lead to rupture and bleeding of the vessels. In 2018, the International Society for the Study of Vascular Anomalies divided vascular anomalies into tumors and malformations. Vascular tumors were divided into three

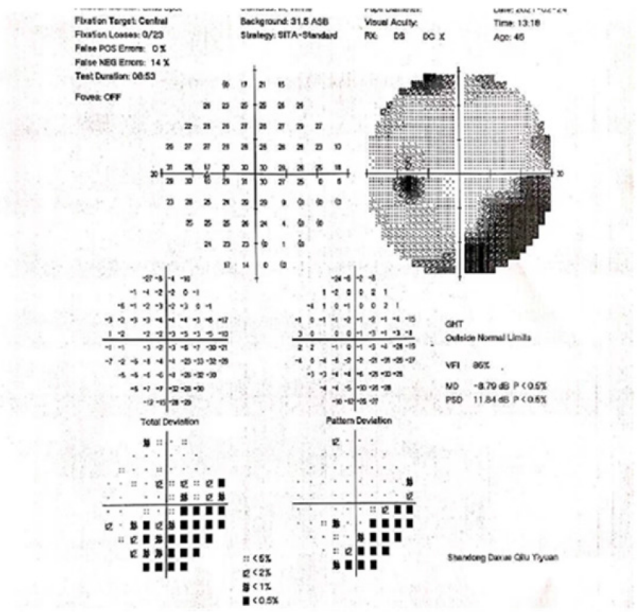

Figure 4 Visual field examination. Visual field examination revealed a visual field defect below the temporal of the left eye.

subtypes: benign, locally aggressive or borderline and malignant. Vascular malformations were divided into simple vascular malformation, mixed vascular malformation, well-known macrovascular malformation, vascular malformation combined with other lesions, vascular changes not yet classified and PIK3CA-related overgrowth spectrum [4]. Strictly speaking, to determine the origin of the vascular tissue of the patient's subconjunctival and intraorbital anomalies, a histopathological study is necessary. However, after conservative treatment, the patient's condition was controlled and to avoid further bleeding, pathological samples were not taken.

The onset of spontaneous orbital hemorrhage is usually sudden and can manifest as proptosis, ophthalmoplegia, pain, pressure, vision loss, diplopia, loss of pupillary reflexes, optic disc, retinal pallor, nausea, and vomiting[2,5]. The clinical presentation of our patient was therefore typical and comprehensive.

The Valsalva maneuver has been reported to be a cause of non-traumatic orbital hemorrhage. In 2004, Hass *et al*[2] investigated the incidence of orbital hemorrhage following cosmetic eyelid surgery and found that among 26433 patients, 149 developed orbital hemorrhage. This development was most common within the first 3 h after surgery and related to hypertension, perioperative aspirin use, postoperative vomiting, and increased physical activity. Liovic *et al*[6] reported a case of a 24-year-old female patient with nontraumatic subperiosteal orbital hemorrhage in the 25th week of pregnancy, presenting with painless left globe proptosis and blurred vision after vomiting. Considering that the patient was pregnant and without any signs of optic nerve compression, conservative treatment was adopted.

In the present case, the patient's symptoms did not improve significantly within the first 2 days of treatment. High orbital pressure was thought to induce frequent nausea and vomiting in the patient, which increased the intra-abdominal and intrathoracic pressure, which in turn increased the pressure in the superior vena cava. Since orbital veins do not contain valves, increased pressure in the superior vena cava would cause a rapid increase in orbital vessel pressure and lead to repeated orbital bleeding[1].

Both CT and MRI can be used to observe orbital structures and identify lesion types; however, while MRI is better than CT for enabling faster detection of vascular lesions, CT is the first choice for head and face emergencies (such as retrobulbar hemorrhage [7]).

There are three main options for the treatment of spontaneous retrobulbar hematoma[7]. First, conservative treatment is preferred if the hematoma scope is small and the early stage of the disease has little effect on visual function. Conservative treatments, such as hemostasis, corticosteroids, mannitol, and other treatments can be provided to reduce edema, orbital pressure and subsequently relieve the compression of the optic nerve and blood vessels. It is important to observe the patient's condition closely, and if there is a clear etiology, such as hypertension or blood system disease, the cause should be treated. Second, puncture of hematoma is preferred for a simple hematoma with high ocular prolapse, eye pain, unbearable headache, serious corneal

function, and vision endangering. This procedure is performed under ultrasound guidance or after CT scan positioning, after which pressurized bandages are applied for several days. The main purpose of the pressure dressing is to prevent a sudden decrease in orbital pressure after the puncture, as this may lead to vascular dilatation and rebleeding. Third, orbital decompression is for orbital hematoma complicated with vascular lesions. Surgical treatment should be performed as early as possible to resolve the orbital lesions while the hematoma is being treated. For simple old hematomas with coagulated blood that are difficult to puncture or have a deep location, anterior or lateral wall orbital surgery is often needed. In the case of fresh active bleeding during the operation, adequate hemostasis should be performed, and attention should be paid to protecting the orbital tissue from injury. A drainage bar should be placed 24–48 h after the operation. Sharma *et al*[8] suggested that all non-traumatic spontaneous orbital hemorrhage cases should be urgently assessed for orbital compartment syndrome or optic nerve compression. Urgent lateral cantholysis and division of the orbital septum are necessary.

In our case, considering that the patient's visual acuity recovered significantly after conservative treatment, with a gradual decrease of the ocular protrusion; while also considering that both ultrasound-guided puncture hematoma and surgical treatment have greater risks, we decided to continue the conservative treatment.

Spontaneous retrobulbar hematoma should be differentiated from the following diseases: (1) traumatic intraorbital hemorrhage, most patients have a clear history of trauma, with a rapidly protruding eyeball often accompanied by facial tissue swelling, periorbital fracture, eyelid enclosure, disturbance of eye movement, and diplopia[9]; (2) intraorbital cystic tumors, which include epidermoid cysts, dermoid cysts, and cystic schwannomas. On CT, intraorbital cystic tumors present regular or irregular low-density shadows in homogeneous soft tissue density, while the intraorbital hematoma appears as a soft tissue mass. Enhanced CT or MRI should be performed when the differential diagnosis is difficult. On enhanced CT, the tumors are mostly enhanced overall, while on MRI, long T1 and T2 signals can be seen[10]; (3) orbital cellulitis, a secondary infection of the adjacent orbital tissues, in which sinus infection, especially in the ethmoid sinus, is the most common source of periorbital infection. Other sources include oral, tooth, gingival, or maxillofacial infections[11]. Spontaneous orbital hemorrhage often has no apparent predisposing factor; therefore, it may be misdiagnosed as orbital cellulitis if bleeding progresses rapidly; and (4) sinus mucous cysts, which are primarily found in the frontal and ethmoid sinuses. If the cyst bone wall is weak or disappears, then once the cyst ruptures, cystic fluid easily flows into the orbit, causing rapid protrusion of the eyeball. If the cyst is large, it can protrude directly into the orbit. In addition to the intraorbital mass, the mass connected to the sinus cyst can also be detected through imaging examination. The signal or density of both masses was similar, and the sinus cavity of the affected sinus was enlarged[12].

CONCLUSION

This case report suggests that patients with malformed periorbital vasculature should be alert for the risk of spontaneous intraorbital hemorrhage. In previous literature, we found reports of retrobulbar hematomas caused by sneezing or vomiting[2]. However, to the best of our knowledge, this is the first reported case of apparent bulbar conjunctival vascular malformation combined with retrobulbar hematoma caused by severe coughing.

REFERENCES

1 **Deveer M**, Cullu N, Beydilli H, Sozen H, Yeniceri O, Parlak S. Spontaneous Retrobulbar Haematoma. *Case Rep Radiol* 2015; **2015**: 796834 [PMID: 26090258 DOI: 10.1155/2015/796834]

2 **Hass AN**, Penne RB, Stefanyszyn MA, Flanagan JC. Incidence of postblepharoplasty orbital hemorrhage and associated visual loss. *Ophthalmic Plast Reconstr Surg* 2004; **20**: 426-432 [PMID: 15599241 DOI: 10.1097/01.iop.0000143711.48389.c5]

3 **Sullivan TJ**, Wright JE. Non-traumatic orbital haemorrhage. *Clin Exp Ophthalmol* 2000; **28**: 26-31 [PMID: 11345340 DOI: 10.1046/j.1442-9071.2000.00241.x]

4 **International Society for the Study of Vascular Anomalies**. ISSVA Classification of Vascular Anomalies 2018. [accessed 2019 Jan]. Available from: https://www.issva.org/classification

5 **Richardson K**, Perry M, White S. Post-traumatic eye observations M.C. Bater, P.L. Ramchandani, P.A. Brennan, Br. J. Oral Maxillofac. Surg. 43 (2005) 410-416. *Br J Oral Maxillofac Surg* 2007; **45**:

173-174 [PMID: 16713044 DOI: 10.1016/j.bjoms.2006.02.006]
6 **Liovic M**, Sekelj S, Janjetovic Z, Vukovic Arar Z. A case of nontraumatic subperiosteal orbital hemorrhage following vomiting in pregnancy. *Int J Ophthalmol* 2020; **13**: 1675-1677 [PMID: 33078122 DOI: 10.18240/ijo.2020.10.25]
7 **Atalla ML**, McNab AA, Sullivan TJ, Sloan B. Nontraumatic subperiosteal orbital hemorrhage. *Ophthalmology* 2001; **108**: 183-189 [PMID: 11150286 DOI: 10.1016/s0161-6420(00)00482-6]
8 **Sharma N**, O'Hagan S. Non-traumatic orbital haemorrhage as a complication of emergence from anaesthesia. *Anaesth Rep* 2014; **2**: 49-51 [DOI: 10.21466/ac.NOHAACO.2014]
9 **Murchison AP**, Bilyk JR, Savino PJ. Traumatic Cranial Neuropathies. In: Black E, Nesi F, Calvano C, Gladstone G, Levine M, editors. Smith and Nesi's Ophthalmic Plastic and Reconstructive Surgery. New York: Springer, 2012: 165-197 [DOI: 10.1007/978-1-4614-0971-7_7]
10 **Smoker WR**, Gentry LR, Yee NK, Reede DL, Nerad JA. Vascular lesions of the orbit: more than meets the eye. *Radiographics* 2008; **28**: 185-204; quiz 325 [PMID: 18203938 DOI: 10.1148/rg.281075040]
11 **Baiu I**, Melendez E. Periorbital and Orbital Cellulitis. *JAMA* 2020; **323**: 196 [PMID: 31935029 DOI: 10.1001/jama.2019.18211]
12 **Işık AÜ**, Arslan S, Arslan E, Baykal S. A giant frontoethmoid mucocele with intracranial extension. *Scott Med J* 2015; **60**: e1-e3 [PMID: 25428941 DOI: 10.1177/0036933014561949]

World Journal of Clinical Cases

Submit a Manuscript: https://www.f6publishing.com

World J Clin Cases 2022 February 16; 10(5): 1697-1701

DOI: 10.12998/wjcc.v10.i5.1697

ISSN 2307-8960 (online)

CASE REPORT

Hepatitis B virus in cerebrospinal fluid of a patient with purulent bacterial meningitis detected by multiplex-PCR: A case report

Dai-Quan Gao, Yong-Qiang Hu, Xin Wang, Yun-Zhou Zhang

ORCID number: Dai-Quan Gao 0000-0002-2091-7567; Yong-Qiang Hu 0000-0001-6763-0072; Xin Wang 0000-0001-6779-6152; Yun-Zhou Zhang 0000-0001-9056-9505.

Author contributions: Gao DQ and Zhang YZ were the patient's neurosurgeons, reviewed the literature, contributed to manuscript drafting, and were responsible for the revision of the manuscript for important intellectual content; Hu YQ and Wang X reviewed the literature, and analyzed and interpreted the imaging findings; all authors issued final approval for the version to be submitted.

Informed consent statement: Informed written consent was obtained from the patient for publication of this report and any accompanying images.

Conflict-of-interest statement: The authors declare that they have no conflict of interest to disclose.

CARE Checklist (2016) statement: The authors have read the CARE Checklist (2016), and the manuscript was prepared and revised according to the CARE Checklist (2016).

Country/Territory of origin: China

Specialty type: Infectious diseases

Dai-Quan Gao, Yun-Zhou Zhang, Department of Neurology, Xuanwu Hospital, Capital Medical University, Beijing 100053, China

Yong-Qiang Hu, Department of Critical Care Medicine, Beijing Fengtai You'anmen Hospital, Beijing 100069, China

Xin Wang, Department of Intensive Medicine, Beijing Youan Hospital, Capital Medical University, Beijing 100069, China

Corresponding author: Yun-Zhou Zhang, PhD, Chief Physician, Department of Neurology, Xuanwu Hospital, Capital Medical University, No. 45 Changchun Street, Xicheng District, Beijing 100053, China. bjyuz657@163.com

Abstract

BACKGROUND

Bacterial meningitis (BM) is a common central nervous system inflammatory disease. BM may cause serious complications, and early diagnosis is essential to improve the prognosis of affected patients.

CASE SUMMARY

A 37-year-old man was hospitalized with purulent meningitis because of worsening headache for 12 h, accompanied by vomiting, fever, and rhinorrhea. Head computed tomography showed a lesion in the left frontal lobe. Infectious disease screening showed positivity for hepatitis B surface antigen, hepatitis B e antigen, and hepatitis B core antigen. Cerebrospinal fluid (CSF) leak was suspected based on clinical history. *Streptococcus pneumoniae* (*S. pneumoniae*) was detected in CSF by metagenomic next-generation sequencing (mNGS) technology, confirming the diagnosis of purulent BM. After treatment, multiplex PCR indicated the presence of hepatitis B virus (HBV) DNA and absence of *S. pneumoniae* DNA in CSF samples.

CONCLUSION

We report a rare case of HBV in the CSF of a patient with purulent BM. Multiplex PCR is more sensitive than mNGS for detecting HBV DNA.

Key Words: Purulent meningitis; *Streptococcus pneumoniae*; Hepatitis B virus; Multiplex PCR; Cerebrospinal fluid; Case report

Provenance and peer review: Unsolicited article; Externally peer reviewed.

Peer-review model: Single blind

Peer-review report's scientific quality classification
Grade A (Excellent): 0
Grade B (Very good): B
Grade C (Good): C, C
Grade D (Fair): D
Grade E (Poor): 0

Received: September 8, 2021
Peer-review started: September 8, 2021
First decision: October 27, 2021
Revised: November 26, 2021
Accepted: January 8, 2022
Article in press: January 8, 2022
Published online: February 16, 2022

P-Reviewer: Kao JT, Kumar R, Pham TTT
S-Editor: Li X
L-Editor: Wang TQ
P-Editor: Li X

Core Tip: The advantages of multiplex PCR are rapid detection and high sensitivity and accuracy. Multiplex PCR can assist in the diagnosis of bacterial and viral meningitis in culture-negative cerebrospinal fluid (CSF). Furthermore, this technique can improve the accuracy of diagnosis of acute bacterial meningitis (BM) in the clinical setting in culture-positive or culture-negative CSF. We report a rare case of hepatitis B virus (HBV) in the CSF of a patient with purulent BM and demonstrate that multiplex PCR is more sensitive than metagenomic next-generation sequencing for detecting HBV DNA.

Citation: Gao DQ, Hu YQ, Wang X, Zhang YZ. Hepatitis B virus in cerebrospinal fluid of a patient with purulent bacterial meningitis detected by multiplex-PCR: A case report. *World J Clin Cases* 2022; 10(5): 1697-1701
URL: https://www.wjgnet.com/2307-8960/full/v10/i5/1697.htm
DOI: https://dx.doi.org/10.12998/wjcc.v10.i5.1697

INTRODUCTION

Bacterial meningitis (BM) is a common central nervous system (CNS) inflammatory disease[1] that usually affects infants and immunocompromised adults[2,3]. BM can cause headache, nausea, fever, altered mental status, and sudden death[4] and is diagnosed by cerebrospinal fluid (CSF) examination. Most meningitis patients survive; however, one-fifth to one-third of survivors, especially newborns and children, have long-term neurological sequelae[5]. BM can be caused by different bacterial pathogens, and several bacterial species have become more prevalent in the past few decades, including *Streptococcus pneumoniae* (*S. pneumoniae*)[6], *Haemophilus influenzae*[7], and *Neisseria meningitidis*[8]. Gram-positive *S. pneumoniae* is the main causative agent of BM in many developing countries[9]. Although the mechanism by which *S. pneumoniae* crosses the blood-brain barrier (BBB) is incompletely understood, bacterial adhesion to the vascular endothelium is a crucial event in meningitis progression[10]. Therefore, timely diagnosis and treatment of BM are imperative because of the possibility of severe CNS complications[11].

The gold standard test for detecting BM is CSF bacterial culture[12]. Nonetheless, this method has limitations, including low sensitivity and delayed microbial growth, affecting clinical decision-making. Consequently, other methods are necessary for the diagnosis of meningitis. Metagenomic next-generation sequencing (mNGS) is widely used to detect pathogen nucleic acids in clinical samples[13]. Furthermore, multiplex PCR is fast and highly accurate and sensitive[14]. The early detection and diagnosis of BM are fundamental to improve long-term prognosis in affected patients. In the present case, CSF samples were analyzed by mNGS and multiplex PCR, and our patient had BM and co-infection with hepatitis B virus (HBV).

CASE PRESENTATION

Chief complaints

On 15 December 2020, a 37-year-old man was admitted to the hospital with purulent BM associated with worsening headache for 12 h and altered consciousness for 7 h.

History of present illness

Twelve hours before admission, the patient had a persistent headache without obvious cause, accompanied by nausea, vomiting, fever, and rhinorrhea. His body temperature was 37.8 ℃.

History of past illness

Medical history showed that the patient had fractured the skull and ribs in a car accident 15 years prior. And he was diagnosed with purulent BM accompanied by rhinorrhea and CSF leak 5 years prior.

Personal and family history

The patient had a free previous personal and family history.

Physical examination

The patient was hospitalized at Huairou Hospital (Beijing, China) 4 h later. Head computed tomography (CT) examination showed a lesion in the left frontal lobe. Routine blood examination showed a white blood cell count ≥ 10.02 × 10^9/L, neutrophil count ≥ 89.10%, and procalcitonin ≥ 1.62 ng/mL. The results of liver and renal function, coagulation test, blood ammonia, and blood gas analysis were unremarkable.

Laboratory examinations

The results of infectious disease screening indicated positivity for hepatitis B surface antigen (HBsAg) (250 IU/mL), hepatitis B e antigen (HBeAg) (211.40 S/CO), and hepatitis B core antigen (HBcAg) (1.2 S/CO), confirming the diagnosis of purulent BM.

CSF samples were collected by lumbar puncture[15]. *S. pneumoniae* was detected using mNGS, confirming the diagnosis of purulent BM. Bacterial infection was controlled with vancomycin and meropenem. On January 14, multiplex PCR indicated the presence of HBV DNA and absence of *S. pneumoniae* DNA in CSF samples.

Imaging examinations

CT scanning indicated that intracranial hemorrhage secondary to intracranial infection was observed, accompanied by hearing disorders (Figure 1).

FINAL DIAGNOSIS

The patient was diagnosed with purulent BM and HBV detected in CSF.

TREATMENT

Symptoms worsened, and the patient presented altered consciousness and restlessness. He was given ceftriaxone, acyclovir, diazepam, and dexamethasone to reduce cerebral edema; however, there was no clinical improvement. The patient was transferred to Xuanwu Hospital (Beijing, China). At the emergency department, his body temperature was 39.1 ℃, and hospitalization was recommended.

OUTCOME AND FOLLOW-UP

The patient was discharged from the hospital when clinical symptoms disappeared and CSF test returned to normal status. And a liver specialist treatment was recommended after discharge.

DISCUSSION

In this case, the detection of *S. pneumoniae* in CSF samples by mNGS confirmed the diagnosis of purulent BM. Infectious disease screening indicated positivity for HBsAg, HBeAg, and HBcAg. After treatment, multiplex PCR indicated the presence of HBV DNA and absence of *S. pneumoniae* DNA in CSF samples, demonstrating the high sensitivity of this molecular technique.

Twelve hours before hospitalization, the patient had worsening headache, altered consciousness, rhinorrhea, then intracranial hemorrhage secondary to intracranial infection accompanied by hearing disorders, and was diagnosed with purulent BM. Medical history showed that the patient had fractured the skull in a car accident and was diagnosed with purulent BM 5 years prior. *S. pneumoniae* was detected in the CSF by mNGS, confirming the diagnosis of purulent BM.

S. pneumoniae is one of the most common human pathogens and the causative agent of meningitis and other diseases[16]. Our findings are supported by a previous study, wherein the risk of late-onset BM was higher in adults with head surgeries[17], and the present patient had fractured the skull before. HBV was not detected in the CSF by

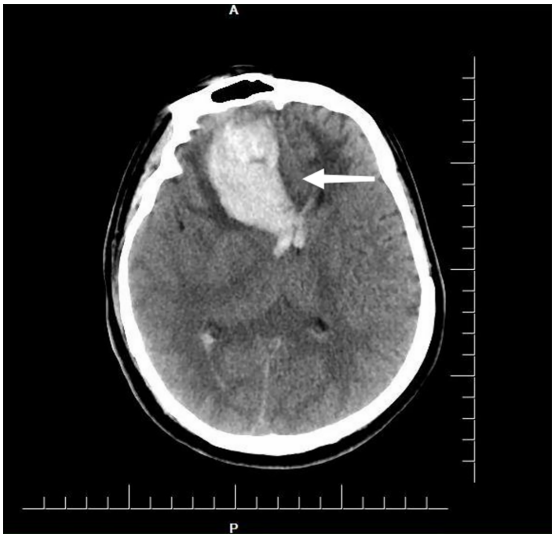

Figure 1 Computed tomography scanning results (intracranial hemorrhage secondary to intracranial infection).

mNGS, consistent with the literature. mNGS has high sensitivity and specificity for detecting *S. pneumoniae* but is less sensitive than RT-PCR for the diagnosis of encephalitis[18].

After antibiotic treatment, multiplex PCR results showed positivity for HBV DNA and negativity for *S. pneumoniae* DNA in the CSF. In this respect, it was reported that HBsAg and HBV viral load were differentially detected in the CSF and blood[19]. Additionally, HBV was detected in the CSF of patients with *S. pneumoniae* infections, demonstrating that HBV can cross the BBB. However, whether HBV can cause more severe complications is unknown.

The advantages of multiplex PCR are rapid detection and high sensitivity and accuracy[20]. Albuquerque *et al*[14] have revealed that multiplex PCR can assist in the diagnosis of bacterial and viral meningitis in culture-negative CSF. Furthermore, this technique can improve the accuracy of diagnosis of acute BM in the clinical setting in culture-positive or culture-negative CSF.

CONCLUSION

We report a rare case of HBV in the CSF of a patient with purulent BM and demonstrate that multiplex PCR is more sensitive than mNGS for detecting HBV DNA.

REFERENCES

1 **Yau B**, Hunt NH, Mitchell AJ, Too LK. Blood–Brain Barrier Pathology and CNS Outcomes in *Streptococcus pneumoniae* Meningitis. *Int J Mol Sci* 2018; **19** [PMID: 30423890 DOI: 10.3390/ijms19113555]

2 **Schuchat A**. Group B streptococcal disease: from trials and tribulations to triumph and trepidation. *Clin Infect Dis* 2001; **33**: 751-756 [PMID: 11512078 DOI: 10.1086/322697]

3 **Ashby LM**, Shepherd BT. Do nurses need mandatory continuing education? *AD Nurse* 1989; **4**: 18-19 [PMID: 2923778]

4 **van de Beek D**, de Gans J, Spanjaard L, Weisfelt M, Reitsma JB, Vermeulen M. Clinical features and prognostic factors in adults with bacterial meningitis. *N Engl J Med* 2004; **351**: 1849-1859 [PMID: 15509818 DOI: 10.1056/NEJMoa040845]

5 **Edmond K**, Clark A, Korczak VS, Sanderson C, Griffiths UK, Rudan I. Global and regional risk of disabling sequelae from bacterial meningitis: a systematic review and meta-analysis. *Lancet Infect Dis* 2010; **10**: 317-328 [PMID: 20417414 DOI: 10.1016/S1473-3099(10)70048-7]

6 **Saavedra-Velasco M**, Tapia-Cruz M, Grandez-Urbina JA, Zegarra Del Rosario-Alvarado S, Mendo-Urbina F, Pichardo-Rodriguez R. [Ceftriaxone-resistant Streptococcus pneumoniae meningitis: case report]. *Rev Peru Med Exp Salud Publica* 2019; **36**: 349-352 [PMID: 31460651 DOI: 10.17843/rpmesp.2019.362.4036]

7 **Sawardekar KP**. Haemophilus influenzae Type a Meningitis in Immunocompetent Child, Oman,

2015. *Emerg Infect Dis* 2017; **23**: 1221-1223 [PMID: 28628438 DOI: 10.3201/eid2307.170311]
8 **Munguambe AM**, de Almeida AECC, Nhantumbo AA, Come CE, Zimba TF, Paulo Langa J, de Filippis I, Gudo ES. Characterization of strains of Neisseria meningitidis causing meningococcal meningitis in Mozambique, 2014: Implications for vaccination against meningococcal meningitis. *PLoS One* 2018; **13**: e0197390 [PMID: 30089105 DOI: 10.1371/journal.pone.0197390]
9 **Scarborough M**, Thwaites GE. The diagnosis and management of acute bacterial meningitis in resource-poor settings. *Lancet Neurol* 2008; **7**: 637-648 [PMID: 18565457 DOI: 10.1016/S1474-4422(08)70139-X]
10 **Iovino F**, Seinen J, Henriques-Normark B, van Dijl JM. How Does Streptococcus pneumoniae Invade the Brain? *Trends Microbiol* 2016; **24**: 307-315 [PMID: 26804733 DOI: 10.1016/j.tim.2015.12.012]
11 **Mook-Kanamori BB**, Geldhoff M, van der Poll T, van de Beek D. Pathogenesis and pathophysiology of pneumococcal meningitis. *Clin Microbiol Rev* 2011; **24**: 557-591 [PMID: 21734248 DOI: 10.1128/CMR.00008-11]
12 **Garcia PCR**, Barcelos ALM, Tonial CT, Fiori HH, Einloft PR, Costa CAD, Portela JL, Bruno F, Branco RG. Accuracy of cerebrospinal fluid ferritin for purulent meningitis. *Arch Dis Child* 2021; **106**: 286-289 [PMID: 32111595 DOI: 10.1136/archdischild-2019-317960]
13 **Fisher AB**, Dodia C, Chander A. Beta-adrenergic mediators increase pulmonary retention of instilled phospholipids. *J Appl Physiol (1985)* 1985; **59**: 743-748 [PMID: 2997104 DOI: 10.1152/jappl.1985.59.3.743]
14 **Albuquerque RC**, Moreno ACR, Dos Santos SR, Ragazzi SLB, Martinez MB. Multiplex-PCR for diagnosis of bacterial meningitis. *Braz J Microbiol* 2019; **50**: 435-443 [PMID: 30796713 DOI: 10.1007/s42770-019-00055-9]
15 **Joffe AR**. Lumbar puncture and brain herniation in acute bacterial meningitis: a review. *J Intensive Care Med* 2007; **22**: 194-207 [PMID: 17712055 DOI: 10.1177/0885066607299516]
16 **Hathaway LJ**, Grandgirard D, Valente LG, Täuber MG, Leib SL. Streptococcus pneumoniae capsule determines disease severity in experimental pneumococcal meningitis. *Open Biol* 2016; **6** [PMID: 27009189 DOI: 10.1098/rsob.150269]
17 **Chu V**, Carpenter DM, Winter K, Harriman K, Glaser C. Increased Risk of Late-onset Streptococcus pneumoniae Meningitis in Adults With Prior Head or Spine Surgeries. *Clin Infect Dis* 2019; **68**: 2120-2122 [PMID: 30452617 DOI: 10.1093/cid/ciy974]
18 **Perlejewski K**, Bukowska-Ośko I, Rydzanicz M, Pawełczyk A, Caraballo Cortès K, Osuch S, Paciorek M, Dzieciątkowski T, Radkowski M, Laskus T. Next-generation sequencing in the diagnosis of viral encephalitis: sensitivity and clinical limitations. *Sci Rep* 2020; **10**: 16173 [PMID: 32999423 DOI: 10.1038/s41598-020-73156-3]
19 **Pronier C**, Guyader D, Jézequel C, Tattevin P, Thibault V. Contribution of quantitative viral markers to document hepatitis B virus compartmentalization in cerebrospinal fluid during hepatitis B with neuropathies. *J Neurovirol* 2018; **24**: 769-772 [PMID: 30097971 DOI: 10.1007/s13365-018-0662-0]
20 **Mahony JB**. Nucleic acid amplification-based diagnosis of respiratory virus infections. *Expert Rev Anti Infect Ther* 2010; **8**: 1273-1292 [PMID: 21073292 DOI: 10.1586/eri.10.121]

World Journal of Clinical Cases

Submit a Manuscript: https://www.f6publishing.com

World J Clin Cases 2022 February 16; 10(5): 1702-1708

DOI: 10.12998/wjcc.v10.i5.1702

ISSN 2307-8960 (online)

CASE REPORT

Aseptic abscess in the abdominal wall accompanied by monoclonal gammopathy simulating the local recurrence of rectal cancer: A case report

Yan Yu, Yong-Dong Feng, Chao Zhang, Ran Li, De-An Tian, Huan-Jun Huang

ORCID number: Yan Yu 0000-0001-5030-4617; Yong-Dong Feng 0000-0001-7686-9480; Chao Zhang 0000-0002-1458-8170; Ran Li 0000-0002-8649-2020; De-An Tian 0000-0002-5782-3417; Huan-Jun Huang 0000-0001-7702-9272.

Author contributions: Yu Y, Huang HJ, and Feng YD were the patient's doctors; Yu Y reviewed the literature and contributed to manuscript drafting; Yu Y, Feng YD, and Tian DA conducted the data analyses and interpretation; Li R and Zhang C performed the microbiological and pathological analyses and interpretation, and contributed to manuscript drafting; Huang HJ was responsible for revising the manuscript for important intellectual content; all authors issued final approval for the version to be submitted.

Informed consent statement: Informed written consent was obtained from the patient for publication of this report and any accompanying images.

Conflict-of-interest statement: The authors declare that they have no conflicts of interest.

CARE Checklist (2016) statement: The authors have read the CARE Checklist (2016), and the

Yan Yu, De-An Tian, Huan-Jun Huang, Department of Gastroenterology, Tongji Hospital, Tongji Medical College, Huazhong University of Science and Technology, Wuhan 430030, Hubei Province, China

Yong-Dong Feng, Department of Gastrointestinal Surgery Center, Tongji Hospital, Tongji Medical College, Huazhong University of Science and Technology, Wuhan 430030, Hubei Province, China

Chao Zhang, Institute of Pathology, Tongji Hospital, Tongji Medical College, Huazhong University of Science and Technology, Wuhan 430030, Hubei Province, China

Ran Li, Tongji Medical College, Huazhong University of Science and Technology, Wuhan 430030, Hubei Province, China

Corresponding author: Huan-Jun Huang, MD, Additional Professor, Department of Gastroenterology, Tongji Hospital, Tongji Medical College, Huazhong University of Science and Technology, No. 1095 Jiefang Road, Wuhan 430030, Hubei Province, China.
ttkxbbmm2013@yeah.net

Abstract

BACKGROUND

Infectious abscesses in the abdominal wall can be secondary to retained foreign bodies (*e.g.*, stones, use of artificial mesh, use of silk yarn in surgical suture), inflammatory diseases (*e.g.*, acute appendicitis), and perforated malignancies of the digestive tract (particularly the colon). Aseptic abscesses (AAs) are relatively rare. To the best of our knowledge, this is the first report of an AA in the abdominal wall accompanied by monoclonal gammopathy of undetermined significance (MGUS) at 5 years after laparoscopic proctectomy.

CASE SUMMARY

A 72-year-old female patient presented with an enlarged painless mass in the lower abdomen for 1 year. She had a history of obesity, diabetes, and MGUS. Her surgical history was laparoscopic resection for rectal cancer 6 years prior, followed by chemotherapy. She was afebrile. Abdominal examination revealed a smooth abdomen with a clinically palpable solid mass under a laparotomy scar in the left lower quadrant. No obvious tenderness or skin redness was spotted. Laboratory data were not remarkable. Computed tomography scan revealed a

manuscript was prepared and revised according to the CARE Checklist (2016).

Country/Territory of origin: China

Specialty type: Medicine, research and experimental

Provenance and peer review: Unsolicited article; Externally peer reviewed.

Peer-review model: Single blind

Peer-review report's scientific quality classification

Grade A (Excellent): 0
Grade B (Very good): B, B
Grade C (Good): 0
Grade D (Fair): 0
Grade E (Poor): 0

Received: September 21, 2021
Peer-review started: September 21, 2021
First decision: December 2, 2021
Revised: December 7, 2021
Accepted: December 31, 2021
Article in press: December 31, 2021
Published online: February 16, 2022

P-Reviewer: Shiryajev YN, Tsimogiannis K
S-Editor: Fan JR
L-Editor: A
P-Editor: Fan JR

low-density mass of 4.8 cm in diameter in the lower abdominal wall, which showed high uptake on positron emission tomography. The preoperative diagnosis was an abscess or tumor, and surgical resection was recommended. The mass was confirmed to be an AA by microbiological and pathological examinations. The patient recovered well after surgery. There was no evidence of recurrence 2 years later.

CONCLUSION
It is important to consider underlying conditions (diabetes, chemotherapy, MGUS) which may contribute to AA formation in the surgical wound.

Key Words: Aseptic abscess; Monoclonalgammopathy of undetermined significance; Abdominal wall; Rectal cancer; Laparoscopic resection; Case report

Core Tip: We report a case of aseptic abscess (AA) in the abdominal wall accompanied by monoclonal gammopathy of undetermined significance (MGUS) at 5 years after laparoscopic proctectomy. This case report describes the clinical characteristics, laboratory findings, computed tomography images, and treatment, and discusses the possible relationship between AAs and a medical history that includes past surgery, MGUS, diabetes, or chemotherapy.

Citation: Yu Y, Feng YD, Zhang C, Li R, Tian DA, Huang HJ. Aseptic abscess in the abdominal wall accompanied by monoclonal gammopathy simulating the local recurrence of rectal cancer: A case report. *World J Clin Cases* 2022; 10(5): 1702-1708
URL: https://www.wjgnet.com/2307-8960/full/v10/i5/1702.htm
DOI: https://dx.doi.org/10.12998/wjcc.v10.i5.1702

INTRODUCTION

Infectious abscesses in the abdominal wall can be secondary to retained foreign bodies (*e.g.*, stones, use of artificial mesh, use of silk yarn in surgical suture)[1], inflammatory diseases (*e.g.*, acute appendicitis[2]), and perforated malignancies of the digestive tract (particularly in the colon)[3]. Patients often present with a painful anterior abdominal wall mass, sometimes with purulent discharge and systemic symptoms (*e.g.*, fever)[2]. A diagnosis is made based on abdominal computed tomography (CT) and is confirmed by surgical pathology[3]. Aseptic abscesses (AAs) are relatively rare. To the best of our knowledge, this is the first report of a sterile AAin the abdominal wall accompanied by monoclonal gammopathy of undetermined significance (MGUS) at 5 years after laparoscopic resection for rectal cancer. The atypical symptoms and imaging findings of an AA mimic a tumor, posing a diagnostic dilemma. The underlying diseases contributing to AA formation and treatments are discussed.

CASE PRESENTATION

Chief complaints

A 72-year-old woman presented to the outpatient department of our hospital complaining of a painless mass in the left lower quadrant of the abdomen.

History of present illness

The patient's symptoms began 10 mo prior and had worsened in the last 1 mo. She denied any changes in bowel habits. She was systemically well, with a good appetite and no fever.

History of past illness

The patient had a history of obesity, hypertension, coronary heart disease, and poorly

controlled type 2 diabetes. She had been diagnosed with MGUS 1 year prior. Regular medications included ramipril, amlodipine, aspirin, and gliclazide. Her surgical history included percutaneous coronary intervention in 2009 and laparoscopic radical resection for rectal cancer approximately 6 years and 4 mo prior to her present admission. Postoperative histopathological examination revealed moderately differentiated adenocarcinoma of the rectum with direct invasion to the deep muscular layer of the intestinal wall. All surgical margins were free of disease, and four lymph nodes were retrieved and found to be non-malignant. The pathological staging was pT3N0M0 stage II, according to American Joint Committee on Cancer Staging. The postoperative course was uneventful. The patient received seven cycles of chemotherapy (capecitabine 3000 mg/d) after surgery with curative intent. She was followed up and free of cancer recurrence at 56 mo after surgery.

Physical examination

The patient was afebrile (36.3 °C). Her body mass index (BMI) was 30 kg/m^2, and her blood pressure and pulse were 127/88 mmHg and 80 beats *per* min, respectively. Abdominal examination at presentation revealed a smooth abdomen with a clinically palpable solid mass (approximately 4 cm in diameter) under a laparotomy scar in the left lower quadrant. No obvious tenderness, skin redness, swelling, or increased skin temperature was observed around the mass. Abdominal auscultation revealed normal bowel sounds.

Laboratory examinations

Serum levels of glycosylated hemoglobin [8.9%, normal range (NR): 4%–6%], triglycerides (6.79 mmoL/L, NR: 0.9-1.7 mmoL/L), and glucose (12.6 mmoL/L, NR: 4.1-6.0 mmoL/L) were elevated. Hemoglobin levels (114 g/L, NR: 115-150 g/L) were decreased. Serum immunofixation electrophoresis revealed the presence of M-protein (11%, NR: 0%) and elevation of monoclonal immunoglobulin G (IgG) lambda (2.36 g/L, NR: 0.9-2.1 g/L). Other laboratory tests were within NR. The laboratory data were not either indicative of acute inflammation (white blood cell count of 5400 cells/μL; neutrophil bands of 66%, serum C-reactive protein level of 0.7 mg/dL) or tumor recurrence (carcinoembryonic antigen level of 2.8 ng/mL).

Imaging examinations

Ultrasonography of the left lower quadrant of the abdominal wall demonstrated a relatively well-demarcated, oval-shaped mass with mixed echogenicity (relatively more hypoechoic) and dimensions of 4.8 cm × 2.2 cm. Blood flow signals were seen in the hypoechoic area. Contrast-enhanced abdominal CT showed a low-density mass with rim enhancement adjacent to the rectus abdominisin the lower abdominal wall (Figure 1A), and ^{18}F-fluorodeoxyglucose-positron emission tomography (^{18}F-FDG-PET)/CT revealed high uptake of fluorodeoxyglucose, with a maximum standardized uptake value of 6.0 (Figure 1B). Colonoscopy showed no cancer recurrence. These findings suggested the possibility of either delayed abscess formation or abdominal wall recurrence of rectal cancer with central necrosis.

FINAL DIAGNOSIS

AA in the abdominal wall.

TREATMENT

Complete resection of the mass for therapeutic and diagnostic purposes was proposed. The patient consented to surgery. She subsequently underwent exploratory laparotomy through a midline incision in an elliptical fashion to include the affected abdominal wall part in the specimen. The lesion was confirmed to be an abscess. Upon exploration, a grey white and irregular-shaped mass with central purulent necrosis in the center was found within the abdominal wall (Figure 2). Postoperative transvenous cefoperazone (2.0 g, twice daily) was administered for 3 d. Pathological examination of the specimen revealed a large number of infiltrated neutrophils, lymphocytes, and macrophages in the adipose and connective tissues, accompanied by focal abscess, inflammatory granulation tissue formation, and interstitial fibrosis (Figure 2C and D). Giant epithelioid cells, granuloma, amyloid substance, un-absorbable yarn, or a

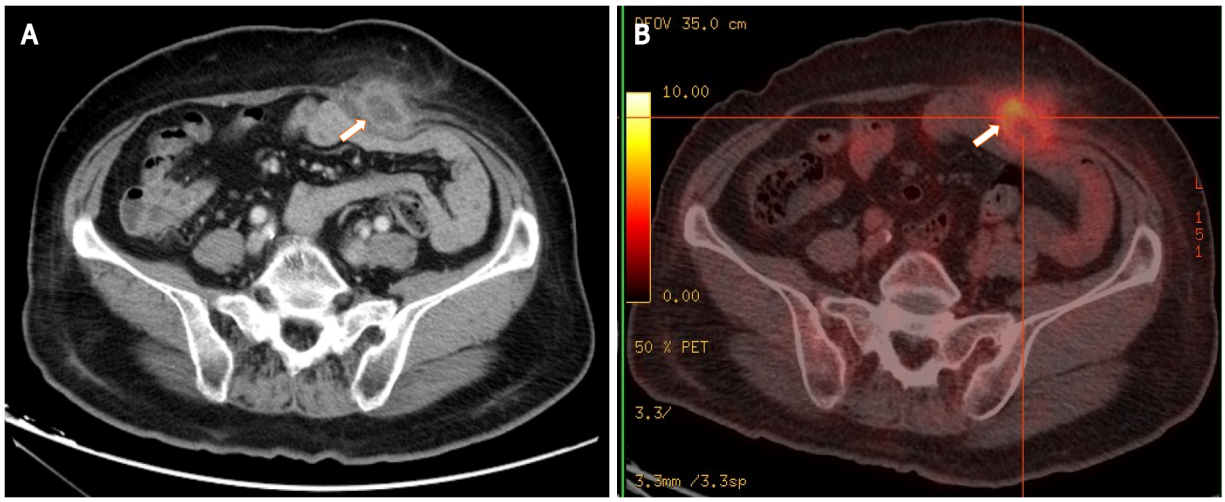

Figure 1 Images of the mass by contrast-enhanced abdominal computed tomography and ^{18}F-fluorodeoxyglucose-positron emission tomography. A: Computed tomography (CT) shows a low-density mass with rim enhancement adjacent to the rectus abdominis in the lower abdominal wall; B: ^{18}F-fluorodeoxyglucose-positron emission tomography/CT shows high uptake of fluorodeoxyglucose by the mass, with a maximum standardized uptake value of 6.0. The white arrows indicate the mass.

foreign body were not found in the specimen. A pus culture produced no bacterial or fungal growth after 7 d. The patient was discharged on the fourth postoperative day.

OUTCOME AND FOLLOW-UP

The patient was in good health at the 2-year follow-up.

DISCUSSION

AA is an inflammatory condition characterized by deep sterile collections of neutrophils, clinically mimicking bacterial abscess[4]. The diagnosis is established by excluding other diseases in different ialdiagnosis[4]. AA can arise in many parts of the body, including the abdominal cavity[5], liver[6], spleen[6], brain[7], lung[8], and extremities[9].

Although the causes of AA are not completely clear, it is known to be accompanied by some conditions such as inflammatory bowel disease (IBD)[6], surgery[5], drug usage (trastuzumab, crizotinib, vaccine)[7,10,11], and MGUS[8], with IBD being by far the most frequently associated condition[6]. AA can antedate, be concomitant with, or follow the diagnosis of IBD[6]; however, AA does not appear to be strongly associated with the disease activity[6]. In our case, ileocolonoscopy was performed, and no IBD was found. Cholecystectomy has been mentioned in intra-abdominal AA, secondary to foreign body reaction to dropped gallstones in gallbladder leakage[5,12,13]. The time of AA presentation canrange from 4 years to 8 years after surgery[5,13]. For example, Hawasli *et al*[12] reported a sterile abscess in the abdominal wall containing gallstones at 4 years and 4 mo after an elective laparoscopic cholecystectomy. In the present case, the AA appeared 5 years after laparoscopic resection for rectal cancer, and was located in the laparoscopic wound. Although no foreign body was retained in the wound, high BMI, diabetes mellitus, and chemotherapy might prevent wound healing, causing local inflammation[14]. Moreover, drug usage is suspected to be one cause as well, as an intracranial AA was formed after the first cycle of trastuzumab in a breast cancer patient[7]. Our patient had received seven cycles of capecitabine and developed AA approximately 4 years after her last chemotherapy treatment. To date, no paper has reportedAA as a side effect of capecitabine.

There is evidence suggesting an association between AA and MGUS. MGUS is a condition characterized by the presence of a monoclonal gammopathy in which the clonal mass has not reached a predefined state in which the condition is considered malignant[15]. It is a precursor to conditions such asmultiple myelomaor lymphoma at a rate of approximately 1% *per* year[15]. MGUS is associated with infections, fractures,

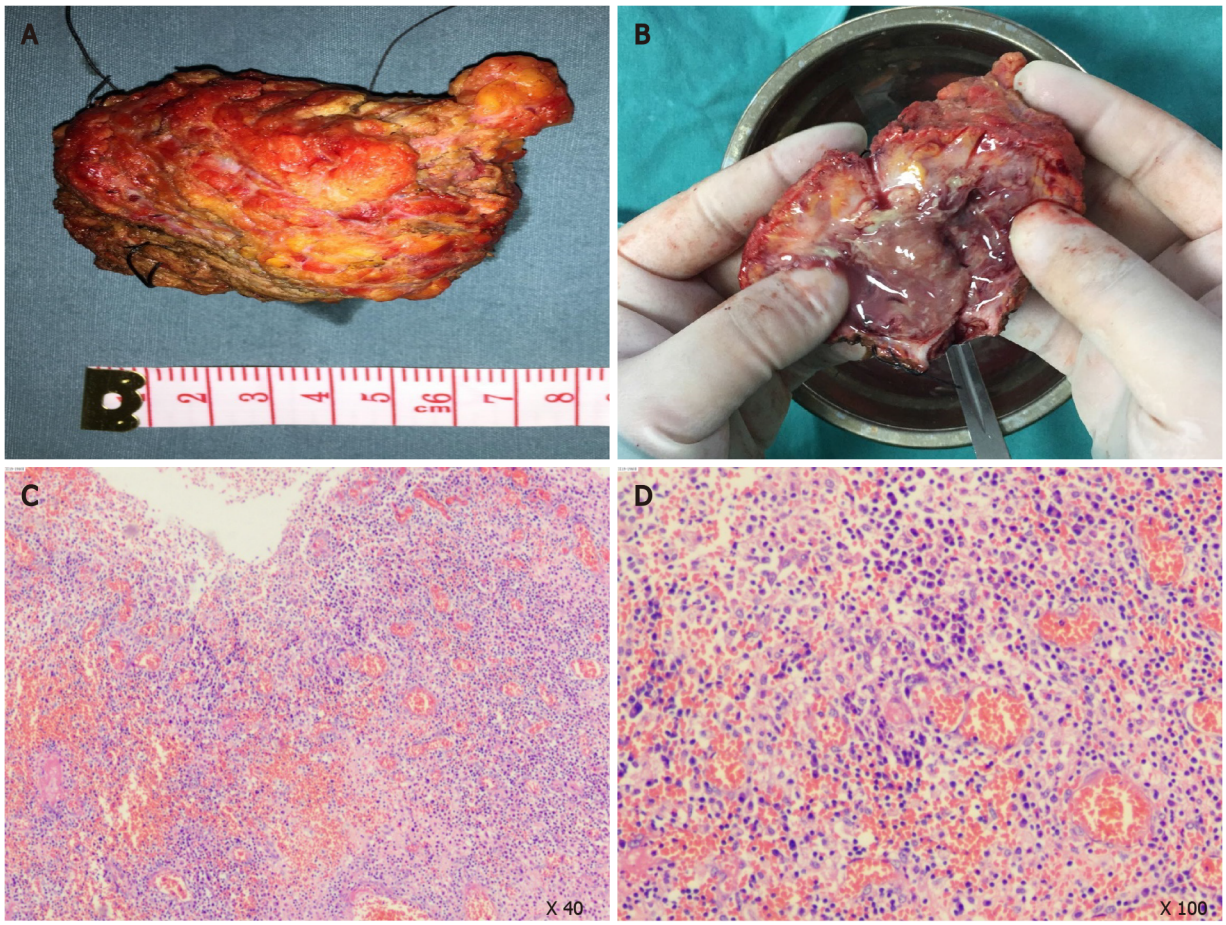

Figure 2 Gross appearance of the mass in surgery. A: The mass was grey white with an irregular shape; B: There were purulent exudates in the center of the mass; C and D: Pathological examination of the specimen revealed a large number of infiltrated neutrophils, lymphocytes, and macrophages in the adipose and connective tissues, accompanied by focal abscess, inflammatory granulation tissue formation, and interstitial fibrosis.

peripheral neuropathy, and thromboembolism[16,17]. Only 4 cases of aseptic organ abscesses (spleen, liver, lung, and pancreas) occurring with MGUS have been reported [6,8]. Neutrophilicdermatoses, which are characterized by neutrophil infiltration in the skin, have been reported in monoclonal gammopathy[18,19]. The strongest association is between IgA monoclonal gammopathies and pyodermagangrenosum, a non-infectious neutrophilicdermatosis[18,20,21]. Interestingly, an abnormal neutrophil increase has also been observed in MGUS patients. A leukemoid reaction presenting as neutrophilic leukocytosis can occur with MGUS, which is attributable to cytokine release by neoplastic plasma cells[22,23]. The prompt and long-lasting regression of neutrophilia observed after short-term chemotherapy suggests that the present case should also be considered as a case of plasma-cell dyscrasia-associated neutrophilia [22]. In our case, one could postulate that the poor healing of the surgical wound may have served as an inducing factor and was enhanced by MGUS-associated neutrophil abnormality, ultimately leading to AA formation.

Pain is the most common symptom in patients with AA[13]. Symptoms vary among the organs involved[8,9]. Weight loss, abdominal pain, nausea, and fatigue suggest involvement of the digestive system[9]. In patients with MGUS, the prevalence of symptomatic neuropathy is 8% to 36%[18]. Most patients with neuropathy and IgG monoclonal gammopathy have IgG MGUS[18]. Both MGUS and diabetes can cause neuropathy, which might explain why the AA was painless in our patient. Multiple lesions in the spleen, liver, and skin are present in IBD and prone to relapse[6,9]. Anti-tumor drugs can cause multiple[10] or single[7] AAs. Surgery or a foreign body can cause a single AA and no recurrence has been reported[13]. Recurrences have occurred with anti-tumor drug usage and vaccination[10,11]. With MGUS, multipleAA lesions have been found in the lung and relapse[8]. In some cases, high fever, weight loss, and pain are the most frequent clinical manifestations associated with severe inflammatory response and elevated polymorphonuclear leukocyte count[6]. Elevated inflammatory markers are mostly seen in patients with IBD[4]. Conversely, the absence of fever or

abdominal pain or lack of a raised leukocyte count does not exclude the possibility of AA[6]. Acute inflammatory symptoms are not obvious and have been observed in patients after surgery[13], anti-tumor drug usage[10], and vaccination[11]. Laboratory tests are unremarkable in patients with AA due to surgery or foreign body[13]. The absence of remarkable inflammatory indicators and pain make it difficult to distinguish AAs from the recurrence of cancer.

Abdominal CT is a very valuable tool for detecting locally advanced colon cancer and its invasion along the tissue planes, which may result in the formation of abdominal wall abscess (AWA)[24]. However, CT is not adequate in distinguishing inflammation and carcinoma in the abdominal wall, especially when the original tumor is absent. Although ^{18}F-FDG-PET/CT is a powerful tool for detecting cancer, ^{18}FDG uptake is not tumor-specific[25]. Our case highlights that sterile AWA-complicating MGUS post-surgerymay pose a diagnostic dilemma mimicking tumors due to their similar radiologic and laboratory appearance.

AA does not respond to antibiotic therapy[9]; however, its response to steroids is excellent[8]. In some cases, AA completely resolves with the combination of cyclophosphamide and prednisone or anti-tumor necrosis factor-alpha therapy in patients with IBD[6]. For surgery-associated AA, *en bloc* resection is also a treatment[5,12,13]. However, for relapsing patients, special attention should be paid to pathologic changes to avoid iterative surgical procedures. The limitation of our case was that corticosteroids were not applied, because the patient had a history of rectal cancer and the lesion could not be preoperatively excluded from a tumor. Therefore, we lack experience on steroid usage in patients with AA. However, our case suggests that AA associated with surgical wound and MGUS can be treated by *en bloc* resection without the aid of corticosteroids.

In conclusion, if local recurrence is suspected by symptoms and imaging modalities in the postoperative period for colorectal cancer patients, although rare, the possibility of AA formation should be considered. Likewise, it is important to consider underlying diseases such as diabetes, chemotherapy, and MGUS, which may contribute to AA formation in the surgical wound, regardless of the time elapsed from surgery.The atypical manifestations of AA lead to difficulties in differentiating from cancer based on the results of imaging modalities. AA associated with surgical wound and MGUS can be treated by *en bloc* resection without the aid of corticosteroids. Greater knowledge of AA among physicians will promote early diagnosis and effective treatment.

CONCLUSION

We reported a rare case of an aseptic AWA with MGUS at 5 years after laparoscopic radical resection for rectal cancer. This case study described the clinical characteristics, laboratory results, imaging findings, and treatment. We also discussed the possible relationship among aseptic abscess, MGUS, and laparoscopic surgery. We believe that this case provides a foundation for further studies on the relationship between MGUS, neutrophils and AA.

REFERENCES

1 **Kawai K**, Sunami E, Nishikawa T, Tanaka J, Tanaka T, Kiyomatsu T, Hata K, Nozawa H, Kazama S, Ishihara S, Yamaguchi H, Kitayama J, Watanabe T. Delayed abdominal wall abscess after abdomino-perineal resection simulating local recurrence of rectal cancer. *Springerplus* 2014; **3**: 681 [PMID: 25520908 DOI: 10.1186/2193-1801-3-681]

2 **Souza IMAG**, Nunes DAA, Massuqueto CMG, Veiga MAM, Tamada H. Complicated acute appendicitis presenting as an abscess in the abdominal wall in an elderly patient: A case report. *Int J Surg Case Rep* 2017; **41**: 5-8 [PMID: 29024841 DOI: 10.1016/j.ijscr.2017.09.023]

3 **Amer E**, Er A, Cengiz F, Karaisli S, Peskersoy M. Colon Cancer Presenting as Abdominal Wall Abscess. *Cyprus J Med Sci* 2018; **3**: 202-203

4 **Snast I**, Ostfeld I, Pavlovsky L, Hodak E, Gafter-Gvili A. Pyoderma Gangrenosum and Extensive Aseptic Chest Wall Abscess in a Patient with Inflammatory Bowel Disease. *Isr Med Assoc J* 2018; **20**: 712-713 [PMID: 30430804]

5 **Kakaty D**, Gosztonyi J, Anthamatten C, Zengaffinen R. Sterile abscess mimicking an abdominal tumor 8 years after laparoscopic cholecystectomy. *J Surg Case Rep* 2017; **2017**: rjx176 [PMID: 28928930 DOI: 10.1093/jscr/rjx176]

6 **André MFJ**, Piette JC, Kémény JL, Ninet J, Jego P, Delèvaux I, Wechsler B, Weiller PJ, Francès C,

Blétry O, Wismans PJ, Rousset H, Colombel JF, Aumaître O; and the French Study Group on Aseptic Abscesses. Aseptic abscesses: a study of 30 patients with or without inflammatory bowel disease and review of the literature. *Medicine (Baltimore)* 2007; **86**: 145-161 [PMID: 17505254 DOI: 10.1097/md.0b013e18064f9f3]

7 **Mezei T**, Hajdu M, Czigléczki G, Lotz G, Kocsis J, Kulka J, Horváth A. Sterile, abscess-like cerebral lesion during trastuzumab therapy after HER2 status switch in a triple negative breast cancer patient: a case report and literature review. *BMC Cancer* 2020; **20**: 615 [PMID: 32611325 DOI: 10.1186/s12885-020-07114-7]

8 **Mitrevski M**, Granata M, Sedati P, Rota F, De Santis A, Remotti D, Callea F, Visentini M. Sterile abscesses complicating monoclonal gammopathy of undetermined significance. *Eur J Haematol* 2008; **81**: 246 [PMID: 18410540 DOI: 10.1111/j.1600-0609.2008.01084.x]

9 **Agirgol S**, Ustaoglu E, Demir FT, Akbulut TO, Turkoglu Z, Kaya H, Pehlivanoğlu F. Aseptic Abscess Syndrome with Severe Skin Involvement: Case Report. *Indian J Dermatol* 2020; **65**: 434-436 [PMID: 33165447 DOI: 10.4103/ijd.IJD_259_18]

10 **Weber D**, Decker M, Schuster M, Folz S, Stürmer CJ, Lutz MP. Crizotinib: aseptic abscesses in multiple organs during treatment of EML4-ALK-positive NSCLC. *J Cancer Res Clin Oncol* 2021; **147**: 3769-3771 [PMID: 34373943 DOI: 10.1007/s00432-021-03664-w]

11 **Kaya A**, Kaya SY. A case of recurrent sterile abscesses following tetanus-diphtheria vaccination treated with corticosteroids. *BMC Infect Dis* 2021; **21**: 53 [PMID: 33430802 DOI: 10.1186/s12879-020-05756-3]

12 **Hawasli A**, Schroder D, Rizzo J, Thusay M, Takach TJ, Thao U, Goncharova I. Remote complications of spilled gallstones during laparoscopic cholecystectomy: causes, prevention, and management. *J Laparoendosc Adv Surg Tech A* 2002; **12**: 123-128 [PMID: 12019573 DOI: 10.1089/10926420252939664]

13 **Bartels AK**, Murali AR, Zamora JG. Subhepatic Sterile Abscess 10 Years After Laparoscopic Cholecystectomy. *ACG Case Rep J* 2015; **2**: 113-115 [PMID: 26157931 DOI: 10.14309/crj.2015.22]

14 **Xu Z**, Qu H, Kanani G, Guo Z, Ren Y, Chen X. Update on risk factors of surgical site infection in colorectal cancer: a systematic review and meta-analysis. *Int J Colorectal Dis* 2020; **35**: 2147-2156 [PMID: 32748113 DOI: 10.1007/s00384-020-03706-8]

15 **Glavey SV**, Leung N. Monoclonal gammopathy: The good, the bad and the ugly. *Blood Rev* 2016; **30**: 223-231 [PMID: 26732417 DOI: 10.1016/j.blre.2015.12.001]

16 **Tete SM**, Bijl M, Sahota SS, Bos NA. Immune defects in the risk of infection and response to vaccination in monoclonal gammopathy of undetermined significance and multiple myeloma. *Front Immunol* 2014; **5**: 257 [PMID: 24917865 DOI: 10.3389/fimmu.2014.00257]

17 **Mouhieddine TH**, Weeks LD, Ghobrial IM. Monoclonal gammopathy of undetermined significance. *Blood* 2019; **133**: 2484-2494 [PMID: 31010848 DOI: 10.1182/blood.2019846782]

18 **Decaux O**, Laurat E, Perlat A, Cazalets C, Jego P, Grosbois B. Systemic manifestations of monoclonal gammopathy. *Eur J Intern Med* 2009; **20**: 457-461 [PMID: 19712843 DOI: 10.1016/j.ejim.2009.01.001]

19 **Gusdorf L**, Lipsker D. Schnitzler Syndrome: the paradigm of an acquired adult-onset auto-inflammatory disease. *G Ital Dermatol Venereol* 2020; **155**: 567-573 [PMID: 33295738 DOI: 10.23736/S0392-0488.20.06692-4]

20 **Montagnon CM**, Fracica EA, Patel AA, Camilleri MJ, Murad MH, Dingli D, Wetter DA, Tolkachjov SN. Pyoderma gangrenosum in hematologic malignancies: A systematic review. *J Am Acad Dermatol* 2020; **82**: 1346-1359 [PMID: 31560977 DOI: 10.1016/j.jaad.2019.09.032]

21 **Velasco-Tamariz V**, Carreño-Tarragona G, Tous-Romero F, Gil-de la Cruz E, Martín-Clavero E, Rivera-Díaz R. Dramatic resolution of disseminated pyoderma gangrenosum associated with monoclonal gammopathy after therapy with bortezomib and dexamethasone. *Int Wound J* 2017; **14**: 1382-1384 [PMID: 28371346 DOI: 10.1111/iwj.12746]

22 **Gnerre P**, Ottonello L, Montecucco F, Boero M, Dallegri F. Nephrotic syndrome in a patient with IgM myeloma with associated neutrophilia. *Eur J Haematol* 2007; **79**: 76-80 [PMID: 17598840 DOI: 10.1111/j.1600-0609.2007.00869.x]

23 **Bain BJ**, Ahmad S. Chronic neutrophilic leukaemia and plasma cell-related neutrophilic leukaemoid reactions. *Br J Haematol* 2015; **171**: 400-410 [PMID: 26218186 DOI: 10.1111/bjh.13600]

24 **Kim SW**, Shin HC, Kim IY, Kim YT, Kim CJ. CT findings of colonic complications associated with colon cancer. *Korean J Radiol* 2010; **11**: 211-221 [PMID: 20191069 DOI: 10.3348/kjr.2010.11.2.211]

25 **Flaus A**, Longo MG, Dematons M, Granjon D, Prevot N. 18F-FDG PET/CT in Urachal Abscess. *Clin Nucl Med* 2019; **44**: e349-e350 [PMID: 30829865 DOI: 10.1097/RLU.0000000000002524]

World Journal of Clinical Cases

Submit a Manuscript: https://www.f6publishing.com

World J Clin Cases 2022 February 16; 10(5): 1709-1715

DOI: 10.12998/wjcc.v10.i5.1709

ISSN 2307-8960 (online)

CASE REPORT

Tacrolimus treatment for relapsing-remitting chronic inflammatory demyelinating polyradiculoneuropathy: Two case reports

Wen-Jia Zhu, Yu-Wei Da, Hai Chen, Min Xu, Yan Lu, Li Di, Jian-Ying Duo

ORCID number: Wen-Jia Zhu 0000-0003-1397-4544; Yu-Wei Da 0000-0002-0318-148X; Hai Chen 0000-0001-9456-8569; Min Xu 0000-0001-8210-0993; Yan Lu 0000-0003-2211-9515; Li Di 0000-0001-6359-7455; Jian-Ying Duo 0000-0002-5709-9545.

Author contributions: Zhu WJ performed the study and drafted the manuscript; Chen H provided technical advice; Xu M, Lu Y and Di L collected clinical data; Da YW designed and supervised the study; all authors have read and approved the final manuscript.

Informed consent statement: Written informed consent was obtained from the patients for publication of this case report.

Conflict-of-interest statement: The authors declare no potential conflicts of interest with respect to the research, authorship, and/or publication of this article.

CARE Checklist (2016) statement: The authors have read the CARE Checklist (2016), and the manuscript was prepared and revised according to the CARE Checklist (2016).

Country/Territory of origin: China

Specialty type: Neurosciences

Provenance and peer review: Unsolicited article; Externally peer

Wen-Jia Zhu, Yu-Wei Da, Hai Chen, Min Xu, Yan Lu, Li Di, Jian-Ying Duo, Department of Neurology, Xuanwu Hospital, Capital Medical University, Beijing 100053, China

Corresponding author: Yu-Wei Da, MD, Doctor, Professor, Department of Neurology, Xuanwu Hospital, Capital Medical University, No. 45 Changchun Street, Xicheng District, Beijing 100053, China. dayuwei100@hotmail.com

Abstract

BACKGROUND

This study describes the efficacy of a tacrolimus treatment regimen used to treat two patients with relapsing-remitting chronic inflammatory demyelinating polyradiculoneuropathy (CIDP).

CASE SUMMARY

Two patients (17-year-old female and 27-year-old male) were enrolled in the current study and were followed up for 12 mo. The first patient was administered tacrolimus (2 mg/d) for 12 mo and prednisolone (40 mg/d) for six months. The second patient was administered tacrolimus (3 mg/d) for six months. Both patients were followed up for 12 mo and the degree of recurrent weakness or normalized motor function was monitored. In addition, nerve conduction studies and tacrolimus levels were recorded. Following tacrolimus treatment, both patients showed marked improvement in clinical outcomes. In the first patient, prednisolone treatment was successfully withdrawn after six months. Sensory as well as motor nerve conduction velocities showed evident recovery following treatment. However, conduction velocities did not completely return to normal, suggesting that electrophysiological recovery can be slower than clinical recovery.

CONCLUSION

Neither patient exhibited any adverse effects due to the tacrolimus therapy. Therefore, tacrolimus can be effective for the treatment of patients with steroid-resistant CIDP.

Key Words: Chronic inflammatory demyelinating polyradiculoneuropathy; Prednisolone; Tacrolimus; Relapsing-remitting; Treatment; Case report

reviewed.

Peer-review model: Single blind

Peer-review report's scientific quality classification
Grade A (Excellent): A
Grade B (Very good): B
Grade C (Good): 0
Grade D (Fair): 0
Grade E (Poor): 0

Received: September 23, 2021
Peer-review started: September 23, 2021
First decision: October 22, 2021
Revised: November 5, 2021
Accepted: January 11, 2022
Article in press: January 11, 2022
Published online: February 16, 2022

P-Reviewer: Oley MH, Şurlin VM
S-Editor: Xing YX
L-Editor: A
P-Editor: Xing YX

Core Tip: Chronic inflammatory demyelinating polyradiculoneuropathy (CIDP) is an immune-mediated motor sensory neuropathy that is characterized by demyelination of the peripheral nerves and secondary axonal damage. Tacrolimus is mainly used in organ transplant patients and autoimmune diseases. Here, we investigate the efficacy of tacrolimus in two CIDP patients. Our results demonstrate the efficacy of tacrolimus treatment without significant adverse events. Therefore, tacrolimus can be used as an alternative treatment option if first line treatments are not effective or in refractory CIDP patients.

Citation: Zhu WJ, Da YW, Chen H, Xu M, Lu Y, Di L, Duo JY. Tacrolimus treatment for relapsing-remitting chronic inflammatory demyelinating polyradiculoneuropathy: Two case reports. *World J Clin Cases* 2022; 10(5): 1709-1715
URL: https://www.wjgnet.com/2307-8960/full/v10/i5/1709.htm
DOI: https://dx.doi.org/10.12998/wjcc.v10.i5.1709

INTRODUCTION

Chronic inflammatory demyelinating polyradiculoneuropathy (CIDP) is an immune-mediated motor sensory neuropathy that is characterized by the demyelination of peripheral nerves and secondary axonal damage[1]. and CIDP patients usually present with numbness and weakness of the extremities as well as a loss of reflexes[2]. The exact pathogenesis of CIDP is not fully understood, but it involves an attack of the myelin sheath by components of both cellular and humoral immunity, ultimately leading to demyelination of nerve fibers[3].

There are several treatment options for CIDP including plasma exchange or the administration of corticosteroids (CS) and intravenous immunoglobulin (IVIg)[4,5]. The failure of first-line treatment strategies to obtain satisfactory outcomes can lead to the consideration of immunosuppressive agents. Immunosuppressive agents include azathioprine, methotrexate, interferon alpha (IFN-α), cyclosporine (CyA), cyclophosphamide, mycophenolate mofetil, rituximab and stem cell transplantation[6-8]. Accumulating evidence has demonstrated that CyA, a calcineurin inhibitor, can selectively inhibit cytokines produced by helper T cells with a quick onset of action[9-11]. However, CyA has also been associated with side effects that may include nephrotoxicity[12]. Tacrolimus, another calcineurin inhibitor, is more bioavailable with a faster onset of action and lower nephrotoxicity than CyA[13]. Tacrolimus has been widely used in organ transplantation and for the treatment of autoimmune diseases [14].

In 1998, Ahlmén *et al*[15] reported the treatment of a patient with CIDP using a combination of glucocorticoids and tacrolimus. However, detailed information regarding the efficacy and safety of tacrolimus in CIDP remains unknown. In this study, the clinical response and follow up evaluation of two CIDP patients treated with tacrolimus were reported.

CASE PRESENTATION

Chief complaints

Case 1: A 17-year-old female was hospitalized with recurrent episodes of numbness and weakness of limbs occurring over the previous 11 mo.

Case 2: A 27-year-old male was admitted to our department complaining of recurrent weakness and numbness in the limbs for 60 mo.

History of present illness

Case 1: In December 2016, the patient presented with numbness in both hands, weakness in the upper extremities, difficulty combing her hair, and difficulty dressing. The patient's symptoms presumably began after she suffered from a common cold. In April 2017, her weakness worsened, and the patient could no longer lift her upper extremities and had trouble sitting upright. The numbness in both hands gradually

progressed toward the proximal extremities. Upon admission, the patient was diagnosed with CIDP at her local hospital, and she was administered methylprednisolone (1000 mg/d for 3 d) and IVIg (0.4/kg/d for 5 d; Table 1). Following treatment, her symptoms subsided and she was discharged with no follow-up treatment. In July 2017, the patient presented with another episode of finger numbness and extremity weakness. After three days, the patient could not walk, and she was admitted to her local hospital. The patient was treated with IVIg (0.4/kg/d for 5 d) and her condition improved. Then, in November 2017 (11 mo after initial onset of symptoms), the patient presented with another CIDP episode and was admitted to our inpatient department one week after symptom onset.

Case 2: The patient presented with gradually progressive numbness and weakness in his extremities and was diagnosed with relapsing-remitting CIDP in February 2014. The patient was treated with multiple courses of IVIg (0.4/kg/d for 5 d, n = 12) and methylprednisolone (1000 mg/d for 3 d) therapy with subsequent dosage reductions. During the steroid treatment periods, the patient's weight increased from 70 kg to 103 kg [body mass index (BMI) of 30.86] and he developed secondary diabetes, hypertension, and hyperlipidemia. In October 2018, he again developed weakness in his extremities that gradually worsened.

History of past illness

Cases 1 and 2: The patient used to be in a good health and had no previous medical history.

Personal and family history

Cases 1 and 2: There were no negative personal habits or customs, and no special family history to note.

Physical examination

Case 1: The patient showed proximal extremity muscle strength values of 2-3 out of 5, distal extremity strength values of 3-4 out of 5, and an absence of tendon reflexes. However, her superficial/deep sensation was normal.

Case 2: The physical examination revealed obesity, an inability to walk on the toes, an inability to squat, a proximal/distal extremity muscle strength of 3 out of 5, and the absence of tendon reflexes as well as sensory anesthesia.

Laboratory examinations

Case 1: Lumbar puncture was performed and the results showed an elevated protein level (59 mg/dL). Routine blood, urine, and stool examinations were normal. Thyroid function, infection, immune findings (ESR, anti-nuclear antibody spectrum, anti-neutrophil cytoplasmic antibody, and anti-cardiolipin antibodies) and tumor screening results were normal. Immunofixation electrophoresis and anti-ganglioside ester antibodies were absent. Nerve conduction velocities were recorded.

Case 2: Lumbar puncture results showed an elevated protein level (82 mg/dL). Routine blood, urine, and stool examinations were normal. Thyroid function, infection, immune findings (ESR, anti-nuclear antibody spectrum, anti-neutrophil cytoplasmic antibody, and anti-cardiolipin antibodies) and tumor screening results were normal. Immunofixation electrophoresis and anti-ganglioside ester antibodies were absent. Nerve conduction velocities were recorded.

Imaging examinations

Case 1: The brain and spinal MRI scan did not reveal any abnormalities. The chest and abdominal Computed tomography (CT) scans were normal.

Case 2: The brain and spinal MRI scan did not reveal any abnormalities. The chest CT scan was normal. The abdominal CT scan showed fatty liver disease.

FINAL DIAGNOSIS

The final diagnosis of both patients was relapsing-remitting CIDP.

Table 1 Clinical features and therapeutic status of two patients with chronic inflammatory demyelinating polyradiculoneuropathy

Case	Sex/age	Disease Course (mo)	Number of recurrences	Pretreatment medication	Prednisone usage and dosage before tacrolimus	Tacrolimus		Therapeutic effect (ONLS score)	
						Dosage (mg/d)	Length of treatment (mo)	Before Tacrolimus	After 6 mo treatment
1	F/17	11	4	IVIg; steroids	40 mg 4 wk, 35 mg 4 wk, 30 mg was associated with onset of symptoms	2	12	1	0
2	M/27	60	4	IVIg; steroids	-	3	6	2	0

ONLS: Overall neuropathy limitation scale; IVIg: Intravenous immunoglobulin.

TREATMENT

Case 1

Following admission, the patient's weakness continued to progress and she was treated with IVIg (0.4/kg/d for 5 d) for the third time. Her extremity weakness and numbness quickly improved. However, her weakened left upper extremity and absence of right knee reflexes persisted. To prevent recurrence, oral prednisone (40 mg/d, reduced by 5 mg per month) was prescribed in November 2017.

Case 2

The patient could not continue steroid pulse therapy or the expensive IVIg treatments. Therefore, oral tacrolimus (3 mg/d) was administered for six months, and his body weight was strictly controlled.

OUTCOME AND FOLLOW-UP

Case 1

In January 2018, the prednisone dose was reduced to 30 mg, but the patient had gained 12 kg (BMI of 26.67). Then, she developed bilateral fingertip numbness and weakness for the fourth time. Physical examination revealed bilateral digital opposition, an extensor strength of 4 out of 5, and extremity tendon reflex attenuation. Other physical examination findings were normal. The patient was treated with tacrolimus (2 mg/d) and prednisone (40 mg/d) was added to her treatment regimen. During treatment, the serum concentration of tacrolimus fluctuated between 1.6 and 2.9 ng/μL (Table 1). Following the initiation of treatment with tacrolimus, the numbness disappeared in the second week, and prednisone was reduced by 5 mg every two weeks. In April 2018, prednisone was decreased to 15 mg and then gradually reduced for discontinuation, but tacrolimus was maintained at 2 mg/d until the end of the 12-month treatment course (January 2019). Prior to treatment, the overall neuropathy limitation scale (ONLS)[9] score was 1 point and it improved to 0 points after six months of treatment (Table 1). In addition, nerve conduction studies were recorded before and after treatment (Table 2). At the one-year follow-up appointment in January 2019, the patient was asymptomatic and the sensory as well as motor nerve conduction velocities had recovered, but did not completely return to normal, suggesting that electrophysiological recovery can be slower than clinical recovery (Table 2).

Case 2

After two months, the patient's weight dropped to 83 kg, and the extremity weakness was markedly improved. His diabetes, hypertension, and hyperlipidemia were controlled with medication. Physical examination revealed symmetrical biceps muscle strength and a finger extension strength ratio of 4/5, a finger abduction/adduction muscle strength of 5/5, a hip flexion and toe dorsiflexion strength ratio of 4/5, muscle strength of 5/5 in the other extremities, and the absence of tendon reflexes. Prior to tacrolimus treatment, the ONLS scores were 2 points, which improved after six months of treatment (Table 1). During treatment, the serum concentration of tacrolimus fluctuated between 5.1 and 6.8 ng/μL. At the one-year follow-up

Table 2 Comparison of nerve conduction velocities before and after treatment in both patients

			Case 1 (one-year)		Case 2 (one-year)	
	Nerve		Before	After	Before	After
MNCV	Median	Distal latency (ms)	5.9	4.7	7.7	6.73
		Velocity (m/s)	22	35	28	38.6
	Tibial	Distal latency (ms)	6.8	7.3	8.2	8.19
		Velocity (m/s)	42	43	45	35
SNCV	Median	Distal latency (ms)	Not elicited	2.9	Not elicited	3.85
		Velocity (m/s)	Not elicited	47	Not elicited	35.8
	Tibial	Distal latency (ms)	5.5	Not performed	Not elicited	Not performed
		Velocity (m/s)	30	Not performed	Not elicited	Not performed

MNCV: Motor nerve conduction velocity; SNCV: Sensory nerve conduction velocity.

appointment, the sensory and motor nerve conduction velocities had recovered but did not completely return to normal, supporting the suggestion that electrophysiological recovery is slower than clinical recovery (Table 2).

DISCUSSION

In this study, two patients were clinically diagnosed with relapsing-remitting CIDP characterized by extremity numbness and weakness, electrophysiological findings consistent with demyelinating peripheral neuropathy, and lumbar puncture findings indicative of cerebrospinal fluid protein-cell separation. Both patients were young and childless (17 and 27 years of age), and the disease courses were 11 and 60 mo in patients 1 and 2, respectively. All other related diseases were excluded.

At the time of admission, both patients experienced CIDP symptoms that had recurred for the fourth time. The clinical features of case 1 were characterized by rapid progression after each recurrence. Following CS and IVIg treatment, her disability score improved by 4 points within five to seven days. However, the patient experienced weight gain following prednisone (40 mg/d) treatment and therefore she disliked the option of long-term CS use. Likewise, the second patient (case 2) developed obesity, diabetes, hypertension, and hyperlipidemia following long-term CS use. Their families could no longer afford the cost of IVIg and plasma exchange. Therefore, a quick-onset non-hormonal immunosuppressive agent was selected.

Ahlmén *et al*[15] used tacrolimus (also known as FK506) in 1998 to treat a 28-year-old woman with relapsing-remitting CIDP. In that particular patient, high-dose IVIg, cyclophosphamide, and azathioprine were ineffective. She had a favorable outcome with high-dose prednisone but she relapsed after discontinuation of the prednisone. Reduction therapy involving a combination of plasma exchange and a high dose of prednisone (80 mg/d) was effective, but the patient developed steroid myopathy. Therefore, she was administered a high dose of tacrolimus (0.42 mg/BMI/d) that was later reduced to 0.08 mg/BMI/d after 1.5 years, and prednisone (40 mg/d) was discontinued after the first six months. This treatment course had a favorable outcome, and the patient did not relapse within the one year of observation. Nevertheless, that patient developed side effects including diarrhea and hand tremors during the high-dose tacrolimus treatment course, but those symptoms disappeared when the tacrolimus dose was reduced[15].

The combination of tacrolimus and FK506 binding protein (FKBP) forms the FK506-FKBP-12 complex, which can prevent T cell proliferation, decrease T-cell mediated tissue damage, and play an immunosuppressive role through the inhibition of various lymphocyte products, such as IL-2[16]. Tacrolimus has been widely used in organ transplantation and may be an effective treatment strategy for CIDP patients. However, several organ transplant patients using tacrolimus developed reversible demyelinating peripheral neuropathy[17-19]. Nevertheless, those symptoms were observed in only 3% of organ transplant patients, and may be attributed to the high doses of tacrolimus that were administered (5-10 mg/d)[20].

In this study, both patients were young adults and childless. Due to possible reproductive toxicity, cyclophosphamide and azathioprine were not optimal treatment options in these younger patients[21,22]. Therefore, the patients preferred treatment with tacrolimus due to its relatively mild side effects and quick onset of action. Among the nonhormonal immunosuppressive agents, tacrolimus has the fastest onset of action [11,13]. In this study, case 2 used a single dose of tacrolimus (3 mg/d) for six months, and the severity of extremity weakness was significantly improved. On the other hand, case 1 used a slightly lower dose of tacrolimus (2 mg/d) for 12 mo. In case 1, although the serum concentration of tacrolimus was lower (fluctuating from 1.6 to 2.9 ng/μL), we were still able to reduce the concentration of prednisone and prevent side effects attributed to prolonged CS treatment. However, this suggests that the serum concentration of tacrolimus is not the only factor that determines the efficacy of treatment, but this point will be addressed in future studies.

CONCLUSION

In conclusion, these results demonstrate the efficacy and safety of low-dose tacrolimus in the treatment of CIDP if first-line treatment options were ineffective or contraindicated. Nevertheless, future multi-center studies that enroll a greater number of patients will be necessary to fully evaluate the role of tacrolimus in the treatment of CIDP.

ACKNOWLEDGEMENTS

Thanks due to the two young patients' support and the trust in our hospital.

REFERENCES

1 **Köller H**, Kieseier BC, Jander S, Hartung HP. Chronic inflammatory demyelinating polyneuropathy. *N Engl J Med* 2005; **352**: 1343-1356 [PMID: 15800230 DOI: 10.1056/NEJMra041347]
2 **Vallat JM**, Sommer C, Magy L. Chronic inflammatory demyelinating polyradiculoneuropathy: diagnostic and therapeutic challenges for a treatable condition. *Lancet Neurol* 2010; **9**: 402-412 [PMID: 20298964 DOI: 10.1016/S1474-4422(10)70041-7]
3 **Koike H**, Katsuno M. Pathophysiology of Chronic Inflammatory Demyelinating Polyneuropathy: Insights into Classification and Therapeutic Strategy. *Neurol Ther* 2020; **9**: 213-227 [PMID: 32410146 DOI: 10.1007/s40120-020-00190-8]
4 **Van den Bergh PY**, Hadden RD, Bouche P, Cornblath DR, Hahn A, Illa I, Koski CL, Léger JM, Nobile-Orazio E, Pollard J, Sommer C, van Doorn PA, van Schaik IN; European Federation of Neurological Societies; Peripheral Nerve Society. European Federation of Neurological Societies/Peripheral Nerve Society guideline on management of chronic inflammatory demyelinating polyradiculoneuropathy: report of a joint task force of the European Federation of Neurological Societies and the Peripheral Nerve Society - first revision. *Eur J Neurol* 2010; **17**: 356-363 [PMID: 20456730 DOI: 10.1111/j.1468-1331.2009.02930.x]
5 **Dyck PJB**, Tracy JA. History, Diagnosis, and Management of Chronic Inflammatory Demyelinating Polyradiculoneuropathy. *Mayo Clin Proc* 2018; **93**: 777-793 [PMID: 29866282 DOI: 10.1016/j.mayocp.2018.03.026]
6 **De Sousa EA**, Brannagan TH 3rd. Diagnosis and treatment of chronic inflammatory demyelinating polyneuropathy. *Curr Treat Options Neurol* 2006; **8**: 91-103 [PMID: 16464406 DOI: 10.1007/s11940-006-0001-2]
7 **Rajabally YA**. Unconventional treatments for chronic inflammatory demyelinating polyneuropathy. *Neurodegener Dis Manag* 2017; **7**: 331-342 [PMID: 29043889 DOI: 10.2217/nmt-2017-0017]
8 **Hodgkinson SJ**, Pollard JD, McLeod JG. Cyclosporin A in the treatment of chronic demyelinating polyradiculoneuropathy. *J Neurol Neurosurg Psychiatry* 1990; **53**: 327-330 [PMID: 2341846 DOI: 10.1136/jnnp.53.4.327]
9 **Barnett MH**, Pollard JD, Davies L, McLeod JG. Cyclosporin A in resistant chronic inflammatory demyelinating polyradiculoneuropathy. *Muscle Nerve* 1998; **21**: 454-460 [PMID: 9533779 DOI: 10.1002/(sici)1097-4598(199804)21:4<454::aid-mus3>3.0.co;2-8]
10 **Visudtibhan A**, Chiemchanya S, Visudhiphan P. Cyclosporine in chronic inflammatory demyelinating polyradiculoneuropathy. *Pediatr Neurol* 2005; **33**: 368-372 [PMID: 16243226 DOI: 10.1016/j.pediatrneurol.2005.05.015]
11 **House AA**, Elmestiri M, Denesyk K, Luke PP, Muirhead N, Rehman F, Boudville N, Jevnikar AM. Apparent low absorbers of cyclosporine microemulsion have higher requirements for tacrolimus in renal transplantation. *Clin Transplant* 2007; **21**: 518-522 [PMID: 17645712 DOI:

10.1111/j.1399-0012.2007.00680.x]
12 **Lee J**. Use of antioxidants to prevent cyclosporine a toxicity. *Toxicol Res* 2010; **26**: 163-170 [PMID: 24278520 DOI: 10.5487/TR.2010.26.3.163]
13 **Kamel M**, Kadian M, Srinivas T, Taber D, Posadas Salas MA. Tacrolimus confers lower acute rejection rates and better renal allograft survival compared to cyclosporine. *World J Transplant* 2016; **6**: 697-702 [PMID: 28058220 DOI: 10.5500/wjt.v6.i4.697]
14 **Dheer D**, Jyoti, Gupta PN, Shankar R. Tacrolimus: An updated review on delivering strategies for multifarious diseases. *Eur J Pharm Sci* 2018; **114**: 217-227 [PMID: 29277665 DOI: 10.1016/j.ejps.2017.12.017]
15 **Ahlmén J**, Andersen O, Hallgren G, Peilot B. Positive effects of tacrolimus in a case of CIDP. *Transplant Proc* 1998; **30**: 4194 [PMID: 9865344 DOI: 10.1016/s0041-1345(98)01389-x]
16 **Schreiber SL**, Crabtree GR. The mechanism of action of cyclosporin A and FK506. *Immunol Today* 1992; **13**: 136-142 [PMID: 1374612 DOI: 10.1016/0167-5699(92)90111-J]
17 **Renard D**, Gauthier T, Venetz JP, Buclin T, Kuntzer T. Late onset tacrolimus-induced life-threatening polyneuropathy in a kidney transplant recipient patient. *Clin Kidney J* 2012; **5**: 323-326 [PMID: 25874089 DOI: 10.1093/ckj/sfs067]
18 **Mahdi-Rogers M**, van Doorn PA, Hughes RA. Immunomodulatory treatment other than corticosteroids, immunoglobulin and plasma exchange for chronic inflammatory demyelinating polyradiculoneuropathy. *Cochrane Database Syst Rev* 2013; CD003280 [PMID: 23771584 DOI: 10.1002/14651858.CD003280.pub4]
19 **Hergüner MO**, Incecik F, Altunbaşak S. Cyclosporin treatment in three children with chronic inflammatory demyelinating neuropathy. *Pediatr Neurol* 2009; **41**: 223-225 [PMID: 19664543 DOI: 10.1016/j.pediatrneurol.2009.03.016]
20 **Wilson JR**, Conwit RA, Eidelman BH, Starzl T, Abu-Elmagd K. Sensorimotor neuropathy resembling CIDP in patients receiving FK506. *Muscle Nerve* 1994; **17**: 528-532 [PMID: 7512691 DOI: 10.1002/mus.880170510]
21 **Moon JI**, Park SG, Cheon KO, Kim SI, Kim YS, Park YW, Park K. Pregnancy in renal transplant patients. *Transplant Proc* 2000; **32**: 1869-1870 [PMID: 11119976 DOI: 10.1016/s0041-1345(00)01469-x]
22 **Srinivas M**, Agarwala S, Datta Gupta S, Das SN, Jha P, Misro MM, Mitra DK. Effect of cyclosporine on fertility in male rats. *Pediatr Surg Int* 1998; **13**: 388-391 [PMID: 9639624 DOI: 10.1007/s003830050346]

World Journal of Clinical Cases

Submit a Manuscript: https://www.f6publishing.com

World J Clin Cases 2022 February 16; 10(5): 1716-1722

DOI: 10.12998/wjcc.v10.i5.1716

ISSN 2307-8960 (online)

CASE REPORT

Vedolizumab-associated diffuse interstitial lung disease in patients with ulcerative colitis: A case report

Jie Zhang, Mei-Hong Liu, Xue Gao, Chang Dong, Yan-Xia Li

ORCID number: Jie Zhang 0000-0002-4244-5660; Mei-Hong Liu 0000-0002-0061-0373; Xue Gao 0000-0002-3894-7561; Chang Dong 0000-0001-5203-0891; Yan-Xia Li 0000-0002-1586-5352.

Author contributions: Dong C and Zhang J reviewed the literature and contributed to manuscript drafting; Liu MH performed the collection and interpretation of the clinical data and material; Gao X analyzed and interpreted the pathological findings; Li YX was responsible for the revision of the manuscript for important intellectual content; all authors contributed to the manuscript and approved the final version to be submitted.

Informed consent statement: Informed written consent was obtained from the patient's proxy for publication of this report and any accompanying images.

Conflict-of-interest statement: The authors declare that they have no conflicts of interest.

CARE Checklist (2016) statement: The authors have read the CARE Checklist (2016), and the manuscript was prepared and revised according to the CARE Checklist (2016).

Supported by the Dalian Municipal

Jie Zhang, Mei-Hong Liu, Chang Dong, Yan-Xia Li, Department of Pulmonary and Critical Care Medicine, First Affiliated Hospital of Dalian Medical University, Dalian 116011, Liaoning Province, China

Xue Gao, Department of Pathology, First Affiliated Hospital of Dalian Medical University, Dalian 116011, Liaoning Province, China

Corresponding author: Chang Dong, MD, Associate Chief Physician, Associate Professor, Department of Pulmonary and Critical Care Medicine, First Affiliated Hospital of Dalian Medical University, No. 222 Zhongshan Road, Xigang District, Dalian 116011, Liaoning Province, China. dongchang8793@163.com

Abstract

BACKGROUND

Vedolizumab, a newer class of integrin antagonist biological agents, has been applied to treat patients with moderate-to-severe Crohn's disease (CD) and ulcerative colitis (UC), especially for patients who are refractory to traditional therapies and tumor necrosis factor antagonists. However, some rare but life-threatening adverse effects warrant pharmacovigilance. We describe the first fatal case of vedolizumab-associated severe diffuse interstitial lung disease in China.

CASE SUMMARY

We present a case of new-onset diffuse parenchymal lung disease developing under treatment with vedolizumab in a patient with UC. After two doses of vedolizumab, he developed persistent fever and progressively worsening dyspnea. Extensive workups, including bronchoalveolar lavage, transbronchial lung biopsy and metagenomic next-generation sequencing, identified no infectious causes, and other potential causes (such as tumors and cardiogenic pulmonary edema) were also excluded. As a result, a diagnosis of vedolizumab-related interstitial lung disease was established. Unfortunately, although corticosteroids and empiric antibiotics were administered, the patient eventually died of respiratory failure.

CONCLUSION

Vedolizumab-related interstitial lung disease in patients with UC is rare but potentially lethal. Gastroenterologists and pulmonologists should be aware of vedolizumab-related adverse drug reactions.

Science and Technology Innovation Foundation, No. 2020JJ27SN072.

Country/Territory of origin: China

Specialty type: Medicine, general and internal

Provenance and peer review: Unsolicited article; Externally peer reviewed.

Peer-review model: Single blind

Peer-review report's scientific quality classification

Grade A (Excellent): 0
Grade B (Very good): B, B
Grade C (Good): 0
Grade D (Fair): 0
Grade E (Poor): 0

Received: October 11, 2021
Peer-review started: October 11, 2021
First decision: November 7, 2021
Revised: December 18, 2021
Accepted: January 5, 2022
Article in press: January 5, 2022
Published online: February 16, 2022

P-Reviewer: Nikolić M, Triantafillidis J
S-Editor: Ma YJ
L-Editor: A
P-Editor: Ma YJ

Key Words: Vedolizumab; Adverse effects; Ulcerative colitis; Inflammatory bowel disease; Interstitial lung disease; Case report

Core Tip: Vedolizumab is the treatment of choice for patients with moderate-to-severe ulcerative colitis who are refractory to tumor necrosis factor antagonists. However, some rare but potentially lethal drug-associated adverse effects warrant pharmacovigilance. We present a case of new-onset diffuse parenchymal lung disease development under treatment with vedolizumab in a patient with ulcerative colitis. After two doses of vedolizumab, he developed persistent fever, progressively worsening dyspnea and eventually died of respiratory failure. The patient was eventually diagnosed with vedolizumab-related interstitial lung disease, in spite of the few case reports found after reviewing the literature. We aim to raise gastroenterologists' and pulmonologists' vigilance to this uncommon adverse event.

Citation: Zhang J, Liu MH, Gao X, Dong C, Li YX. Vedolizumab-associated diffuse interstitial lung disease in patients with ulcerative colitis: A case report. *World J Clin Cases* 2022; 10(5): 1716-1722
URL: https://www.wjgnet.com/2307-8960/full/v10/i5/1716.htm
DOI: https://dx.doi.org/10.12998/wjcc.v10.i5.1716

INTRODUCTION

Vedolizumab is a fully humanized monoclonal antibody. It is currently the only intestinal selective biological agent in the field of inflammatory bowel disease (IBD) that targets α4β7 gastrointestinal integrin receptors and blocks the receptor's interaction with mucosal addressin cell adhesion molecule-1, thereby inhibiting the migration of T lymphocytes into the intestinal parenchymal tissue in order to reduce inflammation[1]. In March 2020, vedolizumab produced by Takeda Pharmaceutical Company was approved for marketing in China for the first time. Although the clinical effectiveness of this brand has been continuously verified and recognized[2], safety and adverse events have also attracted negative attention. Here, we describe one fatal case of vedolizumab-associated severe interstitial lung disease in a patient with ulcerative colitis (UC). We also reviewed the existing literature in English and found only seven case reports of vedolizumab-associated lung diseases, mainly in patients with IBD.

CASE PRESENTATION

Chief complaints

A 61-year-old Chinese male was initially admitted to the gastroenterology department of our hospital with chief complaints of recurrent abdominal pain, diarrhea, mucopurulent hematochezia and weight loss.

History of present illness

The patient was diagnosed with UC 12 years prior to admission, and he had been treated with multiple conventional therapies, including, oral and topical aminosalicylates, dexamethasone enema, oral corticosteroids, selective leukocyte absorption treatment and intestinal flora adjustment treatment. In spite of these treatments, he experienced frequent flare-ups and was admitted to the hospital 3 times over the past 9 mo. Due to these failed conventional therapies, the patient was administered adalimumab 160 mg by subcutaneous injection. However, the symptoms continued with 10 to 20 bowel movements daily, and the modified Truelove and Witts severity index suggested moderately to severely active UC. As a result, the patient was started on vedolizumab. After the first dose of vedolizumab (300 mg intravenous infusion), fever at 39 °C and fatigue occurred the next day. He was treated with intravenous

mezlocillin, foscarnet sodium, and ornidazole, but the fever persisted. The second dose of vedolizumab was administered 2 wk later, and the patient responded well regarding his intestinal symptoms; however, he presented with new-onset dyspnea at rest and nonproductive cough 2 d after the second vedolizumab treatment. Half a month later, the patient was admitted to the Department of Respiratory and Intensive Care Unit (RICU) due to severe dyspnea.

History of past illness

There was no significant medical history.

Physical examination

Upon arrival to the RICU, a body temperature of 36.8 degrees Celsius, a blood pressure of 128/90 mmHg, a heart rate of 97 beats/min, and a respiratory rate of 28 times/min were noted. The remaining physical examination was unremarkable except for diffuse inspiratory crackles in both lungs.

Laboratory examinations

Lab data revealed the following: white blood cells 11.10 × 10^9/L, neutrophils 68.6%, lymphocytes 23.2%, hemoglobin 130 g/L and platelets 328 × 10^9/L. Serum C-reactive protein was increased at 111 mg/L (normal range ≤ 8 mg/L), erythrocyte sedimentation rate at 64 mm/h (normal range ≤ 15 mm/h), fecal calprotectin at 250.9 ug/g (normal range 0-50 ug/g) and procalcitonin was normal at 0.07 ng/mL (normal range ≤ 0.5 ng/mL). A fecal occult blood test showed positive occult blood with 0-1 white blood cells per high-power field. Stool cultures for *Salmonella, Shigella and Campylobacter* were all negative. Arterial blood gas analysis showed that pO_2 was 41 mmHg breathing ambient air. Extensive microbiology assays (blood and sputum culture, 1,3-beta-D-glucan, galactomannan testing, aspergillus antibody, cryptococcal capsular polysaccharide antigen, mycoplasma antibody, human immunodeficiency virus antibody, cytomegalovirus, Epstein–Barr virus, A and B influenza virus PCR assays, and, antibodies of Toxoplasma gondii, rubella, herpes simplex virus and legionella) identified no infectious causes. Serologic examination included rheumatoid factor, antinuclear antibody panel, ds-DNA antibodies, anti-extractable nuclear antigen antibodies, myositis antibody panel, antineutrophil cytoplasmic antibody panel, and immunoglobulin, which were not elevated to pathologic levels. Cardiogenic pulmonary edema was excluded due to normal myocardial enzymes, B-type natriuretic peptide, echocardiogram and echocardiography. Some tumor markers, including, carcinoma embryonic antigen, cytokeratin 19 fragment and neuron-specific enolase, were increased at 7.68 ng/mL (normal range 0-5 ng/mL), 12.37 ng/mL (normal range 0-5 ng/mL) and 26.61 ng/mL (normal range 0-24 ng/mL), respectively, while alpha-fetoprotein and carcinoma antigen 125 and 199 were in the normal range. Bronchoalveolar lavage (BAL) and transbronchial lung biopsy (TBLB) were also performed. Cultures from the BAL were negative for bacteria, mycobacteria and fungi. Samples from the BAL and the peripheral blood were sent together for metagenomic next-generation sequencing (mNGS). This sequencing uses an untargeted DNA/RNA sequencing method to detect all potential pathogens, including, bacteria, fungi, viruses, and parasites[3]. In brief, the negative results of both mNGS and multiple microbiological cultures together effectively excluded infection.

Imaging examinations

On high-resolution computed tomography (HRCT), new-onset diffuse infiltrates, interlobular thickening and fibrosis were noted compared to a HRCT from one month prior (Figure 1).

Pathology

On histopathology, irregular glandular structures in the hyperplastic fibrous tissue were noted with scattered lymphocytes infiltrated in the interstitium. Intranuclear vacuoles, nuclear fragmentation, binuclear cells were seen (Figure 2). No tumor cells were noted and immunohistochemistry showed that adenoid structures were positive for cytokeratin AE1/AE3; epithelial cells were positive for the epidermal growth factor receptor (EGFR), p53 and negative for vimentin; positive immunostaining for Ki67 in some larger epithelial cells accounted approximately 15%; negative immunostaining for desmin was detected.

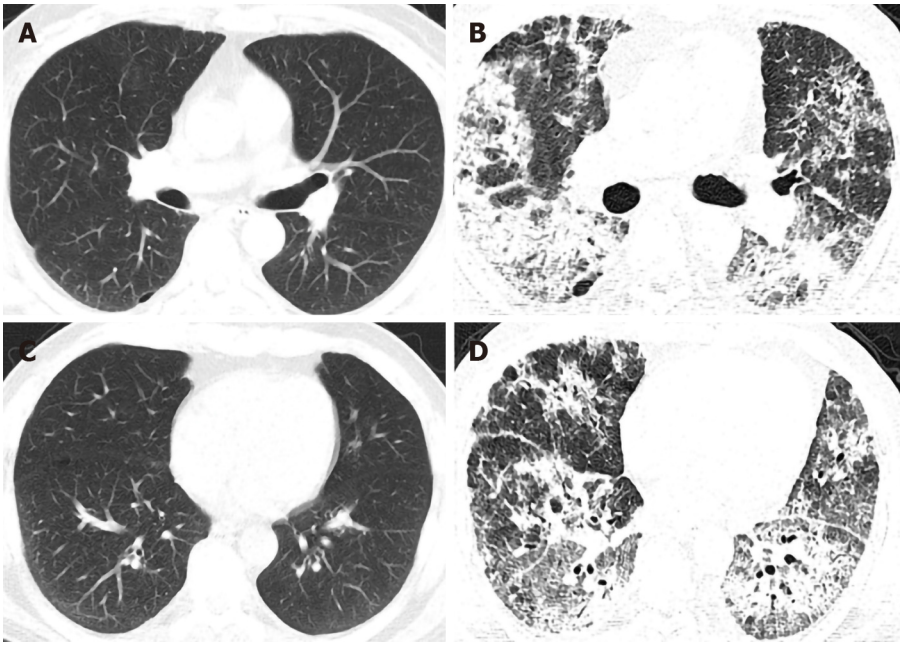

Figure 1 High-resolution computed tomography of the patient before and after vedolizumab administration. A and B: The lung window of the patient in the high-resolution computed tomography (HRCT) before vedolizumab administration was basically normal except for some scattered miliary nodules and localized emphysema; C and D: the lung window of the patient in the HRCT after two doses of vedolizumab administration showed the new-onset severe diffuse infiltrates, interlobular thickening and fibrosis.

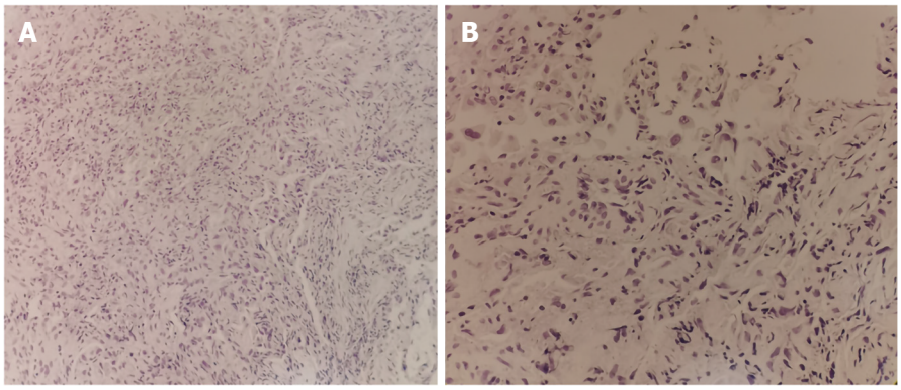

Figure 2 Pathology of transbronchial lung biopsy. A: Irregular glandular structures in the hyperplastic fibrous tissue and infiltrated lymphocytes scattered throughout the interstitium were noted (H&E, x200); B: The glandular cavity was covered with single or stratified epithelium, the epithelial cells were cubic or polygonal, some of the cells had large nuclei and slightly dense chromatin. Intranuclear vacuoles, nuclear fragmentation and binuclear cells were noted. The focal gland cavity contains histiocytes, and the interstitium was infiltrated with scattered lymphocytes. No tumor cells were noted (H&E, x400).

FINAL DIAGNOSIS

A diagnosis of vedolizumab-associated interstitial lung disease was made. The Naranjo adverse drug reaction scale [4] was calculated to be 6 (causality: probable).

TREATMENT

Vedolizumab was discontinued, and the patient was started on methylprednisolone 80 mg/day. Three days later, intubation and mechanical ventilation was initiated due to refractory hypoxia. The anti-infective treatment was adjusted to linezolid, meropenem, caspofungin, compound sulfamethoxazole tablets and foscarnet sodium without any response.

OUTCOME AND FOLLOW-UP

Unfortunately, after nine days of hospitalization, the patient died due to respiratory failure.

DISCUSSION

The efficacy and safety of vedolizumab in patients with moderate to severe IBD have been confirmed in several pivotal clinical trials[5,6]. An integrated study analyzed 2830 IBD patients who used vedolizumab from 2009 to 2013 and showed that vedolizumab did not increase their risk of infection or malignancy, and the most common adverse events were nasopharyngitis, abdominal pain, headache and joint pain[7]. However, in the past 4 years, 7 cases of noninfectious lung injury related to vedolizumab have been reported, including 4 cases of UC and 3 cases of CD. In 2017, Sudheer *et al*[8] first reported a 58-year-old white man with UC who developed acute respiratory distress syndrome requiring intubation and mechanical ventilation after receiving 3 doses of vedolizumab. By withholding vedolizumab and applying the steroid, the patient was successfully discharged home. Another case was described by Eva *et al*[9] of a 52-year-old female with UC who suffered from new onset dyspnea and dry cough with chest CT showing diffuse ground-glass opacities. She was being treated with intravenous vedolizumab every 8 weeks for 2 years. Laboratory work did not identify infection, and the pathology of TBLB showed small bronchiole injury with debris and accumulation of mononuclear cells, macrophages and histiocytes. The fact that a complete resolution of symptoms and radiographic abnormalities was achieved by discontinuation of vedolizumab without any other treatments highly suggested vedolizumab-induced lung toxicity. Another recently published case has a similar clinical course as ours. A 39-year-old male diagnosed with UC presented with acute severe interstitial lung injury while receiving vedolizumab treatment[10]. While vedolizumab cessation and systemic steroid administration helped this patient, our patient was refractory to his therapy and finally passed away. Cucinotta *et al*[11] reported the off-label use of vedolizumab in a 13-year-old child with UC, and after three doses of vedolizumab, the child developed a persistent cough that resolved after vedolizumab discontinuation.

Strictly speaking, drug-induced pulmonary toxicity is not an extraintestinal manifestation of IBD[9,12]. Even so, over half of interstitial lung disease and granulomatous lung disease cases in IBD patients are drug-related; therefore, more differential diagnoses are necessary[13]. On that basis, we also reviewed 3 case reports of patients with CD. They presented with dyspnea, dry cough or fever with new-onset abnormal chest CT results (including pulmonary nodules, ground-glass opacities, pulmonary infiltrates or pleural effusions) after receiving 3-4 doses of vedolizumab[14-16]. On histopathology, lung biopsies from all 3 cases revealed noncaseating granulomatous inflammation. In terms of clinical outcome, 2 patients were successfully treated with prednisone, 1 patient failed systemic steroid treatment but was responsive to infliximab treatment, and complete resolution of pulmonary disease was achieved in all three cases.

In our case, we made a diagnosis of vedolizumab-induced lung injury for the following reasons. First, the patient had no respiratory symptoms or interstitial changes on his previous chest CT, even though his UC was actively relapsing during the past 9 months. Second, the new symptoms following the application of vedolizumab and new-onset diffuse parenchymal changes on CT highly suggested an adverse drug reaction. Third, the resolution of intestinal symptoms and the evolution of respiratory injury occurring directly after the administration of vedolizumab may be attributed to the drug mechanism of vedolizumab itself. One study suggested that vedolizumab could induce an upregulation of β1 expression on lymphocytes (which is an integrin component involved in pulmonary homing)[14], thereby facilitating the development of pulmonary inflammation and injury. Fourth, the abnormalities in the chest CT of our case were the most severe when compared to the above published cases. The reason our patient was not responsive to systemic corticosteroid treatment was due to the devastating damage of the lung tissue and the delay in time to a diagnosis. Last, in addition to conventional microbiological tests, we also utilized the advanced mNGS technique, which has a much higher sensitivity than that of conventional tests in mixed pulmonary infection diagnoses [17]. It has been reported that the sensitivity of mNGS for pathogen detection was 97.1%, with a negative predictive value of 94.1%[18]. Moreover, extensive anti-infective therapy aiming to cover all

possible pathogens was administered without any improvement of symptoms. All the facts discussed above basically excluded the possibility of infection. To the best of our knowledge, this is the first fatal case of vedolizumab-associated interstitial lung disease reported in China. There was an additional death reported in which a 70-year-old man with a UC flare was being treated with prednisone and vedolizumab, but this patient had previously had mild chronic shortness of breath with chest CT showing bilateral interstitial fibrosis before receiving vedolizumab; therefore, we cannot confirm that it was vedolizumab-related[19].

CONCLUSION

Vedolizumab-related interstitial lung diseases in patients with IBD can be potentially fatal (as in our case presentation). Gastroenterologists and pulmonologists should raise their awareness regarding these cases. Timely diagnosis, early discontinuation of the offending drug and systemic corticosteroid treatment could prevent irreversible fibrosis.

REFERENCES

1 **Fischer A**, Zundler S, Atreya R, Rath T, Voskens C, Hirschmann S, López-Posadas R, Watson A, Becker C, Schuler G, Neufert C, Atreya I, Neurath MF. Differential effects of α4β7 and GPR15 on the homing of effector and regulatory T cells from patients with UC to the inflamed gut in vivo. *Gut* 2016; **65**: 1642-1664 [PMID: 26209553 DOI: 10.1136/gutjnl-2015-310022]

2 **Baumgart DC**, Bokemeyer B, Drabik A, Stallmach A, Schreiber S; Vedolizumab Germany Consortium. Vedolizumab induction therapy for inflammatory bowel disease in clinical practice--a nationwide consecutive German cohort study. *Aliment Pharmacol Ther* 2016; **43**: 1090-1102 [PMID: 27038247 DOI: 10.1111/apt.13594]

3 **Gu W**, Miller S, Chiu CY. Clinical Metagenomic Next-Generation Sequencing for Pathogen Detection. *Annu Rev Pathol* 2019; **14**: 319-338 [PMID: 30355154 DOI: 10.1146/annurev-pathmechdis-012418-012751]

4 **Naranjo CA**, Busto U, Sellers EM, Sandor P, Ruiz I, Roberts EA, Janecek E, Domecq C, Greenblatt DJ. A method for estimating the probability of adverse drug reactions. *Clin Pharmacol Ther* 1981; **30**: 239-245 [PMID: 7249508 DOI: 10.1038/clpt.1981.154]

5 **Feagan BG**, Rutgeerts P, Sands BE, Hanauer S, Colombel JF, Sandborn WJ, Van Assche G, Axler J, Kim HJ, Danese S, Fox I, Milch C, Sankoh S, Wyant T, Xu J, Parikh A; GEMINI 1 Study Group. Vedolizumab as induction and maintenance therapy for ulcerative colitis. *N Engl J Med* 2013; **369**: 699-710 [PMID: 23964932 DOI: 10.1056/NEJMoa1215734]

6 **Sandborn WJ**, Feagan BG, Rutgeerts P, Hanauer S, Colombel JF, Sands BE, Lukas M, Fedorak RN, Lee S, Bressler B, Fox I, Rosario M, Sankoh S, Xu J, Stephens K, Milch C, Parikh A; GEMINI 2 Study Group. Vedolizumab as induction and maintenance therapy for Crohn's disease. *N Engl J Med* 2013; **369**: 711-721 [PMID: 23964933 DOI: 10.1056/NEJMoa1215739]

7 **Colombel JF**, Sands BE, Rutgeerts P, Sandborn W, Danese S, D'Haens G, Panaccione R, Loftus EV Jr, Sankoh S, Fox I, Parikh A, Milch C, Abhyankar B, Feagan BG. The safety of vedolizumab for ulcerative colitis and Crohn's disease. *Gut* 2017; **66**: 839-851 [PMID: 26893500 DOI: 10.1136/gutjnl-2015-311079]

8 **Nambiar S**, Karippot A, Oliver T. Vedolizumab-Associated Acute Respiratory Distress Syndrome. *Am J Ther* 2018; **25**: e592-e593 [PMID: 29189313 DOI: 10.1097/MJT.0000000000000627]

9 **De Backer E**, Bode H, Baert F. New-Onset Diffuse Parenchymal Lung Disease in a 52-Year-Old Woman With Ulcerative Colitis. *Gastroenterology* 2020; **158**: 478-479 [PMID: 31560891 DOI: 10.1053/j.gastro.2019.09.016]

10 **Rizos ED**, Antonogiannaki EM, Chatzidakis A, Kallieri M, Tsilogianni Z, Manali ED, Economopoulos N, Triantafyllou K, Papiris SA, Polymeros D. Vedolizumab-induced acute interstitial lung injury in a 39-year-old male with ulcerative colitis. *Eur J Gastroenterol Hepatol* 2021 [PMID: 34074983 DOI: 10.1097/MEG.0000000000002197]

11 **Cucinotta U**, Dipasquale V, Costa S, Pellegrino S, Ramistella V, Romano C. Vedolizumab-associated pulmonary manifestations in children with ulcerative colitis. *J Clin Pharm Ther* 2021 [PMID: 34278581 DOI: 10.1111/jcpt.13494]

12 **Lu DG**, Ji XQ, Liu X, Li HJ, Zhang CQ. Pulmonary manifestations of Crohn's disease. *World J Gastroenterol* 2014; **20**: 133-141 [PMID: 24415866 DOI: 10.3748/wjg.v20.i1.133]

13 **Eliadou E**, Moleiro J, Ribaldone DG, Astegiano M, Rothfuss K, Taxonera C, Ghalim F, Carbonnel F, Verstockt B, Festa S, Maia L, Berrozpe A, Zagorowicz E, Savarino E, Ellul P, Vavricka SR, Calvo M, Koutroubakis I, Hoentjen F, Salazar LF, Callela F, Cañete Pizarro F, Soufleris K, Sonnenberg E, Cavicchi M, Wypych J, Hommel C, Ghiani A, Fiorino G; ECCO CONFER COMMITTEE. Interstitial and Granulomatous Lung Disease in Inflammatory Bowel Disease Patients. *J Crohns Colitis* 2020; **14**: 480-489 [PMID: 31602473 DOI: 10.1093/ecco-jcc/jjz165]

14 **Lissner D**, Glauben R, Allers K, Sonnenberg E, Loddenkemper C, Schneider T, Siegmund B. Pulmonary Manifestation of Crohn's Disease Developed Under Treatment With Vedolizumab. *Am J Gastroenterol* 2018; **113**: 146-148 [PMID: 29311733 DOI: 10.1038/ajg.2017.395]

15 **Myc LA**, Girton MR, Stoler MH, Davis EM. Necrobiotic Pulmonary Nodules of Crohn's Disease in a Patient Receiving Vedolizumab. *Am J Respir Crit Care Med* 2019; **199**: e1-e2 [PMID: 30156859 DOI: 10.1164/rccm.201806-1056IM]

16 **Abu Shtaya A**, Cohen S, Kogan Y, Shteinberg M, Sagool O. Crohn's Disease with Atypical Extra-Intestinal Manifestations Developing Under Treatment with Vedolizumab. *Eur J Case Rep Intern Med* 2021; **8**: 002265 [PMID: 33768073 DOI: 10.12890/2021_002265]

17 **Wang J**, Han Y, Feng J. Metagenomic next-generation sequencing for mixed pulmonary infection diagnosis. *BMC Pulm Med* 2019; **19**: 252 [PMID: 31856779 DOI: 10.1186/s12890-019-1022-4]

18 **Fang X**, Mei Q, Fan X, Zhu C, Yang T, Zhang L, Geng S, Pan A. Diagnostic Value of Metagenomic Next-Generation Sequencing for the Detection of Pathogens in Bronchoalveolar Lavage Fluid in Ventilator-Associated Pneumonia Patients. *Front Microbiol* 2020; **11**: 599756 [PMID: 33335520 DOI: 10.3389/fmicb.2020.599756]

19 **Collins HW**, Frye JW. Interstitial Lung Disease in a 70-Year-Old Man with Ulcerative Colitis. *ACG Case Rep J* 2018; **5**: e28 [PMID: 29670924 DOI: 10.14309/crj.2018.28]

World Journal of Clinical Cases

Submit a Manuscript: https://www.f6publishing.com

World J Clin Cases 2022 February 16; 10(5): 1723-1728

DOI: 10.12998/wjcc.v10.i5.1723

ISSN 2307-8960 (online)

CASE REPORT

Unusual magnetic resonance imaging findings of brain and leptomeningeal metastasis in lung adenocarcinoma: A case report

Na Li, Yu-Jun Wang, Fang-Mei Zhu, Shui-Tang Deng

ORCID number: Na Li 0000-0003-2224-050X; Yu-Jun Wang 0000-0003-3701-0598; Fang-Mei Zhu 0000-0003-0110-455X; Shui-Tang Deng 0000-0002-2858-7400.

Author contributions: Li N and Wang YJ designed research; Li N and Zhu FM performed research; Li N, Zhu FM, Deng ST analyzed data; Li N wrote the letter; Zhu FM and Wang YJ revised the letter.

Informed consent statement: Informed consent was obtained from the patient's guardian for publication of this report and any accompanying images.

Conflict-of-interest statement: The authors declare that they have no conflict of interest.

CARE Checklist (2016) statement: The authors have read the CARE Checklist (2016), and the manuscript was prepared and revised according to the CARE Checklist (2016).

Supported by the Medical and Health Science and Technology Planning Project, No. 2019319609.

Country/Territory of origin: China

Specialty type: Neuroimaging

Provenance and peer review: Unsolicited manuscript; Externally peer reviewed.

Na Li, Fang-Mei Zhu, Shui-Tang Deng, Department of Radiology, Tongde Hospital of Zhejiang Province, Hangzhou 310012, Zhejiang Province, China

Yu-Jun Wang, Department of Radiology, Zhejiang Provincial Hospital of Chinese Medicine, Hangzhou 310012, Zhejiang Province, China

Corresponding author: Yu-Jun Wang, Chief Doctor, Department of Radiology, Zhejiang Provincial Hospital of Chinese Medicine, No. 54 Youdian Road, Hangzhou 310012, Zhejiang Province, China. 981861280@qq.com

Abstract

BACKGROUND

Metastatic tumors are the most common malignancies of central nervous system in adults, and the frequent primary lesion is lung cancer. Brain and leptomeningeal metastases are more common in patients with non-small-cell lung cancer harboring epidermal growth factor receptor mutations. However, the coexist of brain metastasis with leptomeningeal metastasis (LM) in isolated gyriform appearance is rare.

CASE SUMMARY

We herein presented a case of a 76-year-old male with an established diagnosis as lung adenocarcinoma with gyriform-appeared cerebral parenchymal and leptomeningeal metastases, accompanied by mild peripheral edema and avid contrast enhancement on magnetic resonance imaging. Surgical and pathological examinations confirmed the brain and leptomeningeal metastatic lesions in the left frontal cortex, subcortical white matter and local leptomeninges.

CONCLUSION

This case was unique with respect to the imaging findings of focal gyriform appearance, which might be caused by secondary parenchymal brain metastatic tumors invading into the leptomeninges or coexistence with LM. Radiologists should be aware of this uncommon imaging presentation of tumor metastases to the central nervous system.

Key Words: Brain metastasis; Leptomeningeal metastasis; Magnetic resonance imaging; Lung cancer; Epidermal growth factor receptor; Case report

Peer-review model: Single blind

Peer-review report's scientific quality classification
Grade A (Excellent): 0
Grade B (Very good): B
Grade C (Good): C, C
Grade D (Fair): 0
Grade E (Poor): 0

Received: October 18, 2021
Peer-review started: October 18, 2021
First decision: October 27, 2021
Revised: November 4, 2021
Accepted: January 8, 2022
Article in press: January 8, 2022
Published online: February 16, 2022

P-Reviewer: Chu HT, Gokce E, Musoni L
S-Editor: Ma YJ
L-Editor: A
P-Editor: Ma YJ

Core Tip: Patients with non-small-cell lung cancer harboring epidermal growth factor receptor (EGFR) mutations were more susceptible to develop into brain or leptomeningeal metastases when compared to those with wild-type EGFR. However, parenchymal brain metastasis combined with leptomeningeal metastasis (LM) in isolated gyriform appearance is rare. We herein presented a case of a 76-year-old male with EGFR-mutated lung adenocarcinoma metastases of the brain with isolated gyriform appearance in imaging findings. We speculated that the focal gyriform lesions were likely to be caused by secondary leptomeningeal invasion from parenchymal brain metastatic tumors or coexisting of parenchymal brain metastasis with LM.

Citation: Li N, Wang YJ, Zhu FM, Deng ST. Unusual magnetic resonance imaging findings of brain and leptomeningeal metastasis in lung adenocarcinoma: A case report. *World J Clin Cases* 2022; 10(5): 1723-1728
URL: https://www.wjgnet.com/2307-8960/full/v10/i5/1723.htm
DOI: https://dx.doi.org/10.12998/wjcc.v10.i5.1723

INTRODUCTION

Metastatic tumors account for the majority of central nervous system (CNS) neoplasms, which outnumber the primary brain tumors, and the most common source for these is lung cancer[1]. CNS metastasis involves brain parenchyma, dura or leptomeninges. Neuroimaging findings often indicate metastatic diseases. In particular, the gadolinium-enhanced magnetic resonance imaging (MRI) of the brain is regarded beneficial for the detection of leptomeningeal metastasis (LM)[2]. Herein, we presented a case of a 76-year-old male with epidermal growth factor receptor (EGFR) mutated lung adenocarcinoma metastases of the brain with unique appearance in imaging findings.

CASE PRESENTATION

Chief complaints

A 76-year-old male patient with nausea and vomiting without obvious inducement, and dizziness, headache and fatigue was admitted to our hospital for further evaluation.

History of present illness

Patient's symptoms started 3 d ago.

History of past illness

In 2014, the patient underwent radical resection of the right middle lobe lung cancer for the first time. The postoperative diagnosis showed lung adenocarcinoma (T1aN0M0, stage Ia), without adjuvant radiotherapy and chemotherapy. In January 2019, the patient underwent a puncture biopsy because of the newly discovered ground-glass nodule in the right lower lung, and postoperative pathology confirmed lung adenocarcinoma. Polymerase chain reaction of tumor specimens showed EGFR mutations at exon 21. Radiofrequency ablation of right lung cancer was performed after the surgery. At this time, MRI of brain showed no metastatic tumors in the central nervous system.

Personal and family history

The patient had no particular individual or family history.

Physical examination

Neurological examination was conducted, which revealed no obvious pathological signs of tumor metastasis.

Laboratory examinations

The patient underwent cerebrospinal fluid (CSF) tests 2 mo after craniotomy. The CSF results were as follows: Glucose: 0.7 mmol/L; Chloride: 117.4 mmol/L; β-trace protein: 2283 mg/L; White cell: 220 × 10^6/L; Neutrophils: 20%; and Lymphocytes: 80%. The Pandy's test was positive, and CSF cytology showed malignant epithelial cells in the CSF (Figure 1).

Imaging examinations

In October 2019, MRI of the brain (Figure 2) revealed a cortical and subcortical isolated gyriform mass in the left frontal lobe, with T_2/FLAIR hyperintensities, obvious contrast enhancement, subtle perilesional edema, and restricted diffusion, which was unusual for metastatic tumors. Therefore, it was misdiagnosed as glioma or subacute cerebral infarction. In addition, T_1WI enhancement also revealed local leptomeningeal lesions (Figure 2E), which were missed in the process of imaging diagnosis. Magnetic resonance angiography (MRA) showed no obvious abnormalities in the intracranial blood vessels.

Further diagnostic work-up

Due to ambiguity in imaging findings, craniotomy was performed to establish the diagnosis. During operation, the mass was shown to be located in the left frontal lobe and adjacent leptomeninges, with a local gray-white tumor tissue, wherein a small part of it appeared pink fish-like, and had abundant blood supply. Resection of tumor tissue was performed in the frontal lobe, and then along the cerebral gyrus and sulcus to remove the invasive residual tumors and leptomeningeal lesions. The pathological examination results revealed abnormal epithelioid cell nests in the brain tissue (Figure 1). Immunohistochemical stains were positive for cytokeratin 7, thyroid transcription factor-1, Napsin-A, and epithelial membrane antigen and negative for glial fibrillary acidic protein, P53, S-100, Vim and ALK, which was consistent with that of primary lung metastasis. Also 40% proliferative activity was reported with Ki-67.

FINAL DIAGNOSIS

The final diagnosis of the presented case was brain and leptomeningeal metastases in EGFR-mutated lung adenocarcinoma.

TREATMENT

After surgery, the patient's condition was stabilized, but his consciousness was still clouded.

OUTCOME AND FOLLOW-UP

The patient did not receive chemotherapy after surgery and died due to acute brain failure two months later.

DISCUSSION

Lung cancer is the most common primary tumor associated with CNS metastases, and it eventually develops into CNS metastases in 23%-36% of lung cancer patients[3]. LM is rare and occurs in 3%-5% of patients with advanced non-small-cell lung cancer[4]. Patients with non-small-cell lung cancer harboring EGFR mutations were more susceptible to develop brain or leptomeningeal metastases when compared with those bearing wild-type EGFR[5,6]. Patterns of brain metastasis might vary in non-small cell lung cancer patients, as it depends on the tumor nodules and is more or less related to cystic and necrotic lesions[7,8]. However, parenchymal brain metastasis combined with LM in the appearance of isolated gyriform are rare. After all, LM usually presents as more diffused tumor involvement, and isolated one is not frequently seen. A case of EGFR-mutated lung adenocarcinoma with brain parenchymal and leptomeningeal metastases in a focal gyriform appearance was herein presented.

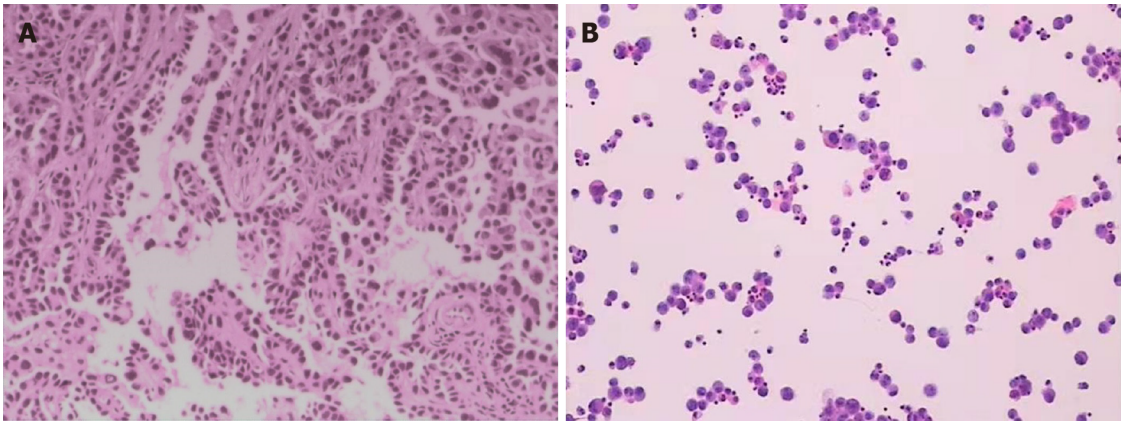

Figure 1 Results of pathologic diagnosis and cerebrospinal fluid cytology. A: H&E staining, magnification 100×, demonstrated abnormal epithelioid cell nests in the left frontal lesion; B: Cerebrospinal fluid (CSF) cytology revealed malignant cells in the CSF.

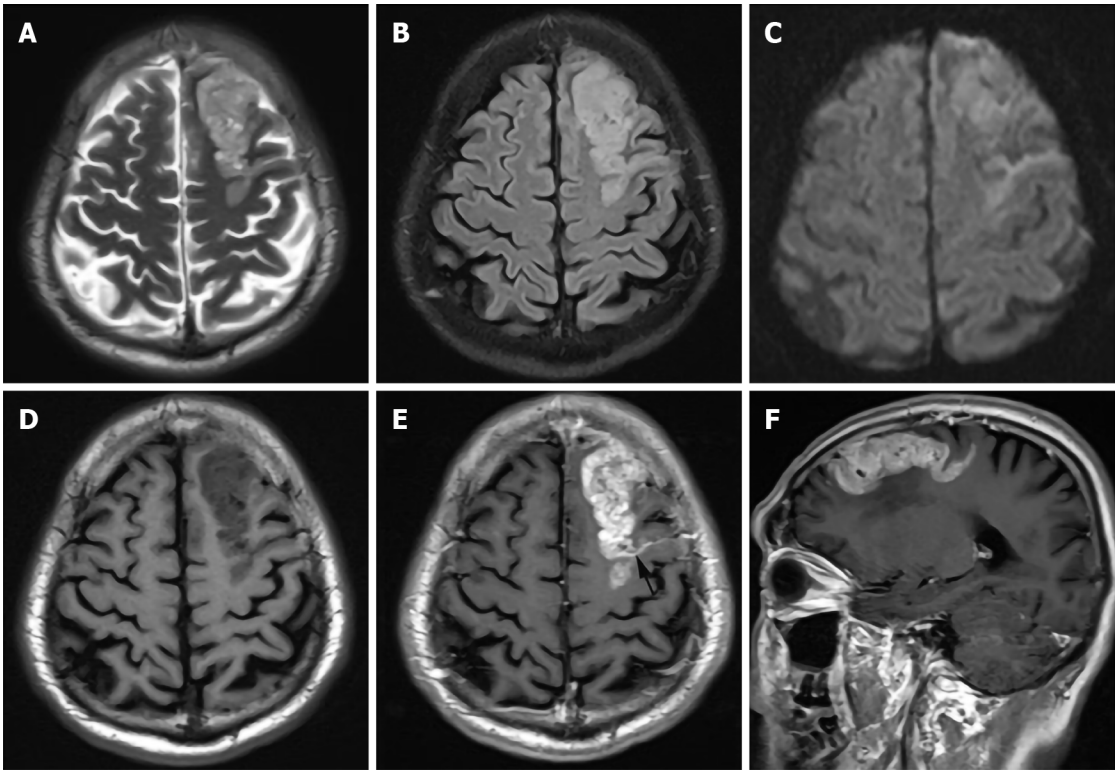

Figure 2 76-year-old male with brain and leptomeningeal metastases. Magnetic resonance imaging (3.0 T) demonstrated a predominately T_2/FLAIR hyperintense gyriform mass in the left frontal lobe (A: T_2WI; B: Axial FLAIR), which is associated with minimal peripheral edema, mild restricted diffusion (C: Diffusion-weighted image), and avid contrast enhancement (D: Non-contrasted Axial T_1WI; E: Sagittal T_1WI after gadolinium administration). Leptomeningeal lesions were also observed (black arrow), (F: Axial post contrast).

The lesions of left frontal cortex, subcortex and local leptomeninges, forming an isolated gyriform, were shown with avid contrast enhancement in our case, which was considered to be rare in tumor metastasis into the CNS. Making a diagnosis of LM is difficult, which is relied on cerebrospinal fluid (CSF) analysis result, and clinical and radiographic findings. CSF cytology remains the gold standard for diagnosing LM, but it is invasive and associated with relatively low sensitivity[9]. Gadolinium-enhanced MRI of the brain is considered to be the best imaging technique for evaluating LM, and the images of LM appear as nodular, linear, arched, focal or diffuse intensification[2, 10]. The clinical manifestations of the patient in this case were non-specific, and cytological examination of CSF was not performed before operation. LM was also neglected during preoperative MRI diagnosis. Compared with T_1WI enhancement sequence, the contrast-enhanced T_2-weighted FLAIR sequence is more sensitive to detect leptomeningeal tumoral or infective-inflammatory involvement. A limitation of

this study was that other smaller areas of metastasis on the leptomeningeal surface may be ignored because contrast-enhanced T_2-weighted FLAIR was not taken. LM was eventually discovered during the surgery. CSF cytology examination also showed malignant tumor cells 2 months later. In fact, preoperative T_1WI enhancement in the present case had significantly revealed LM (Figure 2E).

Similar to the pathophysiology of brain metastases, LM was likely to be a multistep biological process[11]. The spread of cancer cells to leptomeninges might occur *via* multiple routes, including direct metastatic brain tumors infiltration, hematogenous dissemination of tumors, or *via* endoneurial/perineural and perivascular pathways [12]. The imaging and intraoperative findings of this case confirmed the seeding of tumors into the brain parenchyma and leptomeninges. Therefore, we speculated that the isolated gyriform lesions were likely metastatic brain parenchymal tumors with secondary leptomeningeal infiltration or a coexistence of brain metastasis with LM.

Moreover, the patient's MR imaging showed only mild white matter edema below the lesions, which was different from the extensive edema surrounding the typical metastatic tumors. The extracellular space of white matter was wider than that of the gray matter, so white matter was prone to edema. It was speculated that the mild peritumoral edema was related to tumors mainly located in the cortex.

The prognosis of non-small cell lung carcinoma with LM remained poor, and the median overall survival was only 3 mo [5]. Systemic chemotherapy is the preferred treatment choice for lung cancer patients with LM[13]. In this case, the patient had brain and leptomeningeal metastases, and underwent surgical resection without postoperative adjuvant chemotherapy. His condition worsened after surgery and died due to brain failure 2 mo after the diagnosis of CNS metastasis.

Intracranial focal gyriform lesions should be distinguished from cerebral infarction in elderly patients. In subacute infarction, cortical edema and necrosis may lead to enhanced gyral lesions, and may even lead to leptomeningeal enhancement lesions due to meningeal inflammation and early fibrosis[14]. But the enhanced lesions of subacute cerebral infarction demonstrated no obvious mass effect, and the cerebral parenchyma around the enhanced lesions also showed varying degrees of ischemia. However, the mass effect of intracranial enhancement lesions in the present case was obvious, and no adjacent brain parenchyma was involved. Moreover, the clinical manifestations of this patient included only nausea and vomiting, and no symptoms of stroke.

Besides, the diagnosis of this case should be differentiated from high-grade gliomas on imaging. High-grade gliomas tend to occur in the subcortical white matter, and large tumors can cause white matter necrosis, showing circular enhancement images. Furthermore, metastatic peritumoral edema is purely vasogenic, and no infiltrating tumor cells are present outside the perivascular space, which leads to hypoperfusion, with relatively normal magnetic resonance spectrum (MRS) in the peritumoral edema area. The peritumoral edema of high grade gliomas, on the other hand, is a mixture of vasogenic edema, infiltrating neoplastic cells and feeding blood vessels, which is expected to have an increased blood perfusion and higher Cho/NAA and Cho/Cr ratios on MRS, compared to solitary brain metastases[15,16]. Therefore, perfusion-weighted imaging and MRS of peritumoral edema could assist in differential diagnosis of high-grade gliomas versus brain metastases, but the patient didn't receive these tests.

In addition, this case should also be differentiated from cases of leptomeningeal involvement diseases, such as primary central nervous system vasculitis (PCNSV) and tuberculous meningitis (TBM). Unlike the isolated cortical mass in this case, the common MRI features of PCNSV are multiple bilateral supratentorial lesions, involving the gray and white matter, predominantly in the subcortex, deep white matter and corpus callosum, accompanied with focal cerebral infarction[17]. Although PCNSV images could manifest as irregular linear enhancement on subcortical white matter and leptomeninges, there was no obvious mass effect. TBM tended to occur at basal areas, with multiple bilateral foci and obstructive hydrocephalus, which could be differentiated from CNS metastases.

CONCLUSION

A rare case of EGFR-mutated lung adenocarcinoma with cerebral parenchymal and leptomeningeal metastases characterized by isolated gyriform appearance was reported. We speculated that this unique appearance is likely to be due to the induction of secondary leptomeningeal invasion from parenchymal brain metastasis or

coexisted with LM. Therefore, when patients with a history of lung adenocarcinoma were dealt, radiologists should be aware of this uncommon imaging presentation of CNS metastases and carefully observe for the existence of leptomeningeal lesions on T_1 enhancement to avoid missed diagnosis.

REFERENCES

1 **Barnholtz-Sloan JS**, Sloan AE, Davis FG, Vigneau FD, Lai P, Sawaya RE. Incidence proportions of brain metastases in patients diagnosed (1973 to 2001) in the Metropolitan Detroit Cancer Surveillance System. *J Clin Oncol* 2004; **22**: 2865-2872 [PMID: 15254054 DOI: 10.1200/JCO.2004.12.149]

2 **Chamberlain M**, Junck L, Brandsma D, Soffietti R, Rudà R, Raizer J, Boogerd W, Taillibert S, Groves MD, Le Rhun E, Walker J, van den Bent M, Wen PY, Jaeckle KA. Leptomeningeal metastases: a RANO proposal for response criteria. *Neuro Oncol* 2017; **19**: 484-492 [PMID: 28039364 DOI: 10.1093/neuonc/now183]

3 **Ostrom QT**, Wright CH, Barnholtz-Sloan JS. Brain metastases: epidemiology. *Handb Clin Neurol* 2018; **149**: 27-42 [PMID: 29307358 DOI: 10.1016/B978-0-12-811161-1.00002-5]

4 **Remon J**, Le Rhun E, Besse B. Leptomeningeal carcinomatosis in non-small cell lung cancer patients: A continuing challenge in the personalized treatment era. *Cancer Treat Rev* 2017; **53**: 128-137 [PMID: 28110254 DOI: 10.1016/j.ctrv.2016.12.006]

5 **Li YS**, Jiang BY, Yang JJ, Tu HY, Zhou Q, Guo WB, Yan HH, Wu YL. Leptomeningeal Metastases in Patients with NSCLC with EGFR Mutations. *J Thorac Oncol* 2016; **11**: 1962-1969 [PMID: 27539328 DOI: 10.1016/j.jtho.2016.06.029]

6 **Li L**, Luo S, Lin H, Yang H, Chen H, Liao Z, Lin W, Zheng W, Xie X. Correlation between EGFR mutation status and the incidence of brain metastases in patients with non-small cell lung cancer. *J Thorac Dis* 2017; **9**: 2510-2520 [PMID: 28932557 DOI: 10.21037/jtd.2017.07.57]

7 **Essenmacher AC**, Watal P, Bathla G, Bruch LA, Moritani T, Capizzano AA. Brain metastases from adenocarcinoma of the lung with truly cystic magnetic resonance imaging appearance. *Clin Imaging* 2018; **52**: 203-207 [PMID: 30125846 DOI: 10.1016/j.clinimag.2018.07.023]

8 **Sakatani T**, Kage H, Takayanagi S, Watanabe K, Hiraishi Y, Shinozaki-Ushiku A, Tanaka S, Ushiku T, Saito N, Nagase T. Brain Metastasis Mimicking Brain Abscess in ALK-Positive Non-Small-Cell Lung Cancer. *Case Rep Oncol Med* 2019; **2019**: 9141870 [PMID: 31316849 DOI: 10.1155/2019/9141870]

9 **Gil B**, Hwang EJ, Lee S, Jang J, Choi HS, Jung SL, Ahn KJ, Kim BS. Detection of Leptomeningeal Metastasis by Contrast-Enhanced 3D T1-SPACE: Comparison with 2D FLAIR and Contrast-Enhanced 2D T1-Weighted Images. *PLoS One* 2016; **11**: e0163081 [PMID: 27695096 DOI: 10.1371/journal.pone.0163081]

10 **Yang G**, Pan Z, Ma N, Qu L, Yuan T, Pang X, Yang X, Dong L, Liu S. Leptomeningeal metastasis of pulmonary large-cell neuroendocrine carcinoma: A case report and review of the literature. *Oncol Lett* 2017; **14**: 4282-4286 [PMID: 28943940 DOI: 10.3892/ol.2017.6676]

11 **Fidler IJ**, Yano S, Zhang RD, Fujimaki T, Bucana CD. The seed and soil hypothesis: vascularisation and brain metastases. *Lancet Oncol* 2002; **3**: 53-57 [PMID: 11905606 DOI: 10.1016/s1470-2045(01)00622-2]

12 **Chang EL**, Lo S. Diagnosis and management of central nervous system metastases from breast cancer. *Oncologist* 2003; **8**: 398-410 [PMID: 14530493 DOI: 10.1634/theoncologist.8-5-398]

13 **Park JH**, Kim YJ, Lee JO, Lee KW, Kim JH, Bang SM, Chung JH, Kim JS, Lee JS. Clinical outcomes of leptomeningeal metastasis in patients with non-small cell lung cancer in the modern chemotherapy era. *Lung Cancer* 2012; **76**: 387-392 [PMID: 22186628 DOI: 10.1016/j.lungcan.2011.11.022]

14 **Castillo M**, Scatliff JH, Kwock L, Green JJ, Suzuki K, Chancellor K, Smith JK. Postmortem MR imaging of lobar cerebral infarction with pathologic and *in vivo* correlation. *Radiographics* 1996; **16**: 241-250 [PMID: 8966284 DOI: 10.1148/radiographics.16.2.8966284]

15 **Halshtok Neiman O**, Sadetzki S, Chetrit A, Raskin S, Yaniv G, Hoffmann C. Perfusion-weighted imaging of peritumoral edema can aid in the differential diagnosis of glioblastoma mulltiforme *vs* brain metastasis. *Isr Med Assoc J* 2013; **15**: 103-105 [PMID: 23516772 DOI: 10.1016/j.aprim.2012.12.010]

16 **Aslan K**, Gunbey HP, Tomak L, Incesu L. Multiparametric MRI in differentiating solitary brain metastasis from high-grade glioma: diagnostic value of the combined use of diffusion-weighted imaging, dynamic susceptibility contrast imaging, and magnetic resonance spectroscopy parameters. *Neurol Neurochir Pol* 2019; **53**: 227-237 [PMID: 31180131 DOI: 10.5603/PJNNS.a2019.0024]

17 **Wang LJ**, Kong DZ, Guo ZN, Zhang FL, Zhou HW, Yang Y. Study on the Clinical, Imaging, and Pathological Characteristics of 18 Cases with Primary Central Nervous System Vasculitis. *J Stroke Cerebrovasc Dis* 2019; **28**: 920-928 [PMID: 30635219 DOI: 10.1016/j.jstrokecerebrovasdis.2018.12.007]

World Journal of Clinical Cases

Submit a Manuscript: https://www.f6publishing.com

World J Clin Cases 2022 February 16; 10(5): 1729-1737

DOI: 10.12998/wjcc.v10.i5.1729

ISSN 2307-8960 (online)

CASE REPORT

Diffuse invasive signet ring cell carcinoma in total colorectum caused by ulcerative colitis: A case report and review of literature

Zhi Zhang, Peng-Fei Yu, Guo-Li Gu, Yu-Hui Zhang, Yu-Ming Wang, Zhi-Wei Dong, Hai-Rui Yang

ORCID number: Zhi Zhang 0000-0001-5870-1940; Peng-Fei Yu 0000-0002-0528-1839; Guo-Li Gu 0000-0002-9998-047X; Yu-Hui Zhang 0000-0001-7343-1555; Yu-Ming Wang 0000-0001-5108-1494; Zhi-Wei Dong 0000-0001-7009-9331; Hai-Rui Yang 0000-0003-2768-8493.

Author contributions: Gu GL, Zhang Z and Yu PF contributed equally to this study; Gu GL designed the research; Zhang Z, Yu PF, Wang YM, Zhang YH, Dong ZW and Yang HR collected and analyzed the clinical data; Gu GL and Zhang Z wrote the manuscript; Gu GL revised the manuscript; all authors issued final approval for the version to be submitted.

Informed consent statement: The study participants and their legal guardian provided informed written consent prior to study enrollment.

Conflict-of-interest statement: We state that there is no financial or other relationship that might be perceived as leading to a conflict of interest.

CARE Checklist (2016) statement: The authors have read the CARE Checklist (2016), and the manuscript was prepared and revised according to the CARE Checklist (2016).

Zhi Zhang, Peng-Fei Yu, Guo-Li Gu, Yu-Hui Zhang, Zhi-Wei Dong, Hai-Rui Yang, Department of General Surgery, Air Force Medical Center, Chinese People's Liberation Army, Beijing 100142, China

Yu-Hui Zhang, Graduate School, Hebei North University, Zhangjiakou 075000, Hebei Province, China

Yu-Ming Wang, Health Team, 93656 Troop of Chinese People's Liberation Army, Beijing 101113, China

Corresponding author: Guo-Li Gu, FRCS (Gen Surg), Chief Doctor, Department of General Surgery, Air Force Medical Center, Chinese People's Liberation Army, No. 30 Fucheng Road, Haidian District, Beijing 100142, China. kzggl@163.com

Abstract

BACKGROUND

Diffuse invasive signet ring cell carcinoma of the colorectum is extremely rare clinically. This type of colorectal cancer has certain clinical, pathological and biological characteristics that are different from ordinary colorectal cancer.

CASE SUMMARY

A 31-year-old young woman was admitted to the hospital for nearly 1 wk due to recurrent symptoms of mucopurulent bloody stools and abdominal distension. Preoperative colonoscopy showed a ring-shaped intestinal wall mass 10 cm from the rectum to the anus. Three pieces of tumor tissue were removed for examination. The pathological results showed rectal mucinous adenocarcinoma. The patient underwent laparoscopic exploration under general anesthesia, and then laparoscopic total colorectal resection, ileal pouch–anal anastomosis and ileostomy were performed. The patient was switched to a FOLFOX + cetuximab regimen. After the fifth cycle, the patient was unable to tolerate further treatment due to tumor progression and multiple organ dysfunction, and died at the end of May 2020. Overall survival was 7 mo.

CONCLUSION

Carcinogenesis of ulcerative colitis is different from sporadic colon cancer, and the overall prognosis is extremely poor.

Key Words: Ulcerative colitis; Colorectal cancer; Signet ring cell carcinoma; Case report

Supported by Beijing Capital Medical Development Research Fund, No. Shoufa2020-2-5122.

Country/Territory of origin: China

Specialty type: Surgery

Provenance and peer review: Unsolicited article; Externally peer reviewed.

Peer-review model: Single blind

Peer-review report's scientific quality classification
Grade A (Excellent): 0
Grade B (Very good): B
Grade C (Good): C
Grade D (Fair): 0
Grade E (Poor): 0

Received: October 15, 2021
Peer-review started: October 15, 2021
First decision: December 1, 2021
Revised: December 5, 2021
Accepted: December 28, 2021
Article in press: December 28, 2021
Published online: February 16, 2022

P-Reviewer: Brochard C, Habeeb TAAM
S-Editor: Wang JL
L-Editor: Kerr C
P-Editor: Wang JL

Core tip: Primary signet-ring cell carcinoma (SRCC) of the colorectum is extremely rare clinically. This type of colorectal cancer has certain clinical, pathological and biological characteristics that are different from ordinary colorectal cancer. We report a rare case of ulcerative colitis leading to diffuse infiltrating SRCC of the colorectum, and review the relevant literature studying the disease.

Citation: Zhang Z, Yu PF, Gu GL, Zhang YH, Wang YM, Dong ZW, Yang HR. Diffuse invasive signet ring cell carcinoma in total colorectum caused by ulcerative colitis: A case report and review of literature. *World J Clin Cases* 2022; 10(5): 1729-1737
URL: https://www.wjgnet.com/2307-8960/full/v10/i5/1729.htm
DOI: https://dx.doi.org/10.12998/wjcc.v10.i5.1729

INTRODUCTION

Ulcerative colitis (UC) is a chronic nonspecific disease that is immune mediated and has multiple causes[1]. The disease was previously thought to be prevalent in western countries, with a prevalence of about 79–268/10^5 per year[2]; however, the number of cases reported in China has gradually increased in recent years, and it has become a more common gastrointestinal disease. The inflammation of the disease occurs mostly in the colonic mucosa and submucosa, usually involving the rectum first, then spreading to the entire colon. Typical clinical manifestations of the disease include mucopurulent bloody stools, abdominal pain, and diarrhea. A retrospective analysis of a large sample of cases of UC in China in 2007 found that extraintestinal manifestations were rare, causing only 0.4% of cases of colon cancer[3], and about 15% of patients with UC required colectomy[4]. In this paper, we report a rare case of UC leading to diffuse infiltrating signet ring cell carcinoma (SRCC) of the colorectum, and review the relevant literature.

CASE PRESENTATION

Chief complaints

A 31-year-old young woman presented with bloody stools.

History of present illness

The patient was admitted to the hospital for nearly 1 wk due to recurrent symptoms of mucopurulent bloody stools and abdominal distension.

History of past illness

The patient presented to the local hospital 8 years ago with symptoms of mucopurulent bloody stools and abdominal distension. After colonoscopy, she was diagnosed with UC. After taking prednisone acetate tablets orally for > 1 mo and sulfasalazine enteric coated tablets orally for about 1 year according to the doctor's advice, the symptom of bloody stools was largely controlled, and no review or further treatment was performed.

Personal and family history

The patient had no specific history of genetic diseases.

Physical examination

The whole abdomen had mild tenderness and no rebound pain. Digital rectal examination: No obvious mass was palpable on the fingertips, and the fingertips were stained with blood.

Laboratory examinations

Tumor markers: carcinoembryonic antigen: 16.03 ng/mL↑, cancer antigen 72-4: 17.94

U/mL↑. The patient underwent genetic testing before surgery (gene capture hybridization combined with high-throughput sequencing technology). Reference genome: GRCH37/hg19. The number of target genes exceeded 20000. The results are shown in Tables 1 and 2. A test found that the patient's tumor mutational burden (TMB) was 26.2/Mb. A high TMB type that suggested that the patient was more likely to benefit from PD-1 antibody monotherapy.

Imaging examinations

Preoperative colonoscopy: A ring-shaped intestinal wall mass was seen 10 cm from the rectum to the anus (Figure 1). Three pieces of tumor tissue were removed for examination. The pathological results showed rectal mucinous adenocarcinoma.

Preoperative computed tomography (CT): There were no obvious abnormalities in the scan of the chest and upper and lower abdomen. The enhanced CT scan of the pelvis showed that the rectal wall thickened uniformly in stages, visibly strengthened mucosal layer, blurred fat spaces around the intestines, and a small amount of effusion (Figure 2).

FINAL DIAGNOSIS

Rectal cancer caused by UC.

TREATMENT

After discussion by the multidisciplinary team for gastrointestinal tumors in our hospital, the patient underwent laparoscopic exploration under general anesthesia on December 2, 2019. During the operation, there was inflammatory exudative ascites in the abdominal and pelvic cavity, obvious inflammatory hyperplasia and edema throughout the entire sigmoid colon and rectum, cancerous umbilical changes at the peritoneal reflection in the middle of the rectum, and obvious dilation and edema of part of the bowel. Scattered small patchy changes could be seen on the surface of the mesentery (Figure 3). Tissue was taken from the peritoneal reflex and sent for pathological examination, which showed SRCC. Laparoscopic total colorectal resection, ileal pouch–anal anastomosis (IPAA) and ileostomy were performed.

Postoperative pathological examination: The rectum and entire colon showed diffuse invasive SRCC. Rectal tumors invaded the submesangial adipose tissue, and colon tumors were confined to the mucosa and submucosa. Intravascular tumor thrombus and nerve invasion could be seen. The full thickness of the appendix showed SRCC, with visible metastasis to lymph nodes around the bowel (36/37) (Figure 4). The pathological stage was IVB ($T_4N_{2b}M_{1c}$).

The patient started XELOX chemotherapy on the day 23 after surgery (oxaliplatin: Intravenous infusion for 3 h, day 1; capecitabine: Oral, 2 times/d, days 1-14). The first cycle of chemotherapy ended on January 7, 2020. Follow-up treatment was carried out at the local hospital.

OUTCOME AND FOLLOW-UP

Due to the impact of the COVID-19, the time for patients to receive follow-up chemotherapy was delayed by about 6 wk. After the end of the third cycle of chemotherapy, the patient was examined by imaging, the effects were evaluated as progressive disease, and the patient was switched to a FOLFOX + cetuximab regimen. After the fifth cycle, the patient was unable to tolerate further treatment due to tumor progression and multiple organ dysfunction, and died at the end of May 2020. Overall survival was 7 mo.

DISCUSSION

SRCC is a rare histological subtype of adenocarcinoma[5] that contains abundant intracytoplasmic mucin that displaces the nuclei to the periphery, thereby giving the characteristic appearance of an SRC[6]. Primary SRCC of the colon is extremely rare

Table 1 Mutations of gene detection results

Mutant gene	Abundance (%)	Exon	cDNA	Protein	Type
MTOR	0.61	47	c.6617A>G	p.N2206S	Non-synonymous
HRAS	0.85	2	c.81T>C	p.H27H	Synonymous
SLCO1B1	0.79	6	c.597C>T	p.F199F	Synonymous
AKT1	0.57	3	c.103T>C	p.F35L	Non-synonymous
TP53	0.5	8	c.840A>G	p.R280R	Synonymous
STK11	0.51	4	c.524A>T	p.K175M	Non-synonymous
	0.51	4	c.530T>C	p.I177T	Non-synonymous
XRCC1	0.66	10	c.1196A>G	p.Q399R	Non-synonymous
VHL	13.95	2	c.T355C	p.F119L	Non-synonymous
XRCC1	10.34	6	c.C580T	p.R194W	Non-synonymous

Table 2 Mutations of gene detection results

Gene	Mutation detection results
KRAS	Wild
NRAS	Wild
BRAF	Wild
NTRK	Not detected
BAT25	Not detected
BAT26	Not detected
NR21	Not detected
NR24	Not detected
NR27	Not detected

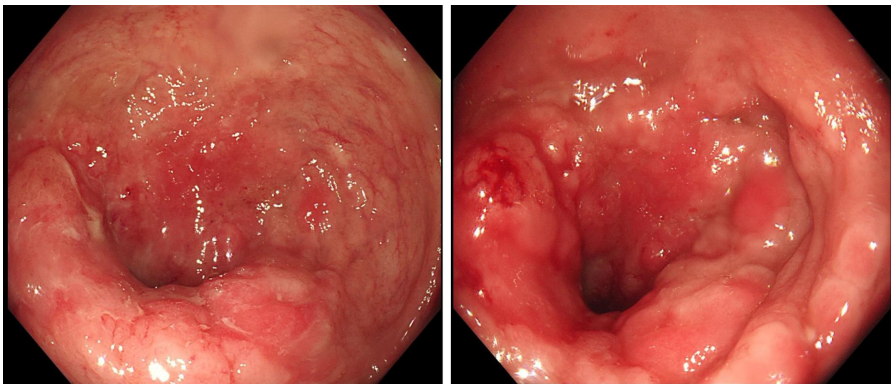

Figure 1 Preoperative colonoscopy. The surface showed nodular or cauliflower-like changes; the rectal mucosa was congested and showed edema; the surface showed longitudinal changes, with many scattered small ulcers and a little mucus-like white coating on the surface or a small amount of bleeding. The intestinal cavity was so narrow that the endoscope was unable to pass.

[7]. A study in the 20th century[8] found that only 11 cases of primary SRCC of the colon were found out of 12000 cases of primary colon cancer, with an incidence rate < 1/1000 cases of common colorectal adenocarcinoma. In about 80% of cases[9], the lesions are seen in the left colon at the distal end of the splenic flexure. This rare colorectal cancer has certain clinical, pathological and biological characteristics that are different from those of ordinary colorectal cancer, and which can be recognized as a stage-independent prognostic factor for adverse outcomes in colorectal cancer[10].

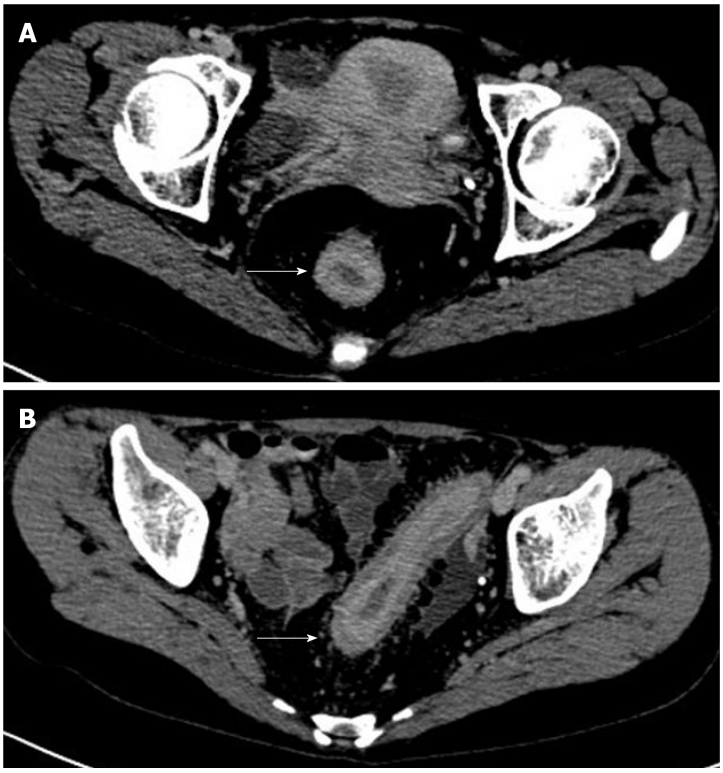

Figure 2 Preoperative computed tomography examination. A: The rectal wall thickened uniformly in stages, and the intestinal cavity was obviously narrowed; B: The rectal mucosal layer was obviously strengthened (the area indicated by the white arrow, 2019/11/28).

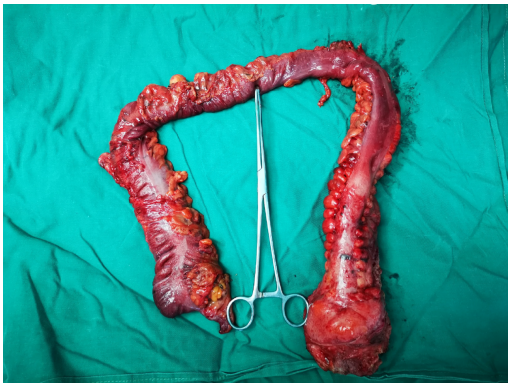

Figure 3 Gross specimen after surgery. The excised intestine had a length of 67 cm and a diameter of 3.5-7.5 cm. The intestine was cut along the opposite side of the mesentery. There were multiple congestions with superficial ulcers on the mucosal surface of the intestinal canal, with a segmental distribution. The wall of the tube 1-16 cm from the rectal stump was diffusely thickened and stiff, with a wall thickness of about 1.2 cm, and the mucosae were polypoid and fused with each other.

Following Laufman and Saphir[11] who first reported SRCC that occurred in the colon in 1951, new cases have been continuously reported[12-16]. Most cases are basically similar in general type, consisting of invasive tumors involving the entire thickness of the colon or rectal wall, leading to obvious thickening and induration. The lesions generally infiltrate the entire cecal wall and involve the proximal part of the appendix. Due to the infiltrative growth and highly aggressive nature of the tumor, most patients are found at an advanced stage, and the overall prognosis is extremely poor[13]. The difference between this patient and previous cases is that she had a clear history of UC, protracted course of disease and irregular follow-up treatment, providing a suitable environment for the later occurrence and development of tumors. Pontes *et al* [17] also reported a similar case to the present one: That patient had a 9-year history of UC, and although undergoing close endoscopic examination and treatment, he was eventually diagnosed with cancer. The pathological examination of the excised specimen showed SRCC of the sigmoid colon. Current research suggests that the

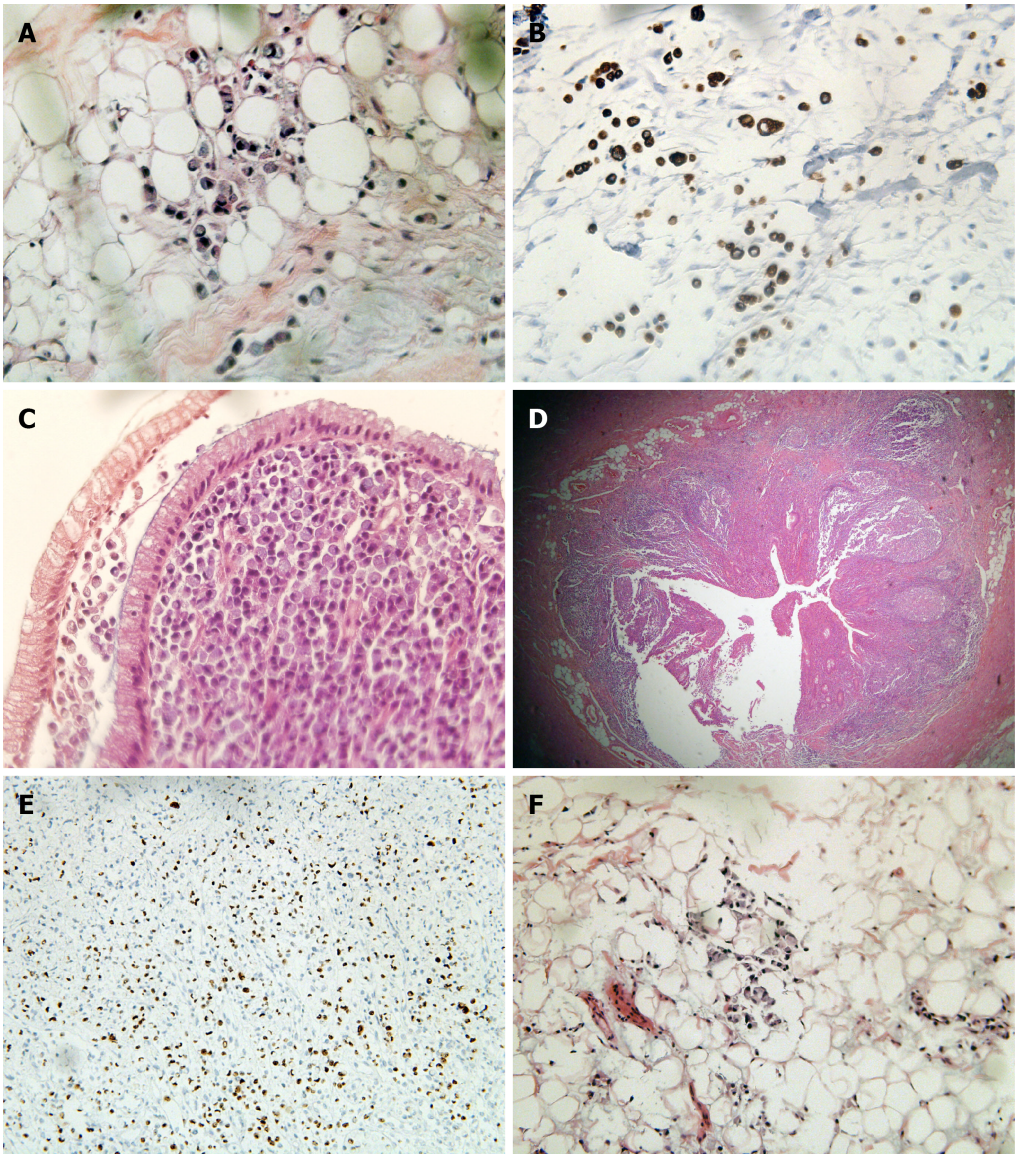

Figure 4 Postoperative pathological section. A and B: Tumor cells infiltrated the tissue stroma. They were rich in cytoplasm and full of mucus, and the nucleus was squeezed on the side of the cytoplasm, resembling a signet ring (hematoxylin and eosin, 10 ×); C: Tumor cells invaded the colonic mucosa and submucosa, and the polarity of the glandular epithelial cells was still normal; D: Tumor cells invaded the entire thickness of the appendix; E: Ki-67 > 90% in the hotspot area; F: The tissue stroma of the upper rectum near the peritoneum reflex was filled with tumor cells, so an intestinal origin was considered in combination with morphology.

occurrence of carcinoma in UC is positively correlated with the duration, degree of inflammation and extent of involvement of the patient[18]; and its occurrence and development experience the process of inflammation-low-grade intraepithelial neoplasia to high-grade intraepithelial neoplasia-carcinogenesis[19], which is different from the mode of gene mutation adenoma canceration of sporadic colorectal cancer [20]. In the same way, the mismatch repair proteins (MLH1, MSH2, MSH6 and PMS2) in this patient were all positive and microsatellite stable, and no mutations closely related to colorectal cancer were detected by genetic testing, yet advanced bowel cancer was detected at such a young age. In addition to the rarity of the case itself, it was more related to the history of UC.

As mentioned earlier, UC is a major type of inflammatory bowel disease (IBD). In the past two decades, the overall incidence of UC in China has been increasing year by year[3], but a consensus has not yet been reached on the exact pathogenesis. It is now believed that a combination of genetic, environmental, intestinal flora and host immune system factors contribute to the development of the disease[21-24]. Studies have shown[25,26] that 8%-14% of patients with UC have a family history of IBD, and the risk of first-degree relatives suffering from the disease is four times higher than that of the general population. To date, genome-wide association studies have confirmed the presence of nearly 200 disease risk genes for IBD; most of which can

cause both UC and Crohn's disease[27,28]. At present, research on IBD susceptibility genes is mainly focused on Crohn's disease, and the internal molecular mechanism of the pathogenesis of UC has not been fully elucidated[29]. Compared with Crohn's disease, UC has a weaker correlation with disease inheritance. Mantovani found that combination of CXC motif chemokine ligand (CXCL) 1 and CXC motif chemokine receptor (CXCR) 2 participates in the malignant behavior of solid and hematological tumors, and these two ligands indirectly act on tumor angiogenesis by regulating the transport of leukocytes that produce angiogenic factors and a variety of inflammatory cytokines[30]. The CXCL1/CXCR2 signaling pathway can regulate inflammation, promote tumor cell proliferation, invasion and transvascular metastasis, and play an important role in the progression of inflammation[31]. In animal experiments, Thaker *et al*[32] found that IDO1 indoleamine 2,3 dioxygenase (IDO)-1 metabolites activate β-catenin signaling to promote the proliferation of mouse cancer cells and induce colitis-related tumors in mice, indicating that IDO1 may play an important role in the progression of colon cancer caused by UC. In addition, the lack of cell regulatory factors, especially anti-inflammatory factors, plays an increasingly important role in the pathogenesis of UC[33-35]. In a study of nearly 2000 subjects, Franke tested > 400000 single nucleotide polymorphisms through genome-wide association and found that interleukin-10 dysfunction is the core cause of UC[36]. With the gradual deepening of research, new susceptibility genes are constantly being discovered, but genetic studies can only explain 7.5% of the disease differences, and the correlation between UC genotype and clinical phenotype is not clear[28,37], indicating that the disease has obvious genetic heterogeneity and a complex genetic background.

CONCLUSION

Primary SRCC of the colorectum is extremely rare clinically. This type of colorectal cancer has certain clinical, pathological and biological characteristics that are different from ordinary colorectal cancer.

REFERENCES

1 **Kobayashi T**, Siegmund B, Le Berre C, Wei SC, Ferrante M, Shen B, Bernstein CN, Danese S, Peyrin-Biroulet L, Hibi T. Ulcerative colitis. *Nat Rev Dis Primers* 2020; **6**: 74 [PMID: 32913180 DOI: 10.1038/s41572-020-0205-x]

2 **Farrokhyar F**, Swarbrick ET, Irvine EJ. A critical review of epidemiological studies in inflammatory bowel disease. *Scand J Gastroenterol* 2001; **36**: 2-15 [PMID: 11218235 DOI: 10.1080/00365520150218002]

3 **Wang Y**, Ouyang Q; APDW 2004 Chinese IBD working group. Ulcerative colitis in China: retrospective analysis of 3100 hospitalized patients. *J Gastroenterol Hepatol* 2007; **22**: 1450-1455 [PMID: 17716349 DOI: 10.1111/j.1440-1746.2007.04873.x]

4 **Magro F**, Rodrigues A, Vieira AI, Portela F, Cremers I, Cotter J, Correia L, Duarte MA, Tavares ML, Lago P, Ministro P, Peixe P, Lopes S, Garcia EB. Review of the disease course among adult ulcerative colitis population-based longitudinal cohorts. *Inflamm Bowel Dis* 2012; **18**: 573-583 [PMID: 21793126 DOI: 10.1002/ibd.21815]

5 **Hugen N**, van de Velde CJH, de Wilt JHW, Nagtegaal ID. Metastatic pattern in colorectal cancer is strongly influenced by histological subtype. *Ann Oncol* 2014; **25**: 651-657 [PMID: 24504447 DOI: 10.1093/annonc/mdt591]

6 **Chew MH**, Yeo SA, Ng ZP, Lim KH, Koh PK, Ng KH, Eu KW. Critical analysis of mucin and signet ring cell as prognostic factors in an Asian population of 2,764 sporadic colorectal cancers. *Int J Colorectal Dis* 2010; **25**: 1221-1229 [PMID: 20686777 DOI: 10.1007/s00384-010-1033-3]

7 **Song W**, Wu SJ, He YL, Cai SR, Zhang CH, Zhang XH, Zhan WH. Clinicopathologic features and survival of patients with colorectal mucinous, signet-ring cell or non-mucinous adenocarcinoma: experience at an institution in southern China. *Chin Med J (Engl)* 2009; **122**: 1486-1491 [PMID: 19719934]

8 **Fahl JC**, Dockerty MB, Judd ES. Scirrhous carcinoma of the colon and rectum. *Surg Gynecol Obstet* 1960; **111**: 759-766 [PMID: 13697905]

9 **Amorn Y**, Knight WA Jr. Primary linitis plastica of the colon: report of two cases and review of the literature. *Cancer* 1978; **41**: 2420-2425 [PMID: 207410]

10 **Kang H**, O'Connell JB, Maggard MA, Sack J, Ko CY. A 10-year outcomes evaluation of mucinous and signet-ring cell carcinoma of the colon and rectum. *Dis Colon Rectum* 2005; **48**: 1161-1168 [PMID: 15868237 DOI: 10.1007/s10350-004-0932-1]

11 **Laufman H**, Saphir O. Primary linitis plastica type of carcinoma of the colon. *AMA Arch Surg* 1951; **62**: 79-91 [PMID: 14789350 DOI: 10.1001/archsurg.1951.01250030082009]

12 **Bonello JC**, Quan SH, Sternberg SS. Primary linitis plastica of the rectum. *Dis Colon Rectum* 1980; **23**: 337-42U [PMID: 6249557 DOI: 10.1007/bf02586841]

13 **Almagro UA**. Primary signet-ring carcinoma of the colon. *Cancer* 1983; **52**: 1453-1457 [PMID: 6311394 DOI: 10.1002/1097-0142(19831015)52:8<1453::aid-cncr2820520819>3.0.co;2-9]

14 **Desai SR**, Tata HR. Primary signet ring carcinoma of the large bowel--a case report. *Indian J Pathol Microbiol* 2004; **47**: 535-537 [PMID: 16295388]

15 **Bianchi G**, Terrinoni V, Lamazza A, Anselmi W, Abate O, Bellini N, Carbone G, Rengo M. [Signet ring cell adenocarcinoma of the colon (signet ring carcinoma): is it really a rare neoplasm? *G Chir* 1997; **18**: 283-285 [PMID: 9312256]

16 **Giacchero A**, Aste H, Baracchini P, Conio M, Fulcheri E, Lapertosa G, Tanzi R. Primary signet-ring carcinoma of the large bowel. Report of nine cases. *Cancer* 1985; **56**: 2723-2726 [PMID: 2996745 DOI: 10.1002/1097-0142(19851201)56:11<2723::aid-cncr2820561137>3.0.co;2-n]

17 **Pontes J**, Fernandes C, Panao E, Castro L, Vicente L, Neto M, Campos M, Pontes F. Synchronic signet ring carcinoma and adenocarcinoma complicating extensive and long-standing ulcerative colitis. *Hepatogastroenterology* 1999; **46**: 236-239 [PMID: 10228799]

18 **Eaden JA**, Abrams KR, Mayberry JF. The risk of colorectal cancer in ulcerative colitis: a meta-analysis. *Gut* 2001; **48**: 526-535 [PMID: 11247898 DOI: 10.1136/gut.48.4.526]

19 **Itzkowitz SH**, Harpaz N. Diagnosis and management of dysplasia in patients with inflammatory bowel diseases. *Gastroenterology* 2004; **126**: 1634-1648 [PMID: 15168373 DOI: 10.1053/j.gastro.2004.03.025]

20 **Vogelstein B**, Fearon ER, Hamilton SR, Kern SE, Preisinger AC, Leppert M, Nakamura Y, White R, Smits AM, Bos JL. Genetic alterations during colorectal-tumor development. *N Engl J Med* 1988; **319**: 525-532 [PMID: 2841597 DOI: 10.1056/NEJM198809013190901]

21 **Nishida A**, Inoue R, Inatomi O, Bamba S, Naito Y, Andoh A. Gut microbiota in the pathogenesis of inflammatory bowel disease. *Clin J Gastroenterol* 2018; **11**: 1-10 [PMID: 29285689 DOI: 10.1007/s12328-017-0813-5]

22 **Hold GL**, Smith M, Grange C, Watt ER, El-Omar EM, Mukhopadhya I. Role of the gut microbiota in inflammatory bowel disease pathogenesis: what have we learnt in the past 10 years? *World J Gastroenterol* 2014; **20**: 1192-1210 [PMID: 24574795 DOI: 10.3748/wjg.v20.i5.1192]

23 **Huang LJ**, Mao XT, Li YY, Liu DD, Fan KQ, Liu RB, Wu TT, Wang HL, Zhang Y, Yang B, Ye CQ, Zhong JY, Chai RJ, Cao Q, Jin J. Multiomics analyses reveal a critical role of selenium in controlling T cell differentiation in Crohn's disease. *Immunity* 2021; **54**: 1728-1744 [PMID: 34343498 DOI: 10.1016/j.immuni.2021.07.004]

24 **Pedersen J**, Coskun M, Soendergaard C, Salem M, Nielsen OH. Inflammatory pathways of importance for management of inflammatory bowel disease. *World J Gastroenterol* 2014; **20**: 64-77 [PMID: 24415859 DOI: 10.3748/wjg.v20.i1.64]

25 **Halme L**, Paavola-Sakki P, Turunen U, Lappalainen M, Farkkila M, Kontula K. Family and twin studies in inflammatory bowel disease. *World J Gastroenterol* 2006; **12**: 3668-3672 [PMID: 16773682 DOI: 10.3748/wjg.v12.i23.3668]

26 **Moller FT**, Andersen V, Wohlfahrt J, Jess T. Familial risk of inflammatory bowel disease: a population-based cohort study 1977-2011. *Am J Gastroenterol* 2015; **110**: 564-571 [PMID: 25803400 DOI: 10.1038/ajg.2015.50]

27 **Liu JZ**, van Sommeren S, Huang H, Ng SC, Alberts R, Takahashi A, Ripke S, Lee JC, Jostins L, Shah T, Abedian S, Cheon JH, Cho J, Dayani NE, Franke L, Fuyuno Y, Hart A, Juyal RC, Juyal G, Kim WH, Morris AP, Poustchi H, Newman WG, Midha V, Orchard TR, Vahedi H, Sood A, Sung JY, Malekzadeh R, Westra HJ, Yamazaki K, Yang SK; International Multiple Sclerosis Genetics Consortium; International IBD Genetics Consortium, Barrett JC, Alizadeh BZ, Parkes M, Bk T, Daly MJ, Kubo M, Anderson CA, Weersma RK. Association analyses identify 38 susceptibility loci for inflammatory bowel disease and highlight shared genetic risk across populations. *Nat Genet* 2015; **47**: 979-986 [PMID: 26192919 DOI: 10.1038/ng.3359]

28 **Jostins L**, Ripke S, Weersma RK, Duerr RH, McGovern DP, Hui KY, Lee JC, Schumm LP, Sharma Y, Anderson CA, Essers J, Mitrovic M, Ning K, Cleynen I, Theatre E, Spain SL, Raychaudhuri S, Goyette P, Wei Z, Abraham C, Achkar JP, Ahmad T, Amininejad L, Ananthakrishnan AN, Andersen V, Andrews JM, Baidoo L, Balschun T, Bampton PA, Bitton A, Boucher G, Brand S, Büning C, Cohain A, Cichon S, D'Amato M, De Jong D, Devaney KL, Dubinsky M, Edwards C, Ellinghaus D, Ferguson LR, Franchimont D, Fransen K, Gearry R, Georges M, Gieger C, Glas J, Haritunians T, Hart A, Hawkey C, Hedl M, Hu X, Karlsen TH, Kupcinskas L, Kugathasan S, Latiano A, Laukens D, Lawrance IC, Lees CW, Louis E, Mahy G, Mansfield J, Morgan AR, Mowat C, Newman W, Palmieri O, Ponsioen CY, Potocnik U, Prescott NJ, Regueiro M, Rotter JI, Russell RK, Sanderson JD, Sans M, Satsangi J, Schreiber S, Simms LA, Sventoraityte J, Targan SR, Taylor KD, Tremelling M, Verspaget HW, De Vos M, Wijmenga C, Wilson DC, Winkelmann J, Xavier RJ, Zeissig S, Zhang B, Zhang CK, Zhao H; International IBD Genetics Consortium (IIBDGC), Silverberg MS, Annese V, Hakonarson H, Brant SR, Radford-Smith G, Mathew CG, Rioux JD, Schadt EE, Daly MJ, Franke A, Parkes M, Vermeire S, Barrett JC, Cho JH. Host-microbe interactions have shaped the genetic architecture of inflammatory bowel disease. *Nature* 2012; **491**: 119-124 [PMID: 23128233 DOI: 10.1038/nature11582]

29 **Chen ZA**, Sun YF, Wang QX, Ma HH, Ma ZZ, Yang CJ. Integrated Analysis of Multiple Microarray Studies to Identify Novel Gene Signatures in Ulcerative Colitis. *Front Genet* 2021; **12**: 697514 [PMID: 34306038 DOI: 10.3389/fgene.2021.697514]

30 **Mantovani A**, Savino B, Locati M, Zammataro L, Allavena P, Bonecchi R. The chemokine system in cancer biology and therapy. *Cytokine Growth Factor Rev* 2010; **21**: 27-39 [PMID: 20004131 DOI: 10.1016/j.cytogfr.2009.11.007]

31 **Acharyya S**, Oskarsson T, Vanharanta S, Malladi S, Kim J, Morris PG, Manova-Todorova K, Leversha M, Hogg N, Seshan VE, Norton L, Brogi E, Massagué J. A CXCL1 paracrine network links cancer chemoresistance and metastasis. *Cell* 2012; **150**: 165-178 [PMID: 22770218 DOI: 10.1016/j.cell.2012.04.042]

32 **Thaker AI**, Rao MS, Bishnupuri KS, Kerr TA, Foster L, Marinshaw JM, Newberry RD, Stenson WF, Ciorba MA. IDO1 metabolites activate β-catenin signaling to promote cancer cell proliferation and colon tumorigenesis in mice. *Gastroenterology* 2013; **145**: 416-25 [PMID: 23669411 DOI: 10.1053/j.gastro.2013.05.002]

33 **Heller F**, Fuss IJ, Nieuwenhuis EE, Blumberg RS, Strober W. Oxazolone colitis, a Th2 colitis model resembling ulcerative colitis, is mediated by IL-13-producing NK-T cells. *Immunity* 2002; **17**: 629-638 [PMID: 12433369 DOI: 10.1016/s1074-7613(02)00453-3]

34 **Sugimoto K**, Ogawa A, Mizoguchi E, Shimomura Y, Andoh A, Bhan AK, Blumberg RS, Xavier RJ, Mizoguchi A. IL-22 ameliorates intestinal inflammation in a mouse model of ulcerative colitis. *J Clin Invest* 2008; **118**: 534-544 [PMID: 18172556 DOI: 10.1172/JCI33194]

35 **Chen Y**, Chen Y, Cao P, Su W, Zhan N, Dong W. Fusobacterium nucleatum facilitates ulcerative colitis through activating IL-17F signaling to NF-κB *via* the upregulation of CARD3 expression. *J Pathol* 2020; **250**: 170-182 [PMID: 31610014 DOI: 10.1002/path.5358]

36 **Franke A**, Balschun T, Karlsen TH, Sventoraityte J, Nikolaus S, Mayr G, Domingues FS, Albrecht M, Nothnagel M, Ellinghaus D, Sina C, Onnie CM, Weersma RK, Stokkers PC, Wijmenga C, Gazouli M, Strachan D, McArdle WL, Vermeire S, Rutgeerts P, Rosenstiel P, Krawczak M, Vatn MH; IBSEN study group, Mathew CG, Schreiber S. Sequence variants in IL10, ARPC2 and multiple other loci contribute to ulcerative colitis susceptibility. *Nat Genet* 2008; **40**: 1319-1323 [PMID: 18836448 DOI: 10.1038/ng.221]

37 **UK IBD Genetics Consortium**, Barrett JC, Lee JC, Lees CW, Prescott NJ, Anderson CA, Phillips A, Wesley E, Parnell K, Zhang H, Drummond H, Nimmo ER, Massey D, Blaszczyk K, Elliott T, Cotterill L, Dallal H, Lobo AJ, Mowat C, Sanderson JD, Jewell DP, Newman WG, Edwards C, Ahmad T, Mansfield JC, Satsangi J, Parkes M, Mathew CG; Wellcome Trust Case Control Consortium 2, Donnelly P, Peltonen L, Blackwell JM, Bramon E, Brown MA, Casas JP, Corvin A, Craddock N, Deloukas P, Duncanson A, Jankowski J, Markus HS, Mathew CG, McCarthy MI, Palmer CN, Plomin R, Rautanen A, Sawcer SJ, Samani N, Trembath RC, Viswanathan AC, Wood N, Spencer CC, Barrett JC, Bellenguez C, Davison D, Freeman C, Strange A, Donnelly P, Langford C, Hunt SE, Edkins S, Gwilliam R, Blackburn H, Bumpstead SJ, Dronov S, Gillman M, Gray E, Hammond N, Jayakumar A, McCann OT, Liddle J, Perez ML, Potter SC, Ravindrarajah R, Ricketts M, Waller M, Weston P, Widaa S, Whittaker P, Deloukas P, Peltonen L, Mathew CG, Blackwell JM, Brown MA, Corvin A, McCarthy MI, Spencer CC, Attwood AP, Stephens J, Sambrook J, Ouwehand WH, McArdle WL, Ring SM, Strachan DP. Genome-wide association study of ulcerative colitis identifies three new susceptibility loci, including the HNF4A region. *Nat Genet* 2009; **41**: 1330-1334 [PMID: 19915572 DOI: 10.1038/ng.483]

World Journal of Clinical Cases

Submit a Manuscript: https://www.f6publishing.com

World J Clin Cases 2022 February 16; 10(5): 1738-1746

DOI: 10.12998/wjcc.v10.i5.1738

ISSN 2307-8960 (online)

CASE REPORT

Neurothekeoma located in the hallux and axilla: Two case reports

Wan-Ying Huang, Yi-Qi Zhang, Xiang-Hong Yang

ORCID number: Wan-Ying Huang 0000000174399825; Yi-Qi Zhang 0000000312407062; Xiang-Hong Yang 0000-0001-9223-3677.

Author contributions: Huang WY and Yang XH designed the study; Huang WY analysed the pathology images and wrote the manuscript; Zhang YQ helped prepare the clinical information; all authors read and approved the final manuscript.

Informed consent statement: Written informed consent was obtained from the patients for the publication of this case report and accompanying images.

Conflict-of-interest statement: The authors have no conflicts of interest to report.

CARE Checklist (2016) statement: We have read the CARE Checklist (2016), and the manuscript was prepared and revised according to the CARE Checklist (2016).

Supported by the National Natural Science Foundation of China, No. 81773108.

Country/Territory of origin: China

Specialty type: Pathology

Provenance and peer review: Unsolicited article; Externally peer reviewed.

Peer-review model: Single blind

Wan-Ying Huang, Xiang-Hong Yang, Department of Pathology, Shengjing Hospital of China Medical University, Shenyang 110000, Liaoning Province, China

Yi-Qi Zhang, Department of Orthopedics, Shengjing Hospital, China Medical University, Shenyang 110000, Liaoning Province, China

Corresponding author: Xiang-Hong Yang, PhD, Professor, Department of Pathology, Shengjing Hospital of China Medical University, No. 36 Sanhao Street, Heping District, Shenyang 110004, Liaoning Province, China. yangxh@sj-hospital.org

Abstract

BACKGROUND

Neurothekeomas (NTKs) are rare benign soft tissue tumours that typically occur in the head, trunk, and upper limbs and are rare in other parts of the body.

CASE SUMMARY

Herein, we present two rare cases in which primary NTKs were located in the hallux and axilla. A 47-year-old woman complained of a verrucous bulge on the plantar side of the left hallux. The surface skin of the tumour was abraded due to poor wound healing. A 6-year-old boy complained of a gradually growing subcutaneous mass in the axilla. The tumours of both patients were completely resected, and the diagnosis of NTK was confirmed by histopathology. At the one-year follow-up, both patients had a good prognosis without local recurrence.

CONCLUSION

To date, NTKs located in the hallux and axilla have rarely been reported in the literature. We describe NTKs that occurred in unconventional areas and summarize the challenges in their diagnosis and differential diagnosis.

Key Words: Neurothekeoma; Hallux; Armpit; Histopathological examination; Immunohistochemical staining; Case report

Core Tip: In these patients, the lack of specificity of clinical symptoms and imaging examination findings as well as the unusual location of neurothekeomas increased the difficulty in diagnosis and treatment. Histopathological examination and immunohistochemical staining may help confirm the diagnosis, but there are still many challenges

Peer-review report's scientific quality classification
Grade A (Excellent): 0
Grade B (Very good): B, B
Grade C (Good): 0
Grade D (Fair): 0
Grade E (Poor): 0

Received: October 16, 2021
Peer-review started: October 16, 2021
First decision: November 17, 2021
Revised: November 29, 2021
Accepted: December 31, 2021
Article in press: December 31, 2021
Published online: February 16, 2022

P-Reviewer: Grawish ME, Vij M
S-Editor: Ma YJ
L-Editor: A
P-Editor: Ma YJ

in the identification of similar diseases.

Citation: Huang WY, Zhang YQ, Yang XH. Neurothekeoma located in the hallux and axilla: Two case reports. *World J Clin Cases* 2022; 10(5): 1738-1746
URL: https://www.wjgnet.com/2307-8960/full/v10/i5/1738.htm
DOI: https://dx.doi.org/10.12998/wjcc.v10.i5.1738

INTRODUCTION

Neurothekeomas (NTKs) are rare, benign, superficial soft tissue tumours that typically present as solitary nodules with a predilection for the head, neck, and upper limbs of females[1,2]. Due to the low prevalence and undefined clinical symptoms of NTKs, it is difficult to accurately distinguish them from other skin tumours. NTKs rarely occur in the lower limbs or axillae and have been reported only once in the areas of the toes and axillae[3,4]. In this report, we describe two different types of NTKs arising in the hallux of a 47-year-old female and the axilla of a 6-year-old boy. Both patients underwent surgical resection, and the final diagnosis was confirmed through histopathological examination.

CASE PRESENTATION

Chief complaints

Case 1: A 47-year-old woman complained of a painless, verrucous bulge on the plantar side of the left hallux for 3 years.

Case 2: A 6-year-old boy visited our hospital and complained of a gradually increasing subcutaneous mass in the axilla for 2 years.

History of present illness

Case 1: The verrucous mass appeared on the plantar side of the left hallux three years previously, and the surface skin of the tumour was abraded due to poor wound healing. Inflammatory granulation tissue formation was observed in the wound. The patient intermittently adhered to conservative treatment, but her condition was not relieved.

Case 2: The subcutaneous mass was found in the axilla two years previously, and the colour of the mass was the same as that of the normal skin. The mass was only 1 cm in diameter when it was first discovered but gradually grew to 2 cm within two years.

History of past illness

Case 1: The patient was diagnosed with tuberculous pleurisy 20 years previously and was cured, and she underwent uterine fibroid surgery 1 year previously.

Case 2: The patient did not complain of any prior specific symptoms.

Personal and family history

Cases 1 and 2: Both patients denied any history of smoking, drinking, or drug abuse. Underlying systemic disease and family genetic history were denied.

Physical examination

Case 1: The patient's general condition was stable with normal vital signs (body temperature 36.8 °C, blood pressure 140/80 mmHg, pulse 110 bpm). A red solid mass with a diameter of 0.8 cm was found on the plantar side of the left hallux with a tough texture, normal skin temperature, and good dorsal artery pulsation.

Case 2: The patient's general condition was stable with normal vital signs (body temperature 36.7 °C, blood pressure 95/65 mmHg, pulse 103 bpm). A subcutaneous mass with a diameter of 2 cm was observed in the left armpit with good mobility, normal surface skin colour and temperature, and mild palpable pain. The superficial

lymph nodes were not enlarged.

Laboratory examinations

Case 1: Laboratory tests revealed signs of inflammation in the urinary system, and the percentage of neutrophils (73.9%) in blood and white blood cell (99.6/μL) and bacterial (1014.5/μL) counts in urine were slightly elevated.

Case 2: No obvious abnormality was noted in the laboratory examination results.

Imaging examinations

Case 1: An ultrasound from the local hospital showed a solid nodule on the plantar side of the left hallux with abundant blood supply.

Case 2: An ultrasound from the local hospital showed a round, well-demarcated soft tissue mass in the left armpit with nosignificant alterations in the surrounding tissue.

Histopathological examination

Case 1: In general, the red, solid, verrucous mass was approximately 0.8 cm in diameter and had a tough texture (Figure 1A). Histopathological examination of the specimen showed that the tumour tissue was in the form of multiple small nodules or clusters. The nodules, which were composed of oval and spindle tumour cells, were abundant in some areas and sparse in other areas. In the cellular area, oval cells were relatively uniform in size with a rich and eosinophilic cytoplasm, a visible nucleolus, and a mild to moderate degree of mitotic activity. In the intermediate area, spindle cells were arranged in bundles and exhibited a benign morphology. Myxoid matrix could be observed in the nodules or interstitium (approximately 40%) (Figure 1B-D). Immunohistochemical examination revealed positive staining for CD10, CD99, transcription factor binding to IGHM enhancer-3 (TFE3) and CD163, indicating NTK (Figure 1E-H). Negative staining for S-100, cytokeratin (CK), epithelial membrane antigen, smooth muscle actin (SMA), desmin, Stat6, anaplastic lymphoma kinase (ALK), and neuron-specific enolase (NSE) can be helpful in differential diagnosis, as this profile distinguishes NTKs from other soft tissue tumours such as dermal nerve sheath myxomas (DNSMs), smooth muscle cell-derived tumours, solitary fibrous tumours, epithelioid fibrous histiocytomas (EFHs), and neuroblastomas (Figure 1I-N). CD34 staining suggested vascular hyperplasia, and the Ki-67 proliferation index was approximately 20% (Figure 1O and P).

Case 2: Histopathological examination of the specimen showed that the tumour tissue was composed of multiple small nodules, and the nodules were separated by hyalinized collagen fibres (Figure 2A). The nodules were composed mainly of uniformly sized eosinophilic oval cells, in which nucleoli and mitosis were observed. A small number of multinucleated giant cells infiltrated the nodules, and no myxoid matrix was observed in the interstitium (Figure 2B and C). Immunohistochemical examination revealed positive staining for CD10, CD68, TFE3, p63 and vimentin (Figure 2D-H) and negative staining for S-100, CK, SMA, glial fibrillary acidic protein (GFAP) and CD1a (Figure 2I-M). The Ki-67proliferation index was approximately 15% (Figure 2N).

FINAL DIAGNOSIS

Case 1

NTK, mixed subtype (left hallux).

Case 2

Cellular NTK (left axilla).

TREATMENT

Case 1

Surgical treatment was performed with local infiltration anaesthesia. The 0.8-cm tumour was located in the superficial layer of the flexor tendon and had an incomplete capsule. The tumour was completely resected and submitted for pathological

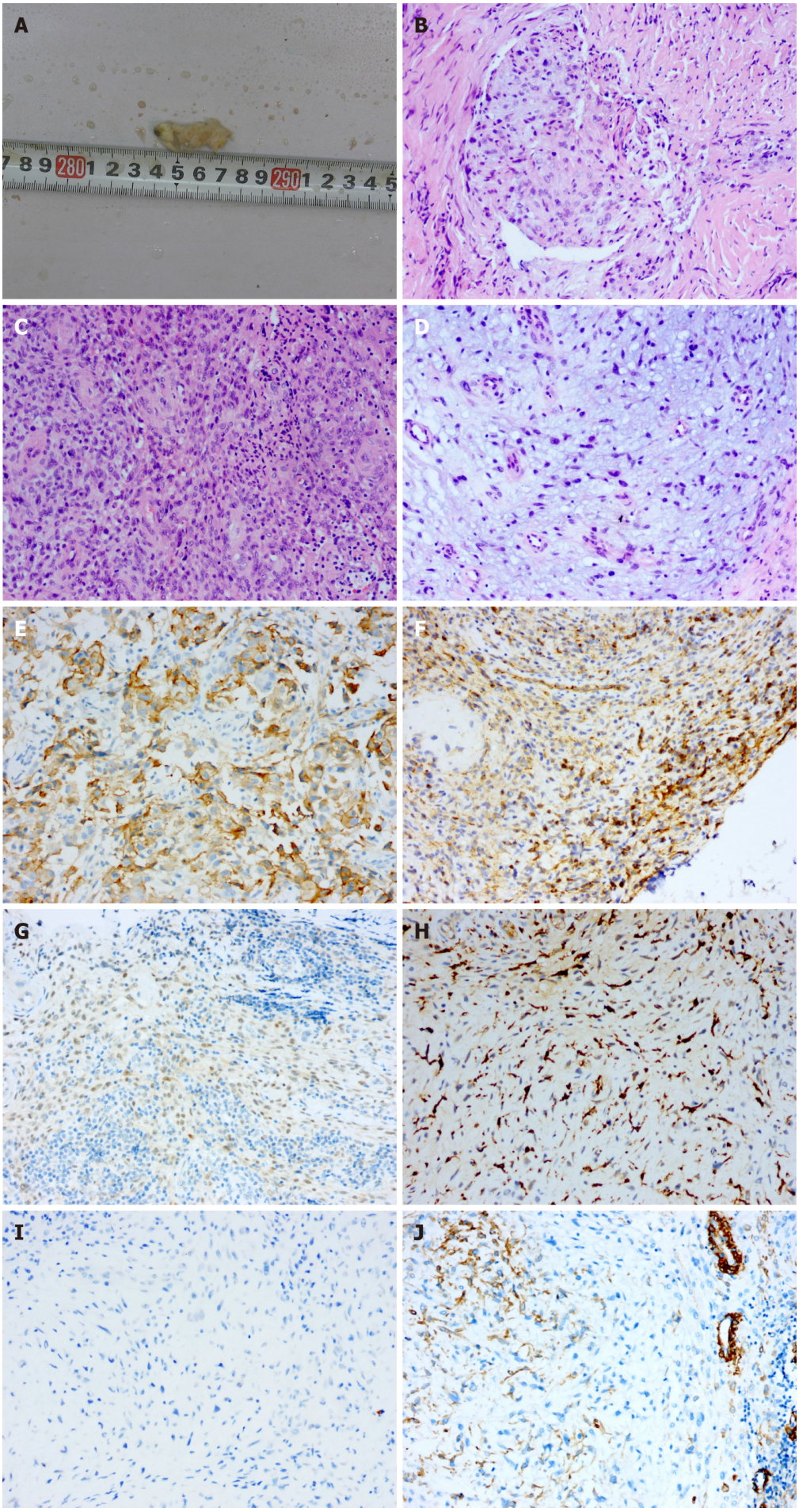
A
B
C
D
E
F
G
H
I
J

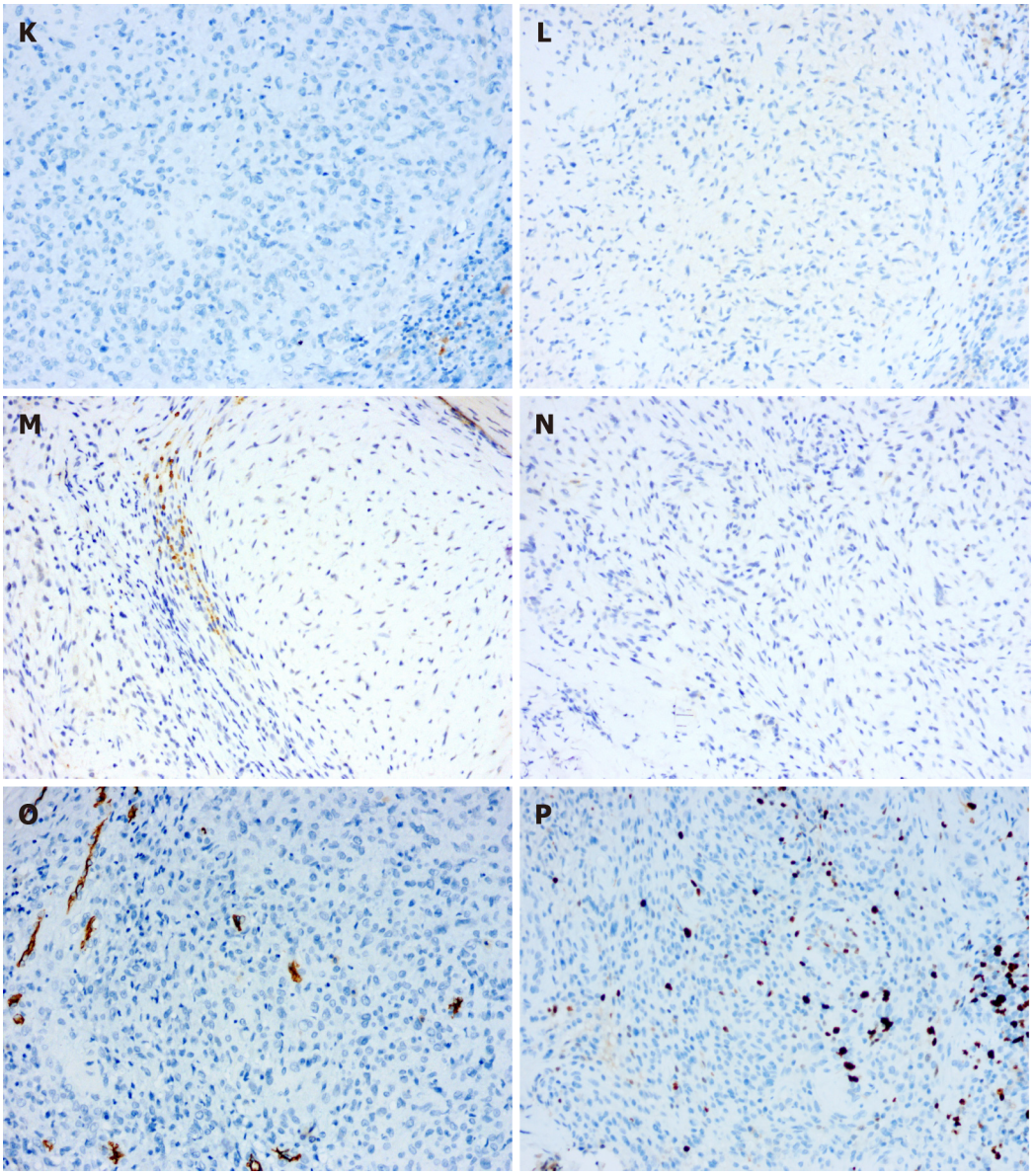

Figure 1 Macropathological and histological analyses of the tumour tissue in case 1. A: Macroscopic image of the verrucous bulge; B-D: Haematoxylin and eosin staining showing the tumour cells (× 200); E-H: Positive immunohistochemical staining for CD10, CD99, transcription factor binding to IGHM enhancer-3 and CD163 (× 200); I-N: Negative immunohistochemical staining for S-100, cytokeratin, EMA, smooth muscle actin, Desmin, Stat6, ALK and NSE (× 200); O and P: Immunohistochemical staining for CD34 and Ki-67 (× 200).

examination.

Case 2

Surgical treatment was performed with local infiltration anaesthesia. The solid, well-defined, 2-cm tumour was located in the subcutaneous soft tissue of the armpit and seemed to lack a defined capsule. After complete removal of the tumour and complete haemostasis, the incision was sutured.

OUTCOME AND FOLLOW-UP

At the 12-mo follow-up, both patients had maintained a favourable postoperative clinical evolution without local pain or motion limitation. The surgical incisions had healed well, and neither patient showed signs of recurrence or metastasis.

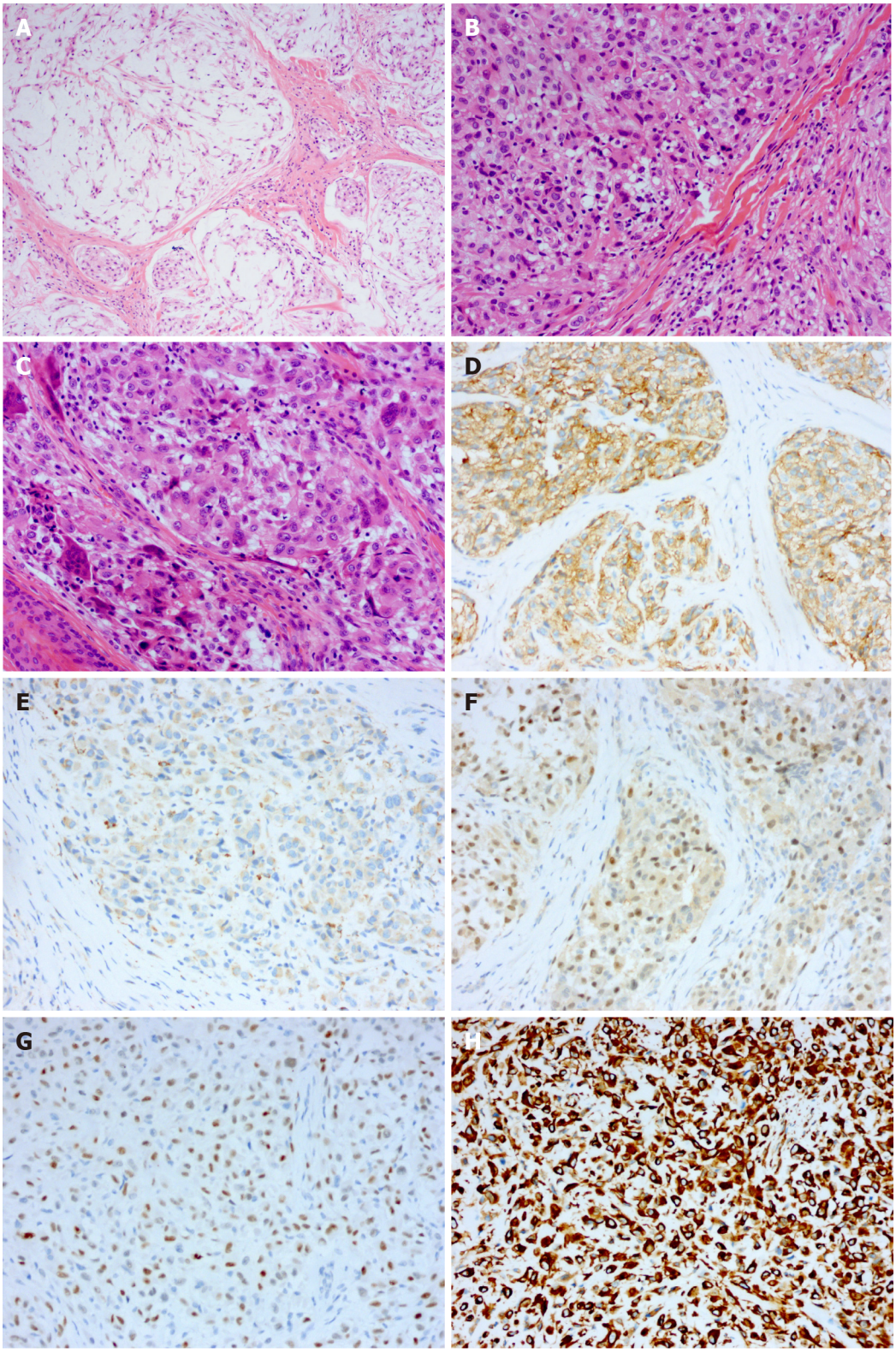
A
B
C
D
E
F
G
H

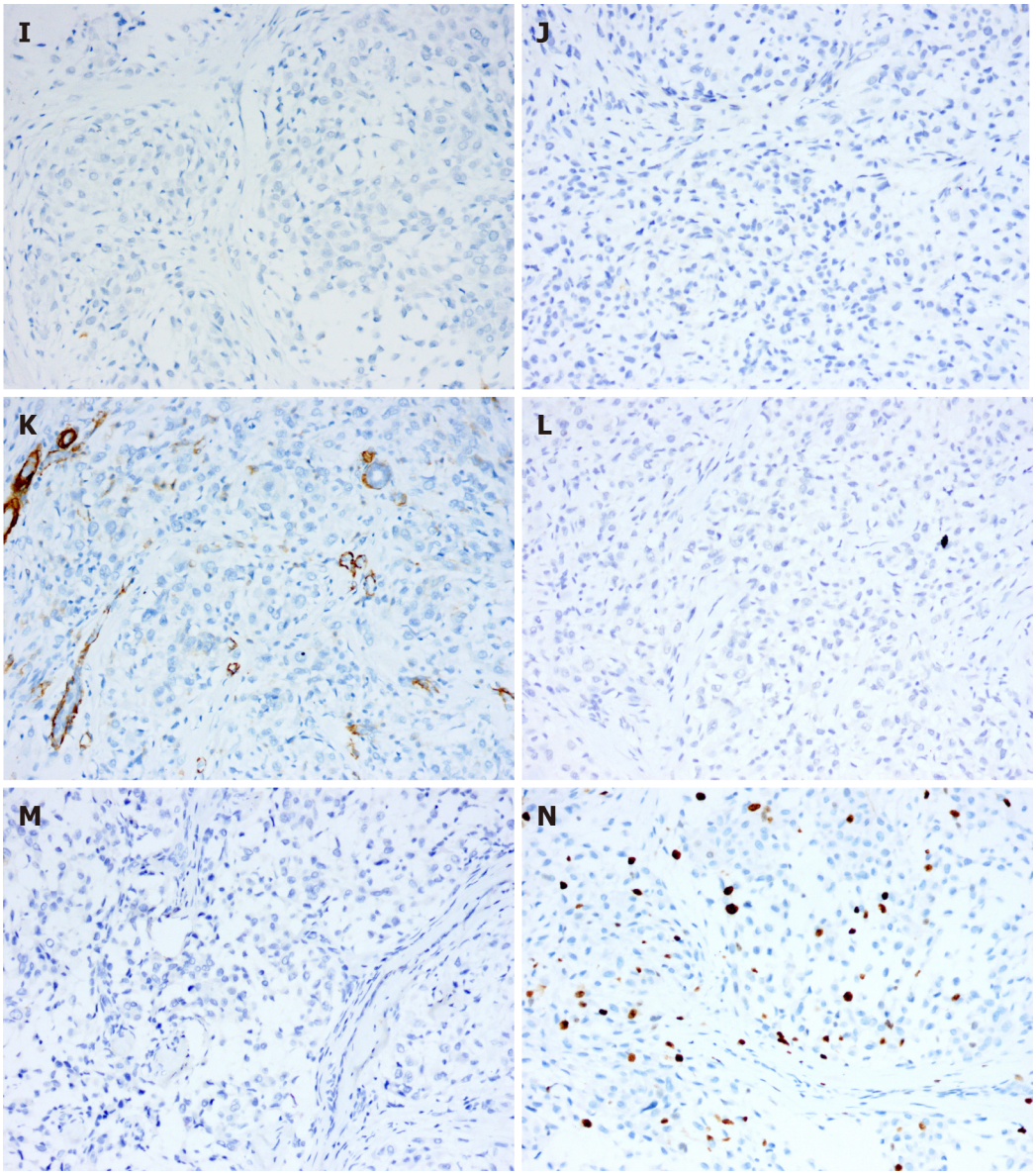

Figure 2 Histological analysis of the tumour tissue in case 2. A-C: Haematoxylin and eosin staining showing the tumour cells (× 200); D-H: Positive immunohistochemical staining for CD10, CD68, transcription factor binding to IGHM enhancer-3, p63 and vimentin (× 200); I-M: Negative immunohistochemical staining for S-100, cytokeratin, smooth muscle actin, glial fibrillary acidic protein and CD1a (× 200); N: Immunohistochemical staining for Ki-67 (× 200).

DISCUSSION

NTKs are rare, benign soft tissue tumours that were first described by Gallager and Helwig in 1980[5]. NTKs were initially considered to be neurogenic tumours originating from Schwann cells, and NTKs were diagnosed and reported for many years as one of the subtypes of dermal nerve sheath myxomas[6]. Recently, studies have shown that, unlike DNSMs, NTKs do not express the S-100 protein[7]. Further analysis of gene expression profiles shows that DNSMs are similar to schwannomas, while NTKs show evidence of myofibroblastic differentiation and possible relation to dermatofibromas[8]. Therefore, NTK was classified as an independent disease for diagnosis. NTKs clinically manifest primarily as painless, slow-growing subcutaneous nodules with good mobility. Clinical diagnosis of these rare neoplasms is challenging because NTKs are not distinctive in physical examinations and imaging examinations. NTK is often mistaken for a sebaceous cyst, a Spitz naevus, a fibrous histiocytoma, a basal cell carcinoma, or a skin adnexal tumour (mainly pilomatricoma)[9,10], and an accurate diagnosis depends on histopathological and immunohistochemical examination.

Histopathologically, NTK is a poorly circumscribed nodule typically composed of fascicles of spindle-shaped and epithelioid tumour cells with a sparse or no mucinous matrix[10]. Epithelioid cells, which present as oval or polygonal eosinophilic cells, are

Table 1 Main points in the differential diagnosis between neurothekeomas and several other diseases

	NTK	DNSM	PFH	EFH	Spitz nevus
Average age	Adult/teenager	Adult	Teenager	Adult/teenager	Teenager/adult under 35
Sex	Female	Both	Female	Female	Female
Predilection site	Head/upper limbs/trunk	Finger/lower limbs	Upper limbs/trunk	Lower limbs	Face/head/lower limbs
Tumour boundary	Blurred	Clear	Clear	Clear	Clear
Arrangement of tumour cells	Lobular/nodular/clump/whirlpool like	Lobular/nodular	Nodular/clump	Mosaic or whirlpool-like	Nested
Tumour cell morphology	Round/oval/spindle	Round/oval/spindle	Round/oval/spindle	Round/oval	Polygon/spindle
Atypia of tumour cells	Mild-moderate	Rare	Rare	Rare	Rare
Mitosis of nucleus	0-25/WHPF	-	Rare	Rare	Rare
Immunohistochemical phenotype	CD10(+); CD63(+); mitf(+)	S-100(+); GFAP(+); SOX10(+)	S-100(+); vimentin(+); lysozyme(+)	ALK(+); TFE3(+); S-100(-)	S-100(+); HMB-45(+)

WHPF: Wide high-power field eyepiece 22 mm, sp 40x objective; NTK: Neurothekeoma; DNSM: Dermal nerve sheath myxoma; PFH: Plexiform fibrous histiocytoma; EFH: Epithelioid fibrous histiocytoma; GFAP: Glial fibrillary acidic protein.

rich in the cytoplasm and arranged in a nodular or plexiform pattern; spindle-shaped cells are arranged in bunches or swirls and have a benign morphology. The stroma is composed of hyalinized collagen fibres often accompanied by mucoid degeneration. Depending on the amount of myxoid matrix, NTKs have been subclassified into three types: myxoid (myxoid matrix > 50%), mixed (10% < myxoid matrix ≤ 50%) and cellular (myxoid matrix < 10%). The myxoid matrix can occasionally superficially infiltrate skin or muscle tissue. The nuclei can show mild to moderate atypia, and approximately 0-25 mitotic nuclei per high power field can be observed.

Immunohistochemical examination demonstrates that tumour cells express CD10, CD63 (NKI/C3), and mitf. Most tumours also express CD99. A few tumours express SMA and are negative for S-100, cytokeratin, Melan-A, and SOX-10 staining[11,12], indicating that NTKs are associated with scattered histiocytes.

Accurate diagnosis of NTKs is essential given that these lesions can be mistaken for malignancies, leading to unnecessary treatment. The differential diagnosis includes mainly various types of cysts, DNSMs, plexiform fibrous histiocytomas (PFHs), EFHs, Spitz nevi, *etc*. The clinical manifestations of these diseases are similar, but the pathological characteristics are different: subcutaneous cysts contain keratinized or necrotic material without tumour cells; DNSMs express S-100, GFAP and SOX10, as assessed by immunohistochemistry[13]; PFHs have spindle-shaped fibroblasts around the nodular-arranged tumour cells[14]; EFH tumour cells are mostly diffusely arranged and do not express CD63[15]; and Spitz nevi are composed of epithelioid or spindle-shaped pigment cells and express S-100[16]. The differential diagnosis of these diseases is shown in Table 1.

CONCLUSION

Herein, we report two rare NTKs; both were completely resected after clinical evaluation, and an accurate diagnosis was obtained after the histopathological and immunohistochemical examination. In addition, we provide a summary of the differential diagnosis and the possible diagnostic pitfalls. The diagnostic and therapeutic experience reported here can be used as a reference for other surgeons and pathologists.

REFERENCES

1 **Lau SK**, Cassarino DS, Koh SS. Multiple myxoid cellular neurothekeomas in a patient with systemic lupus erythematosus. *J Cutan Pathol* 2021; **48**: 980-985 [PMID: 33844324 DOI: 10.1111/cup.14025]

2 **Massimo JA**, Gasibe M, Massimo I, Damilano CP, De Matteo E, Fiorentino J. Neurothekeoma: Report of two cases in children and review of the literature. *Pediatr Dermatol* 2020; **37**: 187-189 [PMID: 31774578 DOI: 10.1111/pde.14057]

3 **Wiemeyer S**, Hafer G. Neurothekeoma of the toe. *Foot Ankle Spec* 2013; **6**: 479-481 [PMID: 24107319 DOI: 10.1177/1938640013507106]

4 **Silva CMM**, Fontenele JPU, Lopes JR, de Brito GCC, Teixeira MJD, Rocha FAC. Neurothekeoma in the Axilla Causing Persistent Shoulder Pain: Case Report. *Rev Bras Ortop (Sao Paulo)* 2020; **55**: 804-807 [PMID: 33364664 DOI: 10.1055/s-0040-1712135]

5 **Cavicchini S**, Guanziroli E, Del Gobbo A, Scaparro M, Gianotti R. Neurothekeoma, a hard to diagnose neoplasm among red nodules. *Australas J Dermatol* 2018; **59**: e280-e282 [PMID: 29527669 DOI: 10.1111/ajd.12800]

6 **Vetrano IG**, Levi V, Pollo B, Chiapparini L, Messina G, Nazzi V. Sleeve-Shaped Neurothekeoma of the Ulnar Nerve: A Unique Case of a Still Unclear Pathological Entity. *Hand (N Y)* 2020; **15**: NP7-NP10 [PMID: 30762430 DOI: 10.1177/1558944719828008]

7 **Abuawad YG**, Saraiva MI, Westin AT, Valente NY. S-100 negative myxoid neurothekeoma: a new type of neurothekeoma? *An Bras Dermatol* 2017; **92**: 153-155 [PMID: 28225982 DOI: 10.1590/abd1806-4841.20176016]

8 **Abdaljaleel M**, North JP. Positive MITF and NKI/C3 Expression in Cellular Neurothekeoma and Dermatofibroma. *Appl Immunohistochem Mol Morphol* 2021; **29**: 440-445 [PMID: 33264109 DOI: 10.1097/PAI.0000000000000889]

9 **Fetsch JF**, Laskin WB, Hallman JR, Lupton GP, Miettinen M. Neurothekeoma: an analysis of 178 tumors with detailed immunohistochemical data and long-term patient follow-up information. *Am J Surg Pathol* 2007; **31**: 1103-1114 [PMID: 17592278 DOI: 10.1097/PAS.0b013e31802d96af]

10 **Tran P**, Mclemore M. Atypical cellular neurothekeoma: A potential diagnostic pitfall for benign and malignant spindle cell lesions in skin. *J Cutan Pathol* 2018; **45**: 619-622 [PMID: 29744902 DOI: 10.1111/cup.13274]

11 **Murphrey M**, Huy Nguyen A, White KP, Krol A, Bernert R, Yarbrough K. Pediatric cellular neurothekeoma: Seven cases and systematic review of the literature. *Pediatr Dermatol* 2020; **37**: 320-325 [PMID: 31930561 DOI: 10.1111/pde.14043]

12 **See TRO**, Stålhammar G, Grossniklaus HE. Neurothekeoma of the eye, conjunctiva, and periorbital adnexa: A report of two cases and brief review. *Surv Ophthalmol* 2019; **64**: 852-857 [PMID: 30978337 DOI: 10.1016/j.survophthal.2019.04.002]

13 **Khashaba H**, Hafez E, Burezq H. Nerve Sheath Myxoma: A rare tumor, a case report and literature review. *Int J Surg Case Rep* 2020; **73**: 183-186 [PMID: 32693231 DOI: 10.1016/j.ijscr.2020.07.030]

14 **Ghuman M**, Hwang S, Antonescu CR, Panicek DM. Plexiform fibrohistiocytic tumor: imaging features and clinical findings. *Skeletal Radiol* 2019; **48**: 437-443 [PMID: 30145610 DOI: 10.1007/s00256-018-3050-1]

15 **Dickson BC**, Swanson D, Charames GS, Fletcher CD, Hornick JL. Epithelioid fibrous histiocytoma: molecular characterization of ALK fusion partners in 23 cases. *Mod Pathol* 2018; **31**: 753-762 [PMID: 29327718 DOI: 10.1038/modpathol.2017.191]

16 **Harms KL**, Lowe L, Fullen DR, Harms PW. Atypical Spitz Tumors: A Diagnostic Challenge. *Arch Pathol Lab Med* 2015; **139**: 1263-1270 [PMID: 26414472 DOI: 10.5858/arpa.2015-0207-RA]

World Journal of Clinical Cases

Submit a Manuscript: https://www.f6publishing.com

World J Clin Cases 2022 February 16; 10(5): 1747-1753

DOI: 10.12998/wjcc.v10.i5.1747

ISSN 2307-8960 (online)

CASE REPORT

Subclavian artery stenting *via* bilateral radial artery access: Four case reports

Tao Qiu, Sheng-Qi Fu, Xiao-Yong Deng, Ming Chen, Xiao-Yan Dai

ORCID number: Tao Qiu 0000-0002-7841-4479; Sheng-Qi Fu 0000-0001-9770-6648; Xiao-Yong Deng 0000-0003-2680-5280; Ming Chen 0000-0002-7645-1911; Xiao-Yan Dai 0000-0002-5197-7773.

Author contributions: Qiu T was guarantor of integrity of the entire study, controlled the study design, literature research, definition of intellectual content, experimental studies, data acquisition, data analysis, statistical analysis, manuscript preparation, manuscript editing; Dai XY concepted study; Qiu T, Fu SQ, Deng XY and Chen M prepared the clinical studies; Qiu T and Dai XY controlled the manuscript review; all authors issued final approval for the version to be submitted.

Informed consent statement: Written Informed consent was obtained from all the participatants.

Conflict-of-interest statement: The authors declare that there are no conflicts of interest associated with this manuscript.

CARE Checklist (2016) statement: The authors have read the CARE Checklist (2016), and the manuscript was prepared and revised according to the CARE Checklist (2016).

Tao Qiu, Sheng-Qi Fu, Xiao-Yong Deng, Ming Chen, Department of Neurology, Zigong First People's Hospital, Zigong 643000, Sichuan Province, China

Xiao-Yan Dai, Department of Equipment Management, Zigong First People's Hospital, Zigong 643000, Sichuan Province, China

Corresponding author: Xiao-Yan Dai, MM, Chief Doctor, Department of Equipment Management, Zigong First People's Hospital, No. 42 Shangyihao 1st Branch Road, Ziliujing District, Zigong 643000, Sichuan Province, China. dxy_zgyyy@163.com

Abstract

BACKGROUND

Subclavian artery stenosis refers to the stenosis in the lumen caused by the presence of plaque or thrombus in the subclavian artery. It is a common problem in endovascular interventions. In fact, conventional subclavian artery stenting *via* the femoral artery approach is effective and safe. Nevertheless, because femoral artery puncture is not easy to stop bleeding, it requires longer femoral artery compression or more expensive hemostatic materials, such as staplers. Patients need to be catheterized and bedridden for a longer time, which may lead to many complications, such as pseudoaneurysm.

CASE SUMMARY

Herein, we reported a new interventional therapy of subclavian artery. From March 1, 2020 to August 31, 2021, we operated on four patients with subclavian artery stenting *via* bilateral radial artery access.

CONCLUSION

After reviewing four cases of successful placement of clavicular artery stents *via* bilateral radial arteries, we concluded that bilateral radial artery approach is feasible. Clavicular artery stenting is safe, effective, and timesaving. It is an excellent alternative to the traditional femoral artery procedure, with few complications and high comfort degree.

Key Words: Subclavian artery stenosis; Bilateral radial artery; Stenting; Subclavian artery steal syndrome; Case report

Country/Territory of origin: China

Specialty type: Neurosciences

Provenance and peer review: Unsolicited article; Externally peer reviewed.

Peer-review model: Single blind

Peer-review report's scientific quality classification
Grade A (Excellent): A
Grade B (Very good): B
Grade C (Good): 0
Grade D (Fair): 0
Grade E (Poor): 0

Received: November 1, 2021
Peer-review started: November 1, 2021
First decision: November 17, 2021
Revised: December 4, 2021
Accepted: January 6, 2022
Article in press: January 6, 2022
Published online: February 16, 2022

P-Reviewer: Diana F, Wang P
S-Editor: Wang JL
L-Editor: A
P-Editor: Wang JL

Core Tip: In this study, we reported a new interventional therapy of subclavian artery. we concluded that bilateral radial artery approach is feasible. Clavicular artery stenting is safe, effective, and timesaving. It is an excellent alternative to the traditional femoral artery procedure, with few complications and high comfort degree.

Citation: Qiu T, Fu SQ, Deng XY, Chen M, Dai XY. Subclavian artery stenting *via* bilateral radial artery access: Four case reports. *World J Clin Cases* 2022; 10(5): 1747-1753
URL: https://www.wjgnet.com/2307-8960/full/v10/i5/1747.htm
DOI: https://dx.doi.org/10.12998/wjcc.v10.i5.1747

INTRODUCTION

Subclavian artery stenosis refers to the stenosis in the lumen caused by the presence of plaque or thrombus in the subclavian artery. Its prevalence in the general population is less than that in the patients with peripheral artery stenosis (2% *vs* 11.5% to 19%)[1]. Occlusion or stenosis in the subclavian artery can lead to some serious complications that endanger the upper extremities, brain and heart[2]. For example, subclavian steal syndrome (SSS) can result in ischemia of the vertebrobasilar system, with the manifestation of vertigo, syncope, diplopia, blurred vision, dysarthria, and tinnitus. The treatment of subclavian artery stenosis mainly includes open surgery, percutaneous transluminal angioplasty (PTA) and percutaneous transluminal stenting. Currently, endovascular intervention is more commonly accepted by clinicians and patients because of its minimal trauma, rapid recovery, and few complications[3].

Traditionally, the right femoral artery is the preferred therapeutic approach for subclavian artery stenting. However, the traditional femoral artery approach still has many limitations, including the need to expose the patient's private site, bed rest, and increased financial burden[4,5]. Moreover, there are also some rare complications, such as retroperitoneal hemorrhage. PTA and subclavian artery stenting *via* brachial approach has also been attempted to overcome those shortcomings[6]. However, previous studies have shown that brachial artery is mainly used as the blood supply to the upper extremity, with a high incidence of complications in access sites and ischemic complications[7]. Therefore, it is considered less favorable. In this case report, we described a new interventional therapy of subclavian artery. Subclavian artery stenting *via* bilateral radial artery access is an excellent alternative to the traditional femoral artery procedure, with few complications and high comfort degree.

CASE PRESENTATION

Chief complaints

Treating Subclavian artery stenosis. From March 1, 2020 to August 31, 2020, we operated on four patients with subclavian artery stenting *via* bilateral radial artery access. All participants signed the informed consent. When necessary, the legal guardian of volunteers signed the informed consent on their behalf. The case report was as follows.

Case 1: A male patient, 68 years old, had hypertension for 10 years and smoking history for 40 years. He was admitted to the hospital after 10 d of dysphonia with right-sided limb weakness. Magnetic resonance imaging (MRI) showed left pontocerebral lacunar cerebral infarction. The blood pressure of the right upper extremity was 186/92 mmHg, and that of the left upper extremity was 156/85 mmHg. Transcranial color Doppler (TCD) suggested steal of the left subclavian artery at stage 2. On March 30, 2020, the patient underwent subclavian artery stenting *via* bilateral radial artery access (Figure 1A-C). Consumables included 5F radial artery sheath (Terumo, Terumo Corporation, Tokyo, Japan), 6F radial artery sheath, 2.6 m long 0.035 guidewire, 5F Simon2 contrast catheter (Terumo, Terumo Corporation, Tokyo, Japan). Moreover, dynamic 9/25 mm ball expansion stent (Biotronika, Ackerstrasse, Bulach, Switzerland) and pressure pump were also used. The total procedure took 13 min.

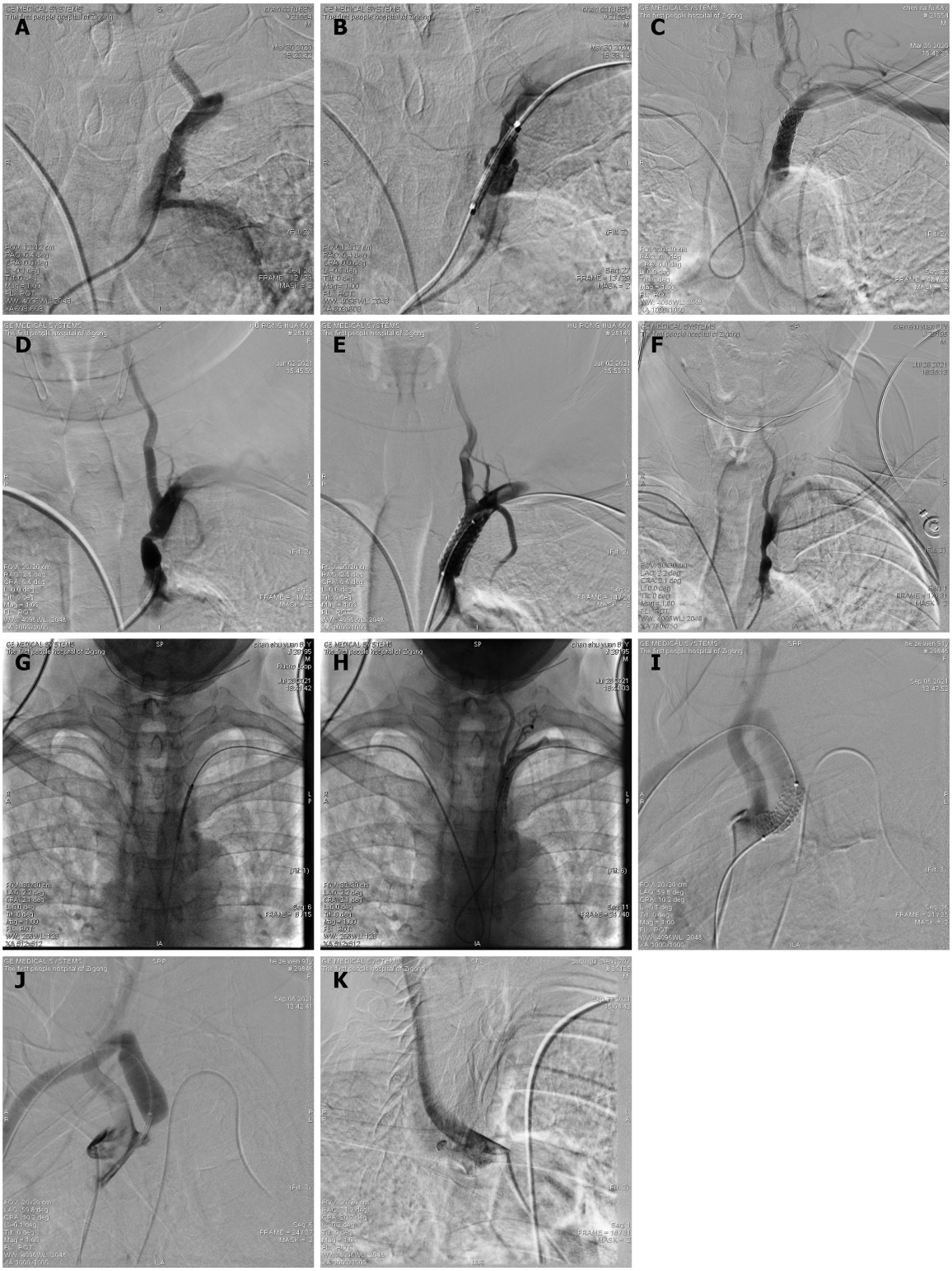

Figure 1 The imaging of cases. A-C: Case 1. At 15:29, right radial artery puncture was inserted into 5F arterial sheath, and Simon2 catheter was selected for left subclavian artery angiography (A); At 15:33, the left radial artery was punctured and a 6F arterial sheath was inserted. A 2.6 m 0.035 guidewire was used for stenting to the left subclavian artery ulcerated plaque with stenosis under Simon2 catheterization positioning (B); At 15:42, 12 ATM dilated the balloon to release the stent. The stent was in good shape. The total procedure took 13 min (C); D and E: Case 2. At 15:45, the right radial artery was punctured and inserted into the 5F arterial sheath, and the Simon2 catheter was selected for left subclavian artery angiography (D); At 15:53, the 6F arterial sheath was inserted *via* left radial artery puncture. The stent was guided into the place with a 2.6-length 0.035 guidewire and successfully released under Simon2 catheter angiographic positioning. Its morphology was good (E); F-H: Case 3. At 18:35, the right radial artery was punctured and a 5F arterial sheath was inserted. The Simon2 catheter was selected for left subclavian artery angiography (F); At 18:41, the 6F arterial sheath was inserted by left radial artery puncture. A 2.6-length 0.035 guidewire was used to guide the stent to the subclavian artery stenosis under Simon2 catheterization positioning (G); At 18:44, 13 ATM dilated balloon to release the stent. Its morphology was good (H); I-K: Case 4. At 13:28, the left radial artery was punctured and a 5F arterial sheath was inserted. The Simon2 catheter was selected into the unnamed artery for imaging (I); At 13:39, the 6F arterial sheath was inserted through the right radial artery puncture. A 2.6-length 0.035 guidewire was used to guide the stent into place

under Simon2 catheterization positioning (J); At 13:48, 14 ATM stent was released accurately. Its morphology was good (K).

Case 2: A female patient, 66 years old, had hypertension for three years. She was admitted to the hospital with dizziness for 10 d. On admission, the blood pressure of the right upper extremity was 130/73 mmHg, and that of the left-sided upper extremity was 103/58 mmHg. TCD suggested steal in the left subclavian artery at stage 2. On June 2, 2020, the patient underwent subclavian artery stenting *via* bilateral radial artery access (Figure 1D and E). Consumables included 5F radial artery sheath, 6F radial artery sheath, 2.6 m long 0.035 guidewire (APT, Hunan, China), 5F Simon2 contrast catheter (Yixinda, Shenzhen, China), Omnilink Elite9/19mm ball Expandable stent (Abbott Vascular, Santa Clara, CA, United States), and pressure pump. The total procedure took 9 min.

Case 3: A male patient, 81 years old, had hypertension for three years. He was admitted to the hospital with recurrent dizziness for 15 d. On admission, the blood pressure of the right upper extremity was 137/85 mmHg, and that of the left upper extremity was 115/61 mmHg. TCD suggested steal of the left subclavian artery at stage 2. On July 28, 2021, he received subclavian artery stenting *via* bilateral radial artery access (Figure 1F-H). Consumables included 5F radial artery sheath, 6F radial artery sheath, 2.6 m long 0.035 guidewire (APT, Hunan, China), 5F Simon2 contrast catheter (Yixinda, Shenzhen, China), Omnilink Elite8/29mm ball-expandable stent (Abbott Vascular, Santa Clara, CA, United States), and pressure pump. The total procedure took 9 min.

Case 4: A female patient, 91 years old, had hypertension for five years. She was admitted to the hospital with recurrent dizziness for six months and exacerbated for two days. on admission, the blood pressure of right upper limb was 95/52 mmHg and that of the left upper limb was 146/78 mmHg. TCD suggested steal of right subclavian artery at stage 3. On August 30, 2021, she received subclavian artery stenting *via* bilateral radial artery access (Figure 1I-K). Consumables included 5F radial artery sheath, 6F radial artery sheath, 2.6 m long 0.035 guidewire, 5F Simon2 contrast catheter, Omnilink Elite10/29 mm ball Expandable stent (Abbott Vascular, Santa Clara, CA, United States), and pressure pump. The total procedure took 20 min.

History of present illness

Case 1: He was admitted to the hospital after 10 d of dysphonia with right-sided limb weakness.

Case 2: She was admitted to the hospital with dizziness for 10 d.

Case 3: He was admitted to the hospital with recurrent dizziness for 15 d.

Case 4: She was admitted to the hospital with recurrent dizziness for six months and exacerbated for 2 d.

History of past illness

Case 1: He had hypertension for 10 years and smoking history for 40 years.

Cases 2 and 3: The patients had hypertension for 3 years.

Case 4: She had hypertension for 5 years.

Laboratory examinations

Case 1: The blood pressure of the right upper extremity was 186/92 mmHg, and that of the left upper extremity was 156/85 mmHg.

Case 2: On admission, the blood pressure of the right upper extremity was 130/73 mmHg, and that of the left-sided upper extremity was 103/58 mmHg.

Case 3: On admission, the blood pressure of the right upper extremity was 137/85 mmHg, and that of the left upper extremity was 115/61 mmHg.

Case 4: On admission, the blood pressure of right upper limb was 95/52 mmHg and that of the left upper limb was 146/78 mmHg.

Imaging examinations

Case 1: MRI showed left pontocerebral lacunar cerebral infarction. TCD suggested steal of the left subclavian artery at stage 2.

Cases 2 and 3: TCD suggested steal in the left subclavian artery at stage 2.

Case 4: TCD suggested steal of right subclavian artery at stage 3.

FINAL DIAGNOSIS

There were satisfactory results and without any complications. The patients were able to get out of bed right after the operation with high comfort degree. Moreover, the radial artery access procedure allows the use of no-guiding catheter.

TREATMENT

The patients underwent subclavian artery stenting *via* bilateral radial artery access.

OUTCOME AND FOLLOW-UP

There were satisfactory results and without any complications. The patients were able to get out of bed right after the operation with high comfort degree. Moreover, the radial artery access procedure allows the use of no-guiding catheter. It avoids the use of hemostatic devices, such as vascular blockers or anastomoses.

DISCUSSION

Nowadays, transradial artery access has been widely used in interventional treatment of the heart. Numerous studies have proven that radial artery puncture is safe and feasible[7,8]. Although the radial artery is small, it is superficial and easy to puncture, and the actual puncture success rate is similar to that of the femoral artery[9-11]. Moreover, the access to the subclavian artery from the radial artery is very easy, especially for the right subclavian artery in type 3 arch. The problem that needs to be addressed is how to deliver larger-diameter stents. In a Korean study, the radial artery diameter was 2.74 ± 0.41 mm in men and 2.26 ± 0.42 mm in women[12]. There is no problem matching the radial artery with an arterial sheath of 6F, with maximum inner diameter of 2.2 mm and outer diameter of 2.46 mm. Furthermore, 8F arterial sheath (2.67 mm ID) is not matched in most people. The only option available to us is the 6F arterial sheath. However, the diameter of the stent needed for subclavian artery stenosis is usually above 8 mm. How to deliver the stent to the stenosis is a problem.

There are currently two options. One is to choose a long 6F sheath (2.2-mm inner diameter and 2.6-mm outer diameter). Due to the large outer diameter, a large percentage of patients are not suitable. Another way is to deliver the stent directly to the stenosis site through the guide wire guidance. Since the upper extremity vessels are generally straight, it is relatively easy to stent in place, and it is more advantageous for the right subclavian artery in type 3 arch. However, because there is no guiding catheter, it is not possible to do the angiographic localization. Therefore, it is necessary to first do a good map of the pathway through the angiographic catheter or localize it using bony markers. After delivery, the balloon or stent is dilated or released under the guidance of the roadmap or bony marker. However, actual patient movement, vascular pulsation, and respiration can cause the roadmap to shift from its actual position. Moreover, as the guidewire and stent are delivered, the vessel morphology will change accordingly. The road map and bony markers do not represent the actual vascular situation, which can easily lead to inaccurate stent positioning. Herein, we thought to perform a dual access procedure, with a Simon2 catheter to access the subclavian artery. A 6F arterial sheath is inserted through the radial artery on the side of the lesion, and a guidewire is passed directly through the stenosis to guide the balloon and stent to the stenosis.

We actually reviewed the relevant literatures and found few reports. A single-center Croatian study on subclavian artery stenosis with a total of 50 SSS was basically performed through the femoral and brachial arteries[1]. The right femoral approach was the most commonly used (62%), followed by the left brachial approach (17%), without transradial procedures. In a Italian study, the opening of the left subclavian artery *via* unilateral radial access was performed with a stent positioned using bony markers, which was clearly more blinded[13]. A relatively large number of Canadian study have been reported[14]. From February 2010 to February 2015, there were 54 patients with stenosis or chronic occlusion of the subclavian artery. In 35 patients, a bilateral radial artery approach was used. However, a 6F guiding catheter was used on the lesion side in all cases, which is different from the present study. A single ipsilateral radial artery approach was used in the other 19 patients. The procedural success rate was 97% in the bilateral group in comparison with 95% in the single group. None of them had major complications except for a small hematoma. It was effective and safe with single femoral access or combined femoral and brachial access, with vascular complications (6.3%) and neurological complications (0.6%-9%).

We have performed more than 2000 cases of whole brain angiography *via* radial artery access in our hospital. We are very proficient in both left radial artery and right radial artery puncture. In combination with the above studies, we demonstrated that it is safe and effective to perform subclavian stenting with bilateral radial artery access. After the approval of the hospital ethics committee, we performed four cases of subclavian stenting *via* bilateral radial artery access. There were satisfactory results and without any complications. The patients were able to get out of bed right after the operation with high comfort degree. Moreover, the radial artery access procedure allows the use of no-guiding catheter. It avoids the use of hemostatic devices, such as vascular blockers or anastomoses. Excluding the cost of an additional radial artery sheath, the cost of per patient is reduced by approximately $500.

CONCLUSION

The case report suggested that subclavian artery stenting can be done quickly from either left or right subclavian artery *via* bilateral radial artery puncture. Through the application experience and literature review, we believe that the treatment of the clavicular artery *via* bilateral radial artery access is safe, effective, and timesaving, with few complications and high comfort degree. It deserves further studies to confirm its safety and efficacy in comparison with the femoral artery.

REFERENCES

1 **Dobrota S**, Filipovi-Gri L, Perkov D, Dobrta VD, Lukinovic-Skudar V, Kirhmajer MV, Coce N, Soldo SB. Endovascular treatment of subclavian stenosis-single center experience. *Medicinske znanosti* 2021; **547**: 32-37 [DOI: 10.21857/m8vqrtqv89]

2 **Noutsias M**, Rigopoulos AG, Ali M, Ukkat J, Sedding D, John E. Acute myocardial ischemia in a patient with coronary-subclavian steal syndrome treated by retrograde percutaneous recanalization of the chronic total occlusion of the left subclavian artery. *Hellenic J Cardiol* 2021; **62**: 225-227 [PMID: 32580019 DOI: 10.1016/j.hjc.2020.06.006]

3 **Rafailidis V**, Li X, Chryssogonidis I, Rengier F, Rajiah P, Wieker CM, Kalva S, Ganguli S, Partovi S. Multimodality Imaging and Endovascular Treatment Options of Subclavian Steal Syndrome. *Can Assoc Radiol J* 2018; **69**: 493-507 [PMID: 30318458 DOI: 10.1016/j.carj.2018.08.003]

4 **Stone JG**, Zussman BM, Tonetti DA, Brown M, Desai SM, Gross BA, Jadhav A, Jovin TG, Jankowitz B. Transradial *versus* transfemoral approaches for diagnostic cerebral angiography: a prospective, single-center, non-inferiority comparative effectiveness study. *J Neurointerv Surg* 2020; **12**: 993-998 [PMID: 31974282 DOI: 10.1136/neurintsurg-2019-015642]

5 **Li Y**, Chen SH, Spiotta AM, Jabbour P, Levitt MR, Kan P, Griessenauer CJ, Arthur AS, Osbun JW, Park MS, Chalouhi N, Sweid A, Wolfe SQ, Fargen KM, Dumont AS, Dumont TM, Brunet MC, Sur S, Luther E, Strickland A, Yavagal DR, Peterson EC, Schirmer CM, Goren O, Dalal S, Weiner G, Rosengart A, Raper D, Chen CJ, Amenta P, Scullen T, Kelly CM, Young C, Nahhas M, Almallouhi E, Gunasekaran A, Pai S, Lanzino G, Brinjikji W, Abbasi M, Dornbos Iii D, Goyal N, Peterson J, El-Ghanem MH, Starke RM. Lower complication rates associated with transradial *versus* transfemoral flow diverting stent placement. *J Neurointerv Surg* 2021; **13**: 91-95 [PMID: 32487766 DOI: 10.1136/neurintsurg-2020-015992]

6 **Dragicevi'c D**, Skori'c M, Koli'c K, Titli'c M. A case of acquired right-sided subclavian steal syndrome successfully treated with stenting using brachial approach. *Case Rep Clin Med* 2014; **2014** [DOI: 10.4236/crcm.2014.32017]

7 **Lee CW**, Cho SC. The Transradial Approach for Coronary Intervention: More Comfort, Better Outcome. *Korean Circ J* 2018; **48**: 728-730 [PMID: 30073811 DOI: 10.4070/kcj.2018.0118]

8 **Mason PJ**, Shah B, Tamis-Holland JE, Bittl JA, Cohen MG, Safirstein J, Drachman DE, Valle JA, Rhodes D, Gilchrist IC; American Heart Association Interventional Cardiovascular Care Committee of the Council on Clinical Cardiology; Council on Cardiovascular and Stroke Nursing; Council on Peripheral Vascular Disease; and Council on Genomic and Precision Medicine. An Update on Radial Artery Access and Best Practices for Transradial Coronary Angiography and Intervention in Acute Coronary Syndrome: A Scientific Statement From the American Heart Association. *Circ Cardiovasc Interv* 2018; **11**: e000035 [PMID: 30354598 DOI: 10.1161/HCV.0000000000000035]

9 **Sandoval Y**, Bell MR, Gulati R. Transradial Artery Access Complications. *Circ Cardiovasc Interv* 2019; **12**: e007386 [PMID: 31672030 DOI: 10.1161/CIRCINTERVENTIONS.119.007386]

10 **Le May M**, Wells G, So D, Chong AY, Dick A, Froeschl M, Glover C, Hibbert B, Marquis JF, Blondeau M, Osborne C, MacDougall A, Kass M, Paddock V, Quraishi A, Labinaz M. Safety and Efficacy of Femoral Access *vs* Radial Access in ST-Segment Elevation Myocardial Infarction: The SAFARI-STEMI Randomized Clinical Trial. *JAMA Cardiol* 2020; **5**: 126-134 [PMID: 31895439 DOI: 10.1001/jamacardio.2019.4852]

11 **Liu M D**, Gai Y T. Comparison of transradial and transfemoral cerebral angiography. *Brain Hemorrh* 2020; **1**: 95-98 [DOI: 10.1016/j.hest.2020.02.001]

12 **Yoon W**, Kwon WK, Choudhri O, Ahn J, Huh H, Ji C, Do HM, Mantha A, Jeun SS. Complications Following Transradial Cerebral Angiography: An Ultrasound Follow-Up Study. *J Korean Neurosurg Soc* 2017 [PMID: 29207853 DOI: 10.3340/jkns.2017.0209]

13 **Rigatelli G**, Zuin M, Dell'Avvocata F, Giatti S, Daggubati R. Transradial supra-aortic arteries interventions: a good option for elderly patients. *J Geriatr Cardiol* 2018; **15**: 634-638 [PMID: 30416512 DOI: 10.11909/j.issn.1671-5411.2018.10.006]

14 **Kedev S**, Zafirovska B, Petkoska D, Vasilev I, Bertrand OF. Results of Transradial Subclavian Artery Percutaneous Interventions After Bilateral or Single Access. *Am J Cardiol* 2016; **118**: 918-923 [PMID: 27471055 DOI: 10.1016/j.amjcard.2016.06.029]

Published by **Baishideng Publishing Group Inc**
7041 Koll Center Parkway, Suite 160, Pleasanton, CA 94566, USA
Telephone: +1-925-3991568
E-mail: bpgoffice@wjgnet.com
Help Desk: https://www.f6publishing.com/helpdesk
https://www.wjgnet.com